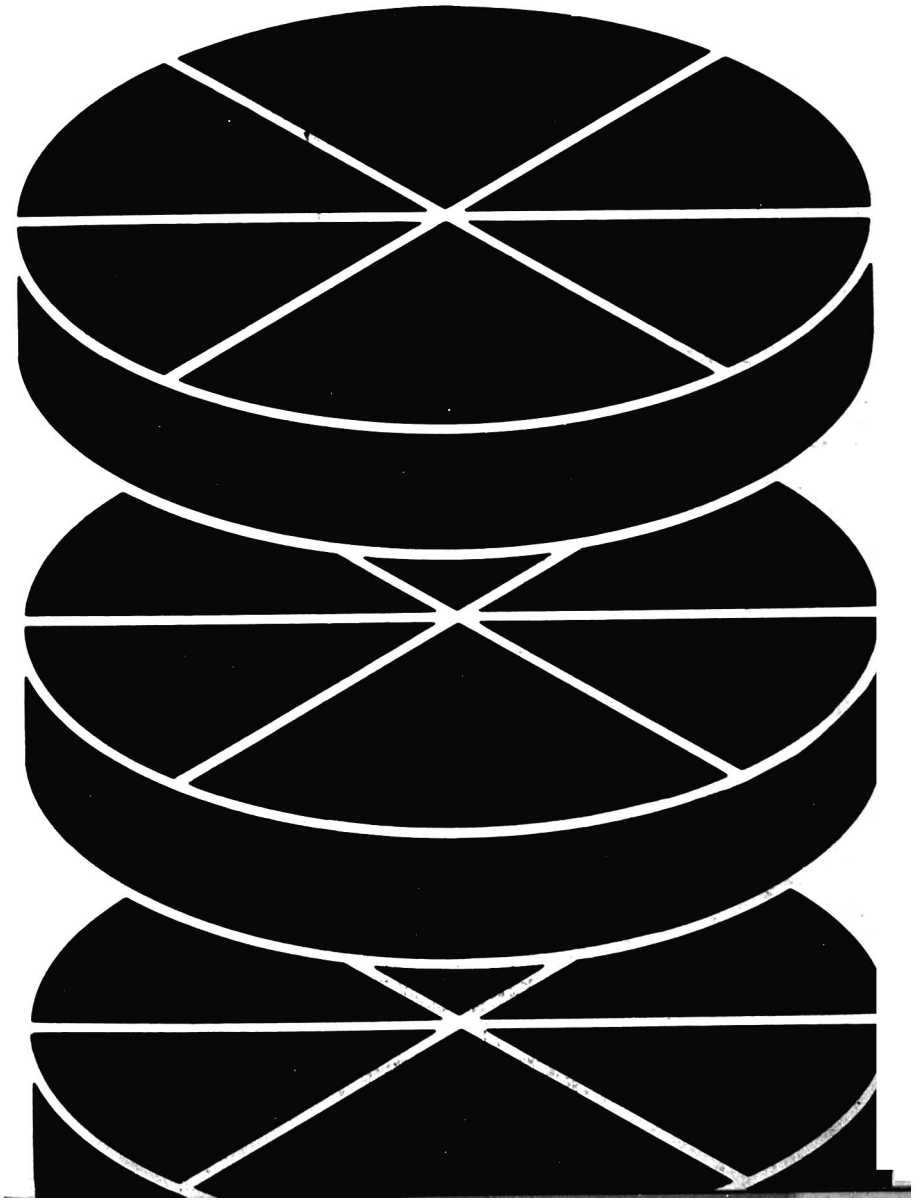
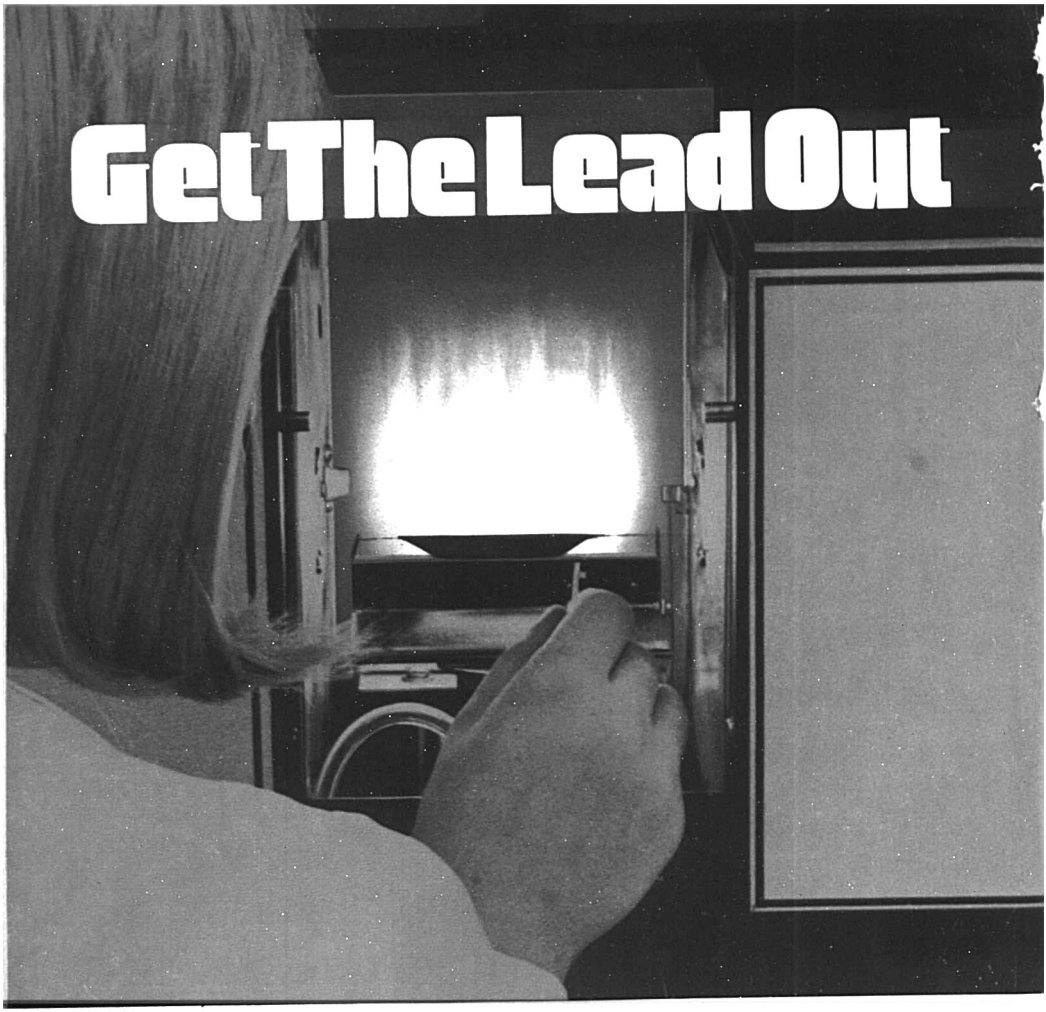
JANUARY 1971

ANALYTICAL CHEMISTRY





There is a quicker, easier and, most important, a more accurate method for making Pb determinations in the laboratory. It combines the use of the IL 353 Atomic Absorption/Emission Spectrophotometer with a new Solid Phase Sampling technique.

The IL 353 provides the acknowledged superiority of a double beam optics system, plus exclusive double beam background correction. Solid Phase Sampling ensures use of small samples, rapidly prepared. The net result is more sensitive, more precise analyses for the determination of possible lead toxicities.

Want to learn more about this new way, this better way, this most accurate way to "get the lead out"? Write today. We'll send you the latest information.

Lead Me To The Lead.

☐ Please send me information regarding the new IL technique for Pb Analysis

Name: _____

Organization: _____

Address: _____

City: _____

State: _____ Zip Code: _____

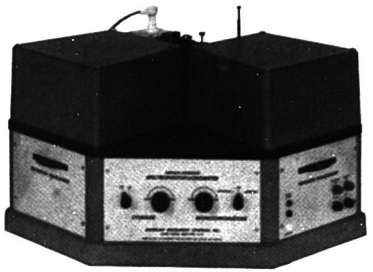
Phone: _____ Area Code: _____

Instrumentation Laboratory Inc./113 Hartwell Avenue/Lexington Mass.

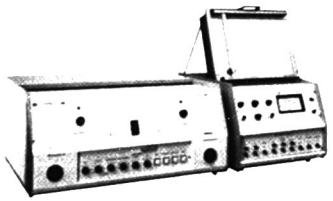
Instrumentation Laboratory Inc. 113 Hartwell Avenue/Lexington, Mass. 02173/Tel. 617-861-0710/Telex 92-3440

Circle No. 93 on Readers' Service Card

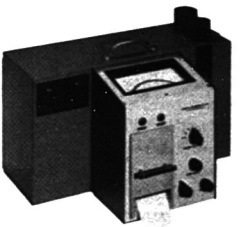
The First Family of Fluorescence Instrumentation



AMINCO-BOWMAN SPECTROPHOTOFLUOROMETER (SPF)
This famous research "workhorse" performs either fluorescence or phosphorescence studies by a simple interchanging of cell compartments. Sensitivity: one part per trillion, quinine sulfate, when excited at 250 or 350nm. Resolution: less than 1nm. Cell compartment and lamp housing provide means to maintain optimum temperature for sample and lamp. Less Noise: low ripple power supply reduces arc wander. Energy-corrected Spectra Accessory compensates for spectral dependence of components. Applications include: fluorescence probes, enzyme assays, phosphorescence studies, thin-layer chromatography, physical chemistry measurements.



AMINCO



AMINCO SPF-1000 HIGH PERFORMANCE SPECTROPHOTOFLUOROMETER
Features: High Resolution: 0.2nm with digital readout; Bandpass of .2, .5, 1, 2, 5, 10, 20 and 40nm. Monochromator wavelength range: 200-1000nm; Spectrum: starting wavelength of 200, 300, 400, 500, 600, 700, 800 or 900nm and spectral width of 100, 200 or 400nm may be selected by front panel switches. Spectra may also be displayed as a function of wavenumber. Large up-front sample compartment. Accessories are on adaptor plates for simple slip-on mounting. Ellipsoidal Condensing System included. Unit accepts 500w xenon lamp. Solid-state blank-subtract Photomultiplier Microphotometer allows use of any side-on or end-on photomultiplier tubes. Photometer responds to phenomena having lifetimes as short as 5 microseconds, allowing the SPF-1000 to be used as a precise phosphorescence lifetime instrument.



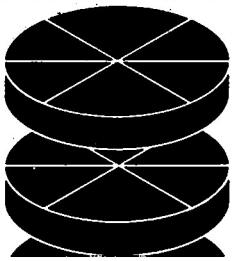
AMINCO FLUORO-MICRO-PHOTOMETER Direct-reading Filter Fluorometer serves as a Turbidimeter, colorimeter, phosphorimeter, nephelometer and liquid-flow monitor and alarm. Permits rapid, quantitative sequential analysis of samples whose luminescence characteristics are known with printed or meter readout. Solid-state blank-subtract model provides for adjustable voltage to the PM tube, ranging from 300 to 1000v within 0.01%. These features provide greatly increased sensitivity and stability.

AMINCO SPF-125 A direct reading spectrofluorometer designed especially to perform standard fluorometric determinations. Two monochromators for independent setting of excitation and emission wavelengths eliminate the guesswork and bother of filter combinations. Disc-mounted fixed slits allow resolution to be adjusted from 1.5 to 44 nm; 85-watt high-pressure mercury lamp is utilized for its high intensity, line-source characteristics. Ideally suited to standard procedures, clinical tests and teaching. Other features include: parts-per-trillion sensitivity for quinine sulfate; wavelength range of 200 to 800 nm, each monochromator; utilizes an S4 tube with a response beyond 600 nm. **SPF-125S** available with Xenon lamp and automatic scanning capability.

AMERICAN INSTRUMENT COMPANY *At the forefront of spectroluminescence technology since its inception.*
DIVISION OF TRAVENOL LABORATORIES, INC., Silver Spring, Maryland 20910
Circle No. 8 on Readers' Service Card

ห้องสมุด กรมวิทยาศาสตร์
2 7 ก.ค. 2514

VOLUME 43, NO. 1 JANUARY 1971



Our Cover Design is based on the Instrumentation column: Data Domains—An Analysis of Digital and Analog Instrumentation Systems and Components by C. G. Enke of Michigan State University. See Page 69 A. The design represents the addition of time to make a three-dimensional data domains map.

Dr. S. Raymond Gambino of Columbia University and Columbia-Presbyterian Hospital offers some provoking ideas in the Report for Analytical Chemists this month, Page 20 A. In discussing Met and Unmet Needs of the Automated Clinical Laboratory, Dr. Gambino stresses the need for automating the handling of matters from the beginning to the end—from admission and the decision to make tests to the evaluation of tests. Further, he feels the patient is entitled to get the results of his own tests. Automated instruments and examples of instruments mentioned by Dr. Gambino in his report are illustrated therein.

Much is happening in the clinical field with increasing automation. The New Products section gives some examples of new instrumentation. Future months will include more of this type of instrumentation since nothing can be of greater importance than the data needed by the doctor to diagnose and treat his patients and since it is becoming increasingly obvious that only automation can handle the amount of work involved in carrying out the nation's goals of good health care for all.

ANCHAM

ANALYTICAL CHEMISTRY

Contents

REPORT FOR ANALYTICAL CHEMISTS

Dr. S. Raymond Gambino of Columbia University discusses the Met and Unmet Needs of the Automated Clinical Laboratory 20 A

NEWS

ANALYTICAL CHEMISTRY appoints five new members to its Advisory Board. They are: C. G. Enke, William C. Purdy, Eugene M. Sallee, Donald T. Sawyer, Lloyd R. Snyder 39 A

BOOK REVIEWS

Books on carboxylic functional group determinations, multicomponent chromatography, spectroscopic methods for organic compound identification, and destruction of organic matter are reviewed by J. G. Hanna, E. Glueckauf, R. M. Silverstein, and E. B. Sandell 49 A

EDITORS' COLUMN

In the future, analytical chemists will require more knowledge about digital and analog instrumentation systems and components 61 A

FEATURED LABORATORY

Northwestern University's consolidation of its analytical services and advanced practices teaching laboratories offers students a strong introduction to chemical instrumentation 28 A

INSTRUMENTATION

C. G. Enke of Michigan State University discusses "data domains" concepts useful in designing and modifying digital and analog measurement systems and devices 69 A

EDITORIAL

Professor Laitinen discusses ANALYTICAL CHEMISTRY's policy on the publication of review papers 1

Author Index 6 A

Briefs 11 A

Calendar of Events 42 A

Future Articles 108 A

Manufacturers' Literature 102 A

New Chemicals 99 A

New Products 87 A

Readers' Information Service 83 A

Scheduled Technical Courses 40 A

General Analysis of Potentiostatic Current–Time Curves for Cylindrical Electrodes. *Sidney Barnartt and C. A. Johnson* 2

Simultaneous Determination of Silicate and Phosphate by an Automated Differential Kinetic Procedure. *J. D. Ingle, Jr., and S. R. Crouch* 7

Radioisotopic X-Ray Analysis of Silver Ores Using Compton Scatter for Matrix Compensation. *P. G. Burkhalter* 10

Application of Field Ionization to Gas-Liquid Chromatography–Mass Spectrometry (GLC-MS) Studies. *J. N. Damico and R. P. Barron* 17

Machine Intelligence Applied to Chemical Systems. Prediction and Reliability Improvement in Classification of Low Resolution Mass Spectrometry Data. *P. C. Jurs* 22

Double Beam Photon Counting Photometer with Dead Time Compensation. *K. C. Ash and E. H. Piepmeier* 26

Chlorine-35 Nuclear Quadrupole Resonance Studies of Trichloromethyl Compounds. *E. G. Brame, Jr.* 35

Cryoscopic Determination of Number-Average Molecular Weight by Quartz Crystal Thermometry. *J. S. Fok, J. W. Robson, and F. C. Youngken* 38

Accuracy of Analysis by Electrical Detection in Spark Source Mass Spectrometry. *R. A. Bingham and R. M. Elliott* 43

Radioactive Tracer Technique for Molecular Diffusion Coefficients in Granular Media. *E. R. Bennett and W. E. Bolch* 55

Spectrophotometric Analysis of Carbonyl Compounds in the Presence of Carbohydrates without Prior Separation. *E. B. Sanders and Jack Schubert* 59

Polarographic Determination of Traces of Nitrilotriacetate in Water Samples. *J. P. Haberman* 63

Selectivity in Liquid–Liquid Chromatography. *D. E. Martire and D. C. Locke* 68

Pyrolysis Gas Chromatography of Phenyl Polymers and Phenyl Ether. *M. T. Jackson, Jr., and J. Q. Walker* 74

Potentiometric Study of Copper(I) Complexes with Univalent Anions in Acetonitrile. *J. K. Senne and Byron Kratochvil* 79

Time-Lapse Spectrometry in Organic Photochemistry. *Nicolae Filipescu, F. L. Minn, and J. W. Pavlik* 83

The Question of Instrumental Artifact in Linear Sweep Voltammetry with Positive Feedback Ohmic Drop Compensation. *E. E. Wells, Jr.* 87

Photon Activation Analysis—A Review. *G. J. Lutz* 93

Use of Static Argon Atmosphere in Emission Spectrochemical Determination of Chromium in Biological Materials. *K. M. Hambidge* 103

Mixed Carrier Gases in Chromatography—A Source of Error. *Raymond Annino, Joseph Franko, and Harry Keller* 107

Micro and Ultramicro Analyses by Null Point Pressuremetry and Coulometry: Hydrogenation and Hydrogenolysis. *D. J. Curran and J. E. Curley* 118

Analysis for Impurities by Nuclear Scattering. *B. L. Cohen and R. A. Moyer* 123

Notes

Sodium Removal as an Aid to Neutron Activation Analysis. *H. R. Ralston and E. S. Sato* 129

Solvent Effects in Gel Permeation Chromatography. *J. G. Bergmann, L. J. Duffy, and R. B. Stevenson* 131

Interference of Lithium in Atomic Absorption Spectrometry. *A. M. Bond and D. R. Canterford* 134

Spectrofluorometric Determination of Traces of Fluoride Ion by Ternary Complex Formation with Zirconium and Calcein Blue. *T. L. Har and T. S. West* 136

Fluorometric Methods for Determination of Europium and Terbium. *D. E. Williams and J. C. Guyon* 139

Spectrophotometric Determination of Sulfide Ion with Organic Disulfides. *R. E. Humphrey, Willie Hinze, and W. M. Jenkines III* 140

Determination of Nitrite by Controlled-Potential Coulometry. *J. E. Harrar* 143

Spectrophotometric Determination of Rhodium with Nitroso R. Formula for the Rh(III)–Nitroso R Complex. *O. W. Rollins and M. M. Oldham* 146





NEW APIEZON
anti-seize greases stop costly laboratory glassware breakage

AP-100 is a high vacuum grease for use down to $5x10^{-11}$ torr at 15°C, with a softening point of 30°C.

AP-101 is an all-purpose stop-cock grease for moderate vacuum use down to 10^{-1} torr and a softening point of 185°C.

These greases are resistant to organic solvents and will not leach out of ground glass joints or stop-cocks. Completely effective in tests against a wide range of aggressive solvents over periods of 72 hours and more.

Also—Apiezon Oils—low vapor pressures—very stable—ideal as vapor-diffusion pump fluids.

Apiezon Compound Q a putty-like, versatile, low cost sealant.

Apiezon Waxes for more permanent vacuum joints.

Write for Bulletin 43-AC. 011

JAMES G. BIDDLE CO.
Electrical and Speed Measuring Instruments
PLYMOUTH MEETING, PENNSYLVANIA 19462
Phone 215/646-9200

Circle No. 24 on Readers' Service Card

The WANG 700 Series



Now a calculator that lets you write your own programs and store them on a tape cassette

It's easy to store, enter or change programs with a 700 Series and there are no language problems. You already have the knowledge in the math steps you're now using to solve your problems.

With the Wang 700 you'll have more than a calculator. There are 16 special function keys that make it personally yours - you can determine the function each performs. And a choice of typewriter or printer/plotter output turns the 700 Series into a fully programmable calculating system.

And to make it even easier, Wang offers a library of preprogrammed cassettes for the many standard needs. Want a demonstration? Call Mr. Courtney collect at 617-851-7211 or send us the coupon.

Wang Laboratories, Inc. Dept. AC-1
836 North Street, Tewksbury, Mass. 01876
I'd like a 700 demonstration as soon as possible. Call me at _____ for a date.
(Phone number)
Name _____
Company _____
Street _____
City _____ State _____ Zip _____

Circle No. 197 on Readers' Service Card

Determination of Polymeric Isocyanate in the Presence of Reactive Halides. *P. M. Beazley* 148

Evaluation of Methods for Determination of Metallic Iron in Reduced Iron Ores. *S. C. Blum and T. D. Searl* 150

Amperometric Titration of Calcium and Magnesium Using the Lead Dioxide Electrode. *C. O. Huber, K. Dahnke, and F. Hinz* 152

Determination of Nitrogen in Vanadium Nitrides and Uranium Nitride (UN). *D. H. Bollman and D. M. Mortimore* 154

Correspondence

Re: "Criteria for Judging Acceptability of Analytical Methods." *T. J. Farrell* 156

Aids for Analytical Chemists

Nonaqueous Electrochemical Cell Capable of Rigorous Exclusion of Water and Oxygen. *J. L. Mills, Roger Nelson, S. G. Shore, and L. B. Anderson* 157

Device to Overcome Spinning Difficulties with Nuclear Magnetic Resonance Sample Tubes at Variable Temperature. *John Barzilay* 160

© Copyright 1971
by the American Chemical Society

MANUSCRIPT REQUIREMENTS published in December 1970 issue, page 1879, outlines scope and copy requirements to be observed in preparing manuscripts for consideration. Manuscript (4 copies) should be submitted to ANALYTICAL CHEMISTRY, 1155 Sixteenth St., N.W., Washington, D. C. 20036.

The American Chemical Society assumes no responsibility for the statements and opinions advanced by contributors to its publications. Views expressed in the editorials are those of the editors and do not necessarily represent the official position of the American Chemical Society.

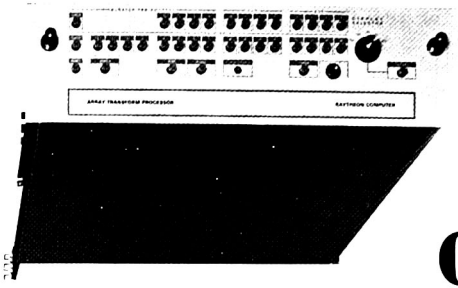
1971 Subscription Rates

	1 yr.	2 yr.	3 yr.
Members, domestic and foreign	$ 5.00	$ 9.00	$12.00
Nonmembers, domestic and Canada	7.00	12.00	16.00
Nonmembers, foreign except Canada	15.00	27.50	40.00

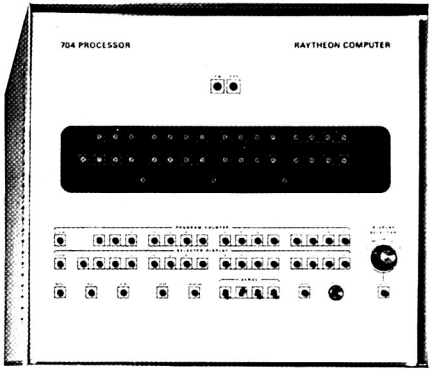
Postage: Canada and Pan-American Union, $2.50; foreign, $3.50. Single copies: current, $2.00 except Annual Reviews, $3.00 each. Rates for back issues and volumes are available from Special Issues Sales Dept., 1155 Sixteenth St., N.W., Washington, D. C. Claims for missing numbers will not be allowed if received more than 60 days from date of mailing plus time normally required for postal delivery of journal and claim. No claims allowed because of failure to notify the Subscription Service Department of a change of address or because copy is "missing from files."

Published monthly with Review issue added in April and a Laboratory Guide in August by the American Chemical Society, from 20th and Northampton Sts., Easton, Pa. 18042; Executive Offices, Editorial Headquarters, and Subscription Service Department, 1155 Sixteenth St., N.W., Washington, D. C. 20036; Advertising Office, 142 East Ave., Norwalk, Conn. 06851. ANALYTICAL CHEMISTRY and other ACS periodicals are available on microfilm. For information write to: MICROFILM, Special Issues Sales, American Chemical Society, 1155 Sixteenth St., N.W., Washington, D. C. 20036. Second class postage paid at Easton, Pa.

CHANGE OF ADDRESS: Notify Subscription Service Department, American Chemical Society, 1155 Sixteenth St., N.W., Washington, D. C. 20036. Such notification should include both old and new addresses, with ZIP code numbers, and be accompanied by mailing label from a recent issue. Allow four weeks for change to become effective.



Our new ATP gives the Raytheon 704 20 times more power than you bargained for.



Raytheon Computer's new Array Transform Processor has made fast Fourier analysis practical and inexpensive. A Raytheon 704 mini with our ATP runs a typical FFT with 2048 complex data points in only 150 milliseconds! And FFT range is 2 to 8192 data points. The Array Transform Processor also performs integration, differentiation, convolution, auto and cross correlation, and signal averaging.

The Raytheon ATP is an auxiliary processor that connects to a Raytheon 704 or 706 computer ready to go to work on your problems immediately. The ATP complete with a Raytheon 704 general purpose computer costs about $40,000.

If you don't need real time processing, we have an ATP software simulator for our 704 computer which will compute FFT's for less than $20,000.

At Raytheon Computer we have all the equipment you need to do signal processing and analysis. Processors. Interfaces. Converters. Peripherals. So write today for Data File C-192. Raytheon Computer, 2700 S. Fairview St., Santa Ana, Calif. 92704. (714) 546-7160.

RAYTHEON

The only thing Raytheon Computer does is your job. Cheaper.

Circle No. 156 on Readers' Service Card

6 new volumes in Chemical Analysis: A Series of Monographs in Analytical Chemistry and Its Applications, edited by P. J. Elving and I. M. Kolthoff

PHOTOMETRIC ORGANIC ANALYSIS
Basic Principles with Applications Part 1
By EUGENE SAWICKI, *National Air Pollution Control Administration*
Furnishes the organic and analytical chemist with the practical spectrophotometric background basic to an understanding of organic analysis by photometric methods.
1970 679 pages $32.50

CHARACTERIZATION OF ORGANOMETALLIC COMPOUNDS
Parts I and II
Edited by MINORU TSUTSUI, *Texas A & M University*
from a review of Part I—
"... an important addition to the library of specialists ..."
—*American Scientist*
Part I: 1969 371 pages $15.00
Part II: 1970 448 pages $19.95

ANALYTICAL CHEMISTRY OF NITROGEN AND ITS COMPOUNDS
Parts 1 and 2
Edited by CARL A. STREULI, *Lederle Laboratories* and PHILIP R. AVERELL
Provides information for the detection, separation, and determination of nitrogen compounds often encountered in the chemical laboratory.
1970 792 pages $35.00 (for the set)

DETERMINATION OF ORGANIC COMPOUNDS
Methods and Procedures
By FREDERICK T. WEISS, *Shell Development Company*
A guide to selected methods and techniques employed in the analysis of organic compounds.
1970 475 pages $17.50

ULTRAMICRO ELEMENTAL ANALYSIS
By GUNTHER TOLG, *Max Planck Institute for Metal Research*
Translated by Conrad E. Thalmayer
"Special care has been taken to provide references to the literature, and this feature alone makes the book a fine addition to any analytical library ..."
from a review of the German Edition in the *Journal of Chemical Education*
1970 216 pages $10.95

MASKING AND DEMASKING OF CHEMICAL REACTIONS
Theoretical Aspects and Practical Applications
By D. D. PERRIN, *Australian National University*
A timely condensation of representative applications relevant to analytical chemistry, industry, biology, and medicine.
1970 211 pages $12.95

Plus the latest volume in

TREATISE ON ANALYTICAL CHEMISTRY
A Comprehensive Account in Three Parts
Volume 14, Part II: Analytical Chemistry of Inorganic and Organic Compounds, edited by I. M. KOLTHOFF, *University of Minnesota* and PHILIP J. ELVING, *University of Michigan*
1971 *In Press*

WILEY MODERN METHODS OF CHEMICAL ANALYSIS FILM SERIES
Executive Editor: Leslie S. Ettre, Editor, *Encyclopedia of Industrial Chemical Analysis*

Nuclear Magnetic Resonance
1968 28 minutes $300.00 Rental: $30.00

Chromatography (in two parts)
Part I, 1970 28 minutes $300.00 Rental: $30.00
Part II, 1970 22 minutes $200.00 Rental: $20.00
Set of Parts I and II: $450.00 Rental: $50.00

Mass Spectrometry
1970 33 minutes $300.00 Rental $30.00
For additional information on films, write to the Audio-Visual Manager.

WILEY-INTERSCIENCE
a division of JOHN WILEY & SONS, Inc.
605 Third Avenue, New York, N.Y. 10016
In Canada: 22 Worcester Road, Rexdale, Ontario

Circle No. 196 on Readers' Service Card

Author Index

Anderson, L. B. 157
Annino, Raymond 107
Ash, K. C. 26

Barnartt, Sidney 2
Barron, R. P. 17
Barzilay, John 160
Beazley, P. M. 148
Bennett, E. R. 55
Bergmann, J. G. 131
Bingham, R. A. 43
Blum, S. C. 150
Bolch, W. E. 55
Bollman, D. H. 154
Bond, A. M. 134
Brame, E. G., Jr. 35
Burkhalter, P. G. 10

Canterford, D. R. 134
Cohen, B. L. 123
Crouch, S. R. 7
Curley, J. E. 118
Curran, D. J. 118

Dahnke, K. 152
Damico, J. N. 17
Duffy, L. J. 131

Elliott, R. M. 43

Farrell, T. J. 156
Filipescu, Nicolae 83
Fok, J. S. 38
Franko, Joseph 107

Guyon, J. C. 139

Haberman, J. P. 63
Hambidge, K. M. 103
Har, T. L. 136
Harrar, J. E. 143
Hinz, F. 152
Hinze, Willie 140
Huber, C. O. 152
Humphrey, R. E. 140

Ingle, J. D., Jr. 7

Jackson, M. T., Jr. 74
Jenkines, W. M., III 140
Johnson, C. A. 2
Jurs, P. C. 22

Keller, Harry 107
Kratochvil, Byron 79

Locke, D. C. 68
Lutz, G. J. 93

Martire, D. E. 68
Mills, J. L. 157
Minn, F. L. 83
Mortimore, D. M. 154
Moyer, R. A. 123

Nelson, Roger 157

Oldham, M. M. 146

Pavlik, J. W. 83
Piepmeier, E. H. 26

Ralston, H. R. 129
Robson, J. W. 38
Rollins, O. W. 146

Sanders, E. B. 59
Sato, E. S. 129
Schubert, Jack 59
Searl, T. D. 150
Senne, J. K. 79
Shore, S. G. 157
Stevenson, R. B. 131

Walker, J. Q. 74
Wells, E. E., Jr. 87
West, T. S. 136
Williams, D. E. 139

Youngken, F. C. 38

The Perkin-Elmer Model 180 Infrared Spectrophotometer. Designed for the world's most demanding spectroscopist.

Here is an instrument with the widest research versatility of any IR instrument ever offered.

Its unique capabilities give you unrestricted selection of instrumental parameters. You have total freedom to set the precise combination of resolution, speed, time constant and gain that you need.

Its large sample space—with unequalled accessibility from front, back and floor—permits you to place almost any configuration of sampling accessory into the instrument; and its chopping system even lets you run very hot or cold samples without loss of transmittance accuracy.

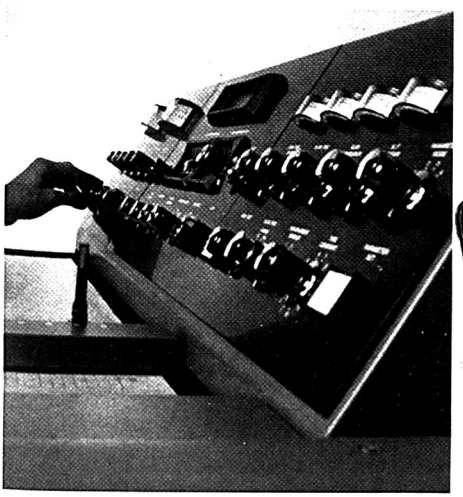
You can operate in either a single beam or a double beam mode—either way with full system energy. And you have total flexibility in the choice of energy mode —choose constant I_0, or programmed or manual slit control, with or without automatic gain.

The dual recorder gives you either an XY or a strip chart recording. And you have exceptionally wide control of spectrum presentation. A digital indexing system lets you quickly set the scan limits, and you have continuous visual display of frequency while scanning.

The Model 180 has excellent data logging capability in which data are presented in ASCII code for interface with data loggers through the standard Perkin-Elmer interface option. An accessory Digital Magnetic Recorder permits recording of high resolution spectra at rates 5 to 100 times faster than is possible on the chart.

If you require the ultimate in flexibility, precision and operator convenience in your IR instrument, you owe it to yourself to investigate the Model 180. For full details write: Instrument Division, Perkin-Elmer Corporation, 702 Main Avenue, Norwalk, Conn. 06852.

PERKIN-ELMER

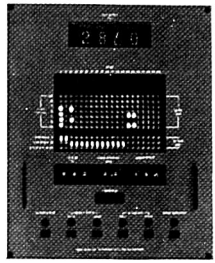




Circle No. 138 on Readers' Service Card


All 207 variations
of our new Moduline 2800
Series GC fit here.

At last count, we came up with 207 different versions of our new 2800 Series Gas Chromatograph. Each able to do a very specific GC job reliably well. With remarkable reproducibility.



MULTILINEAR TEMPERATURE PROGRAMMER

Built around a truly modular mainframe (left), the entire 2800 Series shares an impressive list of standard features. Among them are a newly redesigned electrical system that's not only compatible with any commonly used voltage in the world, but which also produces the cleanest signal ever to come out of a GC. A unique all solid state dual/differential electrometer (above right). A greatly simplified flow control system. A spacious 1090 cubic inch column oven. And dual column, dual detector capability.

But that's just the beginning.

You can choose from four different temperature programmers, plus four versions of our computer-compatible MultiLinear Temperature Programmer (MLTP) pictured above on the left.

We currently have five detectors – four ionization and one TC – from which a variety of combinations can be made. Significantly, all four ionization detectors fit on a common base for speed and ease of interchangeability.

In the end, regardless of versatility, a GC is only as good as the results it produces.

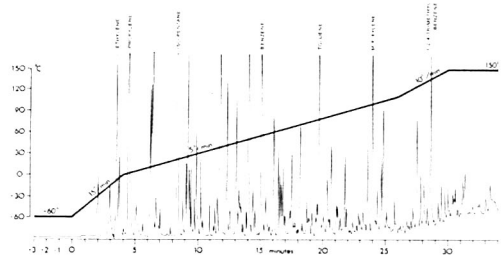
The automobile exhaust emission analysis, below, is just one example of the tough jobs the 2800 handles with authority. This particular analysis is the result of four different capabilities working at once. Cryogenic operation. Capillary capability. Multi-linear temperature programming. And computer controlled operation. The results speak for themselves. (We might also note that in 18 runs of similar samples over a period of 48 hours, the *worst* cumulative retention time error was less than two seconds over a retention time of 1100 seconds.)



DUAL/DIFFERENTIAL ELECTROMETER

We've published a booklet detailing all 207 variations of the new Moduline 2800 Series GC. For your copy, simply write on your letterhead to Varian Aerograph, Walnut Creek, California 94598; Tokyo, Japan; Malton, Ontario, Canada; Crows Nest, N.W.S., Australia; or Zug, Switzerland.

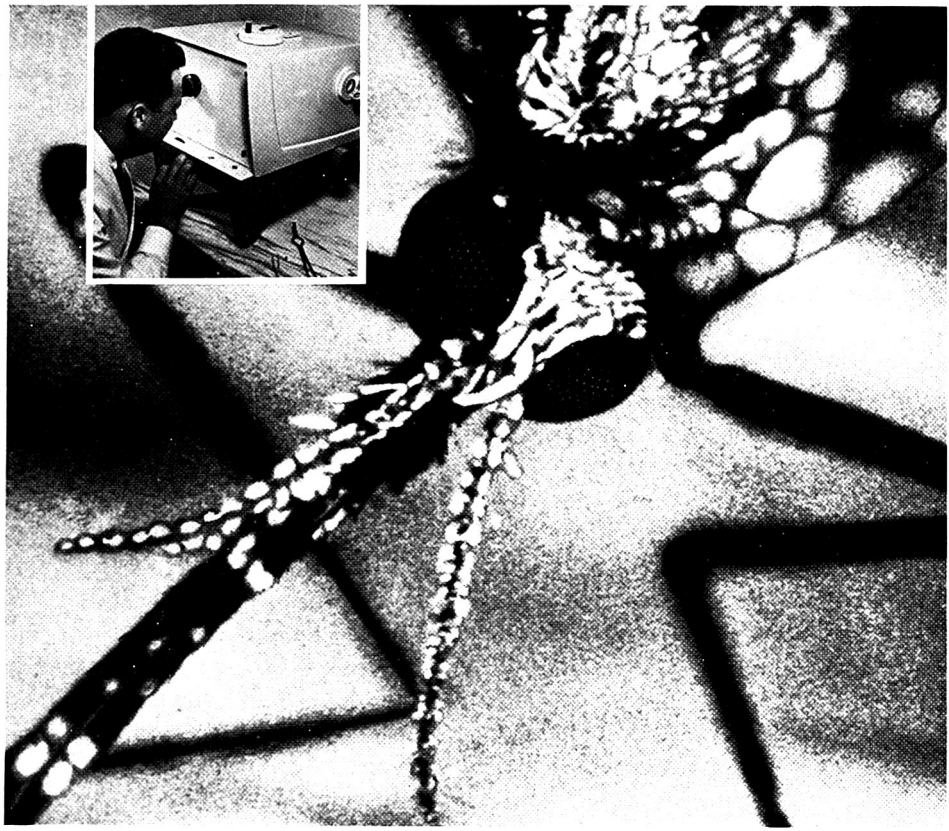
And, if you find 207 combinations aren't enough, we'll be glad to sit down with you and work out Number 208.



AUTOMOBILE EXHAUST ANALYSIS FOR HYDROCARBONS
Conditions: Flame ionization detector; 200' x 0.020" i.d. capillary column with DC 200 (50CS) liquid phase; He carrier gas at 7 ml/min; temperature program as shown.

varian aerograph

Circle No. 190 on Readers' Service Card



We're not weighing the mosquito. We're weighing its lunch.

A 0.2346-mg repast . . . weighed in just two seconds on a UM-7 ultra-micro balance, the most accurate analytical balance in the Mettler line.

If you're in the market for a new balance, chances are your weighing requirements don't call for the UM-7's ten-millionth of a gram accuracy. So Mettler offers 21 other analytical balances for you to choose from. Some have many features in common with the UM-7. Others are unique unto themselves. And collectively, they share the capability of handling any weighing in the analytical spectrum. From 2 mg to 1,000 grams. With precisions from ±0.3 mg to ±0.0001 mg.

Many models feature digital readout. Others . . . analog readout, vernier readout or micrometer readout. One model emits an electrical signal for use with control instrumentation. Many have filling guides for weighing-in at high speed. Some preweigh.

A few feature rapid taring over the entire weighing range with a separate readout for tare weight. There's even a semi micro with macro capacity. And all are fast-weighing, easy-to-use instruments that offer a host of bonus features as standard. Durable sapphire knife edges. Air-dampened optical scales. Corrosion-resistant concentric ring weights. And more.

Choose the one with the specifications and features that tailor it to your weighing needs. Whether you require the precision to weigh the lethal fraction of an insect's lunch. The larger capacity to handle the heavier industrial weighing applications. The durability to survive years of high school freshman chemistry. The versatility to handle the broad variety of weighings that are routine in any analytical laboratory.

For your copy of our analytical balance catalog, or to arrange for a free demonstration, write Mettler Instrument Corporation, 20 Nassau Street, Princeton, N.J. 08540.

Mettler®

Circle No. 124 on Readers' Service Card

A C BRIEFS

Highlights of Articles in This Issue

General Analysis of Potentiostatic Current–Time Curves for Cylindrical Electrodes

A general method is developed for analyzing electrode kinetic curves as measured at constant potential with cylindrical electrodes. A prior knowledge of reaction orders or diffusivities is not required.

SIDNEY BARNARTT and CHARLES A. JOHNSON, Edgar C. Bain Laboratory for Fundamental Research, United States Steel Corporation, Monroeville, Pa. 15146

Anal. Chem., 43, 2 (1971)

Simultaneous Determination of Silicate and Phosphate by an Automated Differential Kinetic Procedure

An automated differential rate procedure is presented for the determination of silicate and phosphate in mixtures. Phosphate results are accurate to 1%, while silicate determinations show accuracies of beter than 3%.

J. D. INGLE, Jr., and S. R. CROUCH, Department of Chemistry, Michigan State University, East Lansing, Mich. 48823

Anal. Chem., 43, 7 (1971)

Radioisotopic X-Ray Analysis of Silver Ores Using Compton Scatter for Matrix Compensation

Silver determinations with accuracies of ±10% in quartz-type ores and ±20% in heavy-matrix ores were achieved using monoenergetic excitation, high-resolution X-ray detectors, and computer data processing.

P. G. BURKHALTER, U. S. Department of the Interior, Bureau of Mines, College Park, Md. 20740

Anal. Chem., 43, 10 (1971)

Application of Field Ionization to Gas–Liquid Chromatography–Mass Spectrometry (GLC–MS) Studies

Field ionization spectra were obtained on components in GLC effluents which complement the electron impact spectra; sensitivity studies for a variety of carbonyl compounds suggest that some types of compounds are more sensitive to field ionization than others.

J. N. DAMICO and R. P. BARRON, Division of Food Chemistry and Technology, Food and Drug Administration, U. S. Department of Health, Education, and Welfare, Washington, D. C. 20204

Anal. Chem., 43, 17 (1971)

Machine Intelligence Applied to Chemical Systems. Prediction and Reliability Improvement in Classification of Low Resolution Mass Spectrometry Data

The predictive ability and reliability of binary pattern classifiers working with low resolution mass spectra have been improved by employing data transformations, thresholds, and layered systems of threshold logic units.

PETER C. JURS, Department of Chemistry, The Pennsylvania State University, University Park, Pa. 16802

Anal. Chem., 43, 22 (1971)

Double Beam Photon Counting Photometer with Dead Time Compensation

A low cost double beam photon counting photometer is discussed and compared with a single beam instrument. Counting rate linearity is extended by a discriminator that compensates for dead time losses.

K. C. ASH and E. H. PIEPMEIER, Department of Chemistry, Oregon State University, Corvallis, Ore. 97331

Anal. Chem., 43, 26 (1971)

Chlorine-35 Nuclear Quadrupole Resonance Studies of Trichloromethyl Compounds

A spectra-structure correlation was developed between ^{35}Cl NQR spectra at 77°K and structures of trichloromethyl groups. Shifts to higher frequency are also seen to be directly correlatable with similar effects known to operate in NMR spectra.

EDWARD C. BRAME, Jr., E. I. du Pont de Nemours and Company, Inc., Elastomer Chemicals Department, Experimental Station, Wilmington, Del. 19898

Anal. Chem., 43, 35 (1971)

Cryoscopic Determination of Number-Average Molecular Weight by Quartz Crystal Thermometry

A freezing point assembly incorporating a quartz crystal thermometer is described. Details of a cryoscopic procedure producing accurate values with a relative error of ±2–3% for the M_n range, 50–2000 are reported.

JOHN S. FOK, JOHN W. ROBSON, and FLORA C. YOUNGKEN, E. I. du Pont de Nemours and Company, Wilmington, Del. 19898

Anal. Chem., 43, 38 (1971)

Accuracy of Analysis by Electrical Detection in Spark Source Mass Spectrometry

The method gives a precision of 35% for survey analysis and 2% for individual elements. Absolute accuracy of 4% is demonstrated for steels. Detective limits are 0.01 ppm atomic for surveys, 0.001 ppm atomic for individual elements.

R. A. BINGHAM and R. M. ELLIOTT, AEI Scientific Apparatus Limited, Barton Dock Road, Manchester, England

Anal. Chem., 43, 43 (1971)

Radioactive Tracer Technique for Molecular Diffusion Coefficients in Granular Media

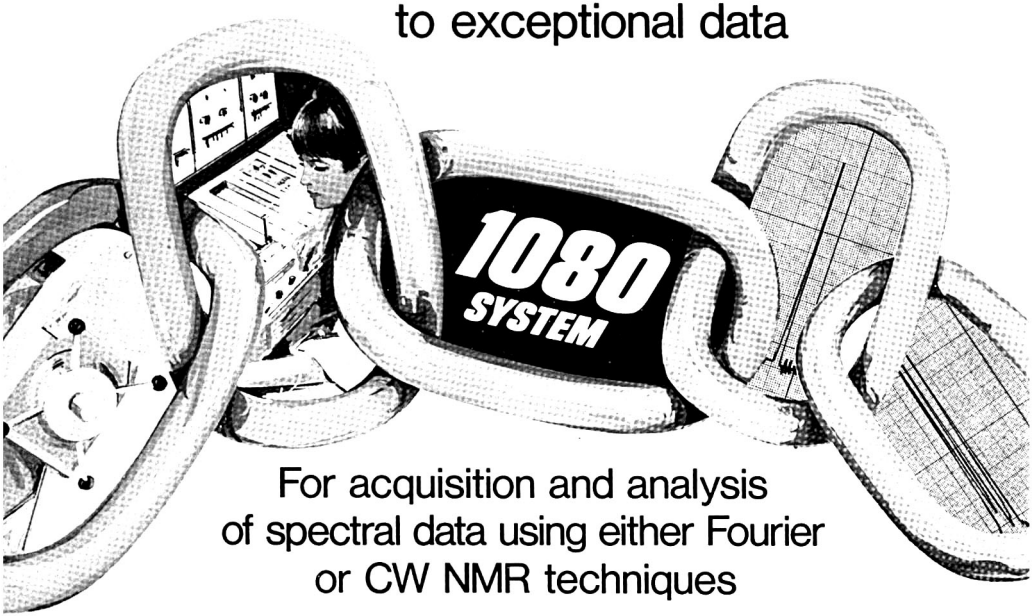
Gaseous molecular diffusion coefficients show a lower value in granular media than in open columns due to the obstruction effect. The size distribution and uniformity of the media were found to have a significant effect on the obstructive factors relating to the diffusivity.

E. R. BENNETT and W. E. BOLCH, Sanitary Engineering Research Laboratory, University of California, Berkeley, Calif.

Anal. Chem., 43, 55 (1971)

FABRI-TEK®

announces
a new way to link your NMR spectrometer to exceptional data



For acquisition and analysis of spectral data using either Fourier or CW NMR techniques

A major design innovation in the 1080 System is its use of a single main frame to perform both stored program **and** wired program computations. Wired programming and conventional instrument controls regulate many data acquisition parameters where high speed, on-line processing is required. Stored program operations are used where complex arithmetic computations are required. If you're so inclined, the 1080 is completely programmable (like any GP computer) with a powerful repertoire of instructions and its own program assembly language.

Additional features include 20-bit word length; input signal filtering; field-expandable memory capacities from 8,192 to 45,056 words (even larger in the future); and versatility through the use of plug-in digitizers and sweep modules to meet future measurement requirements.

The 1080 System has all the required hardware and software to:

- acquire data through analog-to-digital conversion;
- improve signal-to-noise ratio by on-line signal (ensemble) averaging;
- provide off-line baseline correction and/or exponential filtering;
- transform free induction decay data to frequency spectra using fast Fourier algorithm;
- manipulate real (absorption) and imaginary (dispersion) portions of the transformed spectra to yield phase- and amplitude-corrected absorption spectra;
- integrate or perform background subtraction on the absorption spectra;
- provide oscilloscope display of input data or processed memory contents;
- read out data to an X-Y plotter, ASR-33 Teletype, or a computer-compatible magnetic tape unit.

Complete 1080 Systems capable of an 8,192-word Fourier transform start at just over $30,000. For full details write or call collect to discuss your specific NMR data problems.

FABRI-TEK INSTRUMENTS, INC.

5225 VERONA ROAD • MADISON, WIS. 53711 • PHONE: 608/271-3333

Circle No. 61 on Readers' Service Card

Spectrophotometric Analysis of Carbonyl Compounds in the Presence of Carbohydrates without Prior Separation

Normal carbonyl compounds and α-dicarbonyl compounds are determined in the presence of carbohydrates without prior separation, using the reagent 2,4-dinitrophenylhydrazine. The method exploits a technique which suppresses formation of carbohydrate 2,4-dinitrophenylhydrazones.

EDWARD B. SANDERS and JACK SCHUBERT, Department or Radiation Health, Graduate School of Public Health, University of Pittsburgh, Pittsburgh, Pa. 15213

Anal. Chem., 43, 59 (1971)

Polarographic Determination of Traces of Nitrilotriacetate in Water Samples

The technique was evaluated by adding 0.0257 to 2.57 ppm NTA to representative samples. The relative standard deviation was approximately 10%, except at the lowest concentration.

JOHN P. HABERMAN, The Procter and Gamble Company, Miami Valley Labs, Cincinnati, Ohio 45239

Anal. Chem., 43, 63 (1971)

Selectivity in Liquid–Liquid Chromatography

A new theory of solution free energies is used to deduce a thermodynamic basis for liquid chromatographic selectivity.

D. E. MARTIRE, Department of Chemistry, Georgetown University, Washington, D. C. 20007 and D. C. LOCKE, Department of Chemistry, Queens College of the City University of New York, Flushing, N. Y. 11367

Anal. Chem., 43, 68 (1971)

Pyrolysis Gas Chromatography of Phenyl Polymers and Phenyl Ether

This paper describes Curie point pyrolysis experiments applied to a complex copolymer and a polymer-like compound.

M. T. JACKSON, Jr., Central Research Department, Monsanto Company, St. Louis, Mo. 63166 and J. Q. WALKER, McDonnell Douglas Research Laboratories, St. Louis, Mo. 63166

Anal. Chem., 43, 74 (1971)

Potentiometric Study of Copper(I) Complexes with Univalent Anions in Acetonitrile

The standard potential of the Cu(I)–(0) couple in acetonitrile was accurately measured, and the formation constants of Cl^-, Br^-, I^-, SCN^-, and NO_3^- complexes with Cu(I) in acetonitrile were determined potentiometrically.

JOHN K. SENNE and BYRON KRATOCHVIL, Department of Chemistry, University of Alberta, Edmonton, Alberta, Canada

Anal. Chem., 43, 79 (1971)

Time-Lapse Spectrometry in Organic Photochemistry

Following spectra of irradiated solutions in time can yield structural information on long-lived intermediates, as well as rate constants and stoichiometry.

NICOLAE FILIPESCU, FREDRICK L. MINN, and JAMES W. PAVLIK, Departments of Chemistry, The George Washington University, Washington, D. C. 20006, and Wisconsin State University, River Falls, Wis. 54022

Anal. Chem., 43, 83 (1971)

The Question of Instrumental Artifact in Linear Sweep Voltammetry with Positive Feedback Ohmic Drop Compensation

A general criterion is established for rejecting ohmic drop compensated linear sweep voltammograms which suffer from instrumental artifact. Also included is a simple means of determining apparent solution resistance for any degree of positive feedback.

EUGENE E. WELLS, Jr., Power Sources Division, Electronic Components Laboratory, USAECOM, Fort Monmouth, N. J.

Anal. Chem., 43, 87 (1971)

Photon Activation Analysis—A Review

The field of photon activation is reviewed. Topics include isotope sources, determination of C, N, and O; analysis of biological, geochemical, and forensic samples and errors and corrections.

GEORGE J. LUTZ, Activation Analysis Section, Analytical Chemistry Division, National Bureau of Standards, Washington, D. C. 20234

Anal. Chem., 43, 93 (1971)

Use of Static Argon Atmosphere in Emission Spectrochemical Determination of Chromium in Biological Materials

Nanogram quantities of chromium are determined spectrochemically in blood, hair, and urine with a precision of 10% or less using a static argon excitation chamber.

K. MICHAEL HAMBIDGE, The B. F. Stolinsky Research Laboratories, Department of Pediatrics, University of Colorado Medical Center, 4200 East Ninth Avenue, Denver, Colo. 80220

Anal. Chem., 43, 103 (1971)

Mixed Carrier Gases in Chromatography—A Source of Error

A serious experimental difficulty is uncovered in the use of differential gas chromatographic procedures which severely limits the general applicability of this technique for routine analysis.

RAYMOND ANNINO, JOSEPH FRANKO, and HARRY KELLER, Research Center, The Foxboro Company, Foxboro, Mass.

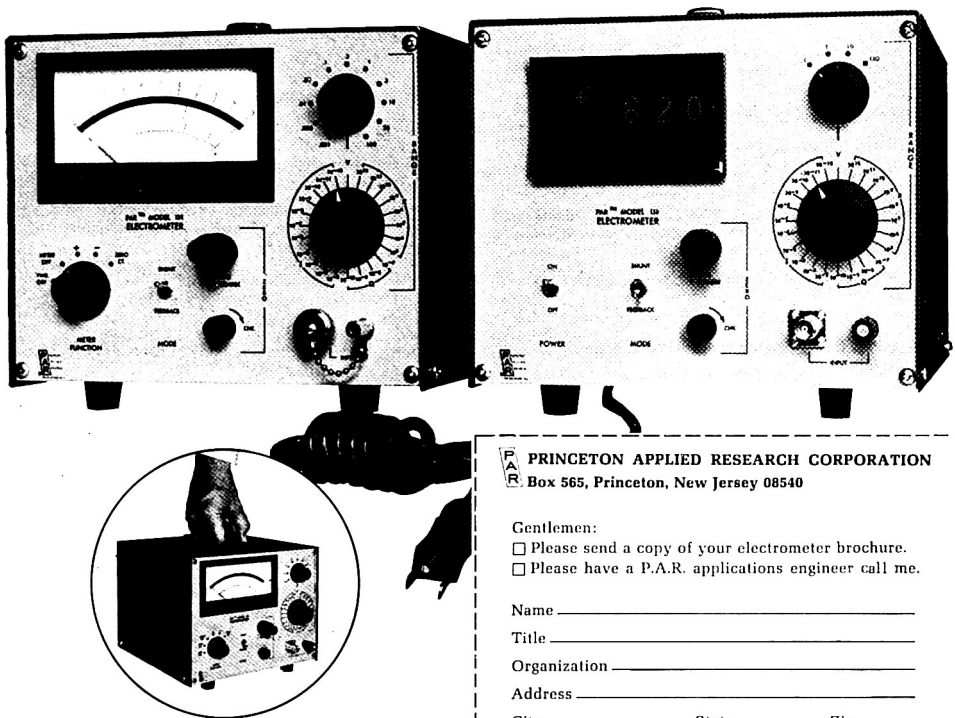
Anal. Chem., 43, 107 (1971)

New family of P.A.R. ELECTROMETERS

Meet our new electrometer family – three models with broad applications flexibility and sensible prices. All with outstanding voltage and current stability for unexcelled resolution. And all offering the quality that has made P.A.R. a leader in low-level signal measurement.

Use our $615 Model 134 when you need a wide range, high stability instrument. Our Model 135 offers the added convenience of a self-contained battery power supply and costs just $675. And, our Model 136 provides a digital display **and** BCD output at only $995.

All three instruments feature extremely low drift and minimum current offset, guarded input circuits, and high overload capacity with fast recovery. A full line of accessories is also available. Send for our new brochure with all the details. Or request a demonstration or applications assistance. Return the coupon below, write or call us collect. Princeton Applied Research Corporation, Box 565, Princeton, New Jersey 08540 ; telephone (609) 452-2111.



PRINCETON APPLIED RESEARCH CORPORATION
Box 565, Princeton, New Jersey 08540

Gentlemen:
☐ Please send a copy of your electrometer brochure.
☐ Please have a P.A.R. applications engineer call me.

Name _____
Title _____
Organization _____
Address _____
City _____ State _____ Zip _____
Phone _____

114

Circle No. 151 on Readers' Service Card

Micro and Ultramicro Analyses by Null Point Pressuremetry and Coulometry: Hydrogenation and Hydrogenolysis

A differential capacitive-type pressure transducer system has been used to follow pressure changes in a closed reactor for the analysis of alkenes, alkynes, organo-halides, nitro- and azo-compounds by hydrogen uptake and coulometric regeneration of hydrogen gas.

D. J. CURRAN and JAMES E. CURLEY, Department of Chemistry, University of Massachusetts, Amherst, Mass. 01002

Anal. Chem., 43, 118 (1971)

Analysis for Impurities by Nuclear Scattering

The use of nuclear scattering to analyze for impurities is investigated. Mass resolutions of 1 AMU at A $\simeq$ 63 and 10 AMU at A $\simeq$ 200 are readily achieved with a sensitivity of $\sim$1 ppm for heavy element impurities in light element materials. By sacrificing mass resolution, 10^{-3} ppm sensitivities are obtained.

B. L. COHEN and R. A. MOYER, University of Pittsburgh, Pittsburgh, Pa. 15213

Anal. Chem., 43, 123 (1971)

Notes

Sodium Removal as an Aid to Neutron Activation Analysis

Fully automated activation analysis is brought nearer [illegible] general applicability by the use of the Girardi and Sabbioni method of sodium removal, which solves the major problem of ^{24}Na contamination. This method can be useful in the analysis of organic and environmental samples.

H. R. RALSTON, Bio-Medical Division, Lawrence Radiation Laboratory, University of California, Livermore, California 94550 and ELAINE S. SATO, Radiochemistry Division, Lawrence Radiation Laboratory, University of California, Livermore, California 94550

Anal. Chem., 43, 129 (1971)

Solvent Effects in Gel Permeation Chromatography

A GPC solvent study has shown that 1,2,4-trichlorobenzene eliminates non-size separations that can occur with other solvents. The elution behaviors of peri-condensed aromatic hydrocarbons and petroleum asphaltenes show similar solvent dependence.

J. G. BERGMAN and L. J. DUFFY, Research and Development Department, American Oil Co., Whiting, Ind., and R. B. STEVENSON, Research and Development, Amoco Chemicals Corp., Whiting, Ind.

Anal. Chem., 43, 131 (1971)

Interference of Lithium in Atomic Absorption Spectrometry

Lithium fusion methods are advantageous for decomposition of geological samples prior to determination of elements by atomic absorption spectrometry. Ionization interference by lithium and its removal are discussed.

A. M. BOND, Department of Inorganic Chemistry, University of Melbourne, Parkville 3052, Victoria, Australia, and D. R. CANTERFORD, Department of Physical Chemistry, University of Melbourne, Parkville 3052, Victoria, Australia

Anal. Chem., 43, 134 (1971)

Spectrofluorimetric Determination of Traces of Fluoride Ion by Ternary Complex Formation with Zirconium and Calcein Blue

An analytical procedure is described which permits fluoride solutions to be analyzed in 10^{-6} to $10^{-7}M$ solution. There are few interferences, and the method is rapid and reproducible.

TAN LAY HAR and T. S. WEST, Chemistry Department, Imperial College of Science and Technology, London, S.W.7., England

Anal. Chem., 43, 136 (1971)

Fluorometric Methods for Determination of Europium and Terbium

Nanogram quantities of Eu and Tb in the presence of other rare earths may be determined by the fluorescence of their chelates with 1,1,1,5,5,5-hexafluoro-2,4-pentanedione.

DORA E. WILLIAMS and JOHN C. GUYON, University of Missouri, Columbia, Mo. 65201

Anal. Chem., 43, 139 (1971)

Spectrophotometric Determination of Sulfide Ion with Organic Disulfides

Sulfide ion can be determined spectrophotometrically in the low μg/ml range by reaction with 2,2′-dithiodipyridine, 2,2′-dithiodipyrimidine, 4,4′-dithiodipyridine, or 5,5′-dithiobis(2-nitrobenzoic acid).

RAY E. HUMPHREY, WILLIE HINZE, and WILLIAM M. JENKINES III, Department of Chemistry, Sam Houston State University, Huntsville, Texas 77340

Anal. Chem., 43, 140 (1971)

Determination of Nitrite by Controlled-Potential Coulometry

Nitrite is determined at the milligram level with an accuracy and precision of 0.1% by controlled-potential coulometry.

J. E. HARRAR, Chemical Department, Lawrence Radiation Laboratory, University of California, Livermore, Calif. 94550

Anal. Chem., 43, 143 (1971)

Spectrophotometric Determination of Rhodium with Nitroso R. Formula for the Rh(III)–Nitroso R Complex

A spectrophotometric method has been developed for determination of rhodium metal employing nitroso R. Beer's law is obeyed at wavelengths of 490 nm, 500 nm, and 520 nm, and in the concentration range 2.06 through 10.4 ppm of rhodium.

ORVILLE W. ROLLINS and MORRIS M. OLDHAM, Contribution from the Department of Chemistry, U. S. Naval Academy, Annapolis, Md. 21402

Anal. Chem., 43, 146 (1971)

Determination of Polymeric Isocyanate in the Presence of Reactive Halides

A titration based upon dicyclohexylamine is used to determine the isocyanate content of polymers in the presence of reactive halides with a precision of 0.2%.

PHILLIP M. BEAZLEY, Marathon Oil Company, Denver Research Center, Littleton, Colo.

Anal. Chem., 43, 148 (1971)

ห้องสมุด กรมวิทยาศาสตร์

First, we give you a better amino acid analyzer. Then we give you a better price. ☐ When you're ready for a totally automated, tabletop amino acid analyzer system, you're ready for Jeolco's JLC-5AH. ☐ The price is right: for $27,350 you get our analyzer, plus our integrator, at less than the cost of a competitive analyzer alone. ☐ And you get more for your money. Take performance. Our unique detection system delivers 10^{-9} mol—4 times the sensitivity of competition. And you can easily adjust the sensitivity during analysis to suit your sample. No other instrument gives you such flexibility. ☐ Or take versatility. You can separate samples for accelerated analysis and physiological fluids with up to 8 programmed buffer changes. Do peptide, nucleotide, or sugar analysis with push-button ease. Run the same program 12 cycles, or vary your program 12 different ways automatically. And in every case, you can clearly pinpoint each stage in the analysis on our lighted indicator panel. No other instrument can do all this, either. To make things even easier, you can order our 36-sampler applicator. And we have a new automated sequenator, as well. ☐ There's more. Our integrator is the only two-channel unit on the market. We design and build it, just as we do all components. That way operation and service are simplified—and you have a better investment for your lab. ☐ At $27,350, you might even call it a bargain. Because it is.



Circle No. 98 on Readers' Service Card

A C BRIEFS

Evaluation of Methods for Determination of Metallic Iron in Reduced Iron Ores

An evaluation of existing and modified metallic iron methods has shown that a modified bromine-methanol procedure is most accurate for analysis of reduced iron ore samples.

S. C. BLUM and T. D. SEARL, Esso Research and Engineering Company, Linden, N. J. 07036

Anal. Chem., 43, 150 (1971)

Amperometric Titration of Calcium and Magnesium Using the Lead Dioxide Electrode

A study of the lead dioxide electrode interaction with EDTA or EGTA in solution allows the formulation of a quick and accurate amperometric titration determination of calcium and magnesium together in solution.

C. O. HUBER, K. DAHNKE, F. HINZ, Department of Chemistry and Laboratory for Surface Studies, University of Wisconsin—Milwaukee, Milwaukee, Wis. 53201

Anal. Chem., 43, 152 (1971)

Determination of Nitrogen in Vanadium Nitrides and Uranium Nitride (UN)

This study shows dissolution procedures for the Kjeldahl determination of nitrogen in vanadium nitrides and uranium nitride. The values obtained are compared with results by other methods.

DEAN H. BOLLMAN and D. M. MORTIMORE, Bureau of Mines, United States Department of the Interior, Box 70, Albany, Ore.

Anal. Chem., 43, 154 (1971)

Correspondence

Re: "Criteria for Judging Acceptability of Analytical Methods"

TERRYL J. FARRELL, Department of Health, Education, and Welfare, Food and Drug Administration, 1521 West Pico Boulevard, Los Angeles, Calif. 90015

Anal. Chem., 43, 156 (1971)

Aids for Analytical Chemists

Nonaqueous Electrochemical Cell Capable of Rigorous Exclusion of Water and Oxygen

JERRY L. MILLS, ROGER NELSON, SHELDON G. SHORE, and LARRY B. ANDERSON, Department of Chemistry, The Ohio State University, Columbus, Ohio 43210

Anal. Chem., 43, 157 (1971)

Device to Overcome Spinning Difficulties with Nuclear Magnetic Resonance Sample Tubes at Variable Temperature

JOHN BARZILAY, Unilever Research Laboratories, Vlaardingen/Duiven, The Netherlands

Anal. Chem., 43, 160 (1971)

Our Infrared Accessories Catalog is free, new and complete.

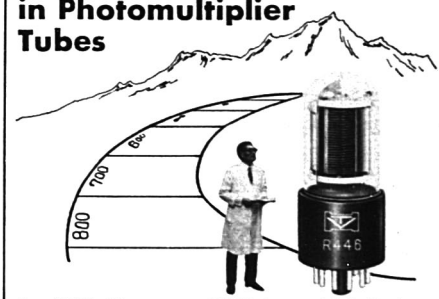


96 pages of text, pictures, diagrams and prices describe Perkin-Elmer's comprehensive line of the finest quality infrared spectroscopy accessories. Includes macro and micro liquid, gas and solid sampling cells, sampling kits, gratings and crystal optics and many special items such as polarizers, internal reflectance units and calibration kits. For your copy write to Instrument Division, Perkin-Elmer Corp., 702 Main Avenue, Norwalk, Conn. 06852.

PERKIN-ELMER

Circle No. 144 on Readers' Service Card

HAMAMATSU Scores a New Milestone in Photomultiplier Tubes



Our NEW side-on type, R446, has multialkali photocathode, hysteresis-free and designed to offer better detection stability in an uncomparable wide spectral response, ranging from 1850 to 8600 Å. These really new characteristics include upgraded sensitivity in the 7000 ~ 8000 Å which enables you to carry out advanced measurement in the red regions. And, is now ready for the highest-level applications in the various fields of photometry.

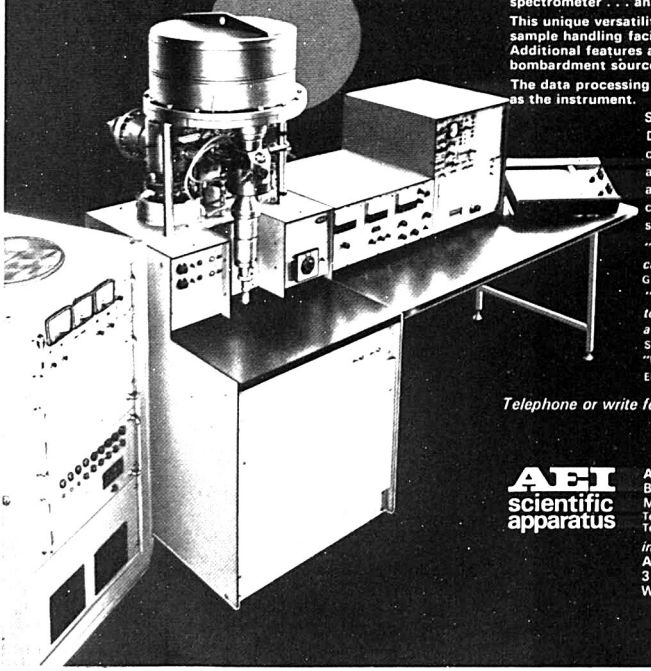
OUR PRODUCTS
Phototubes • Photomultiplier Tubes • Photoconductive cells • Special Vidicons

HAMAMATSU TV CO., LTD.
1126 Ichino-cho, Hamamatsu city, Japan.
Telex: 4225-185 Japan
Cable: HAMA TV HAMAMATSU JAPAN

Circle No. 81 on Readers' Service Card

Introducing the ES100

a new exciting dimension in electron spectrometry



WHAT DIFFERENTIATES THE ES100 FROM OTHER ELECTRON SPECTROMETERS?

It is the first commercially available spectrometer to combine successfully three techniques in one instrument and *fully* exploit the capabilities of each.

The ES100 serves as a high-energy photo-electron spectrometer . . . a low-energy photo-electron spectrometer . . . and Auger spectrometer.

This unique versatility is extended by a range of sample handling facilities without equal. Additional features are ultra-violet and electron bombardment sources.

The data processing system available is as advanced as the instrument.

SOME COMMENTS ON THE ES100

Demonstrations of the ES100's capabilities have aroused much excited and favourable comments. We quote a few remarks to substantiate our claim that no other electron spectrometer is on a par with it.

"Only AEI are thinking of what the customer wants" –
GERMAN ELECTRON SPECTROSCOPIST.
"The ES100 is generally considered to be the best commercial instrument available" –
SWEDISH CHEMIST.
"When can I get one?" –
ENGLISH PHYSICIST.

Telephone or write for full information ;-

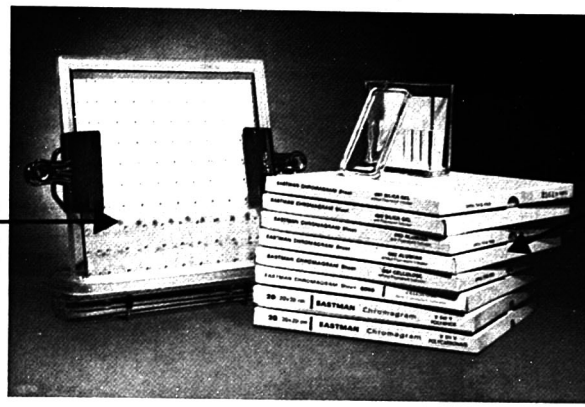
AEI scientific apparatus

AEI Scientific Apparatus Limited,
Barton Dock Road, Urmston,
Manchester M31 2LD, England.
Telephone: 061-865 4466, Telex: 668482.
Telegrams: Sciapp Manchester.

in the U.S.A.
AEI Scientific Apparatus Inc.,
3 Corporate Park Drive,
White Plains, New York 10604.

Circle No. 5 on Readers' Service Card

Fill yourself in on supplies for TLC



☐ A choice of eight types of precoated EASTMAN CHROMAGRAM Sheet—convenient, uniform, flexible.

☐ A choice of two developing chambers.

- ☐ EASTMAN CHROMAGRAM Developing Apparatus—fast equilibrating, easy to use and store.
- ☐ EASTMAN CHROMAGRAM Developing Jar—small and inexpensive; just right for pretesting and short migrations.

☐ Conveniently located local stocks of these TLC supplies are available from:

B&A **HOWE & FRENCH** **SARGENT-WELCH**
CURTIN **NORTH-STRONG** **SCIENTIFIC PRODUCTS**
FISHER **PREISER** **WILL/VW&R**

Use the coupon below to request information on these specific subjects:

- *TLC Visualization Reagents and Chromatographic Solvents* (Kodak Publication No. JJ-5)
- *TLC with* EASTMAN CHROMAGRAM *Sheet and Developing Apparatus* (Kodak Publication No. JJ-6)
- *Bibliography on the Use of* EASTMAN CHROMAGRAM *Sheet in TLC*, revised August, 1970 (Kodak Publication No. JJ-7)
- *TLC Analysis of Toxic Drugs Using* EASTMAN CHROMAGRAM *Sheet* (Kodak Publication No. JJ-37)

West of the Rockies, your dealer can obtain quick delivery of Eastman Organic Chemicals and Laboratory Supplies from our newly established stock in San Ramon, California.

Thank you for reading this advertisement.

Eastman Kodak Company
Eastman Organic Chemicals
Dept. 412L
Rochester, N.Y. 14650

Please send me: ☐ JJ-5 ☐ JJ-6 ☐ JJ-7 ☐ JJ-37

Name _____

Address _____

City _____

State _____ Zip _____

Kodak

Circle No. 51 on Readers' Service Card

This article was reprinted by permission from *Transactions of the New York Academy of Sciences*, Vol 32, No. 8, S.R. Gambino. © The New York Academy of Sciences; 1971

S. RAYMOND GAMBINO, M.D.

College of Physicians & Surgeons,
Columbia University,
630 West 168th St.,
New York, N.Y. 10032

Met and Unmet Needs of the Automated Clinical Laboratory

Development of the automated clinical laboratory should proceed by considering the total system from the ordering to the evaluating of laboratory tests

IN THIS PAPER I attempt to define the met and unmet needs of the automated clinical laboratory to aid in guiding the decisions made by designers, manufacturers, and users. Unless the automated clinical laboratory is developed as a total system we will create pockets of success and pools of chaos (*1*).

What do I mean? If, for example, we continue our logarithmic success in automating ordering, analysis, and reporting of tests, but at the same time do little about automating collection, transportation, identification, separation, evaluation, and required action, we will have the kind of success *cum* chaos that we have in our nationwide transportation system.

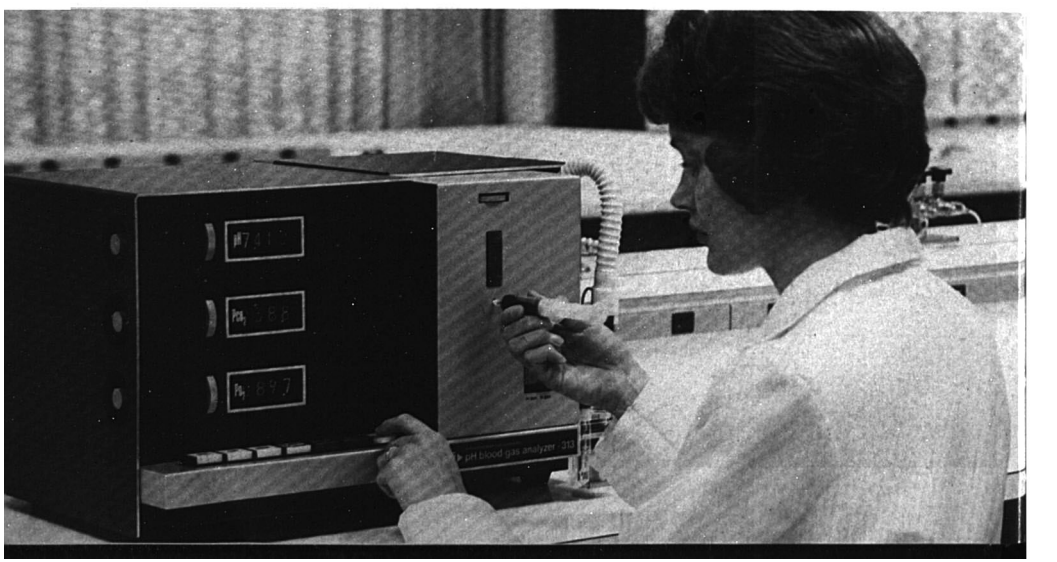
If our automated laboratory is capable of spewing out 6000 test results per hour, but we have no efficient system for interpreting, sifting, cataloging, and acting upon this data, we will then have the same kind of problem one gets when a mechanized parking lot discharges more cars per minute than the street can handle.

What is Available?

When lab tests are performed on patients, the following procedures are carried out: ordering, collection, transport, identification, separation, analysis, reporting, evaluation, and action.

Most of these steps are not automated. However, they must be automated or be eliminated. One way to eliminate them is to make it possible for the physician (and eventually for the patient himself) to obtain his own laboratory data.

Direct operation by the physi-

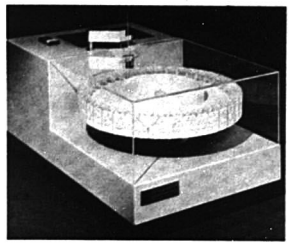


cian is the concept underlying the design of the Instrumentation Laboratory, Inc. (Lexington, Mass.) Model 313 Blood Gas Analyzer.

The Model 313 has a simple push-button control panel. When the operator presses "Calibrate" the instrument is washed with a heparinized cleaning solution equilibrated with oxygen and carbon dioxide. Automatic timing circuits control the movement of specially designed, gas-tight rotary valves that switch from flushing solution to gas. Indicating circuits are kept locked until an equilibration period has passed and a data light indicates it is appropriate to evaluate the calibration data.

When the operator presses "Sample" the instrument automatically pumps the blood sample through a preheater, into the microchamber faced by the P_{CO_2} and P_{O_2} electrodes. Again, automatic timing circuits control the operation of the indicator lights, and after a fixed period the data is locked and the "Data" light glows. If the data light is pushed, the signal can be transmitted directly to the computer. The instrument then cleans itself and returns to the calibrate cycle. By pressing "Standby" the pumps are turned off but the electronics and water bath are kept on.

One Model 313 blood gas analyzer has been used by anesthesiologists and their residents in the recovery room of the Columbia-Presbyterian Medical Center for a 15-mo period. The instrument was used by more than 30 different operators during this time and was operational to the first user 90% of the time. In the remaining 10% of the cases it was easily made operable if a knowledgeable second operator was called. The most common problem was inadequate wash-

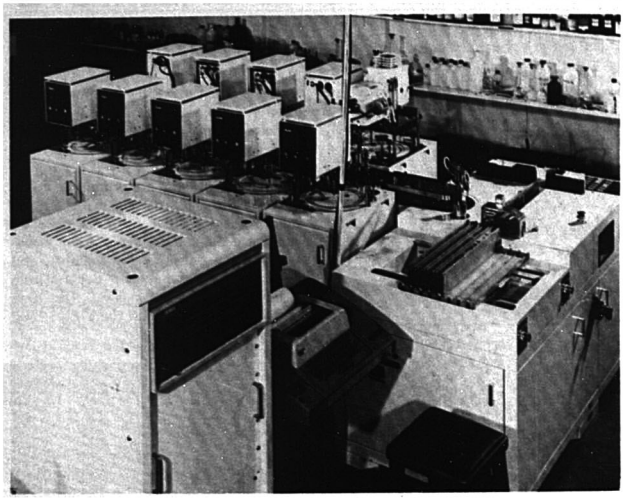


IDee system for positive sample identification eliminates the danger of mismatching samples and results in the laboratory. The system consists of a 40-position sampler that will accommodate either Vacutainers or sample cups, and the optical and electronic equipment necessary to read a coded label, recognize the coding, store the information until test results are available, and print the correct decoded decimal representation on chart paper. The IDee is designed for use with the SMA 12/60 and SMA 6/60 systems



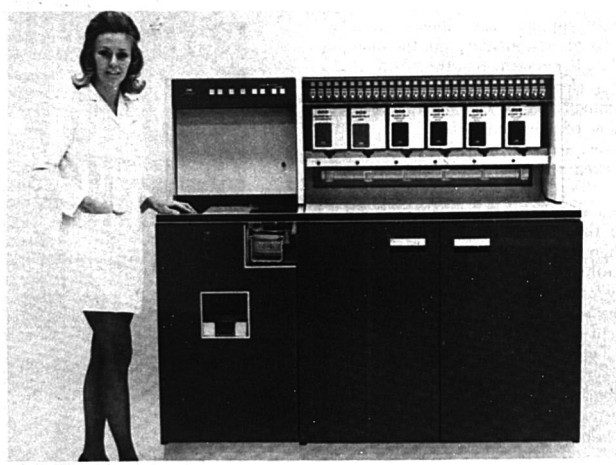
Technicon's SMA 6/60 system (above) may be used alone, or in conjunction with the SMA 12/60 multichannel analyzer. The 6-channel system measures electrolytes, glucose, and BUN. These six determinations may be performed on a 1-ml serum sample in only 9 min. Test can be performed round-the-clock. Results are automatically recorded on precalibrated chart paper, in concentration terms suitable to each parameter. The 12/60 performs 12 determinations on every 1.8-ml serum sample at the rate of 60 samples per hr.

Model 313 pH/blood gas analyzer has simple push button controls and can be operated by assorted personnel. The instrument is made by Instrumentation Laboratory, Inc., of Lexington, Mass.



Multi-Channel 300 clinical analysis system consists of several major modular components including a control console, a distributor system, up to 10 interchangeable analytical reactions consoles, and a process controller. A computer monitors all stages of the analytical cycle, such as sample identification, sample quality control, and selectivity of printout of results in digital form. Up to 300 samples per hr can be processed; with 10 consoles up to 16 different determinations and 4 reagent blanks may be run simultaneously. An initial installation can be increased by adding more reaction consoles as needed. Easy on-line and off-line changes can be made to meet varying workloads. The Vickers Instrument is available in the U.S. from Medi-Computer Corp., Greenwich, Conn.

Du Pont's aca (automatic clinical analyzer) now commercially available is based on a special kit called the analytical test pack. This separate pack is used for each test performed on a sample. The pack contains both the test name for identification by the operator and a binary code to instruct the analyzer. The instrument performs both enzymatic and chemical analyses by using either rate, differential wavelength, or conventional techniques. It has a basic capacity of 30 different methods and an ultimate capacity of 62 procedures. More information on this system is available from the Instrument and Equipment Division, E. I. du Pont de Nemours & Co., Wilmington, Del. 19898



out of the drain lines. The instrument enables physicians to treat critically ill patients with greater ease, and allows any physician to obtain his own blood gas data whenever he wants them, and within 2 min of his request for such information. Thus the essential characteristics of the analyzer are: Simplicity and automaticity of operation; high speed; and functional reliability.

The manufacturers of automated equipment are solving the problem of speed. Each new generation has increased output or turnaround time or both.

The most successful instruments utilize some form of continuous flow first introduced by Technicon (Tarrytown, N. Y.) and currently represented by their SMA 12/60 and 6/60 series. The 12/60 and 6/60 series have been tied to a simple form of sample identification (IDee) with a printout capable of being transferred to the original report. The Technicon system makes it possible for a single laboratory technologist and two bloodclerks to process 300 specimens on each of the two machines. Performance of 18 tests from one blood sample had the following benefits:

(1) A decrease in the number of individual orders to the point where individual requests for such tests as uric acid, calcium, and alkaline phosphatase have decreased more than 10-fold.

(2) A decrease in the number of orders and reports shuttling back

and forth between nursing stations and lab.

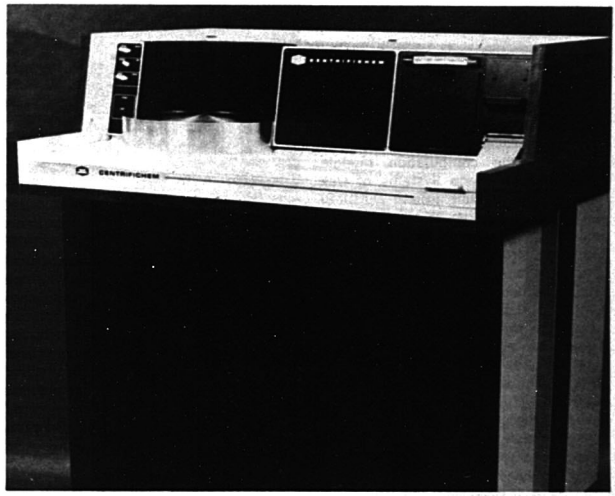
(3) A decrease in the amount of required laboratory space.

(4) An increase in productivity. This is not a false productivity increase based on the addition of previously unmeasured tests, but a true increase based on a decrease in the number of people required to do tests previously ordered individually.

A new approach to an increase in speed has been made by Norman G. Anderson (*2,3*) using continuous rotation rather than continuous flow. Rotors currently available make it possible to measure 16 simultaneous enyzme reactions or any other two-step chemical reaction. Time from start to finish can be as short as one minute. Automatic loading of samples and reagents and automatic printout of results is now available. Larger rotors, and an increase in the number of possible reaction steps, will enable this principle to compete with continuous flow.

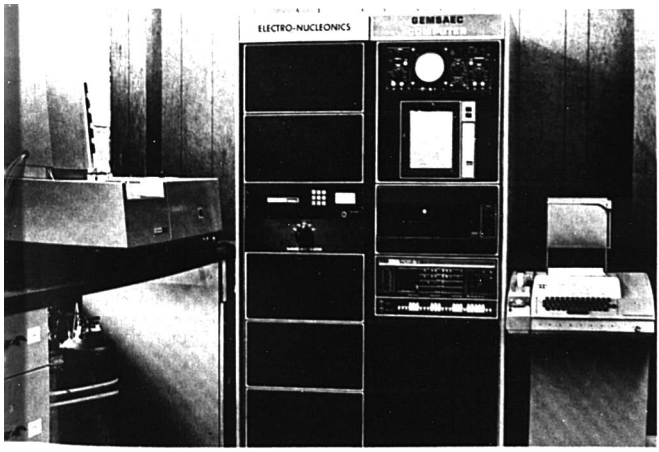
But what about the continued development of discrete sampling? Even after the introduction of continuous flow by L. T. Skeggs, Jr. (*4*), most other attempts at laboratory automation have attempted to reproduce the manual techniques used by chemists. We have had Robot Chemists, AutoChemists, Discrete Sample Analyzers, and other mechanical replacements for manual sampling and delivery.

Of all available discrete sample systems, the two most interesting to me are the Du Pont Automatic Clinical Analyzer and the Vickers



Representative commercial instruments resulting from the work of Norman Anderson and associates at Oak Ridge National Laboratory are shown. These instruments (GEMSAEC) are based on the use of centrifugal force to move and mix samples and reagents concurrently, permitting simultaneous analyses

Union Carbide's (Bioproducts and Research Div., Tarrytown, N. Y.) Centrifichem permits the simultaneous assay of 30 samples at a rate of 120 to 600 per hr. The unit uses a 30-place cuvette rotor. This instrument is designed for routine stat and emergency tests and gives digital printout of absorbance units or concentration units; an oscilloscope displays the analog signal for simultaneous monitoring of all cuvettes. Automatic reaction rate or end-point determinations can be made. The analyzer can be interfaced to dedicated or off-line digital computer systems for further data reduction, analysis, and storage



Electro-Nucleonics of Fairfield, N. J., has just introduced a new programmable high-speed spectrophotometric analyzer for research purposes. The research unit is similar to the company's basic GEMSAEC (ANAL. CHEM., August, 1970, p 70 A, item 405) but integrates a general purpose computer easily programmed with the conversational FOCAL. Programs are provided for data formatting, concentration calculations, and statistical data reduction. Both teletype printout and oscilloscope display of program pages and graphic data permit the review of 16 dynamic reactions simultaneously



American Instrument Co. (AMINCO, Silver Spring, Md.) has designated its instrument the Rotochem. Sample solutions are placed in 15 wells. In this instrument the computation module made by Tennecomp Systems of Oak Ridge, Tenn., is built around a PDP-8i minicomputer with an 8K memory, A/D converter, functional control panel, automatic program loader with magnetic tape cartridge drive, and digital display oscilloscope with light pen. The computer module is completely interfaced to the Rotochem and programmed to acquire end-point and rate data and to output in concentration units. At maximum rotor speed (about 2000 rpm) the minimum time interval between successive measurements on a given sample is 30 msec. The use of a reagent or solvent blank permits automatic baseline correction

Multi-Channel 300 Automated Analysis System (Medi-Computer, 581 W. Putnam Ave., Greenwich, Conn. 06830). The Du Pont instrument is recently available commercially. It is practically self-operable but has a low output. The Vickers instrument has a high output but has not been fully field tested.

But I am not convinced that these discrete devices can really compete with continuous flow or continuous rotation. The history of the internal combustion engine gives us an analogy. The continuous rotary motion of the jet motor is a more reliable, powerful, and simple device than the most sophisticated piston-type internal combustion engine. The complexity of the moving parts in a discrete device sets a low top-limit to speed, and mechanical complexity also increases probability of breakdown.

What is Missing?

Automatic or Self-Collection of Blood. If sample volumes can be brought down to less than 5 μl, then an automatic system for sampling from the capillary bed might be possible. Development of an automatic sampling technique that would sense the heat or flow of blood and then would pass a sterile disposable microprobe into an antecubital vein should be possible. At present the closest we come to this step is in patients with indwelling catheters. But again there is a lack of research on the development of semipermanent indwelling sampling systems for use in hospitals. Such systems would obviate the need for painful, multiple venapunctures.

Automatic or Self-Ordering of Tests. At present most physicians believe that only a physician should order a lab test. On the other hand it makes more sense to make lab orders automatic to suit the problem at hand. It should also be possible for individuals to order their own laboratory tests. We all look at ourselves in mirrors, in photos, and in the reactions of others to us. Why shouldn't we have the right to look at ourselves biochemically and microscopically?

Automatic Transport of Specimens. This area needs develop-

(*Continued on page 27 A*)

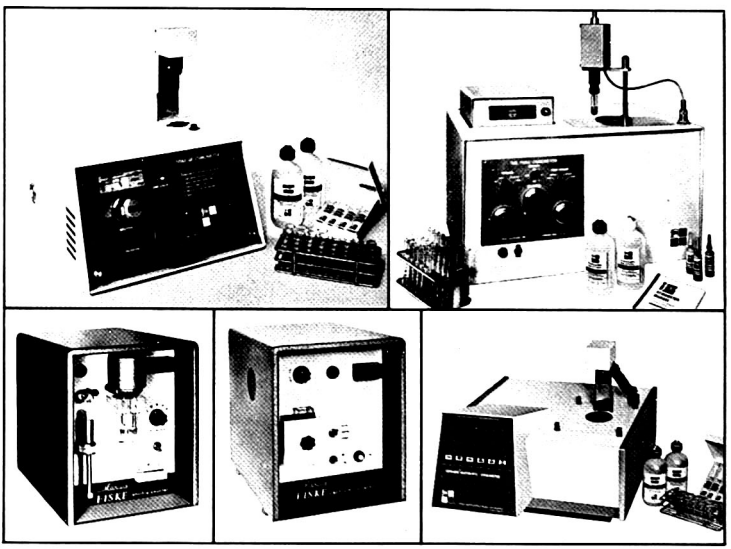
FISKE ASSOCIATES, INC.
Quaker Highway, Uxbridge, Massachusetts 01569

Fiske® Osmometers and Cryoscopes...
standard of the world – since 1952!

Freezing Point, Osmolality, Molecular Weight, Added Water, Total Dissolved Solids, Salinity, Fermentation End Point, Adulterated Solutions, Total Body Water, Pollution, Artificial Sea Water, Tissue Fixative Solutions, Percent Alcohol

These are some of the many applications for which Fiske Osmometers and Cryoscopes are employed. Thousands of Fiske users throughout the world are obtaining useful information vital to their various scientific projects. Fiske has an international reputation for excellence in instrumentation and an international network of authorized Fiske sales and service representatives to back it up. Why not get in touch with your Fiske man today? If you don't find him listed below for your country, write for the Fiske Osmometer and Cryoscope "Fact File."* Your request will receive prompt attention. (617) 278-2482

*Service mark of Fiske Associates, Inc.



Other Fiske specialty instruments for the laboratory include: Chlor-O-Counters and Calcium Titrators.

FOREIGN REPRESENTATIVES **European Sales & Service** — Eurolab Scientific N.V., Coornhertstraat 63 Vlaardingen, Holland

AUSTRALIA — NEW ZEALAND H. B. Selby & Co. Pty. Ltd., Victoria, Australia • Watson Victor Ltd., Wellington, New Zealand • **EUROPE** *(Western)* Arla Trading Co., Bruxelles, Belgium *(also Luxembourg)* • Svend Schrøder, Redovre, Denmark *(also Norway and Sweden)* • V.A. Howe & Company Ltd., London, England *(also Scotland)* • Instrumentarium OY, Helsinki, Finland • Jarre Jacquin Recherches et Laboratoires, Paris, France • Nicholas Sficas & Fils, Thessaloniki, Greece • Joh. Wilten — Utrecht, DeBilt, Holland • Thomas H. Mason & Sons Ltd., Dublin, Ireland • Ing. A. Rastelli e C., Rome, Italy • Ortec, Lisbon, Portugal • Pacisa, Madrid, Spain *(also Balearic Islands)* • **EUROPE** Madag Machinen UND Apparatebau, Dietikon, Switzerland • Eurolab Scientific N.V., Vlaardingen, Holland *(Western Germany and Austria)* • **EUROPE** *(Eastern)* Intertex International, Inc., 270 Madison Ave., New York, New York 10016 • **NEAR AND MIDDLE EAST** Industrial & Research Instrument Co., Bombay, India *(also Pakistan)* • Levant X-Ray Ltd., Tel Aviv, Israel • **FAR EAST** Riko Trading Co., Ltd., Tokyo, Japan • Anthony International Company, New York, New York 10023 *(South Korea)* • **SOUTH AFRICA** Nucleonic Engineering Pty. Ltd., Johannesburg, South Africa • **WEST INDIES** Scott Instruments, Miami, Florida • **CENTRAL AND SOUTH AMERICA** Laboratorio Chemia, La Plata, Argentina • Formed, Rio de Janeiro, Brazil • Victor Mannuel Grez O., Santiago, Chile • **CANADA** O.H. Johns Scientific, Toronto 8, Canada

Circle No. 62 on Readers' Service Card

Students
Instructors
Researchers

will want a copy of

MODERN CLASSICS IN ANALYTICAL CHEMISTRY

A selection from the best feature articles that appeared in recent issues of the American Chemical Society's publications ANALYTICAL CHEMISTRY and CHEMICAL AND ENGINEERING NEWS

Particularly suitable as supplementary reading for the advanced student of analytical chemistry, this reprint volume contains articles on INFRARED SPECTROMETRY, GAS CHROMATOGRAPHY, NMR, COMPUTERS IN CHEMISTRY, and many other topics that are presented only in outline form in most modern textbooks.....

Price: $4.50 per copy, with a discount of 20% for orders of 10 or more (postpaid)

Compiled and Edited by Alvin L. Beilby, Seaver Chemistry Laboratory, Pomona College, Claremont, Calif.....

CONTENTS

Standardization of Acidity Measurements, by Roger G. Bates

Ion-Selective Electrodes and *New Directions for Ion-Selective Electrodes*, by Garry A. Rechnitz

Polarography in Organic Chemistry, by Petr Zuman

Instrumentation of a Spectrophotometric System Designed for Kinetic Methods of Analysis, by Theodore E. Weichselbaum, William H. Plumpe, Jr., and Harry B. Mark, Jr.

Some Aspects of Fluorescence and Phosphoresence Analysis, by David M. Hercules

Circular Dichroism: Theory and Instrumentation, by A. Abu-Shumays and Jack J. Duffield

Shapes of Analytical Curves in Flame Spectrometry, by P. J. T. Zeegers, R. Smith, and J. D. Winefordner

Atomic Absorption Spectrometry: Applications and Problems, by L. L. Lewis

Emission Flame Spectrometry—A New Look at an Old Method, by E. E. Pickett and S. R. Koirtyohann

Infrared Spectroscopy, by Kermit Whetsel

Recent Trends and Developments in Inorganic Far Infrared Spectroscopy, by John R. Ferraro

Microwave Spectroscopy, by William H. Kirchoff

Nuclear Magnetic Resonance, by Frank A. Bovey

Nuclear Quadrupole Resonance, by Russell S. Drago

Electron Spectroscopy, by David M. Hercules

Analytical Potential of Photoelectron Spectroscopy, by D. Betteridge and A. D. Baker

Expanded Analytical Horizons Through Mass Spectrometry, by Fred W. McLafferty and Roland S. Gohlke

Thermal Analysis by Mass Spectrometry, by Roland S. Gohlke and Horst G. Langer

Extraterrestrial Neutron Activation Analysis, by J. S. Hislop and R. E. Wainerdi

New Developments in Chemical Selectivity in Gas-Liquid Chromatography, by Barry L. Karger

Liquid Chromatographic Detectors, by Ralph D. Conlon

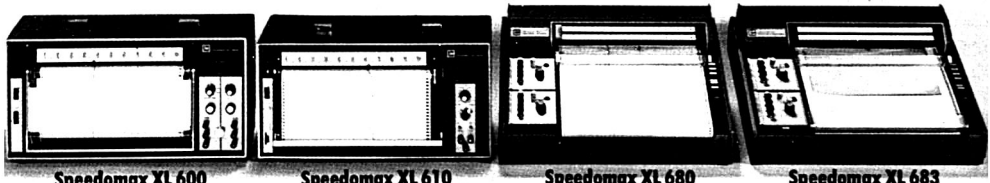
Digital Control Computers in Analytical Chemistry, by Jack W. Frazer

A General-Purpose Laboratory Data Acquisition and Control System, by G. Lauer and R. A. Osteryoung

Proper Utilization of Analytical Instrumentation, by S. Z. Lewin

Send your order to: **Special Issues Sales**
American Chemical Society
1155 Sixteenth St., N.W.
Washington, D. C. 20036

New, dependable Speedomax XL Recorders from Leeds & Northrup to meet all your research and test requirements



Speedomax XL 600
low-profile recorder

One- or two-channel, fixed- or multi-span. Range spans from 100 μV to 100 V, and degrees C.

Speedomax XL 610
low-profile recorder

One- or two-channel, fixed- or multi-span. Range spans from 1 mV to 1250 mV, and degrees C.

Speedomax XL 680
flat-bed recorder

One- or two-channel, fixed- or multi-span. Range spans from 400 μV to 100 V, and degrees C.

Speedomax XL 683
X-Y plus X-t recorder

Two recorders in one. Fixed- or multi-span; range spans from 400 μV to 100 V, and degrees C.

Speedomax® XL Laboratory Recorders offer the best of two worlds.

They are sensitive, highly-precise null-balance potentiometers that incorporate traditional Leeds & Northrup craftsmanship and reliability.

And they are superbly-styled, solidly-built portables that provide maximum versatility and convenience for a broad spectrum of laboratory applications.

Speedomax XL 600 and XL 610 are low-profile recorders with vertical chart travel. They come equipped with a handle and rubber feet for portability, and can be provided with a swivel base, or modified for rack or wall mounting. A tilt-out writing table facilitates jotting notes on the chart. Case dimensions are approximately 18" wide by 9" high by 11" deep.

Speedomax XL 680 and 683 are flat-bed recorders with horizontal chart travel. They come equipped with retractable tilting bracket in base. Rigid plastic dust cover is standard equipment. Case dimensions are 7¾" deep by 17⅜" wide by 6⅜" high (6¾" high with dust cover in place).

A number of standard and optional features are common to all Speedomax XL recorders. They include:

- All-solid-state guarded circuitry.
- Single- or dual-channel recording with full-scale pen travel.
- Accuracy of ±0.25% of span.
- Single or switch-selected multiple spans.
- ±100% zero adjustment.
- mV or thermocouple calibration.
- Optional zero-left (reverse) range.
- Single, dual or multiple chart speeds.
- 250 mm (Nominal 10") calibrated charts.
- Scuff- and chemical-resistant cases.

Want more information? Contact your L&N Field Representative or write Leeds & Northrup, North Wales, Pa. 19454

Circle No. 109 on Readers' Service Card

Circle No. 110 on Readers' Service Card

Circle No. 111 on Readers' Service Card

Circle No. 112 on Readers' Service Card

LEEDS & NORTHRUP
North Wales, Pa. 19454

Now! Automated Sampling for your chromatograph

You can convert your chromatograph into an automatic liquid sampling system by simply adding a Hamilton Autosampler to the face of your instrument. You can introduce samples as small as 0.1 ul with excellent precision and repeatability through a capillary injection device. You can load as many as 48 liquid samples and the Autosampler's built-in logic controller will take over the automatic operation of your GC for the evening or weekend. Samples may be stored for extended periods without fractionation in Hamilton's exclusive piston-sealed sample vials.

For complete information, write for Brochure, Hamilton Company. Post Office Box 307, Whittier, California 90608.

Repeatable Precision: Hamilton's Autosampler



HAMILTON

Circle No. 80 on Readers' Service Card

ment. We can either place inexpensive sensors at, on, or in the patient, and transmit data to a central processor; or we should develop an inexpensive monorail system for rapid transfer of specimens from the patient to a central laboratory. Currently available pneumatic systems are too jarring to specimens. Microbiological specimens, for example, cannot be transported through pneumatic systems. A track system, with controlled acceleration and deceleration, would be capable of transporting microbiological specimens.

Automatic Identification. This area is fairly well developed and Technicon's IDec system illustrates one successful direction. However, what is lacking is what I would like to call the "lock and key" approach. It should be possible to supply an absolutely fail-safe system for identification of patients, samples, and medications. Such a system would make it impossible to get the specimen from the wrong patient, to return the results to the wrong patient, or to give the wrong medication to any patient. Any system that requires a human to make a match is not good enough. What I require is a unique "lock and key" system—either mechanical, electrical, or electronic—that is independent of any transfer of information through a human mind.

Automatic Separation. The time now spent on the preparation of specimens for our automated laboratories consumes a large proportion of our available man-hours. One person can *run* an SMA 12/60 and 6/60 combination, but it requires two people to *feed* these instruments with centrifuged and filtered specimens.

Automatic Analysis. This region is most highly developed, and as mentioned above there is danger that overdevelopment will clog the system. But even in the well developed area of analysis we are spending too much time utilizing human minds to control and operate our instruments. Minicomputers should have more widespread use—not just for data handling but for the myriad operational control functions that could be programmed. Minicomputers are now being used more widely in industry and the cost is below $10,000. Most laboratories could afford to have several.

Automatic Reporting. Much has been done to record raw data automatically and to record patient data in serial fashion, but the current rate of data development threatens to "blow the minds" of the recipients. We need far more compact and efficient ways to present significant data.

Automatic Evaluation. This ties in with improved presentation. Patients should not be at the sole mercy of random access to randomly varying physicians' minds.

Automatic Action. This too ties in with presentation and evaluation. Required action should be signaled automatically in areas where current knowledge justifies such a move.

What About Robots?

An area of automation being developed for industrial use, that should have application in the laboratory, is the robot. Hawker Siddeley Dynamics of Great Britain has a $1500 robot that can make 2000 precise motions an hour (*Business Week,* April 4, 1970, p 50). As wage rates continue to rise and skilled help becomes scarcer, the robot's utility will become more attractive.

What About Space?

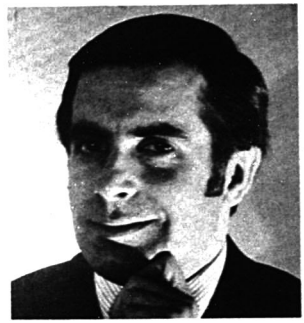
Future automated equipment will be more compact. Currently available equipment has halted the need for ever increasing laboratory space, and miniaturization will probably *decrease* future space requirements.

Conclusions

The manufacturers of equipment for automated clinical laboratories have made great strides in the areas of analysis and reporting. But much work needs to be done in the areas of collection, transport, evaluation, and action. The development of instruments operable by physicians, or by the patients themselves, will simplify and shorten the steps from order to action. For the large laboratory, the use of robots is predicted.

References

(1) J. H. U. Brown and J. F. Dickson, III, *Science* **166**, 334–38 (1969).
(2) N. G. Anderson, *Science* **166**, 317–24 (1969).
(3) D. W. Hatcher, and N. G. Anderson, *Amer. J. Clin. Pathol.* **52**, 645–51 (1969).
(4) L. T. Skeggs, Jr., *Amer. J. Clin. Pathol.* **28**, 311–22 (1957).



S. Raymond Gambino *is Professor of Pathology at Columbia University's College of Physicians & Surgeons and is Director of Clinical Chemistry at Columbia-Presbyterian Medical Center, New York City. He was born in Brooklyn, N. Y., and received his B.S. degree from Antioch College in 1948. He received his M.D. degree from the University of Rochester in 1952 and interned at Bellevue Hospital 1st Medical Division (Columbia University Division). Prior to his positions at Columbia University and Columbia-Presbyterian Hospital, he had been associated with pathology and clinical chemistry laboratory work at Marquette, St. Luke's Hospital in Milwaukee, and Englewood Hospital in Englewood. Dr. Gambino's research interests are in blood gases, acid-base balance, bilirubin, and general laboratory methodology. He is author or coauthor of more than 36 publications. Dr. Gambino is a member of the American Society of Clinical Pathologists, College of American Pathologists, ACS, American Association of Clinical Chemists, New York Academy of Sciences, and the AMA. He is also currently a member of the Committee on Clinical Chemistry of the ACS.*

FEATURED LABORATORY

Chemical Experimentation

Principles and Practice at Northwestern University

CLAUDE A. LUCCHESI, Department of Chemistry, Northwestern University, Evanston, Ill. 60201

Northwestern University's centralized analytical services–advanced practices laboratory introduces students to a wide variety of modern research methods and allows them ready access to high quality analytical instrumentation

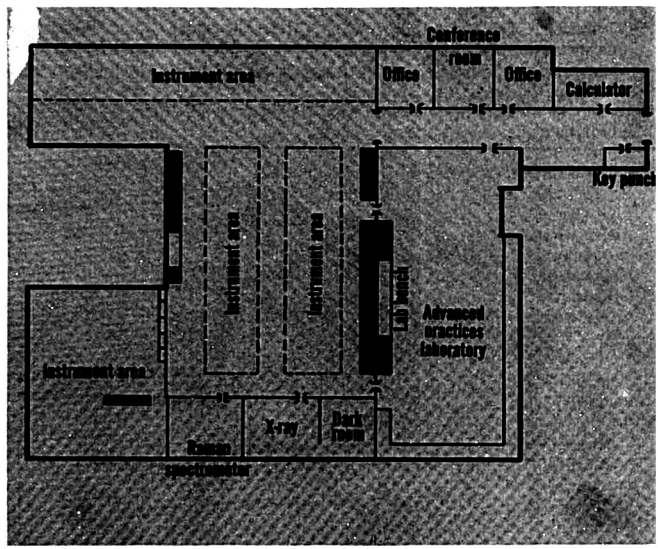


Figure 1. New laboratory unit

THE PRESENTATION of a unified, practical approach to broad-based chemical experimentation has been a continuing goal at Northwestern University for many years. In line with this philosophy, a laboratory course on "advanced practices" was introduced into the undergraduate curriculum about five years ago, and more recently, centralized analytical services were made available for both graduate and undergraduate research students. With last year's completion of a 7000-ft² Chemistry Department addition to house an analytical services laboratory and an adjoining advanced practices teaching laboratory, Northwestern students are now getting a unique introduction to chemical measurement techniques. The new laboratory arrangement gives every student ready access to quality research apparatus and provides a common ground for all research groups—organic, inorganic, biochemical, physical, and analytical—to see the wide array of methods and equipment used in each of the various fields.

The new laboratory unit was established to consolidate the Chemistry Department's analytical instrumentation under a Director of Analytical Services who would manage the services lab and teach in the advanced practices course. The unit is staffed with three technicians and four professionals, including the laboratory director, Dr. Claude A. Lucchesi, who joined the chemistry faculty two years ago after 14 years of industrial experience in the practice and management of chemical analysis. The layout of the Chemistry Department addition is shown in Figure 1.

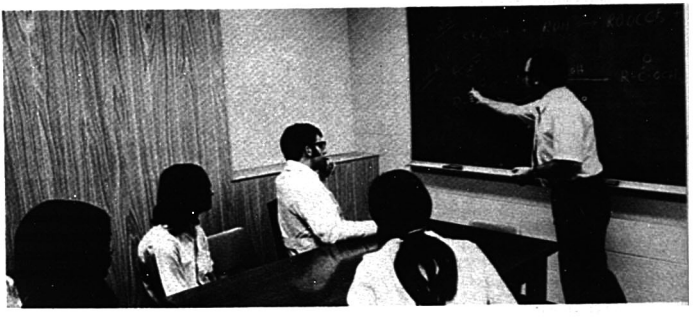
Advanced Practices Laboratory

The advanced laboratory course evolved as a way to lend coherence to the undergraduate curriculum (*1*). The course objective is to provide broad-based experiments that more closely resemble the kind of work a professional chemist actually does rather than just to give the student an exercise illustrating only a single principle. To achieve this scope, the methods and techniques traditionally learned in courses labeled inorganic, physical, and analytical chemistry have been combined to give the student an opportunity to integrate his earlier chemical experience. Topics covered in the course are listed in Table I.

Experimental techniques, including the techniques used in synthesis, are stressed. Most experiments make use of conventional solution preparation methods, but high-temperature syntheses and vacuum-line preparation of air-sensitive compounds also are in-



Instruments in the analytical laboratory have been arranged so that those which are primarily student-operated are most accessible. The area shown above includes most of the spectrometers available to students on a 24 hr/day basis



Included in the analytical services—advanced laboratory area is a conference room which may be used by the graduate teaching assistants who give many of the oral exams required in the chemical experimentation course. It is also used for formal discussions of current research problems. Here, Dr. Lucchesi is discussing a problem with students and a staff member

Table I. Advanced Practices Course

Synthesis
- Coordination compounds
- High temperature preps
- Vacuum line preps

Separations
- Fractional crystallization
- Ion exchange
- Gas chromatography
- Paper chromatography

Determinations
- Titrimetry
- Spectrophotometry
- Gas chromatography
- Optical rotation

Structure-identification
- Line spectra (sodium)
- Band spectra (iodine)
- Vib-rotational spectra (DCl)
- Optical activity (ord-cd)
- Magnetic susceptibility
- Nuclear magnetic resonance
- X-Ray diffraction
- Gas chromatography

Electrochemistry
- Current-voltage curves
- Polarography
- Cyclic voltammetry
- Electrolytic conductance

Chemical kinetics
- Cis-trans isomerization
- Gas phase cyclization
- Rapid proton exchange

Calibration principles
- Reference standards
- Internal standards
- Standard addition technique
- Criteria of purity

Basic electronics
- Operational amplifiers
- Common circuits
- Readout devices

Instrumentation principles
- AC vs. DC systems
- Double/single beam
- Signal averaging

Data treatment
- Statistical evaluation
- Computer programs

Presentation practice
- Formal written reports
- Oral exams

cluded. Methods for performing determinations are utilized in the experiments as are the methods and techniques of structure determination and identification. The determination of the concentration of various species also is used to illustrate the kinetics of the three types of transformations listed in Table I.

Before the institution of the laboratory practices course, there was some question as to where in the undergraduate curriculum certain topics belonged. For example, there had been a question about where to put basic electronics and electrochemistry. A chemical experimentation course turns out to be an ideal place for these topics. Other areas, such as calibration and instrumentation principles as well as data treatment also are readily covered—explicitly or implicitly—in the course. In addition, an especially difficult aspect of an undergraduate's training, oral presentation of his experimental findings, is given special attention.

The experimental units developed to date are listed in Table II. The hope is that with these experiments, the techniques and principles of the

Table II. Experimental Units

Atomic spectra	Gas chromatography
Operational amplifiers	Ion exchange
Current-voltage curves	Synthesis of ND_3 or DCl
Preparation of inorganic complexes	Ir spectral study of DCl or ND_3
Kinetics of cis-trans isomerization	Synthesis of chromous acetate
Preparation and analysis of $CoFe_2O_4$	Magnetic susceptibility
X-Ray powder patterns	Band spectrum of iodine
Polyphosphates	Fluorescence of europium(III)
Formation constants of a complex	Gas-phase kinetics
Polarography and cyclic voltammetry	Chemical dynamics by nmr

Table III. Analytical Laboratory Instruments

- Baird 4-55 infrared spectrophotometer
- Beckman ir-5 infrared spectrophotometer
- Beckman ir-9 infrared spectrophotometer
- Beckman ir-10 infrared spectrophotometer
- Beckman ir-11 infrared spectrophotometer
- Cary Model 11 uv-visible recording spectrophotometer
- Cary Model 14 uv-visible–near ir recording spectrophotometer
- Beckman Model DK-2 uv-visible–near ir recording spectrophotometer
- Perkin-Elmer-Hitachi MPF-2A fluorescence spectrophotometer
- MPF-2A with phosphorescence attachment
- Cary Model 60 optical rotatory dispersion-circular dichroism spectropolarimeter
- Hewlett-Packard automatic carbon, hydrogen, nitrogen analyzer
- Mechrolab Model 302 osmometer
- Barber Coleman programmed temperature gas chromatograph
- CEC Model 21-104 analytical mass spectrometer
- Two Spinco Model E analytical ultracentrifuges, one with photoelectric scanning system
- Two Beckman amino acid analyzers
- Packard Tri-Carb scintillation counter, Model 314E
- Varian Model T-60 nmr spectrometer
- Varian Model A-60 nmr spectrometer
- Bruker Model HFX-10 nmr spectrometer with conventional and high-speed signal averaging capability
- Spex Industries laser-Raman spectrometer
- Two Picker X-ray generators with associated accessories, including an integrating precession camera and a Weissenberg camera

three traditional fields are so well mingled that the student uses many of them without consciously thinking he is doing inorganic, or analytical, or physical chemistry. Rather, he is doing chemistry to solve a problem.

One example of "doing chemistry" involves the preparation of an inorganic complex. The student is given the problem of preparing tris(ethylenediamine) cobalt(III) chloride and resolving the optical isomers produced. In carrying out the work, he learns the principles involved in separating a racemic mixture—*i.e.*, conversion to diastereoisomers which may be separated by fractional crystallization. He learns to use optical rotation as a measure of concentration and as a means for calculating yields. Hopefully, he sees the arbitrariness of the term "pure" because a rather unfamiliar quantity, optical rotation, is used as a measure of purity. He also learns about optical rotatory dispersion and circular dichroism.

Oral Examinations

The laboratory practices course covers two quarters and is taken by chemistry majors in their junior or senior year and by graduate students from other departments. The course meets three days a week, four hours per day, and typically, eight or nine experiments per quarter are required. The student chooses one experiment each quarter for a "long" report which he prepares as a journal-type review or research article, depending on the nature of the experiment. He is expected to do a fair amount of library work for this report. The other experiments are done as "short" reports which means that the student hands the instructor assigned to that particular experiment a carbon copy of the data he obtained and takes an oral exam on the work he did.

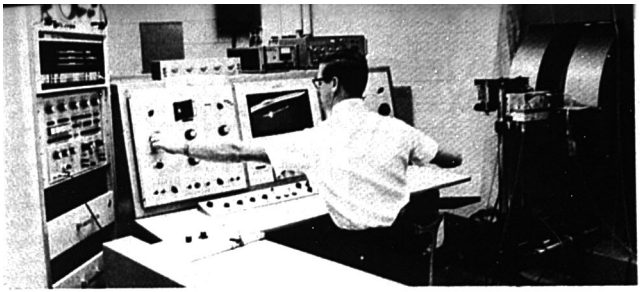
The oral exams are a very significant aspect of the advanced practices course because they serve to inject reality into the student's training. Certainly, in most real-life work situations likely to be encountered—in later graduate work as well as in industry—the student will have to present his work verbally. The oral exams provide the student with practice in thinking on his feet, and give the instructor ample opportunity to find out the extent of his understanding. The disadvantage of the oral exam is that it is very time consuming. This is one reason for a high instructor-to-student ratio for the course. Last year for the 12 students, there were two faculty members and five graduate teaching assistants.

Analytical Services Laboratory

Adjacent to the chemical experimentation teaching laboratory is the analytical services laboratory. The layout of the analytical lab is shown in Figure 2, and the instruments now in use in the lab are listed in Table III. The instruments can be classified broadly as spectrometric or bioanalyti-

The mass spectrometer is one of the instruments operated only by the analytical laboratory staff. The instrument shown here is a medium resolution spectrometer capable of handling gas, liquid, or solid samples. Adjusting the ion accelerating voltage before commencing a run is staff member, Roger Crain





The 90 MHz multinuclide nmr spectrometer is used to study ^{1}H, ^{19}F, ^{11}B, ^{31}P, ^{13}C, ^{17}O resonances. It is equipped with conventional and high-speed Fourier transform signal averaging and is primarily staff-operated. Only specially designated students doing nmr research are trained to operate the instrument in a limited range. The laboratory supervisor, Dan Netzel, is shown making the spectrometer ready for student use.



One of the advantages of having the advanced practices laboratory adjacent to the analytical laboratory is more efficient utilization of equipment. For example, the gas chromatograph was used exclusively in the chemical experimentation course only one quarter a year prior to the present arrangement. It is now located in the analytical lab where it may be used as needed. Adjusting the instrument is Lily Kao who works full-time in the advanced practices lab but is available for special analytical projects.

cal, and they are arranged for the user's convenience. In general, an instrument is operated primarily by one of three groups: students in the chemical experimentation course, research students (graduate and undergraduate), and the analytical laboratory staff. Because of the complexity of the mass spectrometer and the 90-MHz nmr spectrometer, for example, it is impractical to train student operators, and these instruments are used only by analytical staff members.

Most of the apparatus in the lab, however, is available to students on a 24 hr/day basis after suitable instruction by the staff. In addition to providing special instruction on request, the staff is charged with keeping the equipment in operating condition and with enforcing good practices on the part of the student users. Instrument maintenance and repairs are done by the Chemistry Department's electronics shop. The work is supervised by an instrument engineer who also is available for consultation regarding instrument design and construction.

Another function of the analytical laboratory staff is to keep abreast of the latest developments in analytical methods and instrumentation, and each staff member is available to students and faculty for consultation relative to chemical analysis. The laboratory director makes recommendations regarding acquisition of equipment and prepares the NSF Research Equipment Grant Request.

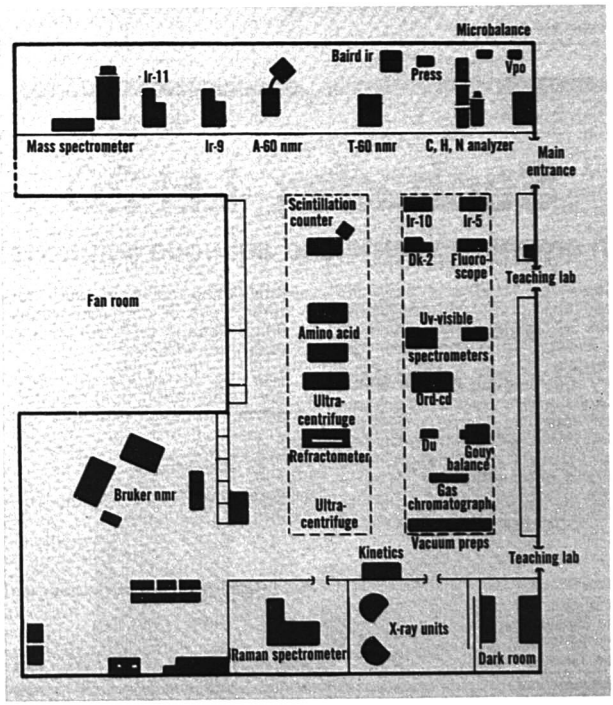
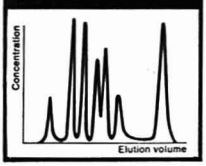


Figure 2. Analytical services laboratory

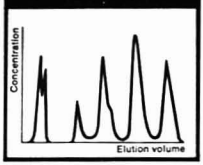
Sephadex®

Partition chromatography



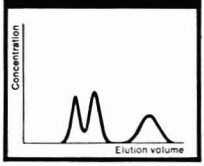
Separation of esterified catecholamine metabolites by partition chromatography in 1,2-dichloroethane: methanol (7:3).
(Ånggård, E., et al., Submitted to J. Chromatog. Reproduced by kind permission of the Authors and the Publisher.)

Gel filtration



Gel filtration of triglycerides and fatty acids in chloroform.
(Adapted from Downey, W.K., et al., J. Chromatog. 46 (1970) 120 - 124. Reproduced by kind permission of the Authors and the Publisher.)

Adsorption chromatography



Separation of oestrogens by adsorption chromatography in distilled water.
(Van Baelen, H., et al., J. Chromatog. 30 (1967) 226-227. Reproduced by kind permission of the Authors and the Publisher.)

Sephadex® LH-20

in organic solvents and aqueous solutions

Sephadex LH-20 is a lipophilic derivative prepared from Sephadex G-25 by hydroxypropylation. It is supplied in bead form (dry particle size 25 – 100 μ) as a dry, free-running powder which swells in water and polar organic solvents. The degree of swelling decreases with decreasing solvent polarity. Although introduced as a medium for gel filtration in organic solvents, Sephadex LH-20 has rapidly become established as a medium for other types of chromatography which depend on partition and adsorption effects.

Sephadex LH-20 is used in polymer fractionation, lipid and steroid separations, aliphatic and aromatic hydrocarbon separation as well as in a host of diverse applications.

Special solvent-resistant columns are available.

Pharmacia Fine Chemicals Inc.
800 Centennial Avenue
PISCATAWAY
New Jersey 08854

Pharmacia Fine Chemicals

Pharmacia (Canada) Ltd. 110 Place Crémazie, Suite 412, Montreal 11, P. Q.
(Inquiries outside U.S.A. and Canada should be directed to PHARMACIA FINE CHEMICALS, Uppsala, Sweden.)

Circle No. 132 on Readers' Service Card

Featured Laboratory

Each incoming graduate student learns about the analytical services as part of his orientation program. The incoming graduate class spends an afternoon in the analytical laboratory learning about the scope and limitations of each instrument and service available. They are instructed in the businesslike operation of the laboratory as well as in the technical factors to be considered in the selection of a particular piece of equipment for a specific measurement problem. For example, if it is decided that an nmr measurement is required, they learn they must choose one of three units which vary in resolution, temperature range, decoupling capability, cost to the user, and in other respects as well. During the orientation session, the student also is reminded of some of the essential factors in considering a particular analytical method, such as reliability, detection limit, sensitivity, and minimum sample size.

New Lab Advantages

The combination of a chemical experimentation teaching laboratory with an analytical services laboratory has advantages for both graduate and undergraduate instruction. For research students, there is the obvious advantage of equal opportunity to use whatever equipment is necessary to solve their particular current problems, including apparatus normally used for the laboratory practices course. Students as well as faculty members and postdoctoral fellows also may use the consulting services of the analytical staff. A number of departments in the University, including astronomy, chemical engineering, civil engineering (environmental sciences), geology, and the medical school, have made use of these services.

The undergraduate has the advantages of ready access to quality research apparatus and exposure to a wide array of methods and equipment. Because about half of the advanced lab experiments are carried out in the analytical lab, the student has almost daily contact with the analytical staff for two quarters and gets a first-hand view of a professionally run analytical laboratory. He also has the opportunity to hear the attitudes of industrially experienced chemists. In short, the analytical lab provides a link with the real world, and the student can see both the preaching and practice of analytical chemistry, side by side.

Reference

(1) F. E. Stafford, D. E. Smith, U. Hofacker, and D. D. DeFord, *J. Chem. Ed.* 44, 162 (1967).

Perkin-Elmer's Model 403 Atomic Absorption Spectrophotometer: A rare blend of workhorse and racehorse.

We questioned a cross-section of users of the Perkin-Elmer Model 403 Atomic Absorption Spectrc-photometer.

"What," we asked them, "do you like about your Model 403 (if anything)?"

The answer was almost unanimous.

"Convenience!" they said. "Speed and ease of operation. The ability to get dependable answers with a minimum of fuss."

How It Starts: Indeed, there's not much to running a 403. You turn the instrument on, and drop in a lamp in its prefocused mount. The lamp current sets itself. The 403 is double-beam, so there's no waiting for warm-up. You press the IGNITE button; the gases start to flow at the proper rates, and the burner ignites itself. You dip the burner capillary into your blank solution and press AUTO-ZERO; seconds later the digits read 0000 and your baseline is set. You aspirate the standard solution and turn a control until the digits read the number you want, and you're ready to go. Elapsed time: less than two minutes.

Operation: For routine work, you'll probably choose the 10-AVERAGE mode. Each reading on the digits is the average of ten individual integrated readings, computed in just over one second, direct in concentration. Precision is better than one percent. You can run a sample every five seconds, and record the answers on a printer-sequencer or on a Teletype-writer/punch tape in any desired format. If you don't use a print-out, you can take data as fast as you can write.

The instrument looks and feels solid. There's only one meter to watch, and if the needle's near the middle of a broad red band, you're OK. Little or nothing needs to be readjusted. You can see the flame clearly through the semi-transparent door, but you're protected from any glare or heat. There's a flame sensor and pressure switches. If the flame goes out or gas pressure drops, everything turns itself off.

Difficult Analyses: With the 403, you do difficult determinations so readily that you have to keep reminding yourself that they're difficult. Need better precision? You switch to the 100-AVERAGE mode, where each digital reading is the average of 100 individual samplings. This takes all of ten seconds per reading. Need to analyze a large range of concentrations? Go to your curve corrector, which straightens the curve with two adjustments, each made only once. Do you have a concentrated sample, which gives unwanted background absorption? Switch on the Background Corrector, and make it go away.

Tricky Samples: Maybe your samples are corrosive. Use the new corrosion-resistant nebulizer, where all parts that touch the sample are made of inert plastic. You may want to use flame emission. Throw a switch, depress a button, and the best emission monochromator built into any instrument is at your service (two 64 mm^2 gratings, UV ruling density 2880 lines/mm, 0.3 A resolution). Need to scan? Set the built-in scan drive to any of four speeds, from 2 to 200 A/min.

Pushing Detection Limits: You may need to determine low levels. Use scale expansion. You can expand scale on the digits until one digit reads 0.0004 absorbance. You can get 0.01 absorbance full-scale on a 10-mv recorder (or 0.001 absorbance *full-scale* on a 1-mv recorder). That's 4000X expansion over the basic range of 0-4 absorbance. And it isn't just electronic one-upmanship. The double-beam stability of the 403 is so good that such expansion is actually useful.

Want to do still better? Wheel up one of two new sampling accessories, the Sampling Boat or the HGA-70 graphite furnace.

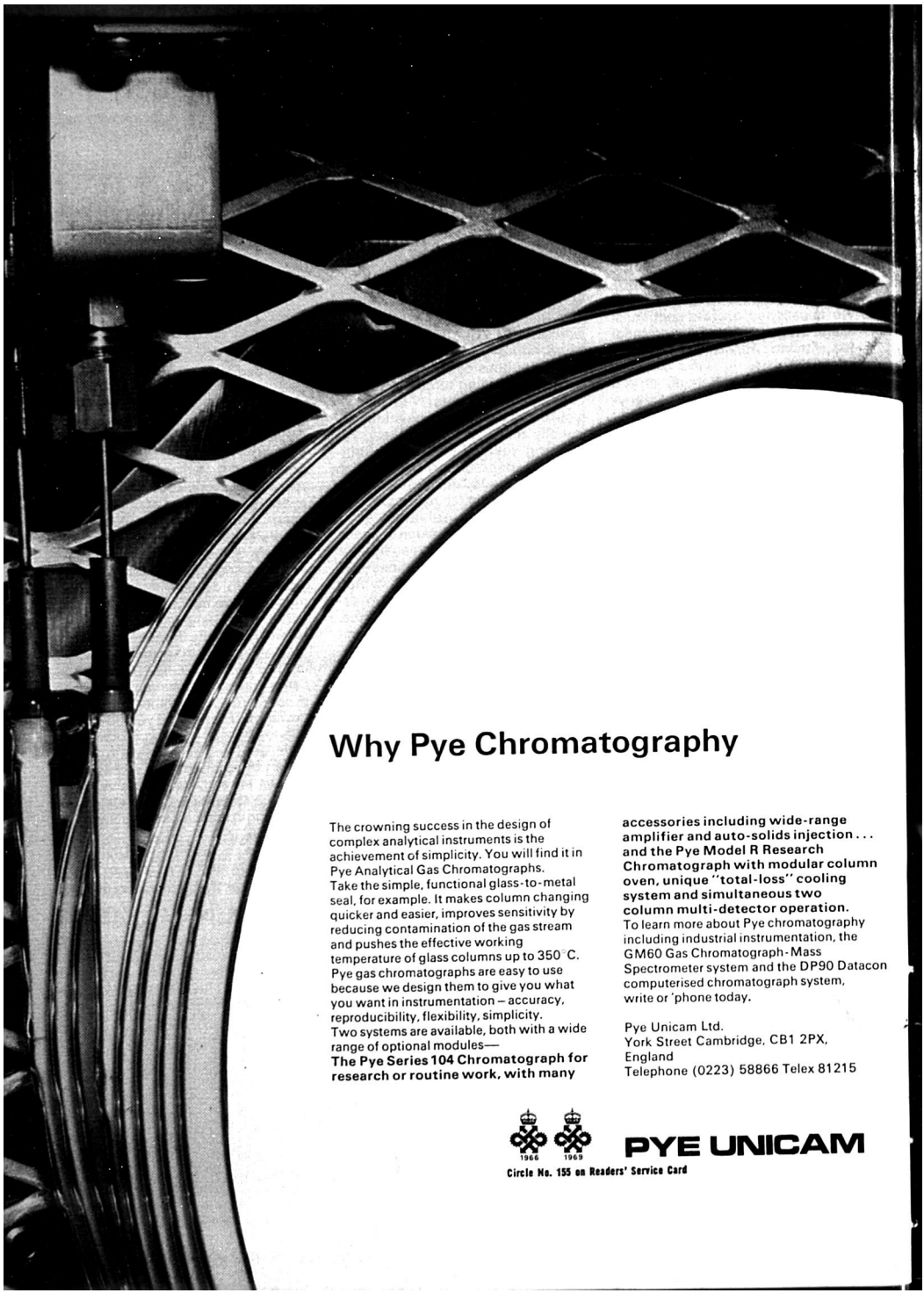
And Finally: When you're done, flip two switches. One turns off the flame gases automatically in the proper order. The other turns the power off. That's what you do if you already have a 403. If you don't yet have one, you may want to send to us for information. If you ask on your letterhead, we'll also send you a free adhesive-backed element wavelength table for absorption and emission.

Write to Instrument Division, Perkin-Elmer Corporation, 702 Main Avenue, Norwalk, Conn. 06852.

PERKIN-ELMER



Circle No. 139 on Readers' Service Card



Why Pye Chromatography

The crowning success in the design of complex analytical instruments is the achievement of simplicity. You will find it in Pye Analytical Gas Chromatographs. Take the simple, functional glass-to-metal seal, for example. It makes column changing quicker and easier, improves sensitivity by reducing contamination of the gas stream and pushes the effective working temperature of glass columns up to 350°C. Pye gas chromatographs are easy to use because we design them to give you what you want in instrumentation – accuracy, reproducibility, flexibility, simplicity. Two systems are available, both with a wide range of optional modules—

The Pye Series 104 Chromatograph for research or routine work, with many accessories including wide-range amplifier and auto-solids injection . . . and the Pye Model R Research Chromatograph with modular column oven, unique "total-loss" cooling system and simultaneous two column multi-detector operation.

To learn more about Pye chromatography including industrial instrumentation, the GM60 Gas Chromatograph-Mass Spectrometer system and the DP90 Datacon computerised chromatograph system, write or 'phone today.

Pye Unicam Ltd.
York Street Cambridge, CB1 2PX,
England
Telephone (0223) 58866 Telex 81215

1966 1969

PYE UNICAM

Circle No. 155 on Readers' Service Card

Even more versatile: Sargent's new Model XVI Recording Polarograph®

Our new Model XVI Polarograph is a strip chart recording instrument suitable for both research and routine analytical applications. Designed to take advantage of recent developments in the technique of D.C. polarography, it provides facilities for recording the derivative polarogram with or without damping and for compensating the residual current to provide materially improved step definition at low concentrations.

For maximum flexibility in experimental conditions, there are 22 current sensitivities ranging through 3 decades from 0.001 to 1.00 μa/mm; 11 fixed ranges of polarizing voltage, 1, 2, or 3 volts in span; 3 scanning rates; 3 chart speeds; 3 degrees of RC damping; and a total zero displacement range of 11X full scale.

We've priced the Model XVI at $1800.00. That includes electrolysis vessels, electrodes, capillaries, mercury reservoir, chart paper, pens, tubing, connecting cable—everything you'll need.

For complete specifications or a demonstration of this instrument, please call your Sargent man or write directly to us. 7-232 REV-2

Polarograph is a registered trademark of Sargent-Welch Scientific Company



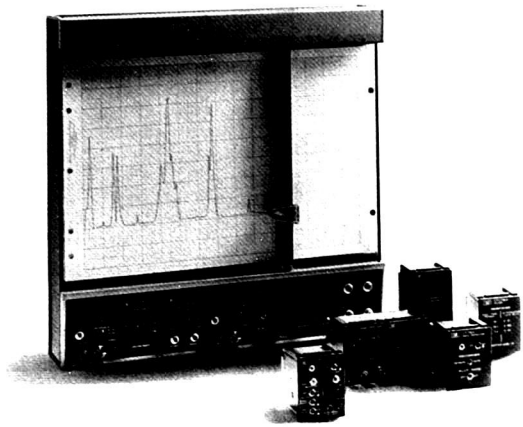
SARGENT-WELCH

Scientific instruments, apparatus, chemicals.
Sargent-Welch Scientific Company
7300 N. Linder Ave.; Skokie, Illinois 60076

Chicago/Anaheim/Birmingham/Cincinnati
Cleveland/Dallas/Denver/Detroit
Springfield, N.J./Toronto/Montreal/Vancouver

Circle No. 166 on Readers' Service Card

You can load up on X-Y recorders.



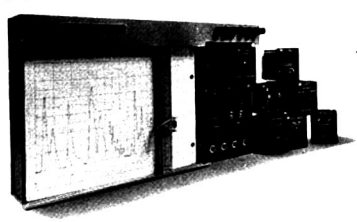
Or get an X-Y recorder you load up.

The world's first plug-in X-Y recorders let you buy modules, not mainframes, when you want to change applications. So you can order a single workhorse instrument to handle any application you have in mind. With the best dynamic performance on the market.

There are eight plug-ins for Hewlett-Packard's 7034A and 7004B X-Y's. You can use two plug-ins per axis. Besides taking care of all the routine tasks, they'll let you plot X-T, Y-T, single channel and discrete analog data. Extract signals superimposed on steady-state DC. Record AC from 5 Hz to 100 kHz. Plot two channels independently. And handle high-speed point plotting, too. You can specify the capability you want now and add to it later.

Dynamic performance is state-of-the-art. There's acceleration of better than 1500 in/sec^2 and slewing speed of 30 in/sec to catch all the transients that most recorders miss. Guarded circuits eliminate the effects of common mode voltages, and IC construction keeps your recorder running perfectly day after day. Autogrip electrostatic paper holddown and mess-free disposable ink pens are standard.

The 8½" x 11" 7034A costs just $1295 and the 11" x 17" 7004B is only $100 more. Modules start at $25. To lighten your load in X-Y recording, call your local HP field engineer. Or write to Hewlett-Packard, Palo Alto, California 94304; Europe: 1217 Meyrin-Geneva, Switzerland.



HEWLETT hp PACKARD

GRAPHIC RECORDERS

11904

Circle No. 82 on Readers' Service Card



Most automatic recording titrators aren't. Beckman's is.

The Beckman Automatic Recording Titrator is *truly* automatic... designed to give you maximum ease of operation, precision, repeatability, versatility. Consider these exclusive Beckman features:

All-electronic automatic mode. You can run completely unknown titration curves without adjustment and without overshoot. Slows automatically as the endpoint nears.

Combination mode. The titrator races to a preset critical point and slows to a preset speed while passing through the endpoint. Extremely precise titrations in only 40 to 60 seconds.

Automatic refill. Completely eliminates mechanical buret stopcocks.

Digital display of titrant added. Fast, simplified reading eliminates operator error.

Widest range. Full, calibrated, 0-14 pH range with expansion scales of 1.4, 2.8, 7 and 14 pH (140, 280, 700 and 1400 mv).

Maximum economy. Buy only what you need, single or double column models. Second column can be added when required. Price: $3200, single column model; $3460, double column model.

Write for Data File 25, Scientific Instruments Division, Beckman Instruments, Inc., 2500 Harbor Boulevard, Fullerton, California 92634.

Now Beckman offers a low-cost Endpoint Titrator System for industrial quality control applications. Ask about it.

Beckman INSTRUMENTS, INC.

HELPING SCIENCE AND INDUSTRY IMPROVE THE QUALITY OF LIFE.

INTERNATIONAL SUBSIDIARIES: AMSTERDAM; CAPE TOWN; GENEVA; GLENROTHES, SCOTLAND; LONDON; MEXICO CITY; MUNICH; PARIS; STOCKHOLM; TOKYO; VIENNA

Circle No. 25 on Readers' Service Card

The Nester/Faust 1240 introduces a new concept in high speed analytical liquid chromatography . . . a complete and self-contained precision instrument with features and capabilities that, until now, were only available on more complex and more costly units. To make our point, let's look at the 1240's outstanding features, one by one. First, easy operation and reproducible analyses are due, principally, to an adjustable 1,000 psi pump, with continuous degassing of solvent, and a zero dead-volume, zero back pressure pulse damper. Second, for gradient elution analysis, there's a precision gradient former available. Third, separation is enhanced by a standard, ambient to 125°C forced air oven with nitrogen purge. Fourth, fountain effect is eliminated by the zero dead-volume on-column septum injector. Fifth, we assure highest resolution by designing and manufacturing all our own columns and fittings. Sixth, the 1240 unit is supplied with a 2000 psi, 12 ul U.V. detector, with internal calibration. Ultimate detector sensitivity is 0.0002 O.D. units. In addition, a complete line of column packings is available. All of these features, plus more that we don't have room to discuss here, add up to some of the reasons why the 1240 is a unique analytical L.C. base priced at $4,900 . . . but don't let the price fool you, we haven't sacrificed quality anywhere in this instrument. For more information about the 1240 and its optional accessories, write or call today. NESTER/FAUST MFG. CORP., Instrument Products Division, 2401 Ogletown Road, Newark, Delaware 19711, (302) 737-6330. In Europe, contact: Steinengraben 44, 4000 Basel, Switzerland.

High speed...self contained...easy to operate high resolution...zero dead volume...and more



Circle No. 137 on Readers' Service Card

New Members Appointed to ANALYTICAL CHEMISTRY's Advisory Board

WASHINGTON, D. C. The rotation policy followed for the Advisory Board of ANALYTICAL CHEMISTRY brings five new members to the 15-member board. The new members are: C. G. Enke, Michigan State University; William C. Purdy, University of Maryland; Eugene M. Sallee, Procter and Gamble Co.; Donald T. Sawyer, University of California, Riverside; and Lloyd R. Snyder, Union Oil Co. of California.

The retiring members who have served for three years are: Lyman C. Craig, The Rockefeller University; Marcel J. E. Golay, consultant for Perkin-Elmer Corp.; Joseph Jordan, Pennsylvania State University; Robert A. Osteryoung, Colorado State University; Robert L. Pecsok, University of California, Los Angeles.

The ten members who continue to serve on the board are: Norman G. Anderson, Oak Ridge National Laboratory; Klaus Biemann, Massachusetts Institute of Technology; James S. Fritz, Iowa State University; John Funkhouser, Arthur D. Little, Inc.; Walter E. Harris, University of Alberta, Canada; W. Wayne Meinke, National Bureau of Standards; A. Lee Smith, Dow Corning Corp.; Edwin P. Przybylowicz; Eastman Kodak Co.; Samuel M. Tuthill, Mallinckrodt Chemical Works; and J. D. Winefordner, University of Florida.

The editorial advisory board, established in the 1940's, is of great assistance to the editors. It meets formally once a year in Washington. This meeting plus special consultations sought by the editors and informal contacts at ACS and other meetings provide valuable suggestions on policy and publication programs. The board is also an important liaison between the editors and readers.

Brief biographical sketches of the new members appear below.

Christie G. Enke is associate professor of chemistry at Michigan State University. He is a native of Minneapolis, Minn. He obtained a B.S. degree from Principia College in 1955 and a Ph.D. in chemistry from the University of Illinois in 1959. At Illinois he worked with Prof. H. A. Laitinen. He was an instructor and assistant professor of chemistry at Princeton University from 1959 until 1966 when he joined the faculty at Michigan State University.

His research interests include electroanalytical chemistry, electrochemical kinetics, instrumentation, and the application of digital techniques and computers in the chemistry laboratory. He has published many papers in ANALYTICAL CHEMISTRY and other specialized technical journals.

Since 1957, he and H. V. Malmstadt (University of Illinois) have collaborated in the development and presentation of courses which will give scientists of all types a working knowledge of the electronics of instrumentation. In this endeavor they have published three books: "Electronics for Scientists," "Digital Electronics for Scientists," and "Computer Logic," and have designed equipment for instrumentation teaching and development. These texts and laboratory equipment form the basis for instrumentation courses in many college technical departments.

He was an Alfred P. Sloan Fellow from 1964 to 1969. He has served on several committees in the ACS and the Electrochemical Society and is currently chairman of the Theoretical Divison of the Electrochemical Society. He is also a member of the AAAS, Phi Lambda Upsilon, and Sigma Xi.

Dr. Enke is the author of our Instrumentation article this month; see page 69 A.

William C. Purdy is professor and head of the Analytical Division of the Department of Chemistry at the University of Maryland. Dr. Purdy was born in Brooklyn. He earned his B.A. at Amherst College in 1951 and his Ph.D. degree at the Massachusetts Institute of Technology in 1955. After serving as an instructor in analytical chemistry at the University of Connecticut from



CHRISTIE G. ENKE



WILLIAM C. PURDY



EUGENE M. SALLEE



DONALD T. SAWYER



LLOYD R. SNYDER

1955 to 1958, he joined the University of Maryland. He became a full professor in 1964 and head of the Analytical Chemistry Division in 1968.

Dr. Purdy's research interests include the application of electroanalytical techniques to biological and clinical systems, coulometric titrations, organic polarography, atomic absorption spectroscopy, separation phenomena, electrode studies in aqueous and nonaqueous media, complexes of the transition elements, and digestion procedures for organic and biological samples. Professor Purdy has directed the research work of 12 candidates for the Ph.D. degree and 15 candidates for the M.S. degree. Currently he has 11 students working for advanced degrees under his direction.

He is author or coauthor of over 80 publications. He has been active in the ACS and is a member of the National Research Council–National Academy of Sciences Committee on Analytical Chemistry. He is also a member of the American Association of Clinical Chemists, the Society for Analytical Chemistry (London), Sigma Xi, the Polarographic Society (London), and the Western Electroanalytical and Theoretical Society.

Eugene M. Sallee is head of the Analytical Research Section in Product Development for the Procter and Gamble Co. He received a B.Ed. from Western Illinois State University in 1940 and a Ph.D. degree in analytical chemistry from Iowa State University in 1948. His technical interests are in the analysis of fats, oils, and detergents. He has been active in committee work for the American Oil Chemists' Society and has served as editor of *Standard Methods* for that organization since 1958. Currently he is a member of the Committee on Fats and Oils, Division of Chemistry and Chemical Technology, IUPAC. Dr. Sallee is coauthor of an undergraduate textbook, "Quantitative Chemistry."

Donald T. Sawyer received his B.S. degree in 1953 and his Ph.D. in 1956, both from UCLA in the field of chemistry. From 1956 until the present he has been a faculty member in the Department of Chemistry at the University of California, Riverside. He served as chairman of the department from 1966 to 1970. Currently he is dean of the College of Physical Sciences. During 1962–63 he was awarded a John S. Guggenheim Fellowship for the study of gas chromatography at the Cambridge University, England. He was appointed Visiting Research Fellow at Merton College, Oxford, England, for the winter and spring quarters of 1970.

Dr. Sawyer is the author of approximately 85 research publications in the areas of electroanalytical chemistry, physical chemical studies of metal chelates, electrochemistry of dissolved gases, and gas chromatography. He is also the coauthor of two books, "Quantitative Analysis," and "Experiments for Instrumental Methods," and is a member of the ACS, AAAS, and Sigma Xi. He is Chairman of the 1971 Gordon Research Conference on Analytical Chemistry.

Lloyd R. Snyder is a senior research associate at the Union Research Center of the Union Oil Co. of California, Brea, Calif. He received his B.S. in 1952 and his Ph.D. in 1954 from the University of California at Berkeley. His major research interests include organic analysis, the molecular composition of petroleum, solution and adsorption thermodynamics, and all aspects of modern liquid chromatography. He has published extensively in these areas, including the book "Principles of Adsorption Chromatography." Dr. Snyder is on the editorial boards of the *Journal of Chromatography* and the *Journal of Chromatographic Science*, and is on the advisory committee to API Research Project 60. He is active in the local section activities of the ACS, currently serving as chairman of the Orange County Section. He is the 1970 recipient of the ACS Award in Petroleum Chemistry.

Scheduled Courses in Analytical Techniques

Information is given in the following order: date, name of course, location of course, professional person(s) in charge of course, and/or sponsoring organizations, and Contact (numbers in parentheses refer to addresses and telephone numbers given at the bottom of the list of scheduled courses).

Jan. 18 to 22—Gas Chromatography. Philadelphia, Pa. Sadtler Research. *Contact (1)*

Jan. 18 to 22—Metallographic Interpretation. Holiday Inn, Dallas, Tex. Metals Engineering Institute. *Contact (2)*

Jan. 19 to 21—Introduction to the Measurement and Control of Electronic Noise. Hilton Inn, San Francisco, Calif. Center for Professional Advancement. *Contact (3)*

Jan. 20 to 22—Basic Gas Chromatography. Millbrae, Calif. *Contact:* Willard Wilson, Varian Aerograph, 1025 Shary Cir., Concord, Calif.

Jan. 21 to 22—Color Technology. Boston, Mass. Diano Corp. *Contact (4)*

Jan. 21 to 23—Fluorescence and Phosphorescence Spectrometry. Philadelphia, Pa. G. G. Guilbault. ACS. *Contact (5)*

Jan. 25 to 26—Instant Thin Layer Chromatography. The Riviera of Atlanta Motor Hotel, Atlanta, Ga. Gelman Instrument. *Contact (6)*

Jan. 25 to 27—Three One-Day Nmr Workshops. Springfield, N. J. Varian. *Contact:* Varian, Analytical Instrument Division, 611 Hansen Way, Palo Alto, Calif. 94303

Jan. 25 to 28— Fractional Distillation. Holiday Inn, Rt. 22, N. J. Center for Professional Advancement. *Contact (3)*

Jan. 25 to 29—Unified Approach to the Engineering of Measuring Systems. Arizona State University. *Contact:* Peter K. Stein, Engineering Center, Arizona State University, Tempe, Ariz. 85281. 602-965-3124

Jan. 25 to 29—Color and Behavior of Colorants. Macbeth Color Photometry Group Research Laboratories, Newburgh, N. Y. *Contact:* Mrs. Sandra Kovacs, Kollmorgen Color Systems Div., Tatamy, Pa. 18085. 215-258-2391

Jan. 25 to 29—Two Separate Courses: Infrared, Part I; Thin Layer Chromatography. Philadelphia, Pa. Sadtler Research. *Contact (1)*

Jan. 26 to 29—Infrared Spectroscopy. Norwalk, Conn. *Contact:* J. L. Bernard, Customer Training Dept., Mail Station 104, Perkin-Elmer Corp., Norwalk, Conn. 06852. 203-762-1000

Jan. 27 to 29—Adsorption and Ion Exchange. O'Hare Inn, Chicago, Ill. Center for Professional Advancement. *Contact (3)*

Jan. 28 to 29—Fourth Annual Particle Characteristics Course. Near New Jersey Airport. Keith Marshall. *Contact:* Shepard Kinsmon, Industrial Applications, Coulter Electronics, 590 W. 20th St., Hialeah, Fla. 33010. 305-887-8131

Jan. 28 to 29—Instant Thin Layer Chromatography. Howard Johnson Motor Lodge. New Orleans, La. Gelman Instrument. *Contact (6)*

Feb. 1 to 3—The Use of Operational Amplifiers in Instrumentation. Oakland, Calif. McKee-Pedersen. *Contact:* Richard G. McKee, McKee-Pedersen Instruments, P. O. Box 322, Danville, Calif. 94526. 415-937-3630

Feb. 2 to 5—Ninth Annual Introductory Course on Gas Chromatography. Chicago, Ill. *Contact:* N. Armstrong, Chicago Gc Discussion Group, 205 Milton St., Hoffman Estates, Ill. 60172

Feb. 6—Column Selection in Gas Chromatography. Baltimore, Md. H. M. McNair, W. R. Supina. ACS. *Contact (5)*

Feb. 8 to 10—Instrumental Methods. Philadelphia, Pa. Sadtler Research. *Contact (1)*

Feb. 8 to 11—Infrared Spectroscopy. Norwalk, Conn. *Contact:* J. L. Bernard, Customer Training Dept., Mail Station 104, Perkin-Elmer Corp., Norwalk, Conn. 06852. 203-762-1000

Feb. 8 to 12—Mass Spectrometry. Casa Ybel Resort, Sanibel Island, Fla. Fred McLafferty. *Contact:* Institute for Scientific Studies, P. O. Box 284, New Paltz, N. Y. 12561. 914-255-6532

Feb. 15 to 16—Color Technology. Edison, N. J. Diano Corp. *Contact (4)*

Feb. 15 to 19—Air Pollution Instrumentation. Philadelphia, Pa. Sadtler Research. *Contact (1)*

Feb. 17 to 19—Basic Gas Chromatography. Houston, Tex. *Contact:* Don Brasseaux, Varian Aerograph, Suite 180, 3939 Hillcroft Ave., Houston, Tex. 77027

Feb. 18 to 20—Computers in Analytical Laboratories. Washington University, St. Louis, Mo. *Contact:* Box 1048, Washington University, St. Louis, Mo. 63130. 314-863-0100 ext. 4779

Feb. 22 to 24—Techniques of Infrared Spectroscopy. Philadelphia, Pa. Sadtler Research. *Contact (1)*

Feb. 22 to 26—Infrared, Part II. Philadelphia, Pa. Sadtler Research. *Contact (1)*

Feb. 27 to 28—Interfacing the Minicomputer. Cleveland, Ohio. R. E. Dessy, D. G. Larsen. ACS. *Contact (5)*

Feb. 27 to 28—Gc/Ms/Computer Techniques. Cleveland, Ohio. F. W. Karasek, W. H. McFadden, W. E. Reynolds. ACS. *Contact (5)*

Mar. 1 to 2—Color Technology. Chicago, Ill. Diano Corp. *Contact (5)*

Mar. 2—Quantitative Thin Layer Chromatography. Cleveland, Ohio. Roy W. Yost. *Contact:* Nester/Faust Mfg. Corp., Box 565, Newark, Del. 19711

Mar. 5—Advanced Infrared Techniques Clinic. Cleveland, Ohio. Coblentz Society. *Contact:* R. W. Hannah, Secretary, The Coblentz Society, Perkin-Elmer Corp., 761 Main St., Norwalk, Conn. 06852

Mar. 8 to 9—Color Technology. Detroit, Mich. Diano Corp. *Contact (4)*

Mar. 8 to 12—Metallographic Interpretation. Los Angeles, Calif. Metals Engineering Institute. *Contact (2)*

Mar. 8 to 12—Two Separate Courses: Gas Chromatography; Infrared, Part I. Philadelphia, Pa. Sadtler Research. *Contact (1)*

Mar. 11 to 12—Color Technology. Pittsburgh, Pa. Diano Corp. *Contact (4)*

(1) Sadtler Educational Div., Sadtler Research Laboratories, Inc., 3316 Spring Garden St., Philadelphia, Pa. 19104. 215-382-7800
(2) William M. Mueller, Director of Education, ASM, Metals Park, Ohio 44073. 216-338-5151
(3) The Center for Professional Advancement, P. O. Box 997, 29 Division St., Somerville, N. J. 08876. 201-722-8111
(4) Diano Corp., P. O. Box 231, 132 Central St., Foxboro, Mass. 02035. 617-543-5383
(5) Education Office, American Chemical Society, 1155 16th St., N.W., Washington, D. C. 20036. 202-737-3337, ext. 258
(6) Scott Himes, Gelman Instrument Co., 600 S. Wagner Rd., Ann Arbor, Mich. 48106. 313-665-0651

The Plenary Session at the Eastern Analytical Symposium, Nov. 18 to 20, New York City, included the following persons (left to right) B. Karger, Chairman, Northeastern University; R. Belcher, University of Birmingham; D. Green, General Chairman, Western Electric Co.; W. Simon, Laboratory for Organic Chemistry, Zurich, Switzerland; and P. W. J. M. Boumans, Philips Research Laboratories, Eindhoven, The Netherlands





John R. Ferraro of Argonne National Laboratory (left) is shown accepting the New York Section Society for Applied Spectroscopy Award from Elias Todd. The award was presented Nov. 18 at the Eastern Analytical Symposium in New York City

John R. Ferraro Receives Annual Award of the SAS, New York Section

Dr. John Ferraro of Argonne National Laboratory and editor of the *Journal of Applied Spectroscopy* received the New York Section Award of the Society for Applied Spectroscopy in New York at the Eastern Analytical Symposium, Nov. 18. In his acceptance remarks, Dr. Ferraro made an impassioned plea for societies acting in concert and individuals in cooperation to use whatever influence and means possible to convey to the nation the seriousness of the unemployment among scientists. What is especially to be deplored is the tendency to release employees in their 40's or 50's, who on reentering the job market find themselves unemployable in their own fields. Dr. Ferraro claims the loss to the country is immeasurable and calls on all professional societies to act in support of their own memberships.

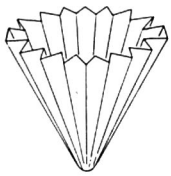
Electronics Division Symposia of The Electrochemical Society

The Electronics Division of the Electrochemical Society is planning the following symposia for the Spring Meeting, May 9 to 14, 1971, at the Sheraton-Park Hotel, Washington, D. C.

Semiconductor General Symposium (materials, processing, dielectrics, metallization)—Chairman: I. A. Lesk, Motorola Semiconductor, Phoenix, Ariz.

Luminescence General Symposium—Chairman: P. M. Jaffe, Zenith Radio R&D, Chicago, Ill.

"Tear-Proof" folded filter papers



S&S folded filter papers have exceptional high wet-strength. Their advantage is a faster flow rate than conventional filters. They are also highly resistant to corrosive solutions and organic solvents. Available in sizes from 12.5 up to 32 cm. They come in six different groups:

NO. 477½ RAPID. CREPED. Suitable for aqueous, alcoholic and oily liquids, pharmaceuticals, beverages. Recommended grade for student use.

NO. 520B½ VERY RAPID. CREPED. THICK. Used in filtration of agar-agar and other culture media, gelatin, fruit juices and syrups. Suitable for coarse precipitates.

NO. 560 MODERATELY RAPID. A pure white folded filter for moderately fine precipitates such as blood sugar and BUN tests in clinical laboratories.

NO. 588 VERY RAPID. A pure white folded filter for coarse precipitates.

NO. 605 DENSE. For very fine precipitates. Suitable for sugar solutions treated with lead acetate, for superphosphates, filtering Dakin's solution.

NO. 606 RAPID, SMOOTH SURFACE. MEDIUM TEXTURE. Pure white filter paper, fairly retentive for filtering solutions which entail no particular difficulties. Recommended grade for student use.

For additional information use coupon below.

S&S **The first name in filtration**
SCHLEICHER & SCHUELL
(603) 352-3810

Schleicher & Schuell, Inc. AC171
Keene, New Hampshire 03431

Please send Bulletin #142 for price information on "Tear-Proof" Folded Filters.

Name_____

Address_____

City_____

State_____ Zip_____

Circle No. 165 on Readers' Service Card

CALENDAR OF EVENTS

Jan. 7 to 15	**ASTM Committee E-10 on Radioisotopes and Radiation Effects and Committee E-7 on Nondestructive Testing.** Ft. Lauderdale, Fla. *Contact:* American Society for Testing and Materials, 1916 Race St., Philadelphia, Pa. 19103. 215-569-4200
Jan. 13 to 16	**ASTM Committee E-15 on Analysis and Testing of Industrial Chemicals.** Atlanta, Ga. *Contact:* American Society for Testing and Materials, 1916 Race St., Philadelphia, Pa. 19103. 215-569-4200
Jan. 18 to 22	**Winter Gordon Research Conference on Electrochemistry.** Miramar Hotel, Santa Barbara, Calif. *Contact:* Dr. Alexander M. Cruickshank, Pastore Chemical Laboratory, University of Rhode Island, Kingston, R. I. 02881. 401-783-4011. Page 71 A, Dec.
Jan. 21	**Joint Meeting American Microchemical Society and Analytical Group, New York Section, ACS.** Fordham University. Topic: What Have We Learned From the Apollo Missions? Dr. Raymond Davies, Brookhaven National Laboratory. *Contact:* Louis M. Brancone, Lederle Laboratories Div., American Cyanamid Co., Pearl River, N. Y. 10965. 914-735-5000, ext. 3443
Jan. 25 to 28	**Louisiana State University Symposium on Air Pollution.** Baton Rouge, La. Will include analytical chemistry. *Contact:* W. J. Robinson, College of Chemistry and Physics, Louisiana State University, Baton Rouge, La. 70803. Page 74 A, Nov.
Jan. 31	**7th Annual Mossbauer Methodology Symposium.** New York Hilton, New York, N. Y. *Contact:* Carl Seidel, Nuclides and Sources Div., New England Nuclear, 601 Treble Cove Rd., North Billerica, Mass. 01862. 617-462-7311. Page 71 A, Nov.

Infrared Excited Visible Luminescence—Chairman: R. Hewes, General Electric Lighting Research, Cleveland, Ohio

Plastics for Environmental Protection and Encapsulation of Electronic Devices—Joint Symposium (Dielectrics and Insulation and Electronics Div.)—Cochairmen: R. Olberg, Fairchild R&D, Palo Alto, Calif. and A. Pfahnl, Bell Labs, Allentown, Pa.

New Techniques for Materials Characterization—Joint Symposium (Electronics and Electrothermics and Metallurgy Div.)—Chairman: V. A. Phillips, General Electric R&D, Schenectady, N. Y.

Further information on these symposia is available from Bruce E. Deal, Fairchild R&D, 4001 Miranda Ave., Palo Alto, Calif. 94304. 415-321-7250.

Coming Events

Feb. 3 to 5—ACS 6th Middle Atlantic Regional Meeting. Baltimore, Md. *Contact:* Howard Cohen, SCM Corp., 3901 Hawkins Pt. Rd., Baltimore, Md. 21226

Feb. 15 to 16—13th Water Quality Conference. Urbana, Ill. *Contact:* V. L. Snoeyink 3230 Civil Engineering Bldg., University of Illinois, Urbana, Ill. 61801

Feb. 21 to 26—2nd International Congress of Pesticide Chemistry. Tel Aviv, Israel. IUPAC. Includes sessions on pesticide analysis. *Contact:* Organizing Committee, P. O. Box 16271, Tel Aviv, Israel

Feb. 23—Symposium on Source Sampling of Atmospheric Contaminants. The Inn on the Park, Toronto, Canada. Sponsor: Toronto Section, Chemical Institute of Canada. *Contact:* H. G. McAdie, Ontario Research Foundation, Sheridan Park, Ontario, Canada

Feb. 28 to Mar. 5—22nd Pittsburgh Conference on Analytical Chemistry and Applied Spectroscopy. Cleveland Convention Center, Cleveland, Ohio. *Contact:* William G. Fateley, Carnegie-Mellon University, 4400 Fifth Ave., Pittsburgh, Pa. 15213. Page 68 A, Sept.

Feb. 28 to Mar. 5—ASTM Committee Week. Sheraton Biltmore Hotel, Atlanta, Ga. *Contact:* American Society for Testing and Materials, 1916 Race St., Philadelphia, Pa. 19103. 215-569-4200

Mar. 9 to 13—Fifth International Exhibition of Industrial Electronics. Basel, Switzerland. Includes special group display for medical science. *Contact:* Sekretariat INEL71, CH-4000, Basel, Switzerland. Page 72 A, Nov.

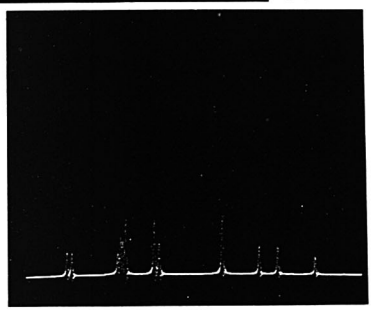
Mar. 11 to 12—Symposium on Advanced Analytical Concepts for the Clinical Laboratory. Oak Ridge, Tenn. *Contact:* Dr. Charles D. Scott, ORNL, P. O. Box X, Oak Ridge, Tenn. 37830. 615-483-8611, ext. 3-6265. Page 73 A, Nov.

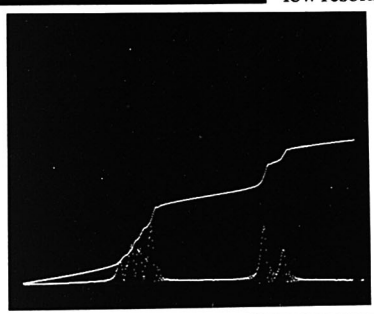
Mar. 16 to 17—Conference on Effectiveness of On-Line Biomedical Computing. International Hotel, Los Angeles. Includes session relating to clinical laboratories. *Contact:* M. J. Miller, AAMI, 9650 Rockville Pike, Bethesda, Md. 20014. 201-530-2800. Page 72 A, Dec.

The PDP-12 Laboratory Data Processor speaks your language.

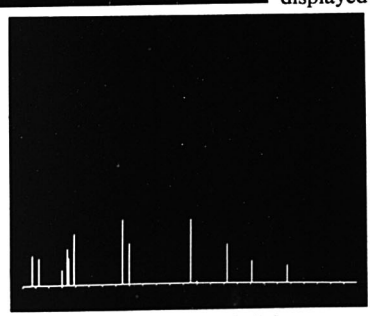
And speaks the language of your lab instruments, too. The PDP12/LDP will automate just about any instrument you've got, then interact with you to examine scope-displayed data.

It'll handle up to eight slow instruments simultaneously and independently; data is stored in raw form directly on the tape or disc for subsequent interactive reduction and analysis. High speed instruments are handled singly, often with some real-time data reduction before storage. Complete software systems are supplied for continuous wave and pulsed NMR, high and low resolution mass spectroscopy, and gas chromatography.





The PDP12/LDP is easy to use. A software system is provided that permits the unsophisticated user to manipulate data using problem-oriented English commands. The results of the operations – including peak stripping, integration, and X axis calibration – are displayed on a cathode ray tube as they are performed. Programs to create and automatically search spectrum libraries are part of the comprehensive software package.



Write for our new 320-page Laboratory Computer Handbook; it'll tell you all about the PDP12/LDP.

digital

Digital Equipment Corporation
Maynard, Mass. 01754 (617)897-5111

Circle No. 41 on Readers' Service Card

Mar. 28 to Apr. 2—161st National ACS Meeting. Los Angeles, Calif. Includes Analytical Chemistry Division sessions. *Contact:* J. C. White, Analytical Chemistry Div., ORNL, Oak Ridge, Tenn. 37830. 615-483-8611, ext. 3-1472

Mar. 30 to Apr. 3—The Chemical Society and Royal Institute of Chemistry Joint Annual Meeting. Brighton, England. *Contact:* John F. Gibson, The Chemical Society, Burlington House, London, W1V OBN, England

Apr. 12 to 17—Federation of American Societies for Experimental Biology. McCormick Place, Chicago, Ill. *Contact:* Steven K. Herlitz, Inc., 850 Third Ave., New York, N.Y. 10022. 212-421-6900

Apr. 14 to 16—National Pollution Control Conference & Exposition. Cobo Hall, Detroit, Mich. *Contact:* Bill Reeves, 1107 S. Loop West, Houston, Tex. 77021

Apr. 19 to 21—17th ISA Analysis Instrumentation Symposium. Marriott Motor Hotel, Houston, Tex. *Contact:* G. A. McNeill, Monsanto Co., 730 Worcester Ave., Springfield, Mass. 01107

Apr. 19 to 23—International Solvent Extraction Conference, SCI. The Hague, The Netherlands. *Contact:* ISEC '71, 14 Belgrave Square, London, W.W.I, England

Apr. 21 to 23—7th Annual Symposium on Vacuum Science. Albuquerque, N. M. *Contact:* D. G. Schreiner, P. O. Box 11451, Albuquerque, N. M. 87112

Apr. 26 to 30—17th Annual Meeting and Equipment Exposition of the Institute of Environmental Sciences. Biltmore Hotel, Los Angeles, Calif. Includes topics on data acquisition and reduction and instruments for environmental measurements. *Contact:* Institute of Environmental Sciences, 940 E. Northwest Hwy., Mt. Prospect, Ill. 60056. 312-255-1561. Page 74 A, Nov.

Apr. 27 to 29—Fourth Annual Scanning Electron Microscopy Symposium. Chicago, Ill. *Contact:* Dr. Om Johari, Metals Div., IIT Research Institute, 10 W. 35th St., Chicago, Ill. 60616. 312-225-9630, ext. 4843. Page 73 A, Nov.

The following meetings are newly listed in ANALYTICAL CHEMISTRY. Meetings previously listed through October 1971 appear in the Coming Events columns of the November and December 1970 issues.

Aug. 9 to 10—13th Annual Rocky Mountain Spectroscopy Conference. Albany Hotel, Denver, Colo. *Contact:* George M. Pachelo, Dow Chemical Co., Bldg. 559, P. O. Box 888, Golden, Colo. 80401

Aug. 16 to 19—8th Australian Spectroscopy Conference. Clayton, Victoria, Australia. *Contact:* J. E. Kent, Dept. of Chemistry, Monash University, Clayton, Victoria 3168, Australia

Oct. 4 to 7—26th Annual ISA Conference. McCormick Place, Chicago, Ill. *Contact:* G. I. Doering, Instrument Society of America, 400 Stanwix St., Pittsburgh, Pa. 15222. 412-281-3171

Industry Items

The Electronic Instruments Division of **Beckman Instruments, Inc.,** 2200 Wright Ave., Richmond, Calif. 94804, has announced a "total service" plan for electronic instruments, computers, computer peripherals, and data systems. Regional service centers have been established for the repair, calibration, and certification of equipment. Major details of the plan are included in a 4-page brochure available from the company.

Evans Electroselenium, Ltd., of Halstead, Essex, has added a comprehensive range of pH meters and electrodes to its extensive line of scientific instruments. The move is a direct result of the company's merger earlier this year with the **Corning Glass Works,** of Corning, U.S.A.

A new type of franchise for professional engineers has been announced by **New York Testing Laboratories, Inc.,** 81 Urban Ave., Westbury, L. I., N. Y. 11590. The laboratory is providing exclusive urban territories to professional engineers or engineering firms anxious to enter the expanding air pollution services and product liabilities field. Equipment, consultation, training, and complete laboratory backup are provided with the franchise arrangement.

Optoelectronics, Inc., of 1309 Dynamic St., Petaluma, Calif. 94952. 707-763-4181, has been appointed by **Mullard, Inc.,** Farmingdale, N.Y., as exclusive national sales representative and distributor for Mullard's full line of infrared detectors and associated electro-optical components.

Science Spectrum, P. O. Box 3003, Santa Barbara, Calif. 93105. 805-963-8605, is a new company formed to apply physics methods, especially light scattering techniques, to the study of structure and dynamics of microparticles. Particular attention is given to microbiology and the firm expects to be an active force in clinical laboratories with a line of automated instruments. Their first major new product is described on page 88 A, this issue.

A realignment of **Miles Laboratories, Inc.,** Elkhart, Ind. 46514 research structure combines the Therapeutics Research Division and the Research Products Division into a new division, Miles Research Division. The new division will operate internationally and research activities will be carried out in molecular biology, organic chemistry, pharmacology, toxicology, immunology, pharmacy, and clinical pharmacology. More than 2000 research chemicals, many available from no other source, are offered for sale to research laboratories. Included are synthetic polynucleotides, blood proteins, research enzymes, immunochemicals, and the stable isotopes of oxygen.

Expert speakers with information about renting, leasing, purchasing, and financing new and reconditioned laboratory equipment and computers are available from the new Telco/Labex Speakers Bureau. **Telco Marketing Services, Inc.,** the parent company, rents and leases new medical and scientific equipment and **Laboratory Instrument Exchange, Inc.** (Labex) buys and sells reconditioned lab equipment. Organizations interested in booking a speaker at no cost should write to Telco/Labex Speakers Bureau, 301 E. Erie St., Chicago, Ill. 60611

A new pollution abatement service involving the use of liquid sodium sulfide for the control of mercury poisoning in streams and estuarine systems has been announced by **The Merichem Co.,** 2727 Allen Pkwy., Houston, Tex. Merichem has the facilities and staff to research mercury and other heavy metal problems.

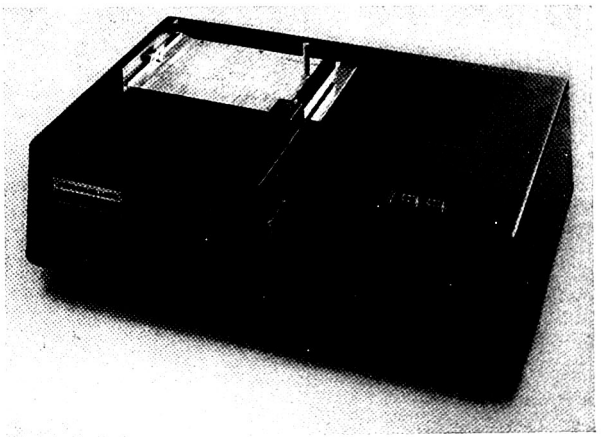
ChemTech Industries, Inc., Dallas-based environmental products and services company, has acquired **Allied Analytical and Research Laboratories.** The latter company will operate as a subsidiary of ChemTech; it has been involved in analyses of industrial plant environmental hazards and the implementation of quality control procedures. Services are provided in all fields of chemistry including air and water pollution studies.

Worthington Biochemical Corp., Freehold, N. J. 07728. 201-462-3838, producer of high-purity enzymes and biochemicals, announces a new service for biochemists. The firm will characterize proteins using advanced methods. Ultracentrifugation services include sedimentation velocity, conventional sedimentation equilibrium, and meniscus depletion sedimentation equilibrium. Amino acid analytical services include analysis of proteins and polypeptides, either intact or prehydrolyzed. Data produced are reduced for final interpretation by the company's electronic data processing equipment.

Adage, Inc., 1079 Commonwealth Ave., Boston, Mass. 02215, plans to expand its line of graphic terminal products by acquiring **Computer Displays, Inc.,** Waltham, Mass. CDI makes the ARDS graphics display terminal, which is complementary to Adage's line of computer terminal systems.

Here's Perkin-Elmer's new Model 710 Infrared Spectrophotometer.

It's a Super 700.

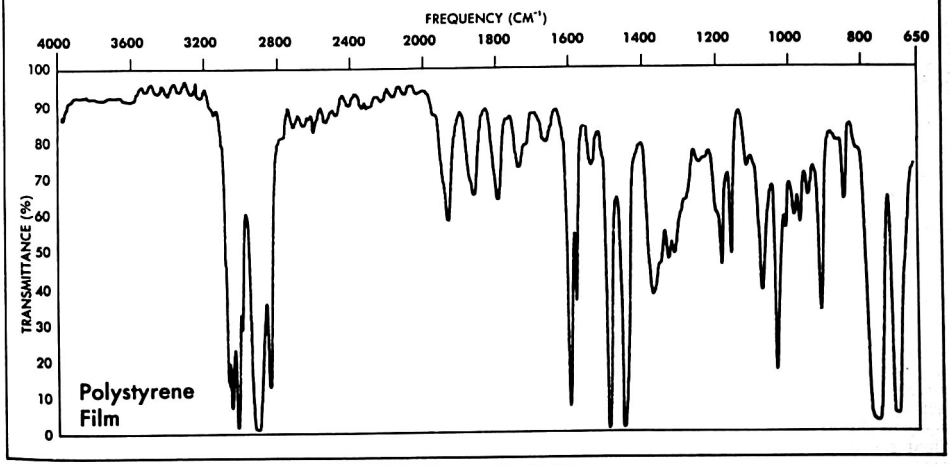


The spectrum below shows the difference.

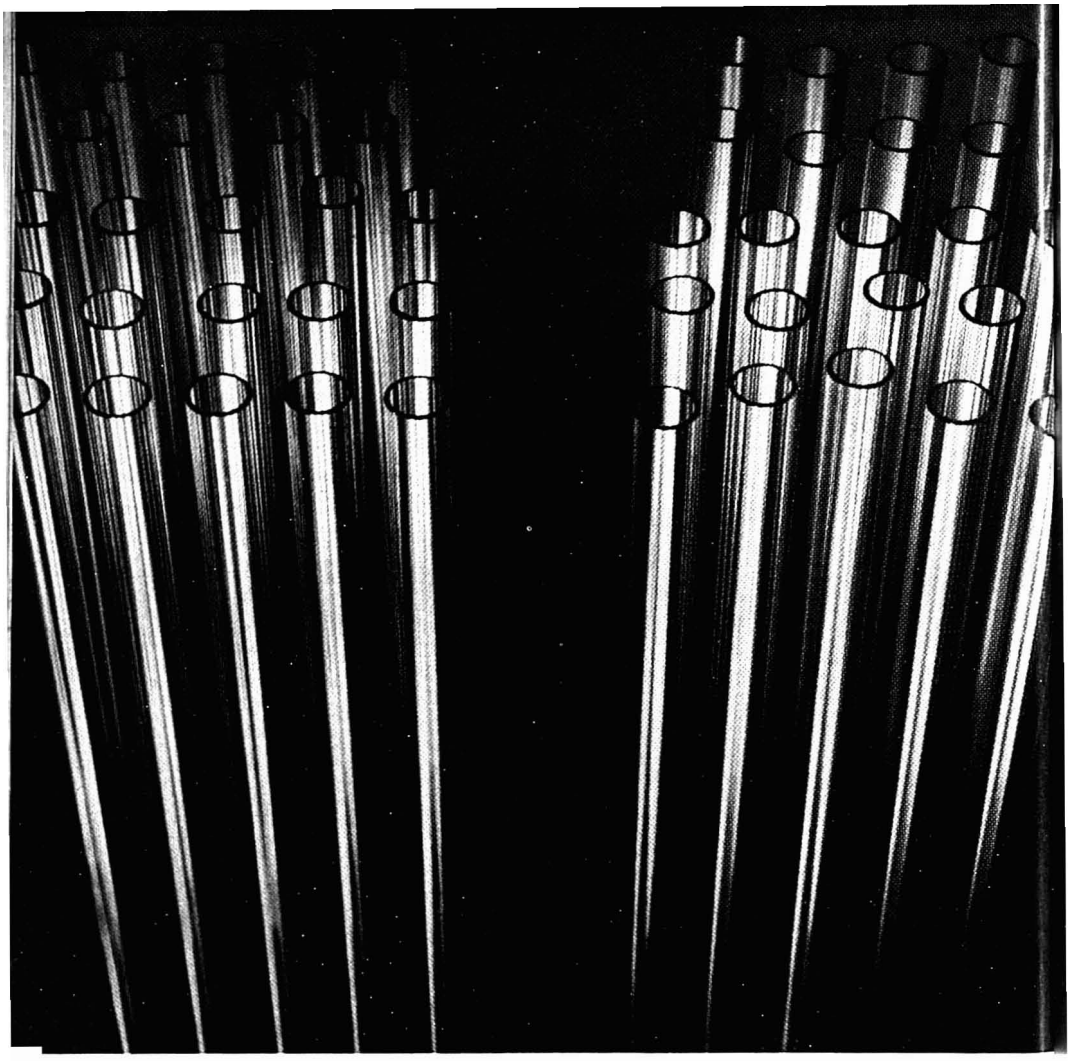
Resolution at 3000 cm^{-1} is now better than 10 cm^{-1}. Resolution at 1000 cm^{-1} is better than 5 cm^{-1}. In other respects, the Model 710 is the same proven 700 you see everywhere in colleges and universities, in industrial research and control laboratories. Same push-button simplicity, compactness and reliability. Same choice of scan speeds. Same unbroken chart presentation, linear frequency recording from 4000-650 cm^{-1} (2.5 to 15.4 microns).

Now, get the Model 710 at $3,150.00 or the Model 700 at $2,760.00. You get outstanding performance both ways. Write for our new brochure. Instrument Division, Perkin-Elmer Corporation, 702 Main Avenue, Norwalk, Conn. 06852.

PERKIN-ELMER



Circle No. 141 on Readers' Service Card



Which NMR tubes are the "best"?

In the precise world of NMR tubes, "best" can be a tricky word. One tube looks just like another. But only the ones with precise, *consistent* tolerances give you the kind of accuracy you need.

Kontes is manufacturing such tubes.

To assure you of the kind of dependability you've come to expect from Kontes, each and every tube is checked for camber and wall variation on an ultra-precision gage specially designed to eliminate human error.

As a result, the variations in your readings will reflect sample differences rather than tube inconsistencies.

Added to this unmatched consistency is competitive pricing and quick delivery from one of our warehouses in New Jersey, Illinois or California.

Which NMR tubes are best? We invite you to compare. Your Kontes salesman will be pleased to give you the details.

Or, write directly for our NMR Bulletin which contains complete data on our growing line of disposables, microcells, precision and ultra-precision tubes and accessories. (The Kontes line more than satisfies the requirements of any NMR system.)

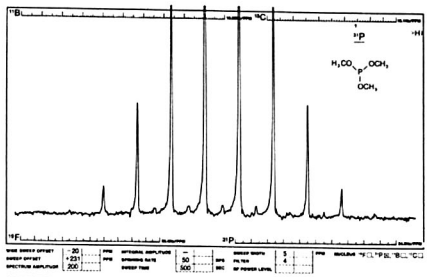
In the meantime, our plant will be turning out the best tube after tube after tube after tube . . .

KONTES
Vineland, N.J. 08360

Regional Distributors: **KONTES OF ILLINOIS,** Evanston, Illinois • **KONTES OF CALIFORNIA,** Berkeley, California

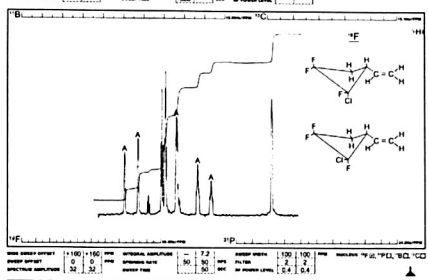
Circle No. 104 on Readers' Service Card

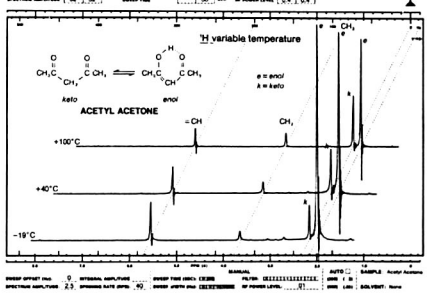
The NMR system that produced all the spectra on this page costs less than $40,000.



^{31}P NMR can be used to analyze pesticides and other phosphorus-containing chemicals such as trimethylphosphite (spectrum shown).

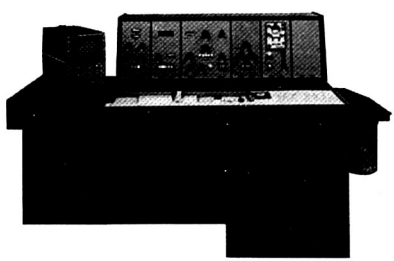
^{19}F NMR analysis is applicable to isomeric mixtures such as shown in this spectrum of 1,1,2-trifluoro-2-chloro-3-vinylcyclobutane. Peaks marked A are of one of the two isomers.





^{1}H NMR analysis of acetyl acetone at −19°C, +40°C, and +100°C shows the temperature dependence of this keto/enol equilibrium.

The multi-nucleus, easy-to-use, under-$40,000, T-60 NMR spectrometer system. You get back a lot more than you put in.



varian
analytical instrument division

For details, or to arrange for a demonstration, write to Varian, Analytical Instrument Division, 611 Hansen Way, Palo Alto, California 94303

Circle No. 192 on Readers' Service Card

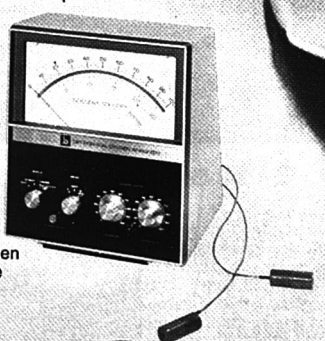
You've never had it so easy

Van Waters & Rogers/Will Scientific brings you the only oxygen analyzers that use convenient, low cost replacement O_2 cartridges with built-in membranes and electrolytes that you replace in seconds.

In addition to ending messy recharge procedures, IBC polarographic Oxygen Analyzers offer many other unprecedented ease and convenience features:

- Unique, built-in calibration reference that takes only seconds.
- Dual sensor models for differential oxygen measurement.
- Unconditionally safe—no external power sources, no possibility of ground loops.
- Complete portability for lab or field use—up to 12 months of continuous use with 4 "D" cells (and a built-in battery tester).
- Plus built-in temperature compensation, all solid-state circuitry, two scale ranges on each instrument: 0-25% and 0-100% oxygen.

Ask your Van Waters & Rogers/Will Scientific representative to give you the full story of the IBC Oxygen Analyzers with the incredible time-saving replacement O_2 cartridges.



VAN WATERS & ROGERS
WILL SCIENTIFIC
VWR UNITED

Serving The West: San Francisco • Albuquerque • Anchorage • Denver • El Paso • Honolulu • Los Angeles • Phoenix • Portland • Salt Lake City • San Diego • Seattle • Tucson • West Sacramento
Serving The East: Rochester • Ann Arbor • Atlanta • Baltimore • Boston • Buffalo • Columbus • New York City

Circle No. 188 on Readers' Service Card

BOOK REVIEWS

The Determination of Carboxylic Functional Groups. R. D. Tiwari and J. P. Sharma. vii + 132 pages. Pergamon Press, Inc., Maxwell House, Fairview Park, Elmsford, N. Y. 10523. 1970. $8

Reviewed by J. Gordon Hanna, The Connecticut Agricultural Experiment Station, New Haven, Conn.

An appropriate place for this succinct book is the immediate vicinity of the chemical laboratory bench where it can be used as a readily available, practical reference. The authors' stated intent is to present, without comprehensive theoretical detail, the key methods useful in general analytical work, specifically for carboxylic acids, acid anhydrides, acid chlorides, esters, and amides.

It is undoubtedly difficult in the preparation of a volume such as this for authors to be prudently selective and probably impossible for them to get unqualified agreement from readers that the best possible selection has been made. This reviewer's most serious disagreement concerns an omission, the failure of the authors to include any of the specific methods for amino acids, especially conspicuous because reference is made in the Introduction to the potential use of the book by workers in the field of natural products and biosynthesis. Otherwise, the authors essentially have attained their objective with this book when allowances are made for objections based on personal preferences of minor significance.

The text of the book is well-organized to help the working chemist select the appropriate approach for his specific situation. The first chapter is a short introduction to the material covered. Subsequent chapters deal separately with carboxylic acids and the derived functions. A final chapter is devoted to the description of methods for binary and ternary mixtures. Details are sufficient so that the general methods (in many cases including semimicro, micro, and submicro adaptations) can be followed directly without recourse to other sources. Literature references and sometimes brief outlines are given for some of the less general methods. Both chemical and physical methods are presented for each type of compound. The importance of separation techniques to the analytical chemist is recognized and adequate attention is given to this area.

A somewhat more expanded Index (or Table of Contents) would have made the book more convenient to use. For example, the reader will fail to find polyethylenic fatty acids and dibasic anhydrides listed in the limited index in spite of the presence of a fairly detailed method for each of these compounds in the text.

The shortcomings cited do not detract significantly from the overall value of the book. This slim monograph, used as a laboratory reference, should give full value for its price.

Multicomponent Chromatography: Theory of Interference. Friedrich Helfferich and Gerhard Klein. viii + 419 pages. Marcel Dekker, Inc., 95 Madison Ave., New York, N. Y. 10016. 1970. $24.50

Reviewed by E. Glueckauf, Atomic Enery Research Establishment, Harwell, England

While there are many text books dealing either entirely or predominantly with "linear chromatography," information on the subject of nonlinear multicomponent chromatography has to be gleaned from a multiplicity of individual research papers. This book therefore fills an important gap, by presenting this subject in a unified theory with a common nomenclature and a single-minded approach.

This subject is of particular importance for all column separations involving a high loading, such as is required in technical or semitechnical column operation. The book will be useful to the chemical engineer and physical chemist rather than to the analyst, though it does also aid the latter by providing a clearer picture of displacement development and of frontal analysis.

The authors have wisely refrained from overloading the text with mathematical equations, and provided, with scholarly precision, a continuous treatment in general terms, relegating lengthy mathematical proofs to the appendix. Yet in multicomponent systems the complexity of the phenomena is such that they can only be described fully in mathematical language, and the reader has to be prepared to do a fair amount of homework in digesting and interpreting the numerous diagrams and conceptual models.

Outstanding in the book are the discussion on the property of "coherence" —*i.e.*, the constant velocity in the column of several components in fixed sets of concentrations—and it is shown that, if "noncoherent" boundaries are provided by the starting conditions, the system will tend toward eventual attainment of "coherence" during subsequent chromatogram development.

Special attention is given to the so-called h-transformation which permits a simpler mathematical treatment in the cases of Langmuir isotherms and is useful where more than three components are involved.

The treatment shows clearly that there has been relatively little progress in this particular section of the chromatographic field during the last 20 years, and one may hope that it will act as a stimulus toward increased research, and in particular, toward the improved understanding of phenomena arising during separation of substances with more complicated forms of mutual interference than is given by multicomponent Langmuir isotherms. The discussion in Part 5 of systems with more involved mass action equilibria shows that while the principles are understood, the detailed evaluation is far from easy.

The book is very well written and can be thoroughly recommended.

An Introduction to Spectroscopic Methods for the Identification of Organic Compounds. Vol. I. Nuclear Magnetic Resonance and Infrared Spectroscopy. F. Scheinmann, Ed. ix + 201 pages. Pergamon Press, Inc., Maxwell House, Fairview Park, Elmsford, N. Y. 10523. 1970. $7

Reviewed by Robert M. Silverstein, College of Forestry at Syracuse University, Syracuse, N. Y. 13210

Since 1963, the teaching of the traditional "qualitative organic analysis" course in this country and abroad has undergone extensive changes by the introduction of spectrometric methods. These methods are widely taught as separate academic courses or are included in organic courses at various levels. Concurrent crash efforts in the form of "short courses" or summer institutes have been used extensively to "retread" teachers and practicing chemists.

A number of excellent texts have been published during the past seven years

BEL-ART
for PLASTIC
safety
products

This is one
of our
products
we hope
you never use...



EYE WASH SAFETY STATION

But...
YOU HAD
BETTER
HAVE IT
HANDY
JUST IN CASE!

See your local laboratory supply house.
Send for NEW 84 page catalog 970.
For your FREE copy write Dept. A-1

BEL-ART PRODUCTS
PEQUANNOCK, N. J. 07440

Circle No. 21 on Readers' Service Card

to implement these teaching activities. The present volume (Volume I) covering nmr and ir spectrometry and a projected volume covering mass, esr, and uv spectrometry grew out of summer institutes at Salford, England. They are a welcome addition to the list. The strong features of Volume I are the extensive correlation tables and a number of worked-out problems (11 for nmr and 14 for ir). The decisions to split the presentation into two volumes and to include the rather specialized esr technique seem unwise, considering the consequent cost increase.

The second volume will contain problems involving the combined use of the methods presented. In my experience, it is the complementary aspects of the spectral probes that make their use so effective and catch the students' interest. The emphasis on this complementarity and on a "Sherlock Holmes" approach to structure elucidation should come as early as possible, even at some initial sacrifice in expertise in an individual area.

The Destruction of Organic Matter. T. T. Gorsuch. viii + 151 pages. Pergamon Press, Inc., Maxwell House, Fairview Park, Elmsford, N. Y. 10523. 1970. $7.50

Reviewed by E. B. Sandell, University of Minnesota, Minneapolis, Minn. 55455

Now that the determination of trace elements in biomaterials is experiencing an upsurge, this monograph appears at an opportune time. It falls in that category of books whose authors have been able to draw on their own experience as well as on the contents of library shelves. The studies of Gorsuch on losses of trace elements in the destruction of organic matter, based on the use of radioactive nuclides, are well known. This method is examined. Accounts are given of wet oxidation, dry oxidation, oxidative fusion, and cognate methods, with comparison of their advantages and drawbacks.

More than half of the monograph deals with the behavior (recovery) of some 50 individual metals and metalloids, particularly at trace levels in the destruction of organic matter. The working analyst will be grateful for succinct directions for the more important decomposition procedures: digestion with nitric–sulfuric acid, perchloric acid mixtures and sulfuric acid–hydrogen peroxide, and by dry ashing.

This book is a valuable source of information, eclectic in approach, and compact in presentation.

Fresh
Pure
Water



Wall Mounting Bracket—
With Research Cartridge $24.95
With Universal Cartridge $22.95

With IWT Cartridges, the pure water flows freshly (5 gph) from the ion exchange cartridge. Only a length of plastic hose links the pure water with the point of use. No contamination can take place. The solvent hunger of pure water has nothing to feed on: no meters; no metal; no storage tanks; no air-carried impurities.

PURITY CAN BE 15 MEGOHMS/CM

A Duplex Mounting Fixture with two Research cartridges in series even removes silica and CO_2 comparing favorably to triple distillation. A single Universal Cartridge delivers water as good as single distilled but silica and CO_2 remain. Both kinds indicate by a color change when resins are exhausted. Then you merely replace the cartridge for $12.95 (Research) or $10.95 (Universal).



Bul. DX-470 describes the expanded IWT cartridge line. Five different models meet the need for varying levels of purity. Six page, 4-color brochure describes fixtures, suggests systems, and contains prices. Yours if you ask for it.

iwt IonXchange

ILLINOIS WATER TREATMENT COMPANY
840 CEDAR ST., ROCKFORD, ILL. 61105

Circle No. 92 on Readers' Service Card

PAPER CHROMATOGRAPHY AND ELECTROPHORESIS

by **GUNTER ZWEIG,** Life Sciences Division, Syracuse Univ. Research Corp., Syracuse, N. Y. and **JOHN R. WHITAKER,** Department of Food Science and Technology, Univ. of Calif., Davis, Calif.
Volume 2: **PAPER CHROMATOGRAPHY**
by **JOSEPH SHERMA,** Lafayette College, Easton, Pennsylvania, **and GUNTER ZWEIG**
CONTENTS: History and Introduction. Theory, Mechanism, and Fundamentals of Paper Chromatography. Techniques of Paper Chromatography, Quantitative Paper Chromatography. Amines, Amino Acids, Peptides, and Proteins. Carbohydrates. Aliphatic Acids. Steroids. Bile Acids, and Cardiac Glycosides. Purines, Pyrimidines, and Related Compounds. Indoles, Phenoles, and Aromatic Acids. Naturally Occurring Pigments. Pesticides. Antibiotics and Vitamins. Miscellaneous Organic Compounds. Inorganic Analysis. Author Index-Subject Index.
January 1971, 604pp., $27.50

THE CHEMISTRY OF NONAQUEOUS SOLVENTS

Volume 3
edited by J. J. LAGOWSKI, Department of Chemistry, University of Texas, Austin, Texas
CONTENTS: MARION MACLEAN DAVIS: Bronsted Acid-Base Behavior in "Inert" Organic Solvents. D. F. BUROW: Liquid Sulfur Dioxide. RAM CHAND PAUL and SARJIT SINGH SANDHU: Acyl Halides as Nonaqueous Solvents. F. FEHER: Liquid Hydrogen Sulfide. ALEXANDER I. POPOV: Anhydrous Acetic Acid as Nonaqueous Solvent. ALEXANDER I. POPOV: Other Carboxylic Acids. Author Index-Subject Index.
1970, 416pp., $21.00

AN INTRODUCTION TO GAS-LIQUID CHROMATOGRAPHY

by **R. ALAN JONES,** School of Chemical Sciences, University of Anglia, Norwich, England
Provides a basis introduction to the practice of gas-liquid chromatography for organic chemists. The book describes the principles of operation of the instrument and the interpretation of the results. An introductory chapter presents sufficient theory for a fundamental understanding of the practical aspects of the technique. The second part of the book comprises tables of reference which will be used for "on the spot" problems during the operation of the gas chromatograph.
1970, 214pp., $8.00

IONIC INTERACTIONS

In Two Volumes
Volumes in **PHYSICAL CHEMISTRY**
Series Editor: E. M. LOEBL
edited by SERGIO PETRUCCI, Dept. of Chemistry, Polytechnic Institute of Brooklyn, Brooklyn, N. Y.
This book is a comprehensive survey of ionic interactions in the entire range of concentrations from dilute solutions to fused salts. The chapters, which deal with the subject both theoretically and experimentally, are written by specialists in the fields of statistical mechanics, inorganic stereochemistry, chemical kinetics, and chemical structure. The first volume surveys the equilibrium and transport properties of dilute electrolytes and fused salts. Volume 2 contains two chapters on chemical kinetics and mechanism, one of which emphasizes the recently developed relaxation tools for the study of ionic association, and two chapters on the spectra and structure of electrolytes.
Volume 1: *Feb. 1971, about 384pp., $19.50*
Volume 2: *Feb. 1971, about 258pp., $16.50*

SPECTROSCOPY IN INORGANIC CHEMISTRY

In Two Volumes
edited by C. N. R. RAO, Department of Chemistry, Indian Inst. of Technology, Kanpur, India, and **J. R. FERRARO,** Chemistry Division, Argonne National Laboratory, Argonne, Ill.
Spectroscopy has become an indispensable tool for inorganic chemists largely because of new and improved techniques and the easy availability of sophisticated commercial instrumentation. This two volume work contains articles on some of the recent innovations and present results of research in some of the specialized and novel areas of inorganic chemistry where spectroscopy has been used effectively.
Volume 1: *1970, 410pp., $19.50*
Volume 2: *April 1971, about 330pp., in preparation*

COMPUTER CALCULATION OF PHASE DIAGRAMS

With Special Reference to Refractory Metals
A Volume in **REFRACTORY MATERIALS**
Series Editor: JOHN L. MARGRAVE
by **LARRY KAUFMAN,** Director of Research, **and HAROLD BERNSTEIN,** Senior Scientist, both at Manlabs, Inc., Cambridge, Mass.
Describes a formal means for computing phase equilibria and lattice stability in metallic systems. Its approach is based on the quantitative definition of the lattice stability of metals. The book also observes and examines the relevance of the lattice stability concept in characterizing solid state transformations. In addition, it is an appreciable source for coursework illustrating the application of computer techniques to problems in metallurgy, ceramics, chemistry, and solid state physics.
1970, 334pp., $15.00

GAS CHROMATOGRAPHY

Second Edition
by **A. B. LITTLEWOOD,** School of Chemistry, The University Newcastle upon Tyne, England
This wholly rewritten version of the author's well-received first edition presents an integrated, up-to-date treatment of all the fundamental aspects of gas chromatography. The first half of the book concerns the ability of gas chromatography to perform separations. The theory of the operation and design of gas chromatographic columns is described in detail. The third quarter of the book deals with detectors, which are the means of obtaining analyses by gas chromatography. The last quarter of the book is a single chapter in a series of sections, each dealing with the chromatography of a particular class of chemical compound.
1970, 521pp., $22.50

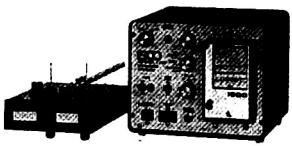
DIFFERENTIAL THERMAL ANALYSIS

Volume 1: **Fundamental Aspects**
edited by R. C. MACKENZIE, The Macauley Institute for Soil Research, Aberdeen, Scotland
This work gives an authoritative and critical assessment of the present position concerning fundamentals and applications. Not only are definitive data given for a very large range of compounds and materials but the processes occurring on heating are discussed in detail and the effects of various, often little appreciated, factors on DTA results are assessed. The book is designed to cover a wide range of disciplines and gives information on basic aspects as well as on advanced problems.
1970, 726pp., $33.00
Volume 2: *in preparation*

ACADEMIC PRESS NEW YORK AND LONDON
111 FIFTH AVENUE, NEW YORK, N.Y. 10003

Circle No. 4 on Readers' Service Card

Final Exam



An ISCO monochromatic UV flow monitor is a reliable assistant which you can trust to give your column effluents a comprehensive examination with a minimum of effort and supervision.

And did you know that of all the instruments of this type, ISCO monitors

- are true absorbance (O.D.) monitors?
- have the narrowest bandwidth and least stray light?
- are the only ones which can operate your fraction collector to automatically deposit separate peaks into separate tubes?
- with an optional channel alternator accessory will monitor two columns at one wavelength, one column at two wavelengths, or one column at one wavelength but with two flow cell light path lengths?
- are priced no higher than instruments having none of these features?

All this adds up to the only fully quantitative UV monitors on the market.

For more information send for brochure UA31.

INSTRUMENTATION SPECIALTIES CO.
4700 SUPERIOR LINCOLN, NEBRASKA 68504
PHONE (402) 434-8231 CABLE ADDRESS: ISCOLAB LINCOLN

Circle No. 94 on Readers' Service Card

New Books

Regular and Related Solutions. Joel H. Hildebrand, John M. Prausnitz, and Robert L. Scott. ix + 228 pages. Van Nostrand Reinhold Co., 450 W. 33rd St., New York, N. Y. 10001. 1970. $10.95

This book is both a revision of and sequel to "Regular Solutions" by Hildebrand and Scott. The title has been altered to go along with the fact that the authors also deal with irregular solutions in terms of their deviation from the behavior of regular solutions considered as reference state. The present book expands the coverage of solubility within a thermodynamic framework using the microscopic or intermolecular potential foundation approach of solubility. Scores of solutions of gases, liquids, and solids are analyzed in the light of this important theory. A large amount of new experimental evidence introduced by the authors within the last eight years is presented. This book will be of value and interest to researchers in chemical engineering, physical chemistry, and polymer chemistry, and specifically in such areas as natural gas, petroleum and petrochemicals, paint and varnish, pharmaceuticals, polymers, chromatography, and plastics.

The Chemistry of Amides. Jacob Zabicky, Ed. xv + 927 pages. John Wiley & Sons, Inc., 605 Third Ave., New York, N. Y. 10016. 1970. $38.50

This volume is part of a series entitled "The Chemistry of the Functional Groups." Each volume tries to cover all aspects of the chemistry of one of the important functional groups in organic chemistry. The emphasis is laid on the functional group treated and on the effects which it exerts on the chemical and physical properties, primarily in the immediate vicinity of the group in question, and secondarily on the behavior of the whole molecule. The amide function as considered in this present volume is based on the trivalent group. To keep the volume within reasonable size, some restrictions were imposed as to the type of radical that might be attached at each site. On the carbonyl side of the group, only bonds to H or C atoms were allowed, while on the amino moiety of the group N could also be attached. These limitations leave compounds such as carbamates, ureas, and semicarbazides, outside the scope of the book, but include in it amides, lactams, imides, diacylamines,

(*Continued on page 55 A*)

plenum
PUBLISHING CORPORATION

AN INTRODUCTION TO MÖSSBAUER SPECTROSCOPY

Edited by **Leopold May,** *Department of Chemistry, The Catholic University of America, Washington, D.C.*

This volume presents articles based on the most current lectures offered at the various institutes conducting courses in Mössbauer spectroscopy.

CONTENTS: Peter G. Debrunner and **Hans Frauenfelder,** Introduction to the Mössbauer Effect • **Jon J. Spijkerman,** Instrumentation • **David W. Hafemeister,** Nuclear Properties Determined from Mössbauer Measurements • **John C. Travis,** The Electric Field Gradient Tensor • **Robert L. Ingalls,** Application to Solid-State Physics • **J. Danon,** Application to Coordination Chemistry • **R. H. Herber,** Application to Organometallic Compounds • **U. Gonser,** Mössbauer Spectroscopy and Physical Metallurgy • **Leopold May,** Application to Biochemical Systems • Appendix A: Nomenclature of Mössbauer Spectroscopy • Appendix B: Bibliographic Sources • Appendix C: Selected References on Mössbauer Spectroscopy • Index.

203 PAGES JANUARY 1971 $15.00
SBN 306-30477-5

LOW-FREQUENCY VIBRATIONS OF INORGANIC AND COORDINATION COMPOUNDS

By **John R. Ferraro,** *Argonne National Laboratory, Argonne, Illinois*

This volume offers a wealth of new information on the correlation of far-infrared vibrations for molecules in inorganic and coordination compounds.

CONTENTS: Introduction • Far-infrared instrumentation • Sampling techniques and instrument calibration in the far-infrared region • New techniques used with far-infrared measurements • Metal-oxygen vibrations • Metal-halide vibration • Metal-nitrogen vibration • Miscellaneous metal-ligand vibrations • Other low-frequency vibrations • Appendices • Index.

309 PAGES JANUARY 1971 $18.50
SBN 306-30453-8

plenum press / consultants bureau
Divisions of Plenum Publishing Corporation
227 W. 17th ST., NEW YORK, NEW YORK 10011
Circle No. 146 on Readers' Service Card

More chromatograms.
(AUTOMATICALLY, TOO.)

Better chromatograms.
(EASIER AND FASTER, TOO.)

And computer compatibility.
(TOO.)

Get it all from Nuclear-Chicago.
(THE UP-AND-COMING CHROMATOGRAPHY PEOPLE.)

Computer compatibility.

Our Series 5000 coiled-column GC is *designed* for smooth interface with all of the most popular computers in laboratory use. Low noise levels and excellent reproducibility are the keys.

All system modules, including our new solid-state electrometer, are better grounded to keep the noise out. The Series 5000 electrometer has temperature-controlled FET's, single-point grounds on individual PCB's, and independent outputs for recorder, integrator, and computer. That means exceptional baseline stability, very low noise level, short warmup time, and *outstanding computer compatibility*. (And our detector systems have unexcelled S/N ratios.)

Necessary reproducibility is built into the Series 5000 in several ways. Our electronic temperature programmer, for instance. It assures column oven temperature reproducibility on a day-to-day basis.

Our cool-down controller returns and *re-equilibrates* the column at the initial temperature before each run can start—truly vital for retention-time reproducibility.

Our flow controllers are insulated *and* isolated from the oven to eliminate changes in controller temperatures caused by oven programming — to provide the best carrier gas flow stability available today.

Better chromatograms.

In addition to the several important advantages mentioned above, all of which can help you get far better results even if you don't use a computer, the Series 5000 has the edge in other ways, too. Some big, some little. But all important.

Ours is the most spacious oven on the market. Over 1300 cubic inches of usable space for your columns, with generous space between turns for air circulation. (Our capillary columns, for instance, are wound on a 6-in. diameter form, with 100 ft. per layer and $\frac{1}{16}$-in. spacing between turns.) And no matter which kind of columns you use — glass or metal, analytical or prep — our design permits the easiest interchangeability around. Experienced hands take no more than two minutes.

Sample temperature remains under tight control from injection to detection. Proportional control of the oven, packed column injection ports, and thermal conductivity detection zone assures stability and rapid equilibration after temperature selection. Tapered thermal bridges prevent cold spots while minimizing heat transfer between zones. And our dual-zone detector oven permits servicing of one zone while operating a detector at full sensitivity in the other zone.

Unique damper control of cool-down, manual or automatic, exhausts hot air at the rear of the oven rather than in the operator's face — at a rate faster than any other oven on the market. And this oven was designed specifically for cryogenic use, by the people who were the first to offer cryogenic gas chromatographs.

We're big on accessory options, too. Radioactivity Monitoring (RAM), Cryogenic Programming, Pyrolysis (with the highest reproducibility of *any* pyrolyzer), Automatic Temperature Programming and Cool-Down, and Automatic Sample Injection (see below). All easily added at minimum expense to our completely modular System 5000. To help you do more things better.

More chromatograms.

Because the Series 5000 Gas Chromatograph does so many things better, it will naturally let you work faster, avoid re-runs, get more done. But our Model 5141 Automatic Injection System can *really* help speed things up. Even when you're in a meeting or home in bed or off for the weekend.

This valuable accessory option permits 24-hour unattended operation for either isothermal or temperature-programmed analyses. It utilizes "Hot Pop" capsules for sample introduction. Is easy to set up. Takes up no additional bench space because it fits right onto your Series 5000.

And it has a *proven record* of accuracy and reliability.

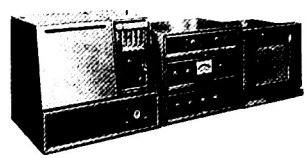
You get it all — and then some.

A complete inventory of chromatography supplies: Columns, phases, supports, syringes, recorders, detectors, column hardware, hydrogen generator, and many others.

More than 25 sales and service offices coast-to-coast.

Complete, detailed, illustrated literature on our Series 5000 Coiled-column Gas Chromatograph. Yours for the asking.

Ask for it. From us. The Up-and-Coming Chromatography People. o-227



NUCLEAR-CHICAGO
A SUBSIDIARY OF G. D. SEARLE & CO.

2000 Nuclear Drive, Des Plaines, Illinois 60018, U.S.A.
Donker Curtiusstraat 7, Amsterdam W. The Netherlands ACS-12

Circle No. 138 on Readers' Service Card

meet our Volks-Royce



3000 Mark A KEVEX-RAY

$2,222 buys the new low cost, high performance KEVEX®-RAY energy dispersive X-ray analyzer.

The new KEVEX-RAY 3000 Mark A saves you a solid $2,000 over the average X-ray analyzer (detector and cryostat). The 3000 Mark A isn't an ultra-high resolution analyzer. But it is a high quality instrument which encourages adventurous applications, not just by its performance and attractive price, but also by its reassurances. Standard 3000 Mark A features include: 30 mm^2 Si(Li) detector ■ 235 eV FWHM resolution for 5.9 KeV X-rays ■ 17-liter LN reservoir ■ 1 mil protected beryllium window ■ minimum microphonics. And that's just a sampling of what the 3000 Mark A offers. Of course, if you need **high resolution—better than 175 eV**—ask about our 3000 Mark AA.

For complete details on the 3000 Mark A plus our **free** 17-page Applications Guide entitled "Analytical Methods for Energy Dispersive X-ray Spectrometry," contact:

kevex

Analytical Instrument Division

898 Mahler Road, Burlingame, CA 94010 • Phone (415) 697-6901

Circle No. 183 on Readers' Service Card

triacylamines, and hydrazides. The thiono analogues of the compounds were also discussed. This volume contains an author index and a subject index.

Infrared Vapour Spectra. D. Welti. xi + 211 pages. Sadtler Research Laboratories, 3314-20 Spring Garden St., Philadelphia, Pa. 19104. 1970. $21

This book contains an extensive compilation of vapor-phase spectra. The preparation of this book stems from the author's interest in the combination of infrared spectrometry with vapor-phase chromatography. The direct collection and examination of chromatographic fractions in the vapor phase, usually in a heated gas cell, is a simple and efficient operation. The only substantial problem that remained in its application as a method of identification of unknowns was the lack of good quality vapor-phase spectra in the literature, and a relative lack of knowledge of the differences to be expected between the spectrum of the vapor and the condensed phase. Not only has Mr. Welti compiled a list of vapor-phase spectra, but he has examined relatively complex materials in the vapor phase, particularly those in which intermolecular hydrogen bonding can occur. The following are the five main topics covered in this book: sample handling; frequency correlations of vapor spectra; introduction to the use of the band contours in vapor spectra; combination of gas chromatography and infrared spectrometry; and vapor spectra. An index to the vapor spectra is also included.

Masking and Demasking of Chemical Reactions. D. D. Perrin. x + 211 pages. John Wiley & Sons, Inc., 605 Third Ave., New York, N. Y. 10016. 1970. $12.95

Masking and demasking techniques are used to improve selectivity in chemical methods ranging over fields as diverse as complexometric titration, gravimetry, polarography, spectrophotometry, solvent extraction, and ion exchange. This book provides a timely condensation of representative applications relevant to analytical chemistry, industry, biology, and medicine. The underlying principles of masking are discussed to serve as a guide to the reader in his choice of masking reagents for use in new systems or under conditions not previously considered. This detailed guide to masking as approached is unique, since previous pub-

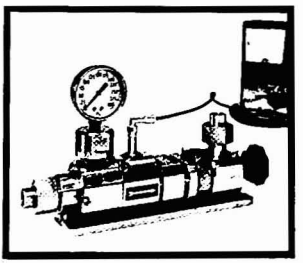
It's new.

A LAB-SIZE DISPERSONIC®

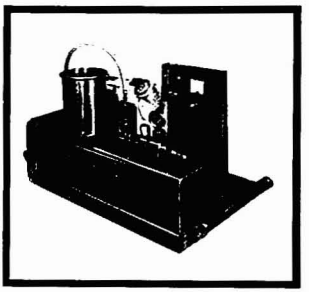
Emulsifies, disperses, homogenizes 1 to 4 liter quantities.

Produces pilot plant data that duplicates effects of production equipment.

Now you can prepare, in the laboratory, the same excellent emulsions, dispersions, suspensions and supermixtures that are produced by Sonic's high-capacity production equipment. You'll find the Lab-Size Dispersonic extremely useful, if not indispensible, in research activities involving chemical, food, rubber, textile, cosmetic and pharmaceutical technology. And, because experimental data can be directly applied to production processes, scale-up problems are a thing of the past.



The heart of our Lab-Size Dispersonic is the new Model "A" Sonolator. It's fully adjustable to permit best utilization of the jet-edge tone principle. Comes with acoustic intensity meter and probe to assure maximum mixing effectiveness. All



stainless steel construction. Strips in minutes for cleaning and changing of internal parts.

Complete, portable, self-contained system includes Sonolator and instrumentation, variable-speed motor, pump, tanks and controls mounted on a 2 x 3 foot base. Place it on a handy bench, plug it in and you're in business.

We'll be happy to send you more detailed operating information, complete specifications and prices. Please write us, or better yet, call. Sonic Engineering Corporation, Connecticut Ave., Norwalk, Conn. 06854. (203) 838-4717.

Sonic

Circle No. 168 on Readers' Service Card

AFS 6™

If this sounds like the most exciting development in flame analysis that you've heard about in recent years you're right. For more information about Technicon's AFS 6 Atomic Fluorescence Spectroscopy system, return this coupon to Technicon Industrial Systems, Dept. 118, Tarrytown, N.Y. 10591. We'll send you a brochure, some recent papers on atomic fluorescence spectroscopy and an application questionnaire.

Name _____

Title _____

Company/Institution _____

Address _____

City _____ State _____ Zip _____

Area Code _____ Phone _____

Ext. _____

Simultaneous multi-element analysis. Technicon® AFS 6 Atomic Fluorescence Spectroscopy System.

- ☐ 6 analytical channels
- ☐ 100 samples/hour...600 analyses
- ☐ Automatic sample handling
- ☐ Easy to operate
- ☐ Fluorescence and/or emission
- ☐ Readout in concentration terms

Technicon Industrial Systems
A Division of Technicon Instruments Corporatio
Tarrytown, New York 10591



Circle No. 172 on Readers' Service Card

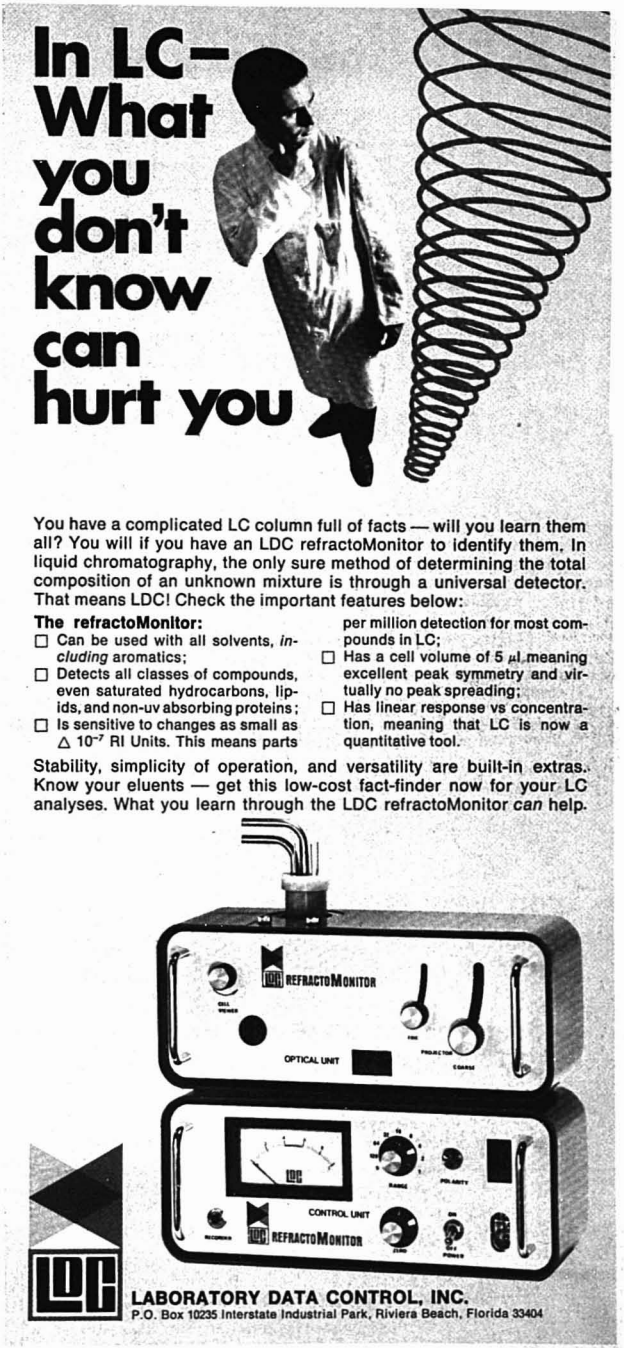
lications have treated the subject matter superficially. It should prove to be a valuable reference for all applied and pure chemical researchers involved with masking reagents.

Chemical Analysis: An Intensive Introduction to Modern Analysis. W. E. Harris and B. Kratochvil. x + 222 pages. Barnes & Noble, Inc., 105 Fifth Ave., New York, N. Y 10003. 1970. $4.25

This manual is designed to complement textbooks which include the theory of modern instrumental and separations techniques. It provides a set of thoroughly tested experiments that bring the laboratory treatment up to the level of the best modern textbooks. No prior analytical experience is assumed; the experiments begin with basic analytical operations and build progressively to include current techniques such as gas chromatography and atomic absorption. This manual is designed for students who have a background of general chemistry and who have gained sufficient appreciation of the need for high quality experimental work to benefit from an intensive course in chemical measurements. The experiments are divided into three parts: (1) a brief study of basic laboratory tools and operations; (2) a study of noninstrumental methods; and (3) a treatment of separations and instrumental methods. The assignments are designed to introduce analytical chemistry through the analysis of samples and to build the confidence of the student in his ability to make accurate chemical measurements at a reasonable rate.

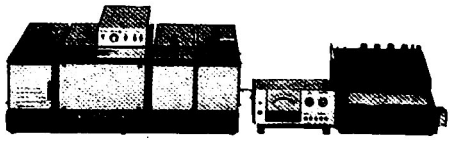
Composition, Reaction, and Equilibrium: Experiments in Chemistry. Norman C. Craig *et al.* x + 341 pages. Addison-Wesley Publishing Co., Inc., Reading, Mass. 01867. 1970. $4.50

This laboratory manual was assembled to serve a wide range of general chemistry programs. There are more experiments in this manual than can be completed in the typical two-term laboratory program. These experiments also differ greatly in the level of mathematical analysis required and in the use of instrumentation. There are 30 experiments; and the general themes include manual stoichiometry, equilibrium, reactivity, structure, and the properties of matter. The manual includes a section on qualitative analysis which contains theory, general proce-

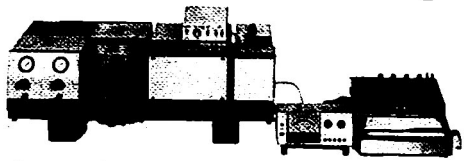


Circle No. 100 on Readers' Service Card

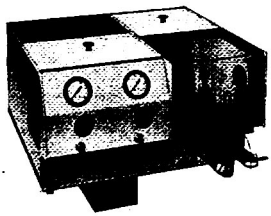
From Heath UV-Vis



...to full AA-AE-AF capability in two low cost, modular steps:



step one:



add the new Heath EU-702-70 module and get complete flame emission capability for only **$835.00***

step two:

add the EU-703-62 power supply ..**$140.00***
EU-703-61 chopper assembly .....**$ 70.00***
EU-703-60 turret assembly **$130.00***
and get complete AA-AE-AF capability for only **$340.00***

another example of how to save money while increasing capability... from the Modular Versatility People — Heath Company

FREE
HEATH SCIENTIFIC INSTRUMENTATION CATALOG
Investigate these and other new ideas in Spectroscopy, Digital Instrumentation, Lab Equipment and Test Equipment. Send for your FREE catalog now.

HEATH COMPANY, Dept. 560-01
Benton Harbor, Michigan 49022
HEATH
a Schlumberger company

☐ Please send free Heath Scientific Instrumentation Catalog

Name_____

Address_____

City_____ State_____ Zip_____

*Mail order prices; FOB factory.
Prices & specifications subject to change without notice. EK-294

Circle No. 85 on Readers' Service Card

dures, and flow charts, and on inorganic qualitative analysis. Quantitative relationships and measurements are emphasized. The experiments allow for considerable flexibility on the part of the instructor, permitting him to determine the order and level of sophistication of the material to be studied. Each of the experiments is self-contained and thereby designed to stimulate experimentation by the student.

Analytical Chemistry of Zirconium and Hafnium. Anil K. Mukherji. xiii + 281 pages. Pergamon Press, Inc., Maxwell House, Fairview Park, Elmsford, N. Y. 10523. 1970. $12

This book presents an up-to-date collection and comparison of published research results on the characterization and analysis of zirconium and hafnium. These two elements have interesting physical and mechanical properties such as corrosion resistance and mechanical strength of metals and alloys at both low and elevated temperatures. The aqueous chemistry of zirconium and hafnium has been discussed to draw attention to the complications of hydrolysis and polymerization and their effect on analytical procedures. Classical methods such as titrimetric, gravimetric, and absorptiometric are presented along with spectrographic, X-ray, and neutron activation methods. Techniques for the separation of zirconium from hafnium also have been discussed.

Programmed Thermodynamics, Vol. 2: Entropy and the Second Law. Charles E. Wales. ix + 275 pages. McGraw-Hill Book Co., 330 W. 42nd St., New York, N. Y. 10036. 1970. $5.95

This is a programmed text composed of a series of numbered sections; each section contains a linear sequence of questions and answers or frames, one or two problem sets, a multiple-choice self-quiz, and a set of content-performance objectives. These programs are designed to be self-sufficient study materials which the student reads outside of class. Topics covered in this volume include: entropy, the second law of thermodynamics and reversible and irreversible heat transfer, reversible and irreversible mixing processes, entropy relationships for real materials, using the thermodynamic transformations to extend state-property data, diagrams which show both S and H, and the general energy balance.

Circle No. 19 on Readers' Service Card →

BAUSCH & LOMB
ANALYTICAL SYSTEMS DIVISION

New! Spectronic 88

with instant concentration
near absorbance to 2.0A, and transmittance

ow, for the first time—direct meter
adings in Concentration, Linear Ab-
orbance and Transmittance in a modestly
riced spectrophotometer.

The Spectronic® 88 is easy to operate. There are
o snap-in blank scales for Concentration, no verifying
oints, no calculations. Just read the meter. One wide set of
cale markings lets you do all your samples in less time, without
onfusion. 0.1× to 3.0× scale expansion in the Concentration mode
ssures accurate readings of samples with low absorbance values.

A single knob selects the operating mode—Concentration, Transmittance
r Linear Absorbance. You can read absorbance values between 0.0-2.0A over
5-inches of meter. The meter is 8-inches in length and reads from 0.0-1.0A. How-
ver if your sample has an absorbance value higher than 1.0A, simply turn the selector
nob to the 1.0-2.0A setting and read the value directly from the meter.

Specifications are excellent . . . an 8nm bandpass, photometric linearity better than .010A
ar .500A, less than 0.2% drift/day, uninterrupted wide wavelength range—no need to switch from
V to Visible to NIR because phototubes and stray light filters are automatically interchanged.

Sampling versatility is superb—interchangeable single and multiple cell compartments. There's virtually no restrictions on glass-
are. The 88 accepts test tubes up to 20mm path length; 1, 5, and 10mm rectangular cuvettes; cylindrical cells up to 100mm; flow-
hru and water jacketed 10mm cuvettes; and filter plates for special applications.

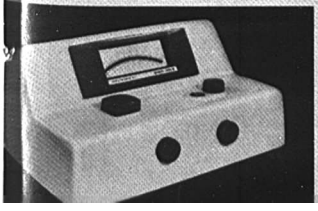
The Spectronic 88 has more features and advantages than anything else within its price range. For the full story, write for catalog
-6059 or request a demonstration. Analytical Systems Division, Bausch & Lomb, 1211-86 Linden Avenue, Rochester, N. Y. 14625.

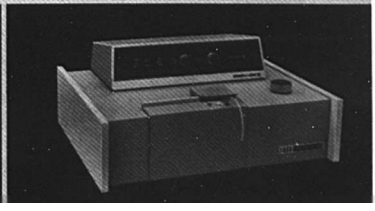
Here's the rest of the family:

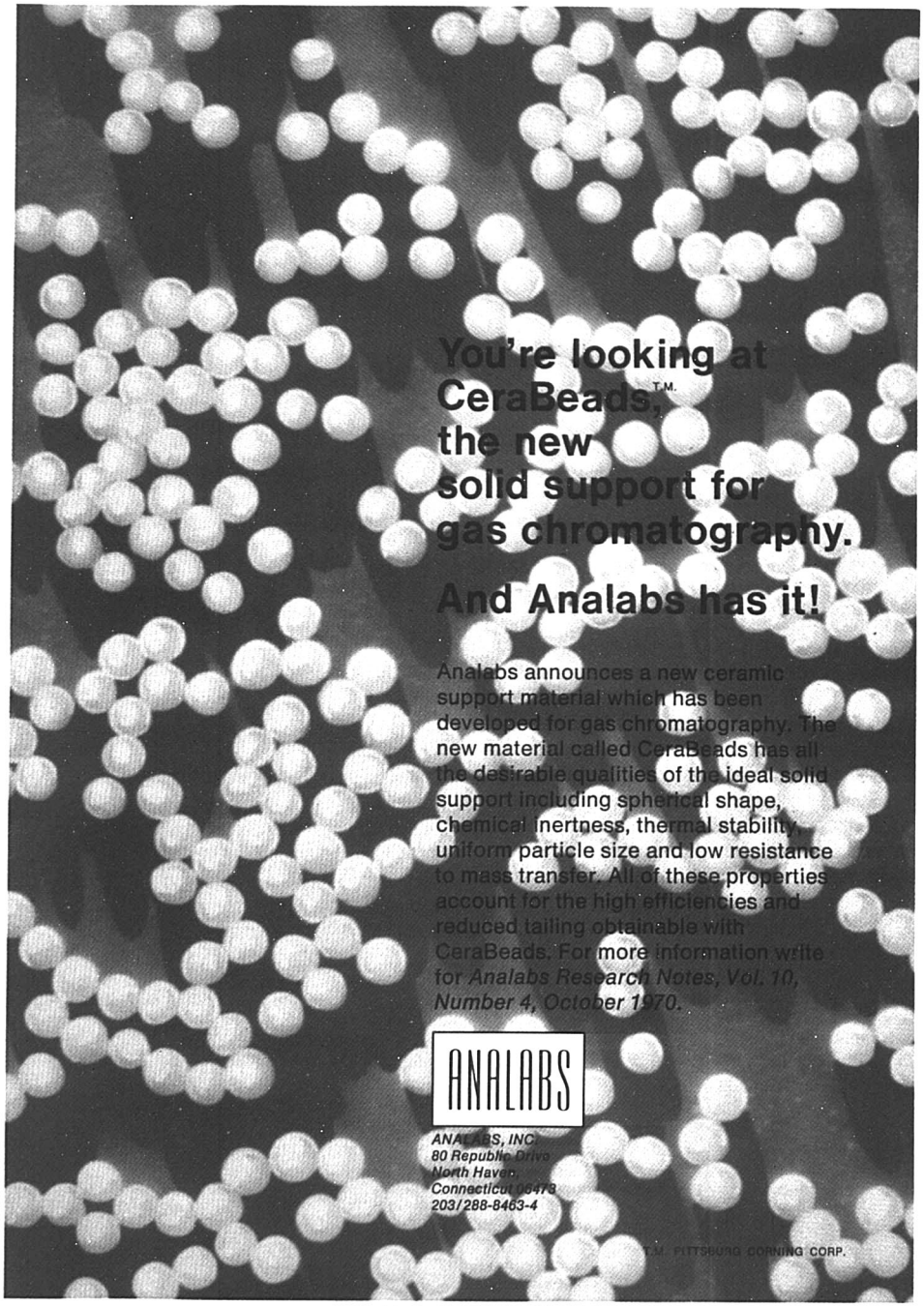
Spectronic 20®
World's most popular Spectrophotom-
ter. Over 85,000 in use.

Spectronic 70®
Direct reading in Transmittance and
Absorbance at low cost.

Spectronic 100®
4-place digital readout—linear Absorbance,
Transmittance and Concentration.







Circle No. 3 on Readers' Service Card

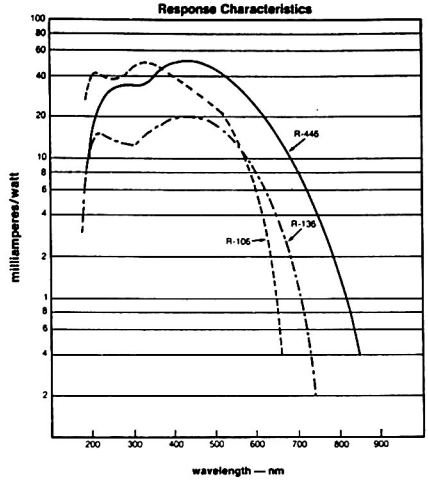
EDITORS' COLUMN

AT LEAST a rudimentary understanding of digital and analog instrumentation systems and components is rapidly becoming a necessity for the practicing analytical chemist. The unwary scientist, tempted by the many new data handling and digitizing devices available today, may incorporate an unwise combination of units into his system and actually degrade the output accuracy!

In this month's Instrumentation feature, page 69A, Professor C. G. Enke of Michigan State University introduces a number of "data domains" concepts which analytical chemists will find most useful in designing and modifying analog, digital, and analog/digital measurement systems and devices. Professor Enke has for a long time been a leader in educating scientists in the intricacies of electronics. His present article provides a means of utilizing the latest electronic devices, such as digital frequency meters, signal averagers, digital pH meters, "digitized" gas chromatographs and double-beam spectrophotometers, and Fourier transform spectrometers, efficiently and effectively, with no more knowledge necessary than an understanding of the basic measurement process.

In the future we shall feature, as a sequel to Professor Enke's article, a discussion and review of the analytical aspects of the digitizing step in digital instrumentation, authored jointly by Professor Stuart P. Cram of the University of Florida and Professor Harry L. Pardue of Purdue University. The quantitative aspects of digitizing and instrumentation performance and specifications will be considered for this important step prior to data acquisition or reduction. The similarities and differences between voltage-to-frequency conversion and analog-to-digital conversion also will be stressed.

We hope that the two-part series of articles mentioned above will



Now, Side-window arrangement in a reliable photomultiplier tube (S-20) by Hamamatsu



Expand the wavelength range of your spectrophotometer with the new HAMAMATSU R-446 Side-Window Photomultiplier Tube. S-20 response — 185-850 nm. Standard direct replacement requires no adaptation. The R-446 eliminates the need for several different-range tubes or time-consuming interchanges. When your UV spectrophotometer analyses require wider wavelength coverage, lower noise, and/or higher sensitivity, plug in the HAMAMATSU Side-Window R-446 and get all the response you need. Dependable, reliable, and available on 48-hour shipment.

Write or call Dept. PT-AC11

OCLI Instruments

132 WATER STREET, SOUTH NORWALK, CONN. 06854 (203) 853-2224

Circle No. 6 on Readers' Service Card



Need a real good HIGH RESOLUTION NMR system?
Want to replace that old 60 or 100 MHz machine?
Looking for a supercon system with more than 220 MHz?

AND NOW... budget cuts?

Here is the solution:

1. **Start** with a BRUKER HX 90 **now.**
   (Delivery: about four months – very attractive price!)
2. **Build up** with additional NMR locks and nuclei **later.**
   (You don't even need grants for that!)
3. **Get** the best FAST FOURIER TRANSFORM SYSTEM for NMR available on the market at **your convenience.**
   (Built for the future! No one else offers 18 and 20 bits/word!)
4. **Add on** a supercon magnet with your **next year's budget.**
   (And let us modify your spectrometer from 90 MHz to 270 MHz.)
5. **Enjoy** this 270 MHz HIGH RESOLUTION SPECTROMETER matching with the FAST FOURIER TRANSFORM system.
   (Which you bought originally for the 90 MHz instrument.)

There is no alternative... right?

GO FOR BRUKER

P.S. If you don't have to worry about the budget, you could, of course, order your new 270 MHz system right now!

For details, call or write:

IN U.S.A. – Bruker Scientific Inc.
1 Westchester Plaza, Elmsford, N.Y. 10523
(914) 592-5470

IN CANADA – Bruker Spectrospin Canada Ltd.
797 Don Mills Road, Don Mills, Ontario
(416) 429-2263

ENGLAND
Bruker Spectrospin Ltd.
19, Nordic Drift
Coventry CV 2 2 DE
Tel. (0203) 32 69 45

FRANCE
Bruker Spectrospin SA
7, rue de la Paix
(67) Wissembourg
Tel. (088) 94.02.42

ITALY
Bruker Spectrospin srl.
Via Pasquale Miglioretti, 2
20161 Milano
Tel.(02) 64 64 261

SWITZERLAND
Spectrospin AG
8117 Zurich-Fallanden
Industriestrasse 26
Tel. (051) 85 48 55/85 45 05

W. GERMANY
Bruker-Physik AG
7501 Forcheim
Tel. (0721) 5 80 70, 5 80 76-9
Tx. (07) 826 836

Circle No. 22 on Readers' Service Card

play a significant role in allaying some of the fears many analytical chemists seem to have regarding the computerization of laboratory instruments. For those who desire more first-hand information about laboratory computerization, the following meeting or the short course described below may be of interest.

The Microwave Research Institute of the Polytechnic Institute of Brooklyn will hold a symposium on "Computers and Automata," April 13–15, 1971, in New York City. The symposium will feature sessions on basic limitations on speed and power, real-time and other time-bounded computations, artificial intelligence and computer creativity, principles of languages, programming and compiling, computer architecture, synthesis of automata and logical circuit design, and machine diagnostics. For more information, contact Jerome Fox, Executive Secretary, MRI Symposium Committee, Polytechnic Institute of Brooklyn, 333 Jay St., Brooklyn, N. Y. 11201.

The Purdue University Chemistry Department will offer a short course on "Digital Computers in Chemical Instrumentation," June 9–26, 1971. The course is designed to provide a sound introduction to the use of the small digital computer in the laboratory. The principles and practices involved in the application of digital techniques will be discussed. Three weeks of intensive lectures will deal with the elements of digital logic, digital data acquisition techniques, and the use of the on-line digital computer in chemical instrumentation. In addition, there will be ample opportunity for laboratory experience with the designing of digital logic circuits, interfacing chemical instrumentation to the digital computer, and programming the small digital computer. Application forms and further information may be obtained from Dr. S. P. Perone, Department of Chemistry, Purdue University, Lafayette, Ind. 47907.

Alan J. Senzel



TAFID
A hot new concept that's 100 times more sensitive than TGA.

And that's only the start. Actually, TAFID (Thermal Analysis Flame Ionization Detection) exceeds TGA in six key areas. These were outlined recently by Dr. F. T. Eggertsen and Dr. F. H. Stross in the October issue of THERMOCHIMICA ACTA*. Here is what they said:

Sensitivity: "... is about 100 times greater than ordinarily obtained by thermogravimetric analysis."

Resolution: "Higher resolution is possible than in TGA because of the smaller samples that can be used . . . Effective one-plate resolution is obtainable."

Specificity: ". . . is specific for reduced [organic] carbon and does not respond to water, carbon oxides, nitrogen oxides and other substances normally associated with inorganic materials."

Analysis Time: ". . . capable of high speed of analysis, owing to the small sample requirement and low thermal lag of the furnace . . . an isothermal mode . . . provides especially rapid and convenient measurements."

Data Readout: "is [directly] expressed as rates of evolution or integrated amounts."

Applications: ". . . high sensitivity and wide range of linear response, together with its specificity and uniformity of response to organic carbon, make it uniquely well suited for the quantitative analysis of organic materials."

Write today if you would like a reprint of this paper and a complete technical description of our new Model 3000 Thermal Analysis System . . . the only instrumentation available that incorporates the TAFID concept.

*Eggertsen, F. T., Stross, F. H., *THERMOCHIM. ACTA*, 1, 451, (1970).

CARLE
INSTRUMENTS, INC.
1141 EAST ASH AVENUE, FULLERTON, CALIFORNIA 92631 (714) 870-8000

Circle No. 30 on Readers' Service Card

Our Model 240 has a new friend.

Model MC-1.

Up to now the Model 240 has done *almost* everything you want in elemental analysis for C,H,N and O. It gives you accuracy far better than classical methods but still uses proven classical combustion chemistry. It gives you the versatility to handle all kinds of samples—liquids, metal organics and other "difficult" materials without elaborate special procedures. You can use the Model 240 in applications such as the analysis of organics in soil, minerals, particulate matter in polluted waters etc. and in routine quantitative analyses of composite materials—polymer blends for example.

But what have we done for you lately?

Well, we've made all of the above simple, efficient and automatic with our new Model MC-1, microanalytical computer. It eliminates the need for signal attenuation and data reduction.

With the MC-1 you enter the sample weight, inject the sample and go and do something else. When you come back in a few minutes the answers in weight, % nitrogen carbon and hydrogen are waiting for you on the digital display! What else is there?

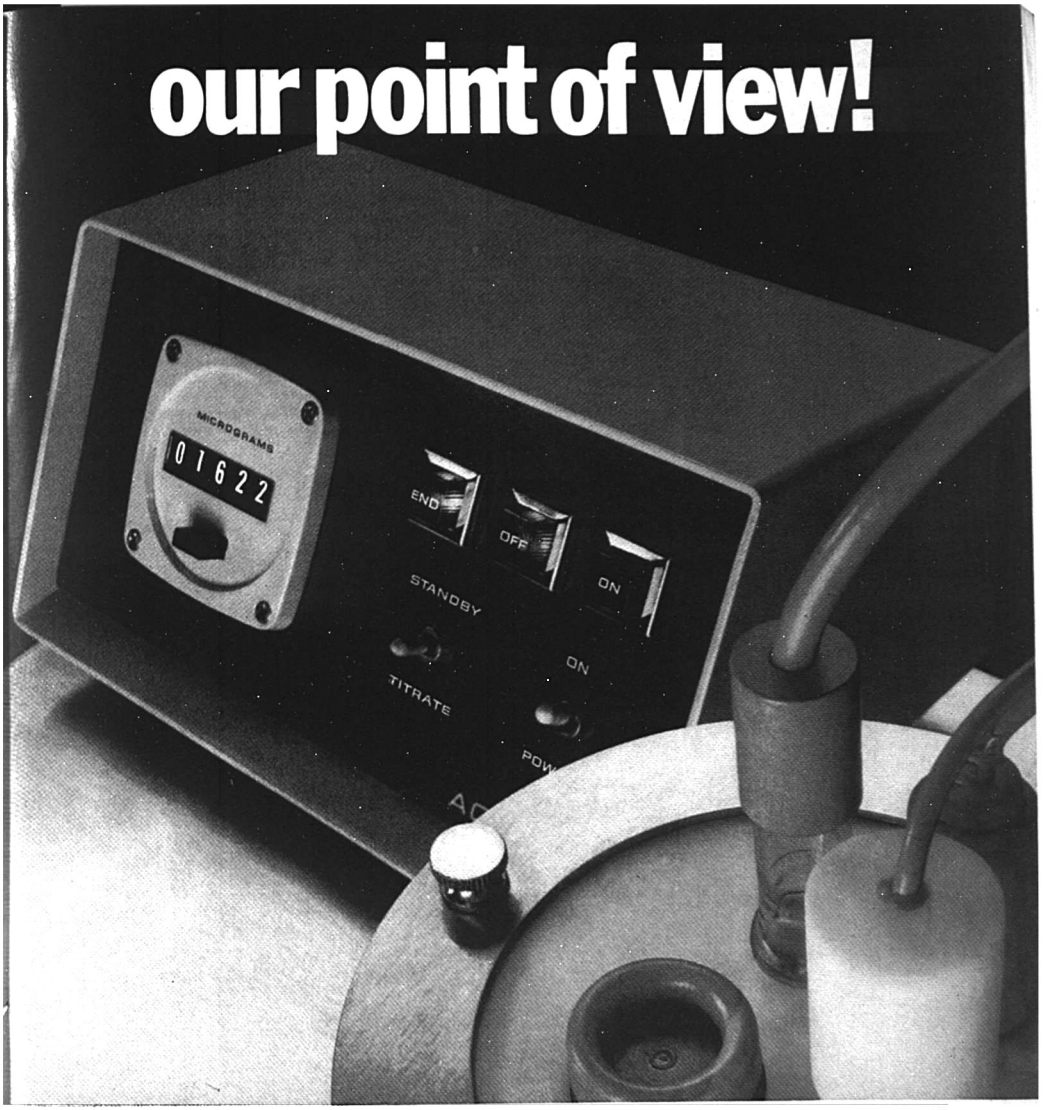
For more information on computerized elemental analysis write to Instrument Division, Perkin-Elmer Corporation, 702 Main Avenue, Norwalk, Conn. 06852.

PERKIN-ELMER



Circle No. 142 on Readers' Service Card

our point of view!



Finding a drop in a bucket is a lead pipe cinch... with AQUATEST

AQUATEST is the only truly automatic Karl Fischer titrator.
Just inject sample... flip switch... step back... read answer!
Digital readout... no standardization... no drying system... no burettes... no measuring... no computations



Accuracy, reproducibility, and sensitivity all within 25 micrograms of water... that's 10 ppm in a 2.5 ml sample!
Our point of view is that "drop in the bucket" water determinations are really a cinch with our AQUATEST. Try one and let us know your point of view.

PHOTOVOLT CORPORATION 1115 Broadway, New York, N.Y. 10010 · (212) 989-2900

Circle No. 152 on Readers' Service Card

Get precise boiling range specs automatically

. . . according to the new ASTM method for simulated distillation by gas chromatography.

Most chemists who have had to obtain boiling range distribution data on petroleum fractions don't like any of the conventional methods because they are not very accurate. HP's new 7600A Gas Chromatograph System — which not only meets or exceeds all requirements for the new ASTM method for simulated distillation by GC but also completely automates it—puts an end to this problem. The 7600A produces results that are much more precise and reproducible than is possible with any conventional distillation method, whether True Boiling Point (TBP), ASTM D-86 or ASTM D-1160.

To test the repeatability of absolute retention times (thus boiling point distribution) produced by the 7600A, 19 runs were made from separate vials of a calibration mixture of normal paraffins whose boiling range is −44°F to 928°F. The results are shown in the photograph below.

Reproducibility of the data is excellent across the entire range. The most critical test of repeatability is the spread between the maximum and minimum values for each of the components. In all cases, the spread is amazingly small. Even in the worst case, the spread is only 0.25 minute for a peak whose retention time was 31 minutes. The worst standard deviation is 0.080.

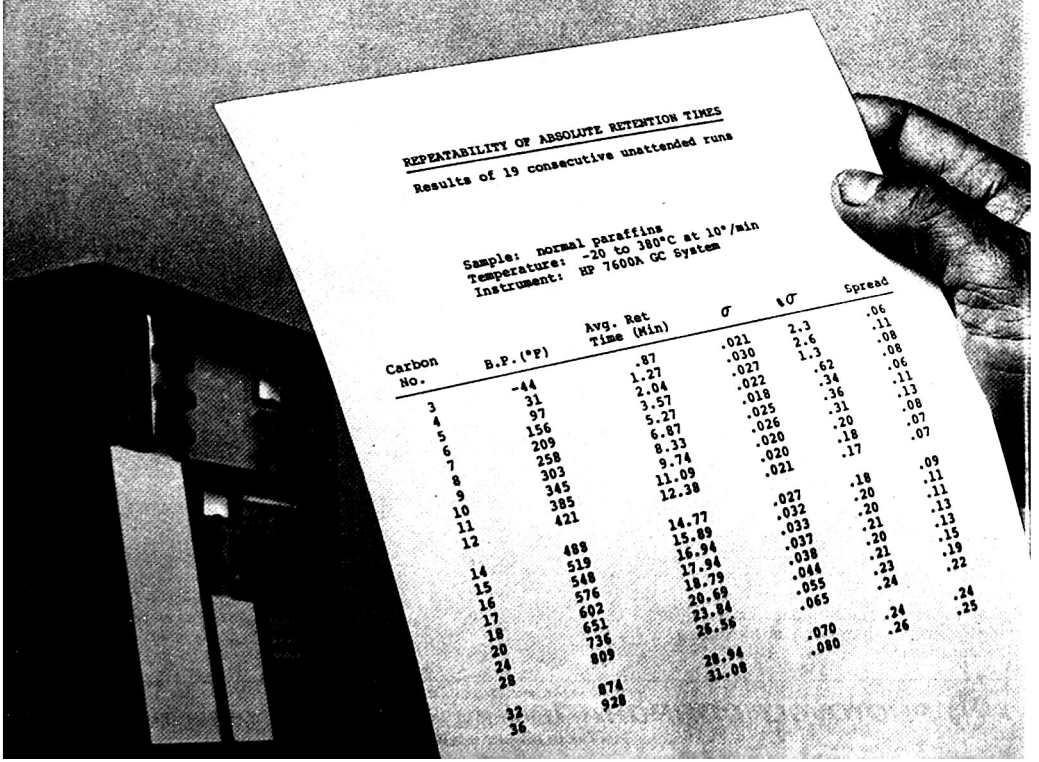
The 7600A operates completely unattended for as many as 36 consecutive samples of widely different boiling ranges. It includes complete sets of programs for automatic data reduction, calculation and reporting of results: any of the principal time-sharing computer services or a dedicated HP mini-computer can be used. An analysis report of boiling range distribution in 1% increments is prepared automatically in less than an hour, for less than 5 dollars per sample, including all costs.

For complete information and a copy of the new ASTM method, call the nearest HP sales office, or write: Hewlett-Packard, Route 41, Avondale, Pa. 19311. In Europe: 1217 Meyrin-Geneva, Switzerland.

HEWLETT hp PACKARD

ANALYTICAL INSTRUMENTS

Circle No. 83 on Readers' Service Card 43013



REPEATABILITY OF ABSOLUTE RETENTION TIMES

Results of 19 consecutive unattended runs

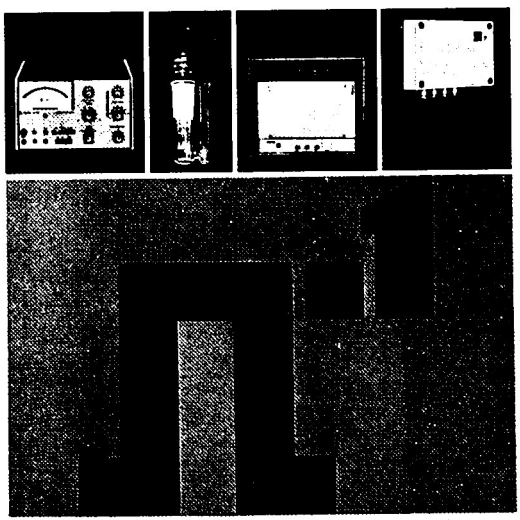
Sample: normal paraffins
Temperature: -20 to 380°C at 10°/min
Instrument: HP 7600A GC System

Carbon No.	B.P.(°F)	Avg. Ret Time (Min)	σ	4σ	Spread
	-44	.87	.021	2.3	.06
3	31	1.27	.030	2.6	.11
4	97	2.04	.027	1.3	.08
5	156	3.57	.022	.62	.08
6	209	5.27	.018	.34	.06
7	258	6.87	.025	.36	.11
8	303	8.33	.026	.31	.13
9	345	9.74	.020	.20	.08
10	385	11.09	.020	.18	.07
11	421	12.38	.021	.17	.07
12	488	14.77	.027	.18	.09
14	519	15.89	.032	.20	.11
15	548	16.94	.033	.20	.11
16	576	17.94	.037	.21	.13
17	602	18.79	.038	.20	.13
18	651	20.69	.044	.21	.15
20	736	23.84	.055	.23	.19
24	809	26.56	.065	.24	.22
28	874	28.94	.070	.24	.24
32	928	31.08	.080	.26	.25
36					

One of the world's two great ranges of electrolytic conductivity measuring equipment

PHILIPS

electrolytic conductivity measuring equipment



When choosing an instrument for measuring electrolytic conductivity, what do you choose *between*?

We don't want to influence you excessively, but it might be worthwhile to review our brand new catalog before making up your mind. It contains some important new additions to the Philips range.

We believe you're going to agree that ours is one of the two great ranges of conductivity instruments . . . and that it compares very favourably with the "other one" . . . no matter which one.

N.V. Philips' Gloeilampenfabrieken, Analytical Equipment Department, Eindhoven, the Netherlands.

PHILIPS ANALYTICAL EQUIPMENT

☐ Please send a copy of your new catalog of Potentiometric Sensors
☐ Please send a copy of your new catalog of pH Measuring Instruments
☐ Please send a copy of your new catalog of Conductivity Measuring Equipment

Name: .....

Position: .....

Please clip this coupon to your company letterhead and mail it today 102

PHILIPS

Circle No. 148 on Readers' Service Card

The ADVANCES IN CHEMISTRY Series...

Excellent Reviews in Book Form of Specialized Chemical Topics

For comprehensive reviews of all the important aspects of a chemical subject... read the books in the ADVANCES IN CHEMISTRY Series.

Ranging up to 750 pages in length, ADVANCES volumes include...

- Authoritative, thought-provoking articles by as many as several dozen scientists per volume.
- Carefully compiled collections of data.
- Groups of related papers presented at important national and international symposia.
- Invited reviews of current work written by researchers eminent in the field discussed.

With the ADVANCES you learn about brand-new chemical subjects... and bring yourself up to date on familiar chemical topics. The numerous scientists contributing to each volume provide you with stimulating reading enriched by a variety of viewpoints. And the ADVANCES bring material together under one cover which would otherwise be scattered among many journals... *or not available at all.*

... Put chemical topics of interest to you in proper perspective. Read the ADVANCES IN CHEMISTRY Series.

The order form lists the 20 most recent titles in the ADVANCES IN CHEMISTRY Series. Use it to order your ADVANCES *now.*

No.	Title	Price	Number of copies ordered	Cost
96	Engineering Plastics and Their Commercial Development 128 pp (1969)	$7.50		
95	Cellulases and Their Applications 460 pp (1969)	$14.50		
93	Radionuclides in the Environment 522 pp (1970)	$15.00		
92	Epoxy Resins 224 pp (1970)	$10.50		
91	Addition and Condensation Polymerization Processes 767 pp (1969)	$19.50		
90	Fuel Cell Systems—II 446 pp (1969)	$17.50		
89	Isotopes Effects in Chemical Processes 278 pp (1969)	$13.00		
88	Propellants Manufacture, Hazards, and Testing 395 pp (1969)	$12.00		
87	Interaction of Liquids at Solid Substrates 212 pp (1968)	$9.50		
86	Pesticidal Formulations Research. Physical and Colloidal Chemical Aspects 212 pp (1969)	$9.50		
85	Stabilization of Polymers and Stabilizer Processes 332 pp (1968)	$12.00		
84	Molecular Association in Biological and Related Systems 308 pp (1968)	$10.50		
83	Chemical Marketing: The Challenges of the Seventies 199 pp (1968)	$9.50		
82	Radiation Chemistry—II 558 pp (1968)	$16.00		
81	Radiation Chemistry—I 616 pp (1968)	$16.00		
81	and 82 ordered together	$30.00		
80	Chemical Reactions in Electrical Discharges 514 pp (1969)	$15.00		
79	Adsorption from Aqueous Solution 212 pp (1968)	$10.00		

TOTAL COST

Postpaid U.S. and Canada; all others please add $0.20 for each volume ordered.

Payment must be in U.S. funds, by international money order, UNESCO coupon, or U.S. bank draft; or order through your book dealer.

Please ship my ADVANCES to:

Name

Address

City State/Country Zip

☐ Bill me. ☐ Payment enclosed.

Return this order form to AMERICAN CHEMICAL SOCIETY, Special Issues Sales, Dept. LG-68, 1155 16th Street, N.W., Washington, D.C. 20036.

... There are over 50 other volumes in the ADVANCES Series. To receive your pricelist for all the ADVANCES, just send us your request... or note it on your order. You'll receive the list by return mail.

Advisory Panel

Jonathan W. Amy, Jack W. Frazer, G. Phillip Hicks, Donald R. Johnson, Charles E. Klopfenstein, Marvin Margoshes, Harry L. Pardue, Ralph E. Thiers, William F. Ulrich

Data Domains—An Analysis of Digital and Analog Instrumentation Systems and Components

Data domains concepts offer a means of effectively utilizing new electronic devices which requires only an understanding of basic measurement processes. These concepts can be used to great advantage in designing or modifying systems and in assessing and minimizing the sources of measurement errors.

C. G. ENKE

Department of Chemistry,
Michigan State University,
E. Lansing, Mich. 48823

SCIENTIFIC INSTRUMENTATION is being revolutionized by the availability of an ever-increasing array of electronic devices which increase measurement speed, accuracy, and convenience while decreasing instrument size and power requirements. Integrated circuits and hybrid circuits have made many measurement techniques, which were previously only theoretically possible, a reality. The continual decrease in the cost of digital and linear circuits has made many sophisticated devices such as frequency meters, digital pH meters, signal averagers, and minicomputers practical for most laboratories. As electronic technology continues to advance, we can expect more and more of the sampling, control, and data analysis of scientific measurements to be performed by the instrument itself.

Digital instrumentation has been the scene of much development and interest because of its inherent accuracy capability, convenient numerical output, and potential digital computer compatibility. However, just "digitizing" an instrument does not insure these advantages. There are literally hundreds of data handling and digitizing devices available today and an unwise combination of units can actually degrade the output accuracy. Also, many digitized measurement systems, while providing excellent accuracy and convenience, are unnecessarily complicated.

Data Domains Concepts

The convenience and power of the amazing new electronic devices are irresistible to almost all scientists, but few are in a position to understand these new tools in detail. A means of applying new devices efficiently and effectively, which requires only an understanding of the basic measurement concepts, is needed for most. The data domains concepts described here are very useful in analyzing, describing, modifying, and designing analog, digital, and analog/digital measurement systems and devices and in assessing and minimizing the sources of measurement errors (*1*). In addition, a much better understanding of the instrumental data handling process is gained as a result of the study and application of the data domains concept. The first four concepts of data domains analysis are given below:

(1) Measurement data are represented in an instrument at any instant by a physical quantity, a chemical quantity, or some property of an electrical signal. The characteristics or properties used to represent the measurement data can be categorized in groups called "data domains."

(2) As the data proceed through the instrument, a change in the characteristic or property used to represent the measured data is called a "data domain conversion."

(3) All electronic measurement systems can be described as a sequence of two or more data domain converters, each of which can be analyzed separately.

(4) Methods of using electrical signals to represent measurement data fall into three major categories or domains: analog, time, and digital.

Since there are only three data domains for electrical signals, the electronic sections of complex measurement systems can be easily analyzed (or designed) as combinations of only a few basic interdomain converters. Also the hundreds of data handling devices available can be shown to be simply various methods of accomplishing the basic interdomain conversions.

Electronics-Aided Measurement

In an electronics-aided measurement, the quantity to be measured is converted into an electrical signal and then amplified or otherwise modified to operate a device which visually displays the value of the measured quantity. This process is illustrated for a typical case in the block diagram of Figure 1. An input transducer such as a photodetector, thermistor, glass pH electrode,

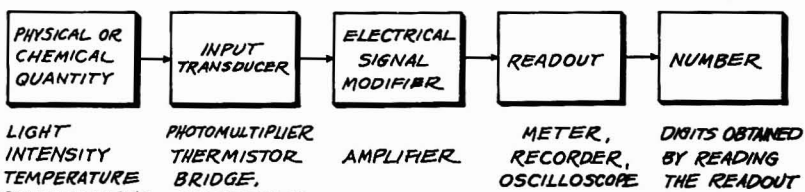


Figure 1. Basic electronic measurement

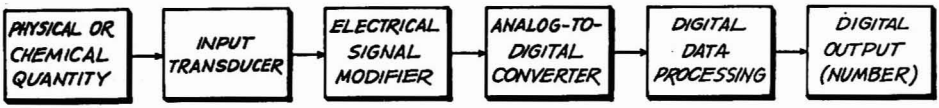


Figure 2. Basic digital electronic measurement

or strain gage is used to convert the quantity to be measured into an electrical signal. The current or voltage amplitude of this signal is related in some known way to the quantity to be measured. The electrical signal from the input transducer is then modified by an electronic circuit to make it suitable to operate a readout device. The electronic circuit is most frequently an amplifier with the appropriate adjustable parameters (zero, standardization, position, etc.) and sometimes with automatic compensation for nonlinearities, temperature variation, etc. of the transducer. The output is a readout device from which a number can be obtained, generally by observing the position of a marker against a numbered scale.

Using the data domains concepts, the basic electronic measurement of Figure 1 is described as follows: The measurement data exist first as the physical or chemical quantity to be measured. At the output of the input transducer, the measurement data are represented by an electrical signal and are thus in one of the three "electrical" domains. The input transducer is thus a device which converts quantities or translates information from a physical or chemical domain into an electrical domain. The measurement data remain in an electrical domain through the electrical signal modifier. However, the output device converts the electrical signal into some readable form such as the relative positions of a marker and a scale—*i.e.*, a nonelectrical domain. Thus the entire measurement can be described in terms of conversions between domains and modifications within domains.

In the basic electronic measurement, at least two converters are required; one to transfer into an electrical domain and one to transfer out. The characteristics of each interdomain converter and each signal modifier affect the quality of the measurement. To take advantage of special input transducers, particular readouts, and available signal processing techniques, an instrument may involve many data domain conversions and signal modifiers. The data domains concept allows each step to be blocked out and analyzed separately. This will be shown to be particularly desirable in assessing sources of errors and the relative advantages of various digitizing or interfacing possibilities.

Digital Measurement. A common form of digital measurement system is shown in block form in Figure 2. At some point after the measurement data have been converted into electrical amplitudes, an analog-to-digital converter is used (*2*). This is an electronic circuit which converts an analog electronic signal (where the measurement data are represented by the signal amplitude) to a digital electronic signal (which represents integer numbers unambiguously by coded binary-level signals). If the digitization was performed to take advantage of the great accuracy, power, and versatility of digital data processing, that will be done next. Finally, the numerical binary-level signal is decoded into a number which is displayed, printed, and/or punched.

Because so many advantages are claimed for digital techniques, many techniques have claimed to be "digital." In fact, any type of device which has dial settings or outputs which are numerals in a row is likely to be called digital. By that standard a decade resistance box is a digital instrument. Since the end result of any measurement is a number, all instruments could be called digital, but the meaning of the word in that sense becomes trivial. Some confine the use of the words "digital instrument" to those instruments which contain binary-level electronic logic circuits of the type developed for digital computers. As will be shown later, it is common for measurement data to be represented by a binary-level electronic signal and still not be "digitized" or numerical. Therefore, in this paper, a digital instrument will be defined as one that uses a digital electronic signal to represent the measurement data somewhere within the instrument. The analysis and design of digital measurement systems necessarily involves an understanding of the ways electrical signals can represent data and how conversions from one form to another are accomplished.

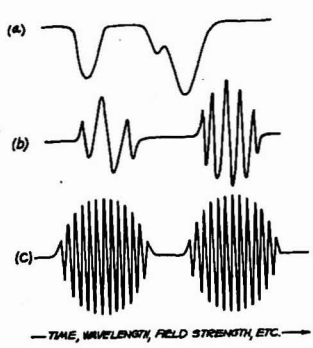


Figure 3. Analog (E_A) domain signals

Electronic Data Domains

There are only three basic ways by which measurement data are represented by an electrical signal: Analog, symbolized E_A, in which the amplitude of the signal current or voltage is related to the data; time, $E_{\Delta t}$, in which the time relationship between signal-level changes is related to the measurement data; and digital, E_D, in which an integer number is represented by binary-level signals. The characteristic signals in each of these domains and examples of their use are described in this section.

Analog, E_A. The measurement data in this domain are represented by the magnitude of a voltage or a current. The analog domain signal is continuously variable in amplitude. Also, the analog amplitude can be measured continuously with time or at any instant in time. Most input transducers used today convert the measurement data from the physical and chemical domains (P) to the E_A domain. Examples of P-to-E_A converters are: photodetectors which convert light intensity to an electrical current, a thermistor bridge which converts temperature difference to an electrical potential, a combination pH electrode which converts solution acidity into an electrical potential, and a flame ionization detector which converts the concentration of ionizable molecules in a gas into an electrical current. Figure 3 shows some typical E_A signals.

At each instant in time, the measured quantity is represented by a signal

amplitude. The variations in the signal amplitude may be plotted against time, wavelength, magnetic field strength, temperature, or other experimental parameters as shown in Figure 3. From such plots, additional information can often be obtained from a correlation of amplitudes measured at different times. Such information would include simple observations like peak height, peak position, number of peaks, or more complex correlations such as peak area, peak separation, signal averaging, and Fourier transformation. The techniques of correlating data taken at different times must be distinguished from the techniques of converting the data taken at each instant into a usable form. It is the latter problem that this paper is primarily concerned with. The former problem is handled by data processing techniques, once the required instantaneous data points have been converted to a useful form and stored.

Signals in the E_A domain are susceptible to electrical noise sources contained within or induced upon the circuits and connections. The resulting signal amplitude at any instant is the sum of the data signals and the noise signals.

Time, $E_{\Delta t}$. In this domain, the measurement data are contained in the time relationship of signal variations, not the amplitude of the variations. Typical $E_{\Delta t}$ domain signals are shown in Figure 4. The most common $E_{\Delta t}$ domain signals represent the data as the frequency of a periodic waveform (a), the time duration of a pulse (b), or as the time or average rate of pulses (c). These are logic-level signals—*i.e.*, their signal amplitude is either in the HI or *1* logic-level region or the LO or *0* logic-level region. The data are contained in the time relationship between the logic-level transitions. The greater the slope (dE/dt) of the signal through the logic-level threshold region, the more precisely the transition time can be defined. Because the data in an $E_{\Delta t}$ domain signal are less amplitude-dependent than in an E_A domain signal, they are less affected by electrical noise sources. A common example of this is the FM radio signal ($E_{\Delta t}$ domain) *vs.* the more noise susceptible AM radio signal (E_A domain). The greater the difference between the average *0* or *1* signal-level amplitude and the logic-level threshold, the less susceptible the signal will be to noise-induced error. In these respects, the signal shown in Figure 4b is better than those of Figures 4a and 4c. The logic-level transitions of signals like Figures 4a and 4c are generally sharpened to those like 4b before the significant time relationship is measured. This is accomplished by a *comparator* or *Schmitt trigger* circuit. Examples of converters producing $E_{\Delta t}$ domain signals from physical domain quantities are: a crystal oscillator that produces a temperature-dependent frequency because of the temperature characteristics of the quartz crystal, an oscillator which has an output frequency dependent upon the value of the capacitance used in the oscillator circuit, and the Geiger tube which converts level of radioactivity to a pulse repetition rate. An example of a E_A-to-$E_{\Delta t}$ domain converter is a voltage-controlled-oscillator or voltage-to-frequency converter which provides an output frequency related to an input voltage.

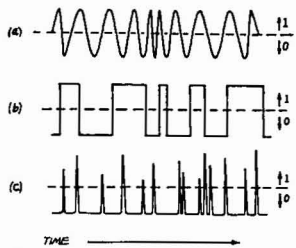


Figure 4. Time ($E_{\Delta t}$) domain signals

The $E_{\Delta t}$ domain signal, like the E_A domain signal, is continuously variable since the frequency or pulse width can be varied infinitesimally. However, the $E_{\Delta t}$ signal variable cannot be measured continuously with time or at any instant in time. The minimum time required for conversion of an $E_{\Delta t}$ domain signal to any other domain is one period or one pulse width.

Digital, E_D. In the digital domain, the measurement data are contained in a 2-level signal (HI/LO, *1/0*, etc.) which is coded to represent a specific integer (or character) (*3*). The digital signal may be a coded series of pulses in one channel (serial form) or a coded set of signals on simultaneous multiple channels (parallel form). Representative digital signal waveforms are shown in Figure 5. The count serial waveform (a) is a series of pulses with a clearly defined beginning and end. The number represented is the number of pulses in the series. The count serial waveform of Figure 5 might represent, for instance, the number of photons of a particular energy detected during a single spark excitation. The count serial form is simple but not very efficient. To provide a resolution of one part per thousand, the time required for at least one thousand pulses to occur must be allowed for each series of pulses.

The most efficient serial digital signal is the binary-coded serial signal shown in Figure 5b. In this signal, each pulse time in the series represents a different bit position in a binary number. The appearance of a pulse at a time position indicates a *1;* the absence of a pulse, a *0*. The data are not represented by the exact time of the pulse as in the $E_{\Delta t}$ domain, but by the signal logic level present within a given time range. The binary number represented by the waveform shown is 101101011 which is decimal 363. A series of n pulse times has a resolution of one

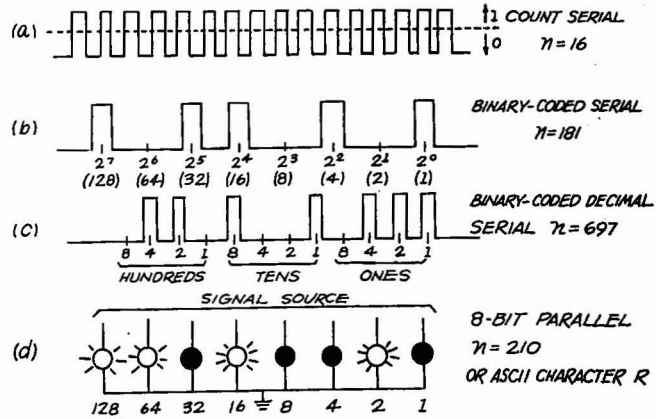


Figure 5. Serial and parallel digital signals

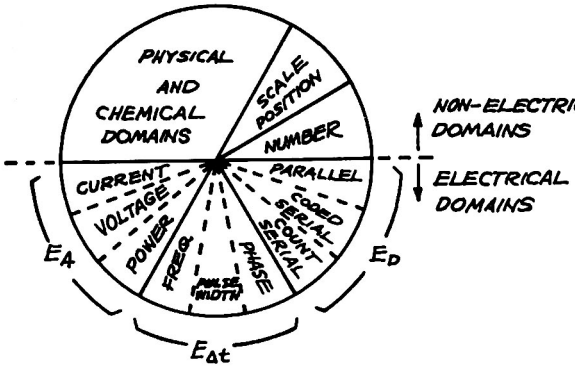


Figure 6. Data domains map

part in $2^{10} = 1024_{10}$, and a 20-bit series has a resolution of better than one part per million.

The binary-coded decimal serial form is somewhat less efficient but very convenient where a decimal numerical output is desired. Each group of four bits represents one decimal digit in a number. Twelve bits can thus represent three decimal digits and provide one part in one thousand resolution.

A parallel digital signal uses a separate wire for each bit position instead of a separate time on a single wire. The principal advantage of parallel digital data connections is speed. An entire "word" (group of bits) can be conveyed from one circuit to another in the time required for the transmission of one bit in a serial connection. An 8-bit parallel data source is shown in Figure 5d connected to indicator lights to show the simultaneous appearance of the data logic levels on all eight data lines. Binary coding (shown), binary-coded decimal coding, and others are used for parallel digital data. Parallel data connections are used in all modern, fast computers. Serial data connections are often used for telemetry and slow computer peripherals such as teletypes.

Mapping Domain Conversions

It has been pointed out that electronic instruments making chemical or physical measurements use no fewer than two data domain conversions. In fact, modern laboratory instruments frequently use three or more domain conversions to perform the desired measurement. Knowing the data domains involved in a particular instrument's operation can help in understanding its operation, applications, limitations, and adaptability as part of a larger measurement system. When analyzing an instrument it is helpful to use the data domains "map" shown in Figure 6. The path of the signal can be traced out on the map as it is followed through the instrument. This process will be illustrated for several chemical instruments of various types.

pH Meter. The block diagram of a conventional pH meter is shown in Figure 7. The combination glass/calomel electrode converts the hydrogen ion activity (chemical composition domain) to an electrical potential (E_A domain). This signal is amplified and converted to a current amplitude that is used to deflect the meter pointer. A number is then obtained by reading the position of the pointer against the calibrated scale. The signal path on the data domains map for the pH meter is also shown in Figure 7. Note that there are two instrumental interdomain conversions, one intradomain conversion, and one "manual" interdomain conversion. It will be shown later that interdomain conversions are more complex and error-prone than intradomain conversions. Recording and "servodigital" pH meters have essentially the same block diagram and domains path except that the servo system can be used to convert the E_A voltage signal from the combination electrode directly into the pen position in the case of the recorder or the position of the turns-counting dial (a rotary scale) in the case of the servodigital meter. Notice that even in the latter case the data are never in the digital domain.

Digital pH Meter. A digital pH meter (Figure 8) differs from an ordinary pH meter in that the meter is replaced by an analog-to-digital (A/D) converter and a digital display. A frequently used A/D converter for this application is the dual slope converter. As is often the case, this A/D converter does not convert directly from the E_A to E_D domains. The dual-slope circuit produces a pulse which has a duration proportional to the input signal voltage—*i.e.*, a $E_{\Delta t}$ signal. The pulse width is converted to a digital signal using the pulse to turn an oscillator on and off, generating a count serial digital signal.

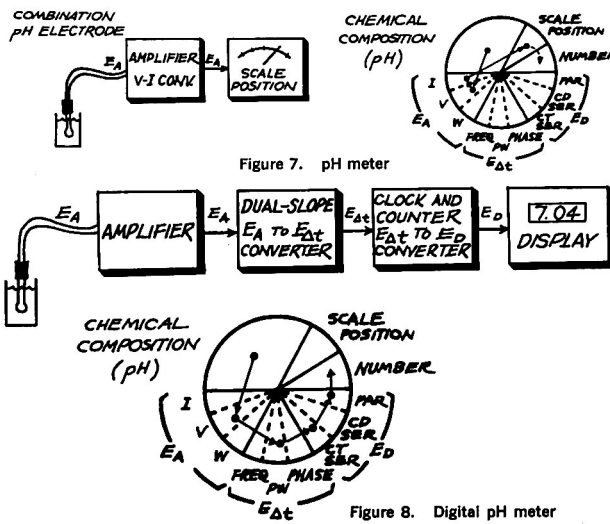


Figure 7. pH meter

Figure 8. Digital pH meter

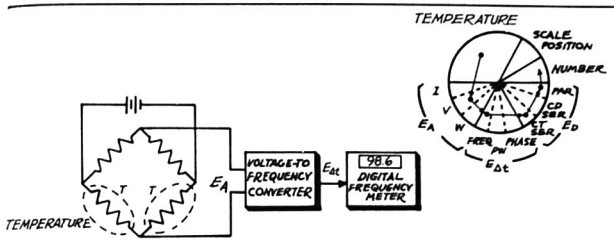


Figure 9. Thermistor-digital temperature measurement

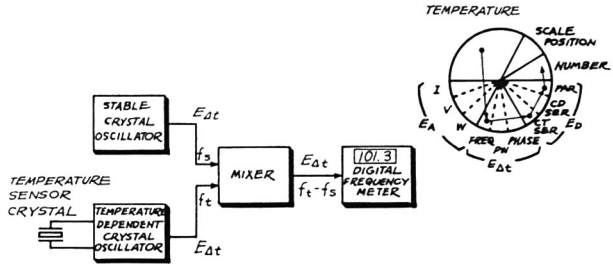


Figure 10. Crystal oscillator temperature measurement

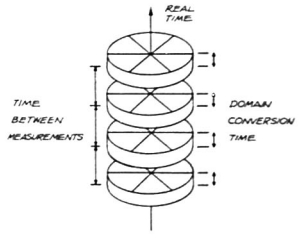


Figure 11. Successive domain conversions

The count serial signal is in turn converted to parallel digital for the display by a counter. From the domains map it is seen that four interdomain and one intradomain conversions are involved in the measurement.

Digital Temperature Measurement. Two approaches to a digital thermometer are compared here. The first is a thermistor bridge connected to a digital voltmeter (E_D) as shown in Figure 9. The thermistor bridge circuit converts temperature to voltage. In this case the E_A-to-E_D (A/D) conversion is accomplished by a voltage-to-frequency converter and a frequency meter. The digital frequency meter operates by counting the number of cycles of an input signal that occur in a specific time. The resulting domain path is shown. There are four interdomain and one intradomain conversions.

The second approach is the use of a quartz crystal which has a temperature-dependent resonant frequency. An oscillator is used to convert the resonant frequency to an electrical signal in the $E_{\Delta t}$ domain. The block diagram is shown in Figure 10. A mixer is used to subtract a standard frequency, f_s, from the temperature-dependent frequency, f_t, to obtain a signal for which the frequency and temperature are related directly. This is an example of signal modification occurring in the $E_{\Delta t}$ domain. Note that this digital thermometer requires one less interdomain conversion than that of Figure 9. Whether this simplification would result in greater accuracy, however, depends upon the accuracy of the converters involved in each case.

Conversions of Varying Quantities

The examples used in the previous section were measurements of steady-state quantities which were not expected to vary perceptibly over the interval of measurement. When the time variation of quantities in the various data domains is considered, a third dimension (time) needs to be added to the data domain map of Figure 6, as shown in Figure 11. Here each interdomain conversion is shown as a slice

CONCEPTS

Data Domains

1. Measurement data are represented in an instrument at any instant by a physical quantity, a chemical quantity, or some property of an electrical signal. The characteristics or properties used to represent the measurement data can be categorized in groups called "data domains."
2. As the data proceed through the instrument, a change in the characteristic or property used to represent the measured data is called a "data domain conversion."
3. All electronic measurement systems can be described as a sequence of two or more data domain converters, each of which can be analyzed separately.
4. Methods of using electrical signals to represent measurement data fall into three major categories or domains: analog, time, and digital.

Measurement Devices

5. All measurement devices employ both a difference detector and a reference standard quantity.
6. Either the difference detector or the reference standard can affect the accuracy of the measurement.
7. The reference standard quantity is the same property or characteristic as that which is being measured.
8. Interdomain converters have the characteristics of measurement devices.

Now Pye Liquid Chromatography has got everything *nearly*

We have modified the claim, of course, because there is always something being developed in the field of liquid chromatography analysis.
Our most recent development is the Pye Eluant Collector. Although designed specifically for Pye liquid chromatograph systems, it is also compatible with certain other column monitors with 0–10mV outputs. Collection of fractions may be initiated by either a change in the detector signal from the column monitor, or a variable timer. Trap indexing, by the emergence of a peak, allows samples to be collected at their maximum concentration and the eluting solvents passed to waste. Overfilling, due to long eluting peaks, is avoided with a pre-set timer which automatically advances the next collector. Manual operation gives facilities for setting-up and calibration and for investigation of non-standard analyses.
Pye liquid chromatographs can detect and analyse practically any known organic substance. Their unique variable-speed, circular-section wire-transport system carries the eluant from the column, via an evaporator pyrolyser, to one of three extremely sensitive detectors. These detectors, with their low noise levels and minimum drift characteristics, allow for substances as small as one part per million to be detected.
If your field of analysis is in liquid or gas chromatography contact Pye Unicam now for further information or a demonstration.

Pye Unicam Ltd.
York Street Cambridge, CB1 2PX, England
Telephone (0223) 58866 Telex 81215

PYE UNICAM

Circle No. 161 on Readers' Service Card



Pye Eluant Collector

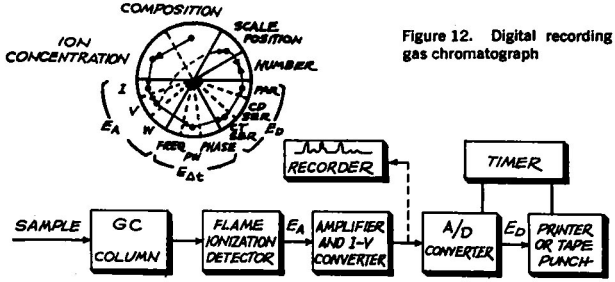


Figure 12. Digital recording gas chromatograph

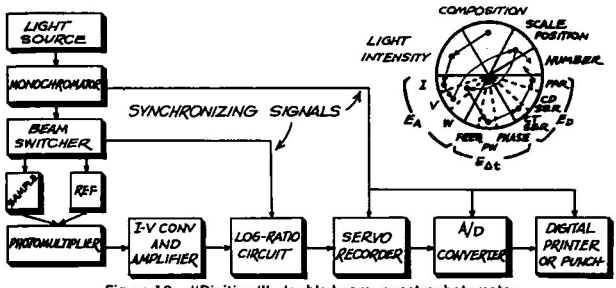


Figure 13. "Digitized" double-beam spectrophotometer

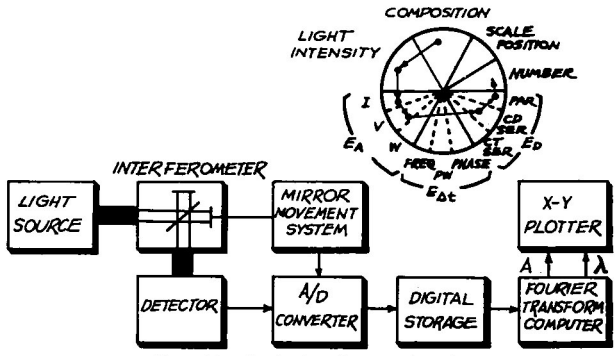


Figure 14. Fourier transform spectrometer

across the real-time continuum. If a quantity that varies continuously with time is to be converted to the digital domain, the resulting number can only be true for a specific instant in time. It is not possible, therefore, to make a truly continuous digital record of a varying quantity. What can be done is to measure the varying quantity at successive instants in time. The numerical result of each measurement is then stored in order in memory registers, or recorded on punched cards or paper tape, or by magnetic recording devices. If the measurements are made frequently enough for the varying quantity to change only slightly between each time, the digital record can quite accurately represent the amplitude *vs.* time behavior of the measured quantity. Of course, the maximum frequency of measurement is limited by the time required to convert the measured quantity into the digital domain and record it. Successive data domain conversions will be illustrated by three examples of digitized measurement systems.

Gas Chromatography. A digital recording gas chromatograph is shown in Figure 12. The components in the sample mixture are separated by the column resulting in a flow of gas of varying composition through the flame ionization detector. The flame in the detector converts the hydrocarbon concentration into an ion concentration (an intradomain conversion) which is then converted by the electric field in the detector to an electrical current (an interdomain conversion). The current signal is amplified and converted to a voltage amplitude suitable for A/D conversion and/or recording. The desired data are a record of detector current *vs.* time. The time relationship of the printed or punched values of the current amplitudes is generally obtained by having the successive A/D conversions performed at precise and regular time intervals. This is accomplished by the timer shown in the block diagram. The domain path for a single conversion (one time slice) is also shown.

Absorption Spectrophotometry. The block diagram of a digitized recording double-beam spectrophotometer is shown in Figure 13. A narrow wavelength range of light from the light source is selected by the monochromator and passed on to the beam switcher and cell compartment. The beam switcher alternately directs the monochromatic beam through the reference and sample cells to the photomultiplier tube detector. This produces an electrical current (E_A domain) which has an amplitude alternating between sample and reference beam intensities P and P_o. The desired output signal for the recorder is absorbance $A = \log_{10}(P_o/P)$, which is accomplished in the log-ratio circuit. This circuit performs a correlation between signal levels measured at two different times. It must, therefore, have a memory and a synchronizing connection to the beam switcher. The recorder is to plot absorbance *vs.* the wavelength of light from the monochromator. The recorder chart drive thus has a synchronizing connection to the monochromator wavelength drive mechanism.

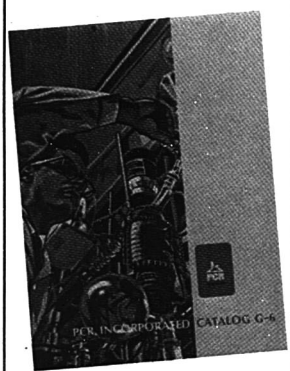
This standard spectrophotometer was later digitized by putting a retransmitting pot assembly on the servorecorder. This converts the recorder pen position to a voltage amplitude which is connected to an A/D converter and printer or punch. Since the absorbance value recorded for precise *wavelength* (rather than time) intervals is desired, the A/D converter and printer are synchronized to the wavelength drive mechanism rather than a timer.

The data domains map for the resulting instrument is shown in Figure 13. It contains nine conversions; seven interdomain and two intradomain. The excursion into the scale position domain is unnecessary to the digitizing process and suggests that the A/D converter would have been better connected to the log-ratio circuit output, if possible. It is interesting to note that if photon

SOMEONE YOU SHOULD KNOW

PCR INCORPORATED

LET OUR CATALOG G6 INTRODUCE YOU TO THE WORLD OF PCR.



Are you engaged in Research on FLUORINE containing compounds? Do SILICON organics hold your attention? Catalog G6 contains one of the most complete listings of these compounds to be found anywhere. We're not limited to these fields of chemistry, many other compounds will be found in this catalog. G6 is more than just a price list, Molecular Weights and Physical Properties are listed for your convenience.

PCR INCORPORATED

For your copy call 904 376-7522 or write
PCR, INCORPORATED
P.O. Box 1466–Gainesville, Florida 32601
Formerly Peninsular ChemResearch Inc.

Circle No. 147 on Readers' Service Card

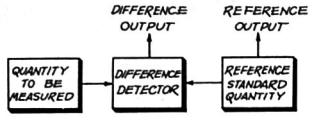


Figure 15. Basic measurement system

counting is used to measure the relative intensities, the number of interdomain conversions is reduced to three and a digital log-ratio circuit is required.

Fourier Transform Spectroscopy. A Fourier transform spectrometer is an example of a conceptually very simple data acquisition system connected to a complex data correlating and processing system. The block diagram is shown in Figure 14. To obtain the interference pattern, the A/D converter converts the detector output signal at constant increments of movement of the reference beam mirror. Each piece of data is stored for use in the Fourier transform calculation. The data domains map as shown is complete for each piece of data as it is acquired and stored. A successive approximations type of A/D converter has been assumed in this map. There are four interdomain and two intradomain conversions in all. After the transform calculation (which involves an intercorrelation of all the measured data points) is complete, a plot of absorbance *vs.* wavelength can be made.

This example demonstrates that Fourier transformation from amplitude *vs.* time or space to amplitude *vs.* frequency (or the reverse) is really an intercorrelation of analog signals which have already been "measured." It is essential to distinguish between the data domains involved in the methods of acquiring each data point and the methods of correlating and displaying groups of data points.

Errors in Domain Conversions

To understand the sources of error in domain conversion, it is helpful to review briefly the basic measurement process. Measurement can be defined as: *The determination of a particular characteristic of a sample in terms of a number of standard units for that characteristic.* The comparison of the quantity to be measured with standard units of that quantity is implicit in this definition. The comparison concept in measurement is illustrated by Figure 15. The quantity to be measured is compared with a reference standard quantity. The difference is converted to another form (domain) such as scale position. The quantity measured is then the sum of the standard units in the reference quantity and the difference output calibrated in the same standard units.

All measurement devices involve both a difference detector and a reference standard, although they differ widely in the degree to which one or the other is relied upon in the measurement. As an example, three mass measuring devices can be compared in this regard. With a double pan balance, the unknown mass is compared with standard weights, whole units and fractional, until the difference detector (beam pointer) points to zero. In this case, the accuracy and resolution of the standard weights determines the accuracy of the measurement as long as the difference detector is sufficiently sensitive. No accuracy requirement is placed on the off-null calibrations of the difference detector. The other extreme is a spring-loaded scale, such as a fish or bathroom scale. In this case, the reference standard weights are used to calibrate the scale markings of the manufacturer's original prototype. In use, the measurement accuracy depends entirely upon the off-null markings on the scale. The reference standard quantity compared by the scale in this case is zero weight. In between these two extremes is the single pan balance with an optical scale for fractional weights. Balances of this type rely upon accurate standard weights for the most significant figures and upon off-null calibrations for the less significant figures.

Similar comparisons and analyses can be made for other types of measurement devices. A potentiometric voltage measurement depends much more upon the slidewire (standard voltage unit adjustment) calibration than upon the galvanometer null detector, while an electrical meter depends much more upon the difference detector calibrations than upon the standard. This kind of analysis is helpful in assessing the sources of errors in measurement devices and in choosing among available devices for a particular application. After considering a variety of measurement systems in this way, some basic concepts concerning measurement devices evolve which can be added to the four data domains concepts listed earlier.

(5) All measurement devices employ both a difference detector and a reference standard quantity.

(6) Either the difference detector *or* the reference standard can affect the accuracy of the measurement.

(7) The reference standard quantity is the same property or characteristic as that which is being measured.

MAKES MERCURY ANALYSIS AN INEXPENSIVE, ROUTINE PROCEDURE



Coleman MODEL MAS-50 MERCURY ANALYZER SYSTEM

- Sensitivity: 0.01 microgram of mercury (equal to or better than atomic absorption)
- Direct reading in micrograms of mercury
- Dynamic range: 0 to 9 micrograms of mercury
- Response time: less than one minute over the full concentration range

Whether you wish to detect mercury in air, water, food, soil, fertilizer or metal—or in urine, blood or tissue, one thing is sure: you'll be able to do it less expensively with this lightweight, compact instrument which boasts a sensitivity equal to or better than can be obtained using the most sophisticated atomic absorption unit.

No special training is required to operate the simple two-control system. No calculations have to be made. The Model MAS-50 Mercury Analyzer System gives a direct meter reading in micrograms of mercury and %T. Even an unskilled operator can easily obtain a sensitivity of 0.01 microgram. *Response time is less than one minute over the full concentration range.*

Model MAS-50, which employs the Hatch and Ott procedure recommended by the Federal Water Quality Administration, is a completely self-contained system requiring no accessories or hook-up. It weighs only ten pounds, has a self-contained circulating pump, comes with procedures, and is available with or without all necessary standards and reagents. A recorder output is provided.

The instrument consists of a metal case finished in gray chemical-resistant enamel measuring 20"x11"x8". It has an all-plastic cell and includes easily demountable plastic windows to facilitate cleaning.

If you're interested in speeding mercury determination procedures while at the same time cutting expenditures, it will pay you to learn more about this new, inexpensive Coleman instrument. Bulletin B-350 will be sent on request. *Ask us for a copy.*

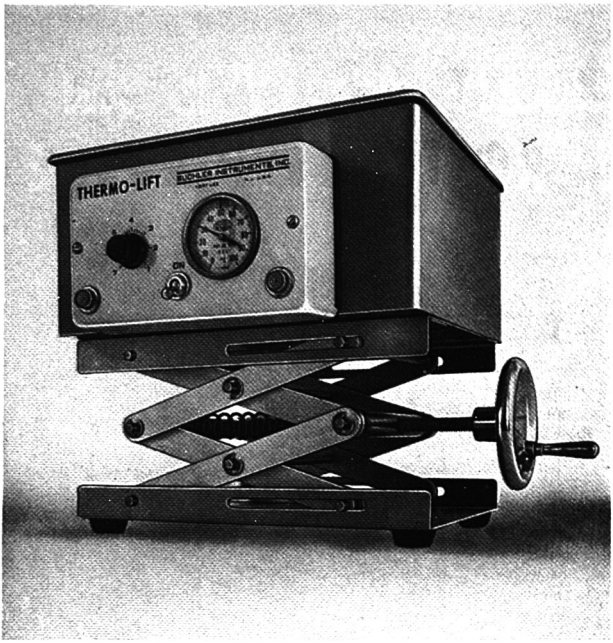
M-2000X Coleman Mercury Analyzer System, Model MAS-50, complete with built-in pump, plastic absorption cell, tubing, and reaction vessel, but without reagents or dispensers. Price $875.00

SCIENTIFIC GLASS APPARATUS CO. INC.
BLOOMFIELD, NEW JERSEY

LABORATORY...
♦ APPARATUS
♦ INSTRUMENTS
♦ CHEMICALS
♦ GLASSWARE

Branches: Boston Mass. • Danbury Conn. • Elk Grove Village Ill. • Fullerton Calif. • Philadelphia Penna. • Silver Spring Md. • Syracuse N. Y.

Circle No. 164 on Readers' Service Card



new from Buchler . . .

THERMO-LIFT™

CONTROLLED HEATING BATH

The new Thermo-Lift is a combination of a lift and a temperature controlled water bath that may be adjusted from a minimum height of 8" to a maximum height of 16". Made of stainless steel, the water bath is 8"x 10" x 4" deep. An automatic thermoregulator controls temperature to within 0.2°C accuracy. This new instrument is useful as a source of heat for rotary evaporators, for distillation procedures and for certain applications where flexibility in operational height is required. The versatile Thermo-Lift may be moved quickly and easily from one application to another.



BUCHLER INSTRUMENTS

BUCHLER INSTRUMENTS DIVISION

NUCLEAR-CHICAGO CORP.

A SUBSIDIARY OF G. D. SEARLE & CO.

1327 SIXTEENTH STREET, FORT LEE, NEW JERSEY, 07024

Circle No. 23 on Readers' Service Card

A data domain conversion is the conversion of a number of units of some physical, chemical, or electrical characteristic into a related number of units of a different characteristic; for instance, the conversion of units of pH into Nernst factor potential units by a combination pH electrode. Devices for converting data from one domain to another are "measuring" one characteristic in terms of another. Therefore,

(8) Interdomain converters have the characteristics of measurement devices.

Using a combination pH electrode as an example of an interdomain converter to illustrate concepts 5–7: 5) The combination pH electrode itself is the difference detector; the reference standard is the standard buffer solution used to "standardize" the voltage output at a given pH. 6) The conversion error (difference between the predicted and actual potential/pH relationship) depends upon the accuracy of the standard solution and upon the accuracy of the electrode response. The greater the pH difference between the standard and unknown solutions, the more the conversion accuracy depends upon the electrode's characteristics. 7) The reference standard is pH, the units which are being converted to electrical potential.

Once one is accustomed to looking for the difference detector, reference standard, and accuracy dependence of interdomain converters, the basis of the conversion and the sources of error are easier to uncover. Every A/D converter contains a standard voltage or current source and every $\Delta t/D$ converter contains a standard clock oscillator, as expected from concept 7 above. In both cases the conversion accuracy depends directly upon the standard sources and, for various types, to a greater or lesser degree upon the other converter characteristics.

Conversions of data within domains can often be accomplished with high accuracy by simple transfer devices that require no comparison or reference standard. For instance, a resistor can be used to convert current to voltage or vice versa; the shift register will convert between serial digital and parallel digital domains.

Domain Converter Classification

A classification scheme for data conversion devices would seem desirable for two purposes: to categorize by function the great many devices available, and to provide a way to organize these devices into complete measurement systems. It is natural and useful to classify converter devices according to the domains which the device converts from

SERIES 7620 GAS CHROMATOGRAPHS

Cryogenic Chromatography Easy and Effective

With the 7620 GC's cryogenic module, sub-ambient oven temperature control is as easy and effective as high-temperature control has been for years.

It's easy because the cryogenic module controls oven temperature continuously down to −70°C and holds it within 0.1°C, for isothermal or programmed operation. It's synchronized with programmer operation: a blinking light tells you when the oven has cooled to the starting temperature, whether cryogenic or near ambient. It operates either with economical liquid CO_2 down to −70°C or with compressed air in the trans-ambient range. And it's a standard option: you can order it installed on a new 7620 or install it yourself later, with relative ease, without modification to the programmer.

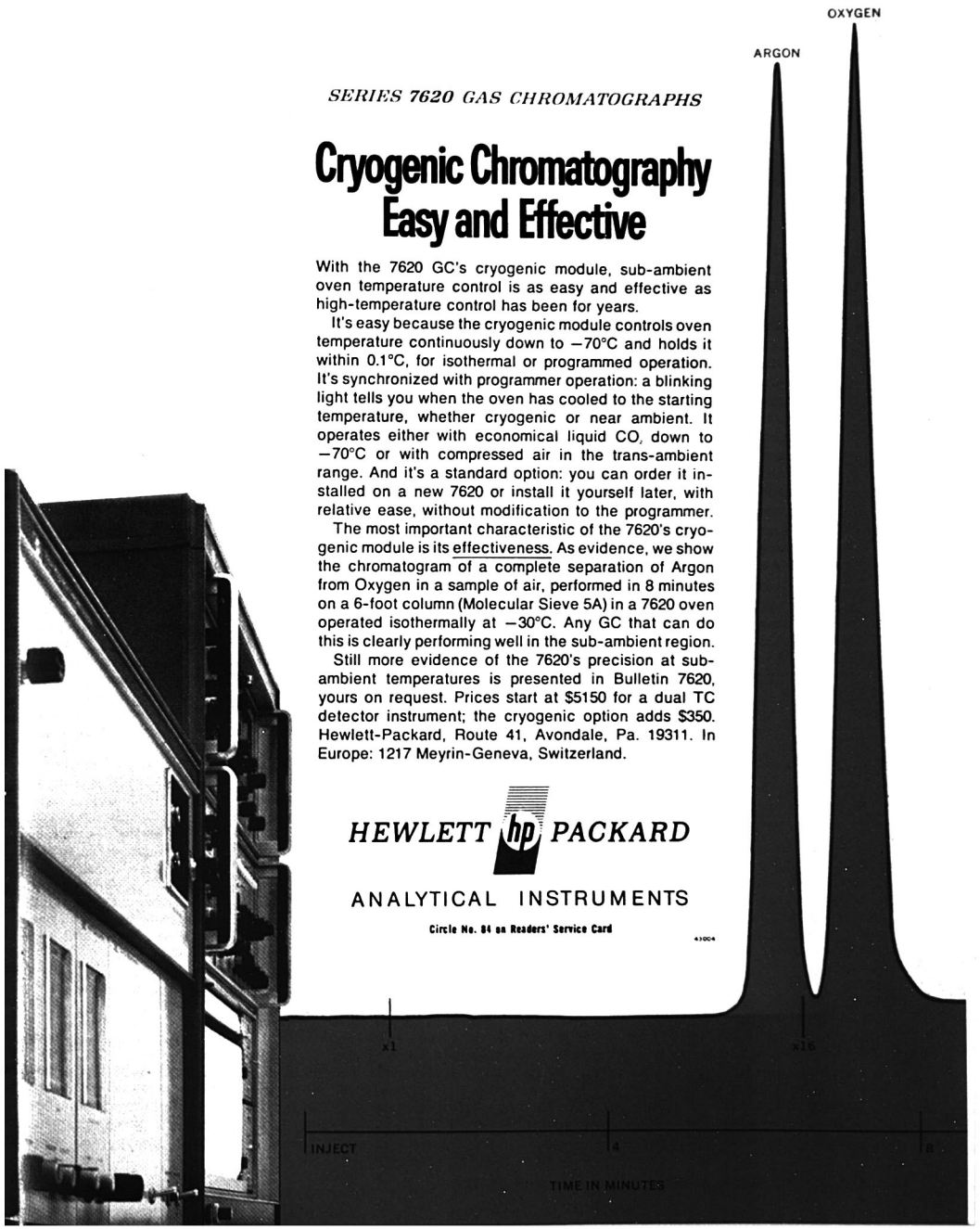
The most important characteristic of the 7620's cryogenic module is its effectiveness. As evidence, we show the chromatogram of a complete separation of Argon from Oxygen in a sample of air, performed in 8 minutes on a 6-foot column (Molecular Sieve 5A) in a 7620 oven operated isothermally at −30°C. Any GC that can do this is clearly performing well in the sub-ambient region.

Still more evidence of the 7620's precision at sub-ambient temperatures is presented in Bulletin 7620, yours on request. Prices start at $5150 for a dual TC detector instrument; the cryogenic option adds $350. Hewlett-Packard, Route 41, Avondale, Pa. 19311. In Europe: 1217 Meyrin-Geneva, Switzerland.

HEWLETT hp PACKARD

ANALYTICAL INSTRUMENTS

Circle No. 84 on Readers' Service Card



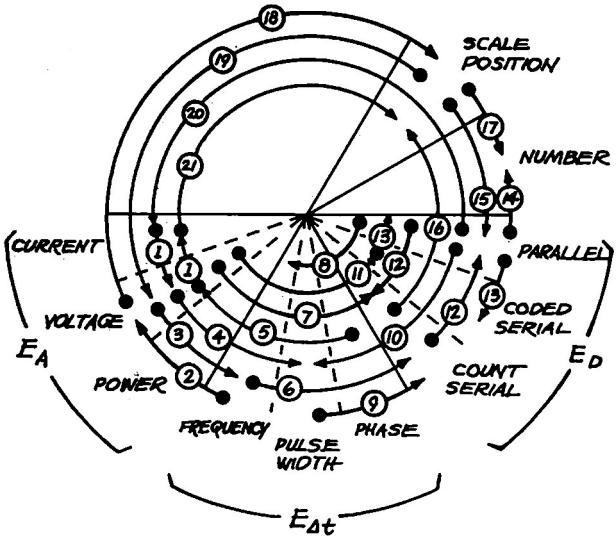


Figure 16. Domain converter classification map

1. Resistor, op amp circuit
2. Count rate meter
3. V-F converter
4. Dual slope A/D converter, ramp A/D converter
5. Phase angle meter
6. Counting gate timer
7. Staircase A/D converter
8. Programmable frequency divider
9. Gated oscillator
10. Preset digital timer
11. Successive approximation A/D converter
12. Counter
13. Shift register
14. Nixie tubes, printer
15. Shaft rotation encoder
16. Stepper motor
17. Mechanical shaft turns counter
18. Recorder
19. Retransmitting potentiometer
20. D/A converter (ladder or weighted sum)
21. Meter

and to. The domains map shows three electrical domains with three subdomains each, the scale position domain, the number domain, and the physical and chemical domains. For this classification, concentrating on electronic instrumentation, only the electrical, scale position, and number domains will be detailed. There are 110 possible interdomain and intradomain conversions among these 11 domains and subdomains. However, direct converters for most of these transitions are rare or unknown. Thus the number of categories required to encompass the common converters is not unwieldy.

The domains map is a very convenient means of organizing domain converter categories. Figure 16 shows 21 categories of converters arranged by input and output domains. Examples of devices for each listed domain transition are given in the accompanying table. This map and table clearly show what direct transitions are possible and which specific devices will do them. In addition, Figure 16 can be used to obtain and compare many possible combinations of devices to achieve a given transition by following connecting paths. Thus voltage-to-parallel digital converters could be made by paths 3–6–12, 7–12, 4–9–12, 11–13, and 18–15. These five types of A/D converters are all currently marketed.

For any required conversion, that path which has the fewest conversions should also be apparent from tracing the possible routes shown in Figure 16. However, the shortest path is not always the path of choice. For example, to go from scale position to parallel digital, the direct path is 15. However, absolute shaft rotation encoders with a high accuracy and ruggedness requirement could cost much more than the devices needed to take route 19–7–12.

Summary

The data domains and measurement concepts discussed here can be used to great advantage to analyze and describe available analog/digital instruments, to design or modify measurement systems, and to determine the sources of measurement errors. The data domains map can serve to show the data path from a block diagram or to devise a possible block diagram for instruments or modules, knowing only the input and output domains.

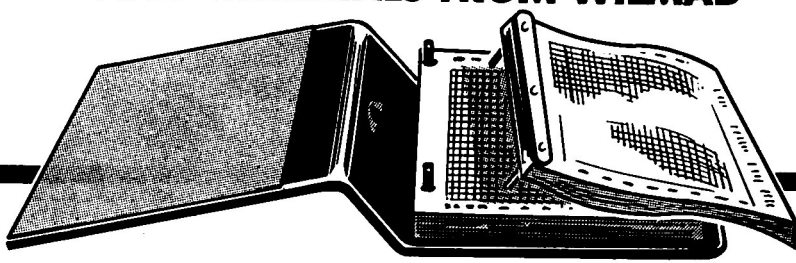
To analyze or describe an instrument, use the instrument description and block diagram to carefully follow the measurement data step-by-step through the instrument. Trace out the path on a domains map as shown in Figures 7–10 and 12–14. Now each converter corresponds to a line segment on the domains map. The conversion errors can be assessed by identifying and studying the reference source and difference detector for each converter. Modifications to instruments can be made by exchanging equivalent converters or by adding appropriate line segments to the instrument's domains map where new domains are to be included. New systems can be designed by completing a chart like Figure 16 for the devices available and comparing all the possible routes between the desired input and output domains.

Readers' comments, criticisms, and discussion on the concepts described in this article are welcomed. The author gratefully acknowledges the many helpful discussions he had with Dr. Howard Malmstadt, Dr. Stanley Crouch, Jim Ingle, and his graduate students during the evolution of these ideas.

References

(1) H. V. Malmstadt and C. G. Enke, "Digital Electronics for Scientists," W. A. Benjamin, New York, N. Y., 1969.
(2) D. Hoeschele Jr., "Analog-to-Digital-to-Analog Conversion Techniques," Wiley, New York, N. Y., 1968.
(3) H. V. Malmstadt and C. G. Enke, "Computer Logic," W. A. Benjamin, New York, N. Y., 1970.

NEW! YOU CAN NOW BUY YOUR NMR CHART PAPER, RECORDING INK, BINDERS AND CHEMICALS FROM WILMAD



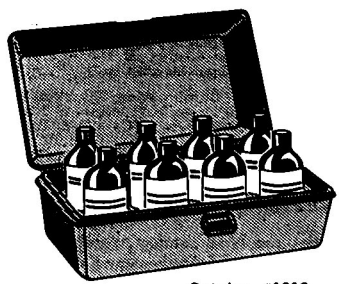
For years we have been known as manufacturers of the world's finest sample tubes and accessories for NMR high resolution spectroscopy. Now we have expanded our accessory line to include: NMR chart paper; recording ink; convenient telescopic post binders; deuterated solvents, reagents, and compounds; and a handy Mini/Chem/Pak containing eight of the most commonly used chemical solvents for NMR investigations.

CHART PAPER

Our chart paper is of excellent quality, with strong, clear grids, and the parameters have been updated to accommodate newer analyses such as time averaging, spin decoupling, and Fourier transformation.

We carry sizes of paper to fit the following spectrometer models: Varian A-60A, HA-100, XL-100, HR-220 and T-60; Jeolco; C-60HL, 4H-100, MH-60 and MH-100; Bruker; HFX-10 and HX-60.

The binders are covered in supported vinyl and will hold 500 sheets of chart paper in filed order at all times. You can read each sheet up to the binding edge without having to rethread sheets on posts after interfiling. Simply insert top posts in hollow bottom posts and snap shut.



Catalog #1010

NMR GRADE CHEMICALS

In addition to NMR chart paper, recording ink, and binders, we have also added to the Wilmad product line deuterated chemicals, reagents, and solvents and our Mini/Chem/Pak which contains eight 100 ml. bottles of the most commonly used NMR solvents and one syringe and needle in a handy, portable, polypropylene case. Additional syringes are available for use with these solvents. Included are NMR grades of chloroform, methanol, carbon tetrachloride, methylene chloride, trichlorofluoromethane, dimethylsulfoxide, trifluoroacetic acid, and isopropyl alcohol.

For complete details on Wilmad NMR chart paper, ink, binders, deuterated chemicals, and the Mini/Chem/Pak, write today to Wilmad Glass Company, Inc., Route 40 & Oak Road., Buena, N.J. 08310. Phone (609) 697-3000.

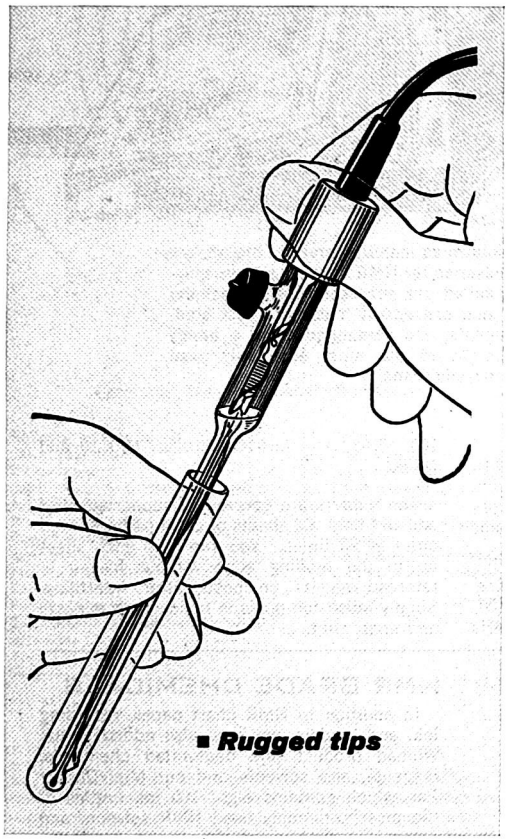
WILMAD

Glassware for NMR Spectroscopy

Circle No. 180 on Readers' Service Card

Thomas... COMBINATION pH ELECTRODES

For samples from 0.2 ml to a tankful



FAST... FAST... FAST

with PRECISION

COMBINATION ELECTRODES, Thomas. Consisting of a glass electrode and a silver-silver chloride reference electrode sealed into a single body. Bulb wall thickness and strength provide a sturdier electrode than heretofore available.

The single ¼-inch stem can be used with samples of small volume as well as with larger quantities, and is more convenient for transfer by hand from sample to sample than bringing the sample to electrodes in a fixed position.

The glass electrode inner element is shielded from electrostatic effects and stray electrical fields by the KCl solution of the reference electrode. Port is provided for KCl refill. Liquid junction is made by a sintered oxide plug sealed into the side of the lower stem 3/16-inch above tip.

The stable, fast response of this low resistance glass electrode and the short fixed distance between it and the reference electrode junction make the Thomas Combination Electrode particularly valuable in avoiding endpoint overshooting in electrometric titrations.* The compactness of the design permits use of small vessels and leaves more room for stirrers and buret tips.

Electrodes are each 6 inches long. Upper section is ½-inch diameter for use in standard electrode holders. Stem is ¼-inch diameter over the lower 4-inch length. Can be used with samples as small as 0.2 ml in narrow tubes.

Connector plug of the glass electrode fits into the jacks of most existing pH Meters, either directly or through available adapters.

4858-L15. Combination Electrode, Thomas, as above, 6 inches long, range pH 0 to 12, temperature range 0 to 75°C, with 30-inch shielded lead..... **40.00**

4858-L60. Ditto, range pH 0 to 14..... **43.00**

*See H. V. Malmstadt and E. H. Piepmeier, *Analytical Chemistry, Vol. 37, No. 1 (January, 1965), p. 34*

Thomas Laboratory Electrodes, see 1968 catalog pages 468-473, 488.
Thomas Industrial Electrodes, information upon request.

Thomas **ARTHUR H. THOMAS COMPANY**

Scientific Apparatus and Reagents

VINE STREET AT 3RD • P.O. BOX 779 • PHILADELPHIA, PA. 19105, U.S.A.

Circle No. 173 on Readers' Service Card

ANALYTICAL CHEMISTRY

January 1971, Vol. 43, No. 1

Editor: HERBERT A. LAITINEN

EDITORIAL HEADQUARTERS
Washington, D.C. 20036
1155 Sixteenth St., N.W.
Phone: 202-737-3337 Teletype: WA 23

Managing Editor: John K. Crum

Associate Editor: Virginia E. Stewart

Assistant Editor: Alan J. Senzel

Editorial Assistant: Sylvia Crawford

PRODUCTION STAFF

Direction of Design: Joseph Jacobs

Production Manager: Bacil Guiley

Associate Production Manager: Charlotte C. Sayre

Art Director: Norman W. Favin

NEW YORK OFFICE
733 Third Avenue
New York, N.Y. 10017
212-867-3161

Associate Editor: Josephine M. Petruzzi

EDITORIAL PRODUCTION OFFICE, EASTON, PA.

Assistant Editor: Elizabeth R. Rufe

ADVISORY BOARD: Norman G. Anderson, Klaus Biemann, C. G. Enke, James S. Fritz, John Funkhouser, Walter E. Harris, W. Wayne Meinke, Edwin P. Przybylowicz, William C. Purdy, Eugene M. Sallee, Donald T. Sawyer, A. Lee Smith, Lloyd R. Snyder, Samuel M. Tuthill, James D. Winefordner

AMERICAN CHEMICAL SOCIETY PUBLICATIONS DIVISION

Director of Publications, Richard L. Kenyon

Director of Business Operations, Joseph H. Kuney

Group Manager, Journals, John K. Crum

Executive Assistant to the Director of Publications, Rodney N. Hader

Circulation Director, Herbert C. Spencer

Assistant to the Director, Publications Division, William Q. Hull

REGIONAL EDITORIAL BUREAUS

PHILADELPHIA, Pa. 19107
Philadelphia National Bank Building
Broad & Chestnut Streets

CHICAGO, Ill. 60603
36 South Wabash Ave.

SAN FRANCISCO, Calif. 94104
57 Post St.

LOS ANGELES, Calif. 90005
422 South Western Ave.

HOUSTON, Texas 77002
514 Main Bldg.
1212 Main St.

FRANKFURT/MAIN, West Germany
32 Grosse Bockenheimerstrasse

LONDON, W. C. 2, England
27 John Adam St.

TOKYO, Japan
Iikura Central Building, 4th Floor
12 Iikura Kata-machi, Azabu
Minato-ku, Tokyo

Advertising Management

CENTURY COMMUNICATIONS CORP.
(for Branch Offices, see page 107 A)

For submission of manuscripts, see page 4 A.

Review Papers

The special review issues each April, alternating between fundamental and applied reviews, have become a well established and appreciated feature of ANALYTICAL CHEMISTRY. Written by recognized authorities in various methodological specialties or in fields of application of analytical methods, the articles have served as a set of biennial progress reports that have proved valuable for established workers to keep up with their fields and for new entrants into the various specialties. We have every intention of keeping these review series going, of course adding and subtracting specialties as changes in their activity appear to warrant.

In addition to these features, articles in the A pages, particularly Reports for Analytical Chemists and the Instrumentation articles, constitute reviews on subjects of interest to analytical chemists. The Reports generally are written in a more popular style than research papers, and serve to give general background for nonspecialists. Instrumentation articles are usually at an intermediate technical level between research articles and general interest features. While A page material is abstracted, it is often not bound permanently with research material in chemical libraries.

Occasionally, there appears to be a review paper that fits none of these categories. If it describes a subject that is not appropriate for periodic review, and makes a substantive contribution by integrating, evaluating, or correlating past research, then it appears appropriate to include such a review in the technical section of the journal. An example of such an article appears on page 93 of the current issue. While it is not intended that review articles shall become a regular feature in the technical section, neither should they be arbitrarily excluded just because they deal with new evaluations of past data rather than presentation of new data.



General Analysis of Potentiostatic Current–Time Curves for Cylindrical Electrodes

Sidney Barnartt and Charles A. Johnson[1]

Edgar C. Bain Laboratory for Fundamental Research, United States Steel Corporation, Monroeville, Pa. 15146

A general equation is developed to approximate the current–time behavior of cylindrical electrodes maintained at constant potential. This equation provides a simple means of analyzing experimental current–time curves to evaluate the charge–transfer current with good inherent accuracy (±2%). *A priori* knowledge of reaction orders or diffusivities is not required. The same form of the current–time equation and the same analytical method apply to spherical and cylindrical electrodes. Also, in the limit of infinite radius, the equation reduces to an equally useful relation for planar electrodes.

A METHOD OF ANALYZING potentiostatic current–time curves for cylindrical electrodes was developed in a previous paper (*1*). That method requires prior knowledge that the electrode reaction being studied is first order with respect to reactant and first order with respect to reaction product. More general analyses, in which the reaction orders can exceed unity and need not be known *a priori*, have been developed for planar electrodes (*2, 3*) and for spherical electrodes (*4*). A similar general analysis is required for cylindrical electrodes, and this is developed in the present paper.

We are concerned here with moderately rapid electrode reactions (exchange current density $\gtrsim 10^{-4}$A cm^{-2}), so that the reaction rate at constant potential decreases with time as a result of concentration changes at the electrode surface. Another contribution to the current variation is the extra current required initially to charge the double layer. The problem is the determination of the current density, i_{ct}, characteristic of the charge-transfer process alone, from the measured current density–time (i–t) curve corresponding to a given applied potential.

APPROXIMATE GENERAL CURRENT–TIME RELATION FOR CYLINDRICAL ELECTRODES

The problem treated here involves general (higher-order) electrode reactions which are controlled by diffusional mass transfer as well as by the charge-transfer process. We consider a reaction of the usual type (*5*):

$$bB^{z+} + xX + ne^- = yY^{[(bz-n)/y]+} + wW \qquad (1)$$

For simplicity it is assumed that the electrical work involved all occurs during the rate-determining step; this restriction is readily lifted when desired (*2, 5*). The electrolyte is formulated to contain a large excess of supporting electrolyte, and also to contain one reactant and one product (W and X) in high concentration so that only substances Y and B change significantly in concentration. For these conditions, the net anodic reaction rate at the electrode surface at time t, expressed as current density $i(t)$, is (*2*)

$$i(t) = i_o \left(\frac{c_Y}{c_Y{}^o}\right)^{y/\nu} \exp\left[(1-\beta)\frac{n}{\nu}\epsilon\eta\right] - i_o \left(\frac{c_B}{c_B{}^o}\right)^{b/\nu} \exp\left[-\beta\frac{n}{\nu}\epsilon\eta\right] \qquad (2)$$

Here i_o is the exchange current density, β the transfer coefficient, and ν the stoichiometric number of the charge-transfer mechanism; $c_Y{}^o$, $c_B{}^o$ are the bulk concentrations of Y and B and c_Y, c_B the concentrations at the electrode surface at time t; $\epsilon \equiv F/RT$. Overpotential η is the potential step applied to the electrode, which is initially at the reversible potential. The reaction order is y/ν with respect to component Y and b/ν with respect to B; it is assumed that the reaction orders are unknown, to be determined from the potentiostatic experiments.

At time zero, just after the potential step is applied but before any concentration changes occur, the theoretical current density at the electrode is the desired charge-transfer controlled current density: (The theoretical current density at $t = 0$ was designated $i_{t=0}$ in our previous papers, and is identical with the present i_{ct}.)

$$i_{ct} = i_o \exp\left[(1-\beta)\frac{n}{\nu}\epsilon\eta\right] - i_o \exp\left[-\beta\frac{n}{\nu}\epsilon\eta\right] \qquad (3)$$

In a real experiment the measured current density at $t \to 0$ is greater than i_{ct} because of the current required to charge the double layer (*6*). This, coupled with the well known distorting effects of potentiostat rise time and of incomplete IR compensation, means that the initial part of a measured i–t curve does not obey Equation 2 and, for our purposes, is unavailable for the determination of i_{ct}. Hence i_{ct} is considered a constant of the experiment, to be obtained by analysis of the later portion of the i–t curve. For this analysis, we sought a general analytic expression for the theoretical i–t behavior.

The general cylindrical diffusion problem, having the current at the electrode boundary as given in Equation 2, can not be solved in closed form by the usual Laplace-transform method. In this paper we propose an approximate general solution of this cylindrical problem which is based upon a solution of the corresponding spherical-electrode problem given in a previous treatment (*4*). In that treatment, higher-order reactions at spherical electrodes are described by the following potentiostatic current–time relation:

$$\frac{i(t)}{i_{ct}} \simeq \frac{\delta}{1+\delta} + \frac{1}{1+\delta} C[\lambda(1+\delta)\sqrt{t}] \qquad (4)$$

$$C[x] \equiv \exp(x^2)\,\mathrm{erfc}(x) \qquad (5)$$

$$\delta \equiv [r_s(\lambda_Y + \lambda_B)]^{-1} \qquad (6s)$$

[1] Present address, Division of Materials Science, Argonne National Laboratory, Argonne, Ill. 60439.

(1) C. A. Johnson and S. Barnartt, *J. Phys. Chem.*, 73, 3374 (1969).
(2) S. Barnartt and C. A. Johnson, *Trans. Faraday Soc.*, 63, 431 (1967).
(3) S. Barnartt and C. A. Johnson, *J. Phys. Chem.*, 71, 4430 (1967).
(4) C. A. Johnson, S. Barnartt, and F. D. Glasser, *J. Electroanal. Chem.*, in press.
(5) R. Parsons, *Trans. Faraday Soc.*, 47, 1332 (1951).
(6) K. B. Oldham, *J. Electroanal. Chem.*, 11, 171 (1966).

Table I. Effect of Reaction Order with Respect to Y on the Range of Validity of Equation 4

$D_Y = D_B = 10^{-5}$ cm^2 s^{-1}, 25 °C

Test No.	$\frac{n}{\nu}$	$\frac{y}{\nu}$	$\frac{b}{\nu}$	i_o, (mA cm^{-2})	γ'[a]	δ	λ, ($s^{-1/2}$)	R_{05}[b]
Group I: $c_Y^\circ = c_B^\circ = 5 \times 10^{-5}$ mol cm^{-3}; $\eta = 10$ mV; $\beta = 0.5$; $a = 0.5$ mm								
1	2	2	1	0.5	1/2	0.220	0.1078	0.529(−)
2	3	3	1	0.5	1/3	0.130	0.1824	0.613(−)
3	4	4	1	0.5	1/4	0.082	0.289	0.650(−)
4	2	1	2	0.5	2	0.346	0.0686	<0.38(+)
5	3	1	3	0.5	3	0.319	0.0744	0.577(+)
6	4	1	4	0.5	4	0.304	0.0780	0.721(+)
Group II: $c_Y^\circ = 4 \times 10^{-5}$, $c_B^\circ = 10^{-5}$ mol cm^{-3}; $\eta = 30$ mV; $\beta = 0.75$; $a = 0.1606$ mm								
7	1	1	1	1	4	0.3	0.246	<0.35(−)
8	2	2	1	0.764	2	0.3	0.246	0.621(−)
9	3	3	1	0.412	4/3	0.3	0.246	0.687(−)
10	4	4	1	0.233	1	0.3	0.246	0.708(−)

[a] $\gamma' = (b/y)(c_Y^\circ/c_B^\circ)$.
[b] The sign of the deviation, given in parentheses, is positive when the approximate current exceeds the true current.

$$\lambda \equiv \lambda_Y \sqrt{D_Y} + \lambda_B \sqrt{D_B} \tag{7}$$

$$\lambda_Y \equiv \frac{(y/\nu)^2 i_o \exp[(1-\beta)(n/\nu)\epsilon\eta]}{(n/\nu)F\, c_Y^\circ D_Y};$$

$$\lambda_B \equiv \frac{(b/\nu)^2 i_o \exp[-\beta(n/\nu)\epsilon\eta]}{(n/\nu)F c_B^\circ D_B} \tag{7a}$$

where D_Y and D_B are the diffusivities of substances Y and B, and r_s is the radius of the sphere. Equation 4 is a good approximation so long as the concentration ratios of reactant (c_Y/c_Y°) and product (c_B/c_B°), which appear in Equation 2, do not deviate significantly from unity. The present treatment of cylindrical electrodes is based on Equation 4, with the assumption that the general i–t relation for a cylinder of radius a can be described approximately by that for a sphere of radius $(8/3)a$. This assumption was shown to be a useful one in the previous treatment of first-order reactions at cylindrical electrodes (*1*). Thus we simply set

$$\delta = 3/8a(\lambda_Y + \lambda_B) \tag{6c}$$

and utilize Equation 4 as our approximate general i–t relation for reactions of any order at cylindrical electrodes. This i–t relation has the same form as that developed for first-order reactions at cylindrical electrodes, and its form makes it suitable for use in analyzing experimental i–t curves (*1*). It remains to be shown how generally valid it is for higher-order reactions, and with what accuracy it permits us to analyze i–t curves.

VALIDITY OF THE APPROXIMATE CURRENT-TIME RELATION

To determine how closely Equation 4 reproduces the true i–t behavior, we compared it with theoretical i–t curves calculated numerically for some 200 particular cases of higher-order reactions at cylindrical electrodes. The true numerical solutions of the boundary-value problem were generated following the Schmidt method (*7*). In comparing the true curve with the corresponding approximate curve from Equation 4, the reaction time t' at which the two curves first deviate by 5% was determined. The corresponding current ratio, $R_{05} \equiv i(t')/i_{ct}$, is utilized below as a single measure of the range of validity of Equation 4, namely the current range $1 > i(t)/i_{ct} > R_{05}$.

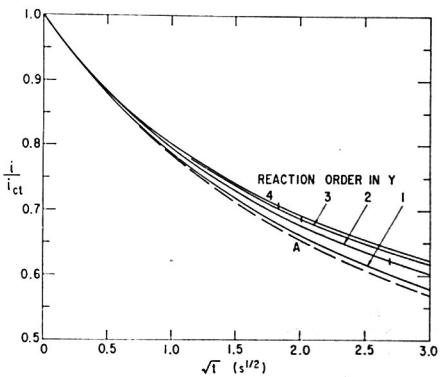


Figure 1. True potentiostatic current–time curves for reactions first-order in B and of order 1–4 in Y. Broken curve A is the approximate curve from Equation 4

The range of validity of Equation 4 contracts as the reaction order with respect to anodic reactant Y or to cathodic reactant B increases, while the other mechanistic parameters (β, ν, and i_o) and the adjustable experimental variables are maintained constant. This is exemplified by the Group I tests listed in Table I. In these tests the two quantities λ and δ, which appear in Equation 4, vary with reaction order. It is possible, however, to maintain λ and δ essentially constant by adjusting the value of i_o only, as was done for the Group II tests of Table I. True i–t curves for the Group II tests are plotted in Figure 1. The single approximate i–t curve corresponding to all Group II tests is also plotted here (broken curve A). A short vertical line on each of the higher-order curves indicates the range of validity. Again, the range of validity of the approximate equation is seen to contract as the reaction order increases This result with cylindrical electrodes parallels that previously found with spherical electrodes and has the same origin (*4*).

(7) H. S. Carslaw and J. C. Jaeger, "The Conduction of Heat in Solids," 2nd Ed., Section 18.3, Clarendon Press, Oxford, England, 1959.

Table II. Effects of Mechanistic Parameters (i_o, β) and Electrode Radius on R_{05}[a]

$y/\nu = n/\nu = 2$, $b/\nu = 1$, $D_Y = D_B = 10^{-5}$ cm² s^{-1}, 25 °C.

Test No.	c_Y^o × 10^5	c_B^o × 10^5	η	β	i_o	a	γ'	δ	λ	R_{05}
1	1	1	10	0.25	0.1	0.302	0.5	0.3	0.1310	0.540(−)
2	1	1	10	0.5	0.1	0.366	0.5	0.3	0.1078	0.540(−)
3	1	1	10	0.75	0.1	0.445	0.5	0.3	0.0888	0.540(−)
4	2	1	20	0.75	0.1	0.739	1	0.3	0.0535	0.599(−)
5	2	1	20	0.5	0.01	0.501	1	0.3	0.00789	0.600(−)
6	2	1	10	0.5	0.1	6.65	1	0.03	0.0595	0.394(−)
7	2	1	10	0.5	0.1	1.994	1	0.1	0.0595	0.455(−)
8	2	1	10	0.5	0.1	0.665	1	0.3	0.0595	0.508(−)
9	2	1	20	0.5	0.3	0.501	1	0.01	0.0789	0.522(−)
10	2	1	20	0.5	0.03	0.501	1	0.1	0.0237	0.561(−)
11	2	1	20	0.5	0.01	0.501	1	0.3	0.00789	0.600(−)

[a] Units: a (mm); c_Y^o, c_B^o (mol cm^{-2}); η (mV); i_o (mA cm^{-2}); λ (sec$^{-1/2}$).

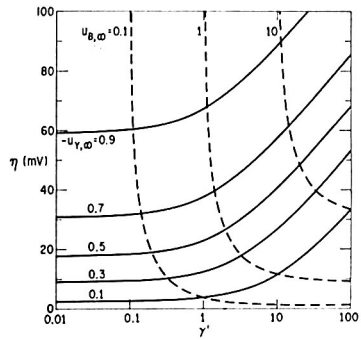


Figure 2. Ultimate concentration changes for reactions second-order in Y and first-order in B, cylindrical electrodes, $D_Y = D_B$, 25 °C

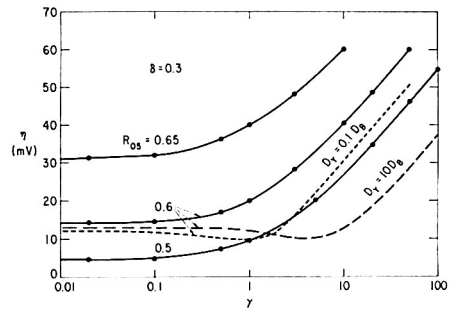


Figure 3. Curves of specified range of validity for Equation 4, reactions second-order in Y and first-order in B. Solid curves: $D_Y = D_B$; 25 °C

In assessing the effects of the other mechanistic parameters (β and i_o) and of the experimental variables (overpotential, cylinder radius, concentration, and diffusivity) on the validity of Equation 4, we make use of the fact that the concentration changes which are possible under potentiostatic conditions are limited. Any change, such as a decrease in η, which reduces the maximum possible concentration changes is expected to yield a greater range of validity, since Equation 4 becomes less accurate as the concentration changes increase. In the special case of equal diffusivities, we can calculate the ultimate concentration changes at the electrode surface (as $t \rightarrow \infty$) for a reaction of any order: relative concentration changes at the electrode as $t \rightarrow \infty$, defined by

$$u_{Y,\infty} \equiv [(c_Y - c_Y^o)/c_Y^o]_\infty, \; u_{B,\infty} \equiv [(c_B - c_B^o)/c_B^o]_\infty$$

are given precisely by the relations:

$$(1 - \gamma' u_{Y,\infty})^{b/\nu}/(1 + u_{Y,\infty})^{y/\nu} = \exp[(n/\nu)\epsilon\eta] \quad (8)$$

$$u_{B,\infty}/u_{Y,\infty} = -\gamma'; \; \gamma' \equiv (b/y)(c_Y^o/c_B^o) \quad (8a)$$

which are derived in the Appendix for the condition $D_Y = D_B$. Surprisingly, Equation 8 shows no influence of electrode radius; it is different in this respect from the corresponding relation for spherical electrodes (*4*). It is, in fact, the same as the planar-electrode relation for the condition of equal diffusivities (*3*).

Equation 8 permits us to make general predictions concerning the effects of the experimental variables on the range of validity of Equation 4. It shows that $u_{Y,\infty}$ and $u_{B,\infty}$ are not affected by i_o or by β at constant η and γ', hence we expect no effect of i_o or of β on the range of validity. This was confirmed, and is demonstrated by tests 1–5 in Table II, which refers to a reaction second-order in Y and first-order in β under the condition $D_Y = D_B$. In fact, even when the diffusivities differed by as much as a factor of 10, the range of validity was found to be independent of i_o and β. (A diffusivity ratio of 10 is greater than that expected in ordinary electrode reactions; it was used here and below to exaggerate any effects of differing diffusivities.)

With varying η and concentration ratio, we might expect that curves of constant range of validity would be similar to the curves of constant $u_{Y,\infty}$ shown in Figure 2, when the diffusivities are equal. This was found to be so as is shown by the solid curves in Figure 3, but with unequal diffusivities the curves of constant R_{05} become displaced as is demonstrated by the two broken curves. The abscissa in Figure 3 is the variable $\gamma \equiv (b/y)(c_Y^o/c_B^o)(D_Y/D_B)$, and is the same as γ' when the diffusivities are equal; γ is so defined when the diffusivities are unequal by analogy with the case of higher-order reactions at spherical electrodes (*4*). The three solid curves show that R_{05} changes much more slowly at the higher overpotentials; changes in η or γ above the curve of $R_{05} = 0.65$ produce little further change in R_{05}. This is clearly demonstrated by

the data in Figure 4, which shows also the existence of a minimum range of validity at large η for all diffusivity ratios from 0.1 to 10. It is evident from Figure 3 that we can extend the range of validity of Equation 4 for a net anodic reaction by increasing the bulk concentration of the anodic reactant (increasing γ).

In the above discussion Equation 8 was utilized successfully to predict effects of experimental variables on R_{0i}, based upon the idea that any variation which reduces the ultimate concentration changes is expected to improve the accuracy of the approximate i–t relation (Equation 4) and hence to reduce the value of R_{0i}. There is one variable, however, namely, the electrode radius a, whose effect on R_{0i} is not indicated by a parallel effect on ultimate concentration changes. Equation 8 shows that variations in radius, at constant η and γ', cause no variation in $u_{Y,\infty}$ or $u_{B,\infty}$; but in fact R_{0i} can be changed markedly by changing the electrode radius (thus changing δ). The fact is clearly demonstrated by tests 6–11 of Table II. Here δ is increased in tests 6–8 by decreasing a and in tests 9–11 by decreasing i_o; in both cases a substantial increase in R_{0i} results. The fundamental basis for this δ effect becomes evident when we consider the form of the approximate i–t relation: Equation 4 requires the current ratio at long times to approach the constant value $\delta/(1 + \delta)$, whereas the current at a cylindrical electrode must approach zero as $t \to \infty$ (proof given in the Appendix). Thus an increase in δ increases the value $\delta/(1 + \delta)$ which the approximate current ultimately attains, and causes the approximate i–t curve to be a poorer fit to the true curve.

ANALYSIS OF CURRENT-TIME CURVES

In the determination of i_{ct} from a potentiostatic current-time curve, the curve at very short times and at relatively long times can not be used. The initial part of an experimental curve must deviate from Equation 4, as discussed above. For analytical purposes we arbitrarily assume here that such deviations become negligible when the faradaic current has fallen to 0.9 i_{ct}; this condition can be realized in practice if the reaction being studied is not too rapid. The charge-transfer process ceases to exert appreciable control over the reaction rate after the current has fallen to 0.5 i_{ct} (*8*, *9*); the curve at longer times, therefore, will not yield an accurate value for i_{ct}. Accordingly, in the numerical analyses presented below, we have utilized the current range $0.9 > i(t)/i_{ct} > 0.5$ when $R_{0i} < 0.5$, and the range $0.9 > i(t)/i_{ct} > R_{0i}$ when $R_{0i} > 0.5$.

A method of evaluating i_{ct}, based upon an i–t relation having the form of Equation 4, has already been described (*1*) for the case of first-order reactions at cylindrical electrodes. This method, called the "difference-ratio" method, was successful in the first-order case, yielding i_{ct} with good accuracy (within ± 2%); hence, the same method was applied in the present study of higher-order reactions.

The difference-ratio method of analysis involves three current measurements, made at times t, $4t$, and $9t$, where t is arbitrary. The three measurements yield the difference ratio

$$\rho \equiv [i(t) - i(4t)]/[i(4t) - i(9t)]$$

This permits us to calculate the quantity $\lambda(1 + \delta)$, appearing in Equation 4, by the use of the relation (*10*)

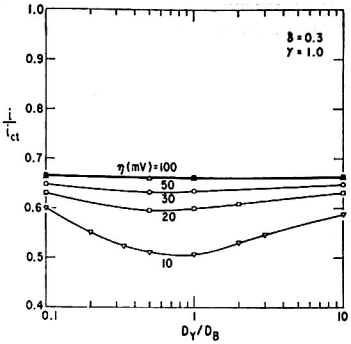


Figure 4. Range of validity of Equation 4, reactions second-order in Y and first-order in B. Plotted points are R_{0i} determinations, 25 °C

$$\lambda(1 + \delta)\sqrt{t} = \frac{b_0(\rho - 1) + b_1(\rho - 1)^2}{1 + b_2(\rho - 1)} \qquad (9)$$

$$b_0 = 0.55735,\ b_1 = -0.25133,\ b_2 = -0.56485$$

Next we calculate δ (whence also λ) from two of the three measured currents using (*11*)

$$\frac{i(t)}{i(4t)} = \frac{\delta + C[\lambda(1 + \delta)\sqrt{t}]}{\delta + C[2\lambda(1 + \delta)\sqrt{t}]} \qquad (10)$$

where $C[x] \equiv \exp(x^2)\,\mathrm{erfc}\,(x)$. Finally i_{ct} is obtained by substituting the values of $i(t)$, λ, and δ into Equation 4. For this analysis, neither the reaction orders nor the diffusivities need be known.

To determine the inherent accuracy of this analysis with higher-order reactions, we used the true i–t curve (obtained numerically) as the "raw" data to be analyzed. In this way, we simulate experimental data of high accuracy indeed, so that any error in i_{ct} can be ascribed to inherent inaccuracies in the analytical method, resulting from the approximations made in arriving at Equation 4. Table III lists calculated mean values of i_{ct}, as obtained by the difference-ratio method, for representative particular cases of higher-order reactions. The inherent accuracy of the analysis is seen to be consistently good. Also there was little variation of the derived value of i_{ct} with selected t, individual values of i_{ct} being all within ±2% of the true value in each of the analyses listed in Table III. Therefore, even in cases where considerably more than the initial 10% of the current fall is inaccessible to the experimenter, we can expect good accuracy from this analytical procedure.

The degree of accuracy found here is the same as was found previously in the analysis of i–t curves for first-order reactions at cylindrical electrodes (*1*), and also for reactions of any order at spherical electrodes (*4*, *10*, *11*). In practice, the approximate nature of Equation 4 is expected to introduce an insignificant error in the analysis for i_{ct}, compared to the error introduced by experimental uncertainties in the current measurements.

In the limit of infinite electrode radius, $\delta = 0$ and Equation 4 reduces to

$$i(t)/i_{ct} = C[\lambda\sqrt{t}] \qquad (11)$$

(8) H. Gerischer and W. Vielstich, *Z. Physik. Chem.*, **3**, 16 (1955).
(9) K. B. Oldham and R. A. Osteryoung, *J. Electroanal. Chem.*, **11**, 397 (1966).
(10) S. Barnartt and C. A. Johnson, *Trans. Faraday Soc.*, **65**, 1091 (1969).
(11) S. Barnartt and C. A. Johnson, *J. Electroanal. Chem.*, **24**, 226 (1970).

Table III. Analysis of Representative Current–Time Curves for Higher-Order Reactions at Cylindrical Electrodes[a]

Test No.	$\frac{\gamma}{\nu}$	$\frac{b}{\nu}$	$\frac{n}{\nu}$	β	η	i_o	D_Y	D_B	c_Y^o	c_B^o	a	δ	λ	$R_{0.5}$	i_{ct} calcd.	Error, %
									$\times 10^5$							
1	2	1	2	0.5	10	0.1	1	1	2	1	1.994	0.1	0.0595	0.455(−)	0.0797	−0.2
2	2	1	2	0.25	45	0.1	1	1	10	0.1	0.249	0.3	0.1590	0.488(−)	1.332	−0.7
3	2	1	2	0.75	30	0.1	0.5	5	10	0.1	3.42	0.3	0.01687	0.554(−)	1.612	−0.5
4	2	1	2	0.75	100	0.1	5	0.5	0.4	20	0.1723	0.3	0.513	0.662(−)	0.702	−0.3
5	1	2	2	0.5	20	0.2	1	1	1	1	0.300	0.3	0.1316	0.361(+)	0.3443	+0.2
6	3	1	3	0.75	60	1	0.5	5	0.3	1	0.1819	0.1725	0.267	0.688(−)	5.743	−0.3
7	4	1	4	0.5	10	0.5	1	1	5	5	0.5	0.082	0.289	0.650(−)	0.858	−0.2

[a] Units: D_Y, D_B(cm^{2}s^{-1}); c_Y^o, c_B^o(mol cm^{-3}); i_o(mA cm^{-2}); η(mV); a(mm); $\lambda(s^{-1/2})$; calcd i_{ct} (mA cm^{-2}) is the mean value for all selected t; 25 °C.

which is the general i–t relation that was developed for planar electrodes (*2, 3, 8*) With planar electrodes, the analysis of an i–t curve based on Equation 11 requires only two current measurements, namely $i(t)$ and $i(4t)$, yielding i_{ct} with an inherent accuracy of ± 2% or better (*3*). Thus Equation 4 is a general potentiostatic i–t relation with very wide applicability. With the appropriate definition of δ, it can be used for analyzing experimental i–t curves obtained with reactions of unknown order and with electrodes of cylindrical, spherical or planar geometry.

We have considered above only the evaluation of i_{ct} at a given overpotential; further measurements at various overpotentials are required to determine the parameters β, i_o, and ν characteristic of the charge-transfer mechanism, but this follows known procedures which will not be restated here.

CONCLUSIONS

It is concluded that a general current–time relation of the form

$$\frac{i(t)}{i_{ct}} \simeq \frac{\delta}{1+\delta} + \frac{1}{1+\delta} \exp\left[\lambda^2(1+\delta)^2 t\right] \operatorname{erfc}\left[\lambda(1+\delta)\sqrt{t}\right]$$

is a good and useful approximation to the true potentiostatic current–time behavior for both cylindrical and spherical electrodes and, in the limit $\delta = 0$, for planar electrodes as well. This equation yields current values which are within 5% of the true values for most of the reaction time over which the charge-transfer process controls the reaction rate to an appreciable extent. It provides an accurate means of analyzing an experimental current–time curve to evaluate the charge-transfer controlled current density, i_{ct}, corresponding to the applied potential.

APPENDIX

Ultimate Concentration Changes and Current at Cylindrical Electrodes. For first-order reactions at cylindrical electrodes, the concentration profiles ultimately reach a steady state and the corresponding reaction current is zero (*1*). We are not able to prove that steady state is achieved for higher-order reactions, but shall make the very plausible assumption that this is, in fact, the case.

The diffusion problem for higher-order reactions at a cylindrical electrode of radius a can be written in terms of the fractional concentration changes

$$u_Y(r,t) \equiv \frac{c_Y(r,t) - c_Y^o}{c_Y^o}; \quad u_B(r,t) \equiv \frac{c_B(r,t) - c_B^o}{c_B^o}$$

as follows:

$$\frac{\partial u_Y(r,t)}{\partial t} = D_Y\left[\frac{\partial^2 u_Y(r,t)}{\partial r^2} + \frac{1}{r}\frac{\partial u_Y(r,t)}{\partial r}\right]$$

$r > a$, $t \geq 0$: (A1)

$$\frac{\partial u_B(r,t)}{\partial t} = D_B\left[\frac{\partial^2 u_B(r,t)}{\partial r^2} + \frac{1}{r}\frac{\partial u_B(r,t)}{\partial r}\right]$$

$t = 0$: $\quad u_Y(r,0) = u_B(r,0) = 0$

$t \geq 0$: $\quad u_Y(r,t)$, $u_B(r,t)$ bounded

[In our previous treatment of first-order reactions one boundary condition (Equation A3 of Ref. *1*) was incorrect; it should be replaced with the bounded condition which is stated here for the general problem of higher-order reactions.]

$$r = a,\ t \geq 0: \quad \frac{i(t)}{nF} = D_Y\frac{c_Y^o}{y}\left(\frac{\partial u_Y(r,t)}{\partial r}\right)_{r=a} = -D_B\frac{c_B^o}{b}\left(\frac{\partial u_B(r,t)}{\partial r}\right)_{r=a} = \frac{i_o}{nF}\left\{(1+u_Y(a,t))^{y/\nu} \times \exp\left[(1-\beta)\frac{n}{\nu}\epsilon\eta\right] - (1+u_B(a,t))^{b/\nu} \times \exp\left[-\beta\frac{n}{\nu}\epsilon\eta\right]\right\} \quad \text{(A2)}$$

With the assumption that steady state is achieved as $t \to \infty$, the time derivatives in Equation (A1) disappear, and the limiting solutions of Equation A1 are

$$\lim_{t\to\infty}[u_Y(r,t)] = u_{Y,\infty} + k_Y \ln r$$

$$\lim_{t\to\infty}[u_B(r,t)] = u_{B,\infty} + k_B \ln r$$

The condition that $u_Y(r,t)$ and $u_B(r,t)$ must remain bounded ensures that k_Y and k_B vanish, so that the concentrations become everywhere the constant values $u_{Y,\infty}$ and $u_{B,\infty}$ as $t \to \infty$. The proportionality of the current $i(t)$ to the gradient of $u_Y(r,t)$ or $u_B(r,t)$ then yields

$$\lim_{t\to\infty}[i(t)] = 0$$

On inserting these results back into Equation A2 we find a relation between the ultimate concentration changes $u_{Y,\infty}$ and $u_{B,\infty}$:

$$(1+u_{B,\infty})^{b/\nu}/(1+u_{Y,\infty})^{y/\nu} = \exp\left[(n/\nu)\epsilon\eta\right] \quad \text{(A3)}$$

This is the Nernst equation, and thus the steady state achieved in the limit $t \to \infty$ is the state of thermodynamic equilibrium corresponding to the potential change η.

In order to obtain expressions for the individual values $u_{Y,\infty}$ and $u_{B,\infty}$, an additional relationship is required. This can be found in the special case $D_Y = D_B = D$. To obtain this relationship we shall suppose that

$$u_B(r,t) \equiv -\frac{b}{y}\frac{c_Y^o}{c_B^o} u_Y(r,t) + f(r,t) \qquad \text{(A4)}$$

where $f(r,t)$ is some unspecified function; in fact, we shall show that $f(r,t)$ is identically equal to zero. Using Equation A1, together with $D_Y = D_B = D$, we find that $f(r,t)$ must satisfy

$$r > a,\ t \geq 0: \quad \frac{\partial f(r,t)}{\partial t} = D\left[\frac{\partial^2 f(r,t)}{\partial r^2} + \frac{1}{r}\frac{\partial f(r,t)}{\partial r}\right] \qquad \text{(A5)}$$

with the initial condition $f(r,0) = 0$, $r \geq a$. Equation A2 similarly yields

$$r = a,\ t \geq 0: \quad \frac{bc_Y^o}{yc_B^o}\frac{\partial u_Y(r,t)}{\partial r} + \frac{\partial u_B(r,t)}{\partial r} = \frac{\partial f(r,t)}{\partial r} = 0 \qquad \text{(A6)}$$

The unspecified function $f(r,t)$ is therefore one which satisfies Equation A5, has initial value zero for all $r \geq a$, and has zero gradient at $r = a$. Taking cognizance of the fact that Equation A5 is linear and of second-order in the variable r, we are at once led to the result that $f(r,t) \equiv 0$.

Returning to Equation A4 we now have

$$D_Y = D_B: \quad u_{B,\infty}/u_{Y,\infty} = -(b/y)(c_Y^o/c_B^o) \qquad \text{(A7)}$$

as the required second relationship between the ultimate fractional concentration changes $u_{Y,\infty}$ and $u_{B,\infty}$. Substitution of Equation A7 into Equation A3 immediately yields Equation 8 of the text.

RECEIVED for review June 19, 1970. Accepted October 1, 1970.

Simultaneous Determination of Silicate and Phosphate by an Automated Differential Kinetic Procedure

J. D. Ingle, Jr., and S. R. Crouch

Department of Chemistry, Michigan State University, East Lansing, Mich. 48823

A differential kinetic method is presented for simultaneous determinations of silicate and phosphate in mixtures. Phosphate and silicate each react with Mo(VI) to form yellow heteropoly acids which can be reduced to heteropoly blues. The initial rate of formation of the heteropoly blue from phosphate can be made much faster than the corresponding silicate heteropoly blue under certain experimental conditions. Thus phosphate can be determined with little interference from silicate. Silicate can be determined under a second set of conditions by measuring the initial rate of formation of β-12-molybdosilicic acid, which forms at a much slower rate than 12-molybdophosphoric acid. Data are presented to illustrate that 1–10 ppm of silicon can be determined in the presence of up to 10 ppm of phosphorus with better than 3% accuracy. Simultaneous phosphate determinations in the 1–10 ppm of P range in the presence of up to 50 ppm of Si can be made with 1% accuracy. Both species can be determined in mixtures in less than five minutes of total analysis time using an automated reaction rate system.

COLORIMETRIC PROCEDURES for the determination of phosphate and silicate are often based on the formation of the yellow heteropolymolybdates of these anions or the reduced heteropoly blues (*1*, *2*). Colorimetric determination of both anions in mixtures is difficult because the heteropolymolybdates of phosphate and silicate have quite similar absorption spectra as do the heteropoly blues (*3*). Mixtures of the two anions have generally been treated by separating the two species, by proper control of reaction conditions, or by adding reagents which destroy or prevent the formation of one of the heteropoly acids. For example, determinations of silicate in the presence of phosphate can involve separation of phosphate by precipitation prior to colorimetric determination of silicate (*4*), control of solution pH so that only the heteropoly blue of silicate is formed (*5*), or destruction of 12-molybdophosphoric acid (12-MPA) with a complexing agent such as oxalic acid (*6*). Phosphate can be determined in the presence of silicate by precipitating the silicate prior to colorimetric determination of phosphate (*4*), addition of tartaric acid to prevent formation of 12-molybdosilicic acid (12-MSA) (*6*), or selective extraction of 12-MPA into a suitable organic solvent (*7*, *8*). Simultaneous analyses of both species in mixture usually involve combinations of these techniques.

Because of the importance of silicate and phosphate determinations in the testing of such samples as natural waters, sewage, and boiler waters, steels, minerals, and soils, a rapid and accurate simultaneous differential kinetic method, which requires no separations, has been developed. The method is based on kinetic differences in the formation reactions of the heteropolymolybdates and the reduced heteropoly blues of phosphate and silicate. By proper pH control, the formation of the heteropoly blue from silicate, molybdate, and ascorbic acid can be made extremely slow in comparison to the formation of the corresponding phosphate heteropoly blue. Thus,

(1) Am. Pub. Health Assoc., Inc. New York, "Standard Methods for the Examination of Water, Sewage, and Industrial Wastes," 11th ed., 1960.
(2) F. Feigl, "Spot Tests In Inorganic Analysis," Elsevier Publishing Company, Amsterdam, the Netherlands, 1958.
(3) D. G. Boltz and M. G. Mellon, IND. ENG. CHEM., ANAL. ED., **19**, 873 (1947).
(4) I. M. Kolthoff, E. B. Sandell, E. J. Meehan, and S. Bruckenstein, "Quantitative Chemical Analysis," The Macmillan Company, London, England, 1969.
(5) H. L. Kahler, IND. ENG. CHEM., ANAL. ED., **13**, 536 (1941).
(6) R. A. Chalmers and A. C. Sinclair, Anal. Chim. Acta, **34**, 412 (1966).
(7) M. A. Desesa and L. B. Rogers, ANAL. CHEM., **26**, 1381 (1954).
(8) J. Paul, Anal. Chim. Acta, **25**, 178 (1960).

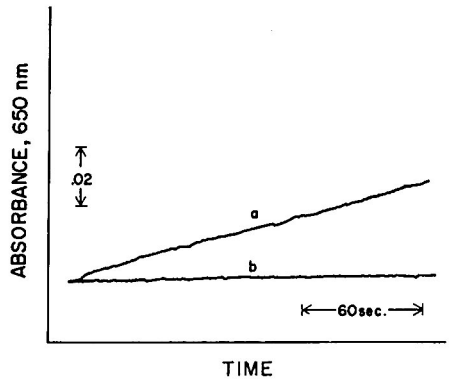


Figure 1. Recorded reaction rate curves for formation of the heteropoly blues of phosphate and silicate measured at 650 nm

(a) **2.5 ppm P and 50 ppm Si**
(b) **100 ppm Si**

measurement of the initial rate of heteropoly blue formation gives information related to the phosphate concentration with very little interference from silicate. With no reducing agent present, the two yellow heteropolymolybdates are formed at significantly different rates. The formation of 12-MPA is complete in a few seconds (*9*), while the formation of 12-MSA requires much longer reaction times. By delaying rate measurements until the 12-MPA formation is essentially complete, silicate can be determined with little interference from phosphate.

The differential rate procedure is precise and accurate for mixtures of phosphate and silicate. Phosphate in the range 2.5–10 ppm of P can be determined in the presence of up to 50 ppm of Si with relative errors of less than 1%. Silicate at the 2.5–10 ppm of Si level can be determined in the presence of up to 10 ppm of P with 1–3% accuracy. Higher concentrations of phosphate cause low results in silicate determinations.

GENERAL CONSIDERATIONS

A mechanistic study of the formation of 12-MPA and its reduction to the heteropoly blue has shown the reaction rate to be first-order in phosphate in both reactions (*9*, *10*). The formation of 12-MPA is fast, and the initial rate must be measured with a stopped-flow apparatus. The reduction of 12-MPA to the heteropoly blue is slower, and the initial rate can be measured with a conventional mixing apparatus. The fact that the 12-MPA formation equilibrium is much faster than the subsequent reduction, results in a steady state concentration of 12-MPA and a first-order dependence of phosphate in the reduction.

Silicate undergoes a similar reaction with molybdate. The kinetics of the formation of β-12-MSA have been studied and the rate was shown to be first-order with respect to silicate in perchloric acid (*11*). The β isomer of 12-MSA forms when the acid to molybdate ratio is greater than 1.5. The β form converts to the α isomer on standing (*12*).

In the present study, the formation of β-12-MSA was found to be first-order with respect to silicate in sulfuric acid solutions and much slower than the formation of 12-MPA. Thus, silicate can be determined by measuring the initial rate of β-12-MSA formation in a conventional mixing apparatus. Since the measurement is made within 1 minute after mixing, the slow conversion of the β-12-MSA to α-12-MSA is negligible.

Attempts to measure the initial rate of the reduction of β-12-MSA to the heteropoly blue and relate this to silicate concentrations failed. This failure can be attributed to the relatively slow rate of formation of β-12-MSA. In order for the reduction to be first-order in silicate, the reversible equilibrium step, formation of β-12-MSA, must be much faster than the irreversible reduction so that a steady state concentration of β-12-MSA exists. This condition is true for the reduction of 12-MPA, but not for β-12-MSA.

For a mixture of phosphate and silicate, both anions contribute to the rates of the heteropoly blue and heteropoly acid reactions as indicated in Equations 1 and 2:

$$\text{Rate}_{(b)} = k_{P(b)}\exp(-k_{P(b)}t)[PO_4^{3-}]_o + k_{Si(b)}\exp(-k_{Si(b)}t)[SiO_3^{2-}]_o \quad (1)$$

$$\text{Rate}_{(y)} = k_{P(y)}\exp(-k_{P(y)}t)[PO_4^{3-}]_o + k_{Si(y)}\exp(-k_{Si(y)}t)[SiO_3^{2-}]_o \quad (2)$$

where the subscripts b and y represent the formation of the heteropoly blues and the yellow heteropoly acids, respectively, and $[PO_4^{3-}]_o$ and $[SiO_3^{2-}]_o$ represent the initial concentrations of phosphate and silicate.

If the reaction conditions are manipulated so that the pseudo-first-order rate constants in Equations 1 or 2 differ significantly, then the kinetic contributions of phosphate and silicate to the total rate can be separated by measurement at the proper times. Differential kinetic methods for studying reaction mixtures with widely differing rate constants and the criteria for neglecting either the slower or faster reacting component have been presented (*13*, *14*).

Experimentally it was found that, under conditions where phosphate has been previously determined by the rate of reduction of 12-MPA (*10*), the rate of formation of β-12-MSA is extremely slow. Figure 1 shows reaction rate curves for a pure silicate sample (curve *b*) and a silicate–phosphate mixture (curve *a*). As can be seen, even a 100 ppm of Si sample gives a negligible reaction rate over the first several minutes after initiating the reaction. A sample containing 2.5 ppm of P, however, gives a relatively large change in absorbance over the same time period. This implies that $k_{Si(b)} << k_{P(b)}$. If the rate of heteropoly blue formation is measured during the initial stages of the reaction, Equation 1 becomes

$$\text{Rate}_{(b)} = k_{P(b)}[PO_4^{3-}]_o \quad (3)$$

Under all reaction conditions studied, the formation of 12-MPA was always much faster than that of β-12-MSA. Thus, the condition $k_{Si(y)} >> k_{P(y)}$ could not be obtained.

(9) A. C. Javier, S. R. Crouch, and H. V. Malmstadt, ANAL. CHEM., 40, 1922 (1968).
(10) S. R. Crouch and H. V. Malmstadt, *ibid.*, 39, 1084 (1967).
(11) L. G. Hargis, *ibid.*, 42, 1494 (1970).
(12) J. D. H. Strickland, J. Amer. Chem. Soc., 74, 862, 868, 872 (1952).
(13) H. B. Mark and G. A. Rechnitz, "Kinetics in Analytical Chemistry," Interscience Publishers, New York, N. Y., 1968.
(14) H. B. Mark, Jr., L. J. Papa, and C. N. Reilley, "Advances in Analytical Chemistry and Instrumentation," Vol. 2, Wiley, New York, N. Y., 1963, pp 255–385.

At lower acidities or higher molybdate concentrations than those used for the phosphate determination, the rate of formation of β-12-MSA is measurable after the phosphate has reacted. Figure 2 illustrates the recorded reaction rate curves for the reaction of molybdate with 10 ppm of P (curve *b*) and a mixture of 10 ppm of P and 2.5 ppm of Si (curve *a*). The reaction to form 12-MPA comes to equilibrium quite rapidly compared to the silicate reaction. Thus, the formation of 12-MPA offers little interference in measuring the rate of formation of β-12-MSA. If the measurement of the rate is made after 12-MPA has formed, but during the initial stages of the silicate reaction, Equation 2 can be written

$$\text{Rate}_{(y)} = k_{\text{Si}(y)}[\text{SiO}_4^{2-}]_0 \qquad (4)$$

EXPERIMENTAL

Spectrophotometric Measurements. The basic spectrophotometric reaction rate measuring system has been previously described (*15*). The absorbance mode was used for all rate measurements. This is necessary for silicate determinations because the % transmittance range over which the measurements are made varies with the phosphate concentration. Thus, nonlinearities would result in the % transmittance mode.

Rate Measurements. A fixed-time digital counting system (*15*) was used to yield a direct digital readout of reaction rates. Appropriate delay and measurement times were chosen as previously discussed (*15*). The progress of reactions was followed on a recorder to ensure that no abnormalities occurred during kinetic runs and to confirm that the automated rate measurements were made during the linear portion of the absorbance *vs.* time curve.

Phosphate Determinations. Reagents for the determination of phosphate were prepared as previously described (*15*). The reaction was followed at 650 nm. Two milliliters of acid–molybdate and 1 ml of the silicate and phosphate mixture were added to the cell and allowed to mix and equilibrate. The reaction was initiated by injecting 100 μl of the ascorbic acid solution into the cell with a hypodermic syringe.

Silicate Determinations. A stock solution of approximately 100 ppm of silicon was prepared by dissolving 1.015 g of $Na_2SiO_3 \cdot 9H_2O$ and diluting to 1 liter. The stock solution was diluted to provide concentrations of 2.5–50 ppm of Si. These working solutions were adjusted to pH 3 with H_2SO_4. Monomeric silicon units have been shown to be most stable in the 1–3 pH range and above pH 13 (*16*). This solution should be standardized by conventional gravimetric techniques for accurate silicate determinations.

A 0.155 Mo(VI) solution in 1.14*N* H_2SO_4 was prepared by dissolving 9.35 g of $Na_2MoO_4 \cdot 2H_2O$ in deionized water in a 250-ml volumetric flask. Eight milliliters of concentrated H_2SO_4 were then added and the solution was diluted to volume. This solution was allowed to stand one day before use. All solutions were stored in polyethylene bottles to prevent silicate leaching. The formation of the yellow heteropolymolybdates was followed at 400 nm. Two milliliters of the acid–molybdate solution were added to the reaction cell. The reaction was initiated by injecting 1 ml of the silicate sample or silicate and phosphate mixture with a syringe.

RESULTS AND DISCUSSION

Silicate Determination. Since the determination of silicate by measurement of the rate of formation of β-12-MSA has not previously been reported, initial experiments were done to determine the accuracy which could be expected for pure Si standards. Under the conditions chosen, the digital rate readout varies linearly with the silicate concentration over the 0–10 ppm of Si range. Results of silicate analyses based on one silicate standard are presented in Table I, and the data indicate 2% or better accuracy.

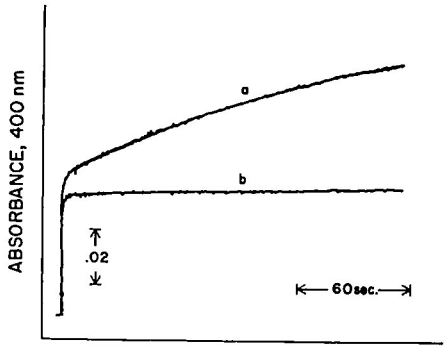


Figure 2. Recorded reaction rate curves for formation of 12-MPA and β-12-MSA measured at 400 nm

(*a*) **10 ppm P and 2.5 ppm Si**
(*b*) **10 ppm P**

Table I. Determination of Silicate

Digital readout[a]	Silicon concentration, ppm: Taken	Found[b]	Rel error, %
7980	3	3.05	+1.6
13338	5	5.10	+2.0
20919	8	...	...
26037	10	9.96	−0.4

[a] Averages of 5 results.
[b] Based on 8 ppm standard: integration time of 40 sec; premeasurement time, 45 sec.

Analysis of Phosphate–Silicate Mixtures. Analysis of phosphate by measurement of the initial rate of 12-MPA formation (*17*) or the initial rate of heteropoly blue formation has been reported (*18*). Mixtures of phosphate and silicate were prepared to determine if synergistic or other effects existed and to determine the concentration ranges over which Equations 3 and 4 are applicable. Results of the simultaneous determinations are shown in Table II. These data indicate that phosphate in the 0–10 ppm of P range can be determined with accuracies of about 1% in the presence of as much as 50 ppm of Si. The data also demonstrate that silicate can be determined with better than 3% accuracy in the presence of up to 10 ppm of P. Relative standard deviations were typically 2–4% for both determinations. For both silicate and phosphate analyses, 40-second measurement times and 45-second premeasurement times are used. The

(15) J. D. Ingle and S. R. Crouch, ANAL. CHEM., **42**, 1055 (1970).
(16) H. R. Skell in "Treatise on Analytical Chemistry," I. M. Kolthoff and P. J. Elving, Ed., Part II, Vol. 2, Wiley and Sons, Inc. New York, N. Y., 1961.
(17) A. C. Javier, S. R. Crouch, and H. V. Malmstadt, ANAL. CHEM., **41**, 239 (1969).
(18) S. R. Crouch and H. V. Malmstadt, *ibid.*, **39**, 1090 (1967).

Table II. Simultaneous Determination of Phosphate and Silicate

Concentration of mixtures taken, ppm		Concentration of mixtures found, ppm[a]			
Silicon	Phosphorus	Silicon	Rel error, %	Phosphorus	Rel error, %
0.0	5.0	...	...	...	...
2.5	10.0	2.57	+2.8	10.04	+0.4
5.0	5.0	4.94	−1.2	5.02	+0.4
5.0	50.0	4.55	−9.0	...	...
10.0	2.5	9.82	−1.8	2.48	−0.8
5.0	0.0	...	...	...	...
50.0	5.0	...	...	5.04	+0.8

[a] Based on 5-ppm silicon standard and 5-ppm phosphorus standard: integration time, 40 sec; premeasurement time, 45 sec.

45-second premeasurement time is sufficient for the reaction to form 12-MPA to come to equilibrium. Once standards have been run, 5 determinations of silicate and phosphate can be made in about 15 minutes.

For the highest phosphate concentration shown in Table II a negative error is evident in the determination of silicate. This error is not attributed to a synergistic effect, but to a "concentration depletion effect," which results because the formation of 12-MPA requires 12 moles of molybdenum for every mole of phosphate. Thus, at high phosphate concentrations, the molybdate concentration after reaction with phosphate is substantially lower than the initial concentration. Since the rate of formation of β-12-MSA is dependent on the molybdate concentration, the depletion of Mo(VI) results in a lower rate and errors in silicate determinations in the presence of large amounts of phosphate. Preliminary results obtained at lower acid and molybdate concentrations were satisfactory for pure silicate solutions. However, the concentration depletion effect became important at lower phosphate concentrations. Higher molybdate concentrations were tried to reduce the concentration depletion effect, but the high densities of these solutions prevented efficient mixing and caused noisy reaction rate curves.

Silicate determinations are not so accurate as phosphate determinations as shown by the data in Table II. There are several possible reasons for the lower accuracy in silicate determinations. The concentration depletion effect mentioned above can give low results if large amounts of phosphate (>25 ppm) are present. Positive errors can result if the phosphate reaction is not complete before the rate of formation of β-12-MSA is measured. The errors due to this latter effect also increase with increasing phosphate concentration. Thus, the silicate procedure is recommended only for phosphate concentrations in the range of 0–25 ppm of P.

Possibly this procedure can be extended to wider concentration ranges. Complete kinetic and equilibrium studies of the formation of the heteropolymolybdates and the heteropoly blues should yield information which can be used to optimize all reaction conditions. Such studies are now in progress in several laboratories.

Also simultaneous determinations of phosphate and silicate can probably be made using only one reaction by employing a stopped-flow apparatus to measure the rate of formation of both 12-MPA and β-12-MSA. Initial rates measured during the first few milliseconds can be related to the phosphate concentration, while after 30 seconds a second reaction rate measurement can be used to determine silicate. Work in this area is in progress.

RECEIVED for review July 23, 1970. Accepted October 5, 1970. Presented at 160th National Meeting, ACS, Chicago, Ill., Sept. 1970. One of us (J. D. Ingle, Jr.) gratefully acknowledges a National Science Foundation traineeship and an ACS Analytical Division Fellowship. This work was partially supported by NSF Grant No. GP-18123.

Radioisotopic X-Ray Analysis of Silver Ores Using Compton Scatter for Matrix Compensation

P. G. Burkhalter[1]

U. S. Department of the Interior, Bureau of Mines, College Park, Md. 20740

Radioisotopic X-ray analysis with semiconductor detectors was evaluated for determining silver in ores. X-ray and scatter peak intensities were obtained using computer processing for curve fitting backgrounds under the Ag Kα peaks and unfolding overlapping spectra. The discrete Compton and coherent scatter peaks obtainable with monoenergetic excitation were evaluated as internal standards for matrix compensation. The Ag Kα-to-Compton ratio provides compensation for X-ray absorption and a single, linear calibration curve can be used for silver determination in both uniform and variable matrix ores. For a set of samples taken from a drill core, silver was determined to within ±10% for concentrations above 3 oz/ton and the detection limit was 0.3 oz/ton (10 ppm). For variable matrix ores, silver can be determined within ±20%.

[1] Presently with U. S. Naval Research Laboratory, Code 7680, Washington, D. C. 20390.

SEMICONDUCTOR DETECTORS combined with radioisotopic sources are being used for nondiffractive X-ray analysis (*1–3*). Laboratory studies at College Park in the area of mineral technology have emphasized delineation of ore deposits (*4, 5*) such as field analysis of drill cores. Semiconductor detectors offer advantages of portability for field usage and have sufficient stability so that the sensitivity for silver (about 10 ppm) is comparable to that obtained by conventional X-ray fluorescent

(1) A. P. Langheinrich and J. W. Forster, *Advan. X-Ray Anal.*, 11, 275 (1968).
(2) J. R. Rhodes, ORNL-11C-10 (V.1), 442 (1967).
(3) J. D. Frierman, H. R. Bowman, I. Perlman, and C. M. York, *Science*, 164, 588 (1969).
(4) P. G. Burkhalter, Symp. Nucl. Techniques Mineral Resources, IAEA, Vienna, STI/PUB/198, p 365 (1969).
(5) P. G. Burkhalter and H. E. Mart III, *Int. J. Appl. Radiat. Isotopes*, 21 (7), 395 (1970).

analysis using diffracting crystals. Radioisotopic excitation replaces a bulky 75- to 100-keV X-ray generator with a compact source that can easily be placed on the detector housing and removed for storage when not in use. The ease in exciting the K spectra of high atomic number (Z) elements with radioisotopes is important because greater X-ray penetration can lessen difficulties of sample heterogeneity and surface roughness that are encountered in field analysis.

Although X-ray analysis provides adequate sensitivity for silver detection in ores, successful field application requires a method to compensate for variable matrix effect. The silver intensity must be corrected for the variable X-ray absorption due to the matrix to obtain linear intensity *vs.* concentration curves. Of the various X-ray techniques to correct for matrix effects, the internal scatter method is suggested because of the large, discrete scatter peaks in ore spectra excited by monoenergetic X-rays from an electron-capture radioisotope such as ^{125}I. Andermann and Kemp (*6*) were first to propose the use of the fluorescence-to-scatter ratio to reduce the effects of variable X-ray absorption in X-ray emission spectrography. In particular, they obtained good results for Ni Kα and Pb Lα intensities in complicated ores using a scatter intensity in the background continuum at an arbitrary energy. Recently, Taylor and Andermann (*7*) determined that compensation by the internal scatter method is strongly dependent on the choice of scatter energy because of the overlapping Compton and coherent scatter intensities using continuum excitation. They obtained good compensation for Ca Kα in a light matrix using the Compton scatter of the primary Cr Kα radiation from a chromium target X-ray tube. In recent years, monoenergetic excitation with radioisotopes has been used for exciting high-Z elements in ores. Large Compton scatter peaks are observed in the ore spectra, and the internal scatter method using the Compton peak has been found to provide good compensation for light matrix ores. However these researchers (*8–10*) found that generally the method undercompensates in heavier matrices, necessitating the use of monographs.

The purpose of this work was a study of nondiffractive X-ray analysis of silver ores. Computer methods were developed for obtaining silver intensities and the use of scatter for matrix compensation was investigated with synthetic silver standards. Two sets of silver ores were used for silver determinations: variable-matrix ores collected from various mining regions in the United States and samples of a relatively constant-matrix ore obtained from a drill core. X-ray intensities were obtained by computer processing of spectral data collected with a multi-channel analyzer. The Ag Kα X-ray peak excited by ^{125}I was superimposed on a rapidly varying scatter background. A computer program BACKGROUND was used to calculate the background under the Ag Kα peaks. A program BANDFIT written by Fraser and Suzuki (*11*) was used for unfolding X-ray interferences arising when cadmium or antimony was present in the silver ore.

EXPERIMENTAL

Instrumentation. Silicon and germanium semiconductor detectors were used in this investigation. A 3-mm thick by 50-mm^2 area Si(Li) detector manufactured by TMC (formerly Technical Measurements Corp.) was used to measure X-ray intensities at high count rate from the set of variable-matrix ores. Operating at 100,000 counts per second the pulse width at half-maximum intensity (FWHM) for Ag Kα was 1080 eV. The electronics used at high count rate were a TMC preamplifier Model 336 having pole-zero cancellation, a TMC linear amplifier Model 341 using bipolar amplification with 0.2 μsec time constants, and a Canberra biased amplifier and pulse stretcher model 1460. The data for the synthetic silver samples and the set of drill-core samples were accumulated at low count rate with a Ge(Li) detection system manufactured by ORTEC. With a 5-mm thick by 80-mm^2 germanium crystal, the system had a pulse resolution of 660 eV for Ag Kα at 5000 counts per second.

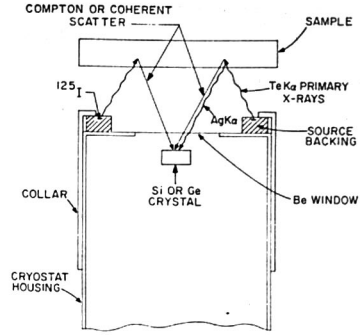


Figure 1. Sample, radioisotopic source, and semiconductor detector geometry

All data were accumulated in a SCIPP 400 channel pulse-height analyzer (PHA) manufactured by Victoreen. The data readout was on paper tape which was converted to cards for processing with the University of Maryland UNIVAC 1108 computer. FORTRAN programs were used that smoothed the spectral data, located the center of the X-ray and scatter peaks, provided background curves under the Ag Kα peak, unfolded overlapping peaks, and calculated X-ray intensities. The computer output was printed intensities, peak-to-background ratios, and spectral curves using a CalComp plotter.

Excitation. Iodine^{125} has been found to be a good radioisotope for exciting Ag Kα radiation (*4*). This electron-capture isotope emits Te Kα (27.5 keV) and Te Kβ (31.0 keV) X-rays plus a low intensity gamma ray at 35.5 keV. The term monoenergetic is used in this paper in respect to ^{125}I in the sense that most of the silver radiation is excited by Te Kα. Other X-rays that could be used for efficient excitation of silver in ores are Sb K and I K radiation. These X-rays could be produced by source-target assemblies but would require source strengths about three orders of magnitude larger than with an electron-capture source. A source strength of 40 mCi of ^{125}I was used. Iodine^{125} has a short half-life of only 56 days which might require frequent replacement in a continuous operation. However, the cost of ^{125}I is only a few dollars per mCi and by ordering a much stronger source than necessary and shielding with a low-Z metal foil, a practical source life of over 6 months can be obtained. For this study a 50-mCi annular source was purchased from the Radiochemical Centre. The radioactive material was prepared as a thin annular ring 1-mm thick by 5.7-cm diameter. A metal collar was used to hold the source on the detector housing and excite samples in a backscatter geometry as shown in Figure 1. Samples were positioned about 2.5 cm from the detector window, thereby irradiating a sample area of about 7.6-cm diameter.

(6) G. Andermann and J. W. Kemp, ANAL. CHEM., **30**, 1306 (1958).
(7) D. L. Taylor and G. Andermann, *Advan. X-Ray Anal.*, **13**, 80 (1970).
(8) P. Martinelli and P. Blanquet, Symp. Radiochem. Methods, IAEA, Vienna, **STI/PUB/88**, p 451 (1965).
(9) B. Holynska and L. Langer, *Anal. Chim. Acta*, **40**, 115 (1968).
(10) A. Lubecki, M. Wasilewskia, and L. Gorski, *Spectrochim. Acta*, **23A**, 831 (1967).
(11) R. D. B. Fraser and E. Suzuki, ANAL. CHEM., **38**, 1770 (1966).

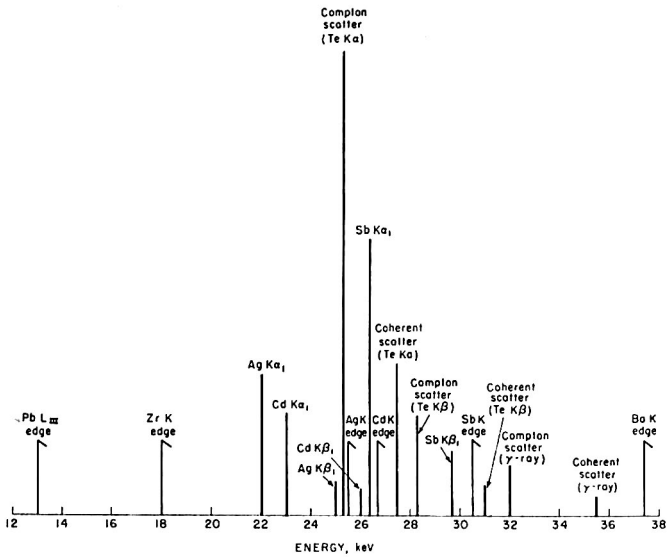


Figure 2. Characteristic X-ray lines, scatter peaks, and absorption edges

The Te Kα primary radiation is very efficient for exciting silver as the Ag K-edge is at 25.5 keV. Other X-rays that are readily excited in silver ores by ^{125}I are the K spectra of iron, copper, and zinc and the L spectra of lead. Barium which has an absorption edge at 37.4 keV is not excited by ^{125}I. Figure 2 shows the positions of the absorption edges, fluorescent X-rays, Compton peaks, and coherent scatter peaks of importance in determining silver in ores. The relative intensities for the X-ray lines and scatter peaks correspond to those of a high-quartz matrix ore containing 26.3 oz/ton of silver. For a back-scatter geometry of 128 degrees, the large Compton scatter peak of Te Kα occurs at 25.3 keV, just below the energy of the Ag K edge. The Compton peak has a FWHM pulse resolution only 44% broader than the Ag Kα X-rays. The Compton peaks are narrow because the angular scatter spread is reduced when using a small detector crystal and a radioactive source in the form of a narrow ring.

COMPTON SCATTER FOR MATRIX COMPENSATION

To obtain silver intensities that vary uniformly with concentration, the measured Ag Kα intensity must be compensated for variations in ore matrix. Scattered radiation whose energy is near that of the desired X-ray but whose intensity is independent of Z would experience X-ray absorption proportional to the characteristic X-ray intensity; and therefore the ratio of characteristic X-ray-to-scatter intensity would be largely independent of X-ray absorption variations. With monoenergetic excitation, distinct Compton and coherent scatter peaks are obtained at higher excitation energies (E_o) using a backscatter geometry. In a light matrix ore, Compton scatter dominates at higher E_o because coherent scatter decreases as E^{-3}. For heavier matrix ores, coherent scatter peaks are large even at higher E_o because coherent scatter varies as approximately Z^3 in the backscatter geometry. On the other hand, Compton scatter is nearly independent of Z but varies as the number of electrons per atomic mass of sample traversed. It is readily apparent that unless the Compton scatter intensity is measured distinctly from coherent scatter that the characteristic X-ray-to-Compton scatter ratio would under-compensate for heavier matrix ores.

To estimate possible success for compensation in silver ores, the X-ray absorption coefficients for Ag Kα and the Compton scatter energy together with the variation in Compton scatter intensity with matrix were examined. As the fluorescent Ag Kα X-rays and Compton scattered radiation traverses the ore matrix before emerging from the sample, the lower energy silver radiation is more strongly absorbed. However, the ratio of the mass absorption coefficients for Ag Kα compared to the Compton scatter energy is nearly constant for the high-Z elements commonly found in silver ores. This ratio of mass absorption coefficients for iron, copper, zinc, zirconium, antimony, barium, and lead varies from 0.690 to 0.705. The same ratio for silica is 0.685. The calculated ratio for a heavy matrix ore consisting of 40% high-Z elements such as barium or lead is 0.693; only about 1% higher than for a quartz-type ore with 15% iron which has a ratio of 0.686. It is because of this constancy of the absorption coefficient ratio that the Compton scatter method can be expected to provide compensation for variable matrix.

The change in matrix, however, will slightly affect the Compton scatter intensity because the Compton scatter varies as Z/A. The value of Z/A varies slowly from 0.499 for quartz to a value of 0.396 for pure lead. Therefore the Compton intensity would be smaller for a heavy matrix ore. The Z/A values were calculated for several of the silver ores used in this work. The Z/A values estimated for light-matrix silver ores such as Crescent or Escalante is 0.494. For several of the heavy matrix ores the Z/A value was lower; about 2% for the Mammoth ores, 4.5% for Baker Property, and 6% for Bunker Hill. This reduction in Compton intensity because of Z/A would over-compensate the fluorescent-to-Compton ratio by

Table I. Intensity Measurements of 1000-ppm Silver Standards

Sample matrix	$I_{Ag\ K\alpha}$, cps	$I_{Compton}$, cps	$I_{coherent}$, cps	$I_{Ag\ K\alpha}/I_{Compton}$	$I_{Ag\ K\alpha}/I_{coherent}$	$I_{coherent}/I_{Compton}$
SiO_2	200.	1890.	642.	0.106	0.31	0.34
SiO_2 + 5% Fe	150.	1420.	510.	0.106	0.29	0.36
SiO_2 + 5% Zr	90.1	854.	350.	0.106	0.26	0.41
SiO_2 + 5% Ba	139.	1440.	547.	0.096	0.25	0.38
SiO_2 + 5% Pb	83.8	754.	369.	0.111	0.23	0.49

Table II. Composition of Variable Matrix Silver Ores

Sample	Oz/ton Ag	Oz/ton Cd	Weight per cent Fe	Cu	Zn	Sb	Ba	Pb	SiO_2	Gangue minerals
Escalante	26.3	*	3.9	0.05	3.9	*	0.35	0.50	79.	Feldspar 10%, calcite 5%, clay 5%
Bunker Hill	24.1	25.6	7.0	0.05	3.6	*	*	28.	32.	Cerussite 20%, chlorite 20%, clay 15%, dolomite 10%
Mammoth 14	19.3	*	4.4	0.09	0.20	3.5	17.	1.3	69.	Barite 25%, siderite 10%, dolomite 5%
Baker Property	18.3	*	3.6	0.10	0.40	*	27.	0.40	35.	Barite 40%, feldspar 10%, pyrite 5%
Crescent	17.6	*	16.	0.34	0.05	0.2	*	0.05	53.	Siderite 40%, sericite 10%
Mammoth Raise	15.1	*	5.0	0.08	0.10	3.0	15.	2.7	68.	Barite 20%, limonite 10%, dolomite 5%
Mammoth 5	14.0	*	33.	2.4	1.5	0.2	2.	0.45	16.	Pyrite 50%, dolomite 15%, barite 5%
Taylor 2	13.4	6.2	0.25	0.06	1.2	1.5	*	0.40	1.2	Dolomite 50%, calcite 40%
Taylor 1	13.2	4.0	1.2	0.38	0.70	3.0	*	1.2	52.	Calcite 40%, dolomite 5%
Mammoth 6	10.9	*	21.	2.1	1.4	0.2	3.	3.6	28.	Pyrite 15%, siderite 25% dolomite 10%
Robinson	5.7	*	4.2	*	0.05	*	*	1.3	83.	Feldspar 10%, calcite 5%
Orphan Girl	4.8	*	2.3	0.05	2.0	*	*	4.8	75.	Cerussite 10%, clay 5%
Flathead	3.9	*	2.8	0.06	0.05	*	0.3	0.80	78.	Calcite 5%, chlorite 10%, mica 10%
Badger	2.7	4.2	3.9	0.26	4.6	*	*	0.40	61.	Feldspar 15%, mica 10%, pyrite 10%
Ward	2.6	5.3	21.	0.06	1.0	*	*	6.2	36.	Limonite 40%, calcite 15%, cerussite 10%

* Values not available.

2 to 6% for heavy matrix silver ores. The absorption coefficient ratio difference of 1.0% between light and heavy ores would also cause over-compensation. For most silver ores we could expect the Compton scatter ratio to provide compensation within a few per cent and that a slight over-compensation may exist for heavy matrix ores.

To test this argument that the Ag Kα-to-Compton scatter ratio will provide compensation, five synthetic silver standards were prepared at the 1000-ppm level in matrices of silica and silica plus 5% additions of several high-Z elements commonly found in silver ores. Intensities were obtained for the silver standards from three separate runs with 5-minute accumulations. The silver and scatter intensities together with the Ag Kα-to-Compton ratios are given in Table I. The 5% high-Z elements in silica standards would correspond in absorption to light matrix silver ores and we find greater than 50% absorption of the Ag Kα intensity in the zirconia and lead containing samples compared to a silica matrix. Exact compensation was found for the iron and zirconia standards using the Ag Kα-to-Compton scatter ratio and a 5% over-compensation for the heavier lead matrix as predicted. The barium containing standard has lower silver-to-Compton and coherent-to-Compton ratios indicating too high a Compton scatter intensity, but no explanation can be given for the lack of compensation for the barium sample. The Ag Kα-to-coherent scatter ratio tends to seriously under-compensate as high-Z elements are added to the matrix.

ANALYSIS OF SILVER ORES

Composition. A set of 21 silver ore samples with silver content ranging from 2.6 to 26.3 oz/ton (1.0 oz/ton equals 34.3 ppm), was collected from mining regions throughout the United States. These samples are classified as variable-matrix ores because of the wide variation in concentration of high-Z elements. In this paper, high-Z is used to designate those elements with atomic number greater than 24 to distinguish from ore matrices composed of principally low-Z elements such as aluminum, silicon, and calcium. Table II lists the concentration of the high-Z elements and the gangue minerals for 15 of these ores. Iron, copper, zinc, barium, lead, and silicon dioxide were determined chemically; cadmium and antimony concentrations were estimated from relative X-ray intensities measured in an X-ray spectrograph. The minerals forming the gangue were qualitatively determined by powder X-ray diffraction and by optical microscopy. Several of these ores such as Escalante, Robinson, and Flathead are light-matrix quartz-type with only 5 to 15% of elements such as iron but small amounts of heavy elements such as barium or lead. Other ores had heavy matrices with abundances of high-Z elements such as Ward with 21% iron and 6% lead, Baker Property with 27% barium, and Bunker Hill with 28% lead. The four Mammoth ores have similar matrices with as much as a 40% high-Z content. The two Taylor ores have light matrices but low silica content. Fire-assay was used to determine the silver content of the ores. To ensure homogeneity, the ores were ground to 100 mesh and thoroughly mixed. Three of the ores were analyzed in duplicate and the silver determinations agreed within ±2%.

A set of 24 silver-ore samples were taken from sections of a drill-hole core from the Westcliffe District, Col. The silver content varied from 0.32 to 41.9 oz/ton. The Westcliffe District ore samples had a relatively uniform matrix consisting of over 50% quartz with 15 to 25% microcline or albite type feldspar and 10 to 15% kaolin. Semiquantitative optical spectrographic analysis gave the following range of concentration for high-Z elements: 1 to 10% manganese, <3% iron, <0.3% copper and zinc, <1% barium and lead. The samples were ground to 100 mesh, split into duplicate sets, and analyzed by fire assay.

Results. Spectral data for the silver ores were accumulated

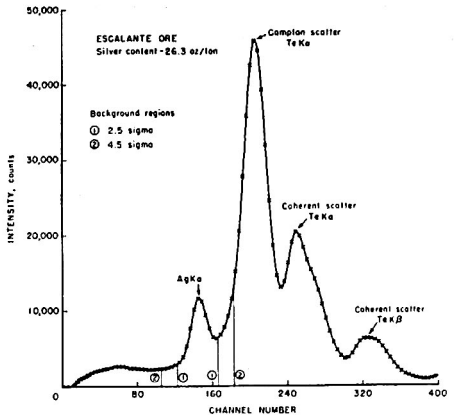


Figure 3. Silver K spectra and scatter peaks measured with a semiconductor detector

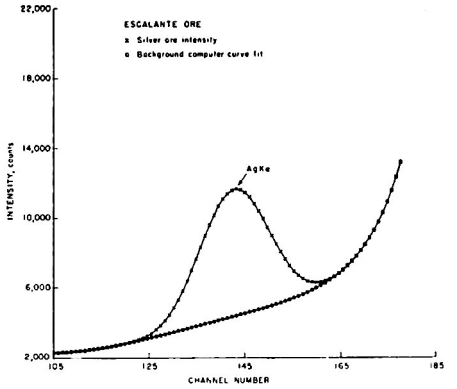


Figure 4. Measured Ag Kα peak intensity superimposed on the computer calculated background

in the 400-channel analyzer for the 17- to 35-keV energy range and read out on punched paper tape for computer processing of the Ag Kα X-ray and scatter peak intensities. The Ag Kα peaks occur on the low-energy side of the strong Compton peak as shown for the Escalante ore in Figure 3. The background under the Ag Kα peak consists of multiple Compton scatter events arising within the sample and electron-hole trapping by impurities within the semiconductor crystal. Standard methods of obtaining a background, such as linear extrapolation, could not be used for such a rapidly varying background. The scatter intensity on the high energy side of the Ag Kα peak is three to six times higher than the background on the low energy side. A technique was developed to curve fit a fifth-order polynomial to the background intensities on both sides of the Ag Kα peak, a process that can easily be handled by least-square regression analysis with a computer. Prior to collecting data from a set of samples, the spectra from a calibration sample consisting of 5000 ppm silver in silica were accumulated in the PHA. A computer program located the peak positions and measured the half-maximum pulse width of the Ag Kα and Compton scatter peaks from this calibration spectra. The X-ray profiles obtained with semiconductor detectors are nearly gaussian in shape. The gaussian shape of the Ag Kα X-ray peaks was used to select the background regions for curve fitting by determining the sigma inflection points (equal to the FWHM value divided by 2.355). The background regions used for curve fitting under the Ag Kα peak were between 2.5 and 4.5 sigma from the centroid of the peak as indicated in Figure 3. The 2.5 sigma value was chosen to separate the peak intensities from the background values as 99% of a gaussian distribution is included between the 2.5 sigma limits. Figure 4 shows the original intensities and the computer calculated background. After background curve fitting, the silver X-ray intensities, $I_{Ag\ K\alpha}$, were obtained by summing channel-by-channel counts under the Ag Kα peak minus the curve-fitted background counts and dividing by the accumulation time in seconds.

Two-minute accumulation times were used to collect spectral data from the 21 variable-matrix samples. Computer curve fitting of backgrounds was achieved with 2.5 to 4.5 background regions for those samples in which Cd Kα interference was not significant. With 1080-eV pulse widths, the Cd Kα peak is 2.26 sigma from the center of the Ag Kα peak. An upper background region of 3.8 to 5.8 sigma allowed curve fitting under both the Ag and Cd Kα composite spectra. The 5.8 sigma value corresponded to 24.9 keV which is near the Compton peak at 25.3 keV. Good background curves were obtained provided the background region did not include the centroid of the Compton peak since even a fifth-order polynomial would fail to match such a sharp inflection.

X-ray interference occurs if cadmium is present in the silver ores in significant amounts. The energy separation of the Ag Kα and Cd Kα X-rays is 1.0 keV; therefore, unfolding of the overlapping peaks would be necessary for pulse widths of 400 eV or greater to avoid systematic errors in measuring the silver peak intensities. After subtracting the background, the composite X-ray peaks were unfolded using the BANDFIT program which processes nonlinear least-square curve fitting by matrix inversion. Pulses produced by the semiconductor detector are nearly gaussian in shape so that accurate unfolding of overlapping X-rays was achieved using gaussian analytical functions. An artificial composite spectra was prepared by adding equal peak intensities of Ag Kα and Cd Kα in the multichannel analyzer. After unfolding, the gaussian peak areas agreed to better than 1% with the original X-ray peak areas.

The relationship of silver Kα intensity to concentration is shown in Figure 5 for the 21 variable-matrix ores. The ratio of the coherent-to-Compton scatter intensity was used to estimate the percentage of high-Z elements in each sample. The coherent-to-Compton ratio was found to be 0.34 for silica and 0.36 for a 5 weight-per cent iron in silica standard. For the low-Z matrix ores, indicated by a solid triangle in Figure 5, the ratio was 0.39 ± 0.02 except for Taylor 1 which had a ratio of 0.44. Within this restricted group of low-Z matrix ores, absorption effects should be small and therefore the silver intensity would be expected to vary linearly with concentration as shown by the solid line in Figure 5. As the high-Z content increases, both absorption of silver intensity and the coherent-to-Compton scatter ratio increased markedly. The Mammoth ores were characterized by scatter ratios of 0.69 to 0.74. The Bunker Hill ore with 28% lead had a scatter ratio of 1.0 and showed the largest deviation from

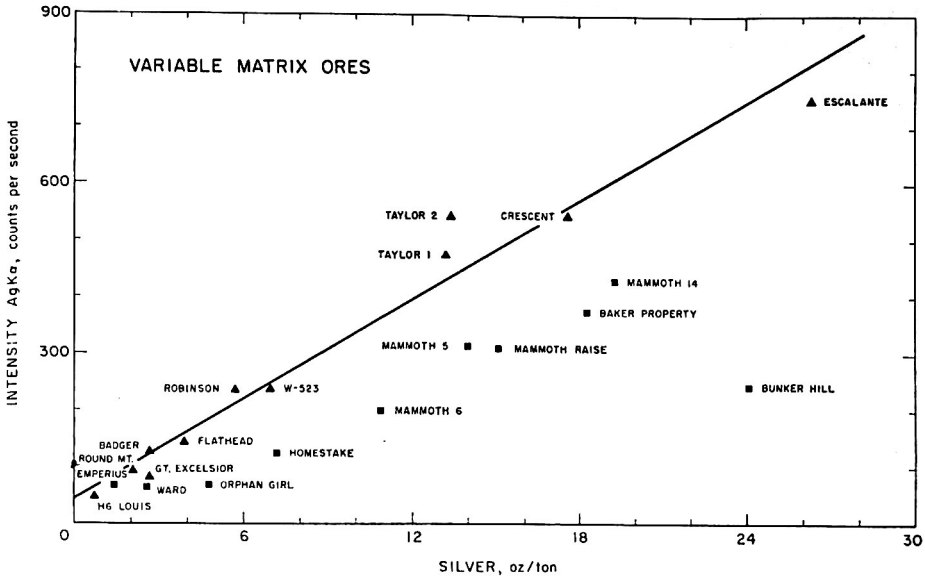


Figure 5. Ag Kα intensity *vs.* concentration for variable matrix ores
▲ Light ore matrix, ■ Heavy ore matrix

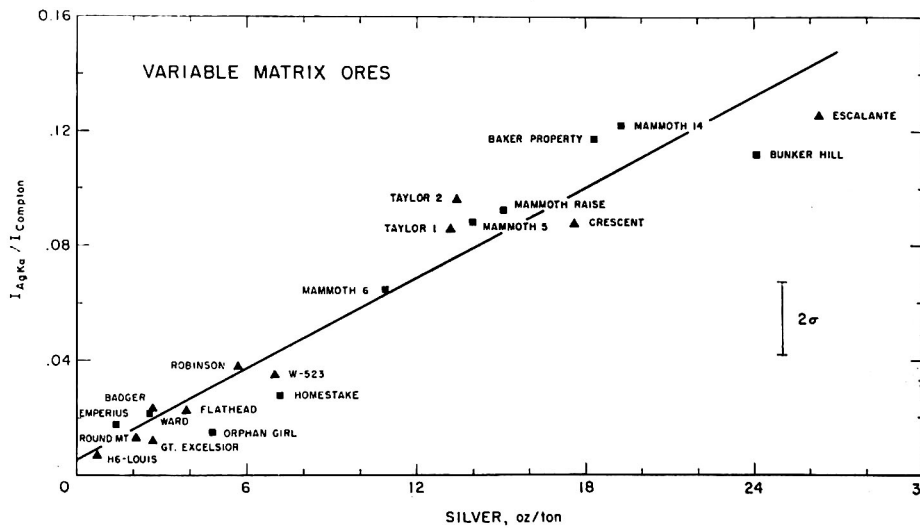


Figure 6. Ag Kα-to-Compton scatter ratio *vs.* concentration for variable matrix ores
▲ Light ore matrix, ■ Heavy ore matrix

the solid line. It is obvious that a single calibration curve is not adequate for these 21 samples because of the strong X-ray absorption by the heavier matrix ores.

The Compton peak intensities, $I_{Compton}$, were measured by summing intensities between FWHM for all samples that do not have a significant amount of antimony. Unfolding techniques were required to obtain discrete scatter peaks for the ores containing greater than about one-half weight per cent of antimony because the Sb Kα peak overlapped with the Compton scatter and the coherent scatter of Te Kα. Antimony is present up to several weight per cent in some silver ores but fortunately antimony is excited by only Te Kβ and the 35.5

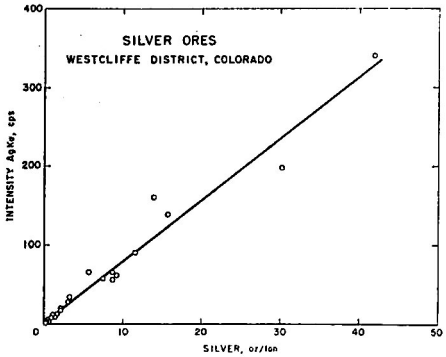


Figure 7. Ag Kα intensity *vs.* concentration for drill core samples

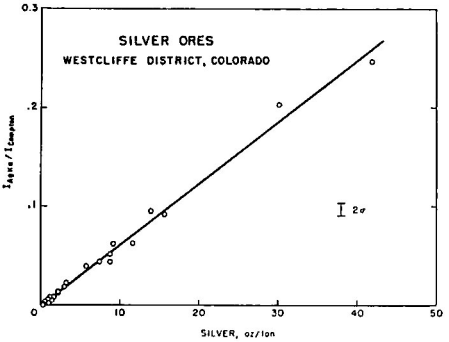


Figure 8. Ag Kα-to-Compton scatter ratio *vs.* concentration for drill core samples

keV gamma ray of ^{128}I. The Sb Kα peak intensity was as high as the Compton peak for the sample containing the largest amount of antimony. The Compton peak deviated from the gaussian shape at lower energies because of tailing. By not allowing the peak widths to change during the matrix inversion process, the Compton and coherent scatter peaks together with the Sb Kα and Kβ X-ray peaks could be simultaneously unfolded to yield good fitting to the upper half of the intensities of the scatter peaks. By these means, accurate Compton intensities between FWHM energies were obtained. The ratio of silver Kα-to-Compton scatter intensity *vs.* concentration for the variable-matrix ores is shown in Figure 6.

The X-ray spectra from the 24 Westcliffe District drill core samples were collected with the Ge semiconductor detector using accumulation times of 15 minutes for the samples having greater than 1 oz/ton silver. X-ray interference was not a problem with the Westcliffe District ores as cadmium and antimony were not present in significant amounts. Background regions of 2.5 to 4.5 sigma were used for samples with greater than 1 oz/ton silver. For the lower grade samples the Ag Kα peak-to-background ratio was less than 0.05 and therefore was difficult to determine accurately. But because of the excellent stability of semiconductor detectors, accumulation times of 150 minutes could be used which provided sufficient counts to distinguish peaks from background. By using background regions of 1.0 to 3.0 sigma, positive silver intensities were obtained for all samples; the lowest one having a silver content of 0.32 oz/ton (11 ppm). The uniformity in ore matrix is indicated by the low variation in the coherent-to-Compton ratio which had a value of 0.48 with a standard deviation of ±0.025. Figure 7 shows the relationship of silver intensity to concentration for the Westcliffe District ores. Although the matrix variation was small, improvement in the intensity-concentration relationship was obtained using the Compton scatter for matrix compensation as seen in Figure 8.

DISCUSSION

The polynomial curve fitting technique gave suitably appearing background fitting for all the silver ores. Blank silica samples with different amounts of high-Z elements were used to determine the accuracy of the curve fitting technique. A fifth-order polynomial gave the best coefficient of correlation as lower-order polynomials always underestimated the actual background intensities from the blank samples. The background intensities were processed by curve fitting across an energy span corresponding to the Ag Kα peak. The computer-calculated background was compared with the actual intensities from the blank samples. The agreement was within 4% with the backgrounds from the blank samples when the background region was 2.5 to 4.5 sigma. If the background region was widened to 3.0 to 5.0 sigma, the agreement was ±7%. When cadmium was present in the ore, the accuracy in background fitting was estimated to be 10%. The precision in determining the Compton intensity was within 2%; however, the accuracy was not that good when overlapping Sb Kα peaks were present. The estimated error for I_{Compton} was ±10% for ores containing high concentrations of antimony and ±5% for those samples in which antimony was not a problem.

The accuracy of the silver intensity measurements depends on both the background determination and the peak-to-background ratio. Because this ratio is small for low-grade silver ores, small errors in the background can result in large errors in the silver intensity value. At the lower concentration levels, a background error of 10% can result in errors in the silver intensity of as much as 25 to 50%. The same per cent background error would result in only a 4% error in silver intensity at a silver concentration of 25 oz/ton. The accuracy in determining the $I_{\text{Ag Kα}}/I_{\text{Compton}}$ ratio depends on the matrix of the ore in addition to the silver concentration as a heavier matrix ore would yield a lower Compton intensity and cadmium and antimony would introduce more difficulty in measurement of both $I_{\text{Ag Kα}}$ and I_{Compton}. For light-matrix ores such as Westcliffe District the estimated accuracy is ±10% for $I_{\text{Ag Kα}}/I_{\text{Compton}}$ at silver concentrations greater than 10 oz/ton. For the variable matrix ores the same ±10% accuracy is estimated for the $I_{\text{Ag Kα}}/I_{\text{Compton}}$ ratio for the quartz type ores and ±15 to 20% for the heavier-matrix ores containing cadmium or antimony.

From measurements of the 5% high-Z synthetic standards, it was anticipated that the Compton scatter method should give good compensation for lighter matrix silver ores. The standard deviation for the Westcliffe District intensity data was a factor of 2 better using the Ag Kα-to-Compton scatter ratio as compared to the silver intensity data. Using the Ag Kα-to-Compton scatter ratio, the deviations from the least square fitted curve were within ±10% for all samples above 3 oz/ton except one at 7.2 oz/ton. For the variable matrix

ores, the Compton scatter method provides matrix compensation within ±20% for silver concentrations greater than 10 oz/ton. The slope of the Ag Kα-to-Compton scatter ratio curves was equal for the both sets of silver ores. The conclusion is reached that silver can be determined in ores with a single calibration curve using the Compton scatter method. The internal scatter technique could not accurately be evaluated in this work for compensation of heavier matrix ores because of uncertainties of 15 to 20% in the intensity measurements. More quantitative work at higher concentration is needed to determine the accuracy of the Compton scatter method for heavier matrix ores. However, it was found that serious under-compensation did not occur for the silver ores as others have reported for heavier matrix ores. In my opinion the under-compensation was absent because measurements of discrete Compton intensities separated from the coherent scatter could be made.

Laboratory results are favorable for nondiffractive X-ray analysis of silver ores. Other high-Z ores could similarly be excited with radioactive sources and at least two other electron-capture isotopes are available with high energy X-rays near those from ^{125}I. Tin ores could be as efficiently excited with the Cs Kα X-rays from ^{133}Ba as Te Kα excites silver. The Sn Kα X-rays would have about equal energy separation from the Compton peak as Ag Kα excited by ^{125}I. Cadmium-109 emits Ag Kα X-rays and could be used for Sr, Y, Zr, Nb, and Mo in ores with results equal to that of silver analysis in light matrix ores provided strong X-ray interferences do not occur and matrix elements are not present which have absorption edges between the desired X-ray and the Compton peak energy. In choosing the excitation energy particularly for trace analysis, one should select E_o sufficiently high that the desired X-ray is well separated from the Compton peak to improve the peak-to-background ratio.

ACKNOWLEDGMENT

I am indebted to C. Mastromonico and W. J. Campbell of the College Park Metallurgy Research Center for their assistance in the computer processing of the data and technical help in preparing this publication, respectively. G. Potter of the Salt Lake City Research Center supplied the variable matrix silver ores. The Westcliffe District ore samples were obtained by C. Roach of the Denver Mining Research Center.

RECEIVED for review July 7, 1970. Accepted October 5, 1970. Reference to specific models of equipment is made for identification only and does not imply endorsement by the Bureau of Mines.

Application of Field Ionization to Gas-Liquid Chromatography—Mass Spectrometry (GLC-MS) Studies

J. N. Damico and R. P. Barron

Division of Food Chemistry and Technology, Food and Drug Administration, U. S. Department of Health, Education, and Welfare, Washington, D. C. 20204

A GLC-MS field ionization system incorporating a permeable membrane interface has been used to obtain spectra of GLC effluents consisting of components that yield relatively weak molecular ions by electron impact. These field ionization spectra complement the electron impact spectra. Field ionization sensitivity studies of the molecular ion (mV/μg) for a variety of carbonyl compounds with relative intensities by electron impact between 0.1 and 6.6% suggest that some types of compounds are significantly more sensitive to field ionization than others. The percentage of sample which permeates the membrane ranged between 30 and 72% for these carbonyl compounds.

COMBINED GLC–ELECTRON impact mass spectrometry is widely used for the analysis of GLC effluents, as evidenced by the excellent review articles and the references therein (*1*, *2*). One of the most important types of information that can be obtained from mass spectral data is the molecular weight of a compound. In electron impact ionization the relative intensity of the molecular ion is very small for many compounds and comprises a small percentage of the total ion yield. Since components of interest in natural products are often present in the parts per million range or lower, the total ion yield will be small and the molecular ion may be of low intensity and difficult to distinguish from column bleed and/or background. Beckey (*3*) was the first to show that field ionization (FI) is effective in enhancing the relative intensity of molecular ions. Other examples and additional information on FI are provided in Table I and in the publications (*4–9*) and references therein which resulted from a symposium on FI mass spectrometry (*10*).

Field ionization is not so convenient a technique as electron impact ionization. First, most FI anodes must be activated before they attain maximum sensitivity, although Chait (*11*) has reported that commercially available chromium-plated razor blades do not require activation to reach full sensitivity. Second, it is not known *a priori* whether activation of a given

(1) W. S. Updegrove and P. Haug, *Amer. Lab.*, pp 8–30 (Feb. (1970).
(2) F. E. Saalfeld, *Ind. Res.*, **11**, 58 (1969).
(3) H. D. Beckey, in "Mass Spectrometry," R. I. Reed, Ed., Academic Press, London and New York, 1965, pp 93–127.
(4) H. D. Beckey, *Int. J. Mass Spectrom. Ion Phys.*, **2**, 101 (1969).
(5) D. F. Barofsky and E. W. Muller, *ibid.*, p 125.
(6) E. M. Chait, W. O. Perry, G. E. Van Lear, and F. W. McLafferty, *ibid.*, p 141.
(7) M. Barber, R. M. Elliott, and T. R. Kemp, *ibid.*, p 157.
(8) J. N. Damico, R. P. Barron, and J. A. Sphon, *ibid.*, p 161.
(9) P. Schulze, B. R. Simoneit, and A. L. Burlingame, *ibid.*, p 183.
(10) Sixteenth Annual Conference on Mass Spectrometry and Allied Topics, ASTM Committee E-14, Pittsburgh, Pa., May 12–17, 1968. Papers numbered 9–12, 21–24.
(11) E. M. Chait and F. Kitson, *Org. Mass Spectrom.*, **3**, 533 (1970).

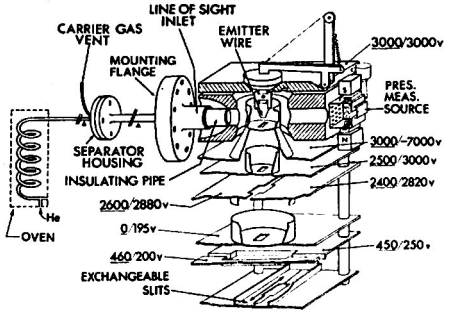


Figure 1. Detailed cut-away drawing of EFO-4B source (ion optic potentials *underlined* are for EI mode), pressure measuring source (GLC) detector, and GLC interface used in FI studies (not drawn to scale)

anode will ensure sensitivity; in addition, the attainable sensitivity varies for different anodes. Tou *et al.* (*12*), using acetone as the reference material, encountered two Wollaston wires (2.5 μm in diameter) which had a field ionization sensitivity ratio of 70 after activation. In their study of the surfaces of the two wires by electron microscopy, they presented some interesting conclusions to account for the striking sensitivity ratio observed. A third disadvantage of FI is its relatively low sensitivity compared to EI.

To our knowledge, no work has been published in which FI was utilized for the analysis of GLC effluents. (Since this manuscript was prepared, we learned that Professor Beckey's group has carried out GLC–FI MS studies of multicomponent mixtures containing several hundred unresolved components.) The object of this report is to demonstrate that FI does have utility in combined GLC–mass spectrometry, despite the disadvantages cited.

EXPERIMENTAL

All studies were made with an Atlas CH-4B mass spectrometer equipped with a dual electron impact/field ionization source (EFO-4B) as supplied with the spectrometer. An exploded drawing of the GLC-MS system is shown in Figure 1.

Instrumental Parameters. Source exit and collector slits were 0.1 mm and 0.3 mm, respectively. The gain of the electron multiplier was usually 10^6. Wires of 2.5-μm diameter, obtained commercially, were used as anodes; they were activated as described previously (*8*) except that maximum sensitivity could usually be approached in only 4 to 5 hours. Three such wire anodes (*A*, *B*, and *C*) were used to obtain the data reported here; wire *B* was preconditioned with benzonitrile. The GLC detector was a pressure measuring source (PMS), an electron impact total ion collector. The electron energy was 20 eV and the trap current was 100 μA. (The total ion monitor, widely used as the GLC detector for EI, is inadequate for FI because the total ion current is very small. For example, the maximum total ion current observed on the total ion monitor from FI of 2 μg of $C_{10}\Delta$ lactone injected on the GLC column was about 10^{-14} A, whereas the maximum response for the same amount of sample using the PMS was about 10^{-10} A.) The column bath for the GLC was a Barber-Colman Model 5360 equipped with temperature programmer and controller. The bath also contained a flame ionization detector (FID); the effluent could be split to the FID and to the mass spectrometer. This made it possible to simultaneously monitor the effluent with the FID and the PMS. The column was a glass coiled column 6 ft × $^1/_4$ in. o.d., packed with 10% diethylene glycol succinate on Gas Chrom Z, 100/120 mesh. The GLC was interfaced to the mass spectrometer with a permeable membrane separator (Varian 5620). The membrane is a methyl silicone polymer layer 0.001-in. thick and has a surface area of 0.4 cm² exposed to the column effluent. [Black *et al.* (*13*) investigated single-stage and double-stage membrane molecular separators in conjunction with columns 0.02 and 0.03 in. i.d. but found that only the single-stage system was satisfactory; severe band broadening was observed for the higher molecular weight compounds (maximum molecular weight *ca.* 250) which was minimized by temperature programming the separator.] Since transmission of the sample through the membrane is decreased at high temperatures, the temperature of the membrane should be maintained as low as possible. Green and Littlejohn (*14*) reported that the membrane could be operated at 50 °C below the column temperature without loss of column efficiency, and this temperature was usually employed in this work. The connecting lines were maintained at 200 °C. The entire interface assembly was mounted line-of-sight to the ionization chamber and was heated by insulated heating wire. The carrier gas vent (see Figure 1) for the effluent, which does not permeate the membrane, was sometimes monitored with a FID.

Procedure. The sensitivity determinations listed in Table I were usually obtained by injecting 30–50 μg on the GLC column. When the component enters the ionization chamber as detected by the PMS, the maximum response of the molecular ion is determined by scanning the mass region of interest at the top of the GLC peak. Although it is sometimes feasible to obtain both electron impact and field ionization spectra on the same sample charge with a dual source, this is not possible when obtaining spectra of GLC peaks because switching between modes of operation requires at least several minutes. Accordingly, the spectra were recorded on separate GC runs. The recorder response of the molecular ion is converted from chart divisions to millivolts from prior calibration data of the recorder. The column temperatures were selected so that the base-line peak widths were between 1 $^1/_2$ and 2 min. All the sensitivity data listed in Table I were obtained with wire anode C. Prior to each sensitivity determination, the anode was reactivated until the collector current (Farady Cage) for *m/e* 58 of acetone was 10^{-11} A at an acetone pressure of 5 × 10^{-6} mm of Hg as measured on the penning gauge of the analyzer tube. [Reactivation is necessary because sample and/or column bleed condenses on the surface of the wire and renders it insensitive. This problem might be alleviated if the wire were heated, preferably by current flow. Beckey *et al.* (*15*) have designed a vacuum lock whereby a wire anode mounted on a sliding rod can be readily interchanged. This design also makes it easy to heat the anode by passing a few milliamperes of current through the wire, a procedure that is not feasible with the system described in this report except by extensive modification.] The transmission of sample through the membrane was determined indirectly. The peak area response was obtained for a given sample injection with the column connected only to the FID in the column bath (C_{FID}), and again with the column

(12) J. C. Tou, L. B. Westover, and E. J. Sutton, *Int. J. Mass Spectrom. Ion Phys.*, 3, 377 (1969).

(13) D. R. Black, R. A. Flath, and R. Teranishi, *J. Chromatogr. Sci.*, 7, 284 (1969).

(14) D. E. Green and D. P. Littlejohn, Pacific Conference on Chemistry and Applied Spectroscopy, Anaheim, Calif., Oct. 6–10, 199.

(15) H. D. Beckey, A. Heindrichs, and H. V. Winkler, *Int. J. Mass Spectrom. Ion Phys.*, 3, App. 9–11, (1970).

Table I. Field Ionization Sensitivity for the Molecular Ion of Some Carbonyl Compounds

Compound	Amount injected, μg	Maximum molecular ion response, mV/μg	Relative intensity of molecular ion, % FI	EI	(Ref No.)
C_8-Δ Lactone	50	45	100	6.6	(16)
C10-γ Lactone	30	100	100	0.3	(17)
C10-Δ Lactone	30	250	100	3.5	(18)
C_{12}-γ Lactone	30	88	100	0.1[a]	(19)
C_{12}-Δ Lactone	30	110	100	4.3	(20)
C_{14}-Δ Lactone	50	200	100	<0.1[a]	(19)
C_{10}-Acid	250	12	100	4.0[b]	(19)
Decyl-acetate	500	0.2	100	<0.3	(19)
C_{10}-Methyl ester	40	62	100	3.6[a]	(19)
C_{12}-Methyl ester	40	62	100	2.7	(21)
C_{14}-Methyl ester	40	62	100	3.2	(22)
C_9-Ketone	50	70	100	4.9	(23)
C_{11}-Ketone	50	200	100	2.5[a]	(19)
C_{15}-Ketone	50	200	100	3.0[c]	(19)
C_8-Aldehyde	50	0.4	100	1.0	(24)
C_{10}-Aldehyde	50	0.8	100	0.5	(24)
C_{12}-Aldehyde	50	2	100	0.3	(24)

[a] Obtained with electron impact E-4B source using GLC–MS inlet.
[b] Obtained with electron impact E-4B source using direct probe.
[c] Obtained with EFO-4B source using GLC–MS inlet.

connected directly to the membrane, the residual sample (RS_{FID}) being measured at the carrier gas vent with a FID. Per cent transmission of sample through the membrane is equal to

$$\frac{\text{Peak area response } (C_{FID}) - \text{peak area response } (RS_{FID}) \times 100}{\text{peak area response } (C_{FID})}$$

The GLC column and membrane temperatures and transmission percentages are listed in Table II.

RESULTS AND DISCUSSION

Although wires of small diameter are fragile and break very easily, Beckey *et al.* (25) have developed a new technique for preconditioning wires which makes feasible the use of 10-μm tungsten wire as anodes. Beckey *et al.* (26) have also pointed out the sparking in the ion source can be minimized by polishing sharp edges in the vicinity of the anode and carefully cleaning the insulators, thus extending the life of 2.5-μm wires.

Leakage current may be a more serious problem; it is always present because of the high potential difference (9–11 kV) between the anode and the cathode. High leakage currents (10 μA) cause the sensitivity to deteriorate markedly, and, if excessive, will make the system inoperable until the ion source is dismantled and the components thoroughly cleaned. Some time ago, all the ion source components of our EFO-4B source were individually electropolished. In subsequent FI experiments, there was no measurable leakage current (<0.5 μA) with 11 kV between the anode and cathode and the sensitivity was enhanced almost 20 times over that usually obtained prior to electropolishing. Previously, only a 9-kV potential difference could be used because at the higher potentials the leakage current became intolerable. In one experiment using acetone, a fourfold increase in sensitivity was achieved by increasing the cathode negative potential from 6 kV to 8 kV. All of these improvements were factors in successful use of FI in GLC–MS for research.

Table II. Sample Transmission of Some Carbonyl Compounds through Polymer Membrane Separator

Compound	Column temperature, °C	Membrane housing, °C	Transmission, %
C_8-Aldehyde	80	30	43
C_9-Ketone	80	30	60
C_{11}-Ketone	95	48	31
Decyl acetate	100	55	61
C_{10}-Aldehyde	100	65	35
C_{10}-Methyl ester	110	65	40
C_{12}-Methyl ester	125	70	59
C_{12}-Aldehyde	135	75	72
C_{15}-Ketone	135	75	57
C_{14}-Methyl ester	145	95	59
C_8-Δ Lactone	155	80	29
C_{10}-γ Lactone	170	85	48
C_{10}Δ Lactone	180	85	46
C_{12}-γ Lactone	195	92	62
C_{12}-Δ Lactone	205	100	54
C_{14}-Δ Lactone	225	100	72

Although the sensitivity of FI is markedly less than that of EI, inspection of Figure 2 shows that the FI spectra complement the EI spectra. Both types of spectra were obtained from a 2-μg injection on the GLC column. It is apparent that the signal-to-noise ratio for the molecular ion response is greater in the FI mode than in the EI mode. Similar results were obtained for C_{10}Δ and C_{14}Δ lactone. Another important feature of the FI spectrum (not apparent in Figure 2) is that no background peaks from column bleed are present. Also, the absence of the M–H_2O peaks in the FI spectra of C_{10}Δ, C_{12}Δ, and C_{14}Δ lactones indicates that the intense M–H_2O peaks which McFadden *et al.* (27) observed in the EI spectra for lactones of this type are not due to thermal processes.

(16) ASTM Uncertified Mass Spectral Data File, No. 1809.
(17) *Ibid.*, No. 1821.
(18) *Ibid.*, No. 1822.
(19) Unpublished data from the authors' laboratory.
(20) ASTM Uncertified Mass Spectral Data File, No. 1836.
(21) *Ibid.*, No. 1081.
(22) *Ibid.*, No. 1084.
(23) *Ibid.*, No. 211.
(24) J. A. Gilpin and F. W. McLafferty, ANAL. CHEM., 29, 990 (1957).
(25) H. D. Beckey, E. Hilt, A. Maas, M. D. Migahed, and E. Ochterbeck, *ibid.*, p 161.
(26) H. D. Beckey, H. Krone, and F. W. Roellgen, *J. Sci. Instrum., Ser. 2*, 1, 118 (1968).
(27) W. H. McFadden, E. A. Day, and M. J. Diamond, ANAL. CHEM., 37, 89 (1965).

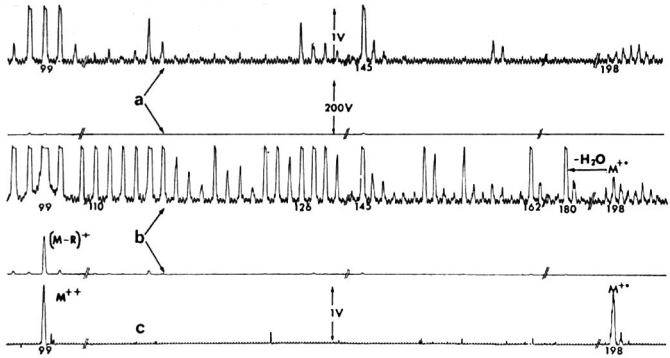


Figure 2. Selected portions of the recorded electron impact and field ionization (wire *A*) spectra of Δ-dodecalactone; spectra are superimposable

***a*, EI background; *b*, EI spectrum (same sensitivities for *a* and *b*); and *c*, FI spectrum**

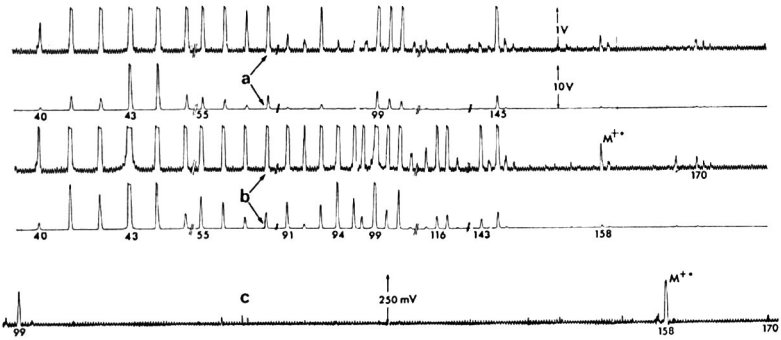


Figure 3. Selected portions of recorded electron impact and field ionization (wire *B*) spectra of *n*-propyl levulenate isolated from an egg extract; EI spectra and FI spectrum are not superimposable

***a*, EI background; *b*, EI spectrum (same sensitivities for *a* and *b*); and *c*, FI spectrum–mass range, m/e 99 to m/e 170**

Intense doubly charged ions were observed by FI but not by EI for all lactones examined. Such phenomena, which are not uncommon in FI, can be useful in characterizing these compounds. (Wanless and Glock (*28*) were able to utilize metastable peaks formed only during FI to characterize some hydrocarbon isomers.) In our work $C_8\Delta$, $C_{10}\gamma$, $C_{10}\Delta$ give abundant ions due to $(M\text{-}O)^{2+}$ with relative intensities between 60 and 90%. In contrast, $C_{12}\gamma$, $C_{12}\Delta$, and $C_{14}\Delta$ give ions due to M^{2+}, but of about the same relative intensity as the $[M\text{-}O]^{2+}$.

The utility of FI can be demonstrated from the spectra shown in Figure 3, in which a component in the GLC effluent from an egg extract was identified as *n*-propyl levulenate. (The component was present in the extract as the acid esterified for GLC analysis.) The EI spectrum shows only a small peak for *m/e* 158, which was corroborated as the molecular ion by FI. Without the FI data, it would not have been possible to assign *m/e* 158 as the molecular weight. Often it is possible to identify a compound using only characteristic peaks and without *a priori* knowledge of the molecular weight by matching with reference spectra; however, the relatively intense peaks at *m/e* 91 and *m/e* 94 in the EI spectrum of this ester are not common to it; accordingly, any attempt to match the relative intensities would probably be unsuccessful. This phenomenon is frequently observed with food isolates.

During GLC–MS field ionization studies of food extracts containing carbonyl compounds, in several instances the response of the PMS and the molecular ion response were inconsistent, suggesting that some types of compounds might be more sensitive to FI than others. Accordingly, an FI sensitivity study was initiated, with the results in Table I. The system described in this paper offers a convenient way of doing this on a microscale. The maximum molecular ion response expressed in millivolts per microgram is intended only for comparison and does not imply that the sensitivity is linear. These results do show significant differences in sensitivity for various types of compounds. The ketones and lactones are the most sensitive and the aldehydes and decyl acetate, the least sensitive of the group. The experiments with decyl acetate were repeated at least ten times with comparable results.

(28) G. G. Wanless and G. A. Glock, Jr., *ibid.*, 39, 2 (1967).

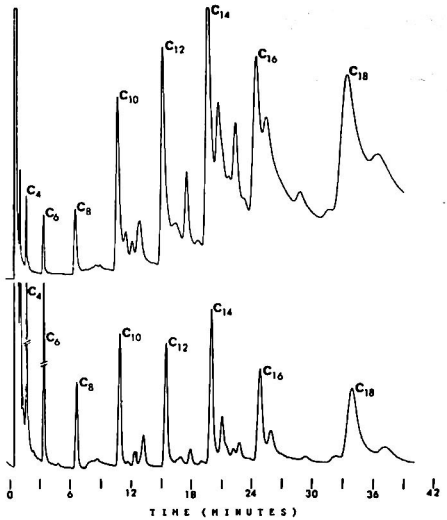


Figure 4. Chromatograms of a cheese extract obtained with the effluent split equally to (*a*) the mass spectrometer through the membrane interface (140 °C), using the pressure measuring source as the GLC detector, and (*b*) a flame ionization detector (glass coiled column 6 ft × 1/4 in. packed with 7.5% EGA + 2.5% H_3PO_4 on Chromosorb W, 80/90 mesh); column temperature programmed from 125 to 200 °C at 40°/min; carrier gas He, 100 ml/min at 125 °C

To ensure the reliability of the sensitivity study (Table I), the amount of sample which permeates the membrane must be known. Table II shows that the aldehydes and decyl acetate, as well as the ketones and lactones, permeate the membrane, indicating that the low sensitivity observed for these compounds is in fact due to FI phenomena.

A few alcohols were examined, although results were too poor to include in this report. A 1-mg injection of decanol yielded only a very weak molecular ion peak (possibly M + 1), and similar results were observed with propanol. Apparently the alcohols made the wire insensitive. Beckey (*3*) reported difficulty in obtaining reproducible peak intensities for alcohols and suggested that this was caused by a monolayer of water on the surface of the wire anode produced by the alcohols. In addition to the decyl acetate studies, poor FI sensitivity was obtained for *cis*-9-tetradecen-1-ol acetate. These results indicate that esterification to the acetates is not an effective means for enhancing the FI sensitivity of alcohols.

If FI (or any mass spectrometric technique) is to be effective for analyzing GLC components which arise from natural products, the interface must provide good enrichment, and not cause the column efficiency to deteriorate to any significant extent. Enrichment has already been shown to be adequate with this system; enrichments are comparable to those of Black *et al.* (*13*). Evidence for absence of deterioration is provided by the chromatograms (obtained in separate runs) shown in Figure 4. The major components of the cheese extract are highly polar and include the free saturated acids up to oleic acid (C_{18}). Inspection of the two chromatograms shows some peak broadening due to the membrane, but the loss in resolution does not preclude mass spectrometric analysis of the various components in the cheese extract.

CONCLUSION

The work described in this paper demonstrates that FI has utility for the analysis of components in GLC effluents. Four of five commercially supplied anodes gave adequate sensitivity. The fragility of the small diameter wire anodes should become less of a problem with the use of the larger diameter tungsten wires made possible by the benzonitrile activation process (*25*).

ACKNOWLEDGMENT

The authors are grateful to N. P. Wong, Dairy Products Laboratory, Agricultural Research Service, United States Department of Agriculture, Washington, D. C., for furnishing the cheese extract and to Walter Staruszkiewicz, Division of Food Chemistry and Technology, Food and Drug Administration, Washington, D. C., for furnishing the egg extract.

RECEIVED for review July 22, 1970. Accepted October 8, 1970. Presented at the Eighteenth Annual Conference on Mass Spectrometry and Allied Topics of the American Society for Mass Spectrometry, San Francisco, Calif., June 14–19, 1970.

Machine Intelligence Applied to Chemical Systems

Prediction and Reliability Improvement in Classification of Low Resolution Mass Spectrometry Data

Peter C. Jurs

Department of Chemistry, The Pennsylvania State University, University Park, Pa. 16802

Several techniques for improving the prediction and reliability of binary pattern classifiers are investigated. The data used are low resolution mass spectra of small organic molecules containing C, H, O, and N atoms. Aspects of pattern classification discussed include transformation of the original data, investigation of the effects of thresholds, and the effects of using layered systems of threshold logic units. A predictive ability as high as 98% on complete unknowns can be obtained by incorporating all these features into one classification system.

PREVIOUS STUDIES have shown that adaptive binary pattern classifiers are capable of learning to usefully classify chemical data derived from low resolution mass spectrometry, infrared spectrometry, and from diverse sources (*1*). Four important attributes of pattern classifiers have been pointed out and studied: recognition ability, reliability, convergence rate, and predictive ability. This paper will discuss some methods whereby the reliability and predictive ability of binary pattern classifiers can be enhanced without undue slowing of the convergence rate.

Data Set. The first and most obvious way to improve the results of any data interpretation technique is to use the best set of data which is available. Previous work dealing with pattern classifiers working on chemical systems used a set of mass spectrometry data which has been previously described (*1*). The present work uses another data set taken from a collection of mass spectra purchased on magnetic tape from the Mass Spectrometry Data Center, Atomic Weapons Research Establishment, United Kingdom Atomic Energy Authority, Aldermaston, Berkshire. A portion of that tape contains 2261 American Petroleum Institute Research Project 44 spectra. These spectra have been digitized with normalized intensities ranging from 99.99 to 0.01 in each spectrum. Throughout this work spectra corresponding to compounds containing only C, H, O, and N atoms were used. In the data selected from the tape for actual tests, there are about 50 to 70 such peaks per spectrum. There are 132 *m/e* positions in which ten or more peaks appear throughout the data set used. In making actual computer runs, an input subroutine is employed to read spectra from a tape, select the ones to be used according to preset criteria, *e.g.* carbon number, and set up the data for the remainder of the program to use. Normally, 600 spectra are thus input, with a training set of 300 and a prediction set of 300.

Data Selection and Transformation. Because of the large quantity of data available, it was possible to select data for inclusion in each problem so as to acquire as homogeneous a data set as possible. In most of the work reported here, the spectra were selected so that they correspond to compounds with three to 10 carbon atoms. (Tests using data sets with spectra of compounds with three to 20 carbon atoms showed that the results obtained in this investigation were not artifacts of the data but worked for the less homogeneous data set also.) Six hundred spectra meeting the criteria of three to 10 carbon atoms were used for each computer run; they were divided evenly between the training and prediction sets. The data set of 600 spectra most often used contained 35,550 peaks spread over 132 *m/e* positions.

Previous pattern classification research has shown that transformations of the intensities of the spectral peaks markedly help the pattern classifiers to find good decision surfaces (*2*). A discussion of the information present in mass spectra from an information theory point of view has been given by Grotch (*3*). Table I shows the results of an investigation of several different transformations.

The investigation shown in Table I used spectra from the purchased collection as described above. For each of the four transformations, a feature selection program was run. The method of feature selection employed has been described in detail previously (*1*). The main points of the feature selection routine are that for each stage in the routine, two weight vectors (initiated with all +1's and all −1's, respectively) are trained, and then the signs of the weight vector components are compared. Only the *m/e* positions corresponding to weight vector components with the same sign are retained for the next stage. The cycle is repeated until no more ambiguous *m/e* positions can be located, and the program then terminates. Each row of Table I shows the results of running this program for the same data, having undergone the transformation listed in column one. The original data have a dynamic range within each spectrum of 10^4 (0.01 to 99.99); the second column gives the dynamic range after the transformation. The third column gives the number of feedbacks necessary for convergence to 100% recognition for the first stage of the feature selection program (when there are 132 *m/e* positions). The fourth column gives the predictive abilities of the two pattern classifiers and the fifth gives the average per cent prediction for this first stage. The logarithmic transformation yields the best predictive ability for the first step of the program. Column five shows the number of ambiguous *m/e* positions found during this first stage; a narrower dynamic range causes the pattern classifier to find few ambiguous *m/e* positions. The program repeats the cycle mentioned above many times for each transformation, and the number of *m/e* positions remaining after all ambiguous positions have been discarded is shown in column six. Again, narrower dynamic range reduces the number of ambiguous *m/e* positions. The final column gives the predictive ability

(1) P. C. Jurs, ANAL. CHEM., 42, 1633 (1970).

(2) P. C. Jurs, B. R. Kowalski, T. L. Isenhour, and C. N. Reilley, ANAL. CHEM., 41, 690 (1969).

(3) S. L. Grotch, "A Computer Program for the Identification of Low Resolution Mass Spectra," 18th Conference on Mass Spectrometry and Allied Topics, San Francisco, Calif., June 1970.

Table I. Effects of Transformations on Properties of Binary Pattern Classifiers

Transformation	Dynamic range	Feedbacks +1 WV/−1 WV[a]	Per cent prediction +WV/−WV	Av % prediction	*m/e* positions discarded	*m/e* positions final	Overall % prediction
Square root	100	123/114	93.7/96.3	95.0	66	43	94.4
Fourth root	10	101/107	94.7/94.3	94.5	49	44	94.6
log	4	141/102	95.3/95.3	95.3	44	57	95.5
Zeroth power	1	235/229	93.7/94.0	93.8	23	83	94.0

	+	−	Total
Training set	121	179	300
Prediction set	126	174	300

132 *m/e* positions
Oxygen presence–absence determinations

[a] Weight vector.

Table II. Comparison of Properties of Four Pattern Classification Methods. Oxygen Presence–Absence Determination

	Randomization	Feedbacks +1WV/−1WV	% prediction +1WV/−1WV	Av % prediction	% recognition σ = 2%	% recognition σ = 5%
Linear machine	1	135/118	96.3/94.0	95.3	98.5	96.4
	2	135/127	95.3/94.0	94.7		
	3	92/172	93.3/94.0	93.6		
Linear machine with threshold Δ = 50	1	239/184	96.0/96.0	96.0	99.6	98.6
	2	286/211	96.3/95.7	95.8		
	3	157/179	95.7/94.3	95.0		
Committee machine	1	180		96.0	95.0	90.7
	2	153		94.0		
	3	95		91.7		
Committee machine with threshold Δ = 50	1	375		98.0	100.0	99.8
	2	297		96.3		
	3	398		95.7		

Randomization	Training set +/−	Prediction set +/−
1	84/216	89/211
2	92/208	81/219
3	78/222	95/205

exhibited by each pattern classifier averaged over all stages of the feature selection process. Once again the logarithmic transformation exhibits the highest predictive ability. This result is consistent with the result obtained by applying information theory to the transgeneration problem. Throughout the remainder of this study, the logarithmic transformation was employed. After the transformation, the magnitude of the peaks was adjusted with constant multipliers for purely computational reasons, and the average peak intensity thus becomes approximately 13.

Dead Zone Training. The binary pattern classifiers used in this research and previous studies are known as threshold logic units, TLU's. The data are represented by *d*-dimensional vectors. They are classified by forming the dot product between a particular pattern vector and the weight vector, a procedure which gives a scalar, *s*. The pattern is classified into one category or the other according to whether the scalar is positive or negative—*i.e.*, the scalar is compared to the threshold level of zero.

A threshold level other than zero, Δ, can also be used. Then, when a dot product is formed between the pattern vector and the weight vector, the scalar is compared to Δ. If $s > \Delta$ then the pattern is said to belong to one category; if $s < -\Delta$ then it is said to belong to the other category; and if $-\Delta < s < \Delta$, then the pattern is not classified. The region between $-\Delta$ and Δ is known as the dead zone. This classification method can be thought of in terms of two hyperplanes, where patterns are classed in one category if they fall on one side of the two planes, are classed in the other category if they fall on the other side of the two planes, and are not classified if they fall between the hyperplanes.

Training is performed using the threshold much as if $\Delta = 0$. Feedback is applied only to correct errors, but now errors include both incorrect classification and failure to make a classification. The new weight vector is calculated from the old one at step *i* in training by the equation

$$\mathbf{W}_{i+1} = \mathbf{W}_i \pm c\mathbf{Y} \qquad (1)$$

where $\mathbf{W}_{i+1}$ is the new weight vector, $\mathbf{W}_i$ is the old one, $\mathbf{Y}$ is the pattern vector being classified, *c* the correction increment, and the sign is chosen according to the sense of the

Table III. Properties of Binary Pattern Classifiers as a Function of Threshold, Δ

Δ	Feedbacks	Average feedbacks	% prediction	Av % Prediction	% recognition σ = 2%	% recognition σ = 5%	m/e positions discarded
0	135/118	126	96.3/94.0	95.3	98.5	96.4	41
25	156/150	153	95.3/96.0	95.7	99.3	97.5	32
50	239/184	206	96.0/96.0	96.0	99.6	98.6	27
75	275/203	239	96.0/96.3	96.1	99.7	98.9	22

Table IV. Enhanced Predictive Ability of Binary Pattern Classifiers by Using Threshold Prediction Process

		+1 weight vector		−1 weight vector		
Δ	Av % prediction	% prediction with threshold	Not attempted	% prediction with threshold	Not attempted	Av % prediction
25	95.7	96.3	3	96.3	4	96.3
50	96.0	97.0	5	96.3	7	96.7
75	96.1	97.6	8	96.3	9	96.9

Table V. Feature Selection Using Threshold Binary Pattern Classifier Δ = 50

		Av % prediction	
m/e	Feedbacks	Δ = 0	Δ = 50
132	239/184	96.0	96.7
105	216/109	95.7	96.8
97	247/99	95.9	96.8
94	196/127	95.7	96.9
91	239/138	96.0	96.7
90	214/129	96.0	97.1
89	207/130	96.0	96.9

error. The correction increment is calculated according to the equation

$$c = \frac{2}{\mathbf{Y}\cdot\mathbf{Y}}(\pm\Delta - s) \qquad (2)$$

where $\mathbf{Y}\cdot\mathbf{Y}$ is related to the length of the pattern vector $\mathbf{Y}$, s is the scalar result which led to the incorrect classification ($s = \mathbf{Y}\cdot\mathbf{W}$), and the sign is chosen according to the sense of the error. This feedback method shifts the decision surface so that after feedback the pattern point is as far on the correct side of the decision surface as it was on the incorrect side before feedback. With assiduous choice of Δ, one would expect predictive ability to rise as compared to the zero threshold case because one is essentially more narrowly defining the hypervolume within which the hyperplane can fall and still be a "good" decision surface. One would also expect an increase in reliability with a nonzero threshold.

Table II shows the results of training binary pattern classifiers with and without the threshold. For each test, 300 spectra were randomly selected from the data set; three different randomizations were used, resulting in three different training and prediction set populations, as shown at the bottom of Table II. The TLU's with Δ = 50 require more feedbacks to train to 100% recognition in each case, and they display higher predictive ability in each case. These TLU's with Δ = 50 are able to correctly classify 95.0, 95.8, and 96.0% of the complete unknowns comprising the prediction set.

The figures given for per cent recognition were obtained as follows. After training to complete recognition, the members of the training set are again fed to the pattern classifier one at a time, but they are varied by a randomly generated Gaussian vector before classification. The σ figure refers to the relative standard deviation of the imposed Gaussian vector. For example, σ = 5% means that approximately one third of the components in each pattern vector are varied more than ± 5% from their original values before variation. The variations are imposed after the logarithmic transformation process, so the occurrence of errors is much more frequent than it would be in an actual laboratory situation where the errors would be introduced before any transformation. It is seen in Table II that the percentage recognition rises when the pattern classifier is trained with the nonzero threshold.

Table III shows the results of investigating the properties of binary pattern classifiers as a function of threshold size. The number of feedbacks required to correctly classify all the patterns in the training set rises as a function of Δ, as would be expected. The predictive ability and reliability both rise also. The last column gives the number of ambiguous m/e positions found out of the 132 used in the training. As Δ increases and the volume in which the final decision surface can fall is more narrowly bounded, the number of m/e positions used by the pattern classifier rises.

When training is done with a threshold, then the threshold can be employed in the prediction process. Table IV shows the results of such an investigation. Column 2 shows the results obtained by using the trained weight vectors to classify the unknown members of the training set with threshold of zero. Then the members of the prediction set were classified using the indicated values for Δ, that is, not classifying those patterns for which the scalar obtained fell between −Δ and Δ. The per cent prediction figures given are the percentage of classifications attempted which were correct. It is seen that in every case the per cent prediction with threshold is higher than that obtained without the threshold. Evidently this is a superior way to perform prediction of unknowns.

Table V shows that the method of feature selection previously described works well when a threshold is imposed on the binary pattern classifier. With Δ = 50, the pattern classifier was able to reduce the number of m/e positions from 132 to 89 while maintaining the same predictive ability. In each case, the predictive ability with Δ = 50 is higher than with Δ = 0.

Committee Machine. The work discussed above utilizes a single threshold logic unit to classify patterns. A slight generalization involves using two levels of TLU's (*4*). In this method the pattern to be classified is presented simul-

(4) N. J. Nilsson, "Learning Machines," McGraw-Hill, New York, N. Y., 1965.

Table VI. Properties of Layered Pattern Classifiers as a Function of Threshold, Δ

Δ	Feedbacks	% prediction	% recognition σ = 2%	% recognition σ = 5%	% prediction σ = 2%	% prediction % fall
0	180	96.0	95.0	90.7	92.8	3.3
25	397	97.0	99.8	98.5	96.7	0.3
50	375	98.0	100.0	99.8	97.7	0.3
75	359	97.3	99.8	100.0	96.5	0.8

Table VII. Training Set Representative Subset Selection

Trial	Training set size	Feedbacks +1WV/−1WV	Spectra fed back	% prediction	% prediction Δ = 50	No. not classified	Prediction Δ = 50	No. not classified	Percentage of all spectra classified correctly
I	300[a]	239/184	80	96.0/96.0	97.0	5	95.1	7	...
II	300[b]	196/206	82	94.3/95.7	94.2	5	97.3	11	...
III	162[c]	622/595	118						98.3
IV	172[d]	1283/1104	126						100.0

[a] Odd indexed members of data set.
[b] Even indexed members of data set.
[c] Spectra fed back in trials I and II.
[d] Training set III plus those predicted incorrectly in trial III.

taneously to three (or five or seven etc.) TLU's which operate in the normal manner. However, the outputs of the first layer of TLU's go to a second layer TLU which follows a majority rule law. Thus, the whole committee of classifiers sends its output to the vote-taker which classifies the original pattern into the category agreed upon by the majority of the first level TLU's.

A useful and simple training method is to make only the minimum necessary error correction feedback at each step in the training. Thus, when an incorrect classification is made during training, then the weights of the TLU's that missed being correct by the smallest amount are altered using Equations 1 and 2 with Δ = 0 substituted. Only enough TLU's are changed to ensure correct classification after the feedback.

Table II shows the results of training a committee machine with three members with the same three sets of data used by the other pattern classification implementations. Convergence to 100% recognition is seen to be fast, and the predictive ability is high. However, this committee machine is evidently quite sensitive to variations in the training set members, as seen from the per cent recognition figures.

Committee Machine with Dead Zone. A pattern classification system combining both features discussed above is a committee machine where each member has a nonzero threshold. Training is as before—the scalars of each member of the committee must be outside the dead zone (−Δ to Δ) to register any classification and the vote-taker registers an overall classification only when a majority of the committee members agrees on a classification. One would expect this to be somewhat more powerful pattern classification system than the simpler systems.

Table II shows the results of training a committee of three TLU's with Δ = 50 and with the same three sets of data as the other implementations in the table. The number of feedbacks is seen to rise, although it remains at a reasonable level. However, the per cent prediction is quite a bit better. This pattern classifier could correctly classify 95.7, 96.3, and 98.0% of the members of the prediction set, which are complete unknowns. The percentage recognition is seen to be very high also; this implementation is nearly impervious to errors in the patterns of this size.

A study was made of some of the properties of committee machines as a function of threshold size. The results are shown in Table VI. The number of feedbacks necessary for convergence jumps dramatically for Δ = 25 and then remains at approximately the same level. The predictive ability goes through a maximim for Δ = 50. The per cent recognition is very high for all nonzero thresholds. The sixth column gives the results of testing the predictive ability with random errors imposed on the prediction set members, and the last column gives the per cent drop in predictive ability with these errors compared to the predictive ability on the prediction set members themselves. Thus, a committee of machines each operating with nonzero threshold is seen to be superior in terms of predictive ability and reliability.

Data Pool Characteristics. For routine use of pattern classifiers, the goal would be to have at all times the best possible weight vectors for classification purposes. When new compounds were run on the mass spectrometer, they would be classified with probability of success approximated by the predictive ability. However, if these new spectra were then to be included in the (expanded) data pool, then it would be necessary to retrain the weight vectors, which requires access to the entire previous data pool. Because storage of the entire data pool may be inconvenient (or impossible) it was decided to see whether the entire data pool could be represented by a subset of its members. This was found to be so in a series of tests summarized in Table VII.

In trial I, the odd indexed members of the data set were used in the training set with the results shown. A tabulation was kept of the members of this training set which were fed back at some time during training; 80 of the 300 spectra participated in the training process. In trial II, the training set was composed of the even indexed members of the data set; 82 spectra participated in training. In trial III, the 80 spectra from trial I and the 82 spectra from trial II were used as a training set; then 10 spectra were missed out of the 438 remaining spectra. These 10 spectra were incorporated into the training set to make a training set of 172 members. In trial IV training was accomplished with these 172 spectra, of which 126 participated in training. The resulting weight vector could then classify not only the 172 members of the

training set but the other 428 spectra also. This is not called predictive ability because of the selection process employed in the training. However, the 126 spectra which participated in training are completely representative of the overall data set with regard to the question of oxygen presence–absence. By going through a feature selection routine identical to those described above, the number of *m/e* positions used in these 126 spectra can be reduced to 104, and the number of spectra used to 114. Thus, the entire data set of 600 spectra of 132 *m/e* positions (600 × 132 = 79,200) can be completely represented by 114 spectra of 104 peaks (144 × 104 = 11,856), a substantial savings.

RECEIVED for review June 26, 1970. Accepted October 19, 1970.

Double Beam Photon Counting Photometer with Dead Time Compensation

K. C. Ash[1] and E. H. Piepmeier

Department of Chemistry, Oregon State University, Corvallis, Ore. 97331

A low cost double beam photon counting photometer has been built with integrated circuits. The improved regulation of the double beam instrument is compared to single beam operation of one of its beams, and the limitations of double beam compensation are discussed. The counting precision due to shot noise for the double beam instrument compared to that of a similar single beam instrument is found to be worse by a factor of $<\sqrt{2}$. The influence of pulse overlap on a Beer's law calibration curve is shown for counting rates up to 2.75 MHz. Pulse width is <0.1 μsec. Dead time losses are partially compensated by gains due to overlapping pulses when the pulse height discriminator is set to reject about one half of the total pulses. A theoretical model that includes the influence of the discriminator is developed to account for the resulting increase in linearity up to medium counting rates.

PRECISION single beam photometers using photon counting detection systems have recently been built and discussed in detail (*1–3*). Among the advantages of a photon counting photometer are its abilities to reject most dark current pulses and to precisely measure low light levels such as might be found in portable or remote instruments that require low power light sources. Photon counting has been used in fluorescence microspectrophotometry (*4*, *5*) where low light levels are found, and may find use in other microanalytical techniques. Winefordner and Vickers (*6*) have reviewed recent articles concerning photon counting.

A double beam photon counting photometer, in addition to having the advantages of a single beam system, can automatically compensate for undesired changes in the light source and power supplies. In addition to a single beam instrument, a simple double beam photometer, such as the one described below, requires only a stationary optical beam splitter, a reference beam photomultiplier, and its discriminator/amplifier. The power supplies can be beneficially shared if they are decoupled. No additional digital circuitry is required because the pulses from the second beam replace the stable time base crystal oscillator needed in a single beam instrument.

In both the single and double beam instruments, a number proportional to the radiant power of the sample beam is obtained by counting the photoelectric pulses of the sample beam during a precisely controlled time base interval. In a single beam instrument, the time interval is produced by dividing the pulse frequency from a stable crystal oscillator. In a double beam instrument, the crystal oscillator is directly replaced by the photon rate pulses from the reference beam amplifier. In this way the ratio of the sample and reference beam signals is obtained directly. If the beams are adjusted so that the pulse rates are equal when a blank solution is in each cell, and the dark current pulse rate is negligible, the digital readout will numerically equal transmittance, the ratio of the beams. This is a distinct advantage over dc signal current measuring instruments, which must further process the sample and reference signals with log amplifiers, servo systems, or analog/digital circuits to obtain the ratio. Also the ratio $1/T$ can be obtained directly by simply throwing a switch that interchanges the sample and reference pulse trains, or by placing the sample in the reference beam.

Inexpensive integrated circuits (IC's) have made photon counting comparable in cost and simplicity to the conventional measurement methods. IC pulse amplifiers which smooth the pulses into an average dc signal current or voltage eliminate the need to build the discrete component amplifiers that have been used previously (*1–3*). Their compact size helps to provide faster response, which decreases dead time counting losses. Some pulse height discriminators, used to eliminate small noise pulses, may also provide sufficient amplification to eliminate the need for an additional amplifier (*7*). Inexpensive IC voltage regulators, such as the U5R-7723393 (Fairchild Semiconductor Div., Mountain View, Calif.) provide sufficient current and well regulated voltages to power the amplifiers and discriminators. For convenience, all of the digital processing of the amplifier pulses can be

[1] Present address, Teledyne Wah Chang Albany Corp., Albany, Ore., 97321

(1) M. L. Franklin, G. Horlick, and H. V. Malmstadt, ANAL. CHEM., 41, 2 (1969).
(2) R. H. Eather and D. L. Reasoner, *Appl. Opt.*, 8, 227 (1969).
(3) E. H. Piepmeier, D. E. Braun, and R. R. Rhodes, ANAL. CHEM., 40, 1667 (1968).
(4) J. R. Kemplay, *Electron. Eng.*, 34, 820 (1962).
(5) F. W. D. Rost, University of London, personal communication, 1968.
(6) J. D. Winefordner and T. J. Vickers, ANAL. CHEM., 42, 206 R (1970).
(7) D. L. Akins, S. E. Schwartz, and C. B. Moore, *Rev. Sci. Instrum.*, 30, 715 (1968).

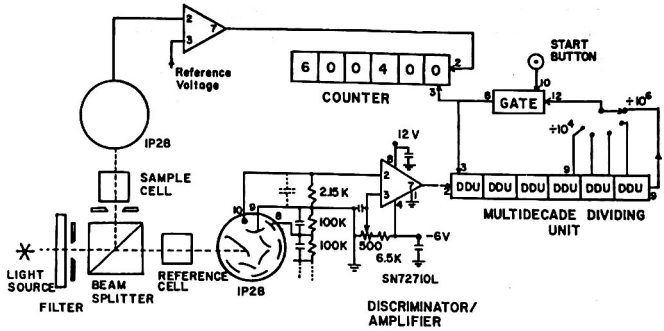


Figure 1. Double beam photon counting photometer

done by any sufficiently fast commercial digital counter with at least 6-digit readout and capable of operating in a frequency ratio X/Y mode for double beam operation, or with a stable crystal oscillator time base for single beam operation. Less expensive 4- or 5-digit counters can also be used without loss of significant figures if the frequency of the amplifier pulses is divided by one or two IC decade dividing units prior to entering the counter. A digital counter for this instrument was built using low power IC's to evaluate their use in a portable instrument.

DOUBLE BEAM COMPENSATION

Optical Changes. A double beam photon counting photometer compensates for changes in light source intensity with time by automatically adjusting the time base interval during which the sample beam photoelectric pulses are counted (Figure 1). Complete compensation however is achieved only when the dark count can be neglected. The way in which compensation is achieved and the influence of dark pulses are shown in the following example. Assume that both beams are matched for photon rates of 0.999 MHz when a blank is in the cell and the dark pulse rates are 0.001 MHz. A sample having a transmittance of 0.6 gives a corresponding photon rate of $0.999 \times 0.6 = 0.5994$ MHz. The total count rates including dark pulse rates of the beams are 1.000 MHz and 0.6004 MHz. The count rate of the reference beam may be electronically divided by 10^6 in this case to produce a time base counting interval of exactly one second. The gate (Figure 1) is opened by pushing the start button allowing the counter to accumulate pulses from the sample beam amplifier and the multidecade dividing unit (MDU) to accumulate pulses from the reference beam amplifier. In one second, 10^6 counts are accumulated by the MDU shutting the gate OFF and 600,400 counts are recorded in the digital counter used for readout, indicating the transmittance to a good approximation, <0.07% relative error. The correct transmittance can be calculated by subtracting 1000 dark pulses from each beam and taking the ratio of the results.

Now let the source photon rate decrease so that the reference photon rate is 0.499 MHz. The sample photon rate correspondingly decreases to $0.499 \times 0.6 = 0.2994$ MHz. The total rates including dark pulse rates are 0.500 MHz and 0.3004 MHz. It takes exactly 2 seconds for the reference beam to produce the necessary 10^6 counts to shut off the gate that controls the counting interval, and 600,800 counts from the sample beam are recorded by the digital counter, still indicating a transmittance of 0.6 within a relative error of 0.14%. If a single beam system had been used, the crystal oscillator would have maintained the counting interval at 1 second and an incorrect reading of about 300,000 would have resulted.

Since the counting interval has doubled, 2000 dark pulses have occurred in each beam and must be subtracted from the accumulated counts in each beam to obtain the correct value for transmittance. Assuming that the change in source photon rate was not known, the original correction of 1000 dark pulses might have been applied to the beams. This would have given a calculated transmittance of 0.6004, 0.067% in error. In either case the correct dark pulse correction can be obtained by blocking the sample beam and observing the accumulated count. It is important to note that dark pulse corrections become more important at low light levels and as the transmittance decreases.

Power Supply Changes. Since most dark current pulses are small compared to most photoelectric signal pulses, a pulse height discriminator is usually used to reject the smaller pulses. Since some dark pulses are counted and some signal pulses are rejected, the stability of the count rate depends upon the stability of the pulse height distributions of the signal and dark pulses, and upon the stabilities of the amplifier gain and discriminator level. The pulse height distributions are determined by the secondary electron emission multiplication processes in the dynode chain, which are influenced by the dynode voltages. Changes in these variables with power supply changes can be compensated by using common power supplies for the components of both beams. The degree of compensation that is achieved will depend upon how well regulated each component is by itself and how well the regulation characteristics of the respective components of each beam are matched. When signal counting rates approaching the dark counting rates are used, it may be necessary to consider the regulation characteristics separately for the signal and the dark counting rates. Considerable compensation was achieved in this instrument using the double beam mode compared to the single beam mode even though no attempts were made to obtain ideally matched components.

PRECISION

Franklin *et al.* (*1*) have shown how to calculate the random errors in transmittance and absorbance due to counting statistics for a single beam instrument. For comparable counting rates and counting times, the counting error for a

Table I. Comparison of Relative Per Cent Errors in Absorbance Due to Counting Statistics for Typical Single and Double Beam Instruments[a]

Absorbance	Single beam T method[b]	Double beam T method[b]	Single beam $1/T$ method[c]	Double beam $1/T$ method[c]
0.0044	14%	20%	14%	20%
0.0088	7.0	9.9	7.0	9.9
0.0177	3.5	4.9	3.5	4.9
0.0458	1.4	1.0	1.3	1.8
0.1549	0.44	0.59	0.40	0.54
0.3010	0.25	0.32	0.20	0.27
0.5229	0.17	0.21	0.12	0.15
1.0000	0.15	0.16	0.062	0.077
2.0000	0.24	0.24	0.033	0.039
3.0000	0.77	0.77	0.038	0.041

[a] Blank count 10^6. Dark count for blank 10^3.
[b] Reference beam controls counting interval.
[c] Sample beam controls counting interval.

double beam instrument is greater than the counting error for a single beam instrument. This is because the counting time interval is precisely fixed for the single beam instrument but has slight random variations for the double beam instrument.

When the sample and blank are alternately placed in the sample beam to give a readout directly in T, the transmittance for the double beam instrument is given by

$$T = \frac{N_s}{N_{rs}} \cdot \frac{N_{rb}}{N_b} \tag{1}$$

where N_s is the sample count minus dark pulses, N_b the blank count minus dark pulses, N_{rs} the reference beam count with the sample in the sample beam minus dark pulses, and N_{rb} the reference beam count with a blank in the sample beam minus dark pulses. Although N_{rb} and N_{rs} are equal and cancel when the direct transmittance readout method is used, each produces a counting interval that has a random error determined by counting statistics. These errors do not cancel. The counting statistics error (ΔT) in transmittance can be calculated using Equation 1 and the fact that the relative variance is additive in multiplication (*8*):

$$\Delta T = \frac{N_s N_{rb}}{N_b N_{rs}} [V_s + V_b + V_{rb} + V_{rs}]^{1/2} \tag{2}$$

In Equation 2, each V_i denotes the relative variance for the factor N_i and can be calculated from the equation

$$V_i = \frac{N_i + 2D_i}{N_i^2} \tag{3}$$

where D_i is the dark count. For counting statistics the absolute variance equals the count (*9*). Since the absolute variance is additive in addition/subtraction of counts (*8*) the term $N_i + 2D_i$ is the absolute variance in N_i corrected for dark count. N_i is obtained from $N_i = (N_i + D_i) - D_i$ where $(N_i + D_i)$ is the observed count uncorrected for dark pulses. When the instrument is stable so that the average counting rate for the reference beam is constant, N_{rs} and N_{rb} need not be corrected for dark count and their relative variances become simply $1/N_i$. For a single beam instrument the terms V_{rb} and V_{rs} in Equation 2 are negligible. Their appearance for the double beam instrument causes ΔT to increase by $\sqrt{2}$ when comparing both instruments for a sample having a transmittance of one.

When the sample and reference beams are interchanged so that the sample beam controls the counting interval for the pulses from the reference beam the readout equals $1/T$, when the dark pulses are negligible. In this case Equation 1 is inverted to give

$$1/T = \frac{N_{rs}}{N_s} \cdot \frac{N_b}{N_{rb}} \tag{4}$$

In this case when dark pulses are negligible, N_s and N_b are equal and fixed since this channel accumulates a predetermined number of pulses to control the counting interval. The counting statistics error in $1/T$ is similar to Equation 2; or

$$\Delta 1/T = \frac{N_b N_{rs}}{N_s N_{rb}} [V_s + V_b + V_{rs} + V_{rb}]^{1/2} \tag{5}$$

Equation 3 is used to find V_s and V_b. The dark pulse count can be found from

$$D_i = N_{pi} \cdot \frac{N_{ri}}{N_{rd}(N_{pi}/N_{pd})} \tag{6}$$

where N_{pd} and N_{pi} are the preset number of counts accumulated by the sample beam when the beam is dark and with a sample (or blank) respectively, N_{ri} is the reference beam count when the sample or blank is in the sample beam, and N_{rd} is the reference beam count when the sample beam is dark. Ordinarily $N_{pd} = N_{pi}$. However if D_i is a small fraction of N_b or N_s, the counting time for N_{rd} might be unnecessarily long unless N_{pd} is decreased. When the instrument is stable so that the average counting rate for the readout beam is constant, N_{rs} and N_{rb} need not be corrected for dark count in which case their relative variances are $1/N_i$.

When the $1/T$ method is used with a single beam instrument, the pulses for the readout beam are replaced by pulses from a stable oscillator. Equation 5 is still valid but $V_{rs} = V_{rb} = 0$.

The relative per cent error in absorbance ($\%\Delta A$) is calculated from ΔT as

$$\%\Delta A = \frac{-\log (T + \Delta T) + \log T}{-\log T} \times 100\% \tag{7}$$

or from $\Delta(1/T)$ using the similar Equation 6 in reference (*1*). The results of an error analysis for a single beam and a double beam instrument using the T and $1/T$ readout methods are presented in Table I. For ready comparison the blank count (10^6) and dark count (10^3) of the single beam instrument and the two beams of the double beam instrument are assumed to be identical. For either the T or $1/T$ method, the error in absorbance due to counting statistics for the double beam is always less than $\sqrt{2}$ times the error of the single beam instrument. For either instrument the $1/T$ method gives a lower counting statistics error in absorbance than the T method. This is due primarily to the increase in counting time caused by the absorbing sample in the reference beam; similarly low errors could be achieved by increasing the predetermined number of counts accumulated by the reference beam and hence the counting time when the T method is used. The shallow minimum in the error curve is reached at higher absorbances for the $1/T$ method compared to the T method. The increase in error at high absorbance values for the $1/T$

(8) H. A. Laitinen, "Chemical Analysis," McGraw-Hill, New York, N. Y., 1960, p 545.
(9) L. J. Rainwater and C. S. Wu, *Nucleonics*, 1, 60 (1947).

method is due primarily to the increasing importance of dark count as it approaches the sample count.

DEAD TIME COMPENSATION

The useful dynamic range of a photon counting system is limited at the low intensity end by the dark current pulse rate and at the high end by pulse overlap. When a pulse height discriminator is used, pulse overlap can cause both positive and negative deviations from a linear relationship between count rate and photon rate. A count results when a pulse is high enough to exceed the discriminator level. If a second pulse arrives before the discriminator resets, the second pulse will be interpreted as a continuation of the first and will not be counted. This causes loss of a count, commonly known as a dead time loss. A gain of one count can occur when neither pulse is high enough to exceed the discriminator level, but their overlapping produces a pulse that does exceed it.

Both pulse losses and pulse gains significantly influence the observed counting rate when the photon rates are moderately high. A theoretical model in the next section considers the interaction of the gains and losses and shows how their influences are affected by the discriminator level setting. Although the model is simplified by certain assumptions, it correctly predicts the experimentally observed fact that the linear range of the observed counting rate can be extended to higher rates by setting the discriminator level to pass about one half of the total number of pulses. The extended linear range occurs when the pulse gain effect compensates for the dead time losses. The extended linear range allows the double beam instrument to be used at higher counting rates, which shortens the measurement intervals for a given counting precision.

Pulse Gain Model. Counting losses due to pulse overlap have been considered in detail by Rainwater and Wu (*9*), De Lotto (*10*), and others. The following model not only includes the commonly considered counting losses but also considers the influence of a pulse height discriminator and the accompanying pulse gain effect. This influence has not been treated quantitatively in the literature. Since some discrimination is inherent in any electronic counting system, the prediction of pulse gains should not be overlooked.

Although simplifying assumptions are used to facilitate the derivation of a mathematical expression for the response curve (observed counting rate *vs.* pulse rate), the result adequately predicts the general shape of the experimental response curves over the range of analytically useful discriminator settings. The new model also provides a better estimate of pulse overlap time than commonly used dead time models.

A mathematical model derived by Rainwater and Wu for pulse losses provides the initial step in our derivation, and a brief review of their approach is presented. It is assumed that the pulses occur randomly in time and that the width of each pulse is the same. Let the true pulse rate N be the total average rate that would be counted if there were no pulse overlap and no discriminator were necessary. Let N' be the observed average counting rate when each pulse has an overlap time width of τ, and no discriminator is used.

Rainwater and Wu find the relationship of N' to N by equating the occurrence of a countable pulse to the event of a pulse having sufficient time to return to the base line. The probability that the trailing edge of a pulse will return to the base line is equal to the probability that zero pulses will occur during the width τ of the pulse. When the pulses arrive randomly with time, this probability is found from the Poisson distribution

$$P = \frac{u^m e^{-u}}{m!} \tag{8}$$

where P is the probability of obtaining exactly m pulses within a time interval τ and u is the mean number of pulses $N\tau$ expected within the time τ. The probability of zero counts is $e^{-N\tau}$ from Equation 8.

The rate of returning pulses equals the total pulse rate times the probability that a pulse returns to the base line, or

$$N' = Ne^{-N\tau} \tag{9}$$

Their assumption is that each time a returning pulse occurs, it is followed by a countable pulse and therefore N' is also numerically equal to the rate of counted pulses. Notice that the countable pulse may be a single pulse or the first pulse of a series of overlapped pulses which form a single countable pulse.

When a discriminator is used, however, the pulse that follows the returning pulse may be too small to be counted, and a count is lost. The frequency of such lost events can be found as follows. It is assumed that the height of a given pulse is independent of the heights of previous pulses so that the heights occur randomly. It is also assumed that the pulse duration τ is constant and determined by the pulse shape prior to entering the discriminator, and that the discriminator and counter are fast enough to prevent additional losses due to pulse overlap. When the discriminator is set to pass at low pulse rates, a fraction A of all individual pulses, the probability of a single pulse being too small to be counted is $(1 - A)$. In order to remain uncounted, a small pulse must return to the base line before it becomes overlapped by another pulse, which might cause the total overlapped pulse to be large enough to trigger the discriminator and be counted. The probability of any pulse being allowed to return to the base line within a time τ is $e^{-N\tau}$ as shown above. Therefore the probability that a pulse is both small and returning is $(1 - A)e^{-N\tau}$. The frequency of such lost events is equal to the frequency $F1$ with which any returning pulse is followed by a small returning pulse. $F1$ is equal to the frequency N' with which any returning pulse is followed by any pulse times the probability that this second pulse is a small returning pulse or

$$F1 = N'(1 - A)e^{-N\tau} = N(1 - A)e^{-2N\tau} \tag{10}$$

where N' is obtained from Equation 9. Since each of these events results in the loss of a count the predicted observed count rate now becomes $N' - F1$.

A counting loss may also occur when a small pulse following a returning pulse is overlapped by one other small pulse, but the resulting pulse is still not large enough to be counted. The probability that one pulse occurs within a time τ is $N\tau e^{-N\tau}$ from Equation 8. The probability that this or any pulse is a small returning pulse is $(1 - A)e^{-N\tau}$ as shown above. Therefore, the probability that one small returning pulse occurs within a time τ after a previous pulse is $(1 - A)e^{-N}$ $N\tau e^{-N\tau}$. The frequency $F2$ with which a returning pulse is followed by a small pulse which itself is followed and overlapped by another small but returning pulse is

$$F2 = (1 - A)N'(1 - A)e^{-N\tau}N\tau e^{-N\tau} \tag{11}$$

(10) I. De Lotto, P. F. Manfredi, and P. Principi, *Energ. Nucl.*, **11** 557 (1964).

Let the fraction of these double small-pulse events which are large enough to be counted be C. Then from Equations 11 and 9, the frequency with which uncounted double small-pulse events occur is

$$F3 = (1 - C)F2 = (1 - C)(1 - A)^2N^2\tau e^{-3N\tau} \quad (12)$$

It can be shown that the ratio of correction terms $F3/F1$ is always less than $1/e$ and for common values of $A > 0.2$ and $C > 0.5$, the ratio is always less than 0.04. The contributions of correction terms for overlapped pulses that are formed by more than two small pulses should be considerably smaller than $F3$ for these values of A and C and therefore will be neglected. This is equivalent to assuming that such pulses are all large enough to be counted. The final expression for the observed count rate n then becomes

$$n = N' - F1 - F3$$

$$n = Ne^{-N\tau} - N(1 - A)e^{-2N\tau} - (1 - C)(1 - A)^2N^2\tau e^{-3N\tau} \quad (13)$$

Note that when $A = 1$, Equation 13 degenerates to Equation 9. This corresponds to the usually undesired and unattainable experimental case where the discriminator is set to pass all pulses.

Further discussion of Equation 13 is facilitated by expanding its exponential terms into infinite series and multiplying the terms together. The final expression is an infinite series in $N\tau$. When $N\tau$ is small, quadratic and higher order terms in the final expression can be neglected giving the simplified result

$$n = AN\left[1 + \frac{N\tau}{A}(1 - 2A - (1 - C)(1 - A)^2)\right] \quad (14)$$

When $\tau = 0$, no overlap occurs and the ideal linear relationship $n = AN$ results. The second term in the brackets represents an error term that can be used to predict deviations from linearity for various discriminator level settings. For instance when the discriminator is set to pass most of the pulses, A approaches unity, the error term becomes negative and the commonly observed downward curvature of the response curve results as N increases. When the discriminator is set to reject most of the pulses, A is close to zero, the error term becomes positive, and an upward curvature results. No curvature is predicted when the error term is zero. Realistic values of C range from 0.5 to 1.0 as shown in the Appendix. For $C = 0.5$, 0.833, and 1.0, the error term is zero when $A = 0.414$, 0.475, and 0.500 respectively. Therefore, for realistic values of C, Equation 14 predicts linear results for small $N\tau$ when the discriminator is set to pass somewhere between 40 to 50% of the total number of pulses.

Because Equation 14 is valid only for small $N\tau$, the relative deviations from the ideal linear relationship $n = AN$ were calculated using Equation 13 for various values of A using $C = 0.5$, 0.833, and 1.0. The relative deviations were found to be independent of τ when $N\tau$ was used as the independent parameter. When the values of A calculated above from Equation 14 were used with the respective values of C, the maximum relative deviation was only 0.01% up to values of $N\tau = 0.01$ and 0.8% up to $N\tau = 0.1$. By using values of A that were 5% lower than these, the maximum relative deviation of all $N\tau$ up to 0.1 was found to be less than 0.15%. These results predict considerable improvement in linearity over commonly used Equation 9 which predicts a relative deviation of 1% at $N\tau = 0.01$ and about 10% at $N\tau = 0.1$. For instance when $\tau = 0.07$ μsec and the discriminator is set to optimize linearity, Equation 13 predicts good linearity up to $N = 1.4$ MHz while Equation 9 predicts a deviation of 10% for the same pulse rate and τ.

Evaluating Dead Time. As A approaches unity, for low discriminator settings, Equation 14 degenerates to

$$n = AN[1 - AN\tau], \text{ or } n = N[1 - N\tau] \quad (15)$$

which is a first order approximation to Equation 9. This approximation is often used with small values of $N\tau$ to evaluate τ. However when a discriminator is used, for instance to minimize dark pulse counts, the response is more linear than predicted by Equation 9, and Equation 15 gives inaccurately low values for τ. When the discriminator is set to pass 40–50% of the pulses, complete dead time compensation is approached for moderate values of $N\tau$ and the apparent value of τ calculated using Equation 19 approaches zero. τ could be in error by orders of magnitude if Equation 15 were used in this case.

For $A < 1$, τ can be more accurately evaluated from the maximum count rate that is observed as the light source is increased to high intensity. Equations 9 and 13 have maxima at

$$n = k\tau^{-1} \quad (16)$$

where k is a constant that depends on the values of A and C used. For Equation 9, $A = C = 1$ and $k = e^{-1} = 0.368$. The constant decreases with decreasing C or decreasing A. When A is as low as 0.2 and $C = 0.5$, $k = 0.267$. Therefore, even when A and C are not accurately known, the value of τ can still be calculated assuming $k = e^{-1}$ without causing an error of more than 40%. For a given A, k depends only slightly on C. If C is unknown and A can be estimated to be greater than 0.2, k can be found to within 4% from the approximation

$$k = 0.24 + 0.128\,A \quad (17)$$

Since counting systems involve some type of discrimination the use of the maximum observed count rate to evaluate τ will generally give more accurate results than the use of Equation 15.

EXPERIMENTAL

Response Evaluation. A modular double beam instrument was used to obtain counting rate as a function of relative intensity for the photomultiplier–discriminator pairs used in the compact double beam instrument described below. A model MP-1019 tungsten light source (McKee-Pedersen Instruments, Danville, Calif.), MP-1018 monochromator MP-1017 sample/filter holder and a MP-1022 prismatic beam splitter were optically connected in that order to provide two proportional beams. One beam was observed by the photon counting detector under evaluation and the other beam by a MP-1021 photomultiplier unit which provided an analog signal directly proportional to relative intensity. The MP-1021 photo-multiplier was powered by the high voltage power supply on a MP-1001 console. A 5-step voltage divider that drew the same current from the power supply for each setting from 250–900 V was added to the output of the power supply for versatility. The anode current was sent to the summing point of a MP-1031 chopper stabilized FET operational amplifier. A MP-1009 precision high impedance selector was used for the feedback resistor to provide an output voltage proportional to anode current. A 0.01 μf capacitor was placed in parallel with the feedback resistor to compensate for cable capacitance.

A model EU-20V recorder (Heath Company, Benton Harbor, Mich.) was used for readout. A 1-K resistor between

the operational amplifier and the recorder eliminated possible operational amplifier oscillation due to the 0.5-μf input capacitance of the recorder without attenuating the signal. A Heath Model EU-805A Universal Digital Instrument was used to observe the counting rate of the photon counting detector. It was preceded by a decade dividing unit (DDU discussed below) to simulate loading of the discriminator by the DDU and decade counting units used in the final instrument. The light intensity was varied by changing the monochromator slit. A 2 × 2-inch frosted glass plate was placed in the sample/filter holder to disperse the light after leaving the monochromator. This helped to provide even illumination of the photocathodes of both detectors regardless of slit width.

Double Beam Instrument. A diagram of the double-beam photon counting photometer is shown in Figure 1.

Optical System. The light source used was a Westinghouse WL22601 neon-filled calcium hollow-cathode tube. It was powered by a Heath EUW-15 regulated power supply in series with ballast resistors which allowed a current range of 1 μA to 20 mA.

A 421-nm interference filter with an 11-nm bandpass and an ultraviolet broad band filter, Corning CS-754, which cuts off above 400 nm were used together to isolate a narrow band of neon lines between 331 and 360 nm (*3*). This wavelength is near the maximum response region of the photomultiplier tubes used.

A 33 × 33 × 20 mm prismatic beam splitter (Edmund Scientific) split the incoming beam into a reference and a sample beam. The sample and reference cells were standard 1-cm path length glass cells. An adjustable slit was placed in the sample beam between the cell and the photomultiplier to match beam intensities.

Counting Detection System. The detectors were RCA-1P28 photomultiplier tubes. Operating voltage was supplied by a Hewlett-Packard–Harrison 6515A variable high-voltage dc power supply. The dynode potentials for both beams were maintained by a series of 1% metal film 100-kilohm resistors. Four 0.05-μf ceramic capacitors were wired in parallel with the last four resistors of each photomultiplier to maintain constant dynode potential during the current pulses. A 1%, 2.15-K resistor was used for each anode load resistance to discharge the load capacitance after each pulse. This value provided a fast fall time for each anode current pulse without significantly decreasing its voltage height from the ideal maximum value that would occur when a very large resistance is used. The stray capacitance, dashed lines, was minimized by using short leads since it influences the voltage height of each current pulse. The 2.15-K resistor also limited the average input voltage to the discriminator to a safe level even at very high light levels.

Texas Instrument SN72710L high speed differential voltage comparitors were used as pulse height discriminators and amplifiers similar to work done by Akins (*7*). They were powered by Heathkit 1P27 regulated low voltage power supplies. The discriminator level was set by the center tap of a voltage divider potentiometer connected between the negative 6-V power lead and ground. The comparator power leads were decoupled to ground with 0.05-μf capacitors and the reference voltage leads were decoupled to ground with 50-pf capacitors. Further amplification of the photomultiplier signal was not necessary.

Multidecade Dividing Unit. The multidecade dividing unit (MDU) is based on the design of Lancaster (*11*). The MC-724P and MC-790P integrated circuits were made by Motorola. The MDU consists of six decade dividing units (DDU) in series. It is tapped in five places by a rotary switch, providing division by 1×10^6, 4×10^5, 1×10^5, 4×10^4, and 1×10^4. A single DDU is shown in Figure 2.

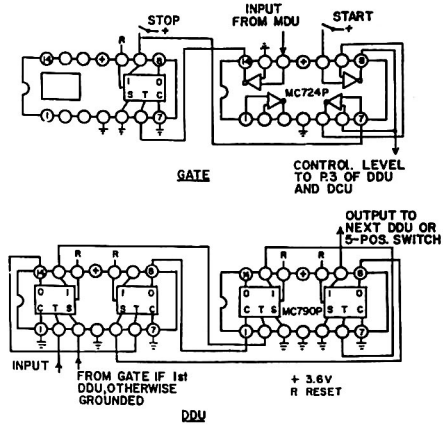


Figure 2. Schematic diagram of the GATE and a Decade Dividing Unit. IC's are viewed from top.

A two-input gate to control the input to the counter is made from two MC-724P quadruple NOR gates connected as a bistable multivibrator. A potential applied to the "stop" lead produces an output signal as the "shutoff" lead. The "shutoff" lead is connected to pin 3 of the first flip-flop in both the MDU and the multidecade counting unit. The signal switches the flip-flops to the set position, thus stopping the counting and dividing units and holds them there.

A potential applied at the "start" lead of the multivibrator flips it so that the output level is zero and the counting and dividing units may begin operating. The units continue counting until the MDU accumulates the predetermined number of pulses indicated by the rotary switch position. The MDU then emits a pulse which is inverted and triggers a flip-flop that supplies a voltage to the "stop" lead of the multivibrator.

Multidecade Counting Unit. The multidecade counting unit (MCU) used is a modification of the decade counting unit (DCU) of Lancaster (*12*). The schematic of the modified counter is shown in Figure 3. The 2N5129 transistors were obtained from Fairchild. The lamps are Grain of Wheat No. 10 bulbs (Aristo-Craft, Newark, N. J.). The counting and dividing units were powered by a Heathkit IP-27 regulated low voltage power supply. Each counting unit draws a current of 190 mA, 80 mA of which is used by the bulb. Six counting units were connected in series, giving a capacity of 999,999 counts.

The operating and reset potential for both counting and dividing units is 3.6 volts. The reset is connected through a momentary contact switch. The power supply need not be especially stable as shown below. Batteries could be used if a portable instrument were desired. The counting and dividing units operate at frequencies greater than 10 MHz and have no lower frequency limit.

Operation. The photometer was allowed to warm up for 1 to 2 hours before use. The hollow cathode light source was allowed 20 minutes to stabilize whenever its current was changed.

The sample and reference cells were not removed during analysis in order to ensure stability of position. Sample solutions were introduced by means of a syringe and removed

(11) D. Lancaster, *Pop. Electron.*, **28**, 92 (1968).

(12) *Ibid.*, p 27.

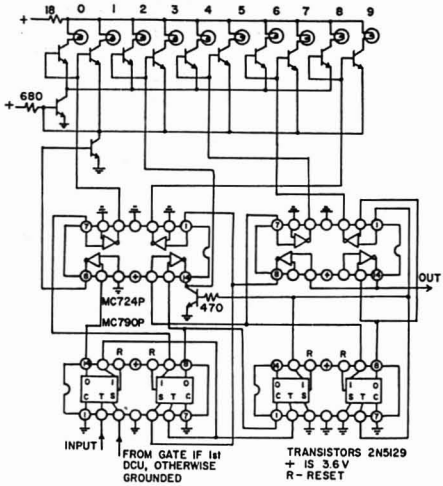


Figure 3. Schematic diagram of a Decade Counting Unit. IC's are viewed from top.

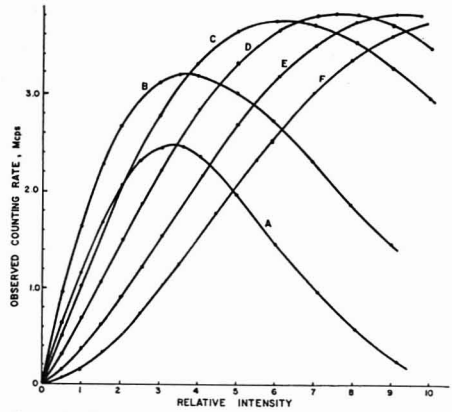


Figure 4. Response of a photon counting channel to relative light intensity.

A. **Discriminator setting 40 mV, $A = 1$, $\tau = 0.15$ μsec**
B. **Discriminator setting 50 mV, $A = 0.9$, $\tau = 0.11$ μsec**
C. **Discriminator setting 55 mV, $A = 0.4$, $\tau = 0.079$ μsec**
D. **Discriminator setting 60 mV, $A = 0.16$, $\tau = 0.071$ μsec**
E. **Discriminator setting 65 mV, $A = 0.1$, $\tau = 0.069$ μsec**
F. **Discriminator setting 70 mV, $A = 0.05$, $\tau = 0.068$ μsec**

with a vacuum suction system both having Teflon (Du Pont) needles.

The total light intensity was adjusted to the desired level by means of a variable slit. The intensity could also be changed by changing the hollow cathode current, but this changes the spectral character of the light. At low currents the neon lines predominate, but at higher currents the calcium lines become more and more prevalent. The sample and reference outputs were matched to equal count rate with the adjustable slit in the sample beam.

The observed count rates of each beam were independently determined by connecting the output of the appropriate discriminator into the counting unit. The reference beam channel of the counting unit was replaced by connecting a 100-KHz square wave from a Heathkit EUW-27 sine-square generator into the dividing unit. A divider setting of 10^5 gives a readout directly in pulses per second.

Reagents. The chemical system studied was potassium dichromate in 0.64*M* nitric acid. Deionized, distilled water and reagent grade potassium dichromate and nitric acid were used.

An acidic potassium dichromate system was chosen because it absorbs strongly in the 330- to 360-nm range of the light source. The solutions were made acidic to prevent conversion of the dichromate to chromate ion. Nitric acid was used as other common strong acids complex with the dichromate ion (*13*).

RESULTS AND DISCUSSION

Response Curves. The photomultiplier power supply voltage was set at 900 V for all measurements to obtain maximum pulse heights. The relative change in output for a variation in this voltage was less at 900 V than at lower voltages. Although dark current count rate is higher at higher voltages, it was only about 1000 cps at 900 V for the tubes used.

Typical response curves at different discriminator level settings for a single channel are shown in Figure 4. Curve *C* demonstrates the improved linearity that results when the discriminator is set at low pulse rates to pass about one half of the total pulses, compared to curve *B* where most of the pulses are passed. The discriminator levels of the double beam instrument were set to obtain extended linear response by visually interpolating response curves similar to those in Figure 4.

Values of A were estimated from the shapes of the curves at low counting rates in Figure 4. The maximum observed count rate and k values from Equation 17 were then used with Equation 16 to find τ for each curve. For comparison with these values of τ, the pulses entering the discriminator were observed at low light levels with a Tektronix 555 oscilloscope with 1A1 plug ins and X10 probe having a nominal capacitance of 7 pf. The pulse rise time equalled that of the oscilloscope and the trailing edge decreased exponentially with a time constant of 0.04 μsec. The time constant is controlled primarily by the parallel combination of stray, anode, amplifier input, and probe capacitances, as the combination discharges through the 2.15-kΩ anode resistor after an anode charge pulse. The effective pulse overlap time of the pulse depends on where the discriminator level intersects the exponentially trailing edge. A low discriminator level, large A, near the wide base of the pulse will cause the effective overlap time to be longer than when a higher discriminator level near the narrow peak of the pulse is used. The values of τ found from the peaks in Figure 4 appear in agreement with the observed pulse width and increase with increasing A as expected from the exponentially decaying pulse shape. The unusually low counting rates at low intensities for curve A, compared to curve B, may be due to the discriminator level approaching the 60-Hz noise level. This might also help to cause the large value of τ for curve A.

The values of A and τ found from the curves in Figure 4 were used in Equation 13 to generate the corresponding theo-

(13) F. A. Cotton and F. R. S. G. Wilkinson, "Advanced Inorganic Chemistry," Interscience, New York, N.Y., 1966, p 1136.

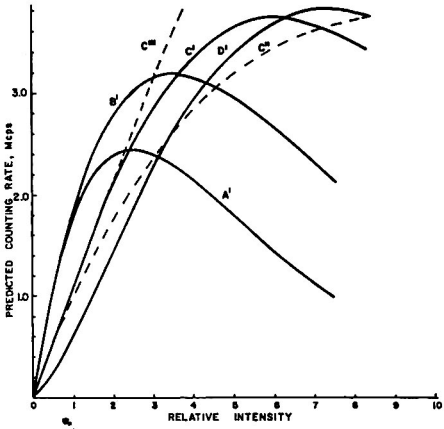


Figure 5. Theoretical response curves. Curves A'–D' from Equation 13 correspond to curves in Figure 4. Curves C'' and C''' are from Equation 9

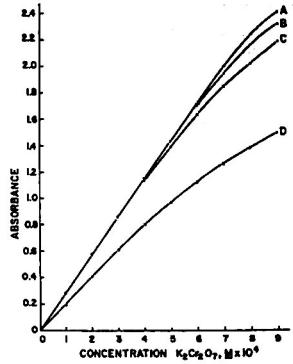


Figure 6. Calibration curves for four different light levels

A. Blank counting rate 0.1 MHz
B. Blank counting rate 0.5 MHz
C. Blank counting rate 1.0 MHz
D. Blank counting rate 2.75 MHz

retical curves A', B', C', and D' in Figure 5. The value of C is not critical except for small values of A and was estimated to be 0.833. A scaling factor was used to adjust the abscissas of the experimental and theoretical curves for comparison purposes because the absolute value of the experimental pulse rate was unknown. For curve C, the ordinates of the experimental and theoretical curves agree to within 1% up to 2 MHz and within 2% throughout. Agreement for curves B and D was 5%. Theoretical curves for curves E and F fit poorly even when values of $A < 0.01$ and $C < 0.833$ were used. This is probably due to the fact that when A is this low it is necessary to include terms in Equation 13 that account for multiple pulses that are made up of more than two small pulses. The fit to curve A was also poor because of the unusually low counting rates at low intensities compared to curve B as discussed above. Better fits to limited portions of curves B, C, and D have been obtained by an iterative least squares technique. These results were obtained at the expense of poorer fits in other regions of the curves and little improvement was obtained to the fit of any curve as a whole. Better agreement between the theory and experiment should be obtained by eliminating the assumption of constant pulse width and including the influence of multiple pulses containing more than 2 small pulses. The assumption of the random occurrence and independence of pulse heights may not be totally valid, particularly if gas ionization after pulses are present in the photomultiplier tube.

For comparison with Equation 13 curves C'' and C''' were generated with Equation 9 using values of τ obtained from the data for curve C. Both curves were normalized to have the same slope as curve C' at low counting rates where pulse overlap is negligible. Curve C'' used a value of τ = 0.098 μsec obtained from Equation 16 using the maximum observed count rate and $k = e^{-1}$. Although the value of τ is not far from what might be expected from the observed pulse width and shape, the curve shows considerable curvature at medium counting rates compared to curve C', or curve C which essentially superimposes on curve C'. Curve C''' used a value of τ = 0.005 μsec obtained from Equation 15 using a deviation from linearity of 1% at 2 MHz. Deviation of curve C''' from curve C' is apparent for medium counting rates and the value of τ is an order of magnitude less than expected from the observed pulse width. These comparisons show that the commonly used dead time counting loss theory expressed by Equation 9 is not able to account for the experimental results. By comparison, the model used to derive Equation 13 that accounts for the presence of a discriminator is able to predict the experimental results reasonably well for values of A from 0.16 to 0.9, which includes the region of analytical interest.

Calibration Curves. Figure 6 shows how the calibration curve for dichromate changes as the incident beam is increased in intensity to high pulse rates. The curvature at high absorbances is due primarily to the polychromatic nature of the incident beam. At high pulse rates the nonlinearity of the pulse rate response curve produces a noticeable decrease in slope and increased curvature for the calibration curve. Where measurements of small differences in concentration are required, increased precision obtained by using higher counting rates for a fixed time interval might be beneficially traded for some nonlinearity of the calibration curve. However, an upper limit of counting rate depending upon overlap time is eventually reached, Figure 4. This region should be avoided since the readout would change very little for even moderate changes in photon rate due to concentration changes.

Double Beam Compensation. The improved regulation of the double beam instrument compared to single beam operation of the sample channel for changes in power supply voltages is shown in Table II. Power supply changes may influence to different extents the signal and dark counting rates. The influences were not separated in Table II because for these instruments the dark count is only a small fraction of the signal except at high absorbances. The minus 6-volt power supply influences the counting rate primarily because it controls the discriminator levels. The response curves are closely related to the discriminator levels. Regulation would be better if the response curves of both photomultipliers were more closely matched.

Changing the counter voltage changes the minimum height and duration of a pulse that is necessary to trigger the counter.

Table II. Regulation[a] of Single and Double Beam Instruments with Respect to Power Supply Changes

	Discriminator power supplies		Photomultiplier power supply	Digital circuit power supply
	+12 V	−6 V	−900 V	+3.5 V
Single beam	0.05	0.85	2.2	0.05
Double beam	<0.09	0.33	0.18	<0.05

[a] Relative change in blank readout + relative change in voltage.

Although most pulses from the discriminator are large enough to trigger the counter, a few smaller ones are present. Therefore the counter takes a minor part in pulse height discrimination. A discriminator/amplifier or photomultiplier with ten times greater gain would help to minimize this problem.

Good regulation with respect to changes in light source intensity is directly dependent upon the slopes of the response curves for both beams and upon low dark pulse rates. For compensation to be achieved in even a narrow range of operation the tangent to the slope must pass through the origin. For compensation over a wide range of operation the response curves must be linear and intersect the origin. This precludes the use of high counting rates to obtain high precision when the light source is not stable. It also emphasizes the advantage of using the discriminator level to extend the effective linear range of the response curves.

APPENDIX

The value of C can be estimated from the pulse height distribution of the small pulses, which overlap to form larger double pulses. Let individual pulses of height h_i occur with a probability or frequency f_i. A typical pulse height distribution curve in the region where the discriminator is ordinarily experimentally set is shown in Figure 7, curve A. It is assumed that the height distribution does not change significantly for succeeding pulses after a given pulse. The abscissa is divided into D equal and sufficiently small intervals of width Δh. The probability P_{ij} that when a small pulse overlaps it will be overlapped with another small pulse having a height between h_j and $h_j + \Delta h$ is approximately

$$P_{ij} = \frac{f_j \Delta h}{\sum_{j=0}^{D} f_j \Delta h} = \frac{f_j \Delta h}{A_T} \tag{18}$$

where A_T in the limit equals the total area under the pulse height distribution curve from the origin to H, i represents the first pulse and j the second pulse of an overlapping double pulse event. The frequency F_{ij} of occurrence of such events is proportional to f_i or

$$F_{ij} = f_i P_{ij} \tag{19}$$

To form a double pulse that exceeds H and is therefore counted, a pulse of height h_i must overlap with any pulse that has a height h_j between H_o and H where H_o is the height

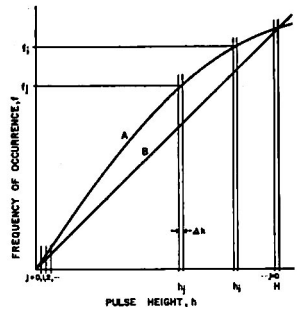


Figure 7. Pulse height distribution curves.

equal to the difference $(H - h_i)$. Taking all possible combinations of j pulses from H_o to H into account for i pulses of a given height, a large countable double pulse occurs with a frequency

$$F_i = \sum_{j=D-i}^{D} f_i P_{ij} = f_i \sum_{j=D-i}^{D} \frac{f_j \Delta h}{A_T} = f_i \frac{A_{Ho}^{H}}{A_T} \tag{20}$$

where A_{Ho}^{H} in the limit is the area under the curve from H_o to H. Summing over all i pulses, the probability C that any double pulse formed from only small pulses will exceed H is given by

$$C = \frac{\sum_i F_i}{\sum_i f_i} \tag{21}$$

where the numerator is the frequency of all of the double pulses (formed from only small pulses) with heights sufficient to exceed the discriminator level and the denominator is the frequency of all double pulses formed from only small pulses.

When all pulse heights have the same probability or frequency of occurrence a value of $C = 0.5$ is obtained from Equation 21. This appears to be a lower limit for C because typical experimental distributions (*3*, *14*) are Poisson shaped and show increasing frequency with increasing pulse height, up to the region where the discriminator level is set to pass more than about half of the pulses. Compared to the flat distribution such distributions increase the probability C of forming larger pulses that exceed the discriminator level. The linearly increasing pulse height distribution curve B in Figure 7 is a better approximation to actual distributions and gives $C = 0.833$. C cannot, of course, exceed unity.

RECEIVED June 10, 1970. Accepted September 28, 1970. This work was partially supported by a grant from the Oregon State University General Research Fund.

(14) R. Foord, R. Jones, C. J. Oliver, and E. R. Pike, *Appl. Opt.*, 8, 1975 (1969).

Chlorine-35 Nuclear Quadrupole Resonance Studies of Trichloromethyl Compounds

Edward G. Brame, Jr.

E. I. du Pont de Nemours and Company, Inc., Elastomer Chemicals Department, Experimental Station, Wilmington, Del. 19898

Chlorine-35 nuclear quadrupole resonance (NQR) spectrometry was applied to the study of trichloromethyl compounds. A correlation of spectra obtained at 77 °K with structure of these trichloromethyl compounds was prepared upon averaging the frequency of the multiplet splitting patterns observed for the trichloromethyl group. A relationship consistent with findings in NMR is seen for the NQR correlation of the trichloromethyl structures.

CHLORINE-35 NUCLEAR QUADRUPOLE RESONANCE (NQR) spectrometry has been used in studying the structure of chlorine-containing compounds to a much greater extent than any of the other isotopes capable of being examined by NQR, because of the frequency range over which ^{35}Cl resonances appear and also because the resonance lines are not easily saturated with high radio-frequency power levels (*1*, *2*). Even with the various NQR studies that have been performed on chlorine-containing compounds, there have been no correlation studies reported involving the trichloromethyl group except for a specific kind of correlation shown by G. K. Semin (*3*) on a homologous series of tetrachloroalkanes. The molecular formula for these tetrachloroalkanes is $Cl-(CH_2)_{n-1}CCl_3$, where n is the number of methylene groups that separates the trichloromethyl group from the chloromethyl group.

In the NQR studies performed by G. K. Semin on these compounds, two interesting phenomena were observed. The first was that a shift to lower frequency was observed for the ^{35}Cl resonances of both the chloromethyl and the trichloromethyl groups as n was varied from 1 to 13. Second, a change in the splitting pattern for the trichloromethyl group was observed as n was varied from 1 to 13. For n equals 1, a three-line pattern of equal spacing was observed. However, on increasing n to 5, the splitting pattern changed to show one of the three lines had shifted to higher frequencies relative to the other two. Then, on increasing n to 9 and beyond, the pattern reversed itself to show that the line separated from the other two was at the low frequency side of the pattern. G. K. Semin attempts to explain the observations by stating that they "may be due to the fact that intermolecular Van der Waals interactions for such large molecules deform one of the CCl_3-group chlorine atoms more than is usually possible." He further states, "it follows from the symmetry of arrangements of the C–Cl and C–H dipoles relative to the chlorine atoms in the trichloromethyl group that the chlorine atom in the symmetry plane of the molecule must differ from the chlorine atoms lying outside this plane. Competition between the contribution of the C–Cl dipole in the chloromethyl group to the electric field gradient and the sum of contributions of the C–H dipoles, which increases with n, apparently results in a large splitting for n equals 2 and n greater than 9 with a slight degree of splitting (of a different type) for intermediate values of n."

Based on the results reported by Graybeal and Cornwell (*4*) for trichloroacetonitrile and Allen (*5*) for chloral hydrate in addition to Semin's results, it is apparent that the splittings of all trichloromethyl group resonances are sensitive to the crystallographic environment. Because of the appearance of multiplet splittings in the nuclear quadrupole resonance spectra of trichloromethyl groups both Graybeal and Cornwell, and Allen stated that the average frequency should be taken in order to calculate quadrupole coupling constants, eQq, or even to discuss relationships with chemical bonding. As a result of these previously reported findings, it is apparent that spectra-structure correlations of the type we reported previously (*2*) for various kinds of chlorine-containing compounds can also be applied to the trichloromethyl group. In this paper we extend our previous correlations to a correlation between average resonance frequencies of trichloromethyl groups and their structures.

EXPERIMENTAL

Data used in the preparation of the spectra-structure correlation chart for trichloromethyl groups were obtained from several literature sources (*3–8*) as well as from studies performed in this laboratory on a variety of trichloromethyl containing compounds. Only data reported at 77 °K were used in the correlations. All samples examined in this laboratory were analyzed at 77 °K except for α and β-parachloral which were examined at ambient temperatures.

The instrument used in our examination of the trichloromethyl containing samples was the Wilks Scientific Corp., Model NQR-1A, spectrometer operating over a frequency range from 30–60 MHz. The quench frequency varied automatically from 30 to 45 KHz during scanning over this frequency range. Time constant used in the detection of the resonance signals was 10 seconds. Chart speed used was 8 inches/hour and the sweep rate used was about 3 MHz/hour.

As discussed previously (*2*) we decided that any data included in correlation charts should be expressed in terms of resonance frequency rather than in terms of the quadrupole coupling constants. This same procedure was used for the correlation chart described herein. For the frequency measurements made on the samples examined in our laboratory we used a standard grid dip meter. The accuracy of the measurement using the grid dip meter was about ±0.1 MHz. Whenever a frequency measurement was made, the marker switch on the console was moved to the right and to the left in order to throw the oscillator out-of-balance. This condition caused the pen to move vertically on the chart. At that precise time the reading was taken on the grid dip meter for the frequency measurement. Interpolations were then required to determine the resonance frequency for each observed peak

(1) E. A. C. Lucken, "Nuclear Quadrupole Coupling Constants," Academic Press, New York, N. Y., 1969.
(2) E. G. Brame, Jr., ANAL. CHEM., 39, 918 (1967).
(3) G. K. Semin and V. I. Robas, *UDC 541.67*, 110 (1966).
(4) J. Graybeal and D. Cornwell, *J. Phys. Chem.*, 62, 483 (1958).
(5) H. Allen, *ibid.*, 57, 501 (1953).
(6) S. L. Segel and R. G. Barnes, *USAEC, IS-1222*, September 1965.
(7) H. O. Hopper and P. J. Bray, *J. Chem. Phys.* 33, 334 (1960).
(8) E. I. Fedin and G. K. Semin, *Zh. Strukt. Khim.*, 1, 464 (1960).

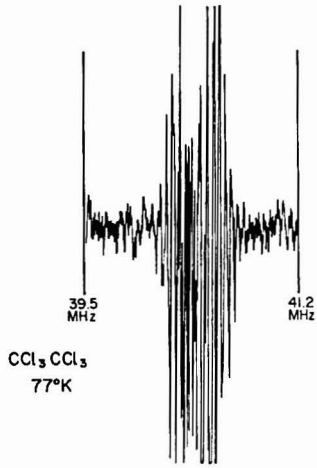


Figure 1. ^{35}Cl NQR spectrum of hexachloroethane at 77 °K

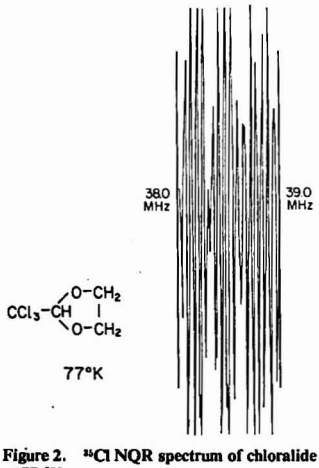


Figure 2. ^{35}Cl NQR spectrum of chloralide at 77 °K

in the spectrum. For the NQR spectra of CCl_3 groups, this meant that several interpolations were required.

RESULTS AND DISCUSSION

In order to prepare a meaningful and useful spectra-structure correlation for use in structure determinations, we followed the work of Graybeal and Cornwell, and Allen in averaging the frequency of the multiplet lines observed for the trichloromethyl group prior to formulating the correlation chart. Three basically different types of multiplet line patterns were observed in our investigation of different kinds of trichloromethyl groups. These different patterns observed are illustrated in Figures 1–3. Figure 1 shows the ^{35}Cl resonance pattern obtained on hexachloroethane. Two lines are seen surrounded by fine structure that is dependent upon the quench frequency (*4*). One line appears at 40.3 MHz and the other line appears at 40.5 MHz. The area ratio is about 1:2 between the lower frequency line and the higher frequency line. The fact that only two lines are seen suggests that only one of the three chlorines in each CCl_3 group is crystallographically different from the other two chlorines. Figure 2 shows the pattern obtained on chloralide. Instead of two lines being observed we find three lines for the CCl_3 group in this compound. One appears at 38.1 MHz, another at 38.4 MHz, and the third at 38.8 MHz. Again fine structure is also observed. Here we see that the lines are not only equivalent in area but they are also evenly spaced. Thus, each chlorine is not only different in a crystallographic sense but there is also a regularity in the degree of difference among the three chlorines.

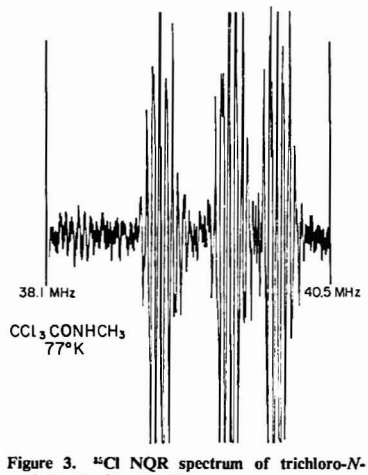


Figure 3. ^{35}Cl NQR spectrum of trichloro-*N*-methylacetamide at 77 °K

The third example as seen in Figure 3 is a spectrum of trichloro-*N*-methylacetamide. Again three lines are observed for the CCl_3 group. They appear at 39.2 MHz, 39.8 MHz, and 40.1 MHz. In this spectrum the three lines are not evenly spaced. The two higher frequency lines are spaced closer together than the two lower frequency lines. In fact there is a factor of 2 difference in the relative difference of the line spacings between the upper two lines and the lower two lines. Since the line intensities are nearly the same for all three lines, each line is assigned to one of the three chlorines in the CCl_3 group. Only through obtaining X-ray data on this material will it be known exactly how the crystal structure can be related to the spacing differences observed in the NQR spectrum. A correlation between X-ray data and NQR data appears to be essentially possible because of the illustration provided by Allen (*5*) on chloral hydrate and because of the kind of difference both we and Semin (*3*) noted in the investigation of trichloromethyl compounds.

The spectra-structure correlation chart which we prepared from our work and from data reported in the literature (*3–8*) is shown in Figure 4. Of the 25 different compounds included in this correlation chart, 10 were analyzed by us for use in

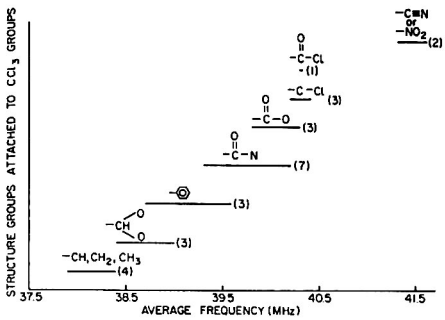
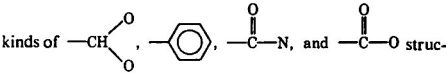
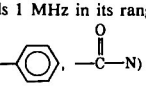


Figure 4. Spectra-structure correlations of ^{35}Cl quadrupole resonances of trichloromethyl compounds at 77 °K

preparing the chart. They included a number of different kinds of  structures. The remaining structures and corresponding data in the chart are from the literature. The numbers in parentheses located to the right of each correlation range indicate the number of compounds used in the correlation. By preparing this spectra-structure correlation chart, it is seen not only more clearly how the different indicated structures affect the ^{35}Cl nuclear quadrupole resonances of trichloromethyl groups but also how the indicated resonance frequencies can be used in determining the kind of groups to which the trichloromethyl groups are attached. This correlation is an extension of the spectra-structure correlation we reported earlier (*2*) for ^{35}Cl resonances in aliphatic compounds.

Upon inspection of the chart in Figure 4 we see that the frequency range over which the ^{35}Cl resonances of CCl_3 groups appear varies from about 38 MHz to about 41.5 MHz. Eight different correlations are included in the chart. None exceeds 1 MHz in its range although only two of the structures () show the relatively large variation of resonance frequency of about 1 MHz. The range for the other structures does not exceed about 0.5 MHz. From this correlation chart, it is seen that there is a shift to higher frequency as groups with greater electronegativity are attached to CCl_3 groups. This relationship which was first indicated by Allen (*5*) for monochloro compounds is consistent with that known for proton NMR; *i.e.*, there is a shift to higher frequency (lower field) as groups with increasing electronegativity are attached to proton groups such as methyl or methylene groups. Since the correlations in this chart show the specific relations between the kind of group to which CCl_3 groups are attached and the average frequency of the NQR resonances for those groups, this chart should find a high degree of usefulness for structure studies of trichloromethyl compounds and it should be an aid in identifying the group to which CCl_3 groups are attached. It is spectra-structure correlations like these that will increase the usefulness of NQR as a structure tool. Up to now NQR has seen only limited use as a means of elucidating structure.

In order to illustrate the use of NQR in determining the structure of isomeric species containing CCl_3 groups, the results obtained on α- and β-parachloral at ambient temperature are given in Table I. These results are compared in the Table with NMR results (*9*) that were reported on dilute solutions of these materials. Even though these two materials are both cyclic trimers of trichloroacetaldehyde the difference between them is in the conformation of the CCl_3 groups. β-Parachloral is the isomer that has all the CCl_3 groups cis to each other and α-parachloral is the isomer that has these CCl_3 groups cis-trans to each other. Three distinct and separate NQR lines were observed for each of these isomers. The difference in the NQR data between these isomers is clearly seen in the average frequency of the three lines observed. It is seen to be 38.7 MHz for β-parachloral and 39.3 MHz for α-parachloral. This difference of 0.6 MHz is not only significant but also shows the substantial difference that can be observed in NQR data for relative subtle changes in structure. The NMR data (*9*) show that β-parachloral, the all cis isomer, has only one line appearing at 5.46 ppm, and that α-parachloral, the cis-trans isomer, has two lines appearing at lower fields (higher frequencies) from the single line of β-parachloral. These lines are at 6.15 ppm and 5.67 ppm relative to the internal standard of TMS. Upon comparing the NQR data with the NMR data for these two isomeric structures, we find that there is a direct correspondence in the shift to higher frequency between the all cis structure and the cis-trans structure. Thus, again we find with this illustration that the frequency (field) shifts observed in the high resolution proton magnetic resonance spectrum not only can be observed in the ^{35}Cl NQR spectrum but also are related directly to each other.

Table I. Comparison of ^{35}Cl NQR Data with ^{1}H NMR Data on Cyclic Trimers of Trichloroacetaldehyde

	NQR of CCl_3 groups (ambient temp.)		NMR of CH groups
Samples	Line frequency, MHz	Average Frequency, MHz	Line position (ppm)
α-Parachloral	39.7		6.15
	39.3	39.3	5.67
	38.8		
β-Parachloral	38.9		
	38.7	38.7	5.46
	38.4		

ACKNOWLEDGMENT

The author wishes to thank Wilks Scientific Company for the use of its Model NQR-1A instrument in this work. Also, the author wishes to thank Drs. O. Vogl, F. M. Sonnenberg, and F. M. Armbrecht for the various chlorine-containing samples supplied for this study on trichloromethyl compounds. Thanks should also be expressed to V. A. Brown who did the measurements on the instrument.

RECEIVED for review May 14, 1970. Accepted September 21, 1970. This work was presented at the 159th National Meeting, American Chemical Society, Houston, Texas, February 1970 and at the 5th Middle Atlantic Regional Meeting, Newark, Del., April 1970.

(9) Varian NMR Spectra Catalog, No. 449 and 450, Varian Associates, Palo Alto, Calif.

Cryoscopic Determination of Number-Average Molecular Weight by Quartz Crystal Thermometry

John S. Fok, John W. Robson, and Flora C. Youngken[1]

Central Research Dept., Experimental Station, E. I. du Pont de Nemours and Company, Wilmington, Del. 19898

Application of a quartz thermometer to the cryoscopic determination of $\bar{M}_n$, 50–2000, has resulted in a simple, rapid method yielding results with a relative error of ±2–3%. The sensitivity and high resolution (1×10^{-4} °C) features of this tool permit precise evaluation of freezing point by the steady-state technique applying exact procedural specifications. Design of an appropriate freezing point assembly is described. Accurate $\bar{M}_n$ values are obtained from a test solution considerably less concentrated than ordinarily specified using a single charge of sample. Solvent interchange requires only a minor adjustment. Solvent purity and solution equilibria are evaluated, and unstable materials create no problems. Representative data substantiate the numerous advantages and analytical accuracy resulting from these innovations. The method is especially suitable where sample supply is limited and sample type random.

QUARTZ CRYSTAL THERMOMETRY has been applied to the cryoscopic determination of number-average molecular weight ($\bar{M}_n$). Accurate values for the $\bar{M}_n$ range, 50–2000, are obtained. Our apparatus has been in operation for approximately four years and an appreciation of its practicality and potential continues. A change in the cooling-bath temperature is the only minor adjustment necessary for quick solvent interchange. Our method is especially suited for evaluation of solvent purity and solution equilibria. It is geared to supply $\bar{M}_n$ values speedily for sample types submitted at random. Ordinarily, a satisfactory determination is accomplished by examination of one optimum solute concentration for $\bar{M}_n < 2000$.

Temperature transducers in common use are glass liquid thermometers of the Beckman (*1*) reset type, a variety of electrical resistance thermometers as introduced by Lakande (*2*) and now including thermistors (*3*), and thermocouple pairs as illustrated by the apparatus of Kraus and his coworkers (*4*). To our knowledge, the only reference to a digital-indicating quartz crystal thermometer (QCT) for the determination of molecular weight is that by Derge (*5*).

A QCT for cryoscopic $\bar{M}_n$ determinations has many advantages. Actual temperature is displayed digitally on nixie tubes to a resolution of 1×10^{-4} °C with an integrating time constant of 10 seconds as compared to a resolution of 2×10^{-3} °C for a Beckmann differential thermometer (BDT). Temperature range is −80 to +250 °C. Temperature output is conveniently printed by a digital recorder. A QCT is considerably more linear than a platinum resistance thermometer, ±0.05% of the span from −40 to +250 °C *vs.* a typical figure of ±0.55% for the same range. Linearity of a QCT is superior to that of thermocouples and thermistors, which have an exponential characteristic (*6*).

Difficulties of standardization or of adaptation are not encountered as with a relative temperature scale. The stainless steel casing of a QCT is far more rugged than any other laboratory temperature-measuring device. It can withstand shock to 10,000 g without change in calibration, so, for our purpose, it can be considered indestructible (*6*). The probe can be cleaned with chromic acid cleaning mixture, if necessary, and thoroughly dried with a heat gun to eliminate adsorbed moisture, a common source of error with a BDT. There is no bridge balancing, limitations in range, nor problems of selfheating as with thermistors. Prior to sample runs, visual display of the actual temperature of the solution under preparation in the freezing point (FP) tube permits monitored application of heat, when indicated, to encourage dissolution of solids without solvent loss or induced change in the nature of the sample. Because FP results are expressed in actual temperatures, solvent purity can be evaluated rapidly by comparison with literature values. Inadvertent contamination of stock solvent is immediately recognized because of the precise repeatability of an individual solvent freezing point.

Relating measurements of an unknown to a standard under similar conditions is general practice. Systematic errors of the apparatus and the technique, solvent properties, molecular weight, and the method of calculation are represented in an overall cryoscopic constant (K). The design of the freezing point assembly combined with the accessory equipment (Figures 1 and 2) we are reporting permits rigid control of this experimental duplication. We use the steady-state temperature (SST) method for determining freezing points. The SST is defined as the maximum temperature of the solvent after the supercooled solvent (solution) begins to crystallize (*7*). Routinely with our method, the SST is the average of a series of 20 temperature observations including and succeeding this maximum temperature over a period of 5 minutes.

The SST is primarily a function of the molal activity of the solute but it is affected to a lesser degree by the rate of cooling and the degree of supercooling. We established stringent control of the two latter factors. For benzene, the cooling bath is maintained at 3.1 ± 0.03 °C. Temperature layering in the cooling bath can be an insidious hazard. The efficiency of the thermoregulator and the circulator should be checked periodically at various levels of the coolant by the QCT. The 20 temperatures of the SST series for this solvent indicate a drift of less than 4×10^{-4} °C.

Substantially lower solute concentrations are used than are ordinarily recommended (*7*). A freezing point differential (ΔT) of 0.1 to 0.2 °C is a meaningful response. With a

[1] To whom requests for reprints should be sent.

(1) E. Beckman, *Z. Phys. Chem.*, **2**, 638, 715 (1888).
(2) A. Lakande, *Compt. Rend.*, **195**, 1267 (1932).
(3) B. M. Zeffert and S. Hormats, ANAL. CHEM., **21**, 1420 (1949).
(4) B. C. Barton, D. A. Rothrock, Jr., and C. A. Kraus, *J. Amer. Chem. Soc.*, **74**, 786 (1952).
(5) K. Derge, *Glas Instrum. Tech.*, **11**(3), 164–170, 173–4; (4) 247–8, 251–2 (1967).
(6) Dymec Division, Hewlett-Packard Co., Palo Alto, Calif., *Technical Data*, "Quartz Thermometer," 4/20/67.
(7) R. W. Bonnar, M. Dimbat, and F. H. Stross, "Number-Average Molecular Weights," Interscience, New York, N. Y., 1958, pp 18, 20, 21, 36.

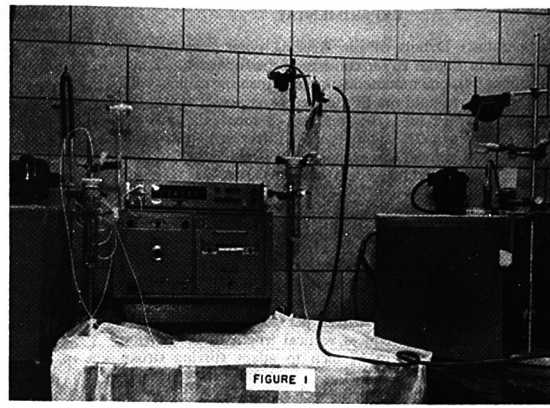


Figure 1. Overall view of a laboratory bench set-up of cryoscopic $\overline{M}_n$ apparatus which utilizes a quartz crystal thermometer as the temperature-measuring tool

solute concentration producing a ΔT of approximately this magnitude, measurements more closely represent ideality than heretofore. Departure from ideal behavior as a function of concentration caused by the normal physical interactions between molecules is minimized.

Routine requirements are satisfied by obtaining sample data from a single-charge, steady-state freezing point measurement calculated by use of an apparent molecular weight constant (*8*). One should remain mindful of the possible experimental errors encountered with an $\overline{M}_n$ determination, such as solute interference with the rate of crystal formation (erratic SST freezing points), solute association or dissociation (discrepancy in $\overline{M}_n$ with different solvents), false appraisal of dissolution of solute, and the problems of multicomponent systems, particularly with materials which include a wide molecular weight range. When these anomalies are encountered, the simplicity and speed of our procedure encourage investigations, in depth, using different solvents and/or examination of a range of solute concentrations. The need for purification or fractionation of sample and other problems are readily recognized by inspection of the drift in the SST series and/or a check of linearity as a function of concentration. More precise methods of calculation (*9*) can be applied but our intent here is to emphasize achievements as to speed, simplicity, and accuracy with samples of normal behavior.

The traditional dimensions applied to the subject determination are °C per mole per 1000 grams of solvent. Measurement of the freezing point depression (ΔT) of a solvent resulting from the addition of a weight of material of known molecular weight (MW) yields a cryoscopic constant ($K_{app\ FP}$).

$$K_{app\ FP} = \frac{\Delta T \times \text{MW of std} \times \text{wt of solvent (g)}}{\text{wt of std (mg)}} \quad (1)$$

Under identical conditions, the $\overline{M}_n$ of an unknown in the same solvent is obtained.

$$\overline{M}_n = \frac{K_{app\ FP} \times \text{wt of sample (mg)}}{\Delta T \times \text{wt of solvent (g)}} \quad (2)$$

(8) J. M. Peterson and W. H. Rodebush, *J. Phys. Chem.*, **32**, 709 (1928).

(9) Ref. 7, Chap. I, IV.

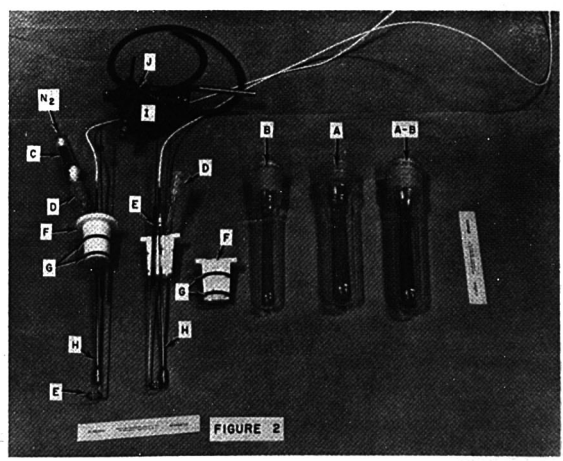


Figure 2. Items of freezing point assemblies arranged to show details of equipment used for the adaption of a quartz crystal thermometer to the cryoscopic $\overline{M}_n$ determination

EXPERIMENTAL

Apparatus. Details of the freezing point assembly are illustrated in Figure 2. It consists of the following: 2 air-bath tubes (*A*), one mounted permanently in the cooling bath and the other to hold the FP tube and accessories at standby (see Figure 1); FP tube (*B*); desiccant chamber (*C*); nitrogen vent attachment (*D*); stainless steel stirrer (*E*); three-hole split Teflon (DuPont) stopper with two guide pins to recombine the stopper and two Viton (DuPont) O-rings as fasteners (*F*) (*G*); Quartz Crystal Thermometer (QCT), H-P Model 2801A (*H*) along with Digital Recorder, Model M84562A (see Figure 1), Dymec Division, Hewlett-Packard Co., Palo Alto, Calif. Mechanical stirring is accomplished by a Cenco stirring motor (Central Scientific Co., Chicago, Ill.) (*I*) attached by a two-way stopcock to a vacuum line permitting fast change from a stirring rate of one stroke per second prior to seeding to two–three strokes per second after seeding. Retooling of part (*J*) reduces vertical length of the stirring stroke by approximately $^3/_8$ inch to adapt stirring stroke to FP tube dimensions.

Refrigerated and heated baths with circulators and thermoregulators designed to control bath temperature within less than ±0.03 °C from approximately −18 to +50 °C in an ambient of 24 °C have fulfilled our needs (Forma-Temp. Jr., No. 2095, Forma Scientific Inc., Marietta, Ohio).

Sample Handling. A Parr pellet press (Parr Instrument Co., Moline, Ill.) is used to produce pellets of a solid sample of $^1/_8$- or $^1/_4$-inch diameter. A sample of high viscosity is manipulated on a split half of a cover glass, approximately $^3/_4$ inch square. A liquid sample is transferred from a microdropping bottle or a microsyringe. Calibrated automatic pipets with Teflon stopcocks, 15 ml and 20 ml, are used for delivery of solvent. Routinely, the method calls for the use of 15 ml of solvent pipetted directly into the FP tube but optimum handling of an unstable sample could require final aliquoting from a previously prepared 20-ml volume of desired solute concentration.

Standards. Benzil (analytical reagent, Eastman Organic Chemicals, Eastman Kodak Co., Rochester, N.Y.) is used with benzene, dimethyl sulfoxide (DMSO), *p*-dioxane, and 100% acetic acid. Anhydrous dextrose and ammonium sulfate (analytical reagent, Mallinckrodt Chemical Works, N.Y.) are used with water and 100% sulfuric acid, respectively. These reagents are prepared in appropriate size pellets, dried 1 hour in a vacuum oven at 60 °C, and stored in a desiccator over "Tel-Tale" silica gel.

Solvents. Benzene (B & A, General Chemical Division, Allied Chemical Co., Morristown, N.J.) is purified by refluxing with excess phosphoric acid anhydride under nitrogen for 10–12 hours. Subsequent distillation under nitrogen yields solvent, FP 5.53 °C.

Dimethyl sulfoxide (Chemical Packaging and Sales Co., Wilmington, Del.) is purified by shaking 2–3 hours with approximately 1 cm depth of basic, activity grade 1, aluminum oxide (Woelm, Eschwege, Germany) added to a pint bottle of the solvent as received from the vendor. It is then filtered by decanting into a fine sintered glass funnel containing an approximately 1-cm layer of Woelm neutral, activity grade 1, aluminum oxide reagent. The latter operation is performed under a dry nitrogen atmosphere.

p-Dioxane (spectroquality, Matheson, Coleman and Bell, East Rutherford, N.J.), FP 11.7 °C, is used as received from the vendor.

Procedure. The digital recorder is set to print every 15 seconds and a record of the latter phase of cooling, the seeding temperature, and a minimum of 19 readings after the maximum observed temperature after seeding are printed for each FP run. A specific FP is the numerical average of the SST series as previously defined.

The following conditions are used for an $\overline{M}_n$ determination in benzene. The cooling bath is maintained at 3.1 ± 0.03 °C, approximately 2.5° below the FP of this solvent. From numerous trial conditions, 4.40 ± 0.01 °C (1.1° below the FP of benzene) was chosen as the optimum seeding point. Under a dry nitrogen atmosphere, a 15-ml aliquot of solvent is pipetted into the FP tube and the Teflon stopper and combined accessories are immediately seated in the tube. A source of nitrogen with flow sufficient to maintain a pressure equivalent to approximately 10 cm of mercury at the outgoing vent is attached. The FP tube is cooled rapidly to approximately 8 °C by immersion directly into the cooling bath. The outside of the FP tube is carefully dried and positioned in the air-bath tube. Stirring is maintained at one stroke per second with the Cenco motor until the seeding temperature is reached. The motor is then stopped. The screw holding the stirrer is loosened, and rapid, manual, vertical manipulation of the stirrer for 15 seconds produces seeding. Mechanical stirring is resumed at an increased rate of 2–3 strokes per second until sufficient temperature output data have been accumulated by the recorder. The stirrer is disconnected and the FP tube removed from the air-bath tube and placed intact in the storage tube.

When possible, sample weight is selected to give approximately a 0.1° FP depression. If the sample is a powder-type, it is now added as a pellet to this same aliquot of benzene. When dissolution is complete, the solution temperature is readjusted to approximately 8 °C, the FP tube is replaced in the air-bath tube and the procedure is repeated to obtain a FP value for the sample solution. $\overline{M}_n$ is calculated by Equation 2 using a $K_{app\ FP}$ value obtained for benzil by this identical procedure.

RESULTS AND DISCUSSION

The $K_{app\ FP}$ for benzil in purified benzene is 5.42 and the standard deviation (σ) is 0.036. Respective values for DMSO are 4.42 and 0.063. In each case, these represent 20 calibrations with several different lots of purified solvents during a recent period of three months. Other representative $K_{app\ FP}$ values are 3.7 for 100% acetic acid, 2.0 for water (dextrose), 5.2 for *p*-dioxane (benzil) and 4.8 for 100% sulfuric acid (ammonium sulfate). $K_{app\ FP}$ for $(NH_4)_2SO_4$ is calculated on the basis of four osmotically active ions.

$$2(NH_4)_2SO_4 + (n + 2)\,H_2SO_4 \rightleftarrows 2(NH_4)(H_2SO_4)_n^+ + 2HSO_4^- \quad (3)$$

$$K_{app\ FP} = \frac{\Delta T \times 132.15 \times \text{wt of solvent (g)}}{\text{wt of } (NH_4)_2SO_4 \text{ (mg)} \times 4} \quad (4)$$

The method of Gillespie *et al.* (*10*) for the preparation of 100% sulfuric acid is accomplished efficiently. The literature value of FP 10.35 °C is confirmed by the QCT. The advantage of observing actual temperatures with a QCT applies equally to the evaluation of 100% acetic acid, FP 16.60 °C.

A detailed study of the behavior of benzil in benzene yielded the results in Table I. These data project a composite appraisal of the capabilities of our method. The validity of establishing a FP from the SST series, justification for our specification for an optimum ΔT, the small amount of material required, the numerical effect on $\overline{M}_n$ and K results with concentration, and the precise control and reproducibility of the FP of solvent are projected. The widening in range of the temperatures in the SST series coincidental with increase in concentration realistically demonstrates departure from "ideality."

(10) R. J. Gillespie, E. D. Hughes, and C. K. Ingold, *J. Chem. Soc.*, 1950, 2473–92.

Table I. K Results for Benzil in Benzene with Cross-Check of $\bar{M}_n$ Values for Benzil

Benzil MW, 210.22
Benzene 15 ml = 12.94 grams
Cooling-bath temp, 3.1 ± 0.03 °C
Seeding temp, 4.40 ± 0.01 °C

Increment, (*i*)	Wt_i	ΣWt_i	Concn g/1000 g	ΔT_i	$\Sigma\Delta T_i$	$K_{app\ FP}$ ΔT_i	$K_{app\ FP}$ $\Sigma\Delta T_i$	SST drift,[a] °C × 10^{-2}	$\bar{M}_n$ (K # 1 and ΔT_i)	Rel error, %	$\bar{M}_n$ (K # 1 and $\Sigma\Delta T_i$)	Rel error, %
	mg			°C × 10^{-2}								
1	48.98	...	3.79	9.82	...	5.45	...	1.5	...	...	...	...
2	47.94	96.92	7.49	9.52	19.34	5.40	5.43	2.8	212.1	+0.89	211.1	+0.40
3	18.12	115.04	8.89	3.70	23.04	5.55	5.45	6.7	206.3	−1.88	210.3	+0.03
1	95.64	...	7.39	19.14	...	5.44		3.4	...	...	...	...
2	16.24	111.88	8.65	3.35	22.49	5.61	5.47	5.8	203.8	−3.05	209.1	−0.51
3	18.96	130.84	10.11	4.01	26.50	5.75	5.51	12.8	198.8	−5.44	207.6	−1.26
4	22.28	153.12	11.83	4.91	31.41	5.99	5.62	28.5	190.8	−9.25	204.9	−2.51

[a] Difference between highest and lowest temperature of SST series.

Table II. $\bar{M}_n$ Results for Dextrose in DMSO

Dextrose MW, 180.16
DMSO 15 ml = 16.36 grams
Cooling-bath temp, 15.1 ± 0.03 °C
Seeding temp, 17.64 ± 0.02 °C

		Wt.	Total wt.	ΔT	SST drift[a]	$K_{app\ FP}$	$\bar{M}_n$ Found	Relative error, %
		mg		°C × 10^{-2}	°C × 10^{-2}			
...	Benzil	91.05	...	11.72	11.0	4.43	...	...
1.	Dextrose	72.48	...	10.85	12.8	...	180.89	+ 0.41
2.	Dextrose	28.56	101.04	16.52	20.3	...	165.62	− 8.07
3.	Dextrose	23.83	124.87	21.30	36.4	...	158.74	−11.89
...	Dextrose	147.06	...	23.41	42.1	...	170.10	− 5.58

[a] See footnote, Table I.

The use of DMSO is restricted to samples which cannot be examined in any other solvent or by another $\bar{M}_n$ method. We have found no better purification procedure than the one previously described. Table II illustrates the behavior of dextrose in this solvent. This example indicates the possible consequences with its indiscriminate use. With a freshly prepared dextrose solution yielding a ΔT (0.1 °C) of the same magnitude as for the benzil standard, an $\bar{M}_n$ very close to theory was obtained. Successive additions of sample to this original solution produced nonlinear values. Also, a freshly prepared dextrose solution, estimated to yield a ΔT double the amount that previously was satisfactory, yielded a result outside the accuracy limits we assign to our method. With DMSO, it is essential to duplicate ΔT values for unknown and standard within a much narrower range than is necessary with benzene. These data indicate degradation in DMSO relative to time as well as demonstrate evidence of a more pronounced molecular activity in a DMSO system than has been noted with benzene.

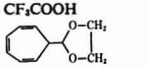
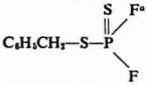
Table III lists representative $\bar{M}_n$ results. Compounds at various $\bar{M}_n$ levels, different cryometric solvents, and various standards are presented in these data. Most values agree within 2–3% of theory, and each is the result of a single determination for $\bar{M}_n$. Recognition of the influence of impurity, water and/or extraneous solvent on an $\bar{M}_n$ result must be emphasized. These effects become more acute with increase in molecular weight. With polymers, the presence of small amounts in terms of weight per cent of low molecular weight molecules can completely dominate an $\bar{M}_n$ value (*11*).

Solvents degassed by a series of freeze-evacuate-thaw cycles are used when samples are unusually sensitive. The following procedure permits evaluation of air- and/or moisture-sensitive compounds and samples otherwise unstable under optimum conditions using degassed solvent when oxygen- or carbon dioxide-sensitivity is recognized. One can assume that the established FP for a solvent and its appropriate K value are precisely reproducible. Solutions of samples of these types are prepared in an appropriate concentration in a container other than the FP tube in a dry box. In these cases, operations are performed in a more sophisticated type of dry box than is routine equipment in most laboratories as for instance, Dri Train (HE-193-2), Vacuum Atmospheres Corp., 7356 Greenbush Ave., North Hollywood, Calif. Later, still in the dry box, an aliquot can be sealed in the FP tube with the QCT and accessories in place. This procedure is equally advantageous for a sample that is slowly soluble or highly colored where a safety margin of time is required to assure complete dissolution in an ordinary dry box, if the sample is an inert type. With foresight, an analyst can continue operation of the equipment with other determinations while awaiting resolution of problems of solubility.

Polymers at low degrees of polymerization are the most frequently encountered sample type for the $\bar{M}_n$ range, 1000–5000. No problems have been attributed to our referencing all unknowns in the $\bar{M}_n$ range applicable to this method, to standards around the 200 molecular weight level. Nevertheless, for purposes of evaluation and coordination of all molecular weight determinations based on colligative properties, we have investigated the possibilities of verifying standards of higher molecular weight, particularly materials representative of polymeric behavior. $\bar{M}_n$ results for three polystyrene samples (designated as standards) by our subject method and by our ebullioscopic (BP) and vapor pressure osmometric (VPO) procedures are listed for comparison in Table IV.

(11) I. M. Kolthoff *et al.*, "Treatise on Analytical Chemistry," Interscience, New York, N. Y., 1968, Part 1, Vol. 8, p 5022.

Table III. Representative $\overline{M}_n$ Results by Cryoscopy

Sample	Solvent	Standard	$\overline{M}_n$ Theory	$\overline{M}_n$ Found	Relative error, %
$(NH_4)_2SO_4$	H_2O	Dextrose	$\frac{132.15}{2}$	63.52	−3.87
CF_3COOH	100% H_2SO_4	$(NH_4)_2SO_4$	114	116	+1.75
 (*12*)	C_6H_6	Benzil	150	152	+1.33
	C_6H_6	Benzil	224	221	−1.34
$Pd(CH_3COO)_2$	100% CH_3COOH	Benzil	225	227	−0.88
$B_{10}H_{10}SCoC_5H_5$[b]	C_6H_6	Benzil	274	272	−0.73
$B_{10}H_{10}SCoC_5H_5$[b]	DMSO	Benzil	274	275	+0.36
$C_{16}H_{32}S_2$[c] (*13*)	C_6H_6	Benzil	288	294	+2.08
$(COCuOOCCF_2)_2$[d]	C_6H_6	Benzil	410	417	+1.71
$[CH_3(CH_2)_3CH_2]_4Pb$ (*14*)	C_6H_6	Benzil	491	489	−0.41
Ethyl ester of Kel-F acid 8114[e]	*p*-dioxane	Benzil	508	501	−1.38
$[(C_6H_5)_3P]_2CuB_3H_8$[f]	C_6H_6	Benzil	629	618	−1.75
$H_2Fe[P(OC_2H_5)_2]_4$ (*15, 16*)	C_6H_6	Benzil	723	698	−3.46
$Ni[P(O\text{-}o\text{-}C_6H_4CH_3)_3]_2$[g]	C_6H_6	Benzil	1116	1145	+2.60

[a,b,d,f,g] Compounds synthesized in these laboratories by H. W. Roesky, W. R. Hertler, C. W. Alegranti, F. Klanberg, and L. W. Gosser respectively.

[c] 1,10-Dithiocyclooctadecane was prepared by R. T. Uyeda.

[e] Kel-F acid 8114, $ClCF_2CFClCF_2CFClCF_2CFClCF_2COOH$, The M. W. Kellogg Co., Chem. Manufacturing Division, Jersey City, N. J. Ethyl ester was prepared by T. A. Ford.

Table IV. $\overline{M}_n$ Values for Polystyrenes

Standard, benzil. Solvents, benzene, toluene*

	$\overline{M}_n$ Supplier[a] data sheet	Cryoscopy Concn by wt	Cryoscopy $\overline{M}_n$ Found	Ebullioscopy $\overline{M}_n \xrightarrow{concn}\infty$ Found	VPO[b] $\overline{M}_n \xrightarrow{concn}\infty$ Found
900-Special	1050 ± 105	1.79%	1030	1270	1130
		1.77	1045	1240	1110
				1270*	
2030-12a	2050 ± 170	1.64%	1525	1777	1640
		2.54	1540	1856	1590
		3.27	1425	1920	
		4.91	1525	1950*	
4000-11a	3690 ± 365	2.46%	2693	4160	3465
		3.27	2634		
		4.91	2513		
		7.37	2464		
		$\xrightarrow{concn}\infty$	2900		

[a] Pressure Chemical Co., Pittsburgh, Pa., Data Sheet No. 107/108, 109/110, March 1966-$\overline{M}_n$ reported as an average.

[b] Hewlett-Packard Model 302 Vapor Pressure Osmometer at 37 °C.

Each BP $\overline{M}_n$ value is based on data from six successive sample additions to solvent not exceeding a final solute concentration of 5% by weight, extrapolated to infinite dilution. Each VPO result is based on four separately prepared solutions, also with highest concentration not exceeding 5% by weight and all data extrapolated to infinite dilution. Each cryoscopic $\overline{M}_n$ result for the 900-Special polystyrene represents a single charge of sample. Freezing points were established by our routine SST procedure. For the two higher molecular weight polystyrenes, freezing points were considered the maximum temperature after seeding and $\overline{M}_n$ was calculated individually for each solution of the strength specified. In these cases, concentrations were obviously beyond proportions where calculation from our SST series could be justified. For the polystyrene 2030, within the concentration range examined, $\overline{M}_n$ values did not appear to be concentration dependent. The value for extrapolation of all data to infinite dilution for the polystyrene 4000 is included.

(12) H. E. Simmons and T. Fukunaga, *J. Amer. Chem. Soc.*, **89**, 5214 (1967).
(13) A. Müller, E. Funder-Fritzsche, W. Konar, and E. Rintersbacher-Wlasak, *Monatsch*, **84**, 1207 (1953).
(14) G. Singh, *J. Organometal. Chem.*, **11**, 140 (1968).
(15) F. N. Tebbe, P. Meakin, J. P. Jesson, and E. L. Muetterties, *J. Amer. Chem. Soc.*, **92**, 1069 (1970).
(16) P. Meakin, L. J. Guggenberger, J. P. Jesson, D. H. Gerlach, F. N. Tebbe, W. G. Peet, and E. L. Muetterties, *ibid.*, p 3482.

Screaton and Seemann (*17*) reported detailed studies on polystyrenes from this same source while searching for reliable standards for gel permeation chromatography. Their data indicated that the nominal molecular weight values of this supplier might be incorrect in some instances. Their fractionation studies of individual polystyrenes and molecular weight results from these fractions, as well as their detection of a range in glass transitions within a given sample, showed the dissimilar composition of their material. This evidence could possibly explain our discrepancies in reproducing $\overline{M}_n$ values among our subject methods. Our results appear to indicate increases in $\overline{M}_n$ values with rise in the level of solvent temperature germane to the particular method, and an association effect appears to be demonstrated. These data illustrate the dilemma of an individual researcher facing the uncomfortable choice of which $\overline{M}_n$ value to apply to each standard when evaluating his own particular method. At this level of molecular weight, there is grave need for dependable calibration standards, particularly materials of narrow molecular weight composition.

The overall result of our adaptation of a QCT to this determination is a well standardized procedure with specifications for apparatus and technique easily duplicated. Not only is demand on sample supply minimal but, since routine determinations are accomplished with a single concentration, analysis time is greatly reduced. Precise, accurate $\overline{M}_n$ values can be obtained without resort to intricate calculations. The fortuitous achievement of a substantial reduction of solute concentration produces with a single charge of sample, an $\overline{M}_n$ value comparable to one from the results of a multiple concentration study, extrapolated to infinite dilution.

(17) R. M. Screaton and R. W. Seemann, *Appl. Polym. Symp.* **8**, 81–110, (1969).

RECEIVED for review August 26, 1970. Accepted October 1, 1970.

Accuracy of Analysis by Electrical Detection in Spark Source Mass Spectrometry

R. A. Bingham and R. M. Elliott

AEI Scientific Apparatus Limited, Barton Dock Road, Manchester, England

The precision and accuracy of Spark Source Mass Spectrometry using electrical detection of the resolved ion beams has been critically examined. Rapid scanning of the spectrum using a logarithmic ratio amplifier system gives a survey of all elements present in the sample within a few minutes. The precision achieved in this rapid survey is shown to be better than 35% for concentrations down to below the 1 ppm atomic level. Precision of 2% for any chosen elements is achieved using the more accurate peak switching technique down to 1 ppm. The limits of detection are 0.001 ppm atomic for the peak switching technique and 0.01 ppm for scanning. Automatic spark discharge control has been developed permitting unattended operation for long periods and giving improved reproducibility. The absolute accuracy of the peak switching technique has been assessed using standard steel samples. The mean difference between the observed and quoted values was 4.2% for impurities in the 500–2500 ppm range.

SPARK SOURCE MASS SPECTROMETRY has been for some time an established technique for the chemical analysis of impurities where trace concentrations are involved or for a survey analysis of all possible impurities (*1*). The combination of extremely high sensitivity and overall element coverage makes it unique among analytical methods. In this paper significant advances in the precision and accuracy of the technique are reported.

The most widely used detector in the past has been the ion sensitive photographic plate, which effectively integrates the fluctuating ion currents produced by the spark discharge; in addition it can record all the elements from mass 7 to 240 in a single exposure. These features made the photographic plate a natural choice initially. However, its use is time-consuming and far from convenient, its linear range is only about 30 to 1, and its precision is limited. The basic precision of the emulsion itself is usually estimated to be of the order of 3–6%; Franzen and Schuy (*2*) have obtained relative standard deviations of 2% but under a strictly defined routine of exposure, development, and measurement.

By contrast the electron multiplier is routinely used for isotopic abundance measurements to 0.1% precision, and the output is immediately accessible in convenient electrical form. Thus, it was natural to investigate the possibility of using the electron multiplier as detector for spark source mass spectrometry; it offered not only improved precision and greater speed and convenience of analysis but also the opportunity for much easier investigation of the other remaining causes of irreproducibility.

Factors such as spark parameters and accelerating voltage had been shown by Halliday *et al.* (*3*) to affect precision, and both Bingham *et al.* (*4*) and Svec *et al.* (*5*) have shown that electrode position was critical. Once these factors were recognized and controlled, the reproducibility improved and analysis could be made with a precision of 5–20%. Removal

(1) A. J. Ahearn, "Mass Spectrometric Analysis of Solids," Elsevier, Amsterdam, 1966, p 5.

(2) J. Franzen and K. D. Schuy, *Z. Anal. Chem.*, **225**, 295 (1967).

(3) J. S. Halliday, P. Swift, and W. A. Wolstenholme, "Advances in Mass Spectrometry," Vol. 3, E. W. Mead, Ed., Institute of Petroleum, London, 1966, p 143.

(4) R. A. Bingham, R. Brown, J. S. Halliday, P. Powers, and P. G. T. Vossen, International Conference on the Characterization of Materials, Pennsylvania State University, University Park, Pa., November 1966.

(5) H. J. Svec, R. J. Conzemius, and G. D. Flesch, 15th Annual Conference on Mass Spectrometry, ASTM E14, Denver, Colo., May 1967.

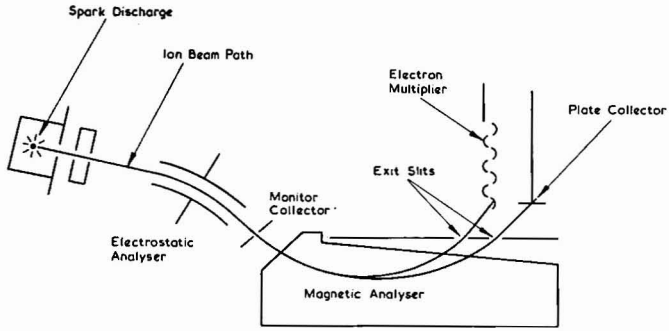


Figure 1. Schematic layout of the AEI MS702 spark source mass spectrometer with electrical detection

of the photoplate contribution to these variables should enable the remaining factors to be studied more precisely.

Several workers have published results of endeavor in the field of electrical detection of spark source mass spectra. Early papers were concerned mainly with isotope ratios [Straus (*6*), Fluegge (*7*), Dupzyk *et al.* (*8*)] or major constituents (Gorman *et al.* (*9*), Chakravarty *et al.* (*10*)] and the first systems for general use in trace analysis were reported by Capellen *et al.* (*11*) and Argyle and Bingham (*12*) in 1965. Svec *et al.* (*5*, *13*, *14*) and Bingham *et al.* (*15–17*) have subsequently described practical systems in which the key factor was the use of the ratios between individual and total ion currents. Both groups have demonstrated precisions in analytical observations of 0.5–5% (*5*, *13*, *15*, *16*), and using a system similar to Bingham *et al.* (*15*), Evans, Guidoboni, and Leipziger (*18*, *19*) have achieved similar precision.

Bingham *et al.* (*17*, *20*), have also shown how the electrical output can readily be processed directly on-line by a computer which can then carry out the entire interpretation of the spectrum. Hull (*21*) has compared electrical detection with photoplate techniques.

The object of this paper is to describe the use of a more fully developed electrical analysis system as now fitted to the AEI MS702 spark source mass spectrometer and to analyze in detail the precision and accuracy of analytical results obtained from a number of different standard materials.

ANALYTICAL PROCEDURE

Figure 1 shows schematically how the electrical detection system is incorporated into the spark source mass spectrometer. The ion source and mass analyzer system are conventional (*22*). The monitor collector, between the analyzers, collects a fixed fraction of the total ion beam before mass separation. The electron multiplier behind the exit slit is used to collect the individual ion species. The alternative plate collector is normally used only for major constituents.

The ratio between the specific ion current at the electron multiplier and the fraction of the total ion current collected at the monitor is a measure of the concentration of that specific element. This ratio has to be corrected for relative sensitivity (*1*, *23*), isotopic abundance, and other factors in the same way as for photographic plate detection. However, comparison with a standard sample eliminates the need for all of these corrections. Owing to the linearity of the method (*3*), a single standard can be used even though the concentration of the elements in the standard may differ by several orders of magnitude from the concentrations being measured. This greatly eases the problem commonly encountered in spectrographic techniques of providing closely similar standards.

Scanning. Two techniques for comparing the individual ion currents with the total ion current have been used. Scanning is generally used for rapid surveys of impurity content

(6) H. A. Straus, *Phys. Rev.*, 59, 430, (1941).
(7) R. A. Fluegge, 9th Annual Conference on Mass Spectrometry, ASTM E-14, Chicago, Ill., June 1961.
(8) R. J. Dupzyk, G. W. Barton, R. D. Carver, and R. A. Thomas, 12th Annual Conference on Mass Spectrometry, ASTM E-14, Montreal, Quebec, June 1964.
(9) J. S. Gorman, J. A. Hipple, and J. E. Jones, ANAL. CHEM., 23, 438 (1951).
(10) B. Chakravarty, V. S. Venkatasubramanian, and H. E. Duckworth, "Advances in Mass Spectrometry," Vol. 2, R. M. Elliott, Ed., Pergamon Press, Elmsford, N. Y., 1963, p 128.
(11) J. Capellen, R. J. Conzemius, and H. J. Svec, 13th Annual Conference on Mass Spectrometry ASTM E-14, St. Louis, Mo., May 1965.
(12) A. Argyle and R. A. Bingham, Proceedings of XII Colloquium Spectroscopium Internationale, Exeter, July 1965, Hilger & Watts Limited, London, p 641..
(13) H. J. Svec and R. J. Conzemius, "Advances in Mass Spectrometry," Vol. 4, E. Kendrick, Ed., Institute of Petroleum, London, 1968, p 457.
(14) R. J. Conzemius and H. J. Svec, *Talanta*, 16, 365–375 (1969).
(15) R. A. Bingham, R. Brown, and P. Powers, 1968 Pittsburgh Conference on Analytical Chemistry and Applied Spectroscopy, Columbus, Ohio, March 1968.
(16) R. A. Bingham and P. Powers, 16th Annual Conference on Mass Spectrometry, ASTM E-14, Pittsburgh, Pa., May 1968.
(17) R. A. Bingham, P. Powers, and W. A. Wolstenholme, 17th Annual Conference on Mass Spectrometry, ASTM E-14, Dallas, Texas, May 1969.
(18) C. A. Evans, R. J. Guidoboni, and F. D. Leipziger, 17th Annual Conference on Mass Spectrometry, ASTM E-14, Dallas, Texas, May 1969.
(19) C. A. Evans, R. J. Guidoboni, and F. D. Leipziger, *Appl. Spectrosc.*, 24, 85–91 (1970).
(20) R. A. Bingham, P. Powers, and W. A. Wolstenholme, Proceedings of the International Conference on Mass Spectrometry, Kyoto, Japan, September 1969.
(21) C. W. Hull, *Int. J. Mass Spectrum Ion Phys.*, 3, 293–307 (1969).
(22) R. M. Elliott, R. D. Craig, and G. A. Errock, "Instruments and Measurements," Vol. 1, Academic Press, New York, 1961, p 271.
(23) R. Brown, R. D. Craig, and R. M. Elliott, "Advances in Mass Spectrometry," Vol. 2, R. M. Elliott, Ed., Pergamon Press, Elmsford, N. Y., 1963, p 141.

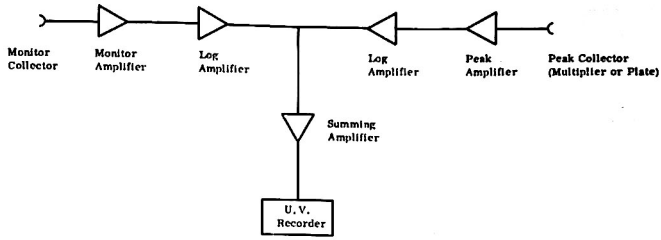


Figure 2. Ratiometer system used in the scanning mode. The output of the summing amplifier is the logarithm of the Collector Current/ Monitor Current ratio

with wide element coverage. In this mode, the ion accelerating voltage is held constant and the magnet field is scanned so that ions of different mass are swept successively over the collector. A wide range of elements, *e.g.* ^{238}U to ^{7}Li, can be covered in a single scan, which is typically covered in a scan time of three minutes.

The ratio of the collector current to the monitor current is recorded continuously by means of the ratiometer system shown in Figure 2. Values proportional to the relative concentrations of the various elements can then be read directly from the recorder chart. A recording of the portion of the mass range from mass 112 to mass 124 is shown in Figure 3. In the example shown here, the electron multiplier and amplifier gains were set so that the concentration range 0.2–200 ppm was displayed on the three-decade logarithmic scale. By adjustment of either the multiplier or amplifier gain, any other concentration ranges covering a factor of 1000 can be recorded; by running three scans covering the ranges 0.1–100, 10–10^4, and 10^3–10^6 ppm the entire concentration range from 0.1 ppm up to the major elements can be covered in a time of about ten minutes. Thus two important advantages of the logarithmic ratiometer system are that it produces the desired ratio of collector current to monitor current directly, and that it has a wide dynamic range covering concentrations differing by up to a factor 1000. A third important advantage is that it compensates for the fluctuations in the spark discharge.

Amplifiers with a logarithmic characteristic are used because the ratio of the two individual currents is given very conveniently by the difference between the two logarithmic signals. In practice the collector current from the electron multiplier is of opposite sign to the monitor current, and the two logarithmic signals therefore have to be added by the summing amplifier to give the logarithm of the ratio. If the plate collector is used, the signal is inverted before the log amplifier.

The most valuable feature of the scanning mode is the ease with which a rapid qualitative survey of all elements in an unknown material can be made from the recorder chart. Comparison with an internal standard or the matrix then permits semi-quantitative determinations of concentration to be made with a precision better than that achieved by visual photoplate analysis, and direct comparison with a standard leads to quantitative determinations of concentration. As already described elsewhere (*17*, *20*), the output signal can also be taken directly to a computer for on-line data acquisition and automatic interpretation of the data by the computer.

The precision and detection limit achieved depend on the scan time. In a later section it will be shown that the precision for a single three minute scan is of the order of 35%, which is at least as good as the analogous readings from a series of exposures on a photographic plate and attained far more conveniently. This precision may be improved to 10% by averaging. The detection limit is of the order of 0.01 ppm for a ten-minute scan over a mass range 7–238 or a three-minute scan covering a narrower mass range, *e.g.* 105–210.

Peak Switching. Peak switching is employed where high precision is required on the few selected elements of interest. In this mode, a number of channels are provided so that the ion accelerating voltage can be switched to preset values at which the ion beams of the elements of interest are tuned on to the exit slit and detected by the electron multiplier. This technique is similar to that used in direct reading emission spectrometers, but is more flexible in that any channel can be quickly tuned in to a different element.

For each mass of interest the collector current is integrated while a predetermined charge is collected at the monitor (see Figure 4), the ion beam then being automatically switched off; the value of integrated peak collector charge is recorded before switching to the next peak. The knowledge of the integrated charge obtained from each peak allows an estimation of the relative concentrations to be made; similar analy-

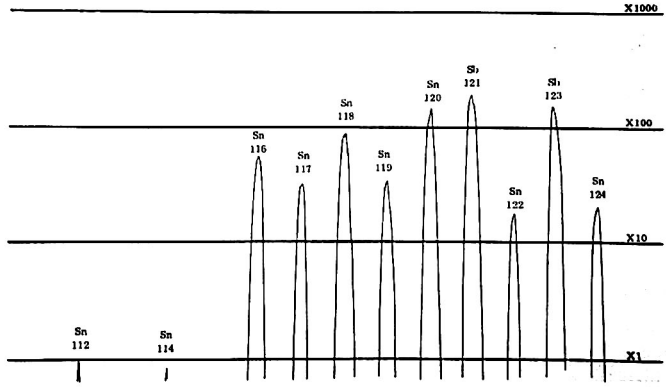


Figure 3. A portion of the ultraviolet recorder chart of the mass spectrum of copper sample CA2 using the scanning mode

The spectrum was scanned at 18 minutes per decade in mass and the portion shown occupied about 1 minute. The intensity scale is logarithmic with X1 corresponding to a concentration level of 0.2 ppm atomic

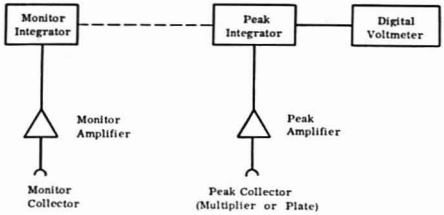


Figure 4. Integration system used in the peak switching mode

The digital voltmeter is read when the monitor integrator has reached a predetermined charge

sis of a standard leads to accurate quantitative analysis of all the elements under consideration. The precision is greatly improved over the scanning mode due to the longer time for which each ion beam is observed.

The choice of integrated monitor charge, and hence of analysis time per element, is governed by the precision required and the concentration level. Figure 5 shows how the reproducibility of the collected charge varies with integrated monitor charge for a wide range of elements in copper. For a monitor charge between 0.3 and 1 nanocoulomb, as normally used, Figure 5 indicates that a precision of the order of 2% or better is achieved for all components greater than 1 ppm. Analytically useful values of precision are still achieved at even lower concentrations. One hundred repeat integrations on ^{204}Pb in copper CA8 at the 0.014-ppm concentration level showed a standard deviation of 9.6%. A detection limit of 0.001 ppm can be achieved for the typical 1-nanocoulomb exposure.

With a 1-nanocoulomb monitor charge, elements can normally be determined at a typical rate of one every ten seconds. Any number of elements may be examined at this rate provided the mass range covered is within a factor 2, *e.g.* ^{209}Bi to ^{107}Ag or ^{100}Mo to ^{50}Cr. To cover masses outside the factor of 2, the magnet current is reset to a new value and another series of elements can then be examined.

Detection Limits and Precision at Low Concentrations. At very low concentrations, the number of ions collected during the observation of a particular peak may be quite small and part of the variations between successive observations is due to the random rate of arrival of these ions. The precision which could be expected under various conditions can be obtained from Table I which indicates the theoretical number of ions to be expected per peak at different concentrations, assuming continuous ion production and perfect sample homogeneity.

The minimum number of ions required for the existence of a peak to be positively established is about 5 (*21*, *24*), pro-

(24) B. N. Green, T. O. Merren, and J. G. Murray, 13th Annual Conference on Mass Spectrometry, ASTM E-14, St. Louis, Mo., May 1965.

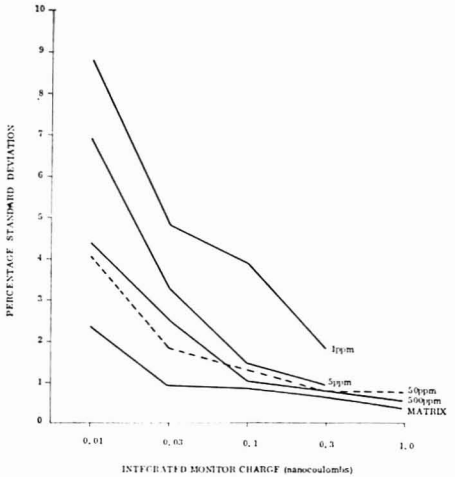


Figure 5. Reproducibility of integrated collector charge measurements for elements in copper present at various concentrations

Data for several elements at similar concentrations are grouped together, *viz*, Ag and Fe at 5 ppm, Ni and Ag at 50 ppm, and Mn, Ag, and Co at 500 ppm. Each estimate of standard deviation is based on 10 or more determinations

vided single ions can be readily detected by the electron multiplier. In practice a single ion gives a signal many times higher than the noise, and the background signal is negligible (except near the matrix lines) under any of the conditions shown in the Table. The conditions in Table I for which 6 ions are observed, therefore, represent realistic detection limits. When one considers an example from the Table, 600 ions would be observed for a 1-ppm impurity and a 0.1-nanocoulomb monitor charge, and the standard deviation for successive observations would be $100\%/\sqrt{N}$ or 4.1%. This is in good agreement with the experimentally observed value in Figure 5.

A sensitivity of 0.001 ppm for peak switching or 0.01 ppm for scanning is achievable even when the impurity line is close to a major line of the matrix elements. Figure 6 shows the intensity of the background close to the major lines in a copper spectrum. The impurity peaks due to $^{60}Ni^+$, $^{61}Ni^+$, $^{62}Ni^+$, $^{64}Zn^+$, $^{66}Zn^+$, $^{121}Sb^{2+}$, $^{123}Sb^{2+}$ can be detected at very low levels since the background is equivalent to less than 0.02 ppm at any of these mass positions, and is indeed less than 0.005 ppm for masses more than 1.5 mass units from the matrix peaks. With photoplate detection the background

Table I. Number of Ions Observed per Peak

Mode	Monitor signal	Ions collected at monitor	Number of ions observed per peak at concentration, ppm					
			100	10	1	0.1	0.01	0.001
	Integrated charge (nanocoulombs)	Total						
Peak switching	1	6×10^9	6×10^6	6×10^4	6×10^2	6×10^2	60	6
	0.1	6×10^8	6×10^4	6×10^3	6×10^2	60	6	...
	Current (Amperes)	Ions/second						
Scanning[a]	10^{-9} (High)	6×10^9	6×10^4	6×10^3	6×10^2	60	6	...
	10^{-10} (Typical)	6×10^8	6×10^3	6×10^2	60	6	...	...
	10^{-11} (Low)	6×10^7	6×10^2	60	6	...	...	...

[a] Three minute scan over mass range 238–7 at 500 resolution.

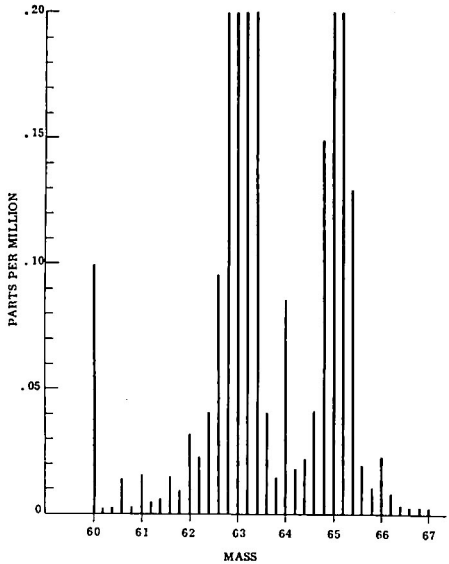


Figure 6. A portion of the spectrum of copper CA2 in the vicinity of the matrix peaks $^{63}Cu^+$ and $^{65}Cu^+$ showing the detectability of trace impurities at the 0.1 ppm level and below

Integrations were made at intervals of 0.2 mass unit. Resolution was 400

level in this region would be of the order of 10 ppm, because of the halation formed around the matrix lines due to secondary particles striking the emulsion.

Automatic Spark Control. In practice, sequential scanning of the peaks in the spectrum will produce quantitative analyses only if the inherent variations in the rf spark discharge are compensated. Although the ratiometer system does compensate for fluctuations, the system would still fail if the spark discharge were not maintained throughout the scan.

The automatic spark control system ("Autospark") developed in our laboratories (*25*) controls the operation of an rf spark discharge in which one electrode is continuously vibrated with respect to the other. A sensing element close to the rf generator detects the magnitude of the electrode gap, and a feedback circuit then causes the mean position of the vibrated electrode to be adjusted accordingly. The discharge will run unattended for long periods, certainly for times corresponding to a large number of scans. A further advantage of this control system is that the characteristics of the discharge are maintained more constant because of the automatic control of the electrode positions.

Both these features can be seen from the traces in Figure 7. Tungsten is normally a difficult material to spark and in the one-hour run under manual conditions, the ion current fell to zero 67 times and the electrode gap needed adjustment 28 times. Under Autospark control no manual electrode adjustment was needed and the signal never fell to zero for a period long enough for the recorder to respond. The limits of fluctuation of the monitor current are also generally reduced. Many other materials including graphite show

(25) P. Powers, R. Graham, and R. A. Bingham, British Patent applied for.

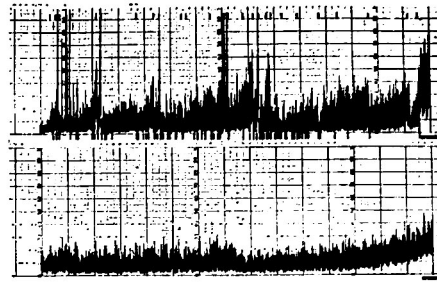


Figure 7. Traces of monitor signal during sparking of a tungsten sample

Upper trace is for manual control, lower trace for Autospark control. Each trace is for a 1-hour run and is recorded from right to left. Vertical ticks above the trace show points where electrode adjustment was needed, below the trace points where the signal fell to zero

similar behavior; samples of copper and steel have been sparked for more than eight hours without operator intervention.

The automatic spark control is clearly an essential requirement for the scanning technique and is also of great advantage for peak switching. While the mean gap is maintained constant, the instantaneous value is continuously varied over a fixed range, typically from close to zero to twice the mean. Although it has been observed in this laboratory, when manual control was used, that the apparent concentration of chromium in a copper standard can vary by a factor of two between a very narrow gap and the widest gap over which breakdown can occur, with Autospark control these variations are controlled and averaged out. During observation of any impurity the entire range of gap widths is covered a number of times, and the signal observed represents an average of all electrode gap conditions. This enables analytical precision to be improved to 1–2%, as shown later.

RESULTS

A number of series of steel, aluminum, and copper standards have been analyzed and the results of the analyses are presented and analyzed below. The purpose of these experiments was to evaluate systematically the basic limits of the technique, which could then serve as a guide to the performance that might be expected for other materials.

Peak switching results on all three materials are described first, since this is the more precise technique and the basic accuracy of the spark source method can therefore be more readily assessed. Scanning results are then presented for some copper standards in order to indicate the performance to be expected in rapid survey analysis.

The BCS Steel standards employed, with concentrations in the range 0.015 to 0.25% by weight, have been extensively examined by analysts using X-ray and emission spectrometry and chemical methods of analysis. The Johnson Matthey aluminum and copper standards used cover a wider concentration range, from 0.00004 to 1% by weight, and have been extensively studied by emission spectrometry.

Analysis of Peak Switching Results on BCS Steels. The chosen spectral peaks were tuned in to their selected channels using the reference standard sample and the channels adjusted in turn for maximum signal. The resolution was set at 500 (10% valley definition). The multiplier gain was adjusted so that for the selected integrated monitor charge of 0.3 nC the

Table II. Analysis of Standard Steel Samples SS12, 14, 15, 16 Using SS17 as Reference Standard

Sample	Loading	Integration	Concentration (% wt) observed Ni	Co	Cr	V
SS12	1	1	0.0420	0.265	0.0250	
		2	0.0431	0.265	0.0238	
		3	0.0431	0.260	0.0234	
	2	1	0.0403	0.230	0.0230	
		2	0.0409	0.232	0.0234	
		3	0.0409	0.226	0.0234	
	Mean observed value		0.04168	0.2462	0.02369	
	Mean quoted value		0.03229	0.2470	0.02671	
SS14	1	1	0.134	0.173	0.215	0.0143
		2	0.134	0.173	0.214	0.0143
		3	0.134	0.175	0.206	0.0143
	2	1	0.131	0.176	0.204	0.0138
		2	0.127	0.177	0.204	0.0141
		3	0.128	0.172	0.202	0.0138
	Mean observed value		0.1314	0.1742	0.2076	0.01409
	Mean quoted value		0.1270	0.1887	0.1833	0.01457
SS15	1	1	0.0939	0.0631	0.191	0.0499
		2	0.0939	0.0631	0.185	0.0495
		3	0.0950	0.0631	0.183	0.0499
	2	1	0.0933	0.0631	0.182	0.0545
		2	0.0939	0.0622	0.175	0.0552
		3	0.0927	0.0627	0.180	0.0535
	Mean observed value		0.09376	0.06290	0.1828	0.05208
	Mean quoted value		0.07871	0.05855	0.1641	0.05050
SS16	1	1	0.176	0.0266	0.118	0.0503
		2	0.183	0.0271	0.113	0.0516
		3	0.178	0.0275	0.113	0.0524
	2	1	0.170	0.0262	0.110	0.0562
		2	0.166	0.0262	0.106	0.0562
		3	0.172	0.0266	0.105	0.0547
	Mean observed value		0.1741	0.02668	0.1108	0.05358
	Mean quoted value		0.1819	0.02660	0.1000	0.05650
Ref SS17	Mean quoted value		0.2334	0.1258	0.02843	0.1053

* The scatter in the quoted values for V in SS12 was so great (standard deviation 41%) that the observations were excluded from the analysis.

collector integrator reading did not exceed full scale deflection.

The reference sample was then re-set in the ion source so that new surfaces could be sparked. Integrations were performed on each element three times taking the elements in rotation, *i.e.*, Ni—Co—Cr—V, Ni—Co—Cr—V, etc., the integrated values being read directly from a meter. The other standards were then run in the same manner, and each "sample" standard was loaded in the ion source twice. The integrated values obtained were compared with the average of 9 integrations for the reference standard, which was loaded three times.

The samples were positioned in the source as carefully as possible. One electrode was clamped to the 20-kV accelerating plate to maintain a fixed position, with the discharge point on the axis of the slit system. Not more than 1 mm of electrode overlap was allowed to ensure that the discharge occurred within the limits of the slits. The position of the discharge was thus controlled as carefully as possible in all directions.

Each integration reading took about ten seconds with source conditions of 20-kV rf spark voltage, 1000 pulses per second, and 200 microseconds pulse length. The discharge was maintained using the manually controlled vibrator.

VARIATIONS AND POSSIBLE CAUSES OF ERROR. The analytically determined values are shown in Table II. Each value is determined by comparing the element/monitor ratio for the particular integration with the corresponding average ratio derived from all three runs on the reference standard.

The variations between successive integrations were estimated from the variations within each group of 3 values for a particular sample loading. The mean standard deviation thus calculated (see Appendix) for variations between successive integrations is 1.6%.

Although care was taken in visually aligning the electrodes, it was expected that some analytical errors from this cause might remain. Analysis of the differences between the two sets of values corresponding to different sample loadings (see Appendix) indicates that the mean standard deviation for variations between sample loadings is 4.1%. Evans *et al.* (*19*) have shown that this variation can be reduced to 1.9% by positioning the electrodes using a telescope and this procedure will be adopted for future analyses.

Thus there are two separate sources of variation in the values shown in Table II, namely random variations of ±1.6% between one integration and the next, and variations of ±4.1% due to changes in sample loading position. Since three integrations and two sample positions have been used for each standard sample, one would expect variations in the mean value to be of the order of $\pm\sqrt{\frac{1.6^2}{3} + \frac{4.1^2}{2}} = \pm 3.0\%$. An additional error is contributed by the reference standard, in this case $\pm\sqrt{\frac{1.6^2}{3} + \frac{4.1^2}{3}} = \pm 2.5\%$ since there were three loading positions. The expected errors in the absolute values of concentrations would therefore be of the order of $\sqrt{3.0^2 + 2.5^2} = 3.9\%$ if only random errors were present. The expected mean error in the absolute values would then be $3.9\sqrt{\frac{2}{\pi}} = 3.1\%$ (see Appendix).

ABSOLUTE ERRORS OBSERVED. The actual differences between the measured mean values and the quoted concentrations for the 15 elements examined in steel have a mean value (irrespective of sign) of 7.9%. Since the random errors considered in the last section amounted to 3.1%, there is some additional source of error either in the measurements or in the quoted values.

The variations in the values quoted by the referee analysts (*26*) using chemical techniques have therefore been examined. The standard deviations of the reported values were calculated together with the overall spread, and these are plotted against concentration in Figure 8. It is clear that in the reported values the scatter increased markedly as the concentration decreased, which must indicate either larger errors in the techniques used, or increased inhomogeneity, at the 0.01–0.05% concentration level.

The percentage standard deviation of these reported values has an average value of 5.8% for the 15 concentration levels involved. Each spark source determination is compared

(26) Certificates of Analysis, Bureau of Analysed Samples Limited, Newham Hall, Middlesbrough, England.

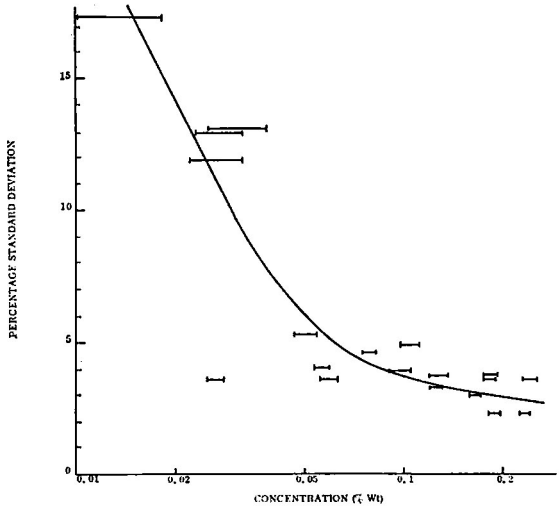


Figure 8. Standard deviations calculated from the analytical values recorded by referee analysts for Ni, Co, Cr, and V in steel standards SS12, 14, 15, 16 and 17

with the ratio between two of the quoted values, and the probable effect of these variations on the reliance to be placed on the ratio can be expressed as a probable mean error e. If σ_1 is the standard deviation for the reported values for the element and sample concerned, σ_2 the corresponding standard deviation for the same element in the reference standard and n_1 and n_2 the number of analysts reporting the values, the probable mean error $e = \sqrt{\frac{2}{\pi}\left(\frac{\sigma_1^2}{n_1} + \frac{\sigma_2^2}{n_2}\right)}$. The individual values of e are listed in Table III. The mean value is 4.4%. If any systematic errors are also present in the chemical techniques used for the reference analyses, the contribution of uncertainties in the quoted values could be higher than 4.4%.

The probable error due to the limited number of significant figures quoted by the referee analysts was also examined, but was found to be small (±0.25%) in comparison with the other possible causes of error.

The errors and their possible sources can be summarized as follows:

Mean difference between observed and quoted values (%) 7.9
Expected mean error in the absolute value due to spark source variations (%) 3.1
Probable mean error in the quoted values (%) 4.4
Average probable error due to rounding-off quoted values (%) 0.25

It is interesting to observe the correlation between the individual values of observed percentage absolute error, which can be calculated from Table II, and the variations in the reference analyses in Table III. The calculated correlation coefficient r is 0.40 (perfect correlation, $r = 1$; no correlation, $r = 0$) which Student's "t" test shows is significant at the 15% level. One is therefore justified in suspecting that many of the higher errors may arise in part from some factor connected with the standard.

If the concentrations with the 9 lowest standard errors of the referee analysts quoted values are selected from Table III,

Table III. Expected Errors Due to Variations in Quoted Values, %

	Ni	Co	Cr	V
SS12	6.1	2.1	8.2	...
SS14	1.8	1.8	6.2	10.0
SS15	2.4	2.1	6.1	4.2
SS16	2.1	2.2	6.2	3.6

the mean difference between the observed and quoted values falls to 4.2%, and the analysis of these errors then appears as follows:

Mean difference between observed and quoted values (%) 4.2
Expected mean error in the absolute value due to spark source variations (%) 3.5
Probable mean error in the quoted values (%) 3.0
Average probable error due to rounding-off of quoted values (%) 0.14

Analysis of Peak Switching Results on Aluminum and Copper Standards. Four of the Johnson Matthey aluminum standards AA1 to AA4, and five copper standards CBO, 1, 2, 3, and 8 were analyzed in a similar way. However, comparison with the quoted values was not made in such detail because the values were quoted to only two significant figures and in many cases only to one.

For a value quoted to one significant figure, *e.g.*, 2 or 0.002, one must assume that the true value may lie anywhere between 25 and 15 or within ±25% of the quoted value. For a number of values quoted in this way, the errors would be evenly distributed between zero and the extreme values, so that in the example quoted here the probable average rounding-off error would be half of the extreme value of 12.5%.

Calculating these rounding-off errors for each quoted elemental concentration in the aluminum standards AA1-3 used as samples, combining these values with the corresponding rounding-off error value for the reference standard

Table IV. Analysis of Standard Aluminium Samples AA1, 2, 3, Using AA4 as Reference Standard

Sample	Loading	Integration	Concentration (% wt) observed Mn	Fe	Ni	Cu	Zn
		1	0.00277	0.0532	0.00258	0.00350	0.00342
	1	2	0.00264	0.0566	0.00255	0.00319	0.00332
AA1		3	0.00249	0.0550	0.00244	0.00355	0.00332
		1	0.00277	0.0581	0.00251	0.00355	0.00300
	2	2	0.00277	0.0581	0.00248	0.00410	0.00295
		3	0.00277	0.0581	0.00251	0.00350	0.00311
	Mean observed value		0.00270	0.0565	0.00251	0.00357	0.00319
	Quoted value		0.002	0.055	0.0025	0.0015	0.002
		1	0.00709	0.105	0.00461	0.00527	0.00514
	1	2	0.00709	0.107	0.00456	0.00459	0.00488
AA2		3	0.00693	0.108	0.00456	0.00542	0.00492
		1	0.00603	0.107	0.00431	0.00510	0.00501
	2	2	0.00618	0.116	0.00409	0.00527	0.00478
		3	0.00632	0.118	0.00394	0.00542	0.00496
	Mean observed value		0.00661	0.110	0.00435	0.00524	0.00495
	Quoted value		0.007	0.10	0.004	0.006	0.005
		1	0.0190	0.199	0.0092	0.0192	0.0105
	1	2	0.0192	0.188	0.0096	0.0190	0.0106
		3	0.0188	0.197	0.0090	0.0196	0.0105
AA3		1	0.0192	0.184	0.0096	0.0176	0.0106
	2	2	0.0192	0.186	0.0094	0.0168	0.0105
		3	0.0188	0.195	0.0092	0.0165	0.0108
	Mean observed value		0.0190	0.192	0.0093	0.0181	0.0106
	Quoted value		0.018	0.19	0.010	0.02	0.010
Ref AA4	Quoted value		0.07	0.76	0.02	0.065	0.025

AA4, and taking an average, one concludes that the probable average error in an analytical determination due to the limited number of significant figures quoted is 6.2%. The corresponding probable average error for the 15 concentration values in copper would be 7.3%.

These uncertainties are themselves higher than those expected from the spark source measurements, which are shown in Table IV and explained in the following paragraphs. Furthermore we have no independent basis for assessing the accuracy of the quoted values in this case, since no list of values obtained by a panel of referee analysts is available for these standards. The analysis of the results is therefore limited to calculation of the variations between integrations and the effects of sample loading and the probable effects on the absolute errors.

The procedure for the aluminium standards was similar to that used with the BCS steels with the following exceptions:

(a) the exposure value used was 1 nanocoulomb
(b) only two integrations were made on the reference standard
(c) the rf spark voltage was 12 kV

The analytically determined values are shown in Table IV. These values were analyzed in the same way as the steel results and indicated variations between integrations of ±3.3% and sample loading variations of ±5.1%. Hence, one would expect variations in the mean value of $\pm\sqrt{\frac{3.3^2}{3} + \frac{5.1^2}{2}} = 4.1\%$. The reference standard would contribute a similar variation and the expected mean errors in the absolute values of concentrations would therefore be of the order of $4.1\sqrt{2}$. $\sqrt{\frac{2}{\pi}} = 4.6\%$ if only random errors were present.

The procedure for the copper standards was similar to that for steel and aluminium except that:

(a) the exposure value used was 0.1 nanocoulomb
(b) five integrations were made on each sample but each sample was only loaded once
(c) the reference standard was run before each sample run
(d) the integrated values were read from a DVM
(e) the rf spark voltage was 40 kV

The analytically determined values are shown in Table V. Analysis of these results can only give a measure of the variations between integrations; the standard deviation is 2.9%.

A further series of measurements was made on silver in copper standard CA4. Silver, which was at a concentration level of 12 ppm atomic, mixes easily in a copper matrix, and represents a fairly homogeneous standard. The sample was loaded, measured, and removed from the source eight times, each measurement being a series of ten integrations. The standard deviation of the variations between integrations was 1.8% and between sample loading 4.0%. These variations correspond closely to those seen for the steel measurements, but in this case at a much lower concentration level.

At even lower concentrations, useful results can still be achieved as shown by the 9.6% standard deviation between successive integrations observed for 0.014 ppm of ^{204}Pb in copper CA8 mentioned earlier.

An example of the linearity of the technique can be seen in Table V where the concentration of the elements in CBO used as the standard are on average 250 times those in CB8.

Summary of Peak Switching Analyses. The sources of the variations to be expected in the values obtained by the spark source mass spectrometry technique are summarized in Table VI.

Table V. Analysis of Standard Copper Samples CB1, 2, 3, 8 Using CB0 as Reference Standard

Sample	Integration	Concentration (% wt) observed Co	Ni[a]	Fe[a]	Mn
CB1	1	0.0224	0.0146	0.0147	0.0183
	2	0.0226	0.0144	0.0145	0.0178
	3	0.0228	0.0143	0.0148	0.0179
	4	0.0227	0.0144	0.0142	0.0176
	5	0.0224	0.0146	0.0146	0.0178
	Mean observed value	0.0226	0.0145	0.0147	0.0179
	Quoted value	0.02	0.015	0.011	0.018
CB2	1	0.0099	0.0064	0.0044	0.0096
	2	0.0104	0.0062	0.0044	0.0097
	3	0.0101	0.0062	0.0043	0.0095
	4	0.0100	0.0062	0.0044	0.0098
	5	0.0100	0.0066	0.0045	0.0098
	Mean observed value	0.0101	0.0063	0.0044	0.0097
	Quoted value	0.01	0.005–0.01[c]	0.005	0.009
CB3	1	0.0054	0.00147	0.0052	0.00425
	2	0.0056	0.00158	0.0048	0.00425
	3	0.0052	0.00158	0.0049	0.00431
	4	0.0053	0.00158	0.0054	0.00414
	5	0.0054	0.00147	0.0044	0.00420
	Mean observed value	0.0054	0.00154	0.00494	0.00423
	Quoted value	0.0052	0.005	0.0025	0.0035
CB8	1	0.000154	0.000185	0.000279	0.000194
	2	0.000154	0.000196	0.000283	0.000180
	3	0.000162	0.000196	0.000271	0.000180
	4	0.000145	0.000175	0.000297	0.000187
	5	0.000137	0.000169	0.000283	0.000180
	Mean observed value	0.000150	0.000184	0.000283	0.000184
	Quoted value	0.0001[b]	0.0002	0.0004	0.00004
Ref CB0	Quoted value	0.052	0.033	0.023	0.046

[a] Evidence of segregation.
[b] Not detected, analysis by dilution.
[c] Quoted range too great for inclusion in absolute error calculation.

RESULTS—SCANNING

Description of Analytical Runs of Johnson Matthey Copper Standards. The starting point of the downward exponential scan of the magnet current was set to cover the mass range 70–24 (gallium to magnesium) in one minute which would embrace the elements to be analyzed. Scans were made at a resolution of 500 (10% valley). Spark conditions used were 25 kV rf spark voltage, 1000 pulses per second, and 200 μsec pulse length with Autospark control. For these copper samples, the scale displayed on the UV recorder corresponded to an approximate concentration range of 1 ppm to 1000 ppm atomic for the samples containing higher concentrations. For the samples containing lower concentrations, the peak amplifier gain was increased by a factor 10 so that the 0.1 ppm to 100 ppm concentration range was covered. The peak height ratios were then read off the ultraviolet recorder chart using a logarithmically engraved scale.

The reference standard was the first sample loaded into the ion source and five scans were recorded. The same procedure was repeated on each of the sample standards. If any series of samples was run on different days, the reference standard was run after each one.

Variation and Possible Causes of Error. The analytically determined values, for one run of five scans on each sample, are shown in Table VII. Each value is determined by comparing the peak height ratio for the particular scan with the corresponding average peak height ratio derived from the five scans on the reference standard. Silicon was determined using the 29 and 30 isotopes since the levels of silicon were higher than the other elements and for some samples the silicon 28 peak was above or near the upper limit of the dynamic range.

Table VI. Sources of Variations in Peak Switching Determinations

	Steels SS12, 14, 15, 16 (reference SS17)	Aluminium AA1, AA2, AA3, (reference AA4)	Copper CB1, CB2, CB3, CB8 (reference CB0)	Copper CA4, ^{109}Ag at 6 ppm Concentration
Variations between integrations (standard deviation, %)	1.6	3.3	2.9	1.8
Variations between sample loadings (standard deviation, %)	4.1	5.1	...	4.0
Expected mean error in absolute value (%)	3.1	4.6	...	1.7

The variations between individual scans are normally considerably greater in the scanning method than the variations between individual integrations in the peak switching mode. Figure 9 shows the standard deviations for repeat scans for all the elements listed in the Johnson Matthey copper standards CA Series (CA0 and CA2-8), CB Series (CB0-8), and CC Series (CC1-5) plotted against concentration. These standard deviations were all derived from 5 repeat scans as in

Table VII. Analysis of Standard Copper Samples CB1, 2, 3 Using CB0 as Reference Standard: One Run of Five Scans

Run 1 Sample	Scan	Concentration (% wt) observed Co	Ni[a]	Fe[a]	Mn	Si
CB1	1	0.0200	0.0138	0.0053	0.0162	0.0133
	2	0.0375	0.0187	0.0096	0.0220	0.0245
	3	0.0265	0.0098	0.0108	0.0239	0.0194
	4	0.0221	0.0200	0.0113	0.0362	0.0227
	5	0.0210	0.0184	0.0150	0.0401	0.0076
	Mean observed value	0.02542	0.01614	0.01040	0.02768	0.01750
	Quoted value	0.02	0.015	0.011	0.018	0.02
CB2	1	0.0175	0.0076	0.0082	0.0210	0.0168
	2	0.0024	0.0066	0.0075	0.0257	0.0153
	3	0.0166	0.0109	0.0066	0.0248	0.0109
	4	0.0150	0.0076	0.0072	0.0100	0.0061
	5	0.0117	0.0081	0.0061	0.0168	0.0122
	Mean observed value	0.01264	0.00816	0.00712	0.01966	0.01226
	Quoted value	0.01	0.005–0.01	0.005	0.009	0.016
CB3	1	0.0071	0.0052	0.0048	0.0130	0.0109
	2	0.0042	0.0043	0.0042	0.0130	0.0053
	3	0.0095	0.0052	0.0030	0.0069	0.0070
	4	0.0062	0.0049	0.0036	0.0069	0.0088
	5	0.0068	0.0046	0.0038	0.0132	0.0079
	Mean observed value	0.00676	0.00484	0.00388	0.01060	0.00798
	Quoted value	0.0052	0.005	0.0025	0.0035	0.004
Ref CB0	Quoted value	0.052	0.033	0.023	0.045	0.049

[a] Evidence of segregation.

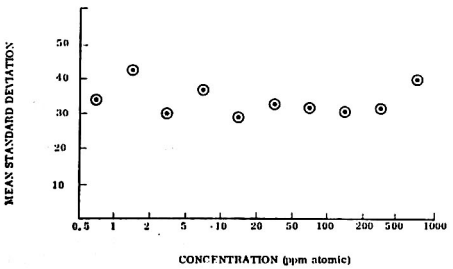


Figure 9. Standard deviations for spark source measurements made on 16 elements in the Johnson Matthey copper standards CA, CB, and CC series over a wide range of concentration using the ratio scanning mode

Table VII. The figure shows very clearly that for the scan conditions used, the reproducibility of individual scans is largely independent of concentration in the range 0.5 to 1000 ppm atomic, the standard deviation for repeat scans on individual elements being in the region of 33% throughout this range.

From the number of ions observed during a peak, given in Table I, one would expect the standard deviation to be smaller, especially at higher concentrations. For example, a 100-ppm component would give typically 6×10^3 ions, and hence on ion statistical grounds alone, one would expect a standard deviation of $100/(6 \times 10^3)^{1/2}$ or 1.3%. The larger variations observed in practice are largely a consequence of the short time (typically 0.1 second) during which each peak is being observed and of the fluctuations in the spark discharge during such short periods of time.

In the case of the CB0–3 standards on which the most detailed examination was carried out, the average standard deviation for repeat scans on individual elements was in fact 42.5%.

One would expect the reliability of the mean of 5 scans to be improved by a factor $\sqrt{5}$ compared with the individual scan values. Such variability would, however, be present in the reference standard runs also, so that the expected variations in the analytical determinations derived from the average of 5 sample scans compared with the average of 5 reference standard scans would be $\frac{42.5}{\sqrt{5}} \times \sqrt{2} = 26.8\%$.

The results from several runs of 5 scans each are shown in Table VIII. In fact, the average standard deviation observed for those determinations is 28.8%, indicating that the variability encountered between runs done with different loadings of the samples, and in some cases on different days, is essentially accounted for by the variation between scans. In view of the fact that the peak switching work for the BCS steels and Johnson Matthey aluminium showed that sample loading effects contributed only a 4–5% variation, this is not surprising.

Absolute Errors Observed. Since the variations observed between runs is 28.8% one would expect the absolute errors in the mean values of the 5 runs to have a mean value of the order of $\frac{28.8}{\sqrt{5}} \times \sqrt{\frac{2}{\pi}} = 10.3\%$ if the only significant errors were random ones. The actual differences between the measured mean values and the quoted concentrations for the 14 determinations have a mean value (irrespective of sign) of 28.3%. Thus, as with the peak switching results for the same standards, there is an additional source of error apart from those due to random variations. As before, there is no list of reported values on which to base an assessment of the source of error, but the mean expected rounding-off error due to the limited number of significant figures quoted is 5.7%.

Table VIII. Analysis of Standard Copper Samples CB1, 2, 3 Using CB0 as Reference Standard: Five Runs of Five Scans Each

Sample	Run	Concentration (% wt) observed				
		Co	Ni[a]	Fe[a]	Mn	Si
CB1	1	0.0254	0.0161	0.0104	0.0277	0.0175
	2	0.0222	0.0043	0.0096	0.0251	0.0100
	3	0.0217	0.0160	0.0124	0.0234	0.0190
	4	0.0265	0.0116	0.0086	0.0168	0.0282
	5	0.0170	0.0098	0.0107	0.0217	0.0315
	Mean observed value	0.02256	0.01156	0.01034	0.02294	0.02124
	Quoted value	0.02	0.015	0.011	0.018	0.02
CB2	1	0.0126	0.0082	0.0071	0.0197	0.0123
	2	0.0122	0.0057	0.0053	0.0122	0.0059
	3	0.0098	0.0128	0.0072	0.0112	0.0076
	4	0.0107	0.0050	0.0049	0.0074	0.0128
	5	0.0157	0.0038	0.0040	0.0148	0.0135
	Mean observed value	0.01220	0.00710	0.00570	0.01306	0.01042
	Quoted value	0.01	0.005–0.01[b]	0.005	0.009	0.016
CB3	1	0.0068	0.0048	0.0039	0.0106	0.0080
	2	0.0053	0.0022	0.0030	0.0083	0.0046
	3	0.0046	0.0062	0.0028	0.0072	0.0054
	4	0.0055	0.0031	0.0028	0.0048	0.0035
	5	0.0049	0.0028	0.0026	0.0078	0.0080
	Mean observed value	0.00542	0.00382	0.00302	0.00774	0.00590
	Quoted value	0.0052	0.005	0.0025	0.0035	0.004
Ref CB0	Quoted value	0.052	0.033	0.023	0.046	0.049

[a] Evidence of segregation.
[b] Quoted range too great for inclusion in absolute error calculation.

CONCLUSIONS

The precision of the spark source mass spectrometry technique has been improved by the use of electrical detection.

By using the scanning mode, a rapid survey of all elements is obtained with a precision and accuracy of 10–35% for all concentrations down to 1 ppm, and with a detection limit of 0.01 ppm. Because the output is immediately available and easy to interpret, the technique is considerably faster and more convenient than the photoplate method even for a complete survey of the elements. Only 10 minutes is required to obtain the data for a complete analysis covering the concentration range from major elements down to 0.1 ppm.

The convenience of the technique is further improved by the use of automatic spark control; after loading the sample, the instrument can be left to run automatically during the scans. On-line interpretation of the data by computer, identifying peaks, and calculating and printing out the concentrations of all elements within a few minutes (*17*, *20*), is also particularly convenient with the immediately accessible electrical output.

When the peak switching technique is used, the precision with which concentrations can be established relative to one another is better than 2%. When all the factors involved in a truly absolute analytical determination are taken into account, including sample loading and comparison with a known standard, the absolute accuracy should be of the order of 2–5%. For four steel standards with impurity concentrations in the range 500–2500 ppm, absolute differences of 4.2% were observed between the concentrations determined and the quoted values. More than half this error could be attributed to residual uncertainties in the quoted values.

This precision and accuracy should be maintained for concentrations down to a few ppm, rising as the concentration decreases further toward the detection limit of 0.001 ppm. This has been borne out by the routine use of the technique in our laboratories over a wide range of materials.

The precision and accuracy of the peak switching technique is thus considerably better than can be obtained using photoplates under routine analytical conditions, and the spark source mass spectrometric method now compares favorably with other analytical techniques such as emission and X-ray fluorescence spectrometry, particularly at lower concentration levels. Further improvements can be expected as the remaining factors influencing accuracy, such as sample inhomogeneity and availability of standards, are investigated and dealt with.

ACKNOWLEDGMENT

The contributions and advice of many colleagues, in particular Mr. P. Powers and Mr. R. Brown, is gratefully acknowledged.

APPENDIX

Statistical Methods of Analysis of Sources of Variation. We can represent any of the sets of 6 values in Table II by x_{i11}, x_{i12}, x_{i13} (1st sample loading) and x_{i21}, x_{i22}, x_{i23} (2nd sample loading) where the suffix i refers to the particular combination of element and sample.

An estimate of the typical variation between successive integrations can be made from the spread in any of the groups of three values x_{ij1}, x_{ij2}, x_{ij3}. In general, where m successive integrations are run, the groups will have the form x_{ijk} (k = 1 to m).

The best estimate of the percentage standard deviation corresponding to this variation which can be made from any one group of m values will be

$$\left\{\frac{\sum_{k=1}^{m}\left(x_{ijk}-\frac{1}{m}\sum_{k=1}^{m}x_{ijk}\right)^2}{m-1}\right\}^{1/2}\times\frac{100m}{\sum_{k=1}^{m}x_{ijk}} \qquad (1)$$

When $m = 3$ as in Table II, any such single estimate will be a poor one. For example, for Ni in SS14 one obtains 0.0% from sample loading 1 (0.134, 0.134, 0.134) but 2.1% from sample loading 2 (0.131, 0.127, 0.128). But an average taken over a considerable number of groups of 3 will give a good estimate of the variation. For $(n \times N)$ such groups corresponding to N combinations of element and sample and n loadings of each sample, the formula becomes:

Best estimate of percentage standard deviation between successive integrations =

$$\left\{\frac{1}{N.n.(m-1)}\sum_{i=1}^{N}\sum_{j=1}^{n}\sum_{k=1}^{m}\left(\frac{mx_{ijk}}{\sum_{k=1}^{m}x_{ijk}}-1\right)^2\right\}^{1/2}\times 100 \quad (2)$$

For $m = 3, n = 2, N = 15$ as in Table II, this formula reduces to 100 and gives a value of 1.6%.

$$100\left\{\frac{1}{60}\sum^{90}\left(\frac{3x_{ijk}}{\sum_{k=1}^{3}x_{ijk}}-1\right)^2\right\}^{1/2} \quad (3)$$

In the same way an estimate of the typical variation between sample loadings can be estimated from the means of the groups, *e.g.* from the values $(0.134 + 0.134 + 0.134)/3 = 0.134$ and $(0.131 + 0.127 + 0.128)/3 = 0.1287$ for Ni in SS14. The best estimate of the percentage standard deviation corresponding to sample loading which can be made from a group of values, from n loadings and m integrations for each loading, is given by

$$\left\{\frac{\sum_{j=1}^{n}\left(\sum_{k=1}^{m}x_{ijk}-\frac{\sum_{j=1}^{n}\sum_{k=1}^{m}x_{ijk}}{n}\right)^2}{n-1}\right\}^{1/2}\times\frac{100n}{\sum_{j=1}^{n}\sum_{k=1}^{m}x_{ijk}} \quad (4)$$

When $n = 2$ as in Table II this becomes

$$\sqrt{2}.\frac{|X_{i1}-X_{i2}|}{X_{i1}+X_{i2}}\times 100 \quad (5)$$

where $X_{ij} = \frac{1}{m}\sum_{k=1}^{m}x_{ijk}$, for example the mean values 0.134 and 0.1287 correspond to X_{i1} and X_{i2} for Ni in SS14. The estimate of percentage standard deviation works out in that case to 2.9%.

Any such estimate from two values only will again be a poor one, but here also a statistically good estimate will be obtained by pooling the N individual estimates. We then obtain the general formula

Best estimate of percentage standard deviation between sample loadings =

$$\left\{\frac{1}{N(n-1)}\sum_{i=1}^{N}\left[\sum_{j=1}^{n}\left(\left(\sum_{k=1}^{m}x_{ijk}-\frac{\sum_{j=1}^{n}\sum_{k=1}^{m}x_{ijk}}{n}\right)\times\frac{100n}{\sum_{j=1}^{n}\sum_{k=1}^{m}x_{ijk}}\right)^2\right]\right\}^{1/2} \quad (6)$$

For $m = 3, n = 2, N = 15$ as in Table II this formula reduces to

$$100\left\{\frac{2}{15}\sum_{i=1}^{15}\left(\frac{\sum_{k=1}^{3}x_{i1k}-\sum_{k=1}^{3}x_{i2k}}{\sum_{k=1}^{3}x_{i1k}+\sum_{k=1}^{3}x_{i2k}}\right)^2\right\}^{1/2} \quad (7)$$

and gives a value of 4.1%.

When the mean value of one of the N groups of $(n \times m)$ values is calculated, the standard error of that mean value is of course reduced compared with the variations in the individual values. If the Bessel-corrected estimates of percentage standard deviations are $\hat{\sigma}_s$ for variations between the n sample loadings, and $\hat{\sigma}_t$ for variations between the m integrations, the best estimate of the percentage standard error of the mean is given by $\hat{s} = \sqrt{\frac{\hat{\sigma}_s^2}{n}+\frac{\hat{\sigma}_t^2}{m}}$. Thus in the case of the steel results in Table II, $n = 2$, $\hat{\sigma}_s = 4.1\%$, $m = 3$, $\hat{\sigma}_t = 1.6\%$, so that $\hat{s} = \sqrt{\frac{4.1^2}{2}+\frac{1.6^2}{3}} = 3.0\%$.

It should be noted that the common expression for the standard error of the mean, $\hat{\sigma}/\sqrt{6}$, where $\hat{\sigma}^2 = \frac{\sum^{6}(x-\bar{x})^2}{5}$, gives a lower value in this case. But this formula applies only when all the samples are independently selected in a random fashion, whereas in the steel results the values in each of the two groups of three are not independent.

The value obtained is in the nature of a standard error of the mean, *i.e.* a Gaussian distribution of errors is implied. For a Gaussian distribution of means it can be shown that the mean deviation from the central value is $\sqrt{\frac{2}{\pi}}$ times the standard error.

Since some of the sources of error can be expressed only as mean deviations and the absolute errors are most conveniently expressed in that form, all sources of variation are expressed as actual or expected mean deviations.

RECEIVED for review July 20, 1970. Accepted September 21, 1970.

Radioactive Tracer Technique for Molecular Diffusion Coefficients in Granular Media

E. R. Bennett[1] and W. E. Bolch[2]

Sanitary Engineering Research Laboratory, University of California, Berkeley, Calif.

A radioactive tracer technique for the measurement of gaseous molecular diffusion coefficients in granular media or in open columns is described. A sealed glass ampoule of radioactive trace component gas was introduced into one end of a column containing granular media and counting gas in the pore volume. The mathematical expression for the arrival of the trace component at the other end of the column is given. The arrival was monitored with a radiation detector. Using this technique, the effect of pore opening obstruction on the molecular diffusion coefficient in granular media was investigated. Gaseous molecular diffusion coefficients in randomly packed, uniform, spherical, media were found to be reduced to a factor of 0.59 ± 0.02. The effect of nonuniformity and nonspherical shape of the granular media was shown to further reduce the molecular diffusion coefficient. The extreme case of a flat plate media was found to produce a diffusion obstruction factor of 0.197. Temperature and pressure correlations with the molecular diffusion coefficient were also made.

MOLECULAR DIFFUSION of a conservative solute from a point source in a three-dimensional medium can be expressed as:

$$\frac{dC}{dt} = D_{med}\nabla^2 C \qquad (1)$$

When the boundary conditions for a particular problem are used, the surface concentration at any location and time can be calculated if the effective media diffusion coefficient, D_{med}, is known. The effective media diffusion coefficient is composed of the molecular diffusion coefficient and selected media parameters.

The molecular diffusion coefficient of a trace component of gas diffusing in another pure gas can be calculated by any of several equations (*1*) relating diffusive transport to the thermodynamic properties (*2–4*) of the gases. (A trace component is a constituent that is present in concentrations that can be measured but are so small as to not change the physical and chemical properties of the carrier gas. In this experiment the radionuclide concentration was approximately $10^{-7}M$.)

In this study a radioactive technique was used. The inert carrier gas required a small percentage of an alkane to serve as the quench gas in the radiation detector. The inert carrier, the quench gas, and the radionuclide therefore produced a three-component diffusion system. Wilke (*5*) has shown that the molecular diffusion coefficient of a multicomponent system can be calculated from the harmonic sum of the ratio of the mole fraction to the molecular diffusion coefficient for each component.

When diffusion takes place in the void area of a packed bed or column, the molecular diffusion coefficient may be modified by a number of media effects. For granular media larger than 200 microns, the Knudsen effect can be considered as negligible. The major effect is that due to obstructed diffusion. This causes a reduction in the molecular diffusion coefficient due to the extra length of travel of the diffusing molecules on the tortuous path around the media granules (*6*) and due to the change in mass flux in the ever changing cross-section size and shape from point to point in the media pores (*7*).

The obstructive factor of molecular diffusion can be defined as a parameter expressing the ratio of the diffusion coefficient in the pore area of granular media to the diffusivity in an open space. From the values presented in Table I (*8–22*), it can be noted that the obstructive factor for randomly packed, uniform spheres has been found to be in the range of 0.5 to 0.8.

EXPERIMENTAL METHOD AND MATERIALS

Packed columns were used to provide a one-dimensional regime in which gas diffusivities and obstructive factors could be measured under varied conditions. The pressure within the column could be maintained over a range of values and measured by means of a manometer. The column assembly was located in a constant temperature and radiological enclosure with a maximum temperature variation less than

[1] Present address, Department of Civil and Environmental Engineering, University of Colorado, Boulder, Colo.

[2] Present address, Department of Environmental Engineering, University of Florida, Gainesville, Fla.

(1) R. B. Bird, W. E. Stewart, and E. N. Lightfoot, "Transport Phenomena," Wiley, New York, N. Y., 1960, p. 505.
(2) "Handbook of Chemistry and Physics, Western Edition, Chemical Rubber Company, Cleveland, Ohio, 1970.
(3) J. O. Hirschfelder, C. F. Curtiss, and R. B. Bird, "Molecular Theory of Gases and Liquids," Wiley, New York, N. Y., 1954, p 539.
(4) S. Chapman and T. C. Cowling, Mathematical Theory of Non-Uniform Gases, 2nd Ed., Cambridge University Press, New York N. Y., 1951.
(5) C. R. Wilke, *Chem. Eng. Progr.*, **46**, 95 (1950).
(6) P. C. Riest, *Environ. Sci. Technol.*, **1**, 567 (1967).
(7) E. E. Peterson, *A.I.Ch.E. J.*, **4**, 343 (1958).
(8) L. J. Klinkenberg, *Bull. Geol. Soc. Amer.*, **62**, 559 (1951).
(9) M. R. T. Wyllie, and A. R. Gregory, *Ind. Eng. Chem.*, **41**, 1379 (1955).
(10) J. M. Coulson, *Trans. Inst. Chem. Eng.* (1949).
(11) R. R. Sullivan and K. L. Hertel, *Advan. Colloid Sci.*, **1**, 37 (1952).
(12) P. C. Carman, *J. Soc. Chem. Ind.*, **57**, 225 (1938).
(13) J. H. Knox and L. McLaren, ANAL. CHEM., **36**, 1477 (1964).
(14) R. J. Blackwell, J. R. Rayne, and W. M. Terry, *Trans. A.I.M.E.*, **216**, 1 (1959).
(15) W. E. Brigham, P. W. Reed, and J. N. Dew, *Soc. Petrol. Eng. J.*, **1**, 1 (1961).
(16) J. Hoogachogen, *Ind. Eng. Chem.*, **47**, 906 (1955).
(17) J. C. Sternberg and R. E. Poulson, ANAL. CHEM., **36**, 1492 (1964).
(18) E. Glueckauf, "Gas Chromatography 1958," K. H. Desty, Ed. Butterworths, London, 1958, p 33.
(19) E. V. Evans and C. N. Kenney, *Trans. Inst. Chem. Eng.* **44**, 189 (1966).
(20) S. J. Hawkes and S. P. Steel, *J. Chromatogr. Sci.*, **8**, 256 (1970).
(21) J. A. Currie, *Brit. J. Appl. Phys*, **11**, 314 (1960).
(22) H. L. Penman, *J. Agr. Sci.*, **30**, 437 (1940).

Table I. Obstructive Factors in Uniform, Spherical Media

Medium	Porosity	Mean size, mm	Obstructive factor	Ref.
Glass spheres	0.435	8	0.71	(8)
Glass spheres	0.368	3	0.72	(9)
Glass spheres	0.402	3	0.71	(9)
Spheres	0.40	...	0.59	(10)
Spheres	0.39	...	0.59	(11)
Spheres	0.36	...	0.575	(12)
Glass spheres	0.38	0.50	0.62	(13)
Glass spheres	0.38	0.50	0.58	(13)
Glass spheres	0.38	0.275	0.62	(13)
Glass spheres	...	0.50	0.80	(14)
Glass spheres	...	0.04	0.71	(15)
Glass spheres	0.35	0.10	0.71	(16)
Glass spheres	...	1 vol 1.0–1.25 1 vol 3.26	0.66	(16)
Glass spheres	...	1 vol 1.0–1.25 4 vol 3.26	0.63	(16)
Glass spheres	...	0.086	0.64	(17)
Glass spheres	0.395	0.21	0.74	(17)
Glass spheres	0.403	0.42	0.66	(17)
Glass spheres	0.418	0.21	0.73	(17)
Glass spheres	0.474	0.42	0.79	(17)
Glass spheres	0.529	0.42	0.76	(17)
Glass spheres	0.643	1.15	0.75	(17)
Glass spheres	...	1.20	0.70	(18)
Glass spheres	0.36	0.81	0.70	(19)
Lead spheres	0.374	1.96	0.70	(19)
Glass spheres	...	0.21	0.73	(20)
Glass spheres	0.405	0.75	0.67	(21)
Glass spheres	0.396	0.75	0.674	(21)
Glass spheres	0.381	0.75	0.672	(21)
Glass spheres	0.395	0.38	0.67	(21)
Glass spheres	0.375	5–6	0.682	(21)
Glass spheres	0.376	5–6	0.67	(21)
Glass spheres	0.397	3	0.803	(22)
Glass spheres	0.364	0.5	0.774	(22)

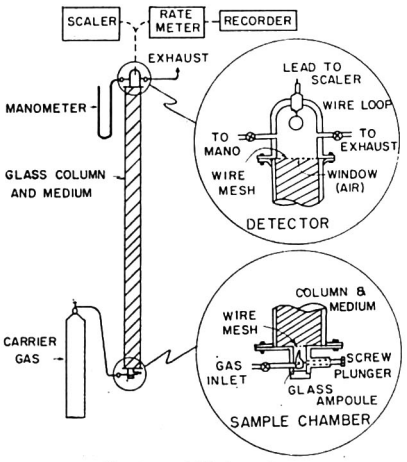


Figure 1. Diffusion column

±1 °C. A schematic drawing of the system is shown in Figure 1 and more complete descriptions are given elsewhere (*23,24*).

(23) E. R. Bennett and W. J. Kaufman, *SERL Rep. No. 67-8*, University of California, Berkeley, Calif., July 1967.
(24) W. E. Bolch, R. E. Selleck, and W. J. Kaufman, *SERL Rep. No. 67-10*, University of California, Berkeley, Nov. 1967.

Table II. Physical Properties of the Media

Media type	Mass mean size, microns	Uniformity coefficient	Solid density, gram/cm³
Glass beads A	6080	1.07	3.00
Glass beads B	380	1.15	2.485
Glass beads C	220	1.20	2.485
Sand I	350	1.26	2.64
Sand II	480	1.32	2.63
Sand IIA	480	2.78	2.64
Sand III	730	1.24	2.63
Sand IV	2640	1.20	2.62
Microplates	800 × 800 × 30	...	2.77

A radioactive trace component gas was released at the sample chamber and the rate of approach to equilibrium at the opposite face was recorded with an internal flow proportional radiation detector. The column voids contained one of three stagnant gas solutions: 99% helium and 1% isobutane (Q gas); 90% argon and 10% methane (P_{10}); or a standard air composition. The trace component radioactive gases used were krypton-85, tritiated hydrogen, and xenon-133.

The properties of the different column packing are given in Table II. Three sizes of uniform, nonporous, glass spheres were selected so as to be similar in shape and size distribution. The two smaller sizes were "3M Superbrite" glass beads, number 100 and 080. The larger size was six-millimeter diameter, laboratory "boiling" beads. Washed, graded, kiln dried, Monterey sands were used as raw material for the second classification of media. Additional grading and separation led to series (I, II, III, IV) of media having the primary variable of particle size. Sand I was selected to yield a natural medium of approximately the same mean size as

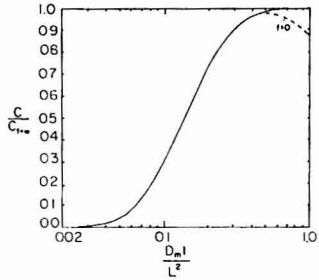


Figure 2. Theoretical molecular diffusion curve

Glass beads B. Sand IIA was prepared to provide a larger uniformity coefficient while retaining the same mean size as Sand II. A third classification consisted of a media from microsized aluminum plates.

For each diffusion measurement, an ampoule containing the radioactive trace component was positioned in the sample chamber, the column was flushed with the appropriate carrier gas, then sealed at the desired static pressure and held at a constant temperature. The ampoule was shattered with the screw plunger and the detection and recording instruments were simultaneously activated. The accumulative total count from the scaler was recorded at time intervals and these data were reduced to a plot of counting rate as a function of elapsed time. The detector was also coupled to a rate meter and a continuous curve was obtained from the chart recorder.

Diffusional transport in an infinitely long, packed column can be considered on the basis of Equation 1. The solution of this equation for diffusion from a plane source in a one-dimensional, single-directional, regime of infinite length is

$$C = \frac{M}{\epsilon A\sqrt{\pi D_m t}} \exp\left(-\frac{X^2}{4\,D_m t}\right) \qquad (2)$$

A "reflection" analogy (*25*) is used to express the effect of closure at some distance L away from the source. Therefore, for a finite column of length L, with a source at one end and the detector at the other, the concentration history can be considered as the superimposed effect of the molecules diffusing from the source and those "reflected" at $x = L$, and "reflected" again at $x = 0$ and returning to the detector at $x = L$, plus molecules that have "traveled" multiples of the two L "reflection lengths" This analogy results in the form of Equation 3.

$$\frac{C}{C_{t\to\infty}} = \frac{2L}{\sqrt{\pi D_m t}} \sum_{f=0}^{f=\infty} \exp\left\{-\frac{[(2f+1)L]^2}{4D_m t}\right\} \qquad (3)$$

with f having positive integer values from zero. The equation has been normalized in terms of a completely mixed concentration.

$$C_{t\to\infty} = \frac{M}{\epsilon AL} \qquad (4)$$

A plot of Equation 3 is shown in Figure 2. The curve rises rapidly until the maximum of the first term is reached and continues to rise until the completely mixed concentration is approached. The time required to reach a specific fraction of the function $C_{t\to\infty}$ is therefore, indicative of the molecular diffusion coefficient. The parameter D_m is replaced by D_{med} for the analysis of a packed column.

DISCUSSION AND RESULTS

Figure 3 is a plot of the counting rate or concentration as a function of time curves for the gas pairs studied and for each of the media and column lengths. Since the detection volume was the same for all portions of the study, the counting rate values can be used to express the concentration terms. The counting rate–time curves were fitted to Equation 3 using Figure 2 to determine the diffusion coefficient. This procedure eliminated the need for a precise value of the total amount of trace component injected or the exact efficiency of the detector.

A summary of the diffusion test results is presented in Table III. Note that runs 1, 9, 19, 23, 24, and 25 were without any media in the column and therefore determined experimental values for the molecular diffusion coefficients for the various tracer-gas solutions. Experimental diffusion coefficients were determined for variations in pressure from 1 atmosphere to 1.72 atmospheres and D_{med} was found to be an inverse function of pressure, as would be expected. A temperature range from 15 to 35° C was studied and D_{med} was found to vary with absolute temperature raised to the 1.55 power.

(25) J. Crank, "Mathematics of Diffusion," Oxford University Press, New York, N. Y. 1956.

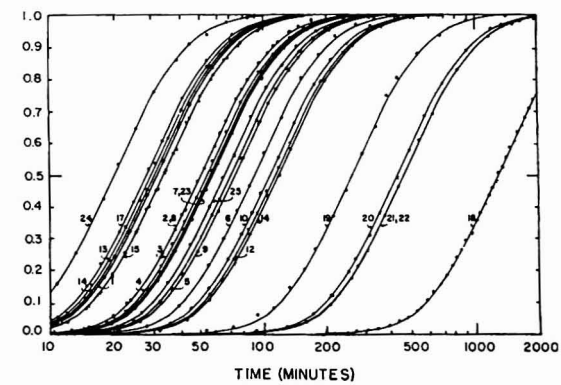


Figure 3. Molecular diffusion measurements

Table III. Diffusion Coefficients in Granular Media

Run No.	Trace gas	Carrier gas	Temp, °C	Press, atm	Media type	Media dia, mm	Porosity	Column length, cm	D_m, D_{med} obsd	D_m calcd	Obstructive factor, γ
1	^3H	He[a]	27	1.00	None	...	1.000	134	1.380	1.580	...
2	^3H	He	27	1.00	Glass A	6.00	0.423	134	0.840	...	0.61
3	^3H	He	27	1.00	Glass B	0.380	0.372	134	0.820	...	0.59
4	^3H	He	27	1.00	Glass C	0.220	0.384	134	0.800	...	0.58
5	^3H	He	27	1.386	Glass C	0.220	0.384	134	0.552	...	...
6	^3H	He	27	1.724	Glass C	0.220	0.384	134	0.444	...	...
7	^3H	He	15.5	1.00	Glass C	0.220	0.384	134	0.750	...	...
8	^3H	He	35	1.00	Glass C	0.220	0.384	134	0.840	...	...
9	^{85}Kr	He	27	1.00	None	...	1.000	123	0.533	0.590	...
10	^{85}Kr	He	27	1.00	Glass A	6.00	0.423	134	0.396	...	0.65
11	^{85}Kr	He	27	1.00	Glass B	0.380	0.372	134	0.362	...	0.59
12	^{85}Kr	He	27	1.00	Glass C	0.220	0.384	134	0.365	...	0.60
13	^{85}Kr	He	27	1.00	Sand I	0.350	0.403	62	0.291	...	0.55
14	^{85}Kr	He	27	1.00	Sand II	0.480	0.398	62	0.293	...	0.56
15	^{85}Kr	He	27	1.00	Sand IIA	0.480	0.375	62	0.264	...	0.50
16	^{85}Kr	He	27	1.00	Sand III	0.730	0.386	62	0.293	...	0.56
17	^{85}Kr	He	27	1.00	Sand IV	2.640	0.350	62	0.302	...	0.57
18	^{85}Kr	He	27	1.00	Microplate	...	0.565	247	0.104	...	0.197
19	^{85}Kr	Argon	27	1.00	None	...	1.000	134	0.162	0.154	...
20	^{85}Kr	Argon	27	1.00	Glass A	6.00	0.423	134	0.100	...	0.62
21	^{85}Kr	Argon	27	1.00	Glass B	0.380	0.372	134	0.094	...	0.59
22	^{85}Kr	Argon	27	1.00	Glass C	0.220	0.384	134	0.094	...	0.59
23	^{85}Kr	Air	27	1.00	None	...	1.000	62	0.157	0.158	...
24	^{133}Xe	He	27	1.00	None	...	1.000	62	0.450	0.550	...
25	^{133}Xe	Air	27	1.00	None	...	1.000	62	0.136	0.125	...

[a] He = 99% helium + 1% isobutane. Argon = 90% argon + 10% methane.

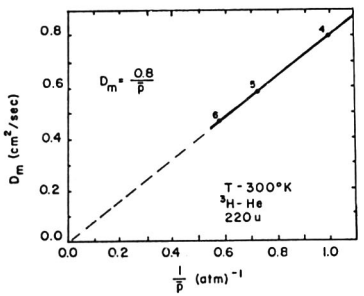


Figure 4. Effect of pressure on the molecular diffusion coefficient

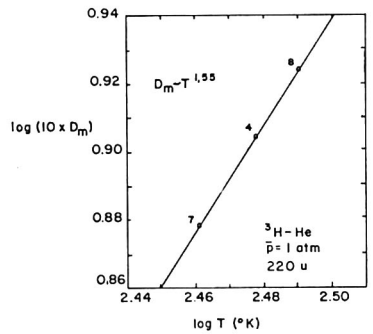


Figure 5. Effect of temperature on the molecular diffusion coefficient

Plots of these results are shown in Figures 4 and 5. Values of the molecular diffusion coefficient calculated from critical constants are also given in Table III. Porosity determinations are also shown. The media diffusion coefficient, D_{med}, determined for molecular transport within each of the granular media, was lower than that for an open tube without media because of the tortuous path and changing size and shape of the void areas. The change can be expressed as $D_{media} = \gamma D_m$. The value of the obstructive factor, γ, was determined for each size medium and gas pair.

The observed values of obstructive factors for the glass spheres are similar to those found by previous investigators. For randomly packed, spherical media, such as the 220-micron and 380-micron sizes, the obstructive factor was found to be 0.59 ± 0.02. With the six-millimeter beads, the column diameter to particle diameter ratio was only 8.4, and edge effects may have caused the increase in porosity and the 6% increase in obstructive factor.

The uniform sands (I, II, III, and IV) have nearly identical obstructive factors. The values of γ for these irregularly shaped particles is about 6% smaller than the value observed for spherical particles of comparable size The uniformity of the medium can produce a substantial change in the obstructive diffusion as seen from the comparison of Sand II and Sand IIA and the extreme case illustrated by the aluminum microplates.

SYMBOLS

A = Cross-sectional area of the column interior
C = Concentration of solute molecules per unit void volume
$C_{t\to\infty}$ = Concentration at the completely mixed condition
D_m = Molecular diffusion coefficient without media in column
D_{med} = Molecular diffusion coefficient with media in column

f = Integration function, integers from zero
L = Length of the sample column
$\bar{p}$ = Total gas system pressure in atmospheres
T = Absolute temperature, °K
t = Time after injection
X = Distance from the source
∇ = Three-dimensional derivatives

ϵ = Porosity
γ = Obstructive factor, equal to D_{med}/D_m

RECEIVED for review April 8, 1970. Accepted October 5, 1970. This work was part of grant AT(11-1)34 Project 30, USAEC completed in the Sanitary Engineering Research Laboratories of the University of California, Berkeley.

Spectrophotometric Analysis of Carbonyl Compounds in the Presence of Carbohydrates without Prior Separation

Edward B. Sanders and Jack Schubert

Department of Radiation Health, Graduate School of Public Health, University of Pittsburgh, Pittsburgh, Pa. 15213

A simple, rapid method is described whereby normal carbonyl compounds can be spectrophotometrically determined in the presence of carbohydrates, without prior separation, using the reagent 2,4-dinitrophenylhydrazine. The method exploits a technique which suppresses formation of carbohydrate 2,4-dinitrophenylhydrazones. The effect of such parameters as pH, temperature, and time of heating on the condensation of both carbonyl compounds and sugars with 2,4-dinitrophenylhydrazine to form 2,4-dinitrophenylhydrazones is discussed. The fraction of α-dicarbonyl compounds present can also be determined.

THE REAGENT 2,4-DINITROPHENYLHYDRAZINE (2,4-DNP) is widely used for the analysis of carbonyl compounds, especially as applied by Lappin and Clark (*1*). In their method, carbonyl compounds are reacted in an acidic media with 2,4-DNP to give a 2,4-dinitrophenylhydrazone (2,4-DNPH) which, after addition of methanolic potassium hydroxide to give the anion, is determined spectrophotometrically. This method has been used, with slight variations, for a number of diverse applications, such as analysis of total carbonyl content in irradiated amino acids (*2*, *3*), ethylene glycol (*4*), and cyclohexane (*5*); analysis of carbonyl functions in polymers (*6*); and the determination of total carbonyl content in foods (*7*). However, the method of Lappin and Clark cannot be directly applied for the analysis of the total carbonyl content when carbohydrates are present, especially in complex systems such as food, DNA, and cellular material. Consequently, analyses for simple aldehydes and ketones in the presence of sugars are carried out only after their prior separation from sugars, usually by volatilization or extraction into an organic phase. Such separations exclude high boiling carbonyl compounds, or highly polar, water soluble compounds such as glyceraldehyde or glycolaldehyde, and in some cases, lead to the chemical loss, destruction, or transformation of certain carbonyls. In our continuing investigations on the chemical changes produced upon gamma-irradiation of carbohydrates and other food components (*8*), it is necessary to determine the total carbonyls known (*9*) to be produced upon irradiation. During our attempts to apply the method of Lappin and Clark (*1*) to irradiated sugar solutions, we developed a rapid and reliable spectrophotometric assay, described here, for total carbonyls in the presence of carbohydrates without requiring the prior separation of the carbonyls.

We are able to eliminate or minimize the interference of sugars in the 2,4-DNP assay of carbonyls by exploiting the fact that carbohydrates, in general, exist in aqueous solution as cyclic hemiacetals rather than open chain aldehydes. Consequently, they react much more slowly with nucleophilic reagents than do carbonyl compounds whose structures either preclude hemiacetal formation or where the hemiacetal-open chain aldehyde equilibrium favors the open chain aldehyde. When we applied the method of Lappin and Clark to aqueous solutions of glucose and fructose, we noted that the visible absorption due to the sugars was considerably less than would be expected for typical carbonyl compounds. This reflected either a lower molar absorptivity for these sugar 2,4-DNPH anions or incompleteness of reaction under these conditions. Examination of the visible spectra of the anions of the 2,4-DNPH's of synthetic glucose and fructose ruled out the former possibility, indicating that proper choice of conditions for the analysis might, and in fact did, result in formation of 2,4-DNPH derivatives of normal carbonyls but not those of the sugars. Further, as described later, since the α-dicarbonyl compounds such as glyoxal necessarily form osazones with a different absorption spectrum and relatively very high molar absorptivity from that of the 2,4-DNPH anions, we are also able to determine the fraction of α-dicarbonyl present in a mixture of carbonyl compounds.

EXPERIMENTAL

Reagents. CARBONYL-FREE METHANOL. To about 500 ml of reagent grade methanol (Fisher), add 5 grams of 2,4-DNP and a few drops of concentrated hydrochloric acid and reflux for 2 hr. The methanol is then distilled through a Vigreux column. When kept tightly stoppered, the methanol remains suitable for use for several months.

2,4-DINITROPHENYLHYDRAZINE REAGENT. 2,4-DNP (Eastman) is recrystallized from carbonyl-free methanol. The recrystallized material melts at 199–200 °C and is pure ac-

(1) G. Lappin and L. C. Clark, ANAL. CHEM., 23, 541 (1951).
(2) B. M. Weeks, S. A. Cole, and W. M. Garrison, *J. Phys. Chem.*, 69, 4131 (1965).
(3) J. W. Harlan, F. Leo Kauffman, and F. Heiligman, "Radiation Preservation of Foods," American Chemical Society, Washington, D. C., 1967, p 39.
(4) M. Ahmud, M. H. Awan, and D. Muhammad, *J. Chem. Soc. (B)*, 1968, 945.
(5) A. J. Bailey, S. A. Barker, R. H. Moore, and M. Stacy, *J. Chem. Soc.*, 1961, 4086.
(6) J. Belisle, *Anal. Chim. Acta*, 43, 515 (1968).
(7) H. P. Fleming, W. Y. Cobb, J. L. Etchells, and T. A. Bell, *J. Food Sci.*, 33, 572 (1968).
(8) J. Schubert, *Bull. W.H.O.*, 41, 873 (1969).
(9) G. O. Phillips, *Advan. Carbohydrate Chem.*, 16, 13 (1961).

Table I. Melting Points of Synthetic 2,4-Dinitrophenylhydrazones

Compound	Melting point, °C Observed	Literature	Reference
Formaldehyde 2,4-DNPH	164–165	164–165	(*12*)
Acetaldehyde 2,4-DNPH	146–148	146	(*13*)
Glycolaldehyde 2,4-DNPH	161–162	157–161	(*14*)
Glyoxal bis(2,4-DNPH)	334–335	336–338	(*14*)
Propionaldehyde 2,4-DNPH	152–153	154.5–155	(*12*)
Glyceraldehyde 2,4-DNPH	168–170	170	(*15*)
Dihydroxyacetone 2,4-DNPH	166–167	168–169	(*15*)
Acetone 2,4-DNPH	125–127	125–126.5	(*12*)
Diacetyl 2,4-DNPH	319 dec.	318 dec.	(*16*)
α-Ketoglutaric acid 2,4-DNPH	210 dec.	203 dec.	(*13*)
Glucose 2,4-DNPH	122–124	122–124	(*17*)
Fructose 2,4-DNPH dioxanate	178–179	176–178	(*18*)

cording to thin layer chromatography. A saturated solution is prepared in carbonyl-free methanol.

POTASSIUM HYDROXIDE REAGENT. Dissolve 10 grams of potassium hydroxide in 20 ml of distilled water and bring the volume to 100 ml with carbonyl-free methanol.

Materials. Sucrose, glucose, fructose, diacetyl, formaldehyde (Fisher), xylose, sorbose, ribose (Nutritional Biochemical), dihydroxyacetone, erythrose, glycolaldehyde, glyceraldehyde, 2-deoxyribose, lyxose, arabinose, α-ketoglutaric acid (Sigma), acetaldehyde and propionaldehyde (Eastman), and glyoxal (Matheson Coleman and Bell) were used without purification. Aldol (Eastman) was chromatographed on silica gel and distilled. Assay of the purified material by iodometric titration (*10*) indicated 99% aldol compared to 80% for the commercial product. Analyses were carried out on solutions of known amounts of the carbonyl compound in distilled water or in an aqueous carbohydrate solution. In cases where solutions could not be obtained by simply weighing out the pure carbonyl compound, chemical methods of standardization were used to ascertain the concentration of the solution. The stock formaldehyde solution was standardized by reaction with sodium sulfite followed by titration of the released base (*11*) while solutions of acetaldehyde, propionaldehyde, and glyoxal were standardized by iodometric titration (*10*).

The 2,4-DNPH's used in this study were prepared by standard methods. Table I lists the 2,4-DNPH's with their melting points and literature melting points for comparison.

Procedure. To a test tube, add 1 ml of an aqueous solution about 10^{-4} to $10^{-3}M$ in the carbonyl compound to be analyzed. Add 1 ml of the 2,4-DNP reagent and 1 ml of 0.01*N* hydrochloric acid. The final pH must be between 2.5 and 2.7. If the final pH is not within this range, it should be adjusted. The final volume is 8.0 ml so that any increase in volume at this stage caused by adjusting the pH can be compensated by adding a correspondingly smaller volume of base. The tube is stoppered, heated at 80 °C for 10 min, and then allowed to cool in an ice bath for 10 min. To the cooled solution, add 5 ml of the potassium hydroxide reagent. Since the color slowly fades with time, 10 min is allowed to elapse before the absorbance is measured at 515 nm on a Unicam SP. 800 ultraviolet spectrophotometer. A reagent blank is run with each sample.

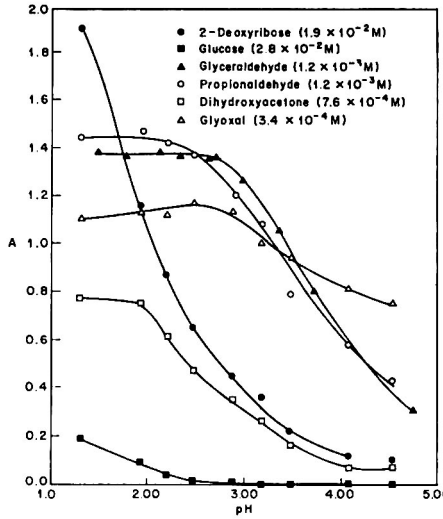


Figure 1. Effect of initial pH on the absorbance at 515 nm of 2,4-DNPH anions of some carbohydrates and carbonyl compounds. All other conditions, temperature, etc., are as described in the analytical procedure

RESULTS AND DISCUSSION

Effect of pH. The condensation of 2,4-DNP with carbonyl compounds to yield 2,4-dinitrophenylhydrazones is an acid-catalyzed reaction. Reaction of 2,4-DNP with carbohydrates, however, would be acid-catalyzed not only with regard to the actual condensation but also because the rate of conversion of the cyclic hemiacetal to the acyclic aldehyde is accelerated at low pH. Two demonstrations of this rate acceleration are the exchange of the aldehydic oxygen of glucose with H_2O^{18} and the mutarotation of glucose. The rate constant for exchange decreases by a factor of ten when the pH is raised from 1.5 to 2.5 while the same pH change decreases the rate of glucose mutarotation by a factor of two (*19*). The pH profiles of the absorbance at 515 nm of the 2,4-DNPH anions of four carbonyl compounds and two sugars are shown in Figure 1. The absorbance due to the two sugars, glucose and 2-deoxyribose, shows a pronounced change as the pH is raised from 1.30 to 2.50. The absorbance of a 0.5% glucose solution treated with 2,4-DNP and potassium hydroxide declines from 0.21 to 0.02 over this pH range while the absorbance of a 0.25% 2-deoxyribose solution

(10) I. M. Kolthoff and R. Belcher, "Volumetric Analyses," Vol. III, Interscience Publishers, Inc., New York, N. Y., 1957, p 120.
(11) *Ibid.*, Vol II, p 385.
(12) J. D. Roberts and C. Green, *J. Amer. Chem. Soc.*, **68**, 274 (1946).
(13) I. Heilbron and H. M. Bunbury, "Dictionary of Organic Compounds," Vol. I, Oxford University Press, New York, N. Y., 1953, p 5.
(14) M. L. Wolfrom and G. P. Arsenault, ANAL. CHEM., **32**, 693 (1960).
(15) H. Reich and B. K. Samuels, *J. Org. Chem.*, **21**, 68 (1956).
(16) R. C. Lindsay, E. A. Day, and W. E. Sandine, *J. Food Sci.*, **29**, 266 (1964).
(17) E. A. Lloyd and D. G. Doherty, *J. Amer. Chem. Soc.*, **74**, 4214 (1952).
(18) L. M. White and G. E. Secor, *ibid.*, **75**, 6343 (1953).
(19) D. Rittenberg and C. Groff, *J. Amer. Chem. Soc.*, **80**, 3370 (1958).

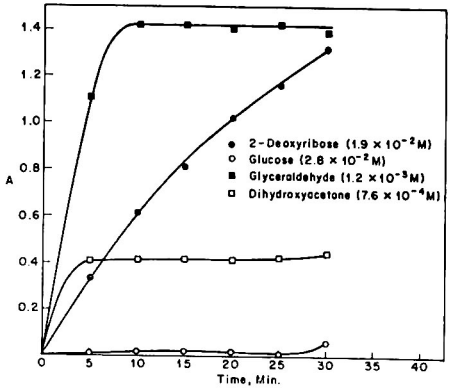


Figure 2. Effect of heating time at 80 °C on the absorbance at 515 nm of 2,4-DNPH anions. All other conditions as described in the analytical procedure

declines from 1.90 to 0.65 over the same range. Of the sugars tested, fructose, xylose, lyxose, arabinose, sorbose, and sucrose also showed absorbance of 0.02 or less between pH 2.5 and 2.7 at 515 nm for a 0.5% solution. Only ribose and 2-deoxyribose, of the sugars tested, gave interference. However, this interference could be successfully blanked out allowing total carbonyl content to be measured in their presence.

As expected, the absorbance of normal carbonyl compounds is also dependent on pH, decreasing as the pH rises. However, in this case the decline in absorbance over the pH range 1.30 to 2.50 is much less marked than for the sugars as can be seen from Figure 1. The absorbance of glyceraldehyde remains relatively constant over the pH range 1.30 to 2.50, glyoxal appears to have a maximum at pH 2.50, while propionaldehyde is about 10% lower at pH 2.50 than at 1.30. Dihydroxyacetone, on the other hand, shows a decline in absorbance from 0.78 at pH 1.30 to 0.47 at pH 2.50. In addition, the absorbance due to dihydroxyacetone decreases significantly from pH 2.50 to pH 2.70, the pH range specified in the procedure. This behavior may well be typical of all ketones which, because of steric effects, react more slowly with 2,4-DNP. Consequently, strict control of pH must be exercised in order to obtain accurate results. Reproducible results can be obtained for stock solutions by simply adding a known amount of hydrochloric acid as indicated in the procedure. However, for complex mixtures, where the initial pH may vary considerably, the pH should be adjusted as close as possible to the stated pH, namely 2.50–2.70, at which the calibration curves were obtained.

Temperature and Time of Heating. The rate of formation of the 2,4-DNPH's is a function of the temperature. Four temperatures were investigated: 25, 50, 80, and 100 °C. The two lower temperatures were unsatisfactory in that too much time is needed for completion of the reaction. On the other hand, sugar interference is appreciable at 100 °C even for a 5-minute heating time. Moreover, methanol evaporation occurs causing significant errors in the analysis. The 80 °C temperature is completely satisfactory in that sugar interference is negligible and the reaction is complete after 10 minutes. The dependence of the visible absorbance with heating time is shown in Figure 2 for two sugars and two carbonyl compounds. Both carbonyl compounds glyceraldehyde and dihydroxyacetone reach a maximum after 10 minutes. No further change is observed up to 30 min. Absorbance due to deoxyribose rises sharply with time, from 0.32 at 5 min to 1.32 after 30 min. Glucose shows an absorbance of 0.02 until 25 min. At 30 min, the absorbance is 0.06.

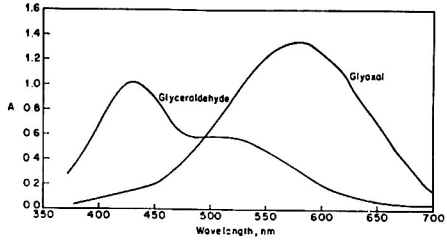


Figure 3. Visible absorption spectra of the 2,4-DNPH anions of glyceraldehyde ($4.1 \times 10^{-4}M$) and glyoxal ($1.4 \times 10^{-4}M$) prepared as described in the analytical procedure

Instability of 2,4-DNPH Color. The visible absorbance of the 2,4-DNPH's decreases slowly with time after being treated with base. That this is an actual property of the 2,4-DNPH anions has been confirmed in that synthetic 2,4-DNPH's show the same effect after treatment with base. Several attempts by other workers have been made to eliminate this instability by altering the solvents for the reaction. Pesez (*20*) carried out the formation of the 2,4-DNPH in acetic acid and utilized the visible spectrum of the 2,4-DNPH itself rather than the anion. We found this method inapplicable to aqueous sugar samples in that very strong sugar 2,4-DNPH absorption resulted. Papa (*21*) has recently published a method which gives stable 2,4-DNPH anions by making the final solution 70% in pyridyne. However, his method is less sensitive.

In our procedure, reproducible results are obtained by simply taking each reading exactly 10 min after addition of the potassium hydroxide reagent. It should be noted that the color produced by the anion of 2,4-DNP itself fades with time. Consequently, a fresh blank should be run with every sample.

The visible absorption spectra for glyceraldehyde and glyoxal are shown in Figure 3. The spectra of glyceraldehyde is typical of all normal aldehyde and ketone 2,4-DNPH anions studied, with a maximum 430 nm and a smaller broader peak at 512 nm. Although the 430-nm peak is more intense, we have chosen to utilize the 515-nm region to completely eliminate sugar interference. Both glucose and fructose show some absorption at 430 nm. The spectrum of glyoxal has a single intense peak at 570 nm which is typical of α-dicarbonyl compounds. The difference is due to the fact that α-dicarbonyl compounds form osazones, bis-2,4-DNPH's, under the conditions of the assay. Even though the α-dicarbonyl compounds do not have a maximum at 515 nm, the absorbance in this region is sufficiently high to utilize this wavelength in the analytical method. The difference between the visible absorption spectra of 2,4-DNPH anions and osazone anions is sufficiently great so that α-dicarbonyl compounds can be easily estimated in the presence of carbonyls if the absorbance at both 430 nm and 570 nm is determined. The absorption of

(20) M. Pesez, *J. Pharm. Pharmacol.*, 71, 475 (1959).
(21) L. J. Papa, *Environ. Sci. Technol.*, 3, 397 (1969).

Table II. Molar Absorptivities, ϵ, of 2,4-DNPH Anions at 515 nm

Compound	From calibration curve[a] Water	0.25% Glucose and 0.25% fructose	From synthetic 2,4-DNPH
Formaldehyde		$5.7 \pm 0.4 \times 10^3$	4.9×10^3
Acetaldehyde		$8.9 \pm 0.2 \times 10^3$	10.1×10^3
Glycolaldehyde	$4.7 \pm 0.3 \times 10^3$	$4.5 \pm 0.4 \times 10^3$	5.4×10^3
Glyoxal	$2.6 \pm 0.2 \times 10^4$		3.2×10^4
Propionaldehyde		$9.4 \pm 0.6 \times 10^3$	10.9×10^3
Glyceraldehyde[b]	$9.3 \pm 0.5 \times 10^3$	$8.6 \pm 0.7 \times 10^3$	9.6×10^3
Acetone		$3.2 \pm 0.3 \times 10^3$	10.5×10^3
Dihydroxyacetone		$5.1 \pm 0.5 \times 10^3$	9.6×10^3
Aldol		$10.6 \pm 0.6 \times 10^3$	
Erythrose	$3.8 \pm 0.6 \times 10^3$	$3.7 \pm 0.5 \times 10^3$	
Diacetyl		$2.3 \pm 0.2 \times 10^4$	5.0×10^4
α-Ketoglutaric acid		$4.9 \pm 0.2 \times 10^3$	16.8×10^3

[a] The error is expressed as the standard deviation calculated from six runs.
[b] ϵ determined in 0.25% 2-deoxyribose is $8.4 \pm 0.6 \times 10^3$.

Table III. Molar Absorptivities, ϵ, of 2,4-DNPH Anions at 430 nm

Compound	From calibration curve[a]	From synthetic 2,4-DNPH
Formaldehyde	$12.5 \pm 0.8 \times 10^3$	12.0×10^3
Glycolaldehyde	$12.1 \pm 0.8 \times 10^3$	12.5×10^3
Glyceraldehyde	$18.3 \pm 1.2 \times 10^3$	18.4×10^3
Dihydroxyacetone	$10.8 \pm 1.2 \times 10^3$	24.0×10^3
Erythrose	$5.3 \pm 0.2 \times 10^2$	
α-Ketoglutaric acid	$13.8 \pm 0.7 \times 10^3$	42.3×10^3

[a] The error is expressed as the standard deviation calculated from six runs.

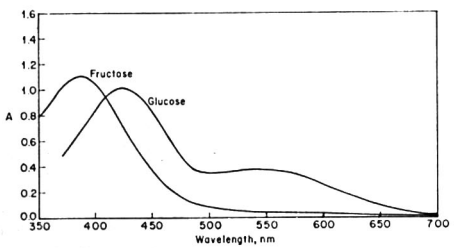


Figure 4. Visible absorption spectra of the 2,4-DNPH anions of glucose ($3.1 \times 10^{-3} M$) and fructose ($1.1 \times 10^{-3} M$)

conjugated carbonyls occurs at higher wavelengths, *e.g.*, 460 nm for crotonaldehyde.

Molar absorptivities at 515 nm for 12 carbonyl compounds obtained from calibration curves are given in Table II. The calibration curves were obtained in either distilled water or a mixture of 0.25% glucose and 0.25% fructose. One calibration curve was run for glyceraldehyde in 0.25% 2-deoxyribose, using the same concentration of 2-deoxyribose in the blank. In all cases, values of the molar absorptivities obtained in different media agree within experimental error. Molar absorptivities at 430 nm for six compounds are shown in Table III.

Molar absorptivities calculated from methanolic solutions of the synthetic 2,4-DNPH anions are also given in Tables II and III. They generally compare well with the molar absorptivities obtained from the analytical procedure for aldehydes as can be seen in Tables II and III. The disparity for ketones is undoubtedly due to incompleteness of formation of the 2,4-DNPH's under the conditions used. In all cases, the spectra obtained by scanning solutions resulting from the analytical method were identical to spectra obtained by treating a methanolic solution of the synthetic 2,4-DNPH with methanolic potassium hydroxide.

An interesting note is that the lack of interference from the carbohydrates is definitely a consequence of lack of reaction of these compounds, and is not due to a difference of the absorption spectra of carbohydrate 2,4-DNPH anions. Figure 4 shows the spectra of synthetic glucose and fructose 2,4-DNPH anions. There is considerable absorption at both 515 and 430 nm for glucose and at 430 nm for fructose. One possible explanation of the interference of ribose and deoxyribose is the position of the acyclic aldehyde–hemiacetal configuration equilibrium. About 8.5% of ribose exists as the open chain aldehyde as compared to 0.003% for glucose in aqueous solution (*22*). The fact that erythrose reacts in the manner of an ordinary carbonyl compound indicates that under the conditions used in the analytical method, erythrose may have a considerable percentage of the open-chain aldehyde present.

ACKNOWLEDGMENT

The authors thank J. L. Meade and S. N. Pagay for technical assistance.

RECEIVED for review September 8, 1970. Accepted October 5, 1970. This work was supported by the U. S. Atomic Energy Commission, Division of Biology and Medicine, under AEC Contract AT(30-1)-3641 and by Contract FDA 68-29 with the Division of Food Chemistry, Bureau of Science, Food and Drug Administration, Department of Health, Education, and Welfare, Washington, D. C. Views expressed herein do not necessarily reflect those of the U. S. Food and Drug Administration or of the U. S. Atomic Energy Commission.

(22) S. M. Cantor and Q. P. Peniston, *J. Amer. Chem. Soc.*, **62**, 2113 (1940).

Polarographic Determination of Traces of Nitrilotriacetate in Water Samples

John P. Haberman

The Procter & Gamble Company, Miami Valley Labs, Cincinnati, Ohio 45239

A sensitive and selective method for determining trace amounts of nitrilotriacetate, a component in detergent formulations, is described. Polarographic analysis of NTA as an In(III)–NTA complex was used. The technique was evaluated in river water and sewage samples from 0.0257 to 2.57 ppm with anion exchange concentration and isotope dilution to correct for incomplete recovery. It was evaluated from 2.57 to 257 ppm without anion exchange concentration. The relative standard deviation was approximately 10%, except for the lowest concentration.

FEW PRACTICAL APPLICATIONS of electroanalytical techniques to environmental analyses have been reported. In this study, nitrilotriacetate (NTA) in sewage and river water samples was converted to a polarographically active complex with In(III) in 1*M* NaCl, 0.1*M* acetic acid (HOAc), and 0.1*M* sodium acetate (NaOAc) buffer. Anion exchange concentration and differential polarography were used to increase the sensitivity. A cation exchange column pretreatment was used as a precaution against interfering cations, and isotope dilution analysis with ^{14}C-labeled NTA (NTA-^{14}C) was used to determine the variability of the concentration step.

Colorimetric methods for NTA analysis based on the bleaching of colored complexes have been described (*1*, *2*). Although sensitive and rapid, they are subject to interference by other chelating agents. Colored material in samples may also interfere. Theoretically, other chelating agents could cause polarographic interference (*3*), but in this study using In(III) there was no interference noted.

EXPERIMENTAL PROCEDURES, MATERIALS AND EQUIPMENT

The following steps constituted the procedure used for the analysis of NTA added to waste water samples. Sample collection and storage were not investigated. Figure 1 is a schematic representation of the complete procedure.

Analytical Procedure below 2.57 ppm. INITIAL PRETREATMENT. One liter of filtered sample was measured into a beaker and analytical studies were performed by adding known amounts of NTA to samples at this point. An aliquot of NTA-^{14}C was added for isotope dilution analysis and the pH was adjusted to 3.0 by the dropwise addition of 6*M* HCl. Nitrogen gas was bubbled through the sample with a gas dispersing tube for 10 minutes at a rate sufficient to give good stirring to remove H_2S.

CATION EXCHANGE PRETREATMENT. The sample was passed through a 60-ml (approximately 1.8 × 26 cm) column of cation exchange resin. After the sample had passed through the column, it was rinsed with 200 ml of distilled water, and this rinse was added to the sample. The flow rate of the column was adjusted so that approximately 1 hour was required for passing the sample and rinse through the column. The resin was discarded after each sample.

ANION EXCHANGE ABSORPTION. The pH of the sample was adjusted to 7.0 by the dropwise addition of 50% NaOH solution and the sample was passed through a 15-ml (approximately 1.4 × 12 cm) column of anion exchange resin. The flow rate was adjusted so that approximately 1 hour was required for the 1.2-liter sample to pass through the column. The column was then rinsed with 100 ml of distilled water, and all column effluent was discarded.

ELUTION OF ANION EXCHANGE COLUMN. The NTA was stripped from the column with 1*M* NaCl in 0.1*M* NaOAc and 0.1*M* HOAc buffer of pH 4.7. The flow rate was adjusted to approximately 10 ml per minute and the first 10-ml fraction contained most of the distilled water from the free volume of the resin, so it was discarded. The next 10-ml fraction contained approximately half of the NTA and the next 50-ml fraction contained almost all of the rest of the NTA. The largest concentration factor was obtained by using the second 10-ml fraction for analysis. The anion exchange resin was discarded after each sample.

ISOTOPE DILUTION ANALYSIS. A small portion of the fraction of eluant (100 μl) was pipetted directly into a scintillation vial for counting. The recovery of NTA-^{14}C compared to the amount added in the "Initial Pretreatment" step was used to calculate the concentration factor.

POLAROGRAPHIC ANALYSIS. The rest of the eluant fraction was used for differential polarographic analysis (the eluant served as the supporting electrolyte solution). Three milliliters were pipetted into the sample and reference cells. Both sample and reference solutions were deaerated by bubbling nitrogen gas through the sample in the cells for 5 minutes. A potential of −0.70 volt *vs.* SCE was applied with the current sensitivity at 0.05 μA full scale. $In(NO_3)_3$ (0.001*M*) in 1*M* NaCl, 0.1*M* NaOAc, and 0.1*M* HOAc (pH 4.7) was added to the sample side of the cell with a 1-ml microburet. After each addition, nitrogen gas was bubbled through the solution for stirring [and removal of dissolved oxygen introduced *via* the In(III) solution] and then stopped. When a polarographic current of 0.005–0.02 μA indicated the presence of excess In(III), addition was stopped and the volume of In(III) solution added to the cell was noted. Note that for some sewage samples, it was necessary to finish "titrating" the sample with 0.01*M* $In(NO_3)_3$. A preliminary potential sweep was manually performed to determine the current sensitivity setting which resulted in the best recorder display. Then a cathodic polarographic sweep was performed from an initial potential of −0.10 volt *vs.* SCE and a polarogram was recorded.

The height of the excess In(III) wave was used as the base line to determine the height of the In(III)–NTA wave and the current was measured at the peak of the wave (Figure 2). It was necessary to correct the polarographic result for dilution by the volume of In(III) solution added. The current was correlated to the solution concentration of NTA as ppm Na_3NTA *via* a standard curve.

Analytical Procedure above 2.57 ppm. The "Initial Pretreatment" step was the same except that solutions of 100-ml volume were used and NTA-^{14}C was not added. All other steps until the "Polarographic Analysis" were deleted.

Materials and Equipment. Four types of waste water sample were used; Ohio River water was collected at Cincinnati and used without further treatment. Cincinnati municipal sewage (Gest Street Plant) was also used without further

(1) J. E. Thompson and J. Duthie, *J. Water Pollut. Contr. Fed.*, 40, Pt. 1, 306 (1968).
(2) R. D. Swisher, M. M. Crutchfield, and D. W. Caldwell, *Environ. Sci. Technol.*, 1, 820 (1967).
(3) W. Hoyle, I. P. Sanderson, and T. S. West, *J. Electroanal. Chem.*, 2, 166 (1961).

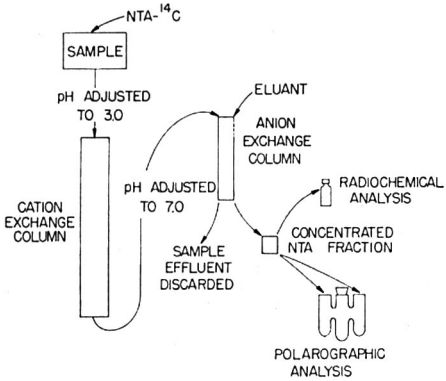


Figure 1. Schematic representation of complete analysis

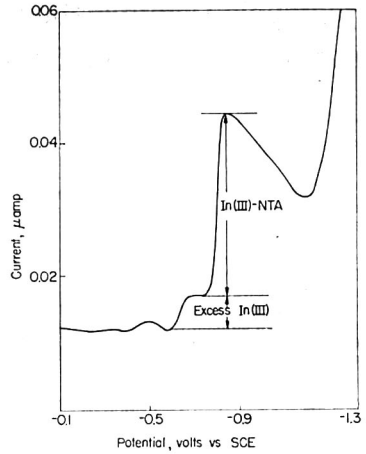


Figure 2. Activated sludge-treated synthetic sewage with 0.0257 ppm of NTA (plus 0.0257 ppm from NTA-^{14}C to give a total of 0.0514 ppm)

It was necessary to add approximately a 30-fold molar excess of In(III) to total NTA before an excess In(III) wave appeared

treatment. Synthetic sewage prepared from a glucose nutrient broth and dipotassium phosphate was treated under laboratory conditions by activated sludge (aerobic). Synthetic sewage with peptone, glucose, urea, disodium phosphate, sodium chloride, and beef extract was treated under laboratory conditions in sludge digesters (anaerobic).

Samples were suction filtered through two thicknesses of glass filter paper. The unlabeled NTA was Matheson Coleman and Bell reagent grade nitrilotriacetic acid and the NTA-^{14}C was an Amersham/Searle Corp. custom preparation with one carboxyl ^{14}C per molecule. Dowex 50 W-X8 (50–100 mesh) cation exchange resin in the hydrogen ion form was used throughout. Dowex 1-X8 (50–100 mesh) anion exchange resin was used for early experiments and Dowex 21 K (50–100 mesh) was used for later experiments including evaluation with waste water samples (both in the chloride ion form). Both cation exchange and anion exchange resins were prewashed with two cycles involving an HCl wash and distilled water rinse, then were rinsed to approximately neutral pH with water. In(III) solutions were prepared by dissolving a weighed quantity of American Smelting and Refining Co. 99.999% indium metal with dropwise additions of concentrated HNO_3 while heating on a steam bath. All other chemicals were reagent grade, and used without further purification. Radioanalytical determinations of NTA-^{14}C were performed with a Packard Tri-Carb Model 3375 liquid scintillation spectrometer. The differential Polarograph (*4*) was a simple one and was programmed on a versatile electrochemical instrument. Details are not given here since a wide variety of commercial electrochemical instruments are available (*5*).

DISCUSSION

Sample collection and storage were not investigated, but if the NTA-^{14}C were added to unfiltered sample at the time of collection, loss of unknown NTA during sample storage would be automatically corrected for if it was in equilibrium with the NTA-^{14}C added.

Ion Exchange of NTA Samples. CATION EXCHANGE REMOVAL OF CATIONS. The pH of samples was adjusted to 3.0 in the initial pretreatment step so that the ionic strength introduced was not appreciable while the pH was low enough to facilitate the displacement of metal ions from NTA complexes (high ionic strength could interfere with the absorption of NTA during the later anion exchange step). The hydrogen ions liberated from the column when the metal ions were absorbed lowered the pH further, with no increase in the ionic strength (after cation exchange treatment, the pH of most samples was in the range of 1.5 to 2.5). The effectiveness of the cation exchange step in removing metal ions was not determined with actual samples but Zn(II) and Mg(II) in the presence of NTA were reduced by a factor of 10^5 in distilled water.

ANION EXCHANGE ABSORPTION OF NTA. Figure 3 illustrates the absorption of NTA-^{14}C onto Dowex 1-X8 resin. NTA is a divalent anion in the pH range of 5–8 (*6*) and a pH of 7.0 was selected for most experiments, but absorption was efficient in the pH range of 5–11. The NTA was taken up by the first part of the resin in spite of the fact that 1 liter of sample was passed through the column in each case.

The optimum size of anion exchange column was not determined during this work. Smaller volumes of resin in the anion exchange column required less eluant to elute the NTA and resulted in higher concentrations of NTA (note that this consideration did not apply to the cation exchange pretreatment step).

ELUTION OF NTA. Figure 4 shows the elution behavior of NTA with sewage samples. Some variability in the elution of NTA from different types of samples was evident from these studies. One of the reasons for selecting anion exchange as a method of concentrating NTA was to have the possibility of a chromatographic elution to separate interferences (*7*). No

(4) L. Meites, "Polarographic Techniques," 2nd ed., Interscience Publishers, New York, N. Y., 1965, p 573.
(5) G. W. Ewing, *J. Chem. Educ.*, **46**, A717 (1969).
(6) "Stability Constants of Metal-Ion Complexes," L. G. Sillen and A. E. Martell, Ed., Chem. Soc. (London), Spec. Publ. No. 17, 1964.
(7) C. Davies, R. D. Hartley, and G. J. Lawson, *J. Chromatogr.*, **18**, 47 (1965).

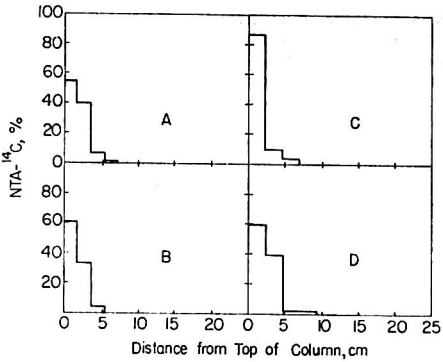


Figure 3. Absorption of NTA onto Dowex 1-X8

A. 25.7 ppm of Na_3NTA in distilled water at pH 11.0; 0.1% of sample in column effluent

B. 25.7 ppm Na_3NTA with 10-fold molar excess of Pb(II) in distilled water at pH 5.0; 0.9% of sample in column effluent; absorption was as a Pb(II) complex

C. 25.7 ppm Na_3NTA in tap water with 7 grain hardness at pH 7.0; pretreated with Dowex 50 W-X8; 0.7% of sample in column effluent

D. 0.257 ppm NTA under same conditions as *C.* above; $\leq$ 3% of sample in column effluent (limit of detection of available NTA-^{14}C)

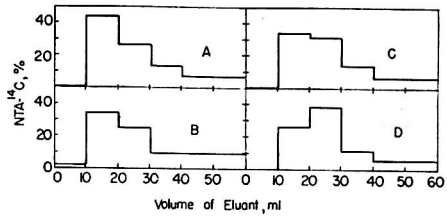


Figure 4. Elution of NTA from Dowex 21 K with 1*M* NaCl, 0.1*M* HOAc, and 0.1*M* NaOAc (pH 4.7)

A. 0.0257 ppm of Na_3NTA in distilled water; 89% recovery in 60 ml of eluant

B. 0.283 ppm of Na_3NTA in untreated municipal sewage; 79% recovery in 60 ml of eluant

C. 0.283 ppm Na_3NTA in activated sludge treated synthetic sewage; 86% recovery in 60 ml of eluant

D. 0.283 ppm Na_3NTA in sludge digester treated synthetic sewage; 87% recovery in 60 ml of eluant

Table I. Average Recovery of NTA-^{14}C during Evaluation

Fraction, No., ml	Recovery, %	RSD, %
2, 10	46	12
3, 50	47	15
2 + 3, 60	93	7

evidence of interference during the polarographic analysis step was found in this study so the practice of using a high concentration of salt to strip the NTA (and presumably other materials) from the column was used. It was found that concentrations of NaCl of 1*M* (and greater) eluted the NTA as soon as the free volume of the resin was displaced. NTA was efficiently stripped from Dowex 21 K resin in this way even when the resin was visibly darkened from material in sewage samples.

Table I is a summary of recoveries observed during an evaluation of the analysis. The first 10-ml fraction contained very little NTA-^{14}C. An average concentration factor of 47 resulted from the second 10-ml fraction and an average concentration factor of 15.5 resulted from a total volume of 60 ml of eluant (not including the first 10-ml fraction). Note that the relative standard deviation (RSD) of the concentration factor in the 60-ml fraction was only 7% while that of the 10-ml fraction was 12%. If it was established in practice that the reproducibility of recovery of a particular fraction was well within the experimental error of the whole procedure, then it would be possible to discontinue the isotope dilution step.

Polarographic Analysis of NTA as In(III)–NTA. Other metal cations were investigated for the polarographic analysis of NTA but In(III) gave the best results during preliminary studies on sewage samples. Without regard for the actual species involved in the equilibrium system and the reduction reactions, they may be represented as follows:

$$In(III) + NTA \rightleftharpoons In(III)-NTA$$

$$\text{Excess } In(III) + 3e^- \rightarrow In(0) \qquad -0.61 \text{ volt } vs. \text{ SCE}$$

$$In(III)\text{–}NTA + 3e^- \rightarrow In(0) + NTA \qquad -0.79 \text{ volt } vs. \text{ SCE}$$

The polarographic wave from excess In(III) in 0.1*M* acetic acid and 0.1*M* sodium acetate (pH 4.7) exhibited a half-wave potential of −0.61 volt *vs.* SCE. The In(III)–NTA reduction wave was well separated from the excess In(III) wave and exhibited an unusual peak shape (*8*). The half-wave potential was found to be −0.79 volt *vs.* SCE and the peak potential was −0.85 volt in the acetate buffer. Apparently the reduction was quasi-reversible and the electroactive species was In(III) $HNTA^+$ (*9*). Polarographic studies of other In(III) complexes which exhibited peak shaped waves have been reported in the literature (*10, 11*). In practice, the peak shape of the waves increased the selectivity of the determination because the peak represented an excellent reference point at which to make the current measurement. Standard curves based on the peak current were linear in appearance but the ratio of the peak current to the NTA concentration changed slightly with the NTA concentration.

The conversion of the NTA to the In(III) complex was an extension of a technique which has already been described (*3*). It was controlled by controlling the amount of excess In(III) in equilibrium with the complex. This was done by adding In(III) to the sample cell until the current at −0.70 volt *vs.* SCE indicated the presence of approximately the same amount of excess In(III) for both calibration standards and unknown samples. Figure 5 illustrates the relatively small effect of the amount of excess In(III) on the reduction current for In(III)–NTA. The horizontal axis represents the excess In(III). The vertical axis represents the magnitude of the reduction current of the In(III)–NTA complex compared to the current when the magnitude of the In(III) wave was in the range used as standard conditions for analyses (0.005–0.02 μA). The points representing standard conditions for each concentration

(8) J. Koryta and I. Kössler, *Collection Czech. Chem. Commun.*, 15, 241 (1950).
(9) R. Staroscik and K. Webs, *Chem. Anal.* (*Warsaw*), 12, 1275 (1967).
(10) A. J. Engel *et al.*, ANAL. CHEM., 37, 203 (1965).
(11) L. Pospisil and R. DeLevie, *J. Electroanal. Chem.*, 25, 245 (1970).

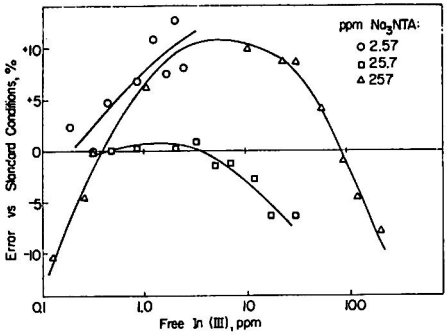


Figure 5. Effect of excess In(III) on height of In(III)–NTA wave

are the symbols centered on the 0% error line. The height of the In(III)–NTA wave was within ±10% of standard conditions for a large range of excess In(III) (0.4 to 100% with 257 ppm Na_3NTA). This was probably due to competing equilibrium and kinetic (*12*) effects.

The relative standard deviation of standards was approximately 5% (with and without temperature control of the cell). The lower limit of NTA which could be measured above background currents (including the current from the excess In(III) wave) was about 0.3 ppm when anion exchange concentration was not used and the measurement was made with a differential polarograph.

INTERFERENCE STUDIES. No evidence of interference was detected in distilled water solutions with a tenfold molar ratio of ethylenediaminetetraacetate (EDTA), ethane-1-hydroxy-1, 1-diphosphonate (EHDP), citrate, maleate, phosphate, carbonate or sulfate to 2.57 ppm Na_3NTA. A solution containing EHDP and EDTA, each with a tenfold molar ratio to NTA resulted in no interference as was also the case for a solution containing all of these compounds, each with a tenfold molar ratio to NTA. Although it was often necessary to add much more In(III) than was necessary for the NTA alone, before excess In(III) was detected, the polarograms were not affected and the analytical results were within experimental error of being the same in these studies.

Anomalous results were observed when In(III) was added to a distilled water sample which had been treated with a particular batch of Dowex 21 K resin. The resin had been left in contact with concentrated HCl for 5 hours during pretreatment. When the resin was retreated with 1*M* HCl in contact with the resin for a short time, normal results were obtained. Benzyltrimethylammonium chloride was added to NTA in distilled water to represent a possible decomposition product of Dowex 21 K resin, but the anomalous results were not reproduced. The wave shapes for the free In(III) and In(III)–NTA were normal but the height of the In(III)–NTA wave was decreased 29% when 200 ppm of benzyltrimethylammonium chloride was present and 41% when 400 ppm was present. In practice, materials of this type which might occur in samples should be efficiently removed during cation exchange treatment.

The polarographic reduction of In(III)–NTA did not appear to be particularly sensitive to interference by surfactants. Linear alkyl benzene sulfonate concentrations of 3.5 and 43.5 ppm did not affect polarograms and an analysis for NTA in a sample of a commercial detergent formulation dissolved in electrolyte solution gave a value which was within experimental error of the expected result.

EVALUATION. The experiments summarized in Tables II and III were performed to evaluate the best set of conditions which evolved from this work. One-liter portions of a river water sample, a laboratory activated sludge treated sewage sample, a raw municipal sewage sample, and a laboratory sludge digester-treated sample were carried through the complete procedure with 0.0257, 0.257, and 2.57 ppm of unlabeled NTA added. The second 10-ml fraction of the anion exchange eluant and a third 50-ml fraction were analyzed. The

(12) C. Auerbach, ANAL. CHEM., 30, 1723 (1958).

Table II. Evaluation with Anion Exchange Concentration

Sample	NTA added, ppm Na_3NTA	Analysis of Fractions: Fraction, No., ml	NTA-^{14}C, %	Total NTA, ppm Na_3NTA	NTA found, ppm Na_3NTA	Error, %
River water	0.0257	2, 10	47	2.38	0.0249	−3
	0.0257	3, 50	61	0.395	0.0072	−72
	0.257	2, 10	56	14.5	0.233	−9
	0.257	3, 50	41	1.98	0.216	−16
	2.57	2, 10[a]	44	11.2	2.52	−2
	2.57	3, 50	55	26.2	2.35	−9
Activated sludge effluent	0.0257	2, 10	46	2.02	0.0182	−29
	0.0257	3, 50	45	0.452	0.0245	−5
	0.257	2, 10	51	12.3	0.215	−16
	0.257	3, 50	45	2.35	0.235	−9
	2.57	2, 10[a]	52	12.6	2.39	−7
	2.57	3, 50[a]	42	2.10	2.47	−4
Raw sewage	0.0257	2, 10	36	1.45	0.0146	−43
	0.0257	3, 50	52	0.585	0.0305	+19
	0.257	2, 10[a]	38	1.05	0.250	−3
	0.257	3, 50	51	2.48	0.217	−16
	2.57	2, 10[a]	44	11.8	2.68	+4
	2.57	3, 50[a]	50	2.53	2.50	−3

[a] Fraction diluted 10-fold before polarographic analysis.

Table III. Evaluation without Anion Exchange Concentration

Sample	NTA added, ppm Na_3NTA	NTA found, ppm Na_3NTA	Error, %
River water	2.57	2.49	−3
	25.7	25.9	+1
	257	239	−7
Activated sludge effluent	2.57	2.55	−1
	25.7	25.3	−2
	257	229	−11
Raw sewage	2.57[a]	2.29	−11
	25.7[b]	25.2	−2
	257[b]	252	−2
Digester effluent	2.57	2.64	+3
	25.7[b]	31.2	+21
	257[b]	267	+4

Sample diluted 5-fold[a] or 10-fold[b] before polarographic analysis.

accuracy of the analytical results for the two fractions was approximately the same. The relative standard deviation of averaged results was 42, 6, and 5%, respectively, for 0.0257, 0.257, and 2.57 ppm Na_3NTA. The analytical results for the digester sample were high but when the NTA added to the samples was subtracted out, a relatively constant blank of 4.0 ppm (13% RSD) was observed. Although contamination was not expected, it was considered more likely that this sample had become contaminated with NTA than that an interference had been encountered. Analytical data from the digester effluent sample were not included in the results on Table II. The results of a second series of the same type of samples (collected at a different time) with 2.57, 25.7, and 257 ppm NTA added are presented in Table III. No NTA-^{14}C was added and all ion exchange steps were deleted. The relative standard deviation of averaged results was 6, 11, and 7%, respectively, for 2.57, 25.7, and 257 ppm Na_3NTA. The results indicate that In(III) has the ability to displace NTA from other metal ions naturally present in these types of samples without the necessity of cation exchange pretreatment. In this series of experiments, the digester sample did not give anomalously high results and analytical data from the digester sample were included with the other types in Table III. In both series of experiments, a precipitate sometimes appeared upon addition of In(III) solution to the sample in the polarographic cell. In order to obtain normal polarographic results, it was then necessary to dilute the sample with electrolyte solution sufficiently that precipitation did not occur.

The polarographic residual current was higher than normal at negative potentials with sewage samples and this effect decreased the negative potential range for reductions at a DME but did not interfere with the reduction of the In(III)–NTA complex (see Figure 2). The analytical results at the 0.0257-ppm level were marginal but the results at the 0.257-ppm level and greater were much better. The NTA-^{14}C added for isotope dilution data was 0.0257 ppm (1 mCi/g specific activity) for all of the results with anion exchange concentration. At the 0.0257-ppm level of unlabeled NTA, the presence of the NTA-^{14}C had the effect of doubling the error in determining the concentration of the unlabeled NTA (which would correspond to the unknown amount in an actual analysis). The use of a smaller amount of a "hotter" sample of NTA-^{14}C would be expected to improve analysis at that level considerably.

Before the excess In(III) wave appeared, it was often necessary to add considerably more In(III) than was necessary to complex the NTA in the representative samples (see Figure 2 caption). Apparently there were large quantities of material in these samples which formed complexes with In(III) which were not polarographically active in the electrolyte used. As long as excess In(III) was present, the presence of polarographically inactive In(III) complexes did not seem to affect the reduction of the In(III)–NTA complex.

For these studies, differential polarography was used as a more sensitive method than dc polarography. Differential polarography also had the advantage of subtracting out residual currents which might be encountered. In practice, there was no evidence of interfering residual currents in samples and there was no evidence that single-cell polarographic techniques could not be used. There was evidence that organic material in sewage samples interfered with the use of stationary mercury drop electrodes and that techniques employing dropping mercury electrodes were to be preferred.

There was no evidence that NTA was lost during the cation exchange step for these studies but large losses were encountered during further development of the method for septic tank samples and the cation exchange step was deleted (*13*). The suggestion was made that better recovery might be obtained with the cation exchange resin in the sodium ion form. The "Initial Pretreatment" step was also discontinued for septic tank samples.

ACKNOWLEDGMENT

The assistance of D. F. Kuemmel and T. R. Williams is gratefully acknowledged.

RECEIVED for review July 30, 1970. Accepted September 28, 1970.

(13) J. E. Thompson, Sanitary Engineering Research Laboratory, Procter & Gamble Co., Cincinnati, Ohio, personal communication, 1970.

Selectivity in Liquid–Liquid Chromatography

D. E. Martire

Department of Chemistry, Georgetown University, Washington, D. C. 20007

D. C. Locke

Department of Chemistry, Queens College of the City University of New York, Flushing, N. Y. 11367

The thermodynamic basis for selectivity in liquid–liquid chromatography is considered in terms of a new approach to solution free energies. The treatment applies to closely-related and difficultly separable molecules, such as isomers. Both athermal (size) and thermal (energy) factors contribute to the relative retention. The results are expressed quite simply in terms of the molar volumes of the solvents and the pair of solutes to be separated, the solvent solubility parameters, and the fractional difference between the solute critical temperatures. LLC solvent systems designed to separate polar molecules inherently offer the greatest selectivity. Reasonably good agreement with experiment is found for a selective LLC system used to separate aromatic hydrocarbons. The fundamental approach taken is shown to be superior to one using conventional regular solution theory.

THE ABILITY of any chromatographic technique to perform separations depends upon both the selectivity and efficiency of the chromatographic system. The former is expressed in terms of the relative retention, α, of the pair of components to be separated, while the efficiency is measured by the number of theoretical plates, N (or plate height H) generated in the chromatographic column by the solutes.

While both are important, achievement of large relative retention values is fundamentally more critical. The very nature of chromatographic systems generally ensures respectable column efficiencies, if reasonable care is taken in constructing and operating the column. Further, any resolution equation shows that resolution, the degree of separation of two peaks, increases directly with $(\alpha - 1)$ but only with $N^{1/2}$. Finally, in practical systems, optimum column efficiency is usually sacrificed for shorter analysis times.

Broadly, plate height depends on operating conditions such as eluent flow rate, packing particle size, stationary phase loading, and so forth—in short, on the dynamics of the system. Relative retention, on the other hand, is an equilibrium property of a specific system, independent of all its extensive properties. Basically, to increase α, it is necessary to change at least one of the chromatographic phases so as to improve the selectivity of the system for one of the solutes of interest.

To this end, we consider the selection and design of the stationary and mobile phases in liquid–liquid chromatography (LLC), in particular as applied to the separation of closely-related molecules such as isomers. Existing solution theories provide an adequate basis for formulating certain principles of selectivity. The results developed apply equally to LLC and to solvent extraction.

Selectivity in GLC has been the subject of recent work (*1–4*) whereas this is the first formulation for LLC as well as the first application of a very recent theoretical development (*5*) to chromatographic separations.

THEORY

Previously, we showed (*6*) that at moderate column pressures, the LLC solute specific retention volume, V_g, is

$$V_g = \frac{\gamma_2^m M_m}{\gamma_2^s M_s \rho_m} \tag{1}$$

where γ_2^m and γ_2^s are, respectively, the infinite dilution solute activity coefficients in the mobile and stationary phases which have molecular weights M_m and M_s; ρ_m is the eluent density at the column temperature. In this paper, all activity coefficients refer to their values at infinite dilution.

The relative retention α of two solutes a and b is

$$\alpha = \frac{(V_g)_a}{(V_g)_b} = \frac{\gamma_a^m \gamma_b^s}{\gamma_b^m \gamma_a^s} \tag{2}$$

Understanding and prediction of selectivity of chromatographic solvent pairs is thus a problem in solution thermodynamics, *i.e.*, the prediction of relative solute activity coefficient values from pure solute and solvent properties.

We are on good grounds for assuming the following additivity (*7–9*):

$$\ln \gamma_2 = \ln \gamma_2^{th} + \ln \gamma_2^{ath} \tag{3}$$

where γ_2^{ath} is the configurational or athermal contribution to the activity coefficient arising from size differences between solute and solvent molecules, and γ_2^{th} is the thermal component which accounts for intermolecular forces between solute and solvent molecules. Whereas the former is strictly an entropic term, $\ln \gamma_2^{th}$ comprises both enthalpic and entropic contributions to solution non-ideality (*9*).

Proceeding, we use the usual Flory–Huggins expression (*8–11*) for the athermal part of the activity coefficient, where

$$\ln \gamma_2^{ath} = \ln (1/r) + [1 - (1/r)] \tag{4}$$

we approximate r as the ratio of molar volumes of solvent (component 1) to solute (component 2), $r = v_1^0/v_2^0$.

The recent theoretical treatment of Luckhurst and Martire (*5*) provides an expression for the thermal contribution. These authors relate γ_2^{th} for some solute 2 of interest to that of a reference solute 2′ in the same solvent under the

(1) P. T. Funke, E. R. Malinowski, D. E. Martire, and L. Z. Pollara, *Separ. Sci.*, **1**, 661 (1966).
(2) S. H. Langer, ANAL. CHEM., **39**, 524 (1967).
(3) L. Rohrschneider, *J. Gas Chromatogr.*, **6**, 5 (1968).
(4) S. H. Langer and R. J. Sheehan, in "Progress in Gas Chromatography," J. H. Purnell, Ed., Interscience, New York, N. Y., 1968, p 289.
(5) G. R. Luckhurst and D. E. Martire, *Trans. Faraday Soc.*, **65**, 1248 (1968).
(6) D. C. Locke and D. E. Martire, ANAL. CHEM., **39**, 921 (1967).
(7) A. J. Ashworth and D. H. Everett, *Trans. Faraday Soc.*, **56**, 1609 (1960).
(8) D. E. Martire, in "Gas Chromatography," L. Fowler, Ed., Academic Press, New York, N. Y., 1963. p 33.
(9) D. E. Martire, in "Gas Chromatography 1966," A. B. Littlewood, Ed., Elsevier, Amsterdam, 1967, p 21.
(10) P. J. Flory, *J. Chem. Phys.*, **10**, 51 (1942).
(11) M. L. Huggins, *Ann. N. Y. Acad. Sci.*, **43**, 1 (1942).

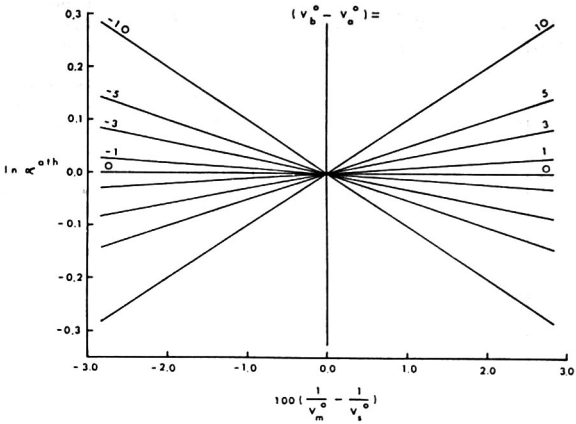


Figure 1. Athermal contribution to relative retention, with $(v_b^\circ - v_b^\circ)$ as a parameter. $\alpha = (V_g)_a/(V_g)_b$

same conditions, by

$$\ln \gamma_{2'}^{th} = \ln \gamma_{2'}^{th} + \frac{v_{2'}^0}{RT}\left[\frac{E_1}{v_1^0} - \frac{E_{2'}}{v_{2'}^0}\right]\left[\frac{T_2^*}{T_{2'}^*} - 1\right] \quad (5)$$

where (E_1/v_1^0) and $(E_{2'}/v_{2'}^0)$ are the cohesive energy densities of the solvent and reference solute, respectively, v_1^0 and $v_{2'}^0$ are their molar volumes, and T_2^* and $T_{2'}^*$ are the critical temperatures (K) of the solute and reference solute, respectively. The reference solute is selected to be closely related in solution behavior to the solute of interest. Now

$$\frac{E_i}{v_i^0} = -\frac{\Delta E_i^v}{v_i^0} = -\frac{(\Delta H_i^v - RT)}{v_i^0} \quad (6)$$

where ΔE_i^v and ΔH_i^v are the molar energy and enthalpy of vaporization of component i. Hildebrand (*12*, *13*), of course, identified $(\Delta E_i^v/v_i^0)^{1/2}$ with the solubility parameter δ_i (see Appendix 1).

Clearly, on this basis we can write Equation 2 as

$$\ln \alpha = (\ln \alpha)^{ath} + (\ln \alpha)^{th} \quad (7)$$

where the activity coefficient contributions to α have been divided into athermal and thermal contributions.

Athermal Contribution to Relative Retention. From Equations 2–4,

$$(\ln \alpha)^{ath} = \ln (\gamma_a^m/\gamma_b^m)^{ath} - \ln (\gamma_a^s/\gamma_b^s)^{ath} = (v_b^0 - v_a^0)\left(\frac{1}{v_m^0} - \frac{1}{v_s^0}\right) \quad (8)$$

Thus the more divergent the values are for the pairs of solvents $(v_m^0$ and $v_s^0)$ and solutes $(v_a^0$ and $v_b^0)$, the greater α will be, especially for small v_m^0 or v_s^0. Experimentally, the eluent in LLC is commonly composed of smaller molecules than is the stationary phase. Energetically identical isomeric solutes are clearly separable by LLC if the molar volumes (densities) are sufficiently different; no selective solute–solvent interactions are required. In this case, the smaller solute is preferentially dissolved in the phase with the larger v^0 because of its larger positive excess entropy of solution (*7–9*). For example, if two isomers a and b of $M = 200$ have respective densities of 1.025 and 1.000, then $(v_b^0 - v_a^0) = 5$ cc/mole; if $v_m^0 = 50$ cc/mole and $v_s^0 = 500$ cc/mole, then $(\ln \alpha)^{ath} = 0.09$, or $\alpha = 1.1$, which corresponds to a straightforward separation requiring roughly only 4300 effective plates for a base-line separation.

In Figure 1, the dependence of $(\ln \alpha)^{ath}$ on $(1/v_m^0 - 1/v_s^0)$ is illustrated for various $(v_b^0 - v_a^0)$. Large separation factors are attainable on the basis of this size effect alone. The athermal contribution to α is readily estimated from the densities and molecular weights of the solutes and solvents.

Thermal Contribution to Relative Retention. From Equation 5, substituting Hildebrand solubility parameters for cohesive energy densities,

$$(\ln \alpha)^{th} = (\ln \gamma_a^m/\gamma_b^m)^{th} - (\ln \gamma_a^s/\gamma_b^s)^{th} = \frac{v_{2'}^0}{RT}(\delta_s^2 - \delta_m^2)\left(\frac{T_a^* - T_b^*}{T_{2'}^*}\right) \quad (9)$$

Since we are restricting attention to energetically closely-related solutes (a and b) which are also both closely related to the reference solute (2′), we can write the following approximate equations,

$$v_{2'}^0 = v_a^0 \qquad T_{2'}^* = T_a^* \quad (10)$$

where we could as easily have equated 2′ and b. Thus

$$(\ln \alpha)^{th} = \frac{v_a^0}{RT}(\delta_s^2 - \delta_m^2)\left(\frac{T_a^* - T_b^*}{T_a^*}\right) \quad (11)$$

where we define $(T_a^* - T_b^*)/T_a^* \equiv f(T^*)$ as the fractional difference between the critical temperatures of pure solutes a and b.

Separation is clearly favored by large differences in the cohesive energy densities of the chromatographic solvents, which must in any event be the case if the two phases are to be immiscible (*12*, *13*). For any given solvent pair, this contribution to resolution of two solutes depends only on the product $v_a^0 f(T^*)$; one criterion of separability in LLC is, on this basis, unequal critical temperatures. Sources of data on critical temperatures and solubility parameters are given in Appendix 1.

(12) J. H. Hildebrand and R. L. Scott, "Regular Solutions," Prentice-Hall, Englewood Cliffs, N. J., 1962.
(13) J. H. Hildebrand and R. L. Scott, "Solubility of Nonelectrolytes," 3rd ed., Reinhold, New York, N. Y., 1950.

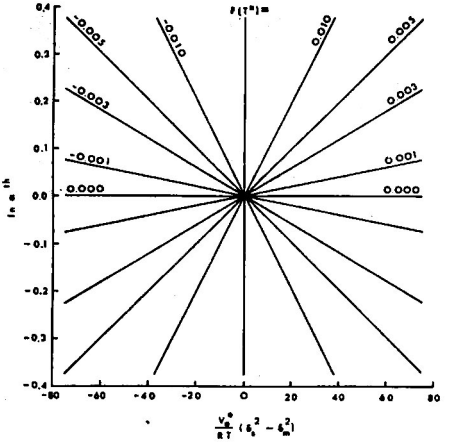


Figure 2. Thermal contribution to relative retention, with $f(T^*)$ as a parameter. $\alpha = (V_a)_a/(V_a)_b$

The behavior predicted by Equation 11 is entirely reasonable. Luckhurst and Martire (*5*) selected T_i^* as a macroscopic measure of the magnitude of the pairwise potential energy of interaction between two molecules of type *i*. Thus the solute molecules of the larger interaction profile (as measured by T^*) will tend to interact more strongly with the solvent of the large interaction profile (measured by δ_i^2); as they say in the old country, "Like dissolves like." If the solvent is the chromatographic stationary phase, this solute will be preferentially retained, and if it is the eluent, the solute will be preferentially eluted. The absence of an explicit solute–solvent interaction term results from the use of a reference solute and the geometric mean assumption for 1–2 interactions.

Equation 11 might be illustrated with a numerical example. If $f(T^*) = 0.01$, $v_a^0/RT = 0.2$ cc/cal, and $(\delta_a^2 - \delta_m^2) = 50$ cal/cc, then $(\ln \alpha)^{ab} = 0.10$, and $\alpha^{ab} = 1.1$, which again is entirely sufficient for the base-line separation of the two equally-sized solute molecules *a* and *b*. The sensitivity of $(\ln \alpha)^{ab}$ to changes in $f(T^*)$ is shown in Figure 2. The ranges of values given in the plot are realistic for practical LLC systems for difficult separations.

DISCUSSION

The validity of the foregoing depends upon the strict applicability of the basic theory (*5*) to these LLC systems. We will consider first the assumptions involved and then compare relative retentions calculated from the theory with experimental values.

First, the reference solute must be chosen such as to have nearly the same strength and nature of interaction with the solvent as the solute of interest. In LLC, of course, this condition must apply to both solvent phases. In other words, our theory applies only to very similar—and difficult to separate—pairs of solutes. A simple means of checking the validity of this assumption is to compare values of v_b^0/T_b^* and v_a^0/T_a^*. This is so because we have arbitrarily identified the reference solute with one of the pair of interest.

The second, and more important, assumption, is that the form of the pairwise intermolecular potential function is the same for both solute–solute and solute–solvent interactions, for identical configurations. If the potential functions above have the same forms, it is reasonable to expect adherence to the geometric mean combining rule for the intermolecular potential functions (*5*). It is this assumption which fundamentally allows the use of the reference solute. In addition, the proportionality between the depth of the potential well and the solute critical temperature can in this case justifiably be used. These two considerations lead to the remarkably simple form of Equation 5 and thus of Equation 11. In LLC, because the two phase solvents must be more or less immiscible, there will generally be different degrees of interaction of the solutes with the two phases. The LLC stationary phase is usually selected to be a "better" solvent for the "average" solute in a mixture than is the mobile phase; this tends in practice to allow the solvent system to differentiate between solutes and produce separations. Consequently, the above assumption may ordinarily hold for one of the phases, but at best less rigorously for both.

We can thus expect agreement of theory with experiment, and also the power of reasonable prediction, for systems in which the distribution coefficients are close to unity. We can also expect the theory to hold where moderately specific interactions exist (see below). In these systems, which are of interest because of their selectivity, one phase interacts or reacts selectively with at least some of the solutes. Here, the second phase is usually a "neutral" solvent for the solutes, possessing the proper solvency to provide reasonable retention volume values. In the example given below, the solutes are aromatic hydrocarbons, the interacting phase is acetonitrile, and the neutral stationary phase is squalane.

Since we are concerned here with selectivity, those systems in which solute–solvent interactions are much weaker than solvent–solvent interactions, or vice versa, need not be considered. An example is given below of the inappropriateness of our theory to such systems. Here, the actual interaction energy would be less than that predicted by the geometric mean rule. At both extremes, then, the theory breaks down. The geometric mean rule does not apply where the solute–solvent interactions are either rather weak or rather strong. In Appendix 2, we consider a modified geometric mean rule.

Finally, to arrive at Equation 8, we have assumed that it is permissible to replace the solute infinite dilution partial molar volume in solution with its molar volume in the pure liquid state. This is justified both because the volume changes on mixing will probably be quite similar for both solutes of interest, and thus introduce only a small error, and additionally because few excess volumes of mixing data exist nor can they be reliably calculated.

Let us now illustrate these considerations with an example. One of the authors (*14*) has published LLC retention data for hydrocarbon solutes using acetonitrile eluent and squalane stationary phase. Tables I and II give the data, and calculated and experimental values of α for the xylenes and diethylbenzenes. While the quantitative agreement of the two sets of α values is hardly perfect, there is uncertainty in the experimental data, and more important, the solute selected as the reference compound may not in all cases be suitable. If values of $(v_a^0/T_a^*)(T_b^*/v_b^0)$ are calculated and ranked in order of magnitude (the values range from 1.004 for *p*/*m*-xylene to 1.046 for *p*/*o*-xylene), the order is nearly the same as the order of increasing percentage deviation of

(14) D. C. Locke, *J. Chromatogr.*, 35, 24 (1968).

Table I. Physical Properties and Chromatographic Data for the System Aromatic Hydrocarbons/Acetonitrile/Squalane

Compound	δ^2, cal/cc	v^0, cc/mol[c]	T^* (K)[d]	V_g, cc/g[f]	K[f]
Acetonitrile	140[a]	52.8	...	...	...
Squalane	66[b]	524	...	...	...
o-Xylene	9.00[e]	121.2	630.3	1.00	0.806
m-Xylene	8.80[e]	123.7	617.0	1.08	0.871
p-Xylene	8.80[e]	124.0	616.2	1.10	0.887
o-Diethylbenzene	...	153.2	662.8	1.71	1.380
m-Diethylbenzene	...	156.2	657.1	1.81	1.460
p-Diethylbenzene	...	156.4	660.5	1.78	1.435

[a] Reference (*15*).
[b] Reference (*16*).
[c] Calculated from data in references (*14*) (acetonitrile), (*16*) (squalane), and (*17*) (hydrocarbons).
[d] References (*18*) (xylenes) and (*17*) (diethylbenzenes).
[e] Reference (*17*).
[f] Reference (*14*).

Table II. Calculated and Experimental Relative Retentions in the Acetonitrile/Squalane System

Solute pair[a]	ln α^{th}	ln α^{th}	α^{calcd}[b]	α^{exptle}
p/*o*-Xylene	−0.049	0.354	1.36	1.10
p/*m*-Xylene	−0.009	0.021	1.01	1.01
m/*o*-Xylene	−0.040	0.333	1.34	1.08
p/*o*-Diethylbenzene	−0.055	0.068	1.01	1.04
p/*m*-Diethylbenzene	−0.003	−0.100	0.902	0.983
m/*o*-Diethylbenzene	−0.051	0.169	1.13	1.06

[a] First-named solute corresponds to solute *a*, second to solute *b*.
[b] $\alpha = (V_g)_a/(V_g)_b$.
[c] Reference (*14*).

the experimental and calculated α values (which range from 0.1% for *p*/*m*-xylene to 21% for *p*/*o*-xylene). The discrepancy is thus mainly attributable to the dissimilarity between the solute of interest and the "reference" solute. Nonetheless, in all cases the correct order of elution is predicted; as expected for specific solute-solvent interactions, the solute interacting more strongly with the acetonitrile has the higher critical temperature. It is interesting that the athermal contribution counteracts the thermal separation. In the case of *p*/*o*-diethylbenzene, the athermal contribution nearly reverses the elution order expected on the basis of molecular interactions between the solutes and acetonitrile.

For comparison, we have calculated α values from the expression for α^{th} based solely on solubility parameter theory (*12*, *13*) as discussed in Appendix 1. The values obtained are *p*/*o*-xylene, 1.44; *p*/*m*-xylene, 1.07; and *m*/*o*-xylene, 1.35; these are all in much poorer agreement with the experimental α values than those based on our α^{th}.

It was suggested above that the theory is inapplicable to systems in which stronger solvent-solvent than solute-solvent interactions occur. Substantiation of this conclusion is readily made using data from the same system (*14*) for saturated hydrocarbon solutes. Table III gives a few of

Table III. Physical Properties, Chromatographic Data, Calculated and Experimental Relative Retentions for Paraffins in the Acetonitrile/Squalane System

Solute	v^0, cc/mol[a]	T^* (K)[b]	V_g, cc/g[c]	α^{exptle}	α^{calcd}
n-Pentane	116.1	469.6	4.32		
				1.05	0.201
2-Methylbutane	117.5	460.4	4.12		
2,3-Dimethylbutane	131.1	499.9	5.15		
				1.15	0.198
2,2-Dimethylbutane	133.8	488.7	4.48		
2-Methylpentane	133.0	504.4	5.54		
				1.02	0.208
3-Methylpentane	130.8	497.5	5.44		

[a] Calculated from data in reference (*18*).
[b] Reference (*18*).
[c] Reference (*14*).
[d] See text.

these results, which are clearly meaningless. For paraffins, the order of elution is no longer the order of decreasing critical temperature, which reflects the fact that paraffins do not enter into specific interactions with acetonitrile and indeed cannot compete effectively with other acetonitrile molecules; they are "rejected" from solution. This is reflected in the magnitude of the activity coefficients in acetonitrile (*14*). There is no satisfactory theory for such systems.

For paraffins of higher molecular weight, interfacial adsorption effects (*14*) preclude even calculation of meaningful and reproducible α values from the experimental retention volumes. Obviously, of course, the actual selectivity of the systems—the observed magnitude of the relative retention—is what is ultimately important, and may in fact be enhanced in some particular systems where adsorption effects, low solubilities, etc., exist.

As shown by the above calculations, the thermal contribution to α is usually more important than the athermal part. The latter can assist or impede separation. Previously (*6*) we showed that, with all else equal, maximum analysis speed is realized in systems with high molecular weight stationary phases and low molecular weight eluents. As we indicated there and have demonstrated here from the point of view of relative retention, the more important consideration is the effect of the athermal part of α on the separation achievable.

In any case, according to Equations 8 and 11, the LLC solvent pair can be characterized by $\left(\frac{1}{v_m^0} - \frac{1}{v_s^0}\right)$ and by $(\delta_s^2 - \delta_m^2)$. Where the stationary phase is less "polar" than the eluent, as would be used for the separation of non-polar or slightly polar solutes, the elution order is that of increasing molecular weight, *i.e.*, $v_a^0 > v_b^0$. Thus when the eluent is smaller than the stationary phase, as is usually the case, α^{ath} is a negative contribution to the overall relative retention. Furthermore, $\delta_m^2 > \delta_s^2$, and since T^* decreases with molecular weight, α^{th} will be a positive contribution, and larger than α^{ath}. For the more favorable case of more polar solutes, a polar fixed phase and a less polar eluent would be in order. For monofunctional compounds, the elution order is that of decreasing molecular weight. If the stationary phase is of higher molecular weight than the eluent, then in this system $v_b^0 > v_a^0$, $\delta_s^2 > \delta_m^2$, $T_a^* > T_b^*$, and both α^{th} and $\alpha^{ath} > 1$. Higher LLC selectivities are intrinsically possible for polar molecules. The two other conceivable cases need not be considered, because as demonstrated above, our theory is

(15) R. F. Blanks and J. M. Prausnitz, *Ind. Eng. Chem., Fundam.*, **3**, 1 (1964).
(16) D. E. Martire and J. H. Purnell, *Trans. Faraday Soc.*, **62**, 710 (1966).
(17) R. R. Dreisbach, Physical Properties of Chemical Compounds, *Advan. Chem. Ser.*, **15** (1955), **22** (1959), and **29** (1961).
(18) A. P. Kudchadker, G. H. Alani, and B. J. Zwolinski, *Chem. Rev.*, **68**, 659 (1968).

inapplicable and unnecessary because one would not ordinarily select such systems for difficult separations.

Our results should in principle apply to mixed and/or partially miscible solvent systems. These are realistically to be encountered more frequently than two effectively immiscible solvents. For predictive purposes, however, we are limited by a lack of information about both molar volumes and cohesive energy densities of mixed solvents. While these may often be simply calculated (*12*), the assumptions underlying our treatment are now clearly suspect, and to expect realistic quantitative predictions is probably presumptuous.

Pursuing our previous assertion (*6*) that LLC has an inherently greater capability for selectivity than GLC, if we apply the Luckhurst-Martire (*5*) treatment to α_{GLC}, Equation 12 results:

$$\ln \alpha_{GLC} = \ln \frac{p_b^0 v_b^0}{p_a^0 v_a^0} + (v_a^0 - v_b^0)\frac{1}{v_s^0} + \frac{v_a^0}{RT}(\delta_s^2 - \delta_a^2) f(T^*) \quad (12)$$

where p^0 is the solute vapor pressure, s refers to the stationary phase [which for comparison purposes we take to be the same compound as is used for the LLC stationary phase (*6*)], and a and b refer to the solutes. Clearly, for very similar solutes, the first term will be very small because it is the logarithm of a number close to unity. The analogous $\alpha_{GLC}{}^{ath}$, the second term, will clearly be smaller than $\alpha_{LLC}{}^{ath}$, if the eluent is a smaller molecule than the stationary phase. If for example $v_m^0 = 100$ cc/mol and $v_s^0 = 500$ cc/mol, then $(v_m^0)^{-1} - (v_s^0)^{-1} = 0.008$ mol/cc whereas $1/v_s^0 = 0.002$ mol/cc. Finally, the last term, $\alpha_{GLC}{}^{th}$, will be smaller than $\alpha_{LLC}{}^{th}$. In general, the pair of LLC solvents will have solubility parameters which bracket those of the solutes; this is so because the two must be mutally less soluble than the solubilities of the solutes in either phase. Consequently, $|\delta_s^2 - \delta_m^2| > |\delta_s^2 - \delta_a^2|$ and $\alpha_{LLC}{}^{th} > \alpha_{GLC}{}^{th}$, which further confirms our original assertion (*6*).

While in principle an important consequence of our results should be the semi-quantitative prediction of α values, screening of solvents for possible use, and designing new solvents, for real analytical problems the required data—molar volumes, critical temperatures, solubility parameters—are scarce. It is, furthermore, a rather ambitious undertaking for an analyst to calculate these parameters from correlations, etc., even when possible, and consequently it would be specious to exhort him to do so. The present state of knowledge concerning solutions often makes it more feasible to experiment than calculate.

In any case, solvent selection in LLC is inherently limited by the dual requirements of low phase miscibility, yet reasonable and differential solvency for the sample components. In our terms, the solubility parameters of the two phases must differ (by approximately 4) and they must bracket the δ values of the solutes. However, they may not diverge excessively or the problem of interfacial adsorption will begin to appear.

This limitation can perhaps be considerably ameliorated by the synthesis of insoluble organic-like stationary phases, the so-called brush (*19*) or fur (*20*) packings which are also used as GC substrates (*21*, *22*). The organo-bentonite clays are also in this category. The organic moiety is chemically bonded to the surface of the support, which is usually siliceous. The product is chemically and physically stable. While they act effectively as solvents, to our knowledge their "solution" properties have not been studied in detail. In principle, it would appear feasible to synthesize any desired property into this LLC substrate.

In conclusion, the results reported here (in particular, Equations 8 and 11) can in principle be used to select solvents for difficult LLC separations, and even to design new solvents. By indicating the dependence of α upon both molecular size and energetic factors, we have shown that separations can be achieved even when the solutes interact identically with the phase solvents. Furthermore, it is now clear that separations entirely feasible on the basis of differential interactions may be confounded if the molar volumes of the two phases are improperly disposed.

APPENDIX 1

Regular Solution Formulation. We have chosen to represent the thermal contribution to the solute activity coefficient by the Luckhurst-Martire formulation (*5*) rather than by the regular solution (solubility parameter) formulation (*12*, *13*) because the former is more general, allowing both negative and positive deviations from Raoult's law; it is directly applicable to the problem of separation of very similar molecules; and it is theoretically more sound.

In order to test these assertions by direct comparison, we have derived an expression analogous to Equation 11. Starting with the expression (*12*, *13*) for the limiting activity coefficient of solute a or b in solvent 1, *e.g.*

$$\ln \gamma_a{}^{th} = \frac{v_a^0}{RT}(\delta_1^2 - \delta_a^2) \quad (A1)$$

substitution as above leads to

$$\ln \alpha^{th} = \frac{v_a^0}{RT}[\delta_m^2 + 2\delta_a(\delta_s - \delta_m) - \delta_s^2] - \frac{v_b^0}{RT}[\delta_m^2 + 2\delta_b(\delta_s - \delta_m) - \delta_s^2] \quad (A2)$$

Assuming $v_a^0 \cong b_b^0$,

$$\ln \alpha^{th} = \frac{2\,v_a^0}{RT}[(\delta_s - \delta_m)(\delta_a - \delta_b)] \quad (A3)$$

which is analogous to Equation 11 (see also Equation 31 in reference *23*).

The most extensive published lists of solubility parameters are those of Burrell (*24*), Lieberman (*25*), Gardon (*26*), Crowley *et al.* (*27*), and Morrison and Freiser (*28*), in addi-

(19) I. Halasz, Fifth International Symposium on Advances in Chromatography, Las Vegas, Nev., January 1969.
(20) H. N. M. Stewart and S. G. Perry, *J. Chromatogr.*, **37**, 97 (1968).
(21) W. A. Aue and C. R. Hastings, *J. Chromatogr.*, **42**, 319 (1969).
(22) E. W. Abel, F. H. Pollard, P. C. Uden, and G. Nickless, *ibid.*, **22**, 23 (1966).
(23) D. C. Locke, in "Advances in Chromatography," Vol. 8, J. C. Giddings and R. A. Keller, Ed., Dekker, New York, N. Y., 1969, p 47.
(24) H. Burrell, *Interchem. Rev.*, **14** (1), 3 (1955); (2), 31.
(25) E. P. Lieberman, *Off. Dig., Fed. Soc. Paint Technol.*, **34**, 30 (1962).
(26) J. L. Gardon, *J. Paint Technol.*, **38**, 43 (1966).
(27) J. D. Crowley, G. S. Teague, Jr., and J. W. Lowe, Jr., *ibid.*, p 269.
(28) G. H. Morrison and H. Freiser, "Solvent Extraction in Analytical Chemistry," Wiley, New York, N. Y., 1957.

tion to the list given by Hildebrand and Scott (*12, 13*) and the cohesive energy densities presented by Polak (*29*). Small (*30*) has deduced a group-contribution type correlation which allows estimation to be made of the solubility parameters of compounds with certain functional groups. Hildebrand and Scott (*12, 13*) also discuss methods by which δ's may be calculated from physical properties, especially the heat of vaporization (Equation 6). These data are compiled in the usual handbooks and references (*17, 31–33*).

The most comprehensive source of critical properties is that of Kudchadker, Alani, and Zwolinski (*18*). In addition to a critical evaluation of experimental data, these authors give means by which critical temperatures may be estimated from pure component properties.

APPENDIX 2

Modified Geometric Mean Combining Rule. In the derivation (*5*) of Equation 5, it is assumed that the pairwise intermolecular potential function for solute–solute and solute–solvent interactions is, for identical configurations, proportional to the depth of the potential well. It is further assumed that the geometric combining rule can be used,

$$\epsilon_{ij} = (\epsilon_{ii}\epsilon_{jj})^{1/2} \tag{B1}$$

In cases where there is a small contribution to the overall interaction energy from, for example, a dipole-induced dipole interaction, we use instead

$$\epsilon_{ij} = (\epsilon_{ii}\epsilon_{jj})^{1/2}(1 + \psi_{ij}) \tag{B2}$$

where ψ_{ij} is a small correction factor, $\psi_{ij} \ll 1$.

Following the derivation of Luckhurst and Martire (*5*), we deduce an expression for $\ln \gamma_2^{th}$ similar to Equation 5 above, plus a third term on the right hand side,

$$+ \frac{2\,v_{2'}}{RT}\,\delta_i^2(\psi - \psi') \tag{B3}$$

where ψ and ψ' are both small. Continuing our procedure as above, we find

$$\ln \alpha^{th} = \frac{v_a^0}{RT}[(\delta_s^2 - \delta_m^2) f(T^*) + 2(\delta_s^2\psi_{ab}^s - \delta_m^2\psi_{ab}^m)] \tag{B4}$$

where $\psi_{ab}^s = (\psi_a^s - \psi_b^s)$, and similarly for phase m, and where the subscripts and superscripts are, respectively, solute and phase indexes.

Because of the requirement that the two chromatographic phases be immiscible, and because the stationary phase is generally selected for its greater solvency for the solutes to be separated, very frequently ψ_a^m and $\psi_b^m \cong 0$. In this case, again selecting solute a as the reference solute,

$$\ln \alpha^{th} = \frac{v_a^0}{RT}[(\delta_s^2 - \delta_m^2) f(T^*) + 2\,\delta_s^2(\psi_a^s - \psi_b^s)] \tag{B6}$$

The last term on the right hand side emphasizes the dependence of α^{th} on rather subtle differences between solute molecules.

An alternate combining rule to Equation B2, *viz.*,

$$\epsilon_{ij} = (\epsilon_{ii}\epsilon_{jj})^{1/2} + \psi''_{ij} \tag{B7}$$

leads to an equation of the same form as B6, except the last term involves $2\,\delta_s^2(\psi''_a{}^s - \psi''_b{}^s)$ only.

Where the eluent is the selective phase, as in the acetonitrile example used above, the last term in Equation B6 is instead

$$-\,2\,\delta_m^2(\psi_a^m - \psi_b^m) \tag{B8}$$

Clearly, in cases such as these, quantitative predictions are difficult. The magnitude of the last term increases in importance with twice the square of the cohesive energy density of the selective phase (the stationary phase in Equation B6), and thus broadly with the polarity of that phase.

(29) J. Polak, *Collect. Czech Chem. Commun.*, **31**, 1483 (1966).
(30) P. A. Small, *J. Appl. Chem.*, **3**, 71 (1953).
(31) J. Timmermans, "Physicochemical Constants of Pure Organic Compounds," Elsevier, New York, N. Y., Vols. 1 and 2, 1950 and 1965.
(32) D. R. Stull and G. C. Stinke, *Advan. Chem. Ser.*, **18** (1956).
(33) American Petroleum Institute, "Selected Values of Physical and Thermodynamic Properties of Hydrocarbons and Related Compounds. API Project 44," Carnegie Press, Pittsburgh, Pa., 1953.

RECEIVED for review July 31, 1970. Accepted October 12, 1970. Presented at the 157th ACS Meeting, Minneapolis, Minn., April 1969. We acknowledge the support of the National Science Foundation, Grant Number GP 17551, and also partial support by a Grant to Queens College from the General Research Support Branch, National Institutes of Health, Number 5-S05-07064-03.

Pyrolysis Gas Chromatography of Phenyl Polymers and Phenyl Ether

M. T. Jackson, Jr.
Central Research Department, Monsanto Company, St. Louis, Mo. 63166

J. Q. Walker
McDonnell Douglas Research Laboratories, St. Louis, Mo. 63166

Pyrolysis in tandem with capillary column gas chromatography–mass spectrometry is a unique and definitive analytical technique for the characterization of various hydrocarbon polymers. We studied the effect of varying parameters affecting the nature of products formed and relative product distribution in routine pyrolysis. These parameters include the effects of pyrolysis temperature rise times, pyrolysis temperatures up to 985 °C, and pyrolysis duration. Temperature rise time (0.1 to 1.5 sec) is not a critical factor in the Curie point pyrolysis of a styrene–isoprene copolymer, either with regard to the products formed or the relative distributions. Additionally, the variation of pyrolysis duration or hold time (2.0 to 12.5 sec) at a fixed Curie temperature reflected no change in the nature of components formed; however, changes in product distributions were observed. Variations in Curie temperature at a fixed pyrolysis duration produced drastic changes in product distributions such as a three-fold change in isoprene dimer formation; however, temperature variance did not change the nature of the products formed. A "polymer-like" compound, bis[*m*-(*m*-phenoxy phenoxy)phenyl] ether, produced two primary pyrolysis products, diphenyl-ether and dibenzofuran.

PHENYL POLYMERS of commercial importance are not readily amenable to chemical degradation. However, they can be readily pyrolyzed to yield the original monomers and/or other volatile fragments. Vinyl or phenyl polymer pyrolysis has been studied by a number of workers (*1–3*).

The major difficulty in pyrolysis studies is obtaining sufficient reproducibility to permit meaningful structure determinations. Good reproducibility requires that all pyrolysis conditions be accurately controlled (*4*). Simon *et al.* (*5*) described that the following pyrolysis conditions must be met. The fragmentation must be conducted at a high dilution sample size in carrier gas and the products quickly transferred to the column to prevent recombination of the products; the sample must be rapidly heated to a constant reproducible temperature; and the pyrolysis temperature must not be so high as to cause catastrophic fragmentation or produce very low molecular weight secondary products.

Rapidly achieved and reproducible pyrolysis temperature can be obtained by the high frequency inductive heating of a wire of ferromagnetic material. With sufficient power input the wire rapidly reaches its Curie point and thereafter absorbs negligible energy (*6*). Such an apparatus is now commonly called a Curie Point pyrolyzer. Because degradation mechanisms are highly temperature dependent, substances which give similar thermal degradation patterns at one temperature will often yield different patterns when the temperature is changed. Hence, a second pyrolysis at a different temperature is often necessary to distinguish clearly between two different materials.

Quantitative analysis of pyrolysis products requires much more stringent control than qualitative identification techniques (*5*). Deviations in handling procedure, such as variation of total sample size and film thickness, can often significantly affect the decomposition pattern (*7*). The metal surface of the wire could have a catalytic effect on the product distribution. However, this has been discounted in at least one instance where the surface area was increased by addition of finely ground metal to the polymer sample and found to have no apparent effect (*8*).

This paper describes Curie point pyrolysis experiments applied to a complex copolymer, polystyrene–polyisoprene, and a polymer-like compound, bis[*m*-(*m*-phenoxy phenoxy)-phenyl]ether, molecular weight 538.6. These experiments included a detailed calibration of Curie point wire composition and temperature, a comparison of three *rf* power supplies with rise times of 0.1 to 1.5 sec, a comparison of pyrolysis time durations of 0.5 to 12.5 sec, and the studies of the effect of temperature on the pyrolysis of copolymer and the phenyl ether, mol wt 538.6.

The combination of a Curie point pyrolyzer and open-tubular capillary column yields adequate separation of most of the olefinic, aromatic, and/or oxygenated products. The flame ionization detector and digital integrator provide quantitative analyses. A medium-resolution mass spectrometer permits positive identification of trace concentrations of pyrolysis product.

EXPERIMENTAL

Apparatus. Three pyrolyzers were used for this work. The three systems showed that Curie point thermal fragmentation patterns were repeatable, at least in the two laboratories. The three units consisted of the following: a pyrolyzer (Philips Electronics) equipped with a 0.05 to 10.0-sec duration timer and a 30-W power supply; a pre-column pyrolyzer (Pye-Unicam) equipped with a 0.2- to 15.0-sec duration timer and a 30-W power supply; and a lab-built pyrolysis chamber equipped with a manual timer and a 2.5-kW *rf* generator (Lepel High Frequency Laboratories, Model T-2.5-1-MC-

(1) J. C. F. Williams, *J. Chem. Soc.*, (*London*), **15**, Pt. 10 (1862).
(2) G. M. Brauer, *J. Polym. Sci.*, **8**, 3 (1965).
(3) M. P. Stevens, "Characterization and Analysis of Polymers of Gas Chromatography," Marcel Dekker, New York, N. Y., 1969, p 64.
(4) S. G. Perry, *Advan. Chromatogr.*, **5**, 221 (1968).
(5) W. Simon, P. Kriemler, J. A. Vollmin, and H. Steiner, *J. Gas Chromatogr.*, **5**, 53 (1967).
(6) W. Simon and H. Giacobbo, *Angew. Chem., Int. Ed. Eng.*, **4**, 938 (1965).
(7) R. S. Lehrle and J. C. Robb, *J. Gas Chromatogr.*, **5**, 89 (1967).
(8) C. E. R. Jones and G. E. J. Reynolds, *ibid.*, p 25.

AP-B). Curie point wires, obtained from Philips Electronics and Varian Associates, were used for all experiments.

The data from the quantitative experiments were obtained using a dual flame detector gas chromatograph (Hewlett-Packard Model 5750) and two digital integrators (Infotronics Models CRS-100 and CRS-108). The qualitative data were obtained with a dual flame detector gas chromatograph (Varian Aerograph Model 1700) and a zero dead-volume column effluent splitter was connected in tandem for gas chromatography/mass spectrometry (GC/MS) operation.

A Biemann–Watson type molecular separator provided the interface between a mass spectrometer (Atlas CH-7) and the gas chromatograph. A block diagram of the pyrolysis GC/MS system is shown in Figure 1.

Samples for pyrolysis were obtained from several different sources: bis[*m*-(*m*-phenoxy phenoxy)phenyl]ether (MW 538.6) was obtained from Varian-Aerograph. The polymer reagents can be obtained from Waters Associates, Inc., (Polystyrene) and Shell Oil Company, (Kraton 1107, styrene–32%, isoprene–68%).

The separation column(s) used for the polymer products were 50 ft × 0.02 in. (i.d.) support-coated open tubular (SCOT) column (Perkin-Elmer Corp.) containing 5-ring polyphenyl ether liquid phase with Apiezon L + Igepal CO 880 added; and 200 ft × 0.02 in. (i.d.) diisodecylphthalate capillary column.

The column used for the separation of the pyrolysis products from the bis[*m*-(*m*-phenoxy phenoxy)phenyl]ether pyrolysis was a 100 ft × 0.02 in. (i.d.) SCOT column (Perkin-Elmer Corp.) containing free fatty acid phase (FFAP) liquid phase.

In the preliminary experiments we used packed separation columns such as a 10 ft × $^1/_8$ in. with 5% methylvinyl silicone liquid phase (UCW-98) on 80–100 mesh chromosorb W-AW. However, this column did not separate the xylene or dimer ($C_{10}H_{16}$) isomers (*9*). Both the diisodecylphthalate and the 5-ring polyphenyl ether-coated open tubular column gave adequate separation of most of the polymer pyrolysis products (*10*). The copolymer pyrolyzate contained 13 compounds having boiling points in a 14 °C range. Thus, detailed analysis of pyrolyzates was necessary to differentiate between very similar structures.

Procedure. The polymer sample is dissolved in a volatile solvent (benzene) to form a 10 weight per cent solution. The chosen pyrolysis Curie point temperature wire is dipped 0.25 in. into the polymer solution. Several samples may be prepared simultaneously. The polymer-coated wires are then placed in a vacuum oven at 75 to 80 °C for 30 min to remove the solvent. Multiple coatings of polymer on the wire were necessary for tandem GC/MS identification of trace products; however, multiple coatings are not recommended for quantitative data. After the sample is positioned in the pyrolyzer, a period of 5 min is allowed for flow rate equilibration.

An auxiliary heating device (heat gun or heating tape) is used to pre-heat the carrier gas line before entry into the pyrolyzer. The pyrolysis chamber is maintained at 174 °C. Asbestos tape and a heating tape were used to eliminate cold spots between the pyrolysis chamber and the GC injection port so that sample and products would not condense prior to entering the column.

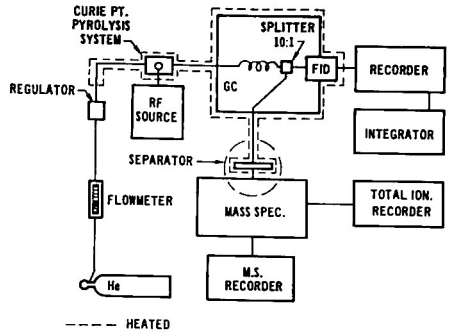


Figure 1. Pyrolysis GC-MS system

Note that the dashed line indicates the heated carrier gas transfer lines and the gas chromatograph heated areas

RESULTS AND DISCUSSION

A prime advantage of the Curie point method (*5, 11*) is the well defined pyrolysis temperature one can obtain with iron or a nickel alloy wire in a *rf* field. Our analyses included a determination of the wire alloy composition by X-ray fluorescence and the determination of Curie temperature by thermal gravimetric analysis. The manufacturer's specifications of eight different wire compositions were similar to our X-ray fluorescence composition data with the exception of the 985 °C wire (see Table I). The Curie temperatures obtained were in

(9) I. N. Nazarov, A. I. Kuznetsova, and N. V. Kuznetosov, *Zh Obshch. Khim.*, **25**, 307 (1955).

(10) W. O. McReynolds, "Gas Chromatographic Retention Data," Preston Technical Abstracts, Evanston, Ill., 1966, pp 71 and 137.

(11) R. L. Levy, *Chromatogr. Rev.*, **1966**, 49.

Table I. Comparison of Curie Point Wires

Manufacturer's specification, °C	TGA,[a] °C	Curie point range, °C	Manufacturer's % composition			X-Ray fluorescence composition[b]		
			Fe	Ni	Co	Fe	Ni	Co
358[c]	352	± 2	0	100	0	0	100	0
480[c]	474	± 2	52	48	0	53.5	46.5	0
510[c]	482	± 2	49	51	0	50.6	49.4	0
600[d]	597	±12	42	42	16	42	42	16
610[c]	601	± 4	30	70	0	29.2	70.8	0
700[d]	707	±12	33	33	33	33	33	33
770[c]	782	± 4	100	0	0	100	0	0
980[c]	985	± 5	0	60	40	39	1	60

[a] Thermal Gravimetric Analyses, (Magnetic transition point, corrected) Perkin-Elmer TGS-1.
[b] Av of three X-Ray Fluorescence analyses from Siemens Crystalloflex IV X-Ray Generator with Vacuum Tunnel Spectrometer.
[c] Philips Electronic Instruments, Mt. Vernon, N. Y.
[d] Fischer Labs (Varian-Aerograph, Walnut Creek, Calif.).

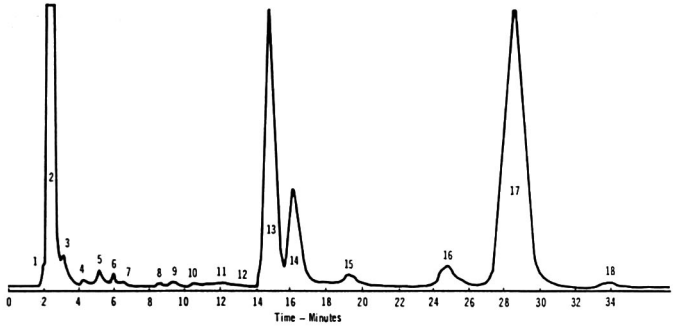


Figure 2. Pyrogram of isoprene–styrene copolymer at 601 °C; 10.0-sec duration

Note that the numbers correspond to the components listed in Table II. The relative areas are also given at 601 °C in Table II

Table II. Repeatability of Thermal Fragmentation Patterns from 601 °C Pyrolysis of Isoprene–Styrene, Copolymer (Relative Per Cent Areas)

Run No. / Component	1	2	3	4	5	6	7	8	9	10	Av	σ
1. C_2–C_4	1.6	1.5	1.7	1.7	1.6	1.5	1.6	1.4	1.6	1.5	1.56	
2. Isoprene	31.8	31.6	32.0	31.8	31.9	31.7	32.0	31.8	32.1	31.6	31.83	0.09
3. Cyclohexadiene + benzene	1.3	1.2	1.4	1.3	1.3	1.4	1.4	1.4	1.5	1.3	1.35	
4. Methylcyclohexadiene	0.4	0.4	0.4	0.4	0.4	0.4	0.4	0.4	0.3	0.4	0.39	
5. Toluene	0.7	0.7	0.6	0.7	0.7	0.6	0.7	0.7	0.7	0.7	0.68	
6. Cyclooctadiene	0.5	0.5	0.5	0.4	0.4	0.5	0.5	0.6	0.5	0.5	0.49	
7. Isopropylcyclohexene	0.6	0.5	0.7	0.6	0.6	0.6	0.7	0.7	0.6	0.5	0.61	
8. Ethyl benzene	0.3	0.2	0.3	0.3	0.3	0.3	0.3	0.3	0.3	0.6	0.32	
9. *p*-Xylene	0.2	0.3	0.2	0.2	0.2	0.3	0.3	0.2	0.2	0.3	0.24	
10. *m*-Xylene	0.3	0.2	0.3	0.2	0.3	0.2	0.2	0.3	0.3	0.2	0.25	
11. *o*-Xylene	0.4	0.3	0.2	0.3	0.3	0.3	0.2	0.4	0.3	0.3	0.30	
12. Isopropylbenzene	0.2	0.2	0.2	0.2	0.2	0.2	0.2	0.2	0.2	0.2	0.20	
13. Styrene	16.1	16.4	15.9	16.2	16.0	15.8	16.3	16.0	15.9	16.0	16.06	0.17
14. 1,4-Dimethyl-1-vinyl-cyclohexene	7.3	7.1	7.4	7.2	7.3	7.1	7.4	7.2	7.2	7.3	7.25	0.11
15. C_3 Alkyl benzene + 1,3-dimethyl-1-vinyl-cyclohexene	1.6	1.7	1.6	1.6	1.7	1.7	1.6	1.7	1.6	1.8	1.66	
16. Diprene and C_3 benzene	3.0	2.8	3.1	2.7	2.8	3.1	3.0	2.9	2.6	2.8	2.88	
17. Dipentene	33.2	33.8	32.9	33.7	33.4	33.7	32.6	33.2	33.5	33.4	33.34	0.37
18. Dimethylcyclooctadienes + isopropenyl benzene	0.5	0.6	0.6	0.5	0.6	0.6	0.6	0.6	0.6	0.6	0.58	
Total area, %	100.0	100.0	100.0	100.0	100.0	100.0	100.0	100.0	100.0	100.0		

good agreement (within 8 to 12°) with the manufacturer's specifications for the wires except for a negative 28° error in the 510 °C wires.

Figure 2 shows a pyrogram of the copolymer (isoprene–styrene) resulting from a 10-sec pyrolysis at 601 °C. One might expect that such a copolymer could yield a product distribution similar to the sum of the two constituent product distributions. For example, when the polymer polyisoprene is pyrolyzed, C_2, C_3, C_4, isoprene, and $C_{10}H_{16}$ dimers are produced (*9*). When polystyrene is pyrolyzed, styrene and aromatic hydrocarbons are the products (*12*). Figure 2 and Table II show that the copolymer product distribution and relative area basis resemble the two individual polymer product distributions.

The pyrolysis patterns observed from the pyrolysis of the copolymer, isoprene styrene, at 601 °C from 10 separate determinations is shown in Table II. These data were obtained over a period of 10 days. The repeatability of the normalized per cent areas is excellent. The average value of the 10 determinations and the standard deviation (σ) are shown at the right. The per cent deviation from the average value for the most abundant products, peak numbers 2, 13, 14, and 17, is 0.28, 1.02, 1.52, and 1.12%, respectively.

The next series of experiments investigated the effect of Curie point rise time on the pyrolysis of the copolymer, isoprene–styrene. Curie point pyrolysis rise time is related to the wattage of the *rf* power supply (*13*). For example, a pure iron wire requires 1.5 sec to reach the final temperature (782 °C) with a 30-W power supply. However, the same iron

(12) G. F. L. Ehlers, K. R. Frisch, and W. R. Powell, *J. Polym. Sci.*, **7**, 2931 (1969).

(13) R. L. Levy and D. L. Fanter, ANAL. CHEM., **41**, 1465 (1965).

Table III. Effect of Pyrolyzer Power on Products (Copolymer Sample)[a]

(Relative per cent area)

Unit Component	Philips 30 W	Pye-Unicam 30 W	Lepel 2.5 kW
C_2–C_4	1.7	1.5	1.4
Isoprene	32.1	31.5	30.2
Cyclohexadiene + benzene	1.3	1.3	1.7
Methylcyclohexadiene	0.4	0.4	0.4
Toluene	0.7	0.7	0.9
Cyclooctadiene	0.5	0.5	0.2
Isopropylcyclohexene	0.7	0.6	0.3
Ethyl benzene	0.3	0.3	0.3
p-Xylene	0.2	0.3	0.2
m-Xylene	0.2	0.3	0.4
o-Xylene	0.2	0.4	0.2
Isopropylbenzene	0.2	0.2	Trace
Styrene	15.7	17.6	18.4
1,4-Dimethyl-1-vinyl-cyclohexene	7.3	7.2	7.5
C_3 Alkyl benzene + 1,3-dimethyl-1-vinyl cyclohexene	1.7	1.7	2.0
Diprene and C_3 benzene	3.2	2.5	2.8
Dipentene	33.0	32.4	32.0
Dimethylcyclooctadienes + isopropenyl benzene	0.6	0.6	1.1
Total area, %	100.0	100.0	100.0

[a] Styrene–isoprene at 601 °C, 10 sec, 200 ft × 0.02 in. (i.d.) diisodecylphthalate (DIDP) capillary, 85 °C, isothermal, flow = 12 ml/min (helium).

Table IV. Effect of Pyrolysis Durations[a]

(Relative per cent area)

Time, sec Component	2.0	5.0	7.5	10.0	12.5
C_2–C_4	1.2	1.4	2.3	3.8	3.4
Isoprene	31.6	32.0	27.0	24.1	21.9
Cyclohexadiene + benzene	1.9	1.4	1.8	2.3	4.0
Methylcyclohexadiene	0.4	0.3	0.4	1.0	1.2
Toluene	0.7	0.2	0.3	1.4	1.6
Cyclooctadiene	0.4	0.8	1.1	1.0	1.3
Isopropylcyclohexene	0.3	0.5	0.7	0.1	Trace
Ethyl benzene	0.2	0.2	0.4	0.2	0.3
p-Xylene	0.3	0.1	0.3	0.2	0.3
m-Xylene	0.2	0.2	0.3	0.2	0.3
o-Xylene	0.3	0.2	0.3	0.1	0.1
Isopropylbenzene	0.2	0.4	1.1	2.3	2.7
Styrene	16.4	16.0	16.0	18.1	20.0
1,4-Dimethyl-1-vinyl-cyclohexene	9.7	9.3	9.2	9.2	9.5
C_3 Alkylbenzene + 1,3-Dimethyl-1-vinyl-cyclohexene	2.9	2.6	3.3	2.0	...
Diprene and C_3 benzene	2.0	1.8	2.1	2.4	2.4
Dipentene	31.3	32.6	33.4	31.1	31.0
Dimethylcyclooctadienes + isopropenylbenzene	Trace	Trace	Trace	0.5	Trace
Total area, %	100.0	100.0	100.0	100.0	100.0

[a] Copolymer (styrene, 32%–isoprene 68%); 782 °C pyrolysis temperature 20 ft × 0.02 in. (i.d.). Diisodecylphthalate (DIDP) capillary, 85 °C isothermal; flow = 12 ml/min (helium).

wire requires only 0.12 sec to reach 782 °C with a 2500-W power supply.

Our results shown in Table III indicate that there is little difference in product distribution normalized on a per cent area basis with this copolymer using the 30-W (rise time of 1.5 sec) and the 2500-W power supply (rise time 0.12 sec). However, it has been suggested (*14*) that faster rise times, on the order of 0.01 to 0.02 sec will yield different polymer product distributions.

The effect of pyrolysis duration has not been reported in the

(14) F. Farré-Rius and G. Guiochon, ANAL. CHEM., 40, 998 (1968).

Table V. Effect of Pyrolysis Temperatures[a]

(Relative per cent areas)

Temperature °C Component	474	482	601	782	985
1. C_2–C_4	0.2	0.4	1.5	3.8	7.6
2. Isoprene	38.0	39.2	31.5	24.1	33.3
3. Cyclohexadiene + benzene	0.3	0.4	1.3	2.3	2.6
4. Methylcyclohexadiene	0.7	0.7	0.4	1.0	0.8
5. Toluene	0.2	0.2	0.7	1.4	0.9
6. Cyclooctadiene	0.3	0.2	0.5	1.0	1.2
7. Isopropylcyclohexene	0.2	0.4	0.6	0.1	0.5
8. Ethyl Benzene	0.1	0.3	0.3	0.2	0.4
9. *p*-Xylene	0.2	0.2	0.3	0.2	0.8
10. *m*-Xylene	0.2	0.2	0.3	0.2	0.3
11. *o*-Xylene	0.4	0.1	0.4	1.1	Trace
12. Isopropylbenzene	0.2	Trace	0.2	2.3	1.4
13. Styrene	2.0	2.2	17.6	18.1	22.9
14. 1,4-Dimethyl-1-vinyl-cyclohexene	6.7	6.8	7.2	9.2	6.5
15. C_3 Alkyl benzene + 1,3-dimethyl-1-vinyl-cyclohexene	1.9	1.4	1.7	2.0	2.2
16. Diprene and C_3 benzene	2.1	1.9	2.5	2.4	1.4
17. Dipentene	45.9	44.8	32.4	31.1	16.6
18. Dimethylcyclooctadienes + isopropenyl benzene	0.4	0.6	0.6	0.5	0.6
Total area, %	100.0	100.0	100.0	100.0	100.0

[a] Copolymer (styrene, 32%–isoprene 68%); 10 sec, pyrolysis duration 200 ft × 0.02 in. (i.d.). Diisodecylphthalate (DIDP) capillary, 85 °C isothermal; flow = 12 ml/min (helium).

Table VI. Effect of Pyrolysis Temperatures[a]

(Relative per cent areas)

Component	Temp, °C 985	782	601	482	474
$CO_2 + C_1$–C_4	17.2	6.2	1.0		
Benzene	11.1	19.1	11.2	Trace	Trace
Toluene	1.5	1.0	Trace		
Indan		Trace			
Indene		Trace			
Benzofuran	2.0	5.5	4.1		
Me Indan		0.9			
Me Indene		0.9			
Naphthalene	13.4	12.3	6.4		
Diphenylether	42.3	41.0	52.5	61.6	65.4
Dibenzofuran	12.5	13.1	24.8	38.4	34.6
Total area, %	100.0	100.0	100.0	100.0	100.0

[a] Bis [*m*-(*m*-phenoxy phenoxy)phenyl]ether. Mol wt 538.60. 100 ft × 0.02 in. (i.d.) free fatty acid phase, (FFAP), SCOT program, 75 to 210 °C at 8 °C/min; flow rate = 20 ml/min (medium).

literature. We studied the effect of pyrolysis duration on the product distribution of the copolymer, isoprene–styrene.

Table IV shows the relative product distribution variation as the pyrolysis duration is changed from 2.0 to 12.5 sec at a temperature of 782 °C. (Note the automatic timer intervals less than 2.0 sec (0.05, 0.1, 0.2, 0.5, and 1.0 sec) were not useful on the Philips and Pye-Unicam pyrolyzers since the rise time to 782 °C was at least 1.2 sec.) The results shown in Table IV show small increases in the relative amounts of polystyrene products (benzene, toluene, styrene, and isopropyl benzene) with increasing pyrolysis time. There are also small changes in the polyisoprene relative pyrolysis product distributions.

The effect of pyrolysis temperature is the most important parameter in pyrolysis gas chromatography (*14*). Our next experiments compared the relative pyrolysis product distributions of the copolymer, isoprene–styrene, at five different temperatures at a constant pyrolysis duration of 10 sec (See Table V). These data show that as the pyrolysis temperature is increased from 474 to 985 °C, there is a three-fold decrease in one polyisoprene degradation product, dipentene, and an increase in C_2 to C_4 products. The polystyrene products also significantly increase with increases in temperature.

The effect of Curie temperature on pyrolysis product distribution was also studied for a phenyl "polymer-like" compound bis[*m*-(*m*-phenoxy phenoxy)phenyl]ether. Table VI shows the relative product distribution variation from 474 to 985 °C. This thermally stable substance yields primarily two high molecular weight compounds, diphenyl ether and dibenzofuran, at 482 and 474 °C. However, at higher temperatures, lower molecular weight products are produced.

CONCLUSIONS

Variation of pyrolysis duration or hold time (2.0 to 12.5 sec) at a fixed Curie temperature reflected no change in the nature of components formed; however, changes in product distributions were observed. Additionally, temperature rise time (0.1 to 1.5 sec) is not a critical factor in Curie point pyrolysis in a styrene–isoprene copolymer, either with regard to the products formed or the relative distributions. Variations in Curie temperature (from 474 to 985 °C) at a fixed pyrolysis duration produced drastic changes in the principal products from the Curie pyrolysis of the copolymer and phenyl ether compound.

In general, the reproducible pyrolysis product distributions of the copolymer resembled the combination of the distributions of the constituent polymers. If this phenomenon is observed in the pyrolysis of other copolymers, it represents an added advantage in copolymer structure determination.

If one uses the wire alloy that Simon originally defined, one obtains the Curie temperature he states with exception of the 510 °C wire.

ACKNOWLEDGMENT

We thank A. H. Bell for technical assistance with the initial experiments. We wish to acknowledge the contributions of J. A. Schoeffel for the X-ray fluorescence analyses and C. E. Scott for the TGA. analyses. Also, we express thanks to W. E. Koerner, C. J. Wolf, J. D. Kelley, and D. R. Beasecker for helpful suggestions concerning the manuscript.

RECEIVED for review July 17, 1970. Accepted October 12, 1970. This research was partially conducted under the McDonnell Douglas Independent Research and Development Program.

Potentiometric Study of Copper(I) Complexes with Univalent Anions in Acetonitrile

John K. Senne and Byron Kratochvil

Department of Chemistry, University of Alberta, Edmonton, Alberta, Canada

The standard potential of the Cu(I)–(0) couple in acetonitrile was found to be −0.5842 ± 0.0005 V *vs.* the standard silver electrode. The stepwise formation constants of several complexes with Cu(I) in acetonitrile were determined by potentiometric titration of Cu(I) solutions with salts of these anions using a saturated copper amalgam indicating electrode. Log β_1 and β_2 values were: Cl^-, 4.3 and 10.2; Br^-, 3.5 and 7.3; I^-, 3.1 and 5.8; SCN^-, 3.6 and 7.2. Nitrate association with Cu(I) is negligibly small. Evaluation of the potentiometric data required knowledge of the ion association constants of the titrant salts in acetonitrile. For NaSCN and Et_4NNO_3 these data were determined by high precision conductance measurements. Analysis of the conductance data by the Fuoss–Onsager equation gave for NaSCN, $K_a = 88 \pm 4$, $\Lambda_o = 189.8 \pm 0.2$; and for Et_4NNO_3, $K_a = 7 \pm 2$, $\Lambda_o = 191.37 \pm 0.03$.

THE BEHAVIOR of copper salts in acetonitrile is of interest since copper(II) perchlorate has been shown to be an analytical oxidant of some utility in this solvent (*1–3*). The oxidizing strength of copper(II) is a function of the anions present, their concentrations, and their interactions with copper(I) as well as copper(II). To date the only formation constants which have been measured are those of chloride with copper(I) and copper(II) by polarographic and spectrophotometric methods (*4*), and those of perchlorate, hexafluorophosphate, and tetrafluoroborate with copper(I) by conductance measurements (*5*). The main purpose of this work was to measure the formation constants of selected monovalent anions with copper(I) in acetonitrile. In conjunction with this study, the standard potential of the copper(I)–(0) couple was accurately determined, and the ion association constants of sodium thiocyanate and tetraethylammonium nitrate were measured.

EXPERIMENTAL

Apparatus. A Sargent Model SR Recorder with a 10-mV full scale deflection was used for measurements of the copper (I)–(0) standard potential. It was provided with a variable and accurately known bucking potential and allowed continuous monitoring of cell potentials with an accuracy of ±0.2 mV.

Potential measurements in the complexation studies were made to the nearest 0.1 mV with a Leeds & Northrup 7554 Type K-4 Potentiometer.

Three cells were used in the determination of the copper (I)–(0) standard potential. All were of the standard H-cell design, with three compartments separated by ultrafine sintered-glass frits. Electrical contact to the amalgam electrodes was made with a platinum wire sealed into the end of soft glass tubing.

The indicating electrode for all potentiometric work was a saturated copper amalgam, prepared by electrolyzing an aqueous 0.1*M* $CuSO_4$ solution, slightly acidified with H_2SO_4, at a current density of about 0.05 A/cm² until the mercury cathode contained about 1% copper by weight. An anode of pure copper wire was used in the electrolysis. When first prepared the amalgam appeared homogeneous but within an hour or two a solid phase separated [the solubility of copper in mercury is about 0.00025% (*6*)]. The amalgam was stored under aqueous 0.1*M* H_2SO_4 in a weighing bottle and exposed to air only when the bottle was opened for removal of amalgam.

Silver electrodes were prepared by sealing platinum foil into soft glass and electroplating silver on the platinum from 50 ml of an aqueous solution containing 0.85 gram of $AgNO_3$, 1 gram of KCN, and 2 grams of K_2CO_3. A current density of 30 mA/cm² was applied for 10 min, after which the electrodes were rinsed with dilute $HClO_4$, water, and finally acetonitrile. When not in use the electrodes were stored in 0.01*M* $AgNO_3$ in acetonitrile. Of four electrodes prepared, one gave significantly different results relative to the other three and was rejected. The average potential difference between any two of the remaining three electrodes when immersed in 0.01*M* $AgNO_3$ in acetonitrile was 0.2 mV.

Unless otherwise specified, the reference electrode was a saturated silver–mercury amalgam in contact with silver perchlorate in acetonitrile. This electrode attained equilibrium quickly. Its reproducibility equals or exceeds that of the silver, 0.01*M* silver nitrate electrode, and it is not affected by jarring or shaking. The amalgam was prepared by placing 25 to 35 cm³ of silver foil into a glass tube with about 30 ml of mercury. The solubility of silver in mercury is about 0.035% (*7*), so the relative amounts are not critical. The tube was sealed with a flame and heated for 8 hours at 110 °C with occasional shaking; it was allowed to cool to room temperature overnight before being opened. The amalgam was stored in contact with silver foil in a dropping bottle, and portions were removed as needed with an eyedropper. Protection from the air was not necessary.

Solid copper electrodes were prepared from pure copper wire by polishing with fine emery cloth immediately before insertion into previously deacrated test solution.

The apparatus, procedure, and method of data analysis for the determination of association constants from conductance measurements have been described previously (*5*). Solution densities, d, were calculated from the equation $d = d_o + A\bar{m}$, where d_o is the solvent density, $\bar{m}$ is the molality, and A is a constant for each salt. The value of A was determined by measuring the density of a 0.01*M* solution of the salt in acetonitrile. For sodium thiocyanate and tetraethylammonium nitrate, the values of A were 0.054 and 0.062, respectively. The density of solid tetraethylammonium nitrate was determined as 1.14 g/cm³.

Chemicals. Acetonitrile was purified by the method previously described (*5*).

Copper (I) perchlorate was prepared by reaction of copper

(1) B. Kratochvil, D. A. Zatko, and R. Markuszewski, ANAL. CHEM., 38, 770 (1966).
(2) B. Kratochvil and P. F. Quirk, *ibid.*, 42, 535 (1970).
(3) H. C. Mruthyunjaya and A. R. V. Murthy, *Indian J. Chem.*, 7, 403 (1969).
(4) S. E. Manahan and R. T. Iwamoto, *Inorg. Chem.*, 4, 1409, (1965).
(5) B. Kratochvil and H. Yeager, *J. Phys. Chem.*, 73, 1963 (1969).
(6) M. Hansen and K. Andergo, "Constitution of Binary Alloys," McGraw-Hill, New York, N. Y., 1958, p 588.
(7) *Ibid.*, p 24.

metal with copper(II) perchlorate in acetonitrile (*8*). It was recrystallized once from purified acetonitrile and dried under vacuum. Analysis for copper by EDTA titration gave 99.8% $CuClO_4 \cdot 4CH_3CN$ (*9*).

Silver perchlorate was prepared as previously described (*5*).

Tetraethylammonium perchlorate was prepared by metathesis from sodium perchlorate and tetraethylammonium bromide. It was recrystallized once from water and dried under vacuum. Silver nitrate tests for bromide were negative.

Tetraethylammonium nitrate was prepared by neutralization of a 10% aqueous solution of tetraethylammonium hydroxide (Eastman Organic Chemicals, Rochester, N. Y.) through dropwise addition of concentrated nitric acid to pH 7.0. The resulting solution was evaporated to near dryness on a hot plate and dried under vacuum at 110 °C overnight. This material was analyzed in two ways, by passage through a strong cation exchange resin in the hydrogen form with subsequent titration of the nitric acid liberated, and by a redox method based on the reduction of nitrate ion by excess Fe(II) in strong acid (*10*). Both methods gave purities of 100 ± 1%. The above material after analysis was recrystallized once from purified acetonitrile, pulverized, and dried at 110 °C under vacuum before use.

Sodium thiocyanate was purified by recrystallization of reagent-grade material first from purified acetonitrile, and then from water. The resulting crystals were dried under vacuum at room temperature, pulverized, and redried under vacuum at 110 °C. A purity of 99.9% was obtained by coulometric titration at constant current with electrochemically generated silver(I).

Tetraethylammonium iodide was prepared by mixing equal volumes of 0.22*M* sodium iodide and tetraethylammonium chloride in technical grade acetonitrile. The sodium chloride precipitate was filtered off and the filtrate reduced to about 50 ml by evaporation on a hot plate. The crystals of tetraethylammonium iodide obtained on cooling were recrystallized once from purified acetonitrile and dried under vacuum at 110 °C.

Reagent grade sodium perchlorate was recrystallized once from purified acetonitrile and dried under vacuum at 110 °C. A silver nitrate test for halides was negative.

Copper(I) nitrate was prepared as described previously (*8*). Because of the instability of $CuNO_3 \cdot 4CH_3CN$, the pure solid could not be isolated. However, a 0.1*M* solution in purified acetonitrile was colorless and clear for several hours after filtration through Whatman No. 2 filter paper; after that time, a blue solid precipitated from solution (*11*). Dilute solutions were prepared by dilution of aliquots of the freshly filtered solution. The exact concentration of copper was determined by EDTA titration after evaporation of the acetonitrile and oxidation of the metal with dilute nitric acid.

Procedure. For the determination of the standard potential of the copper(I)–(0) couple, the following cell was used:

$$\mathrm{Cu(Hg)} \left| \begin{array}{c} \mathrm{CuClO_4},\ M_1 \\ \mathrm{Et_4NClO_4},\ M_2 \end{array} \right| \left| \begin{array}{c} \mathrm{CuClO_4},\ M_1 \\ \mathrm{Et_4NClO_4},\ M_2 \end{array} \right| \left| \begin{array}{c} \mathrm{AgClO_4},\ M_1 \\ \mathrm{Et_4NClO_4},\ M_2 \end{array} \right| \mathrm{Ag(Hg)}$$

The central compartment contained a solution identical to that in the copper half-cell and served to prevent diffusion of silver(I) into the copper half-cell. The solution above the copper amalgam was deaerated by bubbling argon presaturated with acetonitrile through the solution for 15 minutes and then passing the gas over the surface for the duration of the experiment. The silver amalgam half-cell did not require deaeration. The cell potential was continuously monitored for 8–12 hours with a recorder and the best linear portion was extrapolated to zero time. Potential drift during this time was typically on the order of 2 to 3 mV.

Data for the calculation of formation constants were obtained by titration of copper(I) with the appropriate ligand in the following cell:

$$\mathrm{Cu(Hg)} \left| \begin{array}{c} \mathrm{CuClO_4}, \\ M_1 \\ \text{Supp. elec.}, \\ 0.1M \end{array} \right| \left| \begin{array}{c} \mathrm{CuClO_4}, \\ M_1 \\ \text{Supp. elec.}, \\ 0.1M \end{array} \right| \left| \begin{array}{c} \mathrm{AgClO_4}, \\ 0.01M \\ \text{Supp. elec.}, \\ 0.1M \end{array} \right| \mathrm{Ag(Hg)}$$

The titrant contained, in addition to the ligand, the same formal concentration of copper(I) perchlorate, generally $5 \times 10^{-4}M$, and supporting electrolyte as the copper half-cell, as suggested by Manahan and Iwamoto (*4*). By maintaining a constant concentration of copper throughout the titration, treatment of the data is simplified. The ligand concentration typically was varied over the range zero to $4 \times 10^{-3}M$. Titrant was added in milliliter increments to the copper half-cell. The solution in the cell was deaerated continuously by passing argon gas, presaturated with acetonitrile, through it. As before, the central compartment contained solution identical to that in the copper half-cell.

RESULTS AND DISCUSSION

Standard Potential of the Cu(I)–(0) Couple. In the determination of standard potentials, it is important to minimize liquid junction potentials. This can be accomplished by constructing a cell without transference using an electrode of the second kind, or by following one of several extrapolation procedures (*12*). Because suitable electrodes of the second kind are not presently available in acetonitrile, the second method was used.

Three series of measurements were made on the cell

$$\mathrm{Cu(Hg)} \left| \begin{array}{c} \mathrm{CuClO_4},\ M_1 \\ \mathrm{Et_4NClO_4},\ M_2 \end{array} \right| \left| \begin{array}{c} \mathrm{AgClO_4},\ M_1 \\ \mathrm{Et_4NClO_4},\ M_2 \end{array} \right| \mathrm{Ag(Hg)}$$

For simplicity the central compartment is not indicated. In the first series M_1 was varied while the sum of M_1 and M_2 (the ionic strength) was held constant. As M_1 approaches zero, the compositions of the solutions approach that of pure supporting electrolyte and the junction potential approaches zero. Extrapolation of a plot of cell potential *vs.* M_1 to M_1 = zero (Figure 1) yields a potential at a particular ionic strength from which the junction potential has been eliminated. Other series of measurements were taken in the same way as the first but at different values of ionic strength. Slopes and *y*-axis intercepts were calculated for each set of data by least-squares, along with standard deviations for the intercepts. The values obtained at varying ionic strengths were: μ = 0.03, $E^{\circ\prime}$ = 0.6811 ± 0.0005 V; μ = 0.01, $E^{\circ\prime}$ = 0.6815 ± 0.0002 V; and μ = 0.006, $E^{\circ\prime}$ = 0.6811 ± 0.0005 V. Each point on Figure 1 is the average of three measurements, each with a different cell.

It should be possible to obtain the standard potential from an additional plot of potential *vs.* a function of the ionic strength. However, such a plot for this system is not pos-

(8) B. J. Hathaway, D. G. Holah, and J. D. Postlethwaite, *J. Chem. Soc.*, 1961, 3215.
(9) J. S. Fritz, J. E. Abbink, and M. A. Payne, ANAL. CHEM., 33, 1381 (1961).
(10) W. Leithe, *ibid.*, 20, 1082 (1948).
(11) H. H. Morgan, *J. Chem. Soc.*, 1923, 2901.
(12) R. G. Bates, "Determination of pH," John Wiley and Sons, New York, N. Y., 1954, p 47.

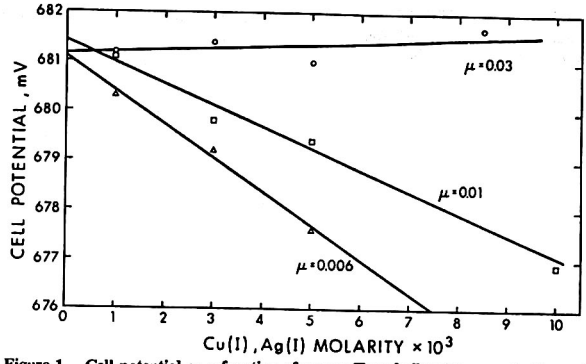


Figure 1. Cell potential as a function of copper(I) and silver(I) concentrations at various ionic strengths

sible because the three intercepts in Figure 1 are the same within experimental error. This indicates that the activity coefficients of the copper(I) and silver(I) species are of the same magnitude since the potential for the cell reaction

$$Cu(Hg) + Ag^+ \rightleftarrows Ag(Hg) + Cu^+$$

is given by

$$E_{cell} = E^\circ_{cell} + 0.0591 \log ([Ag^+]/[Cu^+]) + 0.0591 \log \left(\frac{\gamma_{Ag^+}}{\gamma_{Cu^+}}\right) \quad (1)$$

By maintaining identical concentrations of silver(I) and copper(I), the second term on the right hand side of the equation becomes zero. At the ionic strengths used neither γ_{Ag^+} nor γ_{Cu^+} will be unity. However, upon dilution the ratio of γ_{Ag^+} to γ_{Cu^+} would be expected to approach unity more quickly than the individual activity coefficients, and the cell potential should not be strongly dependent upon the ionic strength. The standard potential of the cell was therefore taken to be the average of the three intercepts, 0.6812 ± 0.0002 V.

To obtain the standard potential of the copper(I)–(0) couple, a correction for the free energy of amalgamation of copper is necessary. The value reported in water by Oku (*13*) is 236 ± 2 calories. This quantity should be independent of the solvent.

To determine the free energy of amalgamation of silver, measurements were made on the cell

$$Ag \left| \begin{array}{l} 0.01M\ AgNO_3 \text{ in} \\ \text{acetonitrile} \end{array} \right| Ag(Hg)$$

A value of 0.0870 ± 0.0005 V was obtained, which corresponds to a Gibbs free energy of −2006 ± 10 calories.

Taking into account the above values, and arbitrarily referring all potentials to the silver, silver(I) couple at unit activity, gives:

Half-Reaction	E°, volts
$Ag^+ + e = Ag(Hg)$	0.0870 ± 0.0005
$Ag^+ + e = Ag$	0.0000
Ag^+ (0.01M $AgNO_3$) + $e = Ag$	−0.133 ± 0.002 (*14*)
$Cu^+ + e = Cu(Hg)$	−0.5942 ± 0.0005
$Cu^+ + e = Cu$	−0.5842 ± 0.0005

The uncertainties in the above values are standard deviations.

(13) M. Oku, *Sci. Rep. Tohoku Imp. Univ. Ser. I*, 22, 288 (1933).
(14) B. Kratochvil, E. Lorah, and C. Garber, ANAL. CHEM., 41, 1793 (1969).

Copper(I) Complexes in Acetonitrile. Overall formation constants, β_1 and β_2, for copper(I) with the halides, thiocyanate, and nitrate were calculated by combining the formation constant expressions with the mass balance equations for total ligand, [L]°, and total copper, [Cu]°. Ion association of the cation of the supporting electrolyte, C^+, with the ligand was also taken into account by including the association constant for C^+L^-, K_a, to give

$$[L^-] = \frac{[L]^\circ - [CuL] - 2[CuL_2^-]}{1 + K_a[C^+]} \quad (2)$$

where $[L^-]$ is the free ligand concentration. Where C^+ was sodium ion, the calculations had to include association with perchlorate [K_a for sodium perchlorate in acetonitrile = 10 (*15*)], but no correction was necessary for tetraethylammonium perchlorate, which is completely dissociated in acetonitrile (*16*). The free copper concentration was obtained from the Nernst equation and the cell potential.

Using these equations, and assuming the concentration of CuL to be negligible at large ratios of ligand to copper(I), β_2 may be calculated either point by point or by a plot based on the equation

$$\Delta E = -0.0591 \log [Cu]^\circ + 0.0591 \log [CuL_2^-]/\beta_2 - 0.0591\ Q \log [L^-] \quad (3)$$

which is readily derived from the Nernst expression and the equations at hand. ΔE is the potential shift from the value observed before any ligand has been added. A graph of ΔE *vs.* log $[L^-]$ will have a slope of 0.0591 Q where Q is the subscript of the highest order complex formed. β_2 may then be calculated from the intercept. The data were analyzed by the latter method and in all cases except nitrate, Q was found to be two.

Values of β_1 were calculated on a point by point basis from data taken at ratios of ligand to copper of less than two. Combining expressions for β_1, β_2, K_a, and total ligand concentration gives

$$\beta_1 = \frac{[L]^\circ - [L^-] - 2\beta_2[Cu^+][L^-]^2 - K_a[C^+][L^-]}{[Cu^+][L^-]} \quad (4)$$

(15) R. L. Kay, B. J. Hales, and G. P. Cunningham, *J. Phys. Chem.*, 71, 3925 (1967).
(16) I. Y. Ahmed and C. D. Schmulbach, *ibid.*, p 2358.

Table I. Complex Formation Constants of Some Anions with Copper(I) in Acetonitrile

Titrant	K_a for titrant salt	Supporting electrolyte, 0.1*M*	Log β_1	Log β_2
Et_4NCl	35 (Ref. *20*)	Et_4NClO_4	4.23, 4.35[a]	10.20, 10.24
Et_4NBr	10 (Ref. *17*)	Et_4NClO_4	3.47, 3.52	7.36, 7.29
Et_4NI	5 (Ref. *17, 18*)	Et_4NClO_4	3.10, 3.13	5.86, 5.96
NaI	0 (Ref. *19*)	$NaClO_4$	3.07	5.69, 5.67
NaSCN	88[c]	$NaClO_4$	3.57, 3.57	7.33, 7.18
Et_4NNO_3	7[d]	Et_4NClO_4	Unassociated	

[a] Previously reported value, 5.9 (*4*).
[b] Previously reported value, 10.8 (*4*).
[c] This work.
[d] This work. Previous estimated value was 25 (*20*).

Table II. Conductance Data for NaSCN and Et_4NNO_3 in Acetonitrile at 25 °C

10^4C NaSCN	Λ	ΔΛ	10^4C Et_4NNO_3	Λ	ΔΛ
	$10^4\kappa$ = 3.98			$10^4\kappa$ = 7.54	
7.580	170.34	0.02	3.524	183.78	0.02
11.182	165.00	−0.04	5.674	181.61	−0.01
14.005	161.44	−0.02	7.704	179.91	−0.06
16.776	158.33	0.03	9.687	178.58	0.02
19.668	155.35	0.03	11.842	177.24	0.04
22.529	152.62	−0.03	14.152	175.88	0.00
25.159	150.36	0.02	16.349	174.73	−0.01
29.029	147.25	−0.01	19.134	173.40	−0.01
NaSCN	$10^4\kappa$ = 3.32		Et_4NNO_3	$10^4\kappa$ = 7.50	
6.991	171.30	0.00	3.338	183.99	0.00
11.248	165.03	−0.01	5.573	181.77	0.00
16.098	159.25	0.05	7.302	180.34	0.00
19.718	155.40	−0.08	9.679	178.65	0.00
24.994	150.71	0.04	11.133	177.74	0.01
28.948	147.52	0.02	12.570	176.86	−0.01
33.581	144.10	−0.06	13.648	176.27	0.00
36.687	142.08	0.02			

Table III. Conductance Parameters and Averaged Conductance Values

Salt	Trial	Λ_0	$\dot{a}$	K_a	σΛ
NaSCN	1	189.63 ± 0.16	2.5 ± 0.5	84 ± 3	0.05
NaSCN	2	189.94 ± 0.13	3.4 ± 0.6	91 ± 3	0.03
Et_4NNO_3	1	191.40 ± 0.09	4 ± 1	9 ± 4	0.04
Et_4NNO_3	2	191.34 ± 0.04	3.5 ± 0.7	5 ± 2	0.01

(17) A. C. Harkness and H. M. Daggett, Jr., *Can. J. Chem.*, 43, 1215 (1965).
(18) G. Kortum, S. G. Gokhale, and H. Wilski, *Z. Phys. Chem.* (Frankfurt am Main) 4, 86 (1955).
(19) R. P. T. Tomkins, E. Andalaft, and G. J. Janz, *Trans. Faraday Soc.*, 65, 1901 (1969).
(20) C. W. Davies, "Ion Association," Butterworths, London, 1962, p 96.

Similarly, expressions for β_1, β_2, and total copper(I) concentration give

$$\beta_1 = \frac{[Cu]^\circ - [Cu^+] - \beta_2[Cu^+][L^-]^2}{[Cu^+][L^-]} \quad (5)$$

Combining Equations 4 and 5 such that β_2 is eliminated results in a quadratic expression from which the free ligand concentration may be calculated.

$$\beta_2[Cu^+][L^-]^2 + (1 + K_a[C^+])[L^-] - [L]^\circ - [Cu^+] + [Cu]^\circ = 0 \quad (6)$$

The free copper concentration may be calculated from the change in cell potential, thus all quantities necessary for the calculation of β_2 are available. Values of β_1 and β_2 are given in Table I for the anions investigated.

Conductance measurements of copper(I) salts of the symmetrical anions perchlorate, tetrafluoroborate, and hexafluorophosphate give association constants of 0, 9, and 15 while the corresponding silver(I) salts are unassociated (*5*). However, silver nitrate has an association constant in acetonitrile of 71 despite appreciable silver(I)–acetonitrile interaction. Therefore the association constant of copper(I) nitrate is of interest. This salt cannot be isolated in sufficiently pure form for high precision conductance work, and so cannot be studied by the technique used for the other copper(I) salts. The potentiometric method described here gave a K_a value of 7 for copper(I) nitrate, but random errors in the measurement technique coupled with possible coordinating trace impurities indicate that the uncertainty in this value is on the order of ±10. Thus, 1 ppt chloride in the tetraethylammonium nitrate would be sufficient to give an association constant of 50.

As an alternate approach, solutions of copper(I) nitrate in acetonitrile were prepared as described in the experimental section and used for potential measurements on the cell

$$Cu(Hg) \left| \begin{matrix} CuClO_4,\ 0.0100M \\ Et_4NClO_4,\ 0.100M \end{matrix} \right|\left| \begin{matrix} CuNO_3,\ 0.01088M \\ Et_4NClO_4,\ 0.100M \end{matrix} \right| Cu(Hg)$$

A potential difference of 2.5 mV was observed, which could be accounted for completely by differences in concentration and by a liquid junction potential of 0.1 mV, estimated by the Henderson equation.

We conclude that the best value for the association constant of copper(I) with nitrate is zero, with an uncertainty of 5. This is on the same order as the association of copper(I) with the symmetrical anions listed above, and indicates that the relatively large K_a value for silver nitrate is not due to unusual behavior of the nitrate ion, but to specific interaction by the silver.

Conductance Measurements. The conductance data for NaSCN and Et_4NNO_3 are given in Table II and the results as analyzed by the Fuoss-Onsager equation in Table III.

RECEIVED for review July 17, 1970. Accepted October 27, 1970. Financial support by the National Research Council of Canada and the University of Alberta is gratefully acknowledged.

Time-Lapse Spectrometry in Organic Photochemistry

Nicolae Filipescu, Fredrick L. Minn, and James W. Pavlik

Departments of Chemistry, The George Washington University, Washington, D. C. 20006, and Wisconsin State University, River Falls, Wis. 54022

Time-lapse spectrometry consists of monitoring absorption spectra after short irradiations, successive determinations of absorption throughout the subsequent dark period, and periodic recording of emission and excitation during and after irradiation. These measurements permit detection of intermediates, calculation of their spectra, quantitative determination of rate constants and reaction orders. The method is invaluable in mechanistic organic photochemistry.

SPECTROMETRY IS AMONG the most valuable analytical tools in chemistry. However, except for flash photolysis, it is used almost exclusively for equilibrium systems. Spectrometric determinations have been used in this laboratory to great advantage, especially in the UV and visible ranges, on systems undergoing chemical changes. These investigations included detection of unsuspected intermediates in complex sequential transformations, quantitative determination of such kinetic parameters as stoichiometry and rate constants, and examination of the behavior of transient species in their reactions with selected analytical reagents.

This procedure was particularly useful for investigating photochemical transformations. Most photochemical processes involve electronically excited molecules originally having energy in excess of the thermal energies required by ground-state reactions. Rather than dissipating by collision, the excess energy tends to remain localized in relatively long-lived intermediates. These species may themselves absorb light and undergo further photochemical reactions or may change to stable products in a dark process. Work on the photoreduction of aromatic ketones (*1–4*) stimulated the use of a technique, time-lapse spectrometry (TLS), which deserves separate discussion; its usefulness, general applicability, and limitations are discussed herein. Although TLS is not restricted to light-induced processes, its use is detailed in organic photochemistry, with some nonphotochemical examples, as well.

EXPERIMENTAL

Reagents. Preparation of 2,3-*exo*(4,5-methylenephenanthrene-11′-*spiro*-1′′-cyclopropane)bicyclo[2.2.1]heptane (*5*), di(4-pyridyl) ketone dimethiodide (*3*), di(*p-tert*-butyl)benzophenone (*2*), and *spiro*(anthrone-10,1′-cyclopropane) (*6*) has been described previously. Spectrograde solvents were used throughout. Irradiations were carried out with a 9W ultraviolet hand lamp (UVS-11 or UVL-22, Ultraviolet Products).

Apparatus and Procedure. Absorption spectra were recorded on Cary Model 14 or 15 Spectrophotometers; emission spectra, on an Aminco-Bowman Spectrophotofluorometer.

In photochemistry, the TLS method consists essentially of three kinds of spectrometric measurements: (1) monitoring absorption spectra of solutions following successive and relatively short intervals of irradiation, (2) consecutive determinations of absorption spectra following a significant photochemical conversion and at intervals throughout the dark until no change is observed for an extended period of time, and (3) periodic recording of emission and excitation spectra, preferrably in the frozen sample but possibly in the liquid phase, in conjunction with or simultaneous to steps 1 and 2. Since many chemical and photochemical reactions are altered by the presence of atmospheric oxygen, it is convenient to degas the reagents under vacuum in reservoirs such as those shown in Figure 1, prior to mixing or irradiation. Although the cell allows examination by emission spectrometry of species detected by absorption, the two spectra could be recorded from separate cells corresponding to "halves" of that illustrated. Dilutions or concentrations of sample can be done conveniently in the sealed cells by cooling the reservoirs in liquid nitrogen.

RESULTS AND DISCUSSION

TLS measurements should probably accompany most mechanistic organic photochemical investigations. Additional valuable information is obtained toward clarifying the overall reaction mechanism, information which cannot be secured by relatively long photolyses followed by product identification. TLS implies a separation of the transformations occurring during irradiation from those taking place in the subsequent dark period. Moreover, the intermediates can be mixed at any chosen time during the transformation with selected coreactants, including acids, oxidizing agents, or chemical trapping agents. Furthermore, quantitative kinetic calculations can easily be performed from TLS data.

The importance of sequential emission measurements should not be minimized. First, analytical measurements based on fluorescence and phosphorescence are in many cases more sensitive and selective than those based on absorption, especially for mixtures (*7–9*). Second, freezing the reacting system may trap transient species physically by arresting diffusion and allow recording of their spectra. Furthermore, low temperatures enhance and clarify fluorescence and add triplet-to-ground-singlet phosphorescence, which is not normally observable in fluids.

There are certain limitations, of course, to the applicability of TLS. First, the transient species must be stable enough that recording time or freezing time be minimal compared to their lifetime. Many reactions will not yield relatively long-lived intermediates. Even in such cases, however, step 1 should be carried out, since it may help to establish stoichiom-

(1) N. Filipescu and F. L. Minn, *J. Amer. Chem. Soc.*, **90**, 1544 (1968).
(2) N. Filipescu and F. L. Minn, *J. Chem. Soc., Sect. B*, **1969**, 84.
(3) F. L. Minn, C. L. Trichilo, C. R. Hurt, and N. Filipescu, *J. Amer. Chem. Soc.*, **92**, 3600 (1970).
(4) N. Filipescu, F. E. Geiger, C. L. Trichilo, and F. L. Minn, *J. Phys. Chem.*, **74**, 4344 (1970).
(5) N. Filipescu, J. R. DeMember, and G. R. Howard, *J. Chim. Phys.*, **1970**, 84.
(6) N. Filipescu and J. W. Pavlik, *J. Chem. Soc., Sect. C*, **1970**, 1851.
(7) C. A. Parker, "Photoluminescence of Solutions," Elsevier, Amsterdam, 1968.
(8) R. S. Becker, "Theory and Interpretation of Fluorescence and Phosphorescence," Interscience, New York, N. Y., 1969.
(9) S. Udenfriend, "Fluorescence Assay in Biology and Medicine," Academic Press, New York, N. Y., 1962.

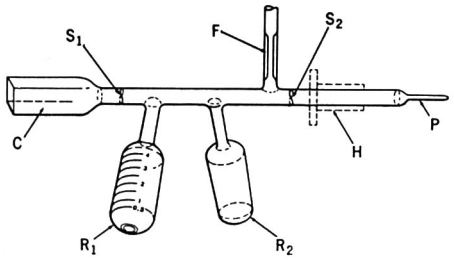


Figure 1. TLS sample cell

C, fused quartz 1-cm² cuvette; R_1 and R_2, degassing side reservoirs, 20 mm i.d. and 50 mm long; *P*, quartz probe for matrix-isolation spectrometry; *F*, flame-sealable constriction tube; S_1 and S_2, quartz-to-borosilicate glass graded seals; *H*, holder for immersion in an Aminco-Bodman or Hitachi-Perkin-Elmer coldfinger Dewar

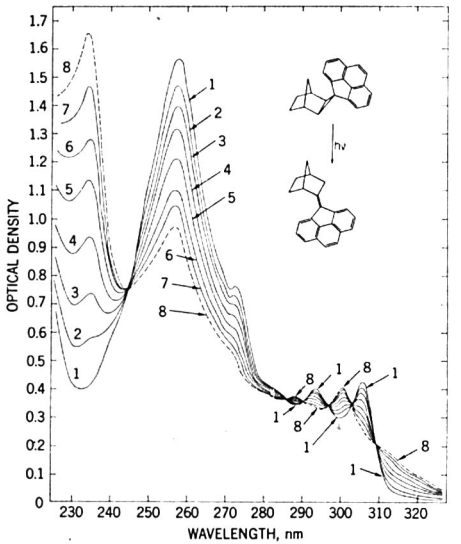


Figure 2 Changes in the UV-absorption spectrum of 1 ($3.0 \times 10^{-5}M$ in isopropyl alcohol) on consecutive irradiation

(1) Before irradiation. (2)–(8) After 1-minute exposures

etry in the first or subsequent photochemical transformations. Second, TLS will not replace flash-photolysis techniques (*10*), which are invaluable for identification of the reacting excited states and of the short-lived products of the primary photoprocess, such as neutral free radicals. Thus TLS essentially borders on the fraction-of-a-second range of flash photolysis. A third limitation is that the results from spectrometric concentration may not necessarily extrapolate to preparative-scale reactions. For instance, during the relatively long irradiation time required to generate sizeable concentrations

(10) See, for example, G. Porter, in "Techniques of Organic Chemistry, Vol. 8," A. Weissberger, Ed., Interscience, New York, N. Y., 1963, p 1055 and references therein.

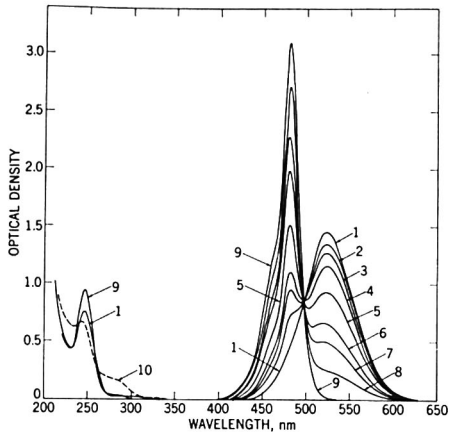
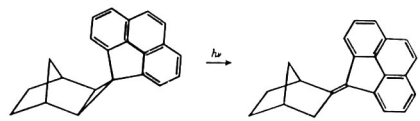


Figure 3. Changes in the UV-visible spectrum of $\sim 10^{-4}M$ solution of 4 in degassed acetonitrile in the presence of zinc

(1) After reaction with zinc was complete. (2)–(9) After 15, 25, 36, 70, 102, 109, 137, and 160 days, respectively, in the dark. (10) After admission of air

of a certain intermediate, the dark reaction may proceed significantly or the intermediate itself may react photochemically. Several other investigations somewhat related to TLS can be found in the recent literature. Time-resolved spectrometry (*11*) yields concentration information from analysis of phosphorescence decay curves. One interesting study (*12*) follows emission spectra in time. Others (*13–17*) refer mainly to thermal reactions, do not exhibit the presence of intermediates, and do not employ emission spectrometry. The examples given below have not been reported previously except for the photoreduction of di-*p*-*tert*-butylbenzophenone, which is included here because it is highly illustrative of TLS.

Illustrative Examples. Figure 2 shows consecutive changes in the UV-absorption spectrum of a rigid model compound **1** undergoing a photorearrangement to **2** upon successive short



1 **2**

(min) irradiations.

This conversion can be followed quantitatively also by monitoring emission spectra either at room temperature or at 77 °K. The characteristic fluorescence of phenanthrene (340–420 nm) is replaced by the intense fluorescence of tri-

(11) P. A. St. John and J. D. Winefordner, ANAL. CHEM., **39**, 500 (1967).
(12) P. F. Jones and A. R. Calloway, 160th National Meeting ACS, Chicago, Ill., Physical Abst 173, 1970.
(13) K. A. Muszkat and E. Fischer, *J. Chem. Soc., Sect. B*, **1967**, 662.
(14) L. Senatore, E. Ciuffarin, and A. Fava, *J. Amer. Chem. Soc.*, **92**, 3035 (1970).
(15) K. R. Huffman, C. E. Kuhn, and A. Zweig, *ibid.*, p 599.
(16) D. K. Lin and C. S. Garner, *ibid.*, **91**, 6637 (1969).
(17) R. D. Temple, *J. Org. Chem.*, **35**, 1275 (1970).

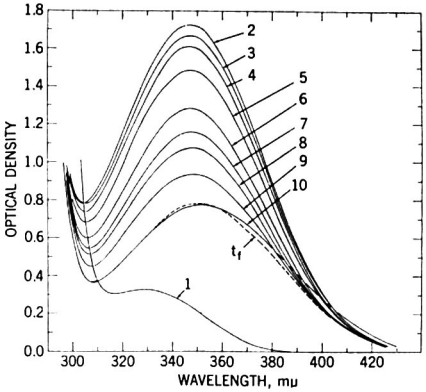


Figure 4*a*. UV absorption spectrum of $1.04 \times 10^{-4}M$ solusolution of TBB in $(CH_3)_2CHOH$ at different times

(1) Before irradiation, (2) after 3-min irradiation (t_0) to 67% conversion, (3) after 30 min of dark reaction (past t_0), (4) after 365 min, (5) 1.8 days, (6) 6.8 days, (7) 9.8 days, (8) 13.8 days, (9) 20.8 days, (10) 33.9 days, (t_f) projected

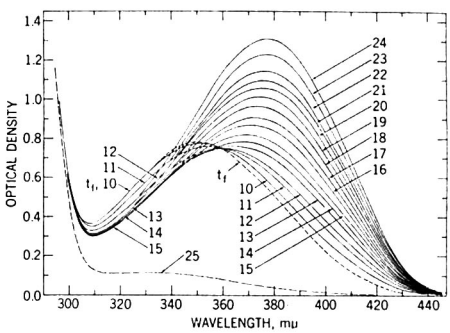


Figure 4b. Continuation of Figure 4a

(t_f) projected, (10) after 33.9 days of dark reaction, (11) 41.8 days, (12) 48.8 days, (13) 55.8 days, (14) 62.7 days, (15) 69.8 days, (16) 76.9 days, (17) 83.8 days, (18) 90.9 days, (19) 97.7 days, (20) 104.7 days, (21) 111.7 days, (22) 118.7 days, (23) 132.7 days, (24) 146.7 and 159.7 (unchanged), (25) after opening and passage of O_2 for 3 min

benzofulvene **2** (structureless band in the 450–540 nm range with λ_{max} 490 nm). The gradual decrease in phenanthrene phosphorescence band (450–580 nm) as the rearrangement proceeds can also be followed by recording emission from samples frozen after each irradiation. Actually, the analogous reaction of *spiro*-linked fluorene–norbornane was used, in connection with TLS, as the photochemical detector for intramolecular energy transfer in two rigid model compounds (*18*, *19*).

Figure 3 illustrates the zero-order conversion of magenta (λ_{max} 523 nm) radical cation **3**, prepared from di(4-pyridyl) ketone dimethiodide **4** and zinc in degassed acetonitrile, to a

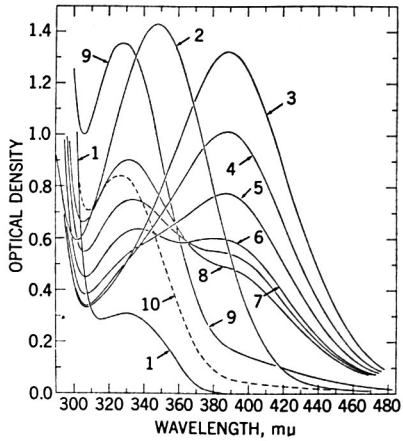
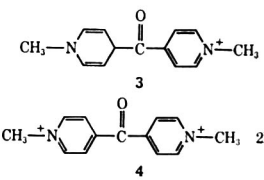


Figure 5. Absorption spectrum of $1.01 \times 10^{-4}M$ solution of TBB in $(CH_3)_2CHOH$. Reaction of the enol intermediate with $(CH_3)_2CHONa$.

(1) Before irradiation, (2) after 3-min irradiation to 52% conversion, (3) after addition of $(CH_3)_2CHONa$ (t_0), (4) 8 min after t_0, (5) 31 min, (6) 66 min, (7) 106 min, (8) 166 min, (9) 1451 min, (10) after 116, 400 min and after bubbling O_2 through the open cell for 1 hour (unchanged)



diamagnetic red species, presumably a zwitterion, (λ_{max} 480 nm) over a period of several months in the dark. The six isosbestic points at 244, 286, 291, 297, 303, and 309 nm in Figure 2 and one at 498 nm in Figure 3 testify to the absence of side reactions and to constant stoichiometry. In addition, they indicate that molecule **2** is photostable. If the behavior is non-isosbestic, the departures may be analyzed by multicomponent absorption spectrometry to give quantitative information regarding the relationship between competitive processes and to determine the absorption spectra of intermediate species.

Figures 4*a* and 4*b* display spectral changes accompanying the dark reaction of the first intermediate generated from di(*p-tert*-butyl)benzophenone (TBB) by an initial brief photolysis. It was demonstrated (*2*) that the intermediate (Curve 2) reacts in a bimolecular process with the residual starting material in competition with a significantly slower reaction in which the enol intermediate (λ_{max} 345 nm) changes in a first-order reaction to a visible-absorbing species (λ_{max} 380 nm). This is illustrated clearly in Figure 4*b*, which gives spectral changes beyond the first stage.

Despite apparent complexity, it was possible to elucidate individual steps responsible for spectral changes in the reaction of the enol intermediate with alkoxide (Figure 5) and to calculate the absorption spectra of three other intermediates,

(18) J. M. Menter and N. Filipescu, *J. Chem. Soc., Sect. B*, **1970**, 464.
(19) N. Filipescu and J. R. Bunting, *J. Chem. Soc.*, in press.

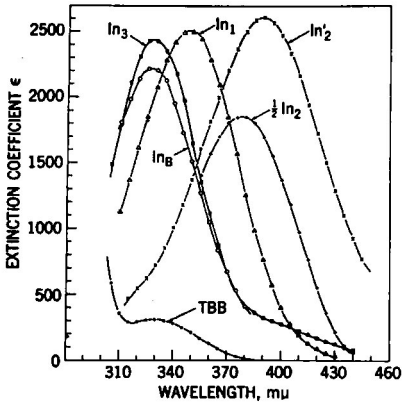


Figure 6. Calculated extinction coefficients for intermediates. The intermediate from unsubstituted benzophenone, In_B, is also included for comparison

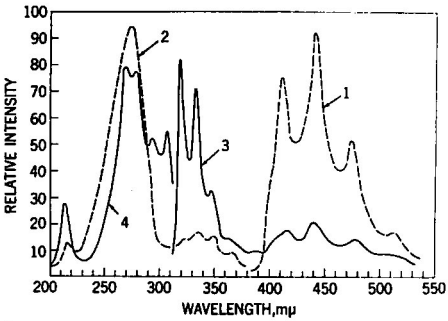


Figure 7. Emission and excitation spectra of $10^{-3}M$ TBB in isopropyl alcohol glass at 77 °K, uncorrected.

Emission (1) and excitation (2) before irradiation. Emission (3) and excitation (4) after 3-min irradiation at room temperature

designated In_2, In'_2, and In_B, in Figure 6. The use of low-temperature emission spectrometry allowed the detection of still another transient fluorescent species in the photoreduction of TBB (Figure 7, Curves 3 and 4).

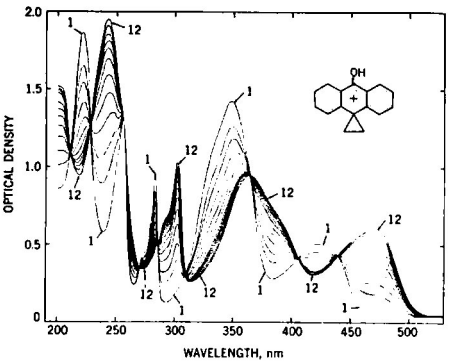


Figure 8. UV-visible absorption spectra of $\sim 10^{-4}M$ of 5 in concentrated H_2SO_4.

(1) Before irradiation. (2)–(12) After consecutive 30-sec exposures to 420-nm light

A final illustration of the wide applicability of TLS to various solvents and solutes is the photolysis of a hydroxycarbonium ion in concentrated sulfuric acid. Figure 8 shows changes in the absorption spectrum of *spiro*(anthrone-10,1′-cyclopropane) in H_2SO_4 upon short exposures to violet light. Again, the gradual changes and the presence of nine isosbestic points at 211, 228, 255, 270, 286, 310, 364, 405, and 439 nm indicated absence of side reactions, constancy of molar relationships among products, photostability and thermal stability of products, and general features of the photoproduct absorption. Furthermore, from knowledge of light intensity, absorbance of solution at the exciting frequency, and duration of the consecutive irradiations, one can estimate the efficiency of the photoreaction.

ACKNOWLEDGMENT

We thank Mr. W. Carrion and Dr. H. Plotkin for their continued interest.

Received for review July 10, 1970. Accepted October 12, 1970. Work partially supported by the Atomic Energy Commission Contract AT-(40-1)-3797. Part of this work was carried out in the Optical Systems Branch of Goddard Space Flight Center, NASA.

The Question of Instrumental Artifact in Linear Sweep Voltammetry with Positive Feedback Ohmic Drop Compensation

Eugene E. Wells, Jr.

Power Sources Division, Electronic Components Laboratory, USAECOM, Fort Monmouth, N. J.

The question of artifact introduced by the severe demands of positive feedback on the instrumentation has been treated for the particular case of linear sweep voltammetry. It was possible to formulate experimentally applicable theoretical criteria for rejecting voltammograms which suffer from either or both of the maladies which define the upper limit of scan rate for this technique: uncompensated solution resistance and bandpass related instrumental artifact. The effect of the faradaic reaction has been specifically included in the treatment.

A GROWING BODY of literature attests to the popularity of positive feedback techniques as a means of conquering the ohmic drop problem in potentiostatic studies (*1*, *2* and references therein). Several attempts to predict, using the criteria for system stability, the amount of resistance which can be "removed" by positive feedback have appeared, and the severe demand of the technique on instrumental bandpass has been duly noted (*1*, *2*). Yet there has been little interpretation of how these problems relate to the user of positive feedback compensation and his goal of obtaining a cell response which is uncontaminated by the masking effect of ohmic resistance, but which is a true measure of the remaining electrochemical parameters.

Zero effective (apparent) solution resistance is virtually impossible to achieve with existing apparatus and normally studied solutions, because if sufficient positive feedback is applied, the system becomes unstable and oscillates (*1*). Thus it is important to determine the effective resistance of each experimental solution at the maximum achievable degree of feedback, for this quantity determines the current which may be passed in a potentiostatic experiment before ohmic drop becomes a detectable artifact. Part of the present work, therefore, describes a convenient procedure for resistance measurements.

A second possible source of artifact, instrumental bandpass, determines how "instantaneously" the apparatus can correct an applied voltage signal for ohmic drop. Consider how the perfect compensator would function in response to the first trickle of current through the cell, itself the result of a changing applied voltage (Figure 1).

A voltage signal proportional to the instantaneous current through the cell would be generated by resistor R_f, amplified by the compensating operational amplifier, A_2, and mixed with the signal from the voltage generator at the potentiostat input. The signal which now appears at the potentiostat control points would not be the instantaneous signal generator voltage, but a signal increased by such an amount that it becomes identical to the (desired) generator voltage in the interphase region, after dropping through the resistance of the solution. The electrochemical system would respond with a current which is dependent upon the kinetics of the electrochemical process, thus providing the beginning of another cycle.

If it is now realized that every real potentiostat has noninfinite frequency response and therefore a propagation delay, it should be clear that for some (large) rate of change of the generator voltage, the correcting signal from the compensating amplifier will be significantly late in arriving at the mixing point. The exact speed at which this behavior becomes detectable as artifact in the observed current would depend on the rate of change of current with voltage (a function of the kinetics of the electrode process) and the sensitivity of the electroanalytical technique to deviations from the assumed voltage input.

The theoretical development of this paper is pointed toward linear sweep voltammetry (*3*), principally because of the almost (*4*) total neglect of the technique in the literature of ohmic drop compensation. However, most of the results are independent of the voltage function, and the approach is applicable to other voltammetric techniques. The significant feature is that the faradaic reaction has been considered in determining bandpass behavior.

THEORY

The present treatment allows for instrumental nonideality by incorporating the potentiostat gain function in terms of its associated time constant. The compensating operational amplifier used in this work has several orders of magnitude greater frequency response than the potentiostat and is assumed to possess an ideal (*i.e.*, frequency independent) gain function.

In the mathematical derivations which follow, extensive use has been made of Laplace transformation (*5*) as a means of obtaining simple algebraic relationships. Thus, the variable parameters appear in terms of the (complex) Laplace variable, s, which has the dimensions of frequency. The theory is most conveniently formulated through the use of an analog electrical circuit to describe the electrochemical portion of the system. An adequate description of working electrode behavior for most cases of interest is provided using the circuit of Figure 2, in which the solution resistance terminates in the double layer capacitance, which is itself shunted by a faradaic impedance (*6* and references therein). In terms of the Laplace variable the impedance function, Z_E, for such a circuit would be written as follows (*1*):

$$Z_E(s) = R_s + \frac{1}{1/Z_F(s) + C_d s} \qquad (1)$$

in which $Z_F(s)$ is the faradaic impedance function. The specific form of Z_F would depend on the type, complexity,

(1) A. A. Pilla, R. B. Roe, and C. C. Herrmann, *J. Electrochem. Soc.*, **116**, 1105 (1969).
(2) E. R. Brown, D. E. Smith, and G. L. Booman, ANAL. CHEM., **40**, 1411 (1968).
(3) R. S. Nicholson and I. Shain, ANAL. CHEM., **36**, 706 (1964).
(4) E. R. Brown, T. G. McCord, D. E. Smith, and D. D. DeFord, *ibid.*, **38**, 1119 (1966).
(5) R. V. Churchill, "Operational Mathematics," McGraw-Hill New York, N. Y., 1958.
(6) A. A. Pilla and G. J. DiMasi, *Advan. Chem. Ser.*, **90**, 1969.

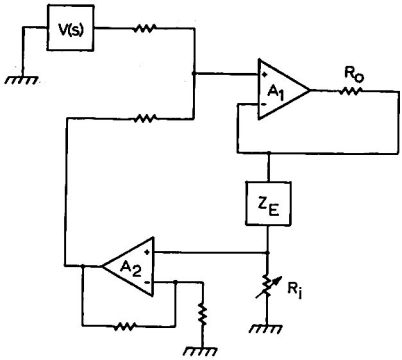


Figure 1. Instrumentation for positive feedback ohmic drop compensation

Z_E represents the working electrode impedance, A_1 and A_2 the potentiostat and feedback amplifier, respectively, R_i the adjustment for degree of feedback and R_o, the potentiostat output impedance

and kinetics of the particular faradaic reaction (*6*), but for reasons which will become apparent momentarily, Z_F need not be specified in detail if we restrict ourselves to the goals stated in the introduction. Note that the component values need not be independent of potential over the several hundred millivolt voltage excursions common in linear sweep voltammetry. Thus, unless otherwise stated, C_d and Z_F have voltage as a functional argument, even though the symbology has been omitted for brevity. Solution resistance is assumed to be independent of electrode voltage.

Equation 1 implies that a separation of current flow between the faradaic and capacitative branches is possible, at least in principle, for by Ohm's law:

$$i_F(s) = \frac{V(s)}{Z_F(s)} \tag{2}$$

$$i_c(s) = \frac{V(s)}{1/C_d s} \tag{3}$$

The ratio of Equations 2 and 3 provides the following convenient working form:

$$k(s) \equiv \frac{1}{C_d s Z_F(s)} \tag{4}$$

where k is a function of potential as are C_d and Z_F. This result will be used later.

The procedure by which the system transfer functions may be combined to provide a meaningful description of the current–voltage behavior of the circuit of Figure 1 has been outlined in some detail (*1*) and will not be repeated here. Thus, the following equation is the result of straightforward procedures and is a general form of an equation already derived and tested for the same instrumentation using the particular case of an RC analog cell (*1*).

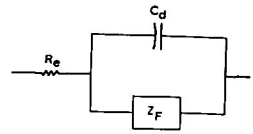


Figure 2. General equivalent circuit representation of the working electrode

R_s is the solution resistance; C_d, the electrode capacitance; and Z_F, a general faradaic impedance

$$i(s) = \frac{K V(s)}{[Z_E(s) + R_o + R_i](s\tau + 1) + [Z_E(s) + R_i - R_i K_2]K} \tag{5}$$

In Equation 5, K is the potentiostat gain, $V(s)$ the signal generator voltage function, τ the potentiostat time constant, and K_2 the (constant) gain of the feedback operational amplifier. Other parameters are as indicated in Figure 1. The equation is applicable to the system whether stable or oscillatory, and if Z_E were known, could be used to theoretically predict the critical damping point following the procedure that has been used successfully for RC cells (*1*). For faradaic cells, the procedure involves considerable difficulty and many assumptions, and for this work a non-oscillating system will be assumed, leaving to the experimentalist the task of assuring that this is indeed the case.

Upon substituting Equation 1 into 5, simplifying, and making the substitutions:

$$\tau_c = (R_s + R_o + R_i) C_d \tag{6}$$

$$\tau_u = (R_s + R_i - R_i K_2) C_d = R_u C_d \tag{7}$$

$$\tau_s = \tau/(K + 1) \tag{8}$$

the current may be expressed as follows:

$$i(s) = \left[\frac{K}{K+1}\right] \frac{V(s)\,[C_d s + 1/Z_F(s)]}{\tau_c \tau_s s^2 + \left[\tau_s + \frac{\tau_c}{K+1} + \tau_u + \left(\frac{R_s + R_o + R_i}{Z_F(s)}\right)\tau_s\right] s + 1 + \frac{R_s + R_o + R_i}{Z_F(s)(K+1)} + \frac{R_u}{Z_F(s)}} \tag{9}$$

Equation 9 predicts the current response to any perturbing voltage function $V(s)$ for a cell of the type of Figure 2 in the circuit of Figure 1.

If Z_F in Equation 4 is expressed in terms of $k(s)$ and the result substituted into Equation 9, the following expression is obtained:

$$i(s) = \left[\frac{K}{K+1}\right] \times \frac{[1 + k(s)]\,V(s)\,C_d s}{[1 + k(s)]\tau_c \tau_s s^2 + \left[\tau_s + \frac{[1 + k(s)]\tau_c}{K+1} + [1 + k(s)]\tau_u\right] s + 1} \tag{10}$$

The goal of this analysis was to determine under what conditions a compensated voltammogram is truly a measure of the cell response. The answer hinges upon finding conditions under which instrumental parameters become insignificant in Equation 10. In mathematical terms frequency derived (bandpass) artifacts will be absent when:

$$\text{ASSUMP} \cong 1 \tag{11}$$

where

$$\text{ASSUMP} = \frac{[1 + k(s)]\tau_u s + 1}{[1 + k(s)]\tau_c\tau_u s^2 + \left[\tau_c + \frac{[1 + k(s)]\tau_c}{K + 1} + [1 + k(s)]\tau_u\right]s + 1} \quad (12)$$

Since the time constants are easily measured in a manner to be described below, further progress depends upon finding $k(s)$ and s, which are functions of the presumably unknown electrochemical mechanism, scan rate, voltage, etc. Unfortunately, it is not convenient to derive these values theoretically because of the nonequilibrium conditions which prevail in linear scan voltammetry. It is possible, however, to measure these parameters, after the fact, from the observed voltammogram. In so doing, the range of s which need be considered is limited to those frequencies actually present to significant degree. Furthermore $k(s)$, which is potentially troublesome because the degree of s is unknown (see Equation 4), is bounded and finite and has observable potential dependence. When evaluated in this manner, Equation 12 becomes a rejection criterion for artifact contaminated data.

Examination of Equation 12 suggests that large values of s are a worst case, as might be expected. Thus, of the frequencies required to synthesize the voltammogram to any given point, it is the maximum significant contributor which should be used to determine if the data is valid. Procedures for finding and using maximum s will be presented in the discussion section. As for $k(s)$, the worst case value depends upon the absolute magnitude of the time constants. Both extremes should therefore be tested. It should also be noted that Equation 12 is a sluggish function of $k(s)$ in any case, and that the significance of this parameter in determining the accuracy of data is usually not as great as that of the frequency.

For the remaining derivations, it is convenient to adopt the fundamental assumption of equivalent circuit impedance analysis that the circuit components are independent of potential (6). In the absence of faradaic reactions, the assumption is reasonable over even moderately large potential excursions, as is evidenced by the nominally flat background traces frequently encountered in linear sweep voltammetry. The assumption of RC cell behavior with potential independent components makes possible the convenient use of Equation 9 for direct analysis of the cell response, an approach which leads to an extremely convenient method of determining solution resistance and capacitance.

From the equivalent circuit point of view, choosing a potential region where faradaic processes are absent corresponds to selecting conditions under which Z_F is infinite. After taking the indicated limit in Equation 9, we have:

$$i(s) = \frac{K}{K + 1} \frac{V(s)\, C_d s}{\tau_c\tau_u s^2 + \left[\tau_c + \frac{\tau_c}{K + 1} + \tau_u\right]s + 1} \quad (13)$$

Assume at this point that

$$\tau_c + \frac{\tau_c}{K + 1} \ll \tau_u \quad (14)$$

$$\tau_c\tau_u s \ll \tau_u \quad (15)$$

which is equivalent to assuming that cell current reflects only effective cell parameters, with no contribution from potentiostat nonideality or inherent cell resistance.

Under these conditions, and since $K/K+1$ is very nearly unity for potentiostats with high gain, Equation 13 reduces to:

$$i(s) = \frac{V(s)\, C_d s}{\tau_u s + 1} \quad (16)$$

Upon substituting the voltage function for a linear sweep:

$$V(s) = \upsilon/s^2 \quad (17)$$

where υ is the scan rate, dV/dt, and converting to the time domain (5), the following result is obtained:

$$i(t) = \upsilon C_d\,[1 - \exp(-t/\tau_u)] \quad (18)$$

Thus the expected current response is exponential in form, attaining a final value of $i(\infty) = \upsilon C_d$. Equation 18 may be rearranged to give:

$$\ln \frac{i(\infty) - i(t)}{i(\infty)} = \frac{-t}{R_u C_d} \quad (19)$$

in which the value of τ_u was obtained from Equation 7. Thus, a plot of $\ln[i(\infty) - i(t)/i(\infty)]$ *vs.* time should be linear with slope $-1/R_uC_d$. Since C_d is simply $i(\infty)/\upsilon$, the value of R_u is calculable. It is important to note that the linearity of the plot of Equation 19 justifies assumptions 14 and 15, and implies the potential independence of C_d, at least over the voltage range traversed in acquiring the data.

It should be clear from examination of Equation 7 that if the effective resistance at any one degree of compensation is also known, the resistance at any other degree of compensation is also known. If R_u represents the unknown effective resistance at R_i, the pertinent relationship is:

$$R_u = R_u^* + (K_2 - 1)(R_i^* - R_i) \quad (20)$$

where R_u^* was measured using Equation 19 at R_i^*.

DISCUSSION

The experimentalist of high speed relaxation techniques is concerned mainly with two problems: how much resistance can be compensated without oscillation and how fast can one make measurements without exceeding the bandpass of the instrument. The two phenomena are of course related, and coupled inseparably to the electrochemical system, a fact which makes absolute prediction of the conditions which will give artifact free voltammograms impossible in the absence of prior knowledge of the mechanism. Nevertheless, it is possible to identify at the bench those data which are free of artifacts of the type considered here, and to define the effective resistance of the solution accurately enough for most practical work.

Effective Resistance Calculation. The successful determination of solution resistance requires attention to two details. It must be ascertained that the cell behaves as an RC circuit, as was assumed, and that artifacts arising from insufficient instrumental bandpass are absent. The fundamental test of both points is a $\ln(i)$ *vs.* t plot, which is predicted by Equation 19 to be linear with slope $-1/R_uC_d$ if the above conditions are satisfied. That these conditions can be met in practice is indicated by representative data from a real electrochemical system, tetrapropylammonium perchlorate in dimethylformamide under a high degree of positive feedback (Figure 3, curve *a*). The remaining curves of the figure were obtained at increasing degrees of compensation, and curve *c* represents the onset of oscillation. At lower degrees of compensation, plots were always linear. Since it is observed that the final current, which is proportional to C_d, does not change with the degree of compensation, the changing

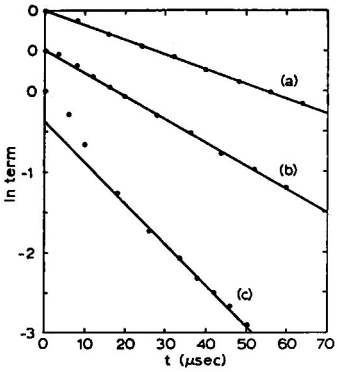


Figure 3. Effect of degree of compensation on plots of Equation 19 for TPAP in DMF

The vertical axis has been displaced 0.5 ln unit per curve. The lines represent the theoretical slope calculated from curve (*a*) using Equation 20; the dots are experimental points. Curves *a*, *b*, and *c*, represent R_u values of 123 ohms, 83 ohms, and 43 ohms, respectively

slope of the plots reflects changes in the value of the effective resistance.

Regrettably, for this and many other systems, the curves taken near the limit of maximum compensation are decidedly nonlinear at short times. This behavior is not as surprising as it would at first seem if a simple calculation based on Assumptions 14 and 15 is made. Using measured values of $\tau_s = 0.22$ microsecond and $K = 3000$ for the potentiostat, and $\tau_c = 183$ microseconds as determined from curve *a* of Figure 3, it may be verified that Equation 14 holds under the conditions ($\tau_u = 36$ microseconds) of Figure 3*b*. Assumption 15, however, is invalid for the 10^6 Hz maximum significant frequency (determined using the rule of thumb to be described below) associated with the raw current–time curve which led to Figure 3*b*. This suggests that under the conditions of Figure 3*b*, the unsimplified Equation 13 must be used to adequately characterize the system. Since Equation 13 describes the system in terms of multiple time constants it is not surprising that the logarithmic plots of Figure 3*b*,*c* seem to involve multiple slopes.

Since it is normally desired to operate at the maximum allowable compensation, means should be available to determine the resistance under just these conditions. This may be accomplished by measuring the (constant) gain of the compensating operational amplifier and using Equation 20 to obtain the effective minimum R_u from that determined at any other degree of compensation using the plot.

A measure of the reproducibility which can be achieved in determining resistance and capacitance values from the charging curves is presented in Table I. The observed R_u and C_d values were obtained at varying degrees of compensation from linear logarithmic plots of Equation 19. Then, using Equation 20, the total electrolyte resistance (R_u at $R_f = 0$) was calculated and checked for constancy. Although the agreement is excellent, it must be remembered that it is the absolute deviation rather than the percentage deviation in a measured R_u which is transmitted to the R_u calculated for maximum compensation. The scan rate at which resistive errors significantly affect the voltammogram is fairly well defined in spite of this large percentage uncertainty in R_u, for the change in the voltammogram is a fairly sluggish function of R_u (*7*). Furthermore, the magnitude of R_u is usually very small since the apparatus described compensates 90–98% of the inherent resistance of the solution (*1*).

Table I. Reproducibility of Resistance–Capacitance Determinations in 0.10*M* TPAP–DMF

Ohms			
R_f	R_u	R_s	C_d, μF
74.6	117	439	0.438
63.5	193	437	0.440
53.5	212	443	0.438
43.5	252	440	0.436
33.5	296	441	0.436
23.5	339	441	0.436
13.5	380	438	0.436
0.0	442	442	0.438
0.0	436	436	0.438

Thus, it is possible to obtain usably accurate values of resistance and capacitance in the absence of faradaic reaction. It is important to realize that the value of R_u should be unchanged by the presence of a faradaic process, for its value is determined solely by the setting of the compensating resistor and the gain of the compensating operational amplifier, unless bandpass or oscillation problems develop. Thus, the value of R_u determined can be expected to remain accurate whatever the electrochemistry, unless stability problems necessitate readjustment of the compensator, and even then the new R_u is easily calculable using Equation 20.

Maximum Usable Scan Rate Problem. As the scan rate increases, the voltammetric current–time plot becomes increasingly steep, a fact which indicates increasingly high frequency content. At some scan rate (the magnitude of which depends in part upon mechanism), the frequencies required to produce the voltammogram will exceed the bandpass of the instrument. At this point the instrument can no longer supply a sufficiently rapid current change, and the observed current response lags the theoretical. The error thus described may be referred to as bandpass artifact, similar in behavior to, but distinct from the effect of an observable iR_u. In order to quantitatively assess whether or not this phenomenon is present in a given voltammogram, two data are needed in addition to the time constants obtained above: the maximum frequency which is significant in a synthesis of the curve and the faradaic to capacitative current ratio $k(s)$, which is a function of the mechanism.

An accurate value of s may be obtained by frequency analysis (*8*) of the experimental waveform, but for most purposes the following rule of thumb, paraphrased from the sampling theorem (*8*), is sufficient: the reciprocal of the minimum time interval over which a significant change in current occurs is greater than or equal to the maximum frequency required to synthesize the curve. For example, suppose there is a voltammogram for which it is desired to study the time interval up to and including the current peak, and that a current accuracy of 1% of the maximum is desired. Locate the time interval of the voltammogram in which this quantity of current is traversed most rapidly. The reciprocal of the time period

(7) R. S. Nicholson, ANAL. CHEM., 37, 667 (1965).
(8) F. H. Raven, "Automatic Control Engineering," McGraw-Hill, New York, N. Y., 1968.

Table II. Maximum Scan Rate for Artifact Free Performance for Various Cells[a]

	Ohms				
	R_s	R_u[b]	C_d, μF	ν_{max}[c], volts/sec	$I/I_{R=0}$[d]
1	1.0	0.69	0.500	145 (5)	0.9982
2	5.0	1.79	0.500	85 (5)	0.9969
3	10.0	2.62	0.500	60 (5), 380 (20)	0.9963, 0.9911
4	50.0	6.10	0.500	25 (5)	0.9945
5	100.0	8.71	0.500	15 (5), 100 (20)	0.9940, 0.9852
6	500.0	19.63	0.500	4 (1), 35 (5)	0.9931, 0.9804
7	1000.0	27.75	0.500	1 (1), 17 (1)	0.9950, 0.9807
8	5000.0	61.37	0.500	0.04 (0.01)	0.9976
9	100.0	18.96	0.100	30 (5)	0.9824
10	100.0	13.60	0.200	20 (5)	0.9895
11	100.0	6.19	1.00	13 (1)	0.9959
12	100.0	2.77	5.00	10 (1), 60 (5)	0.9982, 0.9960
13	100.0	1.95	10.00	10 (1)	0.9986
14	100.0	12.00	0.500	21 (1), 140 (5)	0.9905, 0.9763
15	100.0	15.00	0.500	26 (1), 170 (5)	0.9869, 0.9677
16	100.0	20.00	0.500	36 (1), 210 (5)	0.9798, 0.9533
17	100.0	50.00	0.500	131 (1)	0.9148

[a] Based on calculations using a modification of the method of Nicholson (7). Assumed parameter values were: concentration (1.0 m*M*), electrode area (0.09 cm²), diffusion coefficient (9×10^{-6} cm²/sec). A capacitative current νC_d is included

[b] Except for values 14–17, uncompensated resistances selected are the minimum based on stability criteria, Equation 17, ref (*1*).

[c] Determined by iteration of scan rate using the interval indicated in parentheses. Frequency analysis was by sampling theorem rule of thumb. When two values appear, Fourier analysis was used for the second.

[d] Calculated peak current under the indicated conditions, divided by the peak current for zero resistance. When present, a second value is the result for the Fourier scan rate of the previous column.

thus found is, it should be emphasized, always greater than or equal to the highest frequency needed to synthesize the curve. In other words, the s obtained is a worst case frequency.

The problems encountered in determining $k(s)$ are of a different nature. In deriving the theory, it was assumed that measurement of both faradaic and capacitative currents could be achieved. Yet there are procedural difficulties, for the observed current appears as the sum of the two. If it could be assumed that the value of the capacitance were independent of the faradaic process, then the currents could be separated by subtracting the background, obtained before addition of the electroactive species, from the total current. The success of capacitance compensators (*4*) which subtract the current of a matched cell without electroactive species from the cell response, suggests that the assumption of a background current which is independent of the electroactive material is often a good approximation. Note that any adsorption of the electroactive species is considered by this treatment to be faradaic, and is germane to the present question only inasmuch as it simultaneously alters the electrode capacitance which was present in the background. In any case, we shall continue to assume that the faradaic and capacitative currents are separable by difference of background from the total. Under these conditions, $k(s)$ takes on values from zero at the foot of the wave to a maximum of the peak faradaic current divided by the background current. Since the error criterion Equation 12 is a sluggish function of $k(s)$, small errors due to the problems described above will be insignificant. Nonetheless, the careful worker will examine the error criterion using both extrema of $k(s)$ before concluding that a voltammogram is free of artifact.

Thus far, the point of view of the experimentalist has prevailed. Means were devised to evaluate experimental voltammograms for possible artifact. This approach had the advantage not only of being generally applicable, but also avoided the difficulty of attempting to derive meaningful faradaic impedance functions under the nonequilibrium conditions of cyclic voltammetry. Yet it would be useful if some means were available to predict the conditions under which the compensator could be expected to produce reliable data. Nicholson (*7*) has provided such a means in the form of a computational technique which leads to theoretical reversible voltammograms contaminated by ohmic drop. Thus, for a selected set of time constants it is possible to generate a voltammogram at any given scan rate, test it against Equation 12, and iterate scan rate until conditions are found under which the assumptions just fail. In this manner, maximum scan rates may be determined for any given set of initial resistance and capacitance values. The results of such computations are presented in Table II. The calculations include a time independent capacitative current equal to $C_d dV/dt$ which contributes to the total iR_u, but not to s. The determination of s was, for the most part by use of the sampling theorem, but for comparison certain cases were treated by the more extensive Fourier analysis. The Fortran IV program used in the calculations will be provided on request.

From the results it can be presumed, for example, that a 1000-ohm solution compensated to 28 ohms with a capacitance of 0.5 μF could be studied at scan rates as high as 17 volts/sec with confidence. The companion value of 1 volt/sec based on the sampling theorem serves to indicate the safety margin in the proposed rejection criteria for experimental results. It should be noted that irreversible and other kinetic mechanisms which give broadened voltammograms when compared to the reversible case (*3*) would allow the use of higher scan rates because of the reduced frequency content. Reducing the concentration of reactant, decreasing electrode area, etc., from the assumed values (Table II) would have a similar effect.

Data 9–13 of Table II serve to illustrate the effect of capacitance on the compensated voltammograms. Although the minimum achievable R_u decreases with increasing capacitance as expected (*1*), the cell time constant increases markedly. The result is that the maximum safe scan rate decreases as well. It is possible to achieve increased scan rates by reducing the degree of compensation, as is illustrated by data 14–17, but this sometimes occurs at the expense of a shift in peak potential and a reduction in peak current due to iR_u drop.

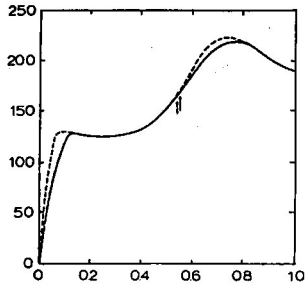


Figure 4. Effect of bandpass artifact on a linear sweep voltammogram at 430 V/sec

The broken line is uncompensated aqueous iron oxalate, the solid line is the same solution, but with 825 ohms added and fully compensated. R_u for both curves is the same. Time is in msec and current in μA

There is clearly an optimal adjustment of the compensator which will maximize achievable scan rate while minimizing observable resistance effects.

Results such as these emphasize the need for a knowledge of specific parameter values in analyzing results obtained with the compensator. The calculations, while adequate to indicate trends, are not sufficiently general or convenient to substitute for the error criteria developed here. They should, however, be useful in the planning stage of a contemplated experiment.

The question remains of the expected behavior of a system in which the bandpass has been exceeded. To provide a valid illustration, it is necessary to eliminate the effect of iR_u, which mimics the behavior of bandpass artifact. This was accomplished by taking voltammograms of the same solution, in one case with zero compensation at the native resistance of the solution and in the other with artificially added resistance just compensated to the same R_u as before. Thus, external resistors were added to a cell containing aqueous iron oxalate with 23 ohms of inherent resistance until the fully compensated effective R_u was 23 ohms. The added resistance at this point was 825 ohms. The voltammograms with added resistance and compensation were then compared to those with neither added resistance nor compensation as the scan rate was incrementally increased. The results for the slowest scan rate at which there is noticeable difference in the two traces (at slower scan rates the traces are superimposable) is presented in Figure 4.

Frequency analysis of the compensated trace of Figure 4 provides, using the rule of thumb mentioned earlier and the interval indicated, a value of 10^3 Hz as the maximum significant frequency. The worst case current ratio for this example occurs if $k(s) = 1$ (its maximum value). Using these data and the observed $\tau_c = 0.25$ microsecond, $\tau_f = 1480$ microseconds, and $\tau_u = 40$ microseconds, it is easily verified that Equation 12 reduces to 0.54. This result suggests that the voltammogram should be rejected, as expected.

Figure 4 serves also to illustrate several points which have not been rigorously explored. Note that the compensated trace shows artifact in the capacitative region, but that the current has managed to "catch up" at the foot of the faradaic wave. This indicates that the voltage form in the interphase region is again linear, and that the artifact early in the capacitative charging does not affect interpretation of the faradaic wave. Note also that beyond the faradaic peak, the two traces of Figure 4 again become superimposable. This behavior reflects the reality that the diffusion gradients, etc. which control the current (*3*) are most sensitive to the immediate past history of the voltage. As the time since deviation from the assumed linear voltage sweep increases, the effect on the current decreases. This suggests that if a second faradaic peak were located just beyond the right hand boundary of Figure 4, it would probably be fair to place quantitative significance upon the current behavior of that peak also, in spite of the earlier deviation. For the same reasons, the reverse scan in compensated cyclic voltammetry may probably be ascribed significance if the forward scan extended sufficiently far beyond the peak, but quantitative treatment of these effects is beyond the scope of the present paper.

EXPERIMENTAL

The potentiostat used for this work was the ultrafast rise Tacussel PIT-20-2A. The compensating operational amplifier was an Optical Electronics, Inc., Model 9186, which features 1 GHz unity gain crossover frequency, operated at a nominal gain of five. The signal generator was a Tacussel GSTP-2A, equipped with a Burr-Brown Model 3018 as voltage follower. Readout was accomplished with the Textronix Model 565 dual beam oscilloscope equipped with 3A7 plug-in preamps. The apparatus was configured as shown in Figure 1.

The compensator is normally adjusted using a low level (5–50 mV), high slope ramp voltage function. A base voltage is selected in a region where faradaic reactions seem to be absent, and the compensating resistor, R_i, is increased until the current rise just overshoots the final value. R_i is then backed off until the current response is flat-topped, with no detectable overshoot. Resistance measurements are normally taken at this point. The measurement of the compensating amplifier gain, K_2, and potentiostat time constant, τ_s has already been described (*1*). All data were obtained at the hanging mercury drop electrode.

Chemicals were purchased from standard sources. Dimethylformamide (DMF), was stored over molecular sieves for several weeks before use. Tetrapropylammonium perchlorate (TPAP) was synthesized from the hydroxide and perchloric acid and crystallized several times from ethanol–water.

ACKNOWLEDGMENT

Thanks are due to A. A. Pilla and R. B. Roe for many helpful discussions.

RECEIVED for review May 14, 1970. Accepted October 19, 1970.

Photon Activation Analysis—A Review

George J. Lutz

Activation Analysis Section, Analytical Chemistry Division, National Bureau of Standards, Washington, D. C. 20234

Prior to the availability of high-energy electron accelerators, photon activation analysis was limited to the determination of deuterium and beryllium with isotopic gamma-ray sources. During the past 15 years, however, the development of high-current cyclic and linear electron accelerators has made possible many analyses not readily acomplished by other methods. These include the determination of carbon, nitrogen, and oxygen at levels well below 1 μg. This review discusses the determination of beryllium and deuterium with isotope sources; accelerator-produced photons and nuclear considerations in photon activation analysis; the determination of carbon, nitrogen, and oxygen; the determination of heavier elements, with emphasis on biological, geochemical, oceanographic, and forensic matrices; and errors and corrections in photon activation analysis.

ACTIVATION ANALYSIS is now being widely used in a variety of analytical problems, particularly where high sensitivity is required. Because of the general availability of nuclear reactors, and the large cross sections of many nuclides for thermal-neutron capture, the greater part of this work is being performed with thermal neutrons. Sensitivities of 10^{-9} gram are not unusual.

There are, however, a number of elements, such as beryllium, carbon, nitrogen, oxygen, iron, and lead, which are not highly activated with thermal neutrons. In addition, severe difficulties due to sample self-shielding are encountered when a mixture to be analyzed contains substantial amounts of elements with large thermal-neutron capture cross sections. Photon activation analysis is useful in many of these situations.

Apparently, the earliest work in photonuclear activation analysis was done by Gorshov and coworkers (*1*), who determined beryllium by prompt neutron emission with a radium source. This work was accomplished in the late 1930's, which makes it contemporary with the experiments of Hevesy and Levi (*2*) and of Seaborg and Livingood (*3*), which are considered the genesis of activation analysis.

The initial efforts utilizing bremsstrahlung from an electron accelerator were made by Basile, Hure, Leveque, and Schuhl (*4*), in 1954. They determined oxygen in various organic materials with a betatron.

Much of the early systematic work in photonuclear activation analysis can be attributed to Engelmann (*5*) and Albert (*6*). They have discussed the practical aspects of bremsstrahlung production with an electron accelerator, the principles of photon activation analysis, and a number of useful determinations. Subsequently, journal articles and conference proceedings numbering almost 200 have described the determination of about 40 of the elements with photons varying in energy from 1.33 to 70 MeV.

This review will consider, in order, the determination of beryllium and deuterium with isotope sources; accelerator-produced photons and nuclear considerations in photon activation analysis; applications in the determination of carbon, nitrogen, and oxygen; applications in the determination of the heavier elements; production and analytical uses of metastable isomers; and errors and corrections in photon activation analysis.

DETERMINATION OF BERYLLIUM AND DEUTERIUM

The only stable nuclides with neutron binding energies less than the energies of gamma rays emitted in radioactive decay are ^{9}Be and deuterium. Their thresholds for (γ,n) reactions are 1.67 and 2.23 MeV, respectively. At photon energies less than about 4 MeV, the photodisintegration of these two nuclides and some isomeric excitations are the only nuclear reactions of consequence to activation analysis.

As noted in the introduction, the determination of beryllium was first accomplished by Gorshov and coworkers in the later 1930's. Contemporary methods were developed by Gaudin *et al.* (*7*, *8*) in the early 1950's. The isotope source used is almost invariably ^{124}Sb, of activity levels ranging from 0.2–2 curies. For most efficient utilization of the source activity, the sample is usually arranged in an annular configuration surrounding the source. The photoneutrons are moderated and detected with BF_3 tubes or scintillation counters, or are captured in a suitable target such as indium or silver and the induced radioactivity in the target is then measured. The whole assembly is shielded so that there is no gamma-ray or neutron hazard to personnel working with the equipment. With efficient neutron detectors and a source strength of about a curie, sensitivities of a few micrograms are possible. A serious potential source of error is absorption of neutrons by elements in the sample.

Useful descriptions of equipment and technique include those by Goldstein (*9*), Bisby (*10*), Knight *et al.* (*11*), Plaksin *et al.* (*12*), and Mountjoy and Lipp (*13*). Brownell (*14*) has described a portable instrument for field work. Mezhiborskaya (*1*) has written a treatise on the determination which contains much worthwhile material on safety considerations as well as on laboratory equipment.

(1) K. B. Mezhiborskaya, "Photoneutron Method for Determining Beryllium," Gosatomizdat, State Press for Literature of Atomic Science and Technology, Moscow (1961).
(2) G. Hevesy and H. Levi, *Math.-Fys. Meddeleser*, **14**, 3 (1936).
(3) G. T. Seaborg and J. J. Livingood, *J. Amer. Chem. Soc.*, **60**, 1784 (1938).
(4) R. Basile, J. Hure, P. Leveque, and C. Schuhl, *Compt. Rend.*, **239**, 422 (1954).
(5) C. Engelmann, French Commissariat a L'Energie Atomique, Report CEA-R 2559, Saclay, France, July 1964.
(6) P. Albert, Proc. 1961 International Conf. on Modern Trends in Activation Analysis, College Station, Texas, Dec. 1961, pp 78–85.
(7) A. M. Gaudin, J. Dasher, J. H. Pannell, and W. L. Freyberger, *Trans. AIME*, **187**, 495 (1950).
(8) A. M. Gaudin and J. H. Pannell, ANAL. CHEM., **23**, 1261 (1951).
(9) G. Goldstein, ANAL. CHEM., **35**, 1620 (1963).
(10) H. Bisby, *Nucl. Power*, **5**, 100 (1960).
(11) A. Knight, J. I. W. Watterson, E. A. Uken, and P. K. Faure, *AEC Rep.* NIM-152, National Institute for Metallurgy, Johannesburg, S. A., Mar. 22, 1967.
(12) I. N. Plaksin, M. A. Belyakov, N. G. Malysheva, and L. P. Starchik, *Dokl. Akad. Nauk USSR*, **141**, 1158 (1961).
(13) W. Mountjoy and H. H. Lipp, *U. S. Geol. Surv. Prof. Pap.*, **424-C**, C379 (1961).
(14) G. M. Brownell, *Econ. Geol.*, **54**, 1103 (1959).

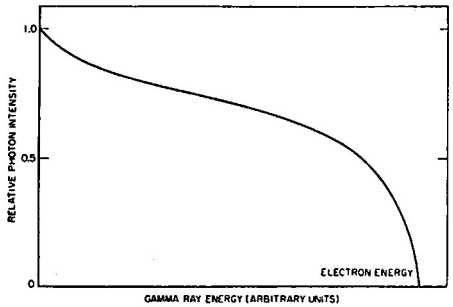


Figure 1. Typical photon intensity *vs.* energy relationship for bremsstrahlung from high-energy electrons

Rook (*15*) and Postma and McMurray (*16*) have developed the techniques for determining beryllium in beryllium metal, thus assessing its purity. Precisions and accuracies of about 2 parts in 1000 are apparently practical, making this the most precise and accurate activation analysis yet accomplished.

Levine and Surls (*17*) have described the determination of trace amounts of beryllium using a Van de Graaff accelerator. The activating photons were produced by converting 2.1 MeV electrons with a tungsten target. Photoneutrons were captured in a silver disk and the radioactive silver was counted with a G-M detector. The photon flux from this machine was about 1000 times that of a typical ^{124}Sb source. The accelerator has the additional advantages of relative freedom from radiation hazards and from frequent source replacements. However, reproducibility of photon flux position, intensity, and energy is not so good as with an isotope source.

The only radionuclides of sufficiently long half-life, whose gamma-ray energies exceed the 2.23 MeV required for deuteron photodisintegration, are ^{24}Na, with a half-life of 15 hours, and ThC″ (^{208}Tl) in equilibrium with ^{228}Th, with a half-life of 1.91 years. The radiothorium mixture is expensive; and most work has been done with ^{24}Na, a technique which was developed by Haigh (*18*, *19*). Source strengths of about a curie are frequently used. The sample-source-detector-shielding configuration is similar to that used in beryllium determinations. Samples are usually water. Detection limits of less than naturally-occurring deuterium in a few milliliters of water are practical. Khristianov and coworkers (*20*, *21*) have used the method for investigating isotopic fractionation of hydrogen in natural waters. Overman *et al.* (*22*) have used the reaction to monitor heavy-water production and have used deuterium oxide in tracing soil moisture.

Guinn and Lukens (*23*) have demonstrated that bremsstrahlung from a 1-mA beam of 3 MeV electrons improves the sensitivity for deuterium determination to 1/500 of its concentration in natural water. Their neutron detector was the ^{55}Mn (n,γ)^{56}Mn reaction.

Mazyukevich and Shkoda-Ul'yanov (*24*) have discussed the possibility of determining hydrogen in metals, utilizing the deuteron photodisintegration. They estimate that with a 50-μA electron beam of 4.5 MeV in energy, metals containing as little as 10^{-4}% hydrogen can be analyzed. It is necessary that the beryllium level in a sample be two or three orders of magnitude lower than that of hydrogen.

NUCLEAR CONSIDERATIONS

The induction of a photonuclear reaction, involving the removal of a nucleon, on stable nuclides other than ^{9}Be and ^{2}H, requires gamma radiation of energies in excess of those available by radioactive decay. These photons must be produced by stopping charged particles, accelerated to high energies, in matter. In photon activation analysis, this is accomplished with electrons, which after acceleration in a linear or cyclic accelerator, are allowed to strike a target, preferably of high atomic-number material. The continuous gamma-ray spectrum produced when the electrons are decelerated in the Coulomb field of nuclei of the target is called bremsstrahlung.

The cross-section equations for production of bremsstrahlung from relativistic electrons were derived by Bethe and Heitler (*25*, *26*), and have been discussed by Koch and Motz (*27*). Some of the considerations of bremsstrahlung production of interest to activation analysis will be summarized.

Figure 1 shows, qualitatively, the energy distribution of bremsstrahlung from a monoenergetic source of electrons. The distribution is continuous and extends up to the electron energy.

Electrons passing through matter lose energy by excitation and ionization, as well as radiative (bremsstrahlung), processes. In the case of a thick target, *i.e.*, a target in which scattering and energy-loss processes occur as the electron traverses the target, a situation which invariably prevails in a photon activation analysis, the efficiency, which is the fraction of the electron energy converted to bremsstrahlung, can be calculated from an expression given by Koch and Motz:

$$\epsilon = \frac{1 - \ln(1 + 1.2 \times 10^{-3}EZ)}{1.2 \times 10^{-3}EZ}$$

where ϵ is the fractional efficiency, Z is the atomic number, and E is the electron energy, in MeV. Results for various atomic numbers at different electron energies are given in Table I.

The angular distribution of bremsstrahlung can be estimated from an equation due to Schiff (*28*), from which the ratio of the radiation intensity per unit solid angle at an angle θ to the intensity at $\theta = 0$, the direction of travel of the electrons, is calculated. Figure 2 shows this distribution

(15) H. L. Rook, ANAL. CHEM., 36, 2211 (1964).
(16) F. W. Postma, Jr., and C. S. McMurray, Jr., *AEC Rep.* TID-7655, pp 90–106, Oak Ridge, Tenn. (1962).
(17) C. A. Levine and J. P. Surls, Jr., ANAL. CHEM., 34, 1614 (1962).
(18) C. P. Haigh, *Nature*, 172, 359 (1953).
(19) C. P. Haigh, Radioisotope Conference, Oxford, 1954, Butterworth, London, Vol. II, pp 101–110 (1954).
(20) V. I. Baranov, V. K. Khristianov, and B. V. Karasev, *U. K. At. Energy Auth. DEG Inf. Ser.* 123 (*CA*) (1961) translated from *Dokl. Akad. Nauk*, 129, 1035 (1959).
(21) V. K. Khristianov, and V. I. Vernadskii, *AEC Rep.* ORNL-tr-1925 (1967) translated from *Isotopenpraxis*, 3, 235 (1967).
(22) R. F. Overman, J. C. Corey, and R. H. Hawkins, *AEC Rep.* DP-MS-68-9, Aiken, S. C. (1968).
(23) V. P. Guinn and H. R. Lukens, *Trans. Amer. Nucl. Soc.*, 9, 106 (1966).
(24) N. P. Mazyukevich and V. A. Shkoda-Ul'yanov, *Sov. At. Energy*, 21, 1069 (1966).
(25) H. Bethe, *Proc. Cambridge Phil. Soc.*, 30, 524 (1934).
(26) H. Bethe and W. Heitler, *Proc. Roy. Soc., Ser. A*, 146, 83 (1934).
(27) H. W. Koch and J. W. Motz, *Rev. Mod. Phys.*, 31, 920 (1959).
(28) L. I. Schiff, *Phys. Rev.*, 70, 87 (1964).

Table I. Approximate Thick-Target X-ray Efficiencies, in Per Cent

Atomic number of target	Electron energy (MeV)				
	10	20	30	40	50
10	5.5	10.4	14.6	18.3	21.7
20	10.4	18.3	24.7	29.9	34.3
30	14.6	24.7	32.2	38.1	42.8
40	18.3	29.9	38.1	44.2	49.0
50	21.7	34.3	42.8	49.0	53.8
60	24.7	38.1	46.7	52.9	57.6
70	27.4	41.3	50.0	56.2	60.7
80	29.9	44.2	52.9	58.9	63.4

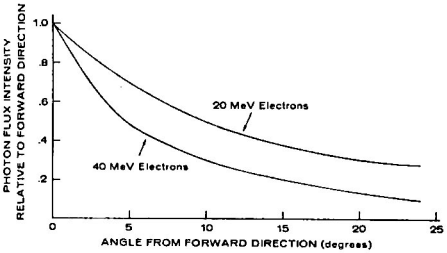


Figure 2. Relative angular distribution of bremsstrahlung from electrons of 20 and 40 MeV striking a tungsten target of 6-mm thickness

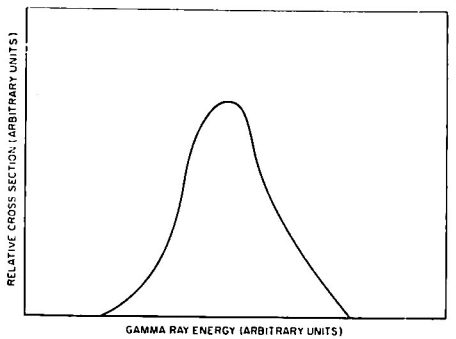


Figure 3. Typical cross-section *vs.* energy relationship for (γ,n) reactions

for electrons of 20 and 40 MeV striking a tungsten target of 6-mm thickness.

In most photon activation work, the target is constructed of a high atomic-number material which has satisfactory mechanical and heat-transfer characteristics. Gold, platinum, tungsten, and tantalum have been used successfully. Since a substantial fraction of the electron-beam energy is deposited in the target *via* excitation and ionization processes, it is usually necessary to water-cool the target. Although the thickness of target for the production of the optimum amount of bremsstrahlung may be less at some energies than the range of electrons in the target, it is generally desirable that the target or an electron absorber stop the electrons

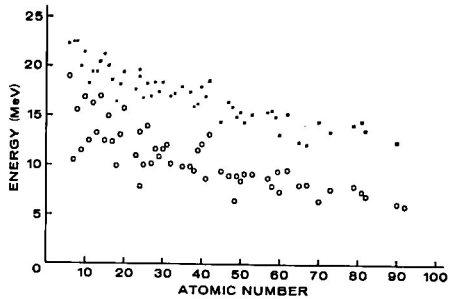


Figure 4. Threshold energy and energy of maximum cross section for (γ,n) reactions

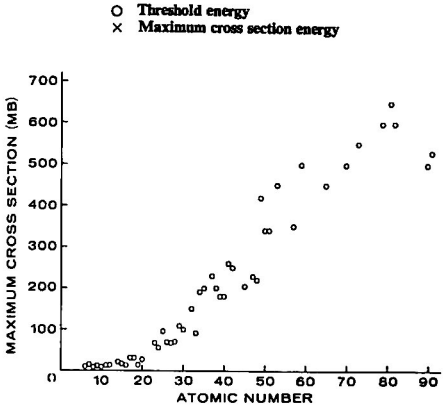


Figure 5. Peak cross section for (γ,n) reactions

completely, so that they do not strike the sample. Several target facilities have been described *(29–31)*.

The cross section-energy relationship for a (γ,n) reaction, the reaction most commonly used in photon activation analysis, is qualitatively shown in Figure 3. The shape is that of a Lorenzian function. The curve is characterized by a threshold energy, an energy of maximum cross section, the cross section at that energy, and a width at half-height. Figure 4 shows the threshold energy of maximum cross section for (γ,n) reactions as a function of atomic number. Figure 5 shows the peak cross section for (γ,n) reactions as a function of atomic number. Widths at half-height are usually in the range of 4–8 MeV.

The production rate for any particular photonuclear reaction is determined by the summation of the product of cross section and flux from the threshold of the reaction up to the

(29) G. H. Andersen, F. M. Graber, V. P. Guinn, H. R. Lukens, and D. M. Settle, Nuclear Activation Techniques in the Life Sciences, Proceedings of a Symposium, Amsterdam, May 1967, IAEA, Vienna, pp 99–113 (1967).
(30) C. Engelmann, P. Graeff, and C. Re, "Proceedings of the 2nd Conference on Practical Aspects of Activation Analysis with Charged Particles, Liege, Sept. 1967," H. G. Ebert, Ed., Brussels, European Atomic Energy Community, pp 403–33 (1968).
(31) F. A. Lundgren and G. J. Lutz, *Trans. Amer. Nucl. Soc.*, **10**, 89 (1967).

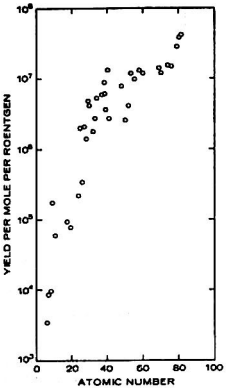


Figure 6. Yields for (γ,n) reactions from 20-MeV bremsstrahlung

electron energy. As would be expected from the trend of cross section with atomic number, and of photon flux with photon energy at a given electron energy, the production rate increases with atomic number. This intrinsic sensitivity has been measured for 20-MeV bremsstrahlung by Oka *et al.* (*32*). Their normalized yield-per-mole data for (γ,n) reactions for many of the elements are shown in Figure 6.

Lutz (*33*) has estimated the specific activities to be expected for most of the elements from bremsstrahlung produced from an electron beam current of 100 μA striking a tungsten target 0.6 cm in thickness, for electron energies of 25, 30, and 35 MeV. The photon-energy distribution was estimated by the method of Hansen and Fultz (*34*). A correction was made for the attenuation of the photons in the target. The angular distribution of the flux was calculated from the Schiff equation. It was assumed that a sample could be positioned to intercept the beam included in the cone described by a five degree angle from the forward direction. Results for irradiations of 10 minutes and 4 hours at the three energies are shown in Table II.

In the range of electron energies from 20–40 MeV, the yield at constant beam current of most (γ,n) reactions will approximately double with a 3–4 MeV increase in electron energy. This is due not only to an increase in the total number of photons of sufficiently high energy, but also to a more favorable (more forward-peaked) angular distribution. The choice of electron energy is usually a compromise between the required sensitivity and the occurrence of interfering reactions. In addition, the operating characteristics of the electron accelerator may be an important consideration.

DETERMINATION OF OXYGEN, NITROGEN, AND CARBON

Photon activation analysts have concentrated a substantial, although perhaps not adequate, portion of their efforts on the determination of three nonmetals: oxygen, nitrogen, and carbon. Although among the least sensitive of the elements for determination by gamma activation, because of their relatively high thresholds and small cross sections, they have nevertheless been determined by photonuclear methods at levels down to less than a microgram. These elements are frequently difficult to determine at very low levels by traditional methods, because of reagent and equipment blanks and the possibility of surface contamination, which would yield a higher result than is representative of the bulk of the sample. In these cases, photon activation is an attractive alternative.

The (γ,n) activation products of carbon, nitrogen, and oxygen all decay exclusively by positron emission, and are detected by the associated annihilation radiation. At low levels, unless the sample is quite simple and its gamma activation products do not yield positron emitters, it is frequently necessary to effect a chemical separation.

(32) Y. Oka, T. Kato, K. Nomura, and T. Saito, *Bull. Chem. Soc. Japan*, **40**, 575 (1967).
(33) G. J. Lutz, ANAL. CHEM., **41**, 424 (1969).
(34) N. E. Hansen and S. C. Fultz, *AEC Rep.* UCRL-6099, Livermore, Calif., Nov. 15, 1960.

Table II. Calculated Sensitivities for Photon Activation Analysis

Element	Reaction	Product half-life	Disintegrations per second (per microgram of element) 10-minute irradiation, MeV 25 M	30	35	4-hour irradiation, MeV 25	30	35
Carbon	$^{12}C(\gamma,n)^{11}C$	20.5m	2×10^{1}	7×10^{1}	1×10^{2}	6×10^{1}	2×10^{2}	5×10^{2}
Nitrogen	$^{14}N(\gamma,n)^{13}N$	10.0m	7×10^{1}	2×10^{2}	4×10^{2}	1×10^{2}	4×10^{2}	8×10^{2}
Oxygen	$^{16}O(\gamma,n)^{15}O$	2.1m	1×10^{2}	3×10^{2}	6×10^{2}	1×10^{2}	3×10^{2}	6×10^{2}
Fluorine	$^{19}F(\gamma,n)^{18}F$	1.83h	3	8	1×10^{1}	4×10^{1}	1×10^{2}	2×10^{2}
Sodium	$^{23}Na(\gamma,n)^{22}Na$	2.6y	9×10^{-4}	2×10^{-3}	4×10^{-3}	2×10^{-3}	5×10^{-3}	9×10^{-3}
Magnesium	$^{24}Mg(\gamma,p)^{24}Na$	15.0h	1×10^{-1}	4×10^{-1}	7×10^{-1}	3	9	2×10^{1}
Magnesium	$^{26}Mg(\gamma,p)^{25}Na$	60s	1×10^{1}	3×10^{1}	7×10^{1}	1×10^{1}	3×10^{1}	7×10^{1}
Silicon	$^{29}Si(\gamma,p)^{28}Al$	2.31m	1×10^{1}	3×10^{1}	5×10^{1}	1×10^{1}	3×10^{1}	5×10^{1}
Silicon	$^{30}Si(\gamma,p)^{29}Al$	6.6m	3	9	2×10^{1}	4	1×10^{1}	3×10^{1}
Phosphorus	$^{31}P(\gamma,n)^{30}P$	2.50m	1×10^{2}	3×10^{2}	6×10^{2}	1×10^{2}	4×10^{2}	6×10^{2}
Sulfur	$^{32}S(\gamma,n)^{31}S$	2.7s	7×10^{1}	2×10^{2}	4×10^{2}	7×10^{1}	2×10^{2}	4×10^{2}
Chlorine	$^{35}Cl(\gamma,n)^{34}Cl$	32.0m	2×10^{1}	5×10^{1}	8×10^{1}	1×10^{2}	2×10^{2}	4×10^{2}
Argon	$^{40}A(\gamma,p)^{39}Cl$	55.5m	1×10^{1}	5×10^{1}	1×10^{2}	1×10^{2}	4×10^{2}	9×10^{2}
Potassium	$^{39}K(\gamma,n)^{38}K$	7.71m	5×10^{1}	1×10^{2}	2×10^{2}	9×10^{1}	2×10^{2}	4×10^{2}
Titanium	$^{46}Ti(\gamma,n)^{45}Ti$	3.09h	5×10^{-1}	1	2	8	2×10^{1}	4×10^{1}
Titanium	$^{48}Ti(\gamma,p)^{47}Sc$	3.4d	8×10^{-2}	2×10^{-1}	5×10^{-1}	2	6	1×10^{1}
Chromium	$^{50}Cr(\gamma,n)^{49}Cr$	42m	2	4	8	1×10^{1}	3×10^{1}	5×10^{1}
Chromium	$^{52}Cr(\gamma,p)^{52}V$	3.76m	8	2×10^{1}	4×10^{1}	9	2×10^{1}	4×10^{1}
Manganese	$^{55}Mn(\gamma,n)^{54}Mn$	303d	1×10^{-1}	2×10^{-1}	4×10^{-1}	2×10^{-1}	6×10^{-1}	1
Iron	$^{54}Fe(\gamma,n)^{53}Fe$	8.5m	1×10^{1}	3×10^{1}	5×10^{1}	2×10^{1}	5×10^{1}	9×10^{1}

(*Continued on next page*)

Table II. (Continued)

Element	Reaction	Product half-life	Disintegrations per second (per microgram of element) 10-minute irradiation, MeV 25 M	30	35	4-hour irradiation, MeV 25	30	35
Cobalt	$^{59}Co(\gamma,n)^{58}Co$	71.3d	3×10^{-3}	7×10^{-3}	1×10^{-1}	8×10^{-1}	2	3
Nickel	$^{58}Ni(\gamma,n)^{57}Ni$	36h	3×10^{-1}	7×10^{-1}	1	7	2×10^{1}	3×10^{1}
Copper	$^{63}Cu(\gamma,n)^{62}Cu$	9.9m	2×10^{3}	5×10^{3}	9×10^{3}	5×10^{3}	1×10^{4}	2×10^{4}
Copper	$^{63}Cu(\gamma,n)^{64}Cu$	12.8h	2	5	9	5×10^{1}	1×10^{2}	2×10^{2}
Zinc	$^{64}Zn(\gamma,n)^{63}Zn$	38.4m	5×10^{1}	1×10^{2}	2×10^{2}	3×10^{2}	7×10^{2}	1×10^{3}
Germanium	$^{76}Ge(\gamma,n)^{75}Ge$	82m	7	2×10^{1}	3×10^{1}	7×10^{1}	2×10^{2}	3×10^{2}
Germanium	$^{70}Ge(\gamma,n)^{69}Ge$	38h	6×10^{-1}	1	2	1×10^{1}	3×10^{1}	5×10^{1}
Arsenic	$^{75}As(\gamma,n)^{74}As$	17.9d	2×10^{-1}	4×10^{-1}	6×10^{-1}	4	8	1×10^{1}
Bromine	$^{79}Br(\gamma,n)^{78}Br$	6.5m	5×10^{2}	1×10^{3}	2×10^{3}	8×10^{3}	2×10^{4}	3×10^{4}
Bromine	$^{81}Br(\gamma,n)^{80m}Br$	4.4h	3	6	1×10^{1}	5×10^{1}	1×10^{2}	2×10^{2}
Rubidium	$^{87}Rb(\gamma,n)^{86}Rb$	18.7d	8×10^{-2}	2×10^{-1}	3×10^{-1}	2	4	7
Strontium	$^{88}Sr(\gamma,n)^{87}Sr$	64d	7×10^{-3}	1×10^{-2}	2×10^{-2}	2×10^{-1}	3×10^{-1}	6×10^{-1}
Yttrium	$^{89}Y(\gamma,n)^{88}Y$	108d	4×10^{-2}	9×10^{-2}	1×10^{-1}	1	2	4
Zirconium	$^{90}Zr(\gamma,n)^{89}Zr$	78.4h	7×10^{-1}	2	3	2×10^{1}	4×10^{1}	7×10^{1}
Niobium	$^{93}Nb(\gamma,n)^{92}Nb$	10.2d	6×10^{-1}	1	2	1×10^{1}	3×10^{1}	5×10^{1}
Molybdenum	$^{92}Mo(\gamma,n)^{91}Mo$	15.5m	2×10^{1}	6×10^{1}	1×10^{2}	6×10^{1}	2×10^{2}	3×10^{2}
Molybdenum	$^{100}Mo(\gamma,n)^{99}Mo$	66h	2×10^{-1}	5×10^{-1}	7×10^{-1}	5	1×10^{1}	2×10^{1}
Ruthenium	$^{96}Ru(\gamma,n)^{95}Ru$	99m	4	9	2×10^{1}	5×10^{1}	1×10^{2}	2×10^{2}
Ruthenium	$^{104}Ru(\gamma,n)^{103}Ru$	40d	3×10^{-2}	6×10^{-2}	1×10^{-1}	7×10^{-1}	2	3
Rhodium	$^{103}Rh(\gamma,n)^{102}Rh$	206d	3×10^{-2}	5×10^{-2}	9×10^{-2}	6×10^{-1}	1	2
Palladium	$^{104}Pd(\gamma,n)^{103}Pd$	17d	4×10^{-2}	9×10^{-2}	1×10^{-1}	1	2	3
Silver	$^{107}Ag(\gamma,n)^{106}Ag$	24m	2×10^{2}	4×10^{2}	6×10^{2}	7×10^{2}	1×10^{3}	2×10^{3}
Cadmium	$^{114}Cd(\gamma,p)^{113}Ag$	3.2h	8×10^{-2}	2×10^{-1}	4×10^{-1}	1	4	6
Cadmium	$^{114}Cd(\gamma,p)^{113}Ag$	5.3h	1×10^{-1}	3×10^{-1}	5×10^{-1}	2	5	9
Indium	$^{115}In(\gamma,n)^{114}In$	50d	2×10^{-1}	4×10^{-1}	6×10^{-1}	5	9	1×10^{1}
Indium	$^{115}In(\gamma,\gamma')^{115m}In$	4.5h	2	4	5	4×10^{1}	7×10^{1}	9×10^{1}
Tin	$^{112}Sn(\gamma,n)^{111}Sn$	35m	3	6	9	2×10^{1}	3×10^{1}	5×10^{1}
Tin	$^{124}Sn(\gamma,n)^{123}Sn$	125d	3×10^{-2}	7×10^{-2}	1×10^{-1}	8×10^{-2}	2×10^{-1}	3×10^{-1}
Antimony	$^{121}Sb(\gamma,n)^{120m}Sb$	5.8d	6×10^{-1}	1	2	1×10^{1}	3×10^{1}	4×10^{1}
Antimony	$^{123}Sb(\gamma,n)^{122}Sb$	2.8d	2	3	5	4×10^{1}	8×10^{1}	1×10^{2}
Iodine	$^{127}I(\gamma,n)^{126}I$	13.2d	8×10^{-1}	2	3	2×10^{1}	4×10^{1}	6×10^{1}
Cesium	$^{133}Cs(\gamma,n)^{132}Cs$	6.58d	1	3	4	3×10^{1}	6×10^{1}	1×10^{2}
Cerium	$^{140}Ce(\gamma,n)^{139}Ce$	140d	6×10^{-2}	1×10^{-1}	2×10^{-1}	1	3	4
Praseodymium	$^{141}Pr(\gamma,n)^{140}Pr$	3.4m	1×10^{2}	3×10^{2}	4×10^{2}	2×10^{3}	3×10^{3}	5×10^{3}
Neodymium	$^{143}Nd(\gamma,n)^{141}Nd$	2.5h	2×10^{1}	4×10^{1}	6×10^{1}	3×10^{2}	5×10^{2}	8×10^{2}
Neodymium	$^{150}Nd(\gamma,n)^{149}Nd$	1.8h	8	1×10^{1}	2×10^{1}	1×10^{2}	2×10^{2}	3×10^{2}
Samarium	$^{144}Sm(\gamma,n)^{143}Sm$	8.9m	2×10^{1}	5×10^{1}	8×10^{1}	5×10^{1}	9×10^{1}	1×10^{2}
Samarium	$^{154}Sm(\gamma,n)^{153}Sm$	47h	1	2	3	2×10^{1}	5×10^{1}	7×10^{1}
Gadolinium	$^{160}Gd(\gamma,n)^{159}Gd$	18h	3	5	7	6×10^{1}	1×10^{2}	2×10^{2}
Terbium	$^{159}Tb(\gamma,n)^{158}Tb$	150y	2×10^{-4}	3×10^{-4}	5×10^{-4}	4×10^{-2}	8×10^{-2}	1×10^{-1}
Dysprosium	$^{162}Dy(\gamma,n)^{161}Dy$	8.1h	2×10^{-2}	4×10^{-2}	7×10^{-2}	5×10^{-1}	9×10^{-1}	1
Holmium	$^{165}Ho(\gamma,n)^{164}Ho$	37m	3×10^{2}	6×10^{2}	1×10^{3}	2×10^{3}	4×10^{3}	6×10^{3}
Erbium	$^{166}Er(\gamma,n)^{165}Er$	10.3h	7	1×10^{1}	2×10^{1}	1×10^{2}	3×10^{2}	4×10^{2}
Thulium	$^{169}Tm(\gamma,n)^{168}Tm$	85d	1×10^{-1}	2×10^{-1}	3×10^{-1}	3	5	8
Ytterbium	$^{168}Yb(\gamma,n)^{167}Yb$	18m	1	2	3	3	5	8
Ytterbium	$^{176}Yb(\gamma,n)^{175}Yb$	4.2d	3×10^{-1}	6×10^{-1}	9×10^{-1}	8	1×10^{1}	2×10^{1}
Lutetium	$^{175}Lu(\gamma,n)^{174}Lu$	300d	1×10^{-2}	3×10^{-2}	4×10^{-2}	3×10^{-1}	6×10^{-1}	1
Tantalum	$^{181}Ta(\gamma,n)^{180m}Ta$	8.1h	4×10^{1}	7×10^{1}	1×10^{2}	8×10^{2}	1×10^{3}	2×10^{3}
Tungsten	$^{184}W(\gamma,n)^{183}W$	75d	5×10^{-2}	9×10^{-2}	1×10^{-1}	1	2	3
Rhenium	$^{187}Re(\gamma,n)^{186}Re$	90h	2	4	6	5×10^{1}	9×10^{1}	1×10^{2}
Osmium	$^{192}Os(\gamma,n)^{191}Os$	15d	3×10^{-1}	6×10^{-1}	1	8	1×10^{1}	2×10^{1}
Iridium	$^{191}Ir(\gamma,n)^{190}Ir$	11d	4×10^{-1}	7×10^{-1}	1	9	2×10^{1}	3×10^{1}
Gold	$^{197}Au(\gamma,n)^{196}Au$	6.2d	2	4	6	5×10^{1}	9×10^{1}	1×10^{2}
Mercury	$^{198}Hg(\gamma,n)^{197}Hg$	65h	5×10^{-1}	9×10^{-1}	1	1×10^{1}	2×10^{1}	3×10^{1}
Thallium	$^{203}Tl(\gamma,n)^{202}Tl$	12d	3×10^{-1}	6×10^{-1}	9×10^{-1}	8	1×10^{1}	2×10^{1}
Lead	$^{204}Pb(\gamma,n)^{203}Pb$	52h	1×10^{-1}	2×10^{-1}	3×10^{-1}	2	4	6

Oxygen. The nuclear reaction involved is

$$^{16}O(\gamma,n)^{15}O$$

The product nuclide has a half-life of 2.05 minutes.

As noted in the introduction, this reaction was used by Basile, Hure, Leveque, and Schuhl in 1953 for the determination of oxygen in organic materials. Much early work in photon activation analysis was concentrated on the determination of oxygen, along with carbon and nitrogen, in beryllium—programs for development of a ductile metal having shown the need for precise analytical methods for these impurities.

The development of this analytical method was furthered by Beard, Johnson, and Bradshaw (*35*), Gilman and Isserow (*36*), and Engelmann and his colleagues (*37*). The method consists of irradiating the sample with bremsstrahlung from 28–40 MeV electrons and counting the resulting annihilation radiation by means of coincidence gamma-ray spectrometry.

(35) D. B. Beard, R. G. Johnson, and W. G. Bradshaw, *Nucleonics*, 17, 90 (1959).
(36) A. R. Gilman and S. Isserow, *AEC Rep.* NMI-1234, Concord, Mass., May 3, 1960.
(37) C. Engelmann, J. Gosset, and M. Loeuillet, *Bull. Soc. Chim. Fr.*, 1967, 544.

The decay curve obtained is resolved graphically or by more sophisticated computer methods. Sensitivities of the order of 1 ppm are claimed, but this is very dependent on the levels of other impurities.

As they have favorable thermodynamic and nuclear properties, the alkali metals have potential use as heat-transfer media for nuclear power reactors. However, they may cause corrosion or embrittlement of structural components with which they come in contact. This is associated with traces of oxygen and other nonmetals in the sodium. Engelmann and Loeuillet (*38*) have pointed out that, for a nondestructive determination of oxygen in sodium, it is necessary to irradiate at energies below the threshold for production of the positron-emitting ^{18}F produced by the reaction $^{23}Na(\gamma, \alpha n)^{18}F$. In addition, the 7.71-minute activity from ^{38}K interferes with counting.

Lutz (*39*) has determined oxygen in sodium at levels of a few ppm with a chemical separation. The sodium sample, after irradiation and etching, is dissolved in water. The radioactive oxygen exchanges with water, a portion of which is rapidly distilled from the sample, and the ^{15}O counted. A small amount of entrainment occurs, and it is necessary to evaluate a long-lived component for subtraction from the oxygen activity.

Holm and Sanders (*40*) determined oxygen at the 30-ppm level by coincidence and gated well techniques. The electron energy was 19 MeV, and the decay curve was analyzed by computer methods. Persiani, Spira, and Bastian (*41*) have described a nondestructive determination of oxygen in cesium, using a 30-MeV betatron. Under optimum conditions, less than 100 ppm of the element could be determined.

Engelmann (*42*) has pointed out that oxygen can be determined in calcium and boron nondestructively. The photonuclear products of these elements do not interfere with the counting of the oxygen activity, and, if other impurities are present only at very low levels, sensitivities of 1 to 0.01 ppm are obtained. Mackintosh and Jervis (*43*) have reported the nondestructive determination of oxygen in a lead-bismuth alloy. Kobayashi *et al.* (*44*) studied the instrumental photon activation analysis determination of oxygen in pure aluminum ingots and oxide films. Utilizing bombarding energies of 31 MeV and a dose of 10^6r/min, it was possible to determine 20 ppm of oxygen.

The betatron at the Karpov Institute has been used for the determination of several per cent of oxygen in natural and butadiene rubbers (*45*, *46*). The method is useful for rapid analysis in the course of processing the rubber.

The fraction of samples that the photon activation analyst encounters in which he can measure trace levels of oxygen nondestructively is certainly very small. Engelmann and his colleagues (*47–49*), and Baker and Williams (*50*), have investigated the application of inert gas-fusion to the separation of ^{18}O from irradiated samples. The usual advantages of activation analysis are present; a massive sample may be etched after irradiation, but before separation and counting, and equipment and reagent contamination do not affect the determination. Engelmann deliberately added iron chips with a high oxygen content to the sample. The added oxygen in the bath acted as a carrier and expedited the ^{18}O extraction. Baker and Williams have pointed out that there is no reason why one may not increase the speed and completeness of the separation by operating the furnace at extremely high temperatures with outgassing, which is unacceptable in traditional inert-gas fusion. They noted that the extracted oxygen is rarely radiochemically pure, and a longer-lived component (usually ^{11}C) appears after several half-lives decay. They analyzed their counting data by a least-squares method for the two components. A sensitivity of about 10^{-7} gram seems to be feasible, but data on precision and accuracy are lacking.

Dorosh *et al.* (*51*) have discussed the possibility of using the reaction, $^{16}O(\gamma,p)^{17}N$, for the determination of oxygen in metals. This is a very attractive nuclear reaction as ^{17}N decays by delayed-neutron emission with a half-life of 4.16 seconds, making its detection in many samples quite simple. The abundance, however, of ^{18}O is only 0.204%, reducing the sensitivity for oxygen to about that available with 14-MeV neutron generators. Nevertheless, it should find utility in determinations where there is an interference with 14-MeV neutrons, such as substantial amounts of boron or fluorine in the sample.

Nitrogen. The nuclear reaction used is

$$^{14}N(\gamma,n)^{13}N.$$

The product nuclide has a half-life of 9.96 minutes.

The nondestructive determination of nitrogen is complicated by the fact that copper and iron both yield photon activation products that also decay by positron emission and have half-lives similar to that of nitrogen-13. Engelmann (*42*) has observed that the yield of nitrogen relative to either copper or iron does not change much with bombarding energy, and it appears that one cannot make corrections for copper or iron this way.

Most nondestructive determinations, therefore, involve the independent determination of copper and iron, and, if necessary, the application of corrections for the two elements. Rocco, Garzon, and Cali (*52*) have determined nitrogen in 40-mg diamond samples. Electron energies of 17.6 MeV, below the threshold for carbon activation, were used. Various nitrogen-containing substances were irradiated and counted to demonstrate a linear relationship between activity and nitrogen content. They were able to conclude from the gamma-ray spectrum that the only possible inter-

(38) C. Engelmann and M. Loeuillet, *Bull. Soc. Chim. Fr.*, **1969**, 680.
(39) G. J. Lutz, ANAL. CHEM., **42**, 531 (1970).
(40) D. M. Holm and W. M. Sanders, *AEC Rep.* LA-DC-7931, Los Alamos, N. M. (1964).
(41) C. Persiani, J. Spira, and R. Bastian, *Talanta*, **14**, 565 (1967).
(42) C. Engelmann, Radiochemical Methods of Analysis, IAEA, Vienna, Vol. I, pp 341–59 (1965).
(43) W. D. Mackintosh and R. E. Jervis, *NBS Spec. Publ.* **312**, Vol. II, Modern Trends in Activation Analysis, pp 835–7 (1969).
(44) M. Kobayashi, T. Sawai, S. Nagatsuka, and S. Maeda, *Proc. Jap. Conf. Radioisotope*, No. 3, pp 179–181 (1963).
(45) L. V. Chepel, B. A. Chapyzhnikov, G. N. Mikhailova, E. V. Zhuravskaya, and A. S. Kuzminskii, *Kauch. Rezina*, **25**, 49 (1966).
(46) L. V. Chepel, B. A. Chapyzhnikov, and B. I. Viting, *J. Anal. Chem. USSR*, **18**, 749 (1963).
(47) C. Engelmann, *Int. J. Appl. Radiat. Isotopes*, **18**, 569 (1967).
(48) C. Engelmann, B. Fritz, J. Gosset, P. Graeff, and M. Loeuillet, "Proceedings of the 2nd Conference on Practical Aspects of Activation Analysis with Charged Particles, Liege, Sept. 1967," H. G. Ebert, Ed., Brussels, European Atomic Energy Community, pp 319–50 (1968).
(49) C. Engelmann, J. Gosset, M. Loeuillet, A. Marschal, P. Ossart, and M. Boissier, *NBS Spec. Publ.* **312**, Vol. II, Modern Trends in Activation Analysis, pp 819–28 (1969).
(50) C. A. Baker and D. R. Williams, *Talanta*, **15**, 1143 (1968).
(51) M. M. Dorosh, N. P. Mazyukevich, and V. A. Shkoda-Ulyanov, *Sov. At. Energy*, 807 (1966).
(52) G. G. Rocco, O. L. Garzon, and J. P. Cali, *Int. J. Appl. Radiat. Isotop.*, **17**, 433 (1966).

ference could be from copper. The diamonds were subsequently analyzed for copper by thermal neutron activation, and it was demonstrated that the copper content was negligible, compared to that of nitrogen.

Post-irradiation separations of nitrogen have followed two courses. Albert (*6*) described the use of the Kjeldahl separation for the determination of nitrogen in aluminum, beryllium, and zirconium. The samples, after irradiation, are dissolved in a suitable acid to which a few milliliters of $HgCl_2$ solution have been added. Ammonium chloride carrier is added, and the solution is neutralized with a large excess of base. The ammonia is distilled out and collected in an acid solution, and the activity of the distillate solution is measured. Samples of highly-purified aluminum were found to have a nitrogen content of 0.1–0.2 ppm.

Engelmann *et al.* (*47*, *48*) have separated nitrogen with oxidizing fusion. After irradiation, the sample is placed in a crucible containing 20–30 grams of an oxidizing flux (87.5% Pb_3O_4–12.5% B_2O_3). During induction heating, the sample is oxidized, nitrogen being converted to molecular nitrogen and nitrogen oxides. These gases are swept in a stream of helium through a glass filter and a halogen trap over copper at 500°C, which reduces nitrogen oxides to nitrogen. The nitrogen is subsequently trapped on liquid nitrogen-cooled molecular sieve. Sensitivities of less than 0.1 ppm are possible.

Carbon. The reaction used is $^{12}C(\gamma,n)^{11}C$, and the half-life of the product nuclide is 20.34 minutes.

Considerations of the nondestructive determination of trace levels of carbon are about the same as for oxygen. Relative to the activity of carbon produced, there must not be much other positron-emitting activity that can interfere. Many of the nondestructive oxygen determinations cited in the section on that element also involved the determination of carbon.

Voigt and Abu-Samra (*53*) have determined carbon nondestructively in a sample taken from a Damascus steel sword of the sixteenth century. A synchrotron was used, and the irradiation energy was 70 MeV. This also induced the 21.1 min ^{52m}Mn activity *via* the reaction $^{54}Fe(\gamma,np)^{52m}Mn$ which interfered with the carbon counting. Fortunately, the interfering radionuclide has a gamma ray of 1.434-MeV energy and, by measurement of the gamma spectrum, it was possible to correct for this interference.

Albert (*6*), Engelmann *et al.* (*47–49*), Revel *et al.* (*54*), Baker and Williams (*50*), and Lutz and Masters (*55*) have all described methods for the separation of ^{11}C activity from a variety of metals. The separations follow, in general, conventional techniques. The sample is burned in a stream of oxygen gas, or oxidized in a Pb_3O_4–B_2O_3 melt, with subsequent trapping of the carbon dioxide in an alkaline solution or a liquid–air trap. In an activation analysis, it is, of course, not necessary to purify the oxygen or other reagents used. One may use fluxes to improve the fluidity of the melt or to initiate and accelerate combustion, without regard for their carbon content.

A large variety of metals have been analyzed for trace levels of carbon by this method. Most of the papers cited give details on specific topics such as monitoring, standards, sample positioning, and counting. Several compare results at higher levels of carbon in samples which have been carefully analyzed by other methods. Sensitivities of 10^{-6} gram are possible.

The separation of ^{11}C activity from irradiated sodium requires a different separation method. It is difficult to extract carbon from sodium oxide at high temperatures, because of the stability of sodium carbonate. In a method described by Lutz and DeSoete (*56*), the irradiated sodium sample is burned in a stream of oxygen to sodium monoxide, the carbon being converted to sodium carbonate. This is then decomposed with acid, the liberated CO_2 being trapped in a dilute alkaline solution. A sulfuric acid–boric acid solution prior to the alkali trap, removes—as a fluoboric acid complex—the ^{18}F that has been produced from the reaction, $^{23}Na(\gamma,\alpha n)^{18}F$.

DETERMINATION OF HEAVIER ELEMENTS

There are a number of elements heavier than oxygen that may be determined more easily, or more advantageously, by photon activation than by activation with reactor neutrons. The following conditions apply:

There may be greater intrinsic sensitivity for photon activation. Examples are fluorine, iron, and lead.

The photon-activation product has a more convenient half-life or decay mode than the thermal-neutron activation product.

Major constituents of the sample have large thermal-neutron cross sections, requiring the evaluation of self-shielding corrections or the handling of large amounts of unwanted radioactivity.

Interfering nuclear reactions may interfere with the neutron determination. The thermal-neutron activation determination of nickel by the reaction, $^{64}Ni(n,\gamma)^{65}Ni$, is subject to interference when copper is present, because of the reaction, $^{65}Cu(n,p)^{65}Ni$. The photon-activation product, ^{57}Ni, produced by the (γ,n) reaction on ^{58}Ni, cannot be produced from any other element at bombarding energies less than about 45 MeV.

Schweikert and Albert (*57*) have irradiated 25 elements with bremsstrahlung from electrons varying between 20 and 27 MeV, and have published specific activities obtained for these elements for five-minute and eight-day irradiations and have described a number of useful analyses. These include the nondestructive determination of zirconium in hafnium, utilizing the 4.18-minute ^{89m}Zr product. They determined titanium in iron and copper; counting the 3.09-hour positron-emitting ^{45}Ti after an oxime extraction. Nickel was determined in copper with chemical separation.

Oka *et al.* (*32*) have used a linear accelerator to irradiate all of the elements from lithium to bismuth, except technetium, promethium, and the inert gases, for 1 hour with bremsstrahlung from 20-MeV electrons. The dose rate was estimated to be 9.4×10^6r/min. After irradiation, the gamma-ray spectra of the elements were measured with a sodium–iodide detector, and prominent gamma rays and specific activities were noted.

Biological Samples. Andersen *et al.* (*29*) surveyed the application of photon activation analysis to biological samples. They have pointed out that most of the major and minor constituents yield either quite short or very long-lived activities

(53) A. F. Voigt and A. Abu-Samra, Proceedings of the 1965 International Conference on Modern Trends in Activation Analysis, College Station, pp 22–25 (1965).
(54) G. Revel, I. Chaudron, J. L. DeBrun, and P. Albert, *NBS Spec. Publ.* 312, Vol. II, Modern Trends in Activation Analysis, pp 838–41 (1969).
(55) G. J. Lutz and L. W. Masters, ANAL. CHEM., 42, 948 (1970).
(56) G. J. Lutz and D. A. DeSoete, *ibid.*, 40, 820 (1968).
(57) E. A. Schweikert and P. Albert, "Radiochemical Methods of Analysis," IAEA, Vienna, Vol. I, pp 323–39 (1965).

after photon bombardment so that radioactivity associated with many trace elements may be readily observed. A number of elements difficult to determine with thermal-neutron activation, such as magnesium, calcium, strontium, and tin were detected in a wide variety of biological materials. Fluorine and strontium were determined instrumentally down to levels of a few tens of ppm in teeth and other samples with 12 MeV photons. This energy is sufficiently low that chlorine, sodium, and carbon do not interfere.

Mulvey, Cardarelli, Burrows *et al.* (*58–61*) have determined iodine and mercury in several biological materials after a pre-irradiation separation of the elements of interest. Dowex 1-X8 resin, in the acetate form, was placed in a polyethylene syringe, and the dissolved sample passed through it. Experiments with known amounts of material demonstrated that the separation was quantitative. The samples were then irradiated for over an hour with bremsstrahlung from 22-MeV electrons. The beam current was 250 μA. The resultant activity was assayed with a sodium–iodide detector. Radioactivities from impurities in the syringe and resin were usually of lower energy and shorter half-life than of the elements of interest, and did not interfere with the counting. These authors have also suggested the use of the reaction, $^{12}C(\gamma, \alpha n)^7Be$ as an internal flux monitor at higher energies for biological samples.

Cooper, Linekin, and Brownell (*58*, *62*) have examined photon irradiated blood and tissue with a Ge(Li) detector. Magnesium, cadmium, lead, iodine, and tin were observed, along with unidentified positron emitters. Asai *et al.* (*63*) examined activated blood with a NaI detector and tentatively identified fourteen elements.

Meyers (*64*) has described a novel application. The composition of fossil bones and teeth buried in the ground is influenced by the ground-water. Nitrogen in bone protein will slowly leave the bones, while fluorine ions in the water will slowly be picked up. A relative age determination of a series of bones from the same ground matrix is possible by determining the content of nitrogen and fluorine. This can be done nondestructively by photon activation analysis, thus preserving the precious samples for other purposes.

Geochemistry and Oceanography. Sulin, Vitozhents, and their colleagues of the All-Union Scientific Research Institute (*65–68*) have used a betatron for the determination of many elements of industrial interest in minerals and ores. Many useful determinations could be done nondestructively by selective activation at different irradiation energies and judicious choice of irradiation and cooling times. Copper, zinc, zirconium, and silver were among the elements determined in this way in complex ores. Servomechanism devices were developed for automatic irradiation and counting. Gerrard (*69*) has reviewed some of this work in English.

Wilkniss and Linnenbom (*70*) developed a method for the photon activation determination of fluorine in seawater. Three-milliliter samples were freeze-dried, encapsulated in aluminum foil, and irradiated for 20 minutes in the bremsstrahlung beam obtained from a 22-MeV, 30-μA electron beam. The reaction induced was the $^{19}F(\gamma,n)^{18}F$ reaction. The low energy was required to prevent interference from the reaction, $^{23}Na(\gamma,\alpha n)^{18}F$, which has a threshold of 23 MeV. The separation consisted of a distillation, followed by a lead chlorofluoride precipitation. The positron activity of ^{18}F was coincidence-counted. The limit of detection was determined to be a few ppb. Wilkniss (*71*) has subsequently developed the methods for the determination of all of the halogens in a single sample.

Meijers and Aten (*72*) instrumentally determined the major constituents, iron, nickel, and cobalt in meteorites. Activities due to the different components were determined by decay curve resolution.

Forensic. Guinn and coworkers (*73*, *74*) have studied a variety of forensic samples by photon activation. Several samples of moonshine whiskey were analyzed for lead using the reaction, $^{204}Pb(\gamma,n)^{203}Pb$. The lead content varied from about four to eighty milligrams per liter of sample. Agreement with colorimetric analysis was good. They have pointed out that an advantage of photonuclear activation of forensic samples over thermal-neutron activation is the avoidance of ^{24}Na production in materials containing large amounts of sodium. They have made exploratory studies on biological samples, drugs, glass, soil, and paper, and have detailed the advantages and problems associated with photonuclear forensic work (*74*).

There has been a great deal of useful work on the determination of the heavier elements in a variety of samples by photon activation. Because of space limitations, the applications of photon activation analysis to the determination of elements heavier than oxygen have not been discussed exhaustively here. Most of the reported applications of photon activation analysis to these elements not referred to in the text are, however, summarized in Table III.

METASTABLE ISOMERS

There are about 40 stable nuclides which have metastable isomers with half-lives greater than 0.5 second. Many of

(58) B. A. Burrows, P. F. Mulvey, Jr., R. D. Cooper, and J. A. Cardarelli, *Strahlentherapie, Sonderb.*, 65, 365 (1967).
(59) J. A. Cardarelli, E. S. Dell, and B. A. Burrows, *NBS Spec. Publ.* 312, Vol. II, Modern Trends in Activation Analysis, pp 847–52 (1969).
(60) P. F. Mulvey, Jr., J. A. Cardarelli, R. A. Meyer, R. D. Cooper, and B. A. Burrows, "Radioisotope Sample Measurement Techniques in Medicine and Biology," IAEA, Vienna, pp 249–258 (1965).
(61) P. F. Mulvey, Jr., J. A. Cardarelli, M. Zoukis, R. D. Cooper, and B. A. Burrows, *J. Nucl. Med.*, 7, 603 (1966).
(62) R. D. Cooper, D. M. Linekin, and G. L. Brownell, Nuclear Activation Techniques in the Life Sciences, Proceedings of a Symposium, Amsterdam, May 1967, IAEA, Vienna, pp 65–80 (1967).
(63) T. Asai, Y. Iwai, R. Miki, Y. Kondo, Y. Sato, and T. Azuma, *Ann. Rep. Radiat. Center Osaka Perfect.*, 8, 120 (1967).
(64) P. Meyers, "Proceedings of the 2nd Conference on Practical Aspects of Activation Analysis with Charged Particles, Liege, Sept. 1967," H. G. Ebert, Ed., Brussels, European Atomic Energy Community, pp 195–224 (1968).
(65) A. K. Berzin, V. V. Sulin, V. I. Belov, G. C. Vitozhents, Y. T. Martynov, V. G. Suslow, and S. I. Shornikov, Radioisotope Instruments in Industry and Geophysics, IAEA, Vienna, STI/PUB/112, pp 323–347 (1966).
(66) A. K. Berzin, G. C. Vitozhents, V. V. Sulin, and S. I. Shornikov, Radiochemical Methods of Analysis, IAEA, Vienna, Vol. I, pp 361–389 (1965).
(67) J. Niewodniczanski, V. V. Sulin, and G. C. Vitozhents, *Nukleonika*, 12, 1153 (1967).
(68) A. Pradzynski, W. W. Sulin, and H. C. Witozenc, *Nukleonika*, 13, 581 (1968).
(69) M. Gerrard, *Isotop. Radiat. Technol.*, 3 (4), 334 (1966).
(70) P. E. Wilkniss and V. J. Linnenbom, *Limnol. Oceanogr.*, 13, 530 (1968).
(71) P. E. Wilkniss, *Radiochim. Acta*, 11, 138 (1969).
(72) P. Meijers and A. H. W. Aten, Jr., *Radiochim. Acta*, 11, 60 (1969).
(73) D. E. Bryan, V. P. Guinn, and D. M. Settle, *AEC Rep.* GA-7041, San Diego, Calif., March 20, 1966.
(74) V. P. Guinn, *AEC Rep.* GA-8013, San Diego, Calif., Oct. 20, 1967.

Table III. Determination of Heavier Elements by Photon Activation Analysis

Element determined		Matrix analyzed	
Arsenic	(*75*)	Alkali halides	(*78*)
Barium	(*76, 77*)	Barium	(*95*)
Cadmium	(*76, 77*)	Calcium	(*95*)
Chlorine	(*78, 79*)	Chromium	(*89*)
Cobalt	(*80*)	Cobalt	(*89*)
Copper	(*81*)	Copper	(*89*)
Europium	(*82*)	Hafnium	(*100, 101*)
Fluorine	(*79, 83, 84*)	Indium	(*85*)
Gadolinium	(*82*)	Iron	(*80, 88, 97*)
Gallium	(*85, 86*)	Niobium	(*96*)
Germanium	(*87, 88*)	Osmium	(*94*)
Indium	(*86*)	Plastics	(*76, 77, 79*)
Iodine	(*78, 83*)	Platinum	(*93*)
Lead	(*76, 77, 83, 89*)	Rare earths	(*99*)
Mercury	(*83*)	Rhodium	(*94*)
Nickel	(*80, 89*)	Selenium	(*75*)
Potassium	(*90*)	Thallium	(*86*)
Rare earths	(*91, 92*)	Titanium	(*87*)
Rhenium	(*93*)	Tungsten	(*84*)
Rhodium	(*93*)	Tungsten bronzes	(*82, 90*)
Ruthenium	(*94*)	Vanadium	(*98*)
Strontium	(*95*)	Zinc	(*81*)
Tantalum	(*96*)		
Thallium	(*85, 89*)		
Titanium	(*97, 98*)		
Yttrium	(*99*)		
Zirconium	(*100, 101*)		

these isomers can be produced from the corresponding stable state by excitation with photons of sufficiently low energy that there will be no photonuclear disintegration reactions produced in any stable nuclides except beryllium and deuterium.

The mechanism of isomer production involves the absorption of a photon by the nucleus. The nucleus is excited to an activation level from whence it decays very rapidly ($<10^{-10}$ sec) to the metastable level. The transition from the metastable state to the ground state then occurs with a characteristic half-life, and with the emission of a photon of energy that is the difference in energy levels of the two states.

The cross section-energy relationship for these reactions, frequently referred to as (γ,γ') reactions, is similar in shape to those of other photonuclear reactions. The peak cross section usually occurs at an energy of about 10 MeV and is usually less than one millibarn. Although the sensitivity is not particularly favorable, the specificity is very good. If irradiations are conducted at a suitably low energy (<7 MeV), the only activities produced will be due to the metastable isomers.

Lukens and coworkers (*102–105*), using a 3-MeV Van de Graaff accelerator and a 15-MeV linear accelerator, and Kaminishi and Kojima (*106*), using a 6-MeV linear accelerator, have examined most of the elements for isomerism, and have published tables of isomers observed, their half-lives, transition energies, and yields. The yield data of Kaminishi and Kojima are shown in Table IV. The irradiation conditions were a 1-minute bombardment with an electron beam current of 1 mA, and the electron energy shown in the table. The samples were counted in the well of a 1.75-inch × 2-inch NaI(Tl) detector. The data imply sensitivities of about 10–100 micrograms for many of the elements.

The amount of activation is very dependent on electron energy. Data by Kaminshi and Kojima show, in the range of 3 to 7 MeV, that the yield from silver is approximately propor-

Table IV. Specific Activities of Metastable Isomers (Ref *106*)

Element	Isotope produced	Half-life	Beam energy, MeV	cpm per gram of element at end of irradiation
Se	^{77m}Se	17.5 sec	5	1.3×10^7
Br	^{79m}Br	4.8 sec	4	1.6×10^7
Sr	^{87m}Sr	2.83 hr	6	3×10^8
Y	^{89m}Y	16 sec	5	9×10^8
Rh	^{103m}Rh	57 min	5	2×10^9
Ag	^{107m}Ag + ^{109m}Ag	44.3 sec 40 sec	5	1.8×10^6
Cd	^{111m}Cd	48.6 min	6	5×10^8
In	^{115m}In	4.5 hr	6	8×10^4
Sn	^{117m}Sn	14 d	6	5
Ba	^{137m}Ba	2.55 min	5	6×10^8
Er	^{167m}Er	2.3 sec	4	4.9×10^7
Hf	^{179m}Hf	18.6 sec	5	1.6×10^7
W	^{183m}W	5.3 sec	5	1.2×10^6
Ir	^{191m}Ir	4.9 sec	5	2.1×10^7
Pt	^{195m}Pt	4.1 d	5	3×10^8
Au	^{197m}Au	7.2 sec	4	4.3×10^7
Hg	^{199m}Hg	43 min	6	9×10^8

(75) Y. Oka, T. Kato, and Y. Konami, *Bunseki Kagaku*, **18**, 971 (1969).
(76) T. Azuma, Y. Sato, J. Tsurugi, R. Miki, Y. Kondo, J. Yoshida, and K. Yamamichi, *ibid.*, p 50.
(77) Y. Kondo, R. Miki, and T. Azuma, The 9th Japan Conference on Radioisotopes (Abstracts of Papers), Nippon Toshi Center, Kozimachi Kaikan, May 1969, Paper A/C-5, pp 35–6 (1969).
(78) S. Abe, *Nippon Kagaku Zasshi*, **87**, 426 (1966).
(79) L. V. Chepel and F. V. Shemarov, *Dokl. Akad. Nauk USSR*, **158**, 682 (1964).
(80) Y. Oka and T. Kato, Nomura, K., *ibid.*, **87**, 147 (1966).
(81) S. Abe, *J. Radioanal. Chem.*, **2**, 275 (1969).
(82) P. J. M. Korthoven, N. A. Wechter, and A. F. Voigt, ANAL. CHEM., **39**, 1594 (1967).
(83) D. Brune, S. Matsson, and K. Liden, *Anal. Chim. Acta*, **44**, 9 (1969).
(84) J. Chin and J. Horsely, *AEC Rep.* GA-8872, San Diego, Calif., October 1968.
(85) *Ibid.*, **87**, 1057 (1966).
(86) *Ibid.*, **86**, 612 (1965).
(87) S. Abe, ANAL. CHEM., **38**, 1622 (1966).
(88) *Ibid.*, **88**, 52 (1967).
(89) J. L. DeBrun and P. Albert, *Bull. Soc. Chim. Fr.*, **1969**, 1020.
(90) M. A. Wechter and A. F. Voigt, ANAL. CHEM., **38**, 1681 (1966).
(91) Y. Oka, T. Kato, and I. Nagai, *Nippon Kagaku Zasshi*, **88**, 871 (1967).
(92) A. Owlya, R. Abdeyazdan, and P. Albert, "Proceedings of the 2nd Conference on Practical Aspects of Activation Analysis with Charged Particles, Liege, Sept. 1967," H. G. Ebert, Ed., Brussels, European Atomic Energy Community, pp 161–94 (1968).
(93) Y. Oka, T. Kato, and T. Saito, *Nippon Kagaku Zasshi*, **87**, 154 (1966).
(94) *Ibid.*, **88**, 866 (1967).
(95) S. Abe, *Yamagata Daigaku Kiyo, Shizen Kagaku*, **7**, 35 (1968).
(96) S. Abe, *Nippon Kagaku Zaisshi*, **86**, 641 (1965).
(97) *Ibid.*, 710.
(98) *Ibid.*, 714.
(99) G. J. Lutz and P. D. LaFleur, *Talanta*, **16**, 1457 (1969).
(100) Y. Oka and T. Kato, *Nippon Kagaku Zasshi*, **86**, 835 (1965).
(101) *Ibid.*, **84**, 588 (1963).
(102) H. R. Lukens, *NBS Spec. Publ.* **312**, Vol. II, Modern Trends in Activation Analysis, 853–9 (1969).
(103) H. R. Lukens, J. W. Otvos, and C. D. Wagner, *Trans. Amer. Nucl. Soc.*, **3**, 414 (1960).
(104) H. R. Lukens, J. W. Otvos, and C. D. Wagner, *Int. J. Appl. Radiat. Isotop.*, **11**, 30 (1961).
(105) J. W. Otvos, V. P. Guinn, H. R. Lukens, and C. D. Wagner, *Nucl. Instrum. Methods*, **11**, 187 (1961).
(106) T. Kaminshi and C. Kojima, *Jap. J. Appl. Phys.*, **2**, 399 (1963).

tional to the eighth power of the electron energy. This is due not only to the production of more photons of sufficiently high energy to cause activation, but also to the more favorable distribution of bremsstrahlung at high energies. Boivin *et al.* (*107*), and Engelmann and Jerome (*108*), have also made systematic studies of the analytical aspects of isomer production with photons.

Bilefield (*109*) has applied this method to the determination of silver in alloys and solders. Abrams and Pelekis (*110*) have described the determination of bromine, silver, and indium in a variety of materials.

Veres (*111, 112*) has described the production of isomers of cadmium, indium, selenium, strontium, and silver with ^{60}Co sources with strengths in excess of 100 curies. Sensitivities of several tens of milligrams of the elements were possible. Veal and Armstrong (*113*) have produced ^{87m}Sr with a 9740-curie ^{60}Co source. A 16-hour irradiation allowed the determination of 0.1% of strontium in a sample of oilfield brine. Yoshihara (*114*) determined indium in alloys by this method. Law and Iddings (*115*) have also studied radionuclide-source photoactivation with sources of 5000 and 30,000 curies.

ERRORS AND CORRECTIONS

Activation analysis is subject to a variety of errors. These include potential errors due to flux gradients, self-shielding, and interfering nuclear reactions.

The angular distribution of bremsstrahlung from a thick target is governed primarily by the multiple scattering of electrons in the target before radiation, and is described by the Schiff equation. This distribution may cause sharp flux gradients in a small space. Unless an internal standard is used, it is necessary that standard and sample occupy well characterized spaces during their irradiation. In the case of an irregularly-shaped sample, an internal standard, utilizing an element whose amount in the sample is known, is useful. This has been used in the determination of carbon and oxygen in sodium (*39, 56*), and in the determination of potassium, gadolinium, and europium in their tungsten bronzes (*82, 90*).

Self-shielding, which can frequently be of great importance in thermal-neutron activation analysis, is usually not critical in photon activation unless the samples are large or very accurate results are required. Niewodniczanski *et al.* (*67*), in their work on the determination of zinc in ores, utilized large samples with copper foils in front of and behind the samples. The average of these foils was taken as a measure of the flux associated with a specific sample. Lutz (*116*) estimated the attenuation to be expected in cylindrical samples of 1-cm diameter irradiated with the beam perpendicular to the axis of the cylinder. A simple expression was developed, giving the ratio of the flux seen by a given sample relative to a hypothetical zero-attenuation sample. This ratio is equal to:

$$e^{-t\Sigma_{\mu\rho}}$$

where t = half of the average thickness of the sample as seen by the flux (= 0.383 × radius for a circular cross section)
Σ = sum over all elements in the sample
μ = gamma-ray absorption coefficient for each element, taken at energy of peak cross section
ρ = density of each element in the sample

Experimental results verified this simple model.

Table V. Nuclear Reactions Used for the Determination of Nitrogen and Carbon, and Interfering Reactions (Ref *49*)

Nuclear reaction used for determination	Threshold in MeV	Principal interfering reactions	Threshold in MeV
$^{12}C(\gamma,n)^{11}C$	18.7	$^{14}N(\gamma,t)^{11}C$	22.7
		$^{16}O(\gamma,\alpha n)^{11}C$	26
$^{14}N(\gamma,n)^{13}N$	10.6	$^{16}O(\gamma,t)^{13}N$	25

Table VI. Amounts of Nitrogen and Oxygen Giving the Same ^{11}C Activity as Given by One Microgram of Carbon by Gamma Activation (Ref *49*)

Electron beam energy, MeV	Oxygen, μg	Nitrogen, μg
30	>6000	>2000
35	680	150
40	180	60
45	90	

Table VII. Amount of Oxygen Giving the Same ^{13}N Activity as Given by One Microgram of Nitrogen by Gamma Activation (Ref *49*)

Electron beam energy, MeV	Oxygen, μg
25	>2500
30	780
35	270
40	140
45	110

The problem of interfering nuclear reactions is more complicated in photon activation analysis than in thermal neutron activation analysis. This is not only because several photonuclear reactions, producing the same radionuclide from more than one stable nuclide, are frequently energetically possible, but also because neutrons are produced in the bremsstrahlung target, the sample, and structural components of the irradiation facility, and may also produce interfering nuclear reactions.

It is not possible to generalize on the extent of interference by neutrons, as this depends substantially on equipment configuration, as well as on electron energy. At the author's laboratory, $^{23}Na(n,\gamma)^{24}Na$ and $^{27}Al(n,\alpha)^{24}Na$ yields are sufficiently large in the energy range of 25–45 MeV so as to make the reaction, $^{25}Mg(\gamma,p)^{24}Na$, for the determination of magnesium worthless in most cases.

Engelmann *et al.* (*49*) have systematically studied the photonuclear interference reactions of oxygen and nitrogen in the determination of carbon, and of oxygen in the determination of nitrogen. The reactions of analytical interest, and the interfering reactions and their Q values are shown in Table V. Ratios of yields are shown in Tables VI and VII. It is neces-

(107) M. Boivin, Y. Cauchois, and Y. Heno, *EURATOM Rep.* EUR 3298.f (1967).
(108) C. Engelmann and D. Y. Jerome, *ibid.*, pp 119–45 (1968).
(109) L. I. Bilefield, *Analyst*, 87, 504 (1962).
(110) I. A. Abrams and L. L. Pelekis, *Latv. PSR. Zinat. Akad. Vestis, Fiz. Teh. Zinat. Ser.*, No. 5, 45 (1967).
(111) A. Veres, *Int. J. Appl. Radiat. Isotop.*, 14, 123 (1963).
(112) A. Veres and I. Pavlicsek, *J. Radioanal. Chem.*, 3, 25 (1969).
(113) D. J. Veal and F. E. Armstrong, *Trans. Amer. Nucl. Soc.*, 11, 95 (1968).
(114) K. Yoshihara, *Doitai To Hoshasen*, 4, 102 (1961).
(115) J. Law and F. A. Iddings, *J. Radioanal. Chem.*, 3, 53 (1969).
(116) G. J. Lutz, *NBS Spec. Publ.* 312, Vol. II, Modern Trends in Activation Analysis, pp 829–34 (1969).

sary, of course, when large amounts of the interfering elements are known or suspected to be present, that the irradiation be carried out at electron energies below the thresholds of the interfering nuclear reactions.

For heavier elements, interfering reactions involving emission of a charged particle become less significant, because of the increasing potential barrier. A cursory study was conducted in the author's laboratory to investigate the interferences from the reactions $^{93}Nb(\gamma,\alpha n)^{88}Y$, $^{90}Zr(\gamma,n^dp)^{88}Y$ and $^{90}Zr(\gamma,2n)^{88}Zr$; ($^{88}Zr \xrightarrow{+} Y^{88}$), in the determination of yttrium, using the reaction, $^{89}Y(\gamma,n)^{88}Y$, with 35 MeV bremsstrahlung. The half-lives of ^{88}Y and ^{88}Zr are 105 days and 85 days, respectively. In the case of niobium, no ^{88}Y was observed, and an upper-limit ratio for production from niobium, relative to production from yttrium, on an atom basis, could be set at 5×10^{-5}. The zirconium sample was counted initially about three hours after irradiation, and an apparent ratio for production, assuming all of the ^{88}Y in the zirconium was produced *via* $^{90}Zr(\gamma,n^dp)$, of ^{90}Zr to ^{89}Y was about 1×10^{-4}. After several weeks, sufficient ^{88}Y had grown into the zirconium sample, that its count rate per atom of target material, corrected for length of irradiation, was of the order of 1% of that due to the yttrium. Since the ratio of the cross sections (not yields) of $(\gamma,2n)$ to (γ,n) reactions of adjacent elements may be as high as 0.20, this type of error may be important in some analyses. Irradiation below the threshold of the $(\gamma,2n)$ reaction eliminates this problem, but sensitivity is substantially reduced. Thresholds for $(\gamma,2n)$ reactions are approximately double those of (γ,n) reactions for the same or adjacent elements.

CONCLUSIONS

Although the emphasis in photon activation analysis is on the determination of trace amounts of the light elements, it should be appreciated that the method determines many elements at trace levels. The author estimates that, at levels of 10^{-7} gram, one may determine approximately as many of the elements with an electron accelerator generating 100 μA of beam current as with a reactor source of 10^{13} n/cm^2-sec. The list for photon activation includes, of course, carbon, nitrogen, and oxygen, for which it may be assumed that reactor activation analysts would be pleased to trade gold, dysprosium, and europium.

Improvements in sensitivity, accuracy, and speed in the determination of the heavier elements by photon activation will come from innovations in separation methods, radiation detector systems, and computer schemes, as well as in improved accelerator irradiation facilities. In the case of the determination of carbon, nitrogen, and oxygen, however, improvements will come almost exclusively from chemistry—rapid and specific separations.

RECEIVED for review June 29, 1970. Accepted September 23, 1970.

Use of Static Argon Atmosphere in Emission Spectrochemical Determination of Chromium in Biological Materials

K. Michael Hambidge

The B. F. Stolinsky Research Laboratories, Department of Pediatrics, University of Colorado Medical Center, 4200 East Ninth Avenue, Denver, Colo. 80220

Major improvements in stability of the direct current arc and in sensitivity and precision of spectrochemical analyses have been achieved by arcing in a static argon atmosphere, with refinements of the excitation chamber described by Gordon. These techniques have been adapted to the trace analysis of ashed biological materials, especially the measurement of nanogram quantities of chromium in blood, hair, and urine. The mean relative standard deviation for quantities of chromium ranging from 1–7 nanograms in 0.2-ml aliquots of serum was 6% (triplicate analyses).

RECOGNITION OF CHROMIUM as an essential micronutrient (*1*) has increased the need for accurate determination at the nanogram level in biological materials. Human deficiency of this trace element, which may be relatively common (*2*), has been implicated in a number of disease processes (*3–5*).

Emission spectrochemical techniques have been used extensively for the determination of trace elements in biological samples, especially in large-scale survey work (*6*) for which the potential for simultaneous multielement analysis is an important advantage. These techniques, particularly with refinements of excitation conditions, are potentially very sensitive, and absolute sensitivities of the order of one nanogram or less have been achieved for many elements (*7*). Routine use of these achievements in the analysis of biological samples has been restricted by such factors as complex sample preparation or impracticable limitations of sample size.

Instability of the primitive direct current (dc) arc, and associated indifferent reproducibility, have limited the value of its inherent sensitivity (*8*). However, the static inert gas atmosphere developed and refined by Gordon (*8–10*) has

(1) W. Mertz, *Physiol. Rev.*, **49**, 163 (1969).
(2) H. A. Schroeder, J. J. Balassa, and I. H. Tipton, *J. Chronic Dis.*, **15**, 941 (1962).
(3) L. L. Hopkins, O. Ransome-Kuti, and A. S. Majaj, *Amer. J. Clin Nutr.*, **21**, 203 (1968).
(4) W. H. Glinsmann and W. Mertz, *Metab., Clin. Exp.* **15**, 510 (1966).
(5) R. A. Levine, D. H. P. Streeten, and R. J. Doisy, *ibid.*, **17**, 114 (1968).
(6) I. H. Tipton, M. J. Cook, R. L. Steiner, C. A. Boye, H. R. Perry, and H. A. Schroeder, *Health Phys.*, **9**, 89 (1963).
(7) E. L. DeKalb, R. N. Kniseley, and V. A. Fassel, *Ann. N.Y. Acad. Sci.*, **137**, 235 (1966).
(8) W. A. Gordon, N.A.S.A., T.N. D-2598, Clearinghouse for Federal Scientific and Technical Information, Springfield, Va. 22151, 1965.
(9) W. A. Gordon, N.A.S.A., T.N. D-5236, Clearinghouse for Federal Scientific and Technical Information, Springfield, Va. 22151, 1967.
(10) W. A. Gordon, N.A.S.A., T.N. D-4769, Clearinghouse for Federal Scientific and Technical Information, Springfield, Va. 22151, 1968.

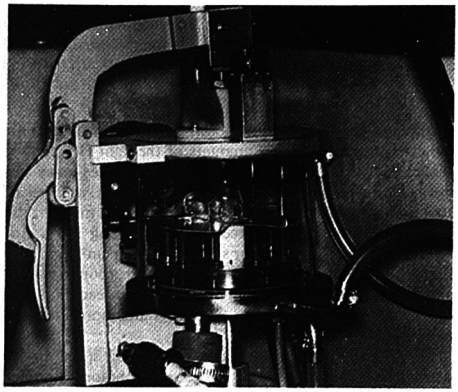


Figure 1. Controlled atmosphere static argon excitation chamber

Table I. Instrumentation

Spectrometer	Jarrell-Ash 1.5-meter direct read-out. Compact atom counter (Model 66-004)
Entrance slit	25 μ
Exit slits	75 μ
Grating	1180 grooves/mm
Spectral dispersion	5.59 Å per mm
Wavelength coverage	2000–8000 Å
External optics	Single spherical quartz lens, 180 mm f 1
DC current source	Jarrell-Ash dr Varisource (modified)
Excitation chamber	Gordon controlled-atmosphere, Static argon arc chamber

resulted in a very stable arc, excellent reproducibility of analyses, and enhancement of line:background ratios for many elements. Moreover, Gordon's techniques permit speed of analysis and simplicity of sample preparation.

This report details preliminary results of the application of these techniques to the quantitative determination of trace elements in biological samples and, in particular, the measurement of chromium in serum, red cells, hair, and urine.

EXPERIMENTAL

Apparatus. The static argon arc chamber (Figure 1) was similar to that previously described by Gordon (*8*). Cyanogen bands were eliminated and background continuum reduced (*8*) by the exclusion of air from this system. Further reduction in background and increase of line:background ratios were achieved by replacing air with argon at a pressure less than atmospheric. Lower argon pressures also resulted in a wider, more stable, positive arc column.

A major improvement in arc stability and reproducibility of analyses was achieved by the introduction of a tantalum sphere at the tip of a graphite counter-electrode (*9*).

The spectrometer employed for these studies was a 1.5-meter direct reading instrument (Table I). No spectrographic facilities were utilized, but vaporization characteristics of individual elements were studied by means of a strip-chart recorder attached to the output of selected photomultiplier tubes.

A low temperature asher (Tracerlab 600) was used for oxidation of organic material prior to analysis.

Table II. Analytical Conditions

Exposure time	12 sec (no preburn)
Argon pressure	300 Torr
Arc current	30 A
Arc gap	12 mm
Region of arc column in optical field	0.5–5.5 mm above anode
Sample electrode (anode)	Pre-purified carbon 1.5- × 0.18-in., pointed tip subtending 90° angle. (Met-Bay 1397 MBC-1)
Counter-electrode (cathode)	Graphite 0.12- in. diam. (Ultracarbon 5001) with tantalum sphere 1.6-mm diam
Spectroscopic buffer	4 mg of AgCl precipitated on anode

Sample Preparation. Preliminary elimination of organic material resulted in a more stable arc together with improved accuracy and reproducibility of analyses. The preconcentration factor and facilitation of sample preparation as a solution are additional features which are advantageous for certain materials. Organic material was oxidized in the oxygen plasma of a low temperature asher; this procedure not only minimized the risks of contamination or loss of trace elements, but yielded a sample which was ideal for subsequent processing. Ashing of serum, urine, and hair samples was rapid and complete, but complete oxidation of red blood cells and solid tissues including liver and muscle was more difficult.

Plasma, urine, and red blood cells in measured volumes ranging from 50 μl to 10 ml, depending on requirements, were pipetted into glass ashing boats of appropriate size and dried in an electric oven prior to oxidation. Hair samples, weighing 100 mg or less and up to 1 inch in length were washed and dried, introduced into glass boats (45 × 20 × 8 mm) with Teflon (Du Pont)-covered forceps and then weighed accurately. It was necessary to ensure that hair did not protrude above the top of the dish, and caution was required in the initial evacuation of the low temperature asher. All samples were routinely ashed overnight, though, depending on sample size, constant ash weights could be achieved in much shorter time intervals. The ash was dissolved directly in the ashing boats with measured quantities of 1.5*N* hydrochloric acid; or, particularly with larger samples all of which was not required for immediate analysis, the ash was weighed *in situ*, then transferred with a Teflon-covered spatula to polystyrene vials, vibrated on a "Wig-L-Bug" to ensure homogeneity of sample, and stored until required for analysis.

Mean recovery of chromium-51 added to 20 serum samples prior to drying was 99.7% with 1 relative standard deviation (rel std dev) of 3.2%. A radiochromium solution (50 μl) was also added onto the top of hair samples already in the ashing boats, and mean recovery for 10 samples, in this instance, was 98.1% (1 rel std dev = 2.9%). Recoveries of sodium (101 ± 2% rel std dev) and potassium (103 ± 2%) from serum samples were equally satisfactory.

Preparation of Electrodes. Solid carbon sample electrodes with a pointed tip subtending a 90° angle were prepurified by arcing for 15 seconds. Silver chloride solution, 4 mg, was precipitated on the tip of each electrode by pipetting 10 μl of silver nitrate solution containing 4.7 mg of the salt, followed by a slight excess of hydrochloric acid (10 μl 6*N* HCl). After drying the buffer on the electrodes, 10- or 20-μl aliquots of standard solution or dissolved sample were added, following which the electrodes were loaded into the arc chamber in batches of ten.

Analytical Conditions. These are summarized in Table II. Exposure times of 12 sec were adequate to ensure complete vaporization of sample. Vaporization of the relatively large quantities of sodium and potassium present in biological

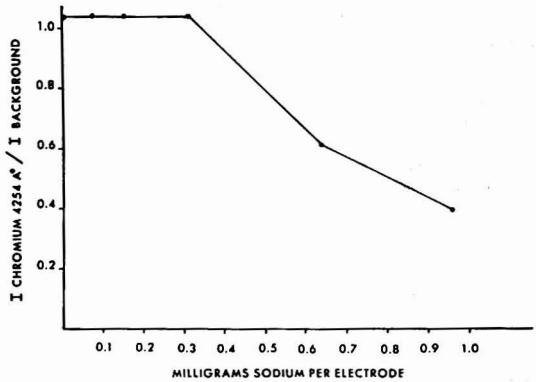


Figure 2. Effect of increasing increments of sodium on line:background ratio for 3 nanograms of chromium

samples commences almost instantaneously and is completed rapidly (approximately 6 sec at 30 A) in comparison with that of the silver buffer (10–12 sec). A study of vaporization curves on a strip chart recorder indicated that vaporization of chromium and other trace elements in the sample paralleled that of these major elements rather than the silver buffer.

Silver chloride functions as a spectroscopic buffer to lower the excitation temperature of the arc in argon (*8*); cooling of this arc by metal ions of relatively low ionization potential was essential in order to achieve optimal conditions for the sensitive neutral atom lines. Though the major cations present in biological materials also contributed to this effect, addition of silver chloride continued to be of major importance in increasing line:background ratios of the neutral atom lines. Larger quantities of this buffer did not improve sensitivity further, and vaporization characteristics of the ashed biological samples were not modified by this means.

RESULTS AND DISCUSSION

The special characteristics associated with the analysis of ashed biological samples in this system were related to sample size and to the principal matrix elements, sodium and/or potassium. For certain materials, such as serum and urine, one milligram or more of ash was required for each sample to ensure that an adequate quantity of chromium (a minimum of approximately one nanogram) was available for analysis. In these circumstances the sodium and potassium had a major influence on the appearance and characteristics of the arc, including vaporization rates. The common matrix effect of the silver buffer was forfeited, and the sensitivity for chromium and other elements was decreased as a result of an increase in background continuum without a corresponding increase in line intensity. Matrix effects of increasing increments of sodium on the line:background ratio for 3 nanograms of chromium are illustrated in Figure 2. Addition of potassium to aqueous standards resulted in a closely comparable effect to that of sodium on a molar basis; this effect of potassium on background adjacent to chromium 4254 Å is illustrated in Figure 3. Phosphate and sulfate, the major anions in the ashed samples were not detrimental to chromium sensitivity in the maximum quantities encountered.

Chromium 4254 Å line:background ratios for increasing increments of serum ash are illustrated in Figure 4. When the sample size is increased to the equivalent of 300 μl of serum or more, there is a decrease in this ratio despite the greater chromium content of the larger samples. This impairment of sensitivity parallels that observed when sodium is added to

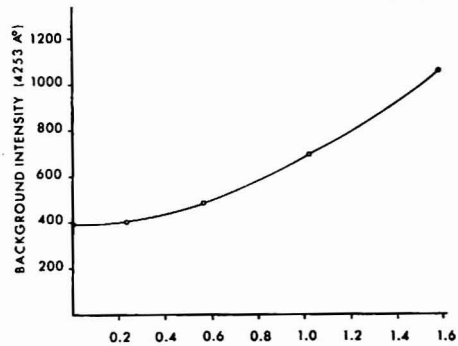


Figure 3. Effect of increasing increments of potassium on background intensity

aqueous solutions in quantities equivalent to those present in the serum ash. Reliable recoveries of sodium following oxidation of serum (rel std dev = 2%) and the negligible variations in sodium levels between different serums ensured that there was no significant variation in matrix effects for equal quantities of different sera. Serum ash samples equivalent to 200 μl of serum (approximately 2.7 mg of ash), though contributing little to signal:background ratio compared with 100 μl of serum, were selected because the larger sample minimized error from variation in the blank signal.

Analytical curves were obtained by the technique of standard additions: dilute chromium solutions, prepared from Matthey "specpure" chromium chloride were added to aliquots of serum prior to drying and ashing. Curves were linear for chromium concentrations ranging from 0 to 25 nanograms per electrode: the chromium concentration of the original serum was determined by extrapolation of the curve to the background-corrected origin. Mean rel std dev for serum chromium concentrations ranging from 5–35 ng/ml serum (1–7 ng/electrode) was 10%. With triplicate analyses, which were routinely employed in practice, there was a 6% rel std dev. Chromium concentrations in early morning serums from 36 normal subjects, determined by these techniques, have ranged from 5 to 31 ng/ml, with a mean of 13 ng/ml. These results are similar to recent values obtained by

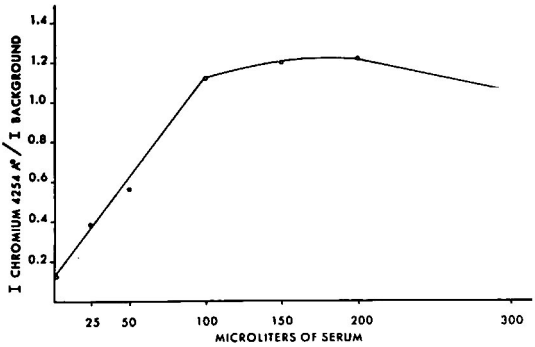


Figure 4. Variation in chromium line:background ratio with increasing increments of serum-ash sample

Table III. Wavelengths and Sensitivities for Elements Studied

Element	Wavelength, Å	Absolute sensitivity,[a] ng
Chromium	4254	1
Manganese	4031	1
Zinc	2138	0.5
Copper	3247	2.5
Iron	3720	4
Molybdenum	3133	13
Magnesium	2802	1

[a] Nanograms of element required for 30% increase in line over background.

other investigators (*11*, *12*), but no direct comparison with other techniques has been undertaken.

Analysis of red blood cells was characterized by similar matrix effects. In this instance, the changes observed with increasing increments of sample ash corresponded with the effect of adding equivalent quantities of potassium, the major intracellular cation, to aqueous standards. Sodium, sulfate, and phosphate did not influence line:background ratios in the maximum quantities present in these samples. Optimal ratios for Chromium 4254 Å were achieved with 2 mg of sample ash. Variation in intracellular potassium concentrations is normally as negligible as that for sodium in serum, resulting in the same analytical advantages; no significant difference in background has been observed between different red cell samples of identical size. Theoretically, these characteristics apply equally to analyses of ash from other cellular tissues, thus permitting extension of these techniques to the analysis of chromium in a wide range of biological materials.

In contrast to serum and intracellular fluids, concentrations of sodium and potassium in a unit volume of urine are highly variable, and the matrix effects observed with equal volumes of different urine samples were not consistent. This problem was minimized by using a constant weight of urine ash; however, to ensure complete exclusion of error from matrix variation, the quantity of urine ash was restricted to 1 mg for each analysis. The total cations present in samples of this size were insufficient to effect sensitivity, and analytical results could be quantitated by comparison with aqueous chromium standards. The mean 24-hour urinary excretion of chromium of ten young adults was 9 μg; individual results ranged from 0 to 18 μg/24 hours. Problems with sample contamination, otherwise minor, have impaired precision of analyses of subnanogram quantities of chromium, which has been of practical importance with respect to urine analyses. The quantity of this element present in 1 mg of urine ash has averaged 0.5 nanogram, with 14% rel std dev. Internal standards have not been evaluated; however, a satisfactory internal standard would be of potential value in the analysis of urine samples, by negating the effects of variable matrix and thus permitting greater flexibility of sample size. Silver from the silver chloride buffer has not proved suitable in practice as an internal standard: it has not been ascertained whether alternative buffers might serve a dual role.

Determination of chromium concentrations in hair was uncomplicated by matrix effects because of the relatively large concentrations of this element, and relatively low concentrations of total ash in hair. Aliquots of dissolved ash (20 μl), corresponding to 5 mg of the original hair sample and containing <100 μg of total ash were added to each sample electrode. Precision of analyses for a pooled hair ash solution, containing 2.5 nanograms per 20 μl, was 6% rel std dev (triplicate analyses). Results of hair chromium determinations in 10 young adult men ranged from 360 to 830 ppb, with a mean of 540 ppb.

COMMENT AND CONCLUSIONS

Though several techniques have been described for the analysis of chromium in biological materials (*1*), the accurate measurement of serum chromium concentrations, which are only a few parts per billion, continues to present major problems. Atomic absorption spectrophotometry (*13*) requires several milliliters of sample, and adequate instrumental sensitivity has been very difficult to achieve; such equipment has been used in this laboratory for the determination of hair chromium concentrations (*14*). Recent reports (*15*) indicate that gas–liquid chromatography of chromium extracted from ashed serum as the fluoro-β-diketone chelate is a very sensitive technique.

(11) W. Mertz, personal communication Agricultural Research Service, 1969.
(12) F. J. Feldman, Presented at the VIII International Congress of Nutrition, Prague, 1969.
(13) F. J. Feldman, E. C. Knoblock, and W. C. Purdy, *Anal. Chim. Acta*, **38**, 489 (1967).
(14) K. M. Hambidge, D. O. Rodgerson, and D. O'Brien, *Diabetes*, **17**, 517 (1968).
(15) J. Savory, P. Mushak, F. W. Sunderman, R. H. Estes, and N. O. Roszel, ANAL. CHEM., **42**, 294 (1970).

The greater sensitivity of the present emission spectrochemical techniques compared with atomic absorption spectrophotometry is an important advantage in the measurement of serum chromium concentrations. Economy of sample size is similar to that achieved with gas–liquid chromatography, but in contrast to the latter, sample preparation does not involve any extraction procedure, and there is only a minimum of handling of the oxidized sample.

A further potential advantage of emission spectrochemical techniques is the capacity for simultaneous multielement analysis. Concurrently with chromium analyses, six other elements have been measured and these are listed in Table III. Sensitivities are expressed as the quantity of element required for a 30% increase of line over background; in practice precision of analyses has permitted realistic detection limits lower than the tabulated figures. Optimization of analytical conditions for these elements has not been attempted. As an example of the economy in sample size which can be achieved with these techniques, only 10 μl of serum are required for the simultaneous determination of zinc, copper, and magnesium concentrations. Initial studies have been restricted to seven elements only because of the lack of spectrographic facilities and the restricted number of photoelectric multipliers available for use in the direct-reading spectrometer.

It is concluded that emission spectrochemical analysis with a static argon arc chamber as described by Gordon is a valuable technique for the quantitative measurement of chromium in biological samples. The inherent sensitivity of this technique is of particular importance for the determination of chromium in serum samples and other tissues in which the concentration of this element is only a few parts per billion.

ACKNOWLEDGMENT

The invaluable advice of W. A. Gordon is gratefully acknowledged. Analyses were performed with the technical assistance of M. Jacobs.

RECEIVED for review August 5, 1970. Accepted October 26, 1970. This work was supported by USPHS Grant No. 1-RO1-AM-12432 from NIAMD.; partly supported by USPHS Grant No. R.R.-00069.

Mixed Carrier Gases in Chromatography—A Source of Error

Raymond Annino, Joseph Franko,[1] and Harry Keller[2]

Research Center, The Foxboro Company, Foxboro, Mass.

Gas chromatography using mixed carrier gases has been evaluated for use as an on-line deviation analysis technique for process control. A serious experimental difficulty is uncovered. Briefly, it is shown that if a particular sample solute is also a component of the carrier gas stream, its elution peak area is not only determined by the difference between its concentration in the sample and in the carrier gas, but also by the identities and the concentrations of all other components of the sample. The origin of this effect is identified and a computer simulation of column behavior, based on the appropriate theoretical model, yields results consistent with those obtained experimentally. Although the observed effect severely limits the general use of chromatographic difference procedures, there are instances where mixed carrier gases provide an excellent solution to a problem. As an example, a method is proposed for the easy resolution of a difficult solute pair by including one of the two solutes in the carrier gas stream.

SUCCESSFUL OPERATION of industrial processes demands reliable means of control. This in turn requires sensing the magnitude of some particular property of the process and, when necessary, initiating a corrective action, the extent and duration of which depends on the sign and magnitude of the difference between the determined value of the property and some reference value. Therefore, if a gas chromatograph is to be used as the sensing element of a control system, there appears to be an advantage in using it in the differential, rather than the conventional mode. Reilley and his colleagues (*1*) in this country, and Zhukhovitskii (*2*) in the USSR, recognized this some time ago. They suggested that if a process sample, suitably diluted with helium, was chromatographed with a helium carrier gas containing fixed percentages of appropriately chosen reference materials, then the response to constituents common to the process stream and the carrier gas stream would appear as difference signals. The sign and magnitude of the difference signals would establish the deviation of the process stream from the desired concentration.

Since the carrier gas contains components which can dissolve in the stationary phase or be adsorbed on an active surface in the column, a base line, elevated with respect to that which would be obtained in a conventional chromatogram, is observed. This corresponds to the plateau of the fully developed frontal chromatogram of the carrier. Either conventional elution or frontal gas chromatograms can be run on this plateau. This type of chromatography is known variously as Difference or Differential Chromatography, Vacancy, Shadow, or Mirror Chromatography and Plateau Elution Chromatography (*1–5*).

There have, as yet, been few accounts of practical application of this form of difference chromatography; among these are the determination of small amounts of water in organic liquids, using water saturated helium carrier gas (*6*) and, more recently, the recommendation that the analysis of sulfur

[1] Present address, Iowa State University, Ames, Iowa.
[2] Present address, Northeastern University, Boston, Mass.

(1) C. N. Reilley, G. P. Hildebrand, and J. W. Ashley, Jr., ANAL. CHEM., 34, 1198 (1962).
(2) A. A. Zhukhovitskii, in "Gas Chromatography, 1964," A. Goldup, Ed., Elsevier, New York, N.Y., 1965, pp 161–169.
(3) A. A. Zhukhovitskii, N. M. Turkel'taub, M. Gaier, M. N. Lagashkina, L. A. Malyasova, and G. P. Shlepuzhnikova, *Zavod. Lab.*, 29, (1) 8 (1963).
(4) J. R. Conder, in "Progress in Gas Chromatography," J. H. Purnell, Ed., Interscience, New York, N.Y., 1968, pp 209–270.
(5) Raymond Annino, "Plateau Elution Chromatography," presented at the Pittsburgh Conference, Analytical Chemistry and Applied Spectroscopy, Cleveland, Ohio, March 1969.
(6) S. Ahuja, G. D. Chase, and J. G. Nikelly, ANAL. CHEM., 37, 840 (1965).

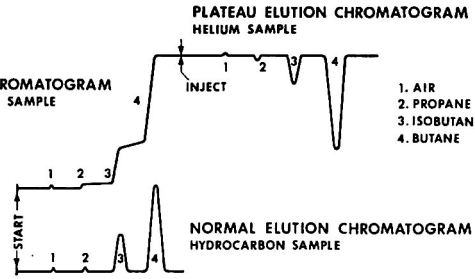


Figure 1. Development of normal elution (helium carrier: 100 μl sample), frontal and plateau elution chromatograms of a mixture of air, propane, isobutane, and butane

Column: 20% w/w squalane on 100/120 mesh Chromosorb P; 6 ft × 0.085-inch i.d. Temperature, 20 °C

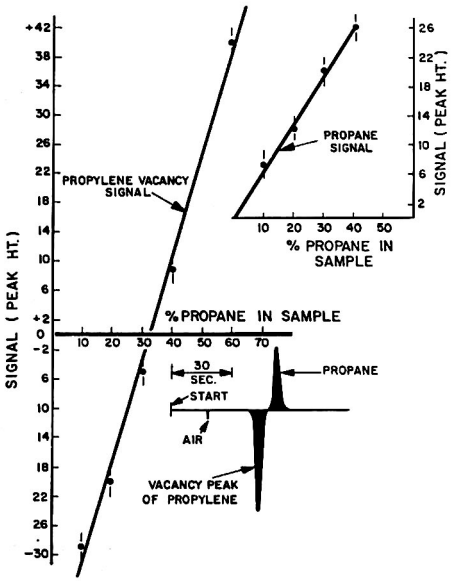


Figure 2. Elution of 100-μl propane–helium samples from a column 6 ft × 0.085-inch i.d. of 20% w/w squalane on 100/120 mesh Chromosorb P. Carrier gas: 20% propylene–80% helium

Bottom right, typical plateau elution chromatogram; sample propane–helium = 20:80%. Left, dependence of propylene vacancy peak height on composition of 100-μl propane–helium sample. Upper right, dependence of propane peak height on composition of sample

dioxide (*7, 8*) can be better performed with helium carrier gas containing a small amount of sulfur dioxide.

The purpose of this paper is to call attention to a serious practical difficulty arising in this mode of chromatographic operation which requires emphasis and elucidation if the method is to be more widely applied in practice. The problem is associated with the fact that the area of the so-called difference peaks (and the side of the base line on which they are seen) depends not only on the difference between the concentrations of the solute in the sample and in the carrier gas, but also on the identities and concentrations of all other components of the sample. This effect may be implicit in the development of finite concentration chromatography theory of recent years (*9–17*). However, to the best of our knowledge, except for this work and that of Helfferich and Klein (*18*), which appeared after the completion of the present investigation, it has never been clearly stated nor studied.

EXPERIMENTAL

Apparatus and Procedure. The gas chromatograph was of conventional design using thermal conductivity detection and incorporating special switches to allow introduction into the column of any one of several premixed carrier gases, either to conduct frontal analysis or to set up a carrier plateau upon which subsequent frontal or elution analyses could be run.

Samples and mixed carrier gases were made up on the basis of partial pressure in large amounts from chromatographically pure components. Mixture compositions were checked by conventional elution gas chromatography using standard analyzed mixtures obtained from The Matheson Company as reference standards for calibration. The results of these analyses were found to be within ±1% relative of the reference standards. A typical set of frontal, plateau elution, and conventional elution chromatograms obtained with the system is illustrated in Figure 1.

RESULTS

In its simplest form, plateau elution chromatography would involve a carrier stream comprising a nonretained gas (*e.g.*,

(7) R. K. Stevens, A. E. O'Keefe, J. D. Mulik, and K. J. Krost, "Gas Chromatography of Reactive Sulfur Gases in Air at the Parts Per Billion Level. II. Differential Response Chromatography," presented at 157th National Meeting, ACS, Anal. Chem. Div., Minneapolis, Minn., April 14–18, 1969; Abstr. Papers, Anal. 56.
(8) E. L. Obermiller and G. O. Charlier, *J. Chromatogr. Sci.*, **7**, 580 (1969).
(9) A. A. Zhukhovitskii, N. M. Turkel'taub, L. A. Malyasova, A. F. Shlyakhov, V. V. Naumova, and T. I. Pogrebnaya, *Zavod. Lab.*, **29**, 1162 (1963).
(10) F. I. Stalkup and H. A. Deans, *AIChE J.*, **9**, 106 (1963).
(11) F. I. Stalkup and R. Kobayashi, *ibid.*, p 121.
(12) D. L. Peterson and F. Helfferich, *J. Phys. Chem.*, **69**, 1283 (1965).
(13) A. A. Zhukhovitskii, M. L. Sazonov, A. F. Shlyakhov, and A. I. Karymova, *Zavod. Lab.*, **31**, 1048 (1965).
(14) K. T. Koonce, H. A. Deans, and R. Kobayashi, *AIChE J.*, **11**, 259 (1965).
(15) A. A. Zhukhovitskii, M. L. Sazonov, A. F. Shlyakhov, and V. P. Shvartsman, *Zh. Fiz. Khim.*, **41**, 2640 (1967).
(16) P. C. Mangelsdorf, Jr., ANAL. CHEM., **38**, 1540 (1966).
(17) J. R. Conder and J. H. Purnell, *Trans. Faraday Soc.*, **64**, 1505 (1968).
(18) F. Helfferich and G. Klein, "Multicomponent Chromatography," Marcel Dekker, Inc., New York, N. Y., 1970, pp 212–213.

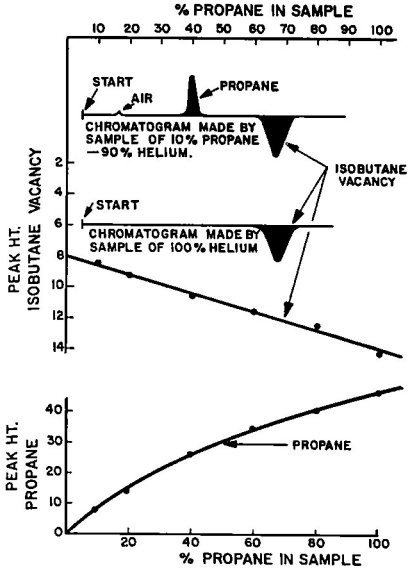


Figure 3. Plateau elution of 100-μl propane–helium samples from column (see Figure 2). Carrier gas: 10% isobutane–90% helium

Upper diagrams show typical chromatograms. Lower diagrams show dependence of isobutane vacancy height and propane peak height on propane–helium sample composition

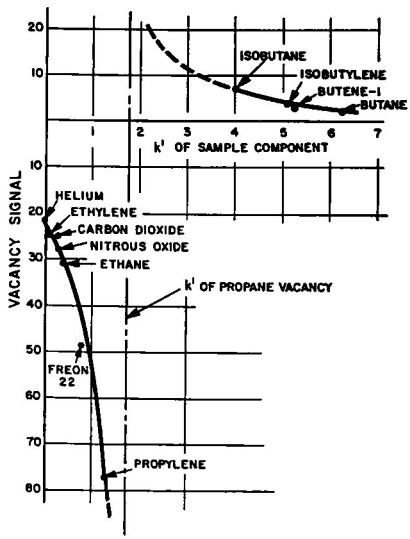


Figure 4. Variation of the vacancy signal as a function of partition ratio k' of injected sample material. Column (see Figure 2). Carrier gas: 20% propane–80% helium. All samples 100 μl of undiluted material.

helium) and a retained gas. Injection of a sample of pure nonretained gas would then create a concentration "vacancy" of the retained material in the flowing stream and this "vacancy peak" would travel through the column, emerging at the correct retention time but being "negative." It is this view which led to the introduction of the term "vacancy" (*3*). In accord with this convention, in all discussion here, the term "vacancy" will be used to describe the chromatographic peak associated with the soluble components of the carrier gas mixture even though, as stated and illustrated below, the signal may be positive or negative depending on the circumstances.

Effect of Sample Partition Coefficient on Area of Vacancy Peak. The results of experiments with a propylene–helium (20:80%) carrier gas stream and 100-μl propane-helium samples are summarized in Figure 2. As is seen (lower right), the positive propane peak is quite normally eluted and peak heights, over a reasonable range, are closely linearly proportional to the propane concentration in the injected sample. In contrast, the propylene vacancy, which occurs at the retention time for propylene, varies in height very markedly with change in propane concentration in the injected sample. This is contrary to what would be expected since, in the simplest view, outlined above, the vacancy size should be dependent on sample size only and not on composition as long as no propylene occurred in the sample. The effect is so marked indeed, that above about 30% propane, the propylene vacancies actually appear as positive peaks and a pure propane sample yielded a positive propylene peak large enough to be interpreted as indicating about 20% propylene in the propane.

The above findings establish clearly that the original simple postulate (*1*, *2*) is inadequate since no obviously simple relation exists between the vacancy peak height or area for the carrier gas component and its concentration in the sample unless other retained substances are absent from the sample.

The results of a series of experiments with isobutane–helium (10:90%) carrier streams with, again, 100-μl propane–helium injected samples, are summarized in Figure 3. The variations of vacancy peak heights or area which occur with changes in the concentration of the sample solute (*i.e.*, propane) are quite different in form from those shown in Figure 2, since here the isobutane vacancy peaks are always negative and the peak areas increase continuously as the concentration of propane in the sample increases. Again, elution of the propane is normal, the fall off of linearity of peak height with propane concentration in the sample over a large concentration range is a detector problem. These observations indicate clearly that the changes in vacancy peak size are dependent not only on sample composition but also in some way on the partition coefficients of the sample solutes.

That the above view is correct is established by the results of experiments summarized in Figure 4. These data are derived from the plateau elutions of a wide variety of sample types (100 μl, undiluted by helium) in a propane–helium (20:80%) carrier gas stream. The partition ratio, k', for propane is about 1.8. As the k' for the various sample materials which were used increases from 0 to 1.8, the size of the negative propane vacancy peak which is created by a fixed sample size, increases. In contrast, when k' for the sample material exceeds 1.8, the propane vacancy peaks are all positive and progressively then diminish in size as k' for the sample material increases beyond 1.8. (The partition ratio expresses the equilibrium ratio of the amount of sample

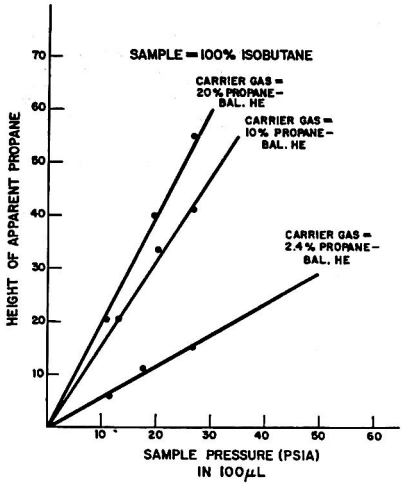


Figure 5. Variation in the height of the vacancy signal for propane in indicated propane–helium streams as a function of amount of pure isobutane sample injected. Note all vacancies are positive under these conditions. Column as described in Figure 2

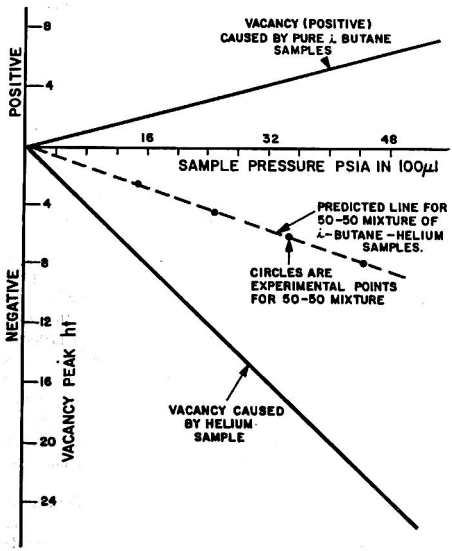


Figure 6. Variation of propane vacancy signal height with sample amount for elution of isobutane, of helium, and of 50–50 mixtures of these two, respectively. Column as described in Figure 2. Carrier gas: 20% propane–80% helium

component in the stationary phase to the amount in the mobile phase.)

The dependence of propane vacancy peak height on the amount of sample injected (undiluted by helium), for a case where the k' of the sample material exceeds that for propane,

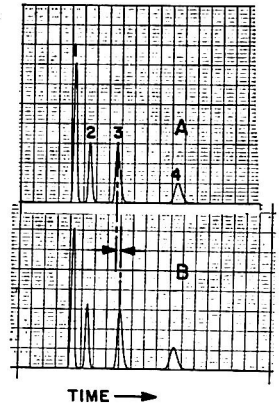


Figure 7. Illustration of the shift in retention time of the vacancy peak for propane with change in its concentration in the carrier gas mixture. Sample components: air (1), ethane (2), propane (3), and isobutane (4).

Chromatograms: *A*, carrier gas is 10% propane–90% helium; *B*, carrier gas is pure helium. Both chromatograms were obtained with a 6 foot × 0.085-inch i.d. column of 20% w/w bis(2-ethoxyethyl) sebacate on 100/120 Chromosorb P at 20 °C

is shown in Figure 5, for several propane–helium carrier gas compositions. The vacancy peak height increases linearly with the amount of sample at all carrier gas compositions. When k' for the sample is less than that for propane, the negative propane vacancy peak is made more negative as the amount of sample is increased. The effect is again linearly related to sample amount. This is illustrated in Figure 6 which shows plots of the effect on propane ($k' = 1.8$) vacancy size for sample injections of both pure isobutane ($k' = 4$) and pure helium ($k' = 0$) when different amounts of these are injected into a propane–helium (20:80%) stream. Shown also are the corresponding data obtained with isobutane–helium mixture (50:50%) as samples. These data points lie exactly on the arithmetic average line for the pure sample materials. These findings establish that the height (and hence also the sign) of the vacancy peak is defined, in the first instance, by the partition ratio of all sample components and, in the second instance, by the relative amounts of these components present in the sample.

In the light of the above findings, it is difficult to visualize any readily applicable practical approach to the application of this form of deviation analysis to the quantitative study of complex mixtures since, minimally, solution of the relevant simultaneous equations would require use of $(n - 1)$ samples of known composition in addition to the one of unknown composition, where n is the number of retained components. In an industrial process, n could be very large.

Retention Time of Vacancy as a Function of Concentration. The chromatograms shown in Figure 7 illustrate something of the extent of the shift in retention time of a vacancy peak (here a positive peak) which can be achieved with a fixed sample size by varying the concentration of the corresponding

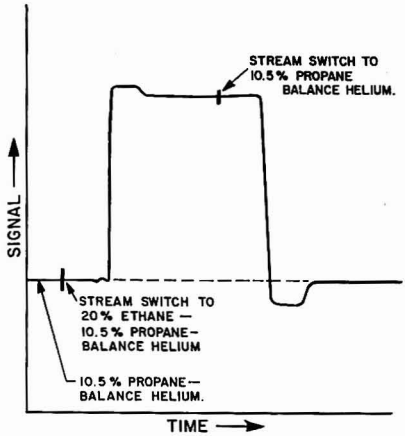


Figure 8. Sorption and desorption frontal chromatograms obtained on 6-ft × 0.085-inch i.d. column as for Figure 7. Sequence of operation and stream compositions as indicated

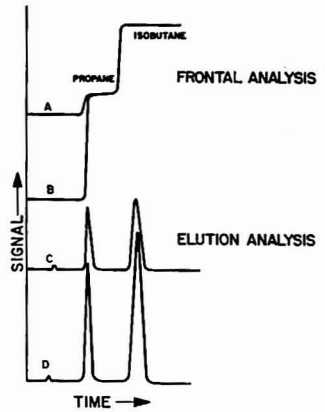


Figure 9. Frontal and elution chromatograms obtained with column as described in Figure 7

***B*, helium stream and *A*, propane–helium (10.5:89.5%) stream replaced by propane–isobutane–helium (10.5:20.0:69.5%) stream. *C* is elution of 100 μl of pure isobutane sample in carrier mixture of propane–helium (10.5:89.5%) and *D* is elution of 100 μl of propane–isobutane–helium (10.5:20.0:69.5%) sample in pure helium.**

soluble component in the carrier gas. This relatively large retention shift is a consequence of the several effects attending the use of high concentrations of the soluble carrier component and can be quantitatively accounted for by developed theory (*10–23*). As would then be expected, in the absence of any significant interdependence of partition coefficients, only imperceptible shifts of retention are noted for the highly dilute sample components which are not also components of the carrier stream. This aspect of the technique requires no theoretical elaboration here and is illustrated only to show an attractive aspect of the method, *i.e.*, the added flexibility of choice of retention to facilitate separation.

Frontal Analysis. A number of experimentally determined frontal chromatograms which exhibit curious peak shapes are shown in Figures 8 and 9. In the former, the initial base line corresponds to the plateau for a propane–helium (10.5:89.5%) stream. After some time, indicated on the diagram, a stream of propane–helium–ethane (10.5:69.5:20.0%) was substituted. Subsequently the new front emerged and eventually set up a new plateau level. This level was maintained for a while but, exactly at the retention time of propane, a fall to a new plateau level occurred. This then was maintained permanently. The hump produced was perfectly reproducible. A subsequent switch back to the original propane–helium stream caused a fall in plateau height which, initially, overshot the original base line and returned only to that level again, exactly at the retention time of propane. In this sequence a negative hump was produced and this, too, was perfectly reproducible. This behavior, that is, the production of positive and negative pulses depending on the relative magnitudes of the k' for the stream components, clearly has affinities with what has been described earlier in the account of the plateau elution experiments.

In Figure 9, *B* shows the switch from pure helium to a stream of propane–helium–isobutane (10.5:69.5:20%) which produces the expected two sharp steps. In *A*, the switch from an initial stream of propane–helium (10.5:89.5%) to the same propane–helium–isobutane stream as above is shown. Again, two steps are seen, although, since the propane concentration in both streams is the same, no propane step should, ideally, appear. Identical anomalous behavior is observed in the corresponding elution experiments, the chromatograms of which are also shown in Figure 9 (lower section). *D* is a conventional elution chromatogram in helium of 100 μl of the quoted propane–helium–isobutane sample while *C* shows the plateau elution of a pure sample of isobutane in a carrier of propane–helium (10.5:89.5%). Since the sample contains no propane, a negative vacancy peak should appear in *C*. In contrast, a positive peak is observed. The elution and frontal anomalies are thus tied together by these experiments, which implies that the usual explanation offered for such anomalies in frontal analysis as are shown in Figures 8 and 9, *i.e.*, competitive sorption, displacement, etc. cannot explain the present findings since in the elution experiment the amount of isobutane in the column is much less than is the case in the frontal experiment. Further, the behavior exemplified in Figures 8 and 9 has evident association with the effects discussed earlier.

DISCUSSION

The effect of finite vapor concentration in gas chromatography has been considered by a number of authors (*9–23*). However, their primary interest has been focused on the con-

(19) C. H. Bosanquet and G. D. Morgan, in "Vapor Phase Chromatography," D. H. Desty, Ed., Butterworth, London, 1957, p 35.
(20) C. H. Bosanquet, in "Gas Chromatography, 1958," D. H. Desty, Ed., Butterworth, London, 1958, p 107.
(21) P. C. Haarhoff and H. J. van der Linde, ANAL. CHEM., 37, 1742 (1965).
(22) *Ibid.*, 38, 573 (1966).
(23) G. Guiochon, L. Jacob, and P Valentin, *J. Chim. Phys. Physicochim. Biol.*, 66, 1097 (1969).

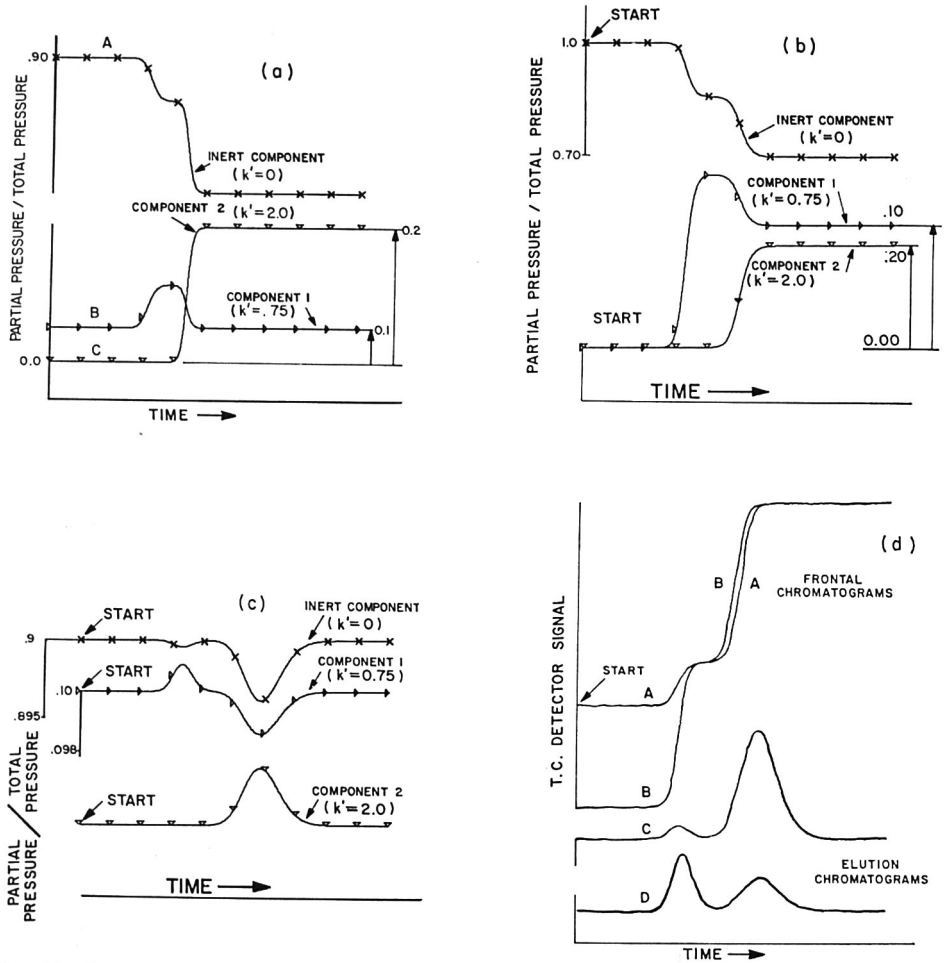


Figure 10. Computer simulation results. Plots of calculated ratios of partial pressure of component/total pressure against time in

(*a*) **Frontal analysis. Original stream composition; inert carrier ($k' = 0$), 90%: component 1 ($k' = 0.75$), 10%. Switched stream composition; inert carrier, 70%: component 1, 10%: component 2 ($k' = 2.0$), 20%.**

(*b*) **Frontal analysis. Original stream composition; inert carrier, 100%. Switched stream composition; inert carrier, 70%: component 1, 10%: component 2, 20%.**

(*c*) **Elution analysis. Carrier gas; inert carrier, 90%: component 1, 10%. Sample, 100% component 2.**

All curves shown were directly drawn on an IBM 1620 plotter. Figure (*d*) represents chromatograms constructed from the data of Figures (*a*)–(*c*). Curve *A* corresponds to (*a*), curve *B* to (*b*), curve *C* to (*c*). Curve *D* is the conventional elution chromatogram of a sample of 50:50% mixture of components 1 and 2 with 100% inert carrier. The corresponding partial pressure ratio plots are not shown for the sake of brevity

sequent band distortions and changes in retention volume which occur in either frontal or elution analysis, as a result of the several physical effects which accompany operation at high solute concentration. Little attention has been given to the impact of such studies on practical analytical application and for this reason the practical consequences established experimentally here have not been explicitly recognized. There are several possible reasons which might be postulated to account for the effects noted in this work, *e.g.*, competitive sorption, concentration dependence of partition coefficients, velocity changes at sorption boundaries, among others. However, it is the postulate of this work that while these may well be contributory, there is a more fundamental underlying problem. To elaborate this view let us first assume (*a*) no mutual interaction of solutes; (*b*) concentration independent partition ratios; (*c*) ideal gas behavior; and (*d*) invariance of pressures throughout the system.

The experimental consequences of operation at a finite

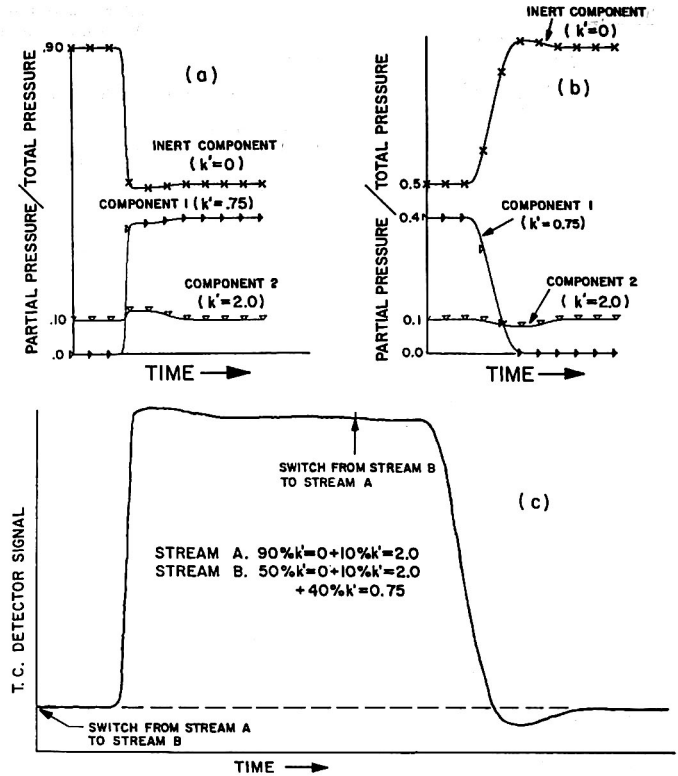


Figure 11. Computer simulation results. Plots of calculated ratios of partial pressure of component/total pressure against time in frontal analyses

(*a*) Original stream composition; inert carrier (k' = 0), 90%: component 2 (k' = 2.0), 10%. Switched stream composition; inert carrier, 50%: component 2, 10%; component 1 (k' = 0.75), 40%

(*b*) Original stream composition; inert carrier, 50%; component 2, 10%: component 1, 40%. Switched stream composition; inert carrier, 90%: component 2, 10%

Operation involved in (*b*) is reverse of (*a*). Combination corresponds to complete sorption–desorption frontal experiment. These data yield the computed chromatogram shown in (*c*). All curves shown were directly drawn by an IBM 1620 plotter

vapor concentration then, quite simply, can be attributed to the sample components having to adjust their contributions to the total gas volume in order to maintain constant total pressure in the gas phase. To illustrate this view, consider a binary carrier gas consisting of 90% inert gas and 10% of a soluble component A, of $k' = 1.0$, flowing at some fixed flow rate x ml/min, and in equilibrium with a liquid phase contained in a column. Then at some appropriate time, this carrier gas is diverted and another carrier mixture containing 80% inert gas, 10% of substance A and 10% of another soluble substance B, of $k' = 2.0$, is passed into the column. As the component B dissolves in the liquid phase, the flow of carrier mixture into the column increases to maintain the total pressure constant. Consequently, there is more of substance A entering the column per unit time than in the original situation where only inert gas and A were present. We can see that this is the case because, in the extreme situation that B had $k' \to \infty$, that is, was completely dissolved, the helium–component A mixture remaining of the original gas packet has the composition 80:10%. Thus, extra A with respect to helium has been introduced. (It must be remembered that fixed inlet and outlet pressures are assumed; that is the rational view to take since it is standard practice.) If the capacity of the column remains constant, the excess quantity of A then breaks through as a positive peak at the retention time corresponding to $k' = 1.0$ and the signal remains anomalous until the column is equilibrated with B. The chromatograms shown in Figures 8 and 9 illustrate this effect and its converse, precisely. Since elution chromatography is the special case of frontal chromatography, corresponding to a momentary switching of the gas streams, the same phenomenon is expected to be evident in this mode also. Thus, as illustrated in Figure 9, the small positive hump evident in the frontal chromatograms has its elution counterpart, in accord with the present theory.

In general then, during a separation (using either inert or

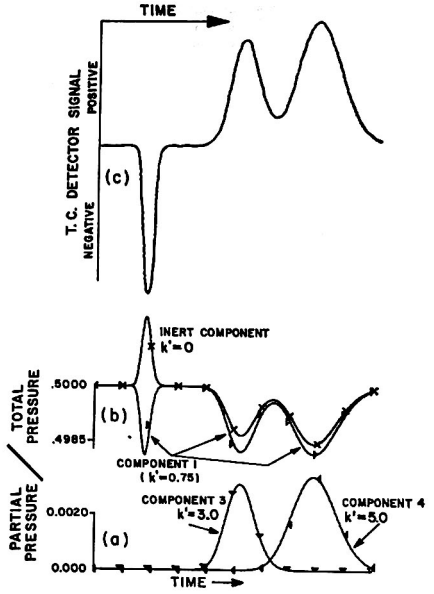


Figure 12. Computer simulation results. Elution of a sample of composition: inert carrier ($k' = 0$), 20%: component 3 ($k' = 3$), 30%: component 4 ($k' = 5$), 50%; using carrier gas of composition; inert carrier, 50%: component 1 ($k' = 0.75$), 50%

Curves for partial pressure of component/total pressure as a function of time for components 3 and 4 are shown in (*a*). Corresponding plots for inert carrier and for component 1 are shown in (*b*). Note correspondence of perturbations. (*c*) shows the resultant chromatogram. All curves shown were directly drawn by an IBM 1620 plotter.

mixed carrier gases), there are zones in the column where the solutes are concentrated and make a significant contribution to total pressure *via* their vapor pressures. Therefore, the partial pressure of the carrier gas must be reduced within these zones so that the total pressure is kept constant over that small region. A similar view has been expressed by Zhukhovitskii and his colleagues in their discussion of "Chromatography Without Carrier Gas" (*9, 13, 15*). The reduction in carrier gas pressure in a zone must also satisfy the equilibrium constant requirements of all components present in the zone. Thus, a concentration perturbation of all carrier components is produced under all peaks and must be satisfied in terms of the material balance of the entire column. Consequently, peak areas, which one expects to represent only the difference in concentration of solutes found in both sample and carrier gas, are drastically influenced by changes in the concentration of the other sample components.

The adequacy of this explanation could, in principle, be demonstrated by theoretical calculational procedures but is much more graphically shown by comparing the type of results obtained in the laboratory experiments previously described with those obtained from a computer column simulation program based on the model outlined above. The mathematical basis of this program was developed from a simple plate model which was subject to the restraints (*a*)–(*d*) previously listed. A detailed account is given in the appendix.

COMPUTER SIMULATION STUDIES

The computer program was designed to accept as inputs the partition ratios (k') of the various components, the carrier gas inlet and outlet pressures, the sample size, and the flow rate at the column exit. All computer outputs were directly plotted on an IBM 1620 plotter. All of the laboratory experiments described earlier, and others, could be simulated.

Figure 10*a* shows the computer output plots of the ratio of individual component partial pressures to total pressure as a function of time for the simulated frontal analysis involving the switch from an initial stream of inert carrier ($k' = 0$) and a component 1 of $k' = 0.75$ (90:10%) to one containing inert carrier, component 1, and a component 2 of $k' = 2.0$ (70:10:20%). Note particularly the hump-shaped perturbation introduced in the plot for component 1, the concentration of which is, of course, unchanged by the switch, as evidenced by the return of the plot to the original level after the perturbation. It is interesting to note also that the return to the original level occurs precisely at the retention time for component 2. These observations correspond exactly to those seen in the laboratory experiment illustrated in Figure 8. This perturbation also is mirrored exactly in the plot for inert carrier. Figure 10*b* shows similar plots for a switch from a stream of pure inert carrier to one of inert carrier, component 1, and component 2 (70:10:20%). Again, the perturbation of the partial pressure curve for component 1 is seen as a hump and this diagram is even more reminiscent of the first half of Figure 8. Again, of course, a balancing perturbation in the plot for inert carrier is seen.

Figure 10*c* shows the same type of plots for simulated elution of a pure sample of component 2 in a carrier stream of inert carrier, component 1 (90:10%). Again balancing perturbations are seen. Finally, Figure 10*d* illustrates the computer plotted chromatograms corresponding to the experiments illustrated in (*a–c*). Curve *A* corresponds to (*a*), curve *B* to (*b*) and curve *C* to (*c*). Included also in *D* is a conventional chromatogram computed for a sample of components 1 and 2 (50:50) eluted by pure helium. Figure 10*d* is to be compared directly with Figure 9, and it is clear that they are essentially identical.

It is to be noted that the initial hump, such as seen for component 1 in Figure 8 and in Figure 10*a*, is hidden in the combined two-component chromatogram of Figure 10*d*. This is because the k' for component 2 exceeds component 1. Thus the breakthrough of component 2 obscures the return of component 1 to its final value. The correctness of this view can be established by computing curves for the reverse process illustrated in Figure 10, *i.e.*, starting with a stream containing component 2 and switching to a stream containing, in addition, component 1. Figures 11*a* and 11*b* show computer derived partial pressure curves for this situation and Figure 11*c*, the composite chromatogram constructed from them. The hump for component 2 which appears in the partial pressure diagrams of 11*a* and 11*b* is now clearly visible in the composite chromatogram of Figure 11*c*. Further verification is found in the similarity of this chromatogram with one obtained experimentally for a similar experiment and shown in Figure 8.

The above findings give substantial support to the model presented here and to the proposal that perturbations in the concentrations of all carrier components occur at times corresponding to the retention times of all components of both

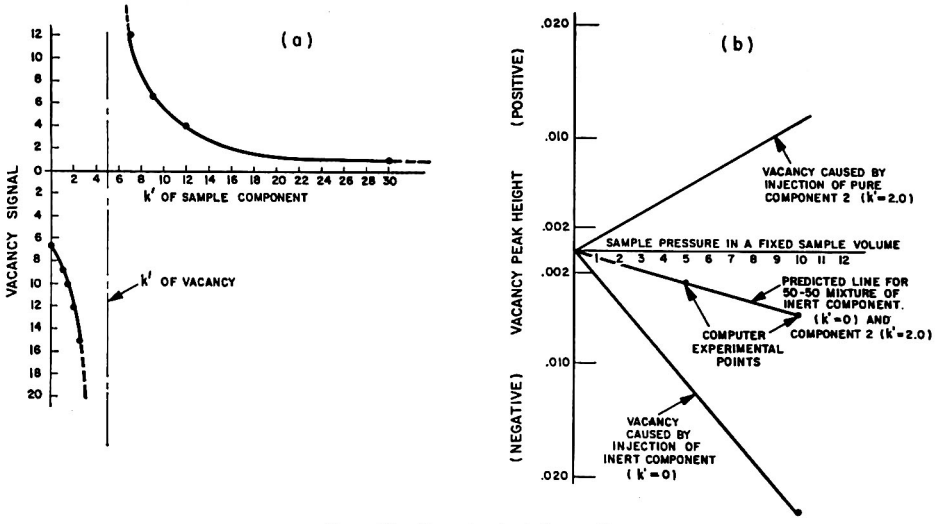


Figure 13. Computer simulation results

(*a*) Summary of calculated data for variation of size of vacancy signal for a carrier gas component with a $k' = 5.0$ diluted in inert carrier (20:80%) which is caused by the injection of pure samples having various k' values

(*b*) Summary of calculated data for dependence of vacancy peak height for carrier component of $k' = 0.75$ diluted in inert carrier (20:80% caused by the injection of varying amounts of pure samples having $k' = 2.0$ and zero, respectively. Shown also is arithmetic mean line and points for 50:50% sample mixture derived from computer simulated chromatograms

carrier and sample. Figure 12, again computer derived, establishes the validity of this view. It depicts in (*a*) and (*b*) the component partial pressure/total pressure ratios as a function of time in a plateau elution of a sample containing components 3 ($k' = 3.0$) and 4 ($k' = 5.0$) in a stream of inert carrier ($k' = 0$) and component 1 ($k' = 0.75$) in the proportions 50:50%. Perturbations in the curves for both inert carrier and component 1 occur at the k' for component 1 and also at those for components 3 and 4 as well. In consequence, the size of the vacancy for component 1 shown in the computed chromatogram in Figure 12*c* is a complex function of the several variables. This accords with the experimental results.

Figure 13 finally establishes without question that the model proposed identifies the essential origin of the anomalies uncovered. Figure 13*a* shows a plot of the computer-calculated size of vacancy peak created by plateau elution of pure samples, having a range of k', in a stream consisting of inert carrier and a component of $k' = 5.0$. This diagram is obviously identical in form with that constructed from the experimental data and illustrated in Figure 4. Figure 13*b* completes the evidence. It shows a plot of computer calculated vacancy peak heights for plateau elution of pure samples of $k' = 0$ and 2.0, respectively, in a stream consisting of inert carrier and a component of $k' = 0.75$. This combination corresponds qualitatively to that for the system used to provide the data employed in constructing Figure 6. Computer calculated values for vacancy peak height produced by plateau elution of 50:50% samples of the components of $k' = 0$ and 2.0 fall exactly on the arithmetic average of the computed lines for the pure samples. The behavior shown is thus identically that illustrated in Figure 6.

The remarkable agreement between the data derived through the model and the experimental information obtained leaves little room for doubt that, despite the approximations involved, the main source of the response anomaly has been identified correctly as the natural requirement for material balance in a system of constant pressure gradient. The assumption of ideal gas behavior introduces little error as is shown by widespread gas chromatographic experience. The success of the present approach indicates that in the systems employed there can be little mutual interaction of solutes. It is a relatively simple matter to establish that the assumption of concentration independent partition ratios introduces little error; in fact, velocity variation due to concentration changes can be shown to be much more significant.

Figure 14 shows the computer derived chromatograms for the vacancies, created by pure inert carrier samples, plateau eluted in carrier mixtures of: *A*, inert carrier 20%, component 1 ($k' = 0.75$) 80% and *B*, inert carrier 80%, component 1, 20%. The results of numerous such computer experiments lead to the finding that retention times are well described by the equation

$$t_r = t_0 + t_0 k' (1 - y)$$

where

y = mole fraction of the soluble component of a binary carrier gas
t_0 = retention time of an unretained substance
t_r = retention time of the soluble component, which has a partition ratio, k'.

This equation is consistent with expressions derived in theoretical studies on the variation of flow rate due to sorption effects (*10–12, 14, 17–23*).

A consequence of this effect is that in plateau elution, with a fixed amount of pure sample, the vacancy size dependence on

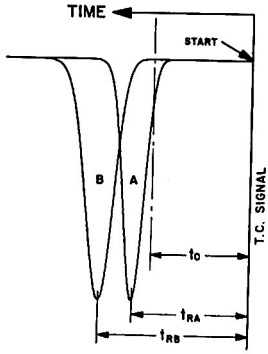


Figure 14. Computer column results

Plateau elution of pure inert carrier samples in carrier streams; *A*, inert carrier, 20%, component 1 ($k' = .75$), 80%; *B*, inert carrier 80%, component 1, 20%. Diagram illustrates substantial dependence of retention volume of the component 1 vacancy peak on carrier composition change due to consequent carrier velocity changes

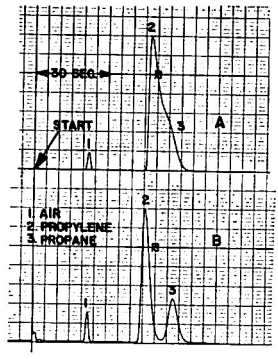


Figure 15. Chromatograms illustrating the improved resolution deriving from the use of mixed carrier gases

Sample composition; 25% propylene, 10% propane, 0.1% air, 64.9% helium. Carrier composition; *A*, 100% helium: *B*, 20% propylene–80% helium. Column: 6-ft × 0.085-inch i.d., 20% squalane on 100/120 Chromosorb P at 25 °C

the amount of soluble component in the carrier mixture is nonlinear. The corresponding laboratory experiments were not pursued in detail because of the complications introduced by nonlinearity of detector response at high solute concentrations in the inert carrier. However, Figure 5 contains implications supporting the above prediction.

CONCLUSIONS

It has been demonstrated both experimentally and theoretically that the area or height of so-called "difference peaks" depends not only on any difference of concentration of the particular component in carrier gas and sample, but also on the identities and concentrations of all other components in the sample. Failure to take this into account leads to totally erroneous results, and analysts using doped carrier gases in differential chromatographic analysis should clearly be aware of this problem. For example, Ahuja *et al.* (*6*), when using water saturated carrier gases, noted a positive peak for water when analyzing a water-free butanol sample and found also, in the analysis of acetone with a tritiated water saturated helium carrier gas, a perturbation of the water under both the acetone peak and at the water (vacancy) peak retention time. These effects are clearly accounted for in the present work, their analog being illustrated in Figure 12 here. Similarly, the use of sulfur dioxide doped carrier gases for the determination of sulfur dioxide (*7*, *8*) will be useful only at levels of sulfur dioxide in the sample which are much above that in the carrier gas. Unless accurately calibrated under conditions of fixed sample composition, inaccurate results will be obtained.

Other examples where unexpected vacancies have been noted have been attributed to impurity of the carrier gas (*24*). A correction scheme has been proposed (*25*) which involves subtracting the peak area of a purified sample from that obtained before purification. In view of the complex nature of the relationship of vacancy size and sign to sample composition, it would appear that this procedure should be adopted with caution.

Although the general use of mixed carrier gases for differential analysis may be in question, there are a number of areas where this technique provides an excellent solution to a problem. Its use for the adjustment of thermal conductivity of the carrier gas in the analysis of hydrogen (*26*) or other gases (*27*, *28*) has been recommended. Also, since it was first suggested (*29*), a number of authors have used carrier gases containing some concentration of the stationary liquid phase to either maintain a constant level on the support or to block active sites. It is proposed here that there are some other aspects of the technique which have not been fully explored. For example, one can take good analytic advantage of the fact that the retention time of the vacancy can be changed by varying the concentration of the solute in the carrier gas. Since it allows selective adjustment of the retention time of one of the peaks of an unresolved pair, it obviates the need for a longer column with the consequent increase in analysis time (*5*). In Figure 15, the analysis of a propane/propylene mixture is shown to be much improved by adjustment of propylene retention time by replacing pure helium with a propylene–helium carrier. Perhaps even more important, trace amounts of materials can be far better analyzed in the presence of large concentrations of interfering components by use of mixed carrier than by recourse to longer columns or the more usual two-column methods. Finally, mixed carrier

(24) B. O. Prescott and H. L. Wise, *J. Gas Chromatogr.*, **4**, 80 (1966).
(25) G. Castello and G. D'Amato, *J. Chromatogr.*, **32**, 625 (1968).
(26) J. E. Purcell and L. S. Ettre, *J. Gas Chromatogr.*, **3**, 69 (1965).
(27) J. Jordan and B. B. Kebbekus, ANAL. CHEM., **37**, 1572 (1965).
(28) B. B. Kebbekus, M. H. Barsky, R. T. Rossi, and J. Jordan, *J. Amer. Chem. Soc.*, **88**, 2398 (1966).
(29) A. Kwantes and G. W. A. Rijnders, in "Gas Chromatography, 1958," D. H. Desty, Ed., Butterworth, London, 1959.

gases with their attendant "vacancies" can also be used to good advantage to provide an internal timing standard for programming purposes (*30*).

APPENDIX I

Equations Used for Column Simulation Program. Equations relating gaseous and dissolved components ($P_{diss} = KP_{gas}$) and total pressure ($\Sigma P_{i,\,gas} = P_{tot}$) are readily obtained for each plate and material balance equations for movement of each component through a plate are derived. The result is $2N + 1$ equations and $2N + 1$ variables, where N is the total number of components.

The program begins with the last plate, this plate being the only one for which a known amount of gas is removed per unit time. It calculates the new composition in this plate and the amount of gas which must be removed from the next plate to maintain constant pressure and to satisfy the other restraints. This procedure continues with each plate up to the first plate. A zero plate is provided to hold the sample; when it has been exhausted, it, too, is filled with carrier.

Let P_{ijk} be the pressure of the jth component in the kth phase of the ith plate. Assume $k = 1$ to be gas and $k = 2$ to be liquid. P°_{ijk} is the present pressure; P'_{ijk} is the new pressure. ΔP_i is the change in total pressure (quantity) between plates i and $i + 1$. Thus it represents the amount of material transferred between these plates. Furthermore, let

m = number of plates
n = number of components
K_j = partition ratio for the jth component
CC_j = fraction of jth component in carrier
SC_j = fraction of jth component in sample
PT_i = total pressure in ith plate

Assuming equilibrium in each plate requires that:

$$K_j P_{ij1} = P_{ij2},\ 0 < i \leq m,\ 0 < j \leq n \tag{1}$$

where K_j is the partition ratio of the jth component. We further require that the total gas pressure in each plate equals the sum of all of the gaseous component pressures.

$$\sum_{j=1}^{n} P_{ij1} = PT_i,\ 0 < i \leq m \tag{2}$$

Finally the change in pressure in each plate of each component in both the liquid and gas phase must, since pressure is proportional to quantity, be equal to the amount of that component entering the plate minus the amount leaving it.

$$P'_{ij1} + P'_{ij2} - P^{\circ}_{ij1} - P^{\circ}_{ij2} = \frac{\Delta P_{i-1}}{PT_{i-1}} P_{i-1j1} - \frac{\Delta P_i}{PT_i} P^{\circ}_{ij1} \tag{3}$$

It is assumed here that the composition of gas leaving the plate is the old composition.

Plate zero is handled in a special fashion. While sample remains, the total amount remaining is simply reduced by ΔP_0 until ΔP_0 is greater than PT_0. At this point an unknown amount of carrier is added to the sample plate to raise the pressure, PT_0, up to ΔP_0 which is the pressure demanded by the first plate. If the amount of added carrier is X, then the $(\Delta P_0/PT_0) P_{0ij}$ term in Equation 3 will change to $\Delta P_0/(X + PT_0)$ $(P_{0ij} + X'CC_j)$ subject to the restriction that $\Delta P_0 = PT_0 + X$. After making these substitutions, Equation 3 becomes (X is eliminated)

$$P'_{ij1} + P'_{ij2} - P^{\circ}_{ij1} - P^{\circ}_{ij2} = P_{i-1j1} + CC_j(\Delta P_{i-1} - PT_{i-1}) - \frac{\Delta P_i}{PT_i} P^{\circ}_{ij1} \tag{3a}$$

There are now, for each plate, $2n + 1$ unknowns. They are P_{ij1} and P_{ij2} for each j and ΔP_{i-1}. There are also $2n + 1$ equations. They are n equations like Equation 1, n equations like Equation 3 or 3a and Equation 2. The simple form of Equation 1 allows its immediate substitution into Equation 3 and 3a, thus reducing the work required to solve the system of equations. The results are, after dividing through by $1 + K$:

$$P'_{ij1} - \frac{P_{i-1j1}}{(1 + K_j)\,PT_{i-1}} \Delta P_{i-1} = P^{\circ}_{ij1} - \frac{P^{\circ}_{ij1}}{(1 + K_j)PT_i} \Delta P_i \tag{4}$$

$$P_{ik1} - \frac{CC_j}{1 + K_j} \Delta P_{i-1} = P^{\circ}_{ij1} + \frac{1}{1 + K_j} \times \left(P_{i-1j1} - CC_j PT_{i-1} - \frac{P^{\circ}_{ij1}}{PT_i} \Delta P_i\right) \tag{4a}$$

To solve the system, the equations of form 4 are subtracted from Equation 2 to determine ΔP_{i-1}.

$$\Delta P_{i-1} \sum_{j=1}^{n} \frac{P_{i-1j1}}{(1 + K_j)\,PT_{i-1}} = \Delta P \sum_{j=1}^{n} \frac{P^{\circ}_{ij1}}{(1 + K_j)\,PT_i} \tag{5}$$

A similar equation results from 4a. Having found ΔP_{i-1}, all remaining unknowns immediately come from Equation 4.

RECEIVED for review June 1, 1970. Accepted October 29, 1970.

(30) Raymond Annino, *J. Chromatogr. Sci.*, 8, 288 (1970).

Micro and Ultramicro Analyses by Null Point Pressuremetry and Coulometry: Hydrogenation and Hydrogenolysis

D. J. Curran and James E. Curley[1]

Department of Chemistry, University of Massachusetts, Amherst, Mass. 01002

A multirange differential capacitive-type pressure transducer system has been used to monitor pressure changes in a hydrogen charged reactor during the reaction of alkenes, alkynes, organo-halides, nitro and azo compounds with hydrogen over palladium-on-charcoal and the subsequent coulometric regeneration of hydrogen gas. Graphical treatment of the strip chart readout yields the time required to generate hydrogen equivalent to that consumed by the sample. Alternatively, a semiautomatic method with digital readout of the micromoles of hydrogen generated is feasible under certain conditions. Precision and accuracy of a few parts per thousand are easily attained in many cases. As little as 0.56 micromole of octene-1 has been determined with an accuracy of about —1% relative.

OUR EARLIER WORK with pressure transducers in analytical hydrogenations has shown that highly accurate and precise analyses can be obtained using null point pressuremetry and volumetric addition of sodium borohydride to regenerate the hydrogen gas consumed in the reaction (*1*). The method has the advantage that it eliminates the assumptions concerning solvent vapor pressures and ideal mixing of solutions which are necessary to calculate the free-space equivalent for solutions or liquids added to the closed reactor. Such corrections are obtained experimentally. However, it was also concluded that further improvements in the method could be obtained if it were possible to eliminate the compression of the gas phase produced by volume additions to the closed system.

The present work combines null point pressuremetry with coulometric generation of hydrogen gas. The latter feature eliminates the need for a free-space equivalent correction due to volumetric addition of reagent to the system for the regeneration of hydrogen gas. A volume compensation technique is used to eliminate a similar correction for the volume of sample introduced. Wherever possible, nonideal mixing of solutions has been avoided by using the same solvent throughout. In those cases where nonadditive volume additions do occur, the method provides a correction. In most cases, a graphical technique is used to locate the null point. For samples that rapidly take up sufficient hydrogen that background drift is negligible, a semiautomatic procedure with digital readout is demonstrated.

Samples of octene-1 ranging in size from 126 to 0.56 μmoles were determined by the graphical technique with an accuracy and precision of a few parts per thousand for the larger samples. Other carbon–carbon unsaturates investigated included cyclohexene, 4-octyne-2-ol, olive oil, cottonseed oil, and corn oil. The reduction of other functional groups was also studied. Samples of azobenzene, nitrobenzene, and picric acid were reduced to the corresponding amines. Several earlier studies of the analytical hydrogenation of nitro groups using gas burets have been reported. Joshel (*2*) found that 1.5 grams of nitrobenzene could be quantitatively reduced in 90 minutes over Adams' catalyst. Hörmann and coworkers (*3*) used a Warburg apparatus to determine dinitrophenols with an accuracy of 4%. Gore and Inamdar (*4*) reduced nitro groups in microsamples of organic compounds with an accuracy of a few per cent.

We have also found that the hydrogenolysis at 42 °C of about 100 μmoles of chloro-, bromo-, and iodobenzene and α-chlorotoluene yields results with a precision and accuracy of 0.8% or better.

EXPERIMENTAL

Reagents. Sources of organic compounds were: octene-1 (Phillips Petroleum Company, Special Products Division, minimum 99 mole %), U.S.P. cottonseed oil (Fisher Scientific Company), olive oil (Matheson, Coleman and Bell), corn oil (a nationally known commercial food product), and 4-octyne-2-ol (K and K Laboratories). Nitrobenzene, azobenzene, picric acid, chlorobenzene, iodobenzene, bromobenzene, cyclohexene, 1-iodopropane, *p*-bromoaniline, and *trans*-cinnamic acid were Eastman White Label; α-chlorotoulene was Eastman Yellow Label (Eastman Organic Chemicals, Distillation Products Industries). Azobenzene and picric acid were recrystallized from absolute ethanol. Purified tank hydrogen was obtained from Air Reduction Company. All other chemicals were reagent grade, except as noted.

Solvents. 2-Propanol was refluxed for 1 hour over sodium borohydride (Fisher Scientific Company) and then distilled. Reagent grade glacial acetic acid (Du Pont) and 2,2,4-trimethylpentane (Eastman White Label) were used without further purification. Laboratory distilled water was redistilled from alkaline permanganate.

Hydrogenation Media. Except as noted, the catalyst was 5% palladium-on-charcoal (Matheson, Coleman and Bell). Seed oils were hydrogenated in 25-ml of 2-propanol containing 50-mg of catalyst and 1 drop of concentrated sulfuric acid. Alkenes and the alkyne, picric acid, and nitrobenzene were reduced in 25 ml of 2-propanol containing 50 mg of catalyst. Azobenzene was reduced in 25 ml of glacial acetic acid containing 50 mg of catalyst. Chlorobenzene and iodobenzene underwent hydrogenolysis in glacial acetic acid that was 1.5*M* in acetate ion. One gram of 5% palladium-on-charcoal and a trace of platinum oxide were placed in 25 ml of this solvent. The platinum oxide was omitted for bromobenzene and α-chlorotoluene.

Sample Solutions. Several compounds were determined as neat liquids. Their densities were determined by weighing known volumes equilibrated at the appropriate reaction temperature. Solutions of other samples were prepared by weight and their densities determined. These data are listed in Tables I and II.

Check Analyses. The Hanus iodine monobromide method as given by Siggia (*5*) was used to determine the iodine values

[1] Present address, Pfizer and Co., Inc., Medical Research Laboratories, Groton, Conn. 06340.

(1) D. J. Curran and J. L. Driscoll, ANAL. CHEM., 42, 1414 (1970).
(2) L. M. Joshel, IND. ENG. CHEM., ANAL. ED., 15, 590 (1943).
(3) H. Hörmann, J. Lamberts, and G. Fries, *Hoppe-Seyler's Z. Physiol. Chem.*, 306, 42 (1956).
(4) T. S. Gore and P. K. Inamdar, *Mikrochim. Acta*, 1968, 883.
(5) S. Siggia, "Quantitative Organic Analysis *via* Functional Groups," 3rd ed., John Wiley and Sons, Inc., New York, N. Y., 1963, pp 316–318.

Table I. Densities of Neat Organic Liquids at Their Reaction Temperatures

Code[a]	Sample	Density-g/ml	Reaction temperature, °C
1a	Octene-1	0.7132	24
1b	Octene-1	0.7061	27
2	4-Octyne-2-ol	0.8691	28
3	Cyclohexene	0.8042	28
4	Chlorobenzene	1.090	42
5	Iodobenzene	1.801	42
6	α-Chlorotoluene	1.084	42
7	Bromobenzene	1.483	42

[a] Code numbers are used for cross referencing between Tables.

(IV) of the seed oils and the mole per cent unsaturation of octene-1 and cyclohexene. The halogen content of the halides was determined by the Office of Research Services, Chemical Analysis Laboratory, University of Massachusetts at Amherst using Schöniger oxygen combustion followed by coulometric titration of the halide with silver ion. Azobenzene, nitrobenzene, and picric acid were determined by a modification of the procedure given by Siggia (*6*). Ti(III) was electrogenerated (*7*) externally and flushed as a batch into a flask containing the sample to be titrated. After refluxing, the excess Ti(III) was titrated with ferric ammonium sulfate solution to a thiocyanate end point.

Apparatus. The equipment used is shown schematically in Figure 1. It consists of a coulometric current source, pressure transducer system, servorecorder, submersible stirring motors, and constant temperature bath. The reactor vessel (Figure 2) is comprised of both a reaction compartment and an electrochemical cell mounted above the former for coulometric generation of hydrogen. Hydrogen gas is generated at the 12-cm² cathode of this cell by the electrolysis of $2N$ H_2SO_4. The 25-cm² platinum anode was depolarized with $1M$ $FeCl_2$ in $2N$ H_2SO_4. Short lengths of glass tubing attached to the electrochemical cell above the electrolyte level and connected to the female ⅎ 14/35 buret mounting joints permitted passage of gas into the reaction compartment. A medium porosity glass frit and an agar–KCl salt bridge separated anolyte from catholyte. Glass stems of the microburets were ring sealed to the male sections of ⅎ 14/35 joints fitted with "O"-ring seals. Side arms permitted hydrogen from the tank source to be passed through the vessel. A reference vessel was similarly constructed. Reaction and reference vessels, stirring motors, and the pressure transducer, mounted as previously described (*8*), were fastened to a ring stand for submersion in the constant temperature bath. The bath was regulated to within ±0.002 °C of its nominal set temperature.

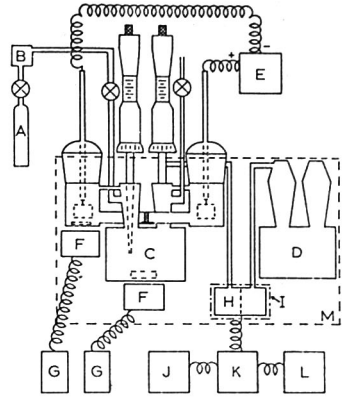


Figure 1. Schematic of equipment for analytical hydrogenation and null point pressuremetry

A. **Tank of H_2 gas.** *B.* **Gas scrubber.** *C.* **Reactor vessel.** *D.* **Reference vessel.** *E.* **Sargent Model IV coulometric current source.** *F.* **Tri-R, MS-7 submersible stirring motor.** *G.* **Stirring motor control.** *H.* **Datametrics Series 511-3, 0–10 psi, Barocel pressure sensor.** *I.* **Waterproof box encasing pressure sensor.** *J.* **Datametrics Type 700 power supply.** *K.* **Datametrics Type 1015 signal conditioner.** *L.* **Photovolt Linear Log Varicord Model 43 Servorecorder.** *M.* **P.M. Tamson, N.V., Model TV 70 constant temperature bath**

Procedure for Null Point Pressuremetry. The appropriate reaction medium and a stirring bar were placed in the reactor. Anolyte was placed in the anode compartment, and a stirring bar and catholyte in the cathode compartment of the electrochemical cell. Microburets and electrodes were secured with a gas-tight seal. The reactor and reference vessels were mounted on the ring stand and their respective transducer connections were made. After immersing the apparatus in the water bath, the transducer was mechanically, electrically,

(6) S. Siggia, "Quantitative Organic Analysis *via* Functional Groups," 3rd ed., John Wiley and Sons, Inc., New York, N.Y., 1963, pp 526–529.

(7) J. J. Lingane and J. H. Kennedy, *Anal. Chim. Acta*, **15**, 465 (1956).

(8) D. J. Curran and J. E. Curley, ANAL. CHEM., **42**, 373 (1970).

Table II. Sample Preparation Data for Organic Solutions

Code	Solute	Solvent[a]	G-sample/ g-solution	Density, g/ml	Mg sample/ μl solution	Reaction temperature, °C
1c	Octene-1	1	0.1305	0.7642	0.09970	27
1d	Octene-1	1	0.04128	0.7718	0.03189	27
1e	Octene-1	1	0.04117	0.7747	0.003189	27
8	Nitrobenzene	1	0.1691	0.8245	0.1394	27
9a	Azobenzene	2	0.08517	1.034	0.08807	25
9b	Azobenzene	2	0.07760	1.041	0.08078	27
10	Picric acid	1	0.02390	0.7846	0.01876	28
11	Olive oil	3	0.6657	0.8163	0.5434	25
12	Cottonseed oil	3	0.4899	0.7822	0.3832	25
13	Corn oil	3	0.5766	0.8064	0.4650	25

[a] 1 = 2-propanol, 2 = glacial acetic acid, 3 = 2,2,4-trimethylpentane.

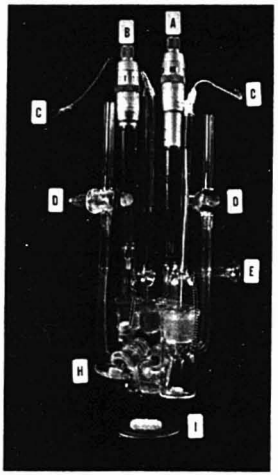


Figure 2. Reactor vessel for null point pressuremetry

A. **Sample microburet, 0.25-ml capacity (Roger Gilmont Instruments, Inc., No. S-3100A).** *B*. **Volume compensation microburet, 0.25-ml capacity (Roger Gilmont Instruments, Inc., No. S-3100).** *C*. **Electrode connections.** *D*. **7 mm 2 stopcocks and side arms.** *E*. **24/5 socket for transducer connection.** *F*. **Anode compartment.** *G*. **Cathode compartment with stirring bar.** *H*. **7 mm 2 stopcock and short side arm with rubber septum.** *I*. **Reactor compartment with stirring bar**

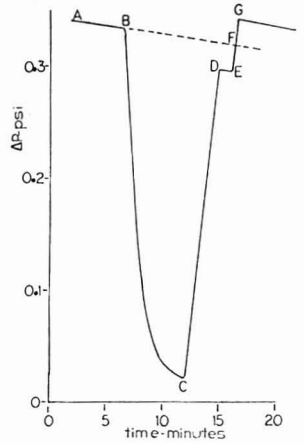


Figure 3. Tracing of the stripchart recording of pressure transducer system output during hydrogenation of cyclohexene

and pressure zeroed. While rapidly stirring the reaction medium and catholyte, hydrogen was passed through the reactor vessel at the rate of 20 ml/min for 10 minutes. To ensure saturation of the catholyte, hydrogen gas was generated coulometrically for 5 minutes with a current of 48 mA. With the transducer set at the appropriate sensitivity, the stopcocks on the side arms were closed and sufficient hydrogen gas electrogenerated to displace the recorder trace to about 80% of the full scale sensitivity chosen. A few microliters of sample were dispensed to adjust the initial microburet setting and test the activity of the catalyst. Hydrogen was generated again to return the pressure to a value approximating that prior to adjusting the buret. Five minutes were allowed to obtain a steady pressure base line. A volume of sample was then added from microburet *A*, and the compression of the gas phase compensated by withdrawing the plunger of microburet *B* an equal volume. After the reaction nears completion, hydrogen gas is coulometrically generated in two increments. More than 10 determinations of a particular sample may be determined in a repetitive fashion.

RESULTS AND DISCUSSION

A tracing of the recorder readout, typical of the method, for the hydrogenation of 10.00 μl of neat cyclohexene is shown in Figure 3. Full scale readout of the recorder was adjusted to 2.500 V, which is one half of the full scale readout of the pressure transducer system for any multiplier setting. Therefore, full scale deflection of the recorder was equivalent to 0.500 psi for this analysis. The slight decrease in pressure with time indicated by base line *AB* was caused by catalyst uptake of hydrogen gas. During the span of an hour or two, this decrease in reactor pressure occurred at a constant rate. At lower transducer sensitivities the negative slope was slight, but at higher sensitivities it became appreciable.

At point *B*, cyclohexene was delivered into the reactor vessel and compensation for the gas phase compression was performed. Curve *BC* indicates the uptake of hydrogen by unsaturate. At point *C*, the system is approaching equilibrium and coulometric generation of hydrogen was begun. Electrogeneration is continued to point *D*, which corresponds to replacing about 90% of the hydrogen consumed. When line *DE* is parallel to line *AB*, equilibrium has been reestablished and another increment of hydrogen was generated. The quantity of gas generated during the second increment was sufficient to make the *total* hydrogen generated by both increments equal to about 110% of the hydrogen consumed by the sample. This second increment is indicated as line *EG*. Line *AB* was extended so that it intersected line *EG* at point *F*. Point *F* is the null point of the determination where the quantity of gas generated to restore the pressure of the system is equal to the quantity of gas consumed by the sample. The coulometric generation time in seconds required to reach the null point was calculated using Equation 1:

$$T_{np} = T_1 + T_2 (L_{ef}/L_{eg}) \quad (1)$$

where T_1 is the seconds of coulometric generation for the first increment, T_2 is the seconds of coulometric generation time for the second increment, L_{ef} is the length of line *EF* in millimeters, and L_{eg} is the length of *EG* in millimeters. The equivalents of hydrogen generated to reach the null point can be calculated from Faraday's law.

This two increment procedure offered several advantages. By assuring that line *DE* is parallel to *AB*, it was demonstrated that the reaction had gone to completion and that the rate of hydrogen uptake by the catalyst had not changed. The resulting lengths of lines *EG* and *EF* were such that they can be conveniently and accurately measured with screw-

Table III. Results of Null Point Pressuremetric Analyses of Seed Oils

Code	Oil	μl taken	No. of detns	Av μmoles H_2 taken up	HIV	Std dev, IV	IV, Hanus method	Std dev, IV
11	Olive oil	10.00	4	17.78	83	±1.4	83	±0.9
		40.00	6	71.68	84	±0.6		
12	Cottonseed oil	40.00	6	68.50	115	±1.3	113	±0.9
13	Corn oil	40.00	5	87.76	120	±1.6	121	±0.3

Table IV. Results of Null Point Pressuremetric Analyses of Organic Compounds

Code	Compound	μl taken	No. of detns	μmoles found	% cmpd	Rel std dev, %	% cmpd, check assay	Rel std dev, %
	Unsaturates							
1b	Octene-1	20.00	6	125.6	99.8	±0.3	99.4	±0.2
1b	Octene-1	10.00	10	62.76	99.8	±0.2		
1c	Octene-1	20.00	6	17.72	99.7	±0.9		
1d	Octene-1	20.00	6	5.690	100.2	±1.2		
1e	Octene-1	20.00	9	0.5597	98.5	±6.0		
2	4-Octyne-2-ol	10.00	6	67.01	97.2	±0.7	...	...
3	Cyclohexene	10.00	5	97.71	99.8	±0.1	99.8	±0.3
	Halides							
4	Chlorobenzene	10.00	5	95.99	99.1	±0.5	99.6	±0.3
5	Iodobenzene	10.00	6	86.46	98.0	±0.5	98.5	±0.3
6	α-Chlorotoluene	10.00	5	85.08	99.3	±0.8	99.4	±0.3
7	Bromobenzene	10.00	6	90.27	95.6	±0.3	95.8	±0.3
	Nitrogen compounds							
8	Nitrobenzene	20.00	6	22.63	99.9	±0.2	100.3	±1.7
9a	Azobenzene	40.00	5	19.47	100.8	±0.8	101.6	±3.6
9b	Azobenzene	20.00	7	8.956	101.0	±0.8		
10	Picric acid	50.00	4	3.858	94.3	±0.3	95.8	±1.3

locking type dividers. It provided an opportunity for any heat generated in the electrochemical cell to be completely dissipated although there were never any experimental indications that heating was a problem. Finally, the procedure saves time. A number of runs were made where the reaction was allowed to go to completion before generation of hydrogen as evidenced by a line parallel to the base line. Although the system did not take an unreasonable length of time to come to equilibrium, it is clearly more efficient to begin hydrogen generation as the system approaches equilibrium.

To test the use of the second microburet for compensating gas phase compressions caused by sample additions, 50.00-μl aliquots of most of the neat and solution samples were added to the hydrogen charged reactor containing 25.00 ml of the appropriate solvent and activated charcoal (without catalyst). The apparatus was thermostated to the appropriate reaction temperature for the compound tested. The transducer sensitivity was set so that 0.030 psi corresponded to 5.000-V output. The servorecorder was calibrated for a full sale deflection equivalent to 5.000 V. After the addition of each 50.00-μl aliquot, the plunger of the volume compensating buret was withdrawn to increase the gas phase by 50.00 μl. Generally, 5 aliquots of each sample were delivered. An average pressure increase of about 0.0060 psi per aliquot was produced. It was interesting to note that the first aliquot of octene-1 delivered into 2-propanol resulted in a slight solution volume contraction, but subsequent additions did not. The volume compensation returned the pressure of the system to that prevailing prior to sample delivery into 2-propanol for neat octene-1, 0.3189 wt/vol % octene-1 in 2-propanol, and the 2-propanol solution of picric acid. The same results were obtained when azobenzene dissolved in glacial acetic acid was delivered into that solvent and when the neat liquids chlorobenzene, α-chlorotoluene, and bromobenzene were added to the acetic acid–acetate medium. As expected, when 2-propanol was delivered into 2-propanol, glacial acetic acid into glacial acetic acid and also into the acetic acid–acetate solvent, no solution volume changes were observed.

It was also possible that the products of hydrogenation did not form ideal solutions. Using the same procedures as above, except omitting the hydrogen atmosphere, no volume contractions or expansions were observed when cyclohexane was added to 2-propanol, aniline to 2-propanol, or benzene to the acetic acid–acetate medium.

When the compensation technique was tested on the seed oils dissolved in 2,2,4-trimethylpentane, solution volume expansions were observed. However, exact compensation was obtained using the solvent alone. Thus the volume change is associated with the seed oils. The result of using microburet *B* was to overcompensate, which had the effect of shifting the pressure base line upward producing low results. The magnitude of the resulting error was small. The pressure decrease observed during the seed oil hydrogenations was about 0.300 psi. In the case of cottonseed oil solution, the pressure base line was shifted an amount corresponding to +0.00144 psi. This is 0.48% of the total pressure decrease, and as a result the apparent null pressure was reached when only 99.52% of the hydrogen consumed was regenerated. Similar calculations for the corn and olive oil solutions showed that the null pressures were obtained at 99.75 and 99.80% of the hydrogen consumed, respectively. These corrections are valid provided the hydrogenated products do not produce a further solution volume expansion or an offsetting volume contraction.

It was also noted that in the absence of catalyst, no negative drift in pressure base line was observed. The pressure base line had a slight positive drift as observed by Curran and Driscoll (*9*).

Tables III and IV summarize the results. Initial investigations with the method were made by determining the unsat-

(9) D. J. Curran and J. L. Driscoll, ANAL. CHEM., 38, 1746 (1966).

uration of olive, cottonseed, and corn oils. For comparison of the pressuremetric results with iodine values found by the Hanus method, the hydrogen iodine value for each oil was calculated using the formula given by Miwa (*10*). Agreement between methods was excellent in all cases. Octene-1 samples of several concentrations (Table IV) were hydrogenated to demonstrate a range of sample sizes over which the method is applicable. For sample sizes of about 100 micromoles, precision and accuracy of a few parts per thousand were easily attained. As little as 0.560 micromole was determined with a precision of ±6% and an accuracy of −1%. The lower limit of sample size that may be taken is governed by the drift rate. At higher transducer sensitivities, the drift rate and the reaction rate become comparable. Generally, the unsaturates were completely hydrogenated in less than 5 minutes. Determinations could be performed at the rate of about 6 an hour.

In addition to alkenes and alkynes, other organic compounds also take up hydrogen under mild conditions in the presence of palladium. Azobenzene (*11*), nitrobenzene, and picric acid (*12*) reacted completely in less than 3 minutes with 4, 6, and 18 equivalents, respectively, of hydrogen. Samples ranging in size from 3.858 to 22.63 micromoles were determined with precisions ranging from ±0.2 to ±0.8% and accuracies of 1.3% or better.

Aryl halides and α-chlorotoluene undergo hydrogenolysis of the carbon–halide bond in a glacial acetic acid–acetate medium (*13*). Ten to fifteen minutes are required for complete reaction at 42 °C. The synergistic effect observed by Pickard and Lochte (*14*) of adding a trace of platinum oxide to the palladium catalyst was used to promote the dehalogenation of chlorobenzene and iodobenzene. The precision for determinations of these compounds ranged from ±0.4 to ±0.8%, with accuracies of −0.5% or better.

For samples that consumed about 250 micromoles of hydrogen in a few minutes, the amount of gas taken up by the catalyst during the course of a reaction is small compared to that consumed by the sample. Under these conditions, semiautomatic analyses were feasible. Neat octene samples were used to test an apparatus. By placing the Sargent Model IV Coulometric Current Source in the remote mode, the cell current can be turned on by supplying a 115-VAC signal to the remote connector of the coulometer. A momentary-off Micro switch (No. 1SM1, Freeport, Ill.) was used to control this 115-VAC signal. The switch was attached to the servorecorder so the recorder pen, *via* a steel band lever, would open the switch at a predetermined potential. This was set at a convenient pressure base line by coulometrically generating hydrogen in the reactor vessel until the ascending recorder pen opened the Micro switch, shutting off the generating current. When an aliquot of octene-1 was added to the reactor, the pressure rapidly dropped, driving the servo pen down scale and turning on the generating current. The rate of hydrogenation was considerably greater than that of the coulometric generation of gas. As a result, the reaction would be complete before the recorder pen returned up scale to open the Micro switch. By selecting a generating current of 193.0 mA, the figure displayed on the digital counter of the coulometer was a factor of 10 greater than the number of micromoles of octene-1 hydrogenated. Analysis of six 40.00-μl samples of octene-1 gave an average per cent compound of 99.8 with a precision of ±0.6% relative standard deviation.

Several compounds, when reacted in the presence of palladium catalyst, did not give satisfactory results. Samples of neat 1-iodopropene readily underwent hydrogenolysis but only to 35% completion. Samples of *p*-bromoaniline dissolved in 2-propanol rapidly took up 1 mole of hydrogen per mole of bromide and then continued to slowly consume hydrogen for an indefinite period. Samples of *trans*-cinnamic acid in 2-propanol gave results that varied from 10 to 20% high.

CONCLUSIONS

The use of null-point pressuremetry in conjunction with coulometry for analytical hydrogenation and hydrogenolysis offers several advantages. In terms of precision and accuracy, the benefits that can be derived from the use of differential measurements, null techniques, and constant current coulometry are well known. The results obtained in this work are highly precise and accurate and compare favorably with the best existing methods. The earlier work of Miller and DeFord (*15*) and Burkhardt and Dirscherl (*16*) using electrolytic hydrogen generation gave results poorer by an order of magnitude than those reported here. For our samples which consumed about 100 micromoles of hydrogen gas, precision and accuracy were a few parts per thousand in most cases. Similar results have been obtained in earlier work in our laboratories (*1*) using volumetric techniques for the generation of hydrogen and in work by Brown (*17*).

The sample size range and the sensitivity of the method are excellent. The work covered a range of better than 400-fold and the minimum sample size studied (0.560 micromole) represents a factor of two improvement over our previous study (*1*) and nearly an order of magnitude improvement over the work of Brown (*17*). The sensitivity is presently limited by the rate of drift of the background signal due to hydrogen uptake by the catalyst. Elimination of this drift would improve sensitivity because present measurements are not at the limit of sensitivity of the pressure transducer system or at the limit of generation of hydrogen gas with 100% current efficiency. Several approaches can be explored to achieve this goal: further efforts to achieve a saturated catalyst, electronic compensation for the drift, and null compensation for the drift by placing catalyst under hydrogen in the reference vessel.

The method has several operational advantages worthy of note. Coulometric generation of hydrogen gas eliminates the need for preparation, standardization and storage of reagents for this purpose. Calculation *via* the ideal gas law of the free space equivalent for reagents or sample delivered to the system is not required. The compensation buret provides an exact correction in those cases where solution volumes are additive and the system provides an experimental correction where volume changes do occur. As demonstrated, the method is easily automated if a sufficiently large sample size is used. We have described the present instrumentation as semiautomatic because operator time is still required for the initial hydrogen gas saturation step and for the introduction of

(10) T. K. Miwa, W. F. Kwolek, and I. A. Wolff, *Lipids*, **1**, 152 (1966).
(11) R. N. Rylander, "Catalytic Hydrogenation Over Platinum Metals," Academic Press, New York, N. Y., 1965, pp 491–493.
(12) R. L. Augustine, "Catalytic Hydrogenation," Marcel Dekker, Inc., New York, N. Y., 1967, pp 91–92.
(13) R. N. Rylander, "Catalytic Hydrogenation Over Platinum Metals," Academic Press, New York, N. Y., 1965, Chap. 24.
(14) P. L. Pickard and H. L. Lochte, *J. Amer. Chem. Soc.*, **69**, 14 (1947).
(15) J. W. Miller and D. D. DeFord, ANAL. CHEM., **30**, 295 (1958).
(16) F. Burkhardt and A. Dirscherl, *Mikrochim. Acta*, **1965**, 353.
(17) C. A. Brown, ANAL. CHEM., **39**, 1882 (1967).

sample. It would appear that full automation is entirely possible. The speed of analysis (6 replicates/hour manually and 8 replicates/hour semiautomatically) is very satisfactory and would justify further development of a completely automatic instrument.

In addition to versatility in terms of automation, the method also has good chemical versatility. The quantitative reduction of several organic functional groups has been accomplished. The reduction of nitro and azo groups with hydrogen gas offers a rapid, accurate, and precise microanalysis that avoids the difficulties due to air oxidation with reagents such as Ti(III) (*6*) and chromous (*6*, *18*) ions. The analytical hydrogenolysis of aryl halides appears to be a novel method which gives a true measure of the organo halide as opposed to the usual combustion or digestion halide determination methods which measure total halide.

(18) R. S. Bottei and N. H. Furman, ANAL. CHEM., 27, 1182 (1955).

ACKNOWLEDGMENT

We thank Gordon Good for technical assistance in the design and construction of the glass vessels.

RECEIVED for review August 10, 1970. Accepted November 2, 1970. Presented in part at the Second Northeast Regional ACS Meeting, Providence, R. I., October 1970.

Analysis for Impurities by Nuclear Scattering

B. L. Cohen and R. A. Moyer[1]

University of Pittsburgh, Pittsburgh, Pa. 15213

Use of elastic proton scattering to analyze for impurities in thin samples is investigated. Mass resolutions of one AMU at A ≲ 63 and 10 AMU at A ≈ 200 are readily achieved. Backgrounds are sufficiently low that 1 part per billion impurities of heavy elements in a light element material are detectable. Sensitivities below one part per million are easily achieved; they can be traded-off against mass resolution to reach the part-per-billion region.

WHEN A PROTON is elastically scattered from a target nucleus of mass number A, application of the principles of momentum and energy conservation in a nonrelativistic approximation easily shows that the target nucleus recoils with an energy E_T given by

$$E_T = \frac{2E_o}{A+1}\{1 - (A-1)[x^2 + x(1+x^2)^{1/2}]\}$$

$$\text{with } x = [(A+1)(A-1)]^{-1/2}\cos\theta$$

where E_o is the energy of the incident proton and θ is the angle at which it is scattered. For $A \gg 1$, this is well approximated by

$$E_T = \frac{2E_o}{A}(1 - \cos\theta) \qquad (1)$$

In analyzing data, this approximation is not used, but rather an accurate and complete relativistic calculation is carried out with a computer. The approximation used here is to lend clarity to the discussion.

The energy of the scattered proton, E, is then

$$E = E_o - E_T$$

$$= E_o\left[1 - \frac{2}{A}(1 - \cos\theta)\right] \qquad (2)$$

which is a function of A. A measurement of E at a given θ therefore determines A for the target nucleus. This method has been used for determining the surface composition of materials (*1–4*), and with alpha particles substituted for protons, for determining the composition of the lunar surface (*5*). In these applications, only the most abundant elements present were detected. The purpose of this paper is to investigate the usefulness of this method for determining amounts of trace element impurities in or below the parts per million range, in thin samples of material.

The application of nuclear techniques to the determination of trace element impurities is most familiar in the form of activation analysis. That method has proved to be highly sensitive, and with the introduction of high resolution detectors, it has become relatively easy (no chemical separations are necessary) to determine abundances of about 20 elements (*6*). However, it is extremely difficult to use for a complete analysis of all, or even most, elements. This limitation is not applicable in the present method as is apparent from the simplicity of Equation 2.

As a first orientation on the type of data that may be obtained by the scattering method, Figure 1 shows the energy distribution of protons observed at $\theta = 90°$ when a 0.0002-inch thick aluminum foil was bombarded with 17-MeV protons. The numbers immediately above the peaks are the mass numbers of the impurities causing the peaks, and above these are shown the elements responsible, and their abundance in atomic parts per million as determined from this measurement.

We next consider some of the properties and limitations of this method.

BACKGROUND LIMITATIONS

There are many effects in nuclear scattering experiments which give scattered particles of lower energy than E as given by Equation 2. For example, the target nucleus can be left in an excited state (this is called "inelastic scattering") or some particles in the incident or scattered beam may be degraded in energy by passing through a slit edge. If one is studying a material of high A, these effects would produce a background in the region where one studies low A impurities,

[1] Present address, Nuclear Chicago Corp., Des Plaines, Ill. 60018

(1) S. Rubin, T. O. Passell, and L. E. Bailey, ANAL. CHEM., 29, 736 (1957).
(2) *Ibid.*, 33, 583 (1961).
(3) O. U. Anders, *ibid.*, 38, 1442 (1966).
(4) M. Peisach and D. O. Poole, *ibid.*, 38, 1345 (1966).
(5) J. H. Patterson, A. L. Turkevich, and E. Franzgrote, *J. Geophys. Res.*, 70, 1311 (1965).
(6) See, for example, "Modern Trends in Activation Analysis," J. R. De Voe, Ed., National Bureau of Standards, Washington, D. C., 1969.

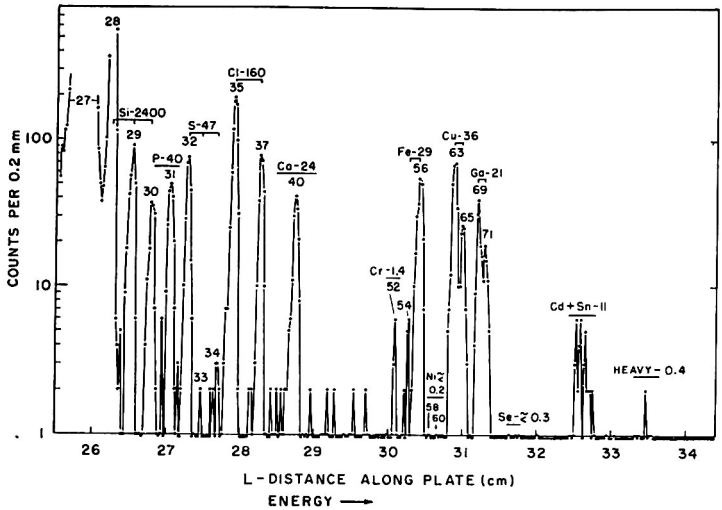


Figure 1. Analysis of an 0.0002-inch thick aluminum foil

This is the energy spectrum of protons scattered from the foil at 90° to the incident direction when it is bombarded with 17-MeV protons. Numbers above peaks are the mass of the nucleus causing the scattering. Above these are the chemical element and the quantity present in parts per million. Points below 1 on the ordinate scale are zero. The bombardment was with a current of about 0.7 μA for 3 hours

so this method would not be very sensitive. On the other hand, in the more usual situation where one is studying high A impurities in a low A material, this background is inconsequential. In such cases, if the energy of the scattered protons is measured by scintillation or semiconductor detectors, there is some background in the high A region due to exothermic (p,α) reactions and due to electronic pile-up. The background problem is therefore reduced to a minimum by determining E with a magnetic spectrograph. In the experiments to be reported here, the scattered particles are detected by photographic plates on the focal plane of the spectrograph—thus eliminating electronic pile-up as a factor—and the plates are covered by sufficient absorber to stop alpha particles from (p,α) reactions. The actual ordinate in Figure 1 is the distance along this plate, L; the energy E varies approximately linearly with L.

Since the principal material of the sample in Figure 1 is aluminum (A = 27), the primary source of background is protons whose energy is such that they would ordinarily strike the plate at $L \simeq 26$ cm but somehow are scattered, causing them to strike the plate at larger L (where higher energy protons ordinarily strike it). However, it is readily shown that scattering from any point near the target causes particles to reach the focal plane at *smaller* L than they would without scattering—this is essentially due to the fact that second order aberrations are dominant. This conclusion applies with reasonable accuracy to the slit S which defines the acceptance solid angle for scattered particles, so the only way for protons scattered from aluminum in the target to reach the focal plane at $L \gg 26$ cm is for them to be scattered again from something far away from the target. If the vacuum is good enough to remove gas scattering as a factor, the only objects in that region from which scattering can occur are the pole faces of the spectrograph magnet. In a double focusing spectrograph, the slit S ordinarily prevents any particles passing through it from reaching the magnet pole faces, so the only reasonable possibility for background in the $L \gg$ 26-cm region is for a proton scattered from the aluminum target to be scattered from the sides of the slit S so as to reach a pole face, and then to be scattered from this pole face into the detector. Even then the proton approaches the detector at an abnormal angle and it may well be discriminated out on that basis. In any case, the probability for two instrumental scatterings would be very small.

In principle, neutrons can cause background by having collisions with hydrogen nuclei or inducing (n,p) reactions in other nuclei in the emulsion. However these tracks are easily discriminated because they do not start in the emulsion surface. Also they are not at the correct angle, or of the correct length. The spectrograph system used in this work has elaborate shielding against neutrons, and they have never been a problem in any work done with it, even when the incident particles are deuterons which give much larger neutron production than protons.

From this discussion it is clear that when a low A sample is being analyzed, background in the high A region is extremely low. Direct evidence for this may be seen in the $L \approx$ 34-cm region of Figure 1 where there can be no true counts, and the observed counts are indeed zero.

In the data of Figure 1, one count corresponds to about 50 parts per billion of a heavy element; in order to investigate the background limitations with higher sensitivity, a relatively thick (0.002 inch) carbon sheet was bombarded, and the results are shown in Figure 2. Other interesting aspects of Figure 2 will be discussed later, but the sensitivity is such that each count corresponds to 0.5 part per billion of a heavy element. If we determine background from the region $L \approx$ 33 cm where true counts are impossible, we conclude that

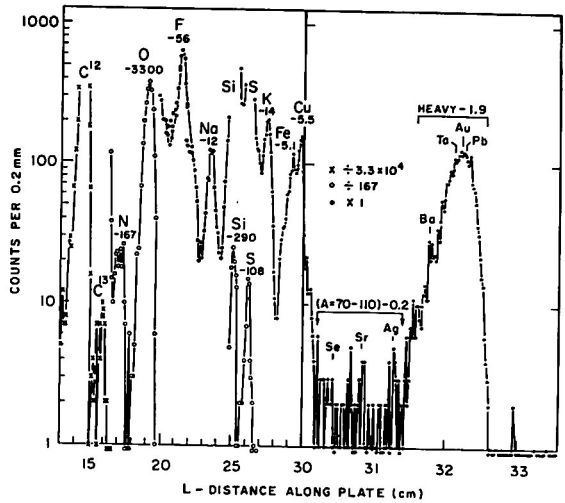


Figure 2. Analysis of a 0.002-inch carbon sheet

See caption for Figure 1. Above peaks are impurity elements and their abundance in parts per million

total heavy element concentrations as low as 1–2 parts per billion would be detectable.

In these measurements, no special care was taken to reduce this background; the spectrograph was used in its normal configuration. Rather obvious steps that would further reduce background would be to improve the vacuum (it was about 10^{-5} mm Hg), to reduce the thickness of the slit S so as to reduce the probability for scattering from its edges (it is about three times thicker than is necessary to stop the protons), and to move S closer to the target (it is about 10 inches away). It therefore seems conservative to say that the background can easily be reduced to the point where impurity concentrations well below one part per billion are detectable.

MASS RESOLUTION

By differentiating Equation 2, we find the change in energy with mass number to be

$$\frac{dE}{dA} = \frac{2E_o}{A^2}(1 - \cos\theta) \tag{3}$$

If the energy resolution of the spectrograph is ΔE, the change in A within this resolution, ΔA, is

$$\Delta A = \frac{\Delta E}{dE/dA} = \frac{\Delta E}{2E_o(1 - \cos\theta)} A^2 \tag{4}$$

For a sample thin enough not to limit the energy resolution, the most favorable angle would be near 180°, where $(1 - \cos\theta) \simeq 2$. A typical energy resolution for a spectrograph is $\Delta E/E_o \simeq 1/2000$; with extensive effort and a very good accelerator, this can be pushed to 1/10,000. Inserting the most favorable values into Equation 4 then gives

$$\Delta A \simeq \frac{A^2}{40{,}000} \tag{5}$$

which means that consecutive masses are resolved up to $A \simeq 200$. This would apply to samples in the thickness range near or below 25 millimicrons when the incident particles are 17-MeV protons. For thicker samples, the energy resolution ΔE is much improved if the scattered particles leave from the side of the sample opposite the entering side, and if the target angle is $\theta/2$; the total energy loss of the incident and scattered proton then becomes independent of where in the target the scattering takes place, so the only loss of energy resolution is that due to straggling. The largest value of θ for which this is readily applicable is 90°, so $(1 - \cos\theta) \approx 1$. For a typical easily achieved energy resolution of $\Delta E/E \approx 1/2000$, we then find

$$\Delta A \simeq \frac{A^2}{4000} \tag{6}$$

which means that consecutive mass numbers can be resolved up to $A \approx 63$. For $A = 100$ and 200, $\Delta A \simeq 2.5$ and 10, respectively, so it is barely possible to resolve Au($A = 197$) from Pb($A \simeq 207$). This is approximately the resolution achieved in Figure 1. The energy resolution assumed here is achievable with 17-MeV protons for sample thicknesses $\lesssim 0.5$ mg/cm² which is $\lesssim 0.6$ micron of Fe or Cu, $\lesssim 2$ microns of Al, or $\lesssim 5$ microns of plastic or other organic material. (These limiting thicknesses increase linearly with the proton energy.) For thicker materials, the mass resolution is reduced as is readily apparent in Figure 2, and also in Figure 3 which shows an analysis of a 0.002-inch thick beryllium metal foil.

SENSITIVITY

The data of Figure 1 were obtained with a bombardment of several hours with maximum available beam (0.7 μA), and we see that the sensitivity is sufficient to detect impurities only $\lesssim 1$ part per million. Here we consider various methods of increasing the sensitivity by increasing the intensity I

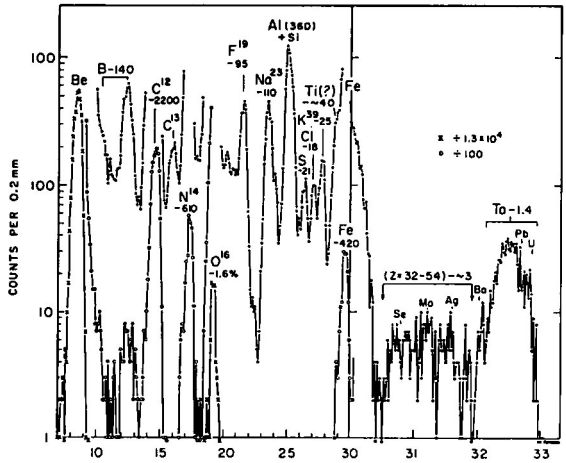


Figure 3. Analysis of a 0.002-inch beryllium sheet

See caption for Figure 1. Above peaks are impurity elements and their abundance in parts per million

of scattered particles, and the consequences of these methods for mass resolution.

Of course the intensity increases linearly with beam current and length of bombardment. We assume that the maximum beam current available and safe with regard to destruction of the target sample is being used. Bombardment times longer than several hours become expensive and therefore impractical. The other variable factors are the scattering angle θ, the bombarding energy E_o, and the sample thickness t.

If we assume as a rough approximation that the scattering cross section is equal to the Rutherford value (it never deviates by as much as an order of magnitude from this, and is usually somewhat closer), we may estimate

$$I \propto E_o^{-2}\,\theta^{-4}t \tag{7}$$

so the sensitivity can be improved by lowering the bombarding energy, decreasing θ, or increasing t. However, each of these measures causes the resolution, ΔA, to deteriorate. For bombarding energies around 17 MeV, the energy resolution is limited by target thickness when the latter is $\gtrsim$0.5 mg/cm², and from that thickness up to about 5 mg/cm², it varies linearly (7) with t. In this region, therefore, $\Delta A \propto t$. (For larger thicknesses, $\Delta A \propto t^{1/2}$). From Equation 4 we see that $\Delta A \propto 1/(1 - \cos\theta)$, which is roughly approximated by $\Delta A \propto 1/\theta^2$. Bombarding energy affects energy resolution because the straggling is proportional to the energy loss (7) in the thickness region under consideration. Since energy loss is inversely proportional to energy, $\Delta A \propto 1/E$. Combining these terms, we find

$$\Delta A \propto tE_o^{-1}\theta^{-2} \tag{8}$$

Combining Equations 7 and 8 we find

$$I \propto \frac{(\Delta A)^2}{t} \tag{9}$$

Thus sensitivity can be improved at the expense of mass resolution roughly as the square of the latter by reducing either the bombarding energy or the scattering angle. We shall see in a later section that a change in scattering angle requires a shift in the focal plane, so it is easier to adjust the energy. Figure 4 shows a run on the same aluminum target used in Figure 1 except at a bombarding energy of 5 MeV and with a ten times shorter exposure. From Equation 7 one would expect the sensitivity to be about the same in the two runs, with the order of magnitude change in E_o^2 approximately compensated by the length of the bombardment; and from Equation 8 or 9, one would expect the resolution to be about three times poorer. A comparison of Figures 1 and 4 reveals that this prediction is roughly verified among the low A impurities, but the sensitivity for high A impurities is improved by lowering the bombarding energy considerably more than predicted by Equation 7. This type of discrepancy is not unexpected since the elastic scattering cross section is not well approximated by the Rutherford value (pure coulomb with no effects of nuclear forces), especially at energies as high as 17 MeV. At that energy, the elastic scattering cross section at 90° is known (8) to be only about 15 and 50% of the Rutherford value for the Ag and Au regions, respectively. Accurate determinations of impurity abundances from Figure 4 were not made because measurements of scattering cross sections at 5 MeV are not available, but use of the Rutherford values gives reasonable agreement with the impurity abundances shown in Figure 1 except for the very heavy elements where there is a factor of two discrepancy. The data of Figure 4 were obtained several weeks later, and it is not impossible for additional impurities to have gotten onto the sample in the interim. Statistical fluctuations and plate reading errors might also be responsible for some of the discrepancy.

(7) B. L. Cohen, *Rev. Sci. Instrum.*, **33**, 85 (1962).

(8) I. E. Dayton and G. Schrank, *Phys. Rev.*, **101**, 1358 (1956).

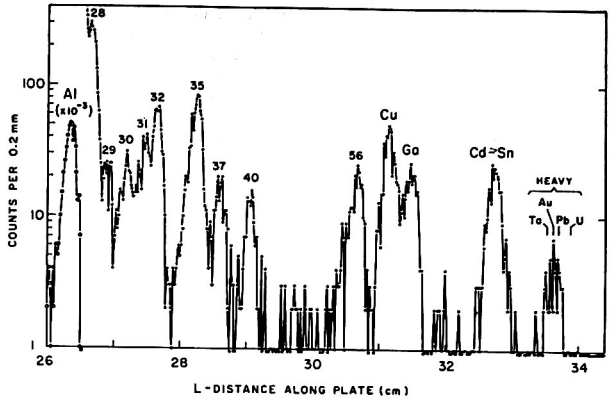


Figure 4. Analysis of the same aluminum foil analyzed in Figure 1, but with 5-MeV incident protons and an exposure 10 times smaller, about 0.4 μA for 30 min

SCALING LAWS FOR PROJECTILES

While all the experimental work reported here was carried out with protons, it is interesting to consider the use of other projectiles. These are especially interesting in applications where samples are very thin or where their thicknesses are easily adjusted; in fact we will assume here that the target thickness is chosen to give the desired mass resolution, and calculate the intensity of scattered particles at a given angle when incident particles of mass m, charge Z, and energy E_o are used. The energy shift per mass unit, ΔE, is obtained from a generalized version of Equations 1 and 2 as

$$\Delta E \propto mE_o \tag{10}$$

and from a generalized form of Equation 7 at a given θ we have

$$I \propto \frac{Z^2 t}{E_o^2} \tag{11}$$

If the rate of energy loss is $-\mathrm{d}E/\mathrm{d}x$, the fact that target thickness limits mass resolution implies that

$$\frac{\mathrm{d}E}{\mathrm{d}x} t = \Delta E \tag{12}$$

From energy loss theory, $-\mathrm{d}E/\mathrm{d}x \propto mZ^2/E_o$, whence with Equation 10 we find

$$\frac{mZ^2}{E_o} t \propto mE_o \tag{13}$$

which may be solved for t to give

$$t \propto \frac{E_o^2}{Z^2} \tag{14}$$

Using this value in Equation 11 we finally obtain

$$I \propto \frac{Z^2}{E_o^2} \cdot \frac{E_o^2}{Z^2} = \text{constant} \tag{15}$$

which is independent of m, Z, or E_o. We therefore conclude that the sensitivity for a given mass resolution (limited by target thickness) is the same for all bombarding particles and energies. On the other hand, if the experimental energy resolution is limited by factors other than target thickness, there is an advantage in using heavier bombarding particles since, from Equation 10, the energy resolution requirement is eased linearly with m. However, it is important to remember that for all particles but protons, exothermal reactions are important and lead to background difficulties when investigating heavy element impurities in low A materials.

DETERMINATION OF IMPURITY CONCENTRATIONS

All measurements reported in this paper were made at $\theta = 90°$; the number of tracks in the peak for element x is designated C_x (90°). During the run, a scintillation monitor located at 38° records the number of particles elastically scattered at that angle, principally by the main element, B, of which the sample is composed; the number of counts recorded in this detector is C_B (38°).

If f is the concentration of element x, from the definition of cross sections

$$f = \frac{C_x(90°)}{C_B(90°)} \times \frac{\sigma_B(90°)}{\sigma_x(90°)} \tag{16}$$

where $\sigma_i(\theta)$ is the elastic scattering cross section for element i at laboratory angle θ. We also have the relation

$$\frac{C_B(90°)}{C_B(38°)} = r \frac{\sigma_B(90°)}{\sigma_B(38°)} \tag{17}$$

where r is the ratio of the solid angles of the spectrograph detection system and the monitor. By solving Equation 17 for $C_B(90°)$ and inserting the result in Equation 16, we obtain

$$f = \frac{C_x(90°)}{C_B(38°)} \frac{\sigma_B(38°)}{r\sigma_x(90°)} \tag{18}$$

If $C_x(90°)$ and $C_B(38°)$ are determined in the experiment, and r is known from geometric measurement, f is determined if the cross sections are known. Measurements of elastic scattering cross sections for various elements at 17 MeV are available in the literature (*8*). These vary smoothly with A so there is little difficulty in making extrapolations where direct measurements are not available. Where higher accuracy is needed, or if experiments are done at an energy for which no cross section measurements are available, elastic scattering cross sections may easily be measured at the angles of interest with targets of individual elements.

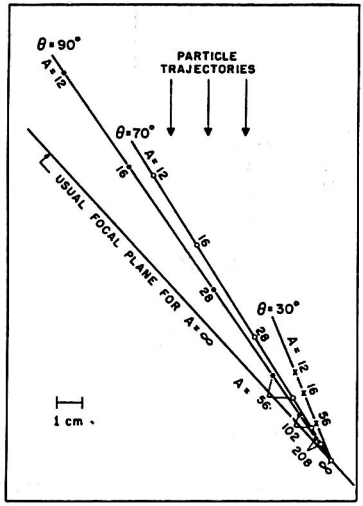


Figure 5. Spectrograph focal planes for impurity by elastic scattering

The three upper lines show the focal planes for $\theta = 90°$, $\theta = 70°$, and $\theta = 30°$, and the points are the focal points for the A values shown

FOCAL PLANE DETERMINATION

It is well known (*9*) that the variation of E with θ in Equation 2 leads to a shift in the focal plane of a magnetic spectrograph for materials of low A. In ordinary situations, the entire energy spectrum from a given target is put into focus by a relatively small shift roughly parallel to the focal plane for $A = \infty$. However, in the present application, it is necessary to have the elastic scattering peak in focus for all A simultaneously. The calculated focal positions for several values of A and θ are shown in Figure 5. Fortunately, the positions for all A and a given θ fall on a straight line so the shape of the detection system does not require modification.

(9) H. A. Enge, *Rev. Sci. Instrum.*, 29, 885 (1958).

However, the drastic change in angle of the detector did require mechanical modifications in the detector support system. The rather steep angle of the focal plane relative to the particle trajectories for $\theta = 30°$ would preclude the use of that small a θ value.

The final location of the focal plane was carried out experimentally by use of a target made from successive evaporations of Al, Cu, Ag, and Au onto a thin carbon backing, the thickness of each material (including C) being about 20 micrograms per cm². After a ten-minute exposure to the beam, the photographic plate used for detection was sufficiently darkened that, after a five-minute development, black lines due to the elastic scattering of protons from each of the target elements could be seen. The focal plane was then found by adjusting the detector position in successive runs until all lines had minimum width.

APPLICABILITY

The method described here should be applicable to the analysis of impurities in materials which are easily prepared in thin samples. Hair and dried blood samples would seem to be reasonable examples; methods for analyzing hair are now under development here. It would seem that analyses in the one part per million range would generally be easy and rapid, and where mass resolution can be sacrificed by using thicker samples, analyses down to the few parts per billion range are practical. One especially simple application of this type is where the only requirement is to know the total amount of heavy element impurity. The authors would welcome suggestions for collaboration in projects where this technique would be useful.

The Los Alamos Meson Physics Facility will operate at 800 MeV, and will be equipped with a high resolution spectrometer with $\Delta E/E \simeq 1/15{,}000$. This should be capable of analyzing materials up to about $^1/_{32}$-in. thick with excellent mass resolution.

ACKNOWLEDGMENTS

The authors are indebted to G. R. Rao and J. A. Penkrot for help in taking data, and to Miss Delores Johnson for carrying out the microscope scanning.

RECEIVED for review June 4, 1970. Accepted November 2, 1970. Work supported by the National Science Foundation.

NOTES

Sodium Removal as an Aid to Neutron Activation Analysis

H. R. Ralston

Bio-Medical Division, Lawrence Radiation Laboratory, University of California, Livermore, California 94550

Elaine S. Sato

Radiochemistry Division, Lawrence Radiation Laboratory, University of California, Livermore, California 94550

THE FULLY AUTOMATED approach to neutron activation analysis has been limited to substances with very low sodium content if the sought-for nuclides have half-lives close to, or less than the 15-hour half-life of ^{24}Na. The presence of ^{24}Na in the irradiated material makes it difficult if not impossible to detect and quantitate the other gamma peaks. For organic materials or environmental samples such as soil or rock, the problem of sodium is overwhelming; the instrumental approach is limited to elements whose activation products have half-lives long enough to allow their measurements after ^{24}Na is lost through decay. Since our activation analysis program is oriented to exploit the instrumental approach, complicated radiochemical separations were excluded from study.

A recently developed simple method for selectively removing sodium from irradiated material (*1*) shows promise for extending the instrumental approach to isotopes of shorter half-life. The method is rapid and involves a minimum of radiochemical procedures. First, a series of simple experiments was done to test the adaptability of the method to biological and environmental analyses and to determine the optimum conditions for this application (see Appendix A). Then the method was tested on nonradioactive materials and in a trial analysis of rock samples, liver, and protein. No effort was made to quantitatively analyze the rock or liver samples; the object was merely to test the efficiency of sodium removal and to gain experience with the method. The protein sample was analyzed to determine its metal content.

This work was done to establish necessary and sufficient conditions for the use of the method for our particular applications. No attempt was made to critically evaluate hydrated antimony pentoxide performance under a wide range of experimental conditions.

EXPERIMENTAL

Column Preparation. Following the method of Girardi and Sabbioni (*1*), a quantity of HAP obtained from commercial suppliers was sieved to about 150 to 250 μ. A glass column, 6 mm inner diameter, was filled to a height of about 3 cm with HAP and preconditioned with 6*M* hydrochloric acid.

Irradiation. The samples as finely ground dried powders were sealed in polyethylene vials by welding the snap-type cap in place with a low-wattage soldering iron. The samples were then exposed in a flux of 10^{13} n/cm^2 sec in the Livermore Pool Type Reactor (LPTR) S-1 irradiation facility.

Sodium Separation. After irradiation, each rock sample was transferred from its polyethylene vial to a platinum crucible. Concentrated hydrofluoric and nitric acids were added and the sample was heated to near dryness. Concentrated perchloric acid was then added with more hydrofluoric acid, and the sample was again heated to dryness. The residue was dissolved in a small amount of 6*M* hydrochloric acid and centrifuged, and the supernate was decanted. This solution procedure was repeated if necessary until no residue remained or until the radioactivity in the residue was negligible. If the solution was over 10 ml in volume, it was boiled to reduce the volume.

Organic samples were dissolved in a solution of concentrated hydrochloric, nitric, and perchloric acids (1:1:2) in a glass beaker. This solution was heated to dryness and the residue was dissolved in 2 ml of 6*M* hydrochloric acid.

One half of each sample was set aside, and the remaining half was then passed through the HAP column with a wash of the beaker. The column was then washed with 1 to 2 ml of 6*M* hydrochloric acid.

Counting. The process of dissolving the rock sample was begun ninety minutes after the end of the irradiation, and the completely dissolved sample was put into the column three hours after irradiation. The column did not function well during the test on the rock sample, however, and the separation process took considerably longer than anticipated. The separated rock sample was not placed on the detector until six hours after the end of the irradiation. The liver and protein samples were ready to count within two hours after the irradiation. All samples for counting consisted of 6 ml of solution placed in a 90-cc polyethylene jar with a 5-cm-diameter bottom to obtain a thin layer of liquid.

The counter was a 12-cc Ge–Li gamma detector with a full width half maximum (FWHM) of 3.5 keV at 1332 MeV. Counting data were collected on a 2048-channel analyzer equipped with a magnetic tape readout. The magnetic tape was computer-compatible; no further treatment was needed prior to analysis by a computer program (*2*).

In the fractions of the dissolved samples eluted from the HAP column, the gamma activities were high enough for adequate counting statistics in counting times of 10 minutes without excessive dead times. Both the untreated half of the dissolved sample and the column containing the sodium adsorbed from the separated fraction were too active to count until a number of half-lives of ^{24}Na had elapsed.

In all of the samples, the sodium-free fraction was counted as soon as possible and the ^{24}Na-active fraction and column were counted as soon as their activities permitted. For the protein sample, which was not only tested for its sodium reduction factor but also was analyzed for Mn Co, Zn, and Cu, standards were irradiated simultaneously.

RESULTS

Rock Sample. The rock sample (100 mg) was irradiated for 10 hours, then dissolved; half of it was separated on HAP,

(1) F. Girardi and E. Sabbioni, *J. Radioanal. Chem.*, **1**, 169 (1968).

(2) H. R. Ralston and G. E. Wilcox, *Nat. Bur. Stand.* (*U.S.*) *Spec. Publ.* 312, **2**, 1238 (1969).

Table I. Na Adsorption Capacity of HAP Column[a]

HAP, grams	Na carrier, mg	Na retained on HAP, mg
0.9	10	9.9
0.9	15	13.6
0.9	20	15.5
0.9	25	14.9
0.9	30	13.9
0.9	35	13.9
0.9	40	14.3

[a] ^{22}Na tracer with $NaNO_3$ carrier was added in 15 ml of 8*M* HCl. Washed with 15 ml of 8*M* HCl.

Table II. Na Adsorption Capacity of HAP Column[a]

HAP, g	Na carrier, mg	Na retained on HAP, mg
1	45	14.5
2		36.0
3		45.0
1	30	15.1
2		30.0

[a] ^{22}Na tracer with $NaNO_3$ carrier was added in 15 ml of 6*M* HCl. Washed with 15 ml 6*M* HCl.

Table III. Na Adsorption Capacity of HAP Column[a]

HAP, g	Na carrier, mg	Na retained on HAP, mg
1	45	21.5
2		45.0

[a] ^{22}Na tracer with $NaNO_3$ carrier was added in 10 ml 1*M* HNO_3. Washed with 10 ml 1*M* HNO_3.

Table IV. Potassium Adsorption Capacity of HAP Column[a]

HAP, g	K carrier, mg	K retained on HAP, mg
0.5	5	4.3
	10	6.9
	15	7.8
	20	7.6
	25	9.9
	30	10.2
	35	11.2
	40	11.7
0.5	20	8.4
1.0		16.1
1.5		20.0
0.5	40	11.7
1.0		21.8
1.5		28.5

[a] K-42 tracer with KNO_3 carrier was added in 10 ml of 1*M* HCl. Washed with 10 ml of 1*M* HCl.

and both halves were counted for 10.0 minutes. The activity was quite high despite the removal of sodium. This high initial activity was found to be ^{56}Mn.

The ratio between the ^{24}Na retained on the column and that counted in the unseparated fraction was 1.06 which is within the probable error of the experiment. The ratio between the sodium counted in the separated sample and that retained on the column was 0.013. This does not represent as complete a separation as that reported in the literature (*1*).

Liver Sample. The sample of dried human liver (148 mg) was irradiated for 8 hours, then dissolved; half of it was separated on HAP. The principal activities remaining in the separated sample were ^{56}Mn, ^{64}Cu, and ^{42}K.

The ratio between the ^{24}Na retained on the column and that in the unseparated fraction was 1.12, which is within the probable errors of the experiment. The ratio between the sodium counted in the separated sample and that retained on the column was 4.2×10^{-4}, which is somewhat better than the ratio obtained for the rock sample but not as low as was expected.

Protein Sample. The sample was 2.67 mg of the enzyme phosphoenolpyruvate carboxylase, which had been extracted from *E. coli* strain B to a specific enzymatic activity of 90 units/mg (*3*, *4*). It was irradiated for 10 hours. Standards for the determination of Mn, Co, Zn, and Cu were included; the Mn and Co standards were mixed in one vial and the Zn and Cu standards in another.

The sodium separation was completed and the first sample was counted 2.0 hours after irradiation. The analysis showed Mn, 3.4 parts per million (0.0091 μg in 2.67 mg); Zn, 288 parts per million (0.77 μg in 2.67 mg); Co, not detected; Cu, not detected.

The estimated probable errors for this determination included errors in counting statistics, irradiation geometry, counting geometry, and recovery. The total estimated errors are: Mn, $\pm$ 23%; Zn, $\pm$ 25%. The ^{24}Na ratio between the treated sample and the column was 3.8×10^{-5}.

DISCUSSION

The sodium separation technique investigated here proved to be effective for the kind of analysis used in the activation analysis program of the Bio-Medical Division, Lawrence Radiation Laboratory. Although our measured decontamination factors were smaller than those reported elsewhere (*1*), the ratios were sufficient to make an otherwise impossible analysis possible.

The observed increase of the decontamination factor when passing from the rock samples to liver tissue to proteins has been tentatively attributed to the decrease in the mineral content (interfering ions) of the sample. The discrepancy between our measured retention and those previously reported (*1*) is probably due to variations in the HAP material. Differences were noted as a function of material preparation and source.

This technique and others of a similar nature promise to greatly extend our capabilities for meaningful activation analyses.

APPENDIX A

Adsorption Parameters for Adaptation of the Girardi–Sabbioni Sodium Removal Procedure. The procedure of Girardi and Sabbioni (*1*) for the removal of sodium from solutions is based on adsorption of sodium on hydrated antimony pentoxide (HAP). The adaptability of the technique to analyses at Lawrence Radiation Laboratory was checked by a series of exploratory experiments, from which suitable and/or optimum conditions for the present application were ascertained.

Sodium was found to be adsorbed on HAP from 6*M* or 8*M* HCl, 1*M* or 8*M* HNO_3, 6*M* HCl/3*M* HNO_3, and 8*M* $HClO_4$. Data for 6*M* and 8*M* HCl and 1*M* HNO_3 are presented in Tables I to III. The adsorption of potassium from 1*M* HCl was also studied (Table IV).

(3) T. E. Smith, *Arch. Biochem. Biophys.*, **128**, 611 (1968).
(4) T. E. Smith, Lawrence Radiation Laboratory, University of California, Livermore, unpublished work, 1969.

Cesium and barium were adsorbed from 1*M* HCl, 1*M* HNO_3, 2*M* HCl/1*M* HNO_3, 1*M* $HClO_4$, and 1*M* H_2SO_4. From solutions of mixed-fission and activation products in 8*M* HNO_3, tantalum was found to be adsorbed along with the sodium.

The conditions employed in the present investigation were selected on the basis of these studies, checked, and found suitable.

RECEIVED for review May 21, 1970. Accepted October 5, 1970. This work was performed under the auspices of the United States Atomic Energy Commission.

Solvent Effects in Gel Permeation Chromatography

J. G. Bergmann and L. J. Duffy

Research and Development Department, American Oil Co., Whiting, Ind.

R. B. Stevenson

Research and Development Department, Amoco Chemicals Corp., Whiting, Ind.

WHEREAS HYDRODYNAMIC VOLUME appears to be the effective parameter for the size separation of high-molecular-weight polymers in Gel Permeation Chromatography (*1*), molar volume is better for low-molecular-weight compounds such as alkanes and aromatics (*2*). However, some of these compounds show unusual elution behavior in tetrahydrofuran (THF), a common solvent in GPC. For example, alkanes and aromatics with similar molar volumes show large differences in retention volumes, which have been attributed to an association between the aromatic and the polystyrene divinylbenzene gel (*3*). Even within the aromatics class, different elution patterns have been observed, not only in THF (*4*), but also in methylene chloride (*5*); with increasing molar volume, retention volumes decrease for the cata-condensed series of polynuclear aromatics, but there is an anomalous increase for the peri-condensed series. Thus, a GPC study of petroleum resids—complex mixtures of high-molecular-weight compounds including homologs of alkanes and aromatics—is hampered by these varied elution patterns.

To simplify the study of elution behavior, we observed the elution of low-molecular-weight model compounds in various solvents and solvent combinations. These studies were supplemented with infrared, ultraviolet, and solubility measurements to determine whether elution order is affected by adsorption, association, and/or differences in the solubilities of the compounds. Conventional GPC equipment (Waters Associates, Models 100 and 200) was used for this work. The results should be useful with more complex systems such as resids.

To date, we have obtained no clear-cut evidence to explain the anomalous behavior of the peri-condensed molecules. However, we have found that the anomalies disappear when 1,2,4-trichlorobenzene (TCB) is used as the GPC solvent.

RESULTS AND DISCUSSION

Figure 1 illustrates the complex elution patterns in THF compared to TCB. Retention volume data for these compounds are presented in Tables I and II. In THF, five distinct elution patterns are observed for these six series of compounds (the sulfur-heterocyclics align with the cata-condensed aromatics). The series of peri-condensed aromatics shows an unusual reversal in elution behavior—the larger the molecule, the later it elutes. This reversal seems to be related to peri-condensation. Further support for this observation lies in the elution behavior of the nitrogen compounds. Elution is in the expected order through carbazole, but benzcarbazole—a peri-condensed molecule—elutes later than carbazole. The hydrogenated pyrenes show a maximum in relative retention and, although less clear, this would again appear to be a function of structure.

By contrast, in TCB these differences between classes of compounds disappear. With that solvent, the retention

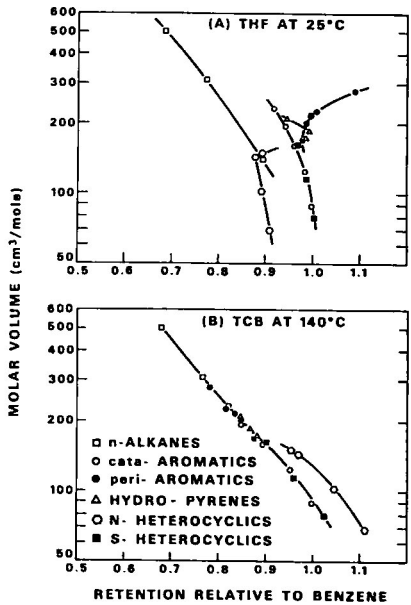


Figure 1. Effect of solvent on elution behavior

(1) Z. Grubisic, P. Rempp, and H. Benoit, *J. Polym. Sci., Part B*, 5, 753 (1967).
(2) J. Cazes and D. R. Gaskill, *Separ. Sci.*, 2, 421 (1967).
(3) G. D. Edwards and Q. Y. Ng, *J. Polym. Sci., Part C*, 21, 105 (1968).
(4) T. Edstrom and B. A. Petro, *ibid.*, p 171.
(5) H. Oelert, presented at the API 60 Summer Meeting, Laramie, Wyo., 1969.

Table I. GPC of Model Compounds in THF at 25 °C

Compound	Molar volume data: cc/mole	Data source[a]	Retention volume, cc
n-Alkanes			
Heptane	141	1	147.5
Hexadecane	311	1	127.4
Octacosane	503	1	113.0
Cata-condensed aromatics			
Benzene	88.9	2	164.5
Naphthalene	125.0	2	162.3
Anthracene	160.2	2	158.6
Naphthacene	196	2	155.0
Picene	232	2	151.5
Peri-condensed aromatics			
Pyrene	171.5	2	161.3
Perylene	202	2	162.7
1,12-Benzperylene	219	2	163.8
Coronene	228	2	166.2
Ovalene	280	2	179.3
Hydrogenated pyrenes			
Pyrene	171.5	2	161.3
1,2-Dihydropyrene	175.1	3	162.5
1,2,3,6,7,8-Hexahydropyrene	186.0	3	163.2
Decahydropyrene	211.3	3	156.0
N-heterocyclics			
Pyrrole	69.3	3	149.8
Indole	102.9	3	147.0
Carbazole	144	2	145.0
4H-Benzo(*def*)carbazole	149.8	3	147.4
S-heterocyclics			
Thiophene	79.0	3	165.4
Benzthiophene	115.2	3	162.6
Dibenzthiophene	162.7	3	159.6

[a] (1) J. Cazes and D. R. Gaskill, Seminar Proceedings, Sixth International Seminar on GPC, Miami Beach, Fla., Oct. 7–9, 1968; (2) H. G. Davis and S. Gottlieb, *Fuel*, **42**, 37 (1963); (3) Calculated from molecular weight and density values.

Table II. GPC of Model Compounds in TCB at 140 °C

Compounds	Molar volume, cc/mole	Retention volume, cc
Thiophene	79.0	170.0
Benzene	88.9	166.0
Benzthiophene	115.2	159.6
Naphthalene	125.0	158.4
Anthracene	160.2	148.8
Dibenzthiophene	162.7	149.5
Pyrene	171.5	145.8
1,2-Dihydropyrene	175.1	146.3
1,2,3,6,7,8-Hexahydropyrene	186.0	143.8
Naphthacene	196	141.0
Perylene	202	140.3
Decahydropyrene	211.3	140.3
1,12-Benzperylene	219	139.1
Coronene	228	136.0
Picene	232	136.3
Ovalene	280	129.7
Hexadecane	311	127.5
Octacosane	503	112.7
N-heterocyclics		
Pyrrole	69.3	184.4
Indole	102.9	173.5
Carbazole	144	161.1
4H-Benzo(*def*)carbazole	149.8	158.3

Table III. Effect of Temperature on Elution Behavior in TCB

Compound	Retention relative to benzene: 140 °C	25 °C
Pyrene	0.877	0.842
Perylene	0.844	0.812
Coronene	0.818	0.787

Table IV. Solubility of Aromatic Hydrocarbons

Solute	Solubility, (grams/liter) at 25 °C: Toluene	THF	TCB
Coronene	1.4	3.6	6.4
Perylene	2.9	7.8	11.0
Pyrene	V. Sol.	V. Sol.	V. Sol.
Picene	2.6	2.8	2.7

volumes of nearly all the compounds show a simple relationship with the log of molar volume. The only exceptions are the nitrogen compounds, which are slightly displaced, undoubtedly because a small adsorption component remains. The displacement could very likely be eliminated if a small amount of a polar solvent is incorporated in the TCB. The ability of TCB to eliminate unusual elution behaviors is temperature independent; Table III shows that at 25° and 140 °C elution orders are identical, although positions are slightly displaced presumably because of differences in swelling characteristics of the gel.

The marked contrast in elution behavior between the cata- and peri-condensed molecules in THF and TCB apparently cannot be explained by adsorption, which is a common reason for delayed retention in liquid chromatography. Such adsorption usually causes pronounced tailing whereas GPC peaks for peri-condensed molecules, although wider than expected, do not show such tailing. Furthermore, the adsorption behavior of a large number of polynuclear aromatics on alumina (*6*) does not reveal any reason for their anomalous GPC behavior.

Studies with other solvents also failed to show reasons for the varied elution pattern. In toluene, coronene is held back even farther with respect to benzene than in THF; the retentions relative to benzene are 1.13 and 1.01. In 10 vol % TCB-in-toluene at room temperature and at 50 °C, retention of coronene relative to benzene is the same as in toluene. Increasing the temperature to 75 °C shifted the coronene peak only slightly toward earlier elution.

Studies to determine whether a relationship exists between solubility and retention of the polynuclear hydrocarbons in TCB, THF, and toluene are summarized in Table IV and in Figure 2. For the peri-condensed molecules, there appears to be a correlation between the degree of solubility in the three solvents and retention. Both coronene and perylene are most soluble in TCB, in which there is apparently no delayed retention; they are least soluble in toluene, in which there is the greatest delay in retention. On the other hand, picene—a cata-condensed molecule—has the same low solubility in all solvents, and it is not delayed. These data suggest that solubility may affect the elution order of the peri-condensed but not of the cata-condensed molecules. This suggestion is made cautiously because pyrene shows some delayed retention even though it is highly soluble in all solvents. But the amount of delayed retention is the smallest of the series.

(6) L. R. Snyder, *J. Phys. Chem.* **67**, 234 (1963).

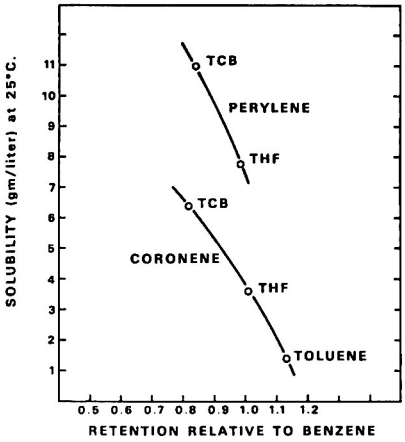


Figure 2. Relation of solubility to retention volume

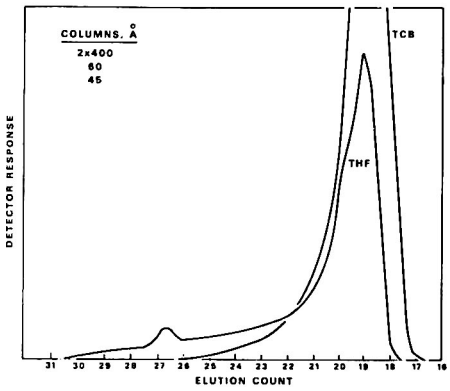


Figure 3. Solvent effect on GPC of asphaltene

An association between the peri-condensed solutes and the gel phase is possible, and it may be enhanced by poor solubility. However, IR examination of a gel upon which coronene had been deposited revealed no evidence for such an association. A solute–solvent interaction could possibly explain the effectiveness of TCB in eliminating association—coronene and TCB are good candidates for a charge transfer complex. But examination of the UV spectra of coronene in TCB, THF, and toluene failed to provide solid support for such complexing.

In preliminary experiments, the elution behavior of petroleum asphaltenes has shown a solvent dependence similar to that for peri-condensed model compounds. In THF, all asphaltenes show a prominent low-molecular weight tail; but in TCB this tail is considerably reduced. These differences are shown in Figure 3. In addition, an asphaltene was fractionated in a preparative column in methylene chloride solvent, and the material represented by the tail was collected and then chromatographed in the analytical GPC instrument. As shown in Figure 4, this material is held back

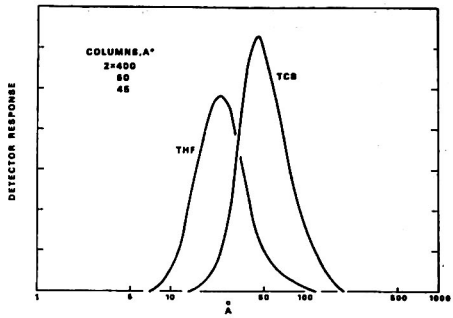


Figure 4. Solvent effect on GPC of asphaltene fraction

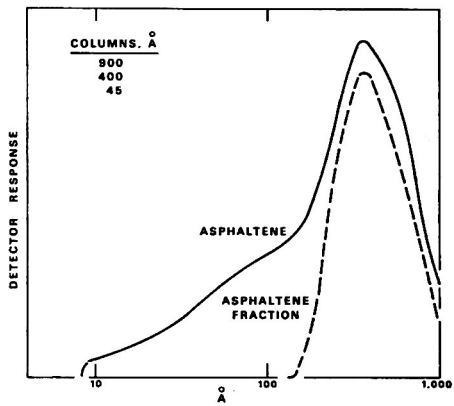


Figure 5. GPC of asphaltene fractions

much more in THF than in TCB; the relative retentions of the peaks compared to benzene are 0.77 for THF and 0.66 for TCB. Possibly the diminution of the asphaltene tail in TCB and the shift in peak position of this material with solvent may be analogous to the elution behavior of the simple peri- and cata-condensed molecules in THF and TCB. Thus, this behavior may well be caused by naturally occurring peri-condensed molecules in asphaltenes. An alternate explanation is that adsorption by sulfur, nitrogen, or oxygen compounds is greater in THF than in TCB. However, this seems unlikely upon examination of the GCP behavior of high-molecular-weight material obtained by fractionation. The chromatogram of such material in THF, together with that of the parent asphaltene, is shown in Figure 5. On the basis of simple adsorption, a tail should still be present in the derived peak if the polar compounds are assumed to be distributed uniformly across the molecular weight spectrum. These results thus imply that the low-molecular-weight tail of an asphaltene in THF is caused by unique species which show different elution behavior in TCB. But we have not yet established by independent means that the low-molecular-weight asphaltenic material actually is enriched in peri-condensed aromatics.

Received for review July 6, 1970. Accepted September 28, 1970.

Interference of Lithium in Atomic Absorption Spectrometry

A. M. Bond

Department of Inorganic Chemistry, University of Melbourne, Parkville 3052, Victoria, Australia

D. R. Canterford

Department of Physical Chemistry, University of Melbourne, Parkville 3052, Victoria, Australia

IN ANALYSIS OF SOLID materials by the atomic absorption method, the sample must first be brought into solution. If this can be achieved successfully, then a wide variety of metals often can be determined by the atomic absorption method from the one solution procedure. For geological samples, fusion techniques are frequently used to obtain the sample in solution form. There are two obvious requisites for a particular fusion method to be suitable: Decomposition must be complete and the fusion process should not introduce any elements to be determined.

Sodium and potassium are commonly occurring elements in geological samples and determination of these elements is often required. Most fusion methods, however, utilize sodium or potassium salts such as the hydroxides, carbonates, peroxides, etc. which eliminates the possibility of determining one or the other of these elements without a separate fusion. Lithium, however, is not as commonly required in routine analysis, and use of lithium salts in the fusion method will often avoid the necessity of a second fusion. Lithium fusions can therefore be quite advantageous.

The fusion method developed by Biskupsky (*1*) using lithium fluoride and boric acid has been found by the authors to provide virtually complete decomposition of a wide variety of rock types and is particularly suitable for geochemical analysis. For instance Bond and coworkers (*2*) recently compared this method with several well-documented fusion techniques, and found that the lithium fluoride–boric acid or sodium fluoride–boric acid methods were the most satisfactory, little or no residue being left after a single fusion. As a fusion method prior to analysis of a wide range of metals by atomic absorption, including sodium, the method is therefore particularly suitable.

Sodium and potassium can often interfere in atomic absorption analysis (*3*). The low ionization potentials of sodium and potassium, relative to other elements, causes an enhancement in the absorption of the other elements if the latter are ionized in the flame being used, but less preferentially than sodium or potassium.

Table I shows the ionization potentials and percentage ionization of the alkali metals in various flames (*4*, *5*). Interference due to lithium ionization would probably be less than that due to the other alkali metals; however, when one considers the very high concentrations of lithium introduced by the lithium fluoride–boric acid fusion, significant ionization interference would be expected.

To utilize the advantages of this fusion method with atomic absorption spectrometry, it is therefore necessary to know to what extent the interference occurs and for those cases where it occurs, how to eliminate it. These aspects of lithium interference were therefore investigated with a number of elements and the results are reported in this paper.

Table I. Ionization Potentials and Percentage Ionization of Alkali Metals in Various Flames

Values as Reported in Ref *4*

Element	Ionization potential (eV)	% Ionization in different flames: Air–propane (2200 °K)	Hydrogen–oxygen (2450 °K)	Acetylene–oxygen (2800 °K)
Li	5.37	0.01	0.9	16.1
Na	5.12	0.3	5.0	26.4
K	4.32	2.5	31.9	82.1
Rb	4.16	13.5	44.4	89.6
Cs	3.87	28.3	69.6	96.4

Table II. Reagents, Resonance Lines, and Flames Used for Each Element

Element	Reagents used	Line, Å	Flame(s)
Zn	Zinc(II) sulfate	2138	air–C_2H_2/N_2O–C_2H_2
Mn	Manganese(II) sulfate	2794	air–C_2H_2
Pb	Lead(II) nitrate	2170	air–C_2H_2/N_2O–C_2H_2
Mo	Molybdenum trioxide	3132	air–C_2H_2/N_2O–C_2H_2
W	Sodium tungstate	2551	air–C_2H_2/N_2O–C_2H_2
Ti	Potassium titanium(IV) oxalate	3642	N_2O–C_2H_2
Zr	Zirconyl chloride octahydrate	3601	N_2O–C_2H_2
Hf	Hafnium nitrate	3073	N_2O–C_2H_2

EXPERIMENTAL

All chemicals used were of reagent grade purity. Lithium was added as both the chloride and perchlorate salt, for tests on lithium interference.

Table II summarizes the chemicals used to provide the elements on which interference tests were carried out along with the resonance lines and types of flame used.

The atomic absorption spectrophotometer used in this work was a modified Techtron Model AA-3 instrument. Techtron burners AB-50 (nitrous oxide–acetylene) and AB-51 (air–acetylene) were used with the AA-5 model nebulizer and spray chamber.

Small bore hollow cathode lamps manufactured by Atomic Spectral Lamps, Melbourne, were used in conjunction with the AA-5 power unit and lamp turret. The operating currents for the lamps and the monochromator slit widths used in each case were those suggested by the lamp manufacturer.

RESULTS AND DISCUSSION

Enhancement of Zinc Absorption by Lithium. According to Fuwa *et al.*, (*6*), a solution containing 100 ppm lithium

(1) V. S. Biskupsky, *Anal. Chim. Acta*, **33**, 333 (1965).
(2) A. M. Bond, T. A. O'Donnell, A. B. Waugh, and R. J. W. McLaughlin, ANAL. CHEM., **42**, 1168 (1970).
(3) J. Ramírez-Muñoz, "Atomic-Absorption Spectroscopy," Elsevier, Amsterdam, 1968, p 269.
(4) J. A. Dean, "Flame Photometry," McGraw-Hill, New York, N. Y., 1960, p 42.
(5) W. H. Foster, Ph.D. Thesis, Massachusetts Institute of Technology, Cambridge, Mass., 1959.
(6) K. Fuwa, P. Pulido, R. McKay, and B. L. Vallee, ANAL. CHEM., **36**, 2407 (1964).

(as the chloride) did not affect the absorbance reading of a standard 0.2 ppm zinc solution in the hydrogen–air flame. However, we have found that as little as 5 ppm lithium caused significant enhancement of the absorbance of a 0.5 ppm zinc solution in the air–acetylene flame. Typical results are shown in Table III.

The enhancement reaches a maximum value at about 1000 ppm lithium and thereafter remains virtually constant. Similar results were obtained in the hotter nitrous oxide–acetylene flame. The presence of lithium was estimated to potentially provide up to a 15% error in the determination of zinc if calibration curves were prepared in the absence of lithium and no correction were to be applied for lithium interference.

Enhancement of Lead Absorption by Lithium. Dagnall and West (*7*) reported no interference on lead by a 1000-fold excess of lithium, in the air–propane flame. In the air–acetylene flame, we have found that lithium causes considerable enhancement of the absorbance of a 5-ppm lead solution, as shown in Table IV. Again a maximum enhancement at about 1000 ppm lithium was found, and similar results were observed in the nitrous oxide–acetylene flame.

Enhancement of Manganese Absorption by Lithium. Lithium was found to enhance the absorbance of a 3.0-ppm manganese solution in the air–acetylene flame. Typical results are shown in Table V.

Enhancement of Other Elements Absorption by Lithium. Results similar to the above were found for titanium, zirconium, and hafnium in the nitrous oxide–acetylene flame. No enhancement of molybdenum or tungsten was observed in either the air–acetylene or nitrous oxide–acetylene flames.

Table III. Enhancement of Zinc Absorbance by Lithium

Zinc concn, ppm	Lithium added, ppm	Av absorbance[a]
0.5	0	0.132
0.5	5.0	0.141
0.5	20.0	0.144
0.5	35.0	0.146
0.5	500	0.149
0.5	1000	0.150
0.5	2000	0.150

[a] Average of three determinations.

Table IV. Enhancement of Lead Absorbance by Lithium

Lead concn, ppm	Lithium added, ppm	Av absorbance[a]
5.0	0	0.300
5.0	600	0.319
5.0	800	0.323
5.0	1000	0.325

[a] Average of three determinations.

Table V. Enhancement of Manganese Absorbance by Lithium

Manganese concn, ppm	Lithium added, ppm	Av absorbance[a]
3.0	0	0.303
3.0	800	0.313
3.0	1000	0.314

[a] Average of three determinations.

ELIMINATION OF LITHIUM INTERFERENCE

Ionization interference can be overcome by using the addition method of analysis or by using standards containing a similar concentration of the interfering element to the standard solutions. Alternatively, as the absorbance of elements was observed to be independent of lithium concentration above 1000 ppm, addition of a standard lithium concentration above this value to all test and standard solutions provides a third and probably the simplest and most convenient method for elimination of interference (*8*, *9*).

The seriousness of this interference and the effective manner in which it can be overcome is demonstrated by the following set of results for determination of zinc in an impure willemite (Zn_2SiO_4) sample. Using standards containing zinc only, the result of five determinations was 58.3 ± 0.6% Zn. By using the addition method on the same sample, a value of 55.6 ± 0.9% Zn was obtained. In the solution analyzed by the addition procedure, the concentration of lithium from the fusion was about 10 ppm, and when zinc standards containing 10 ppm lithium were used, the result was 55.8 ± 0.5% Zn. Addition of 2000 ppm lithium to both standards and unknown solution gave 55.7 ± 0.5%. As this sample contained high concentrations of zinc, the fusion solution was diluted prior to the zinc determination by atomic absorption spectrometry, and the concentration of interfering lithium is not very high. However, even the potential interference that can be caused by 10 ppm lithium is significant, and it can be readily visualized that the apparent result for zinc when it is only a trace constituent of the rock sample and no dilution of the fusion solution is possible, could be exceedingly high unless the lithium interference is eliminated.

When the willemite sample was analyzed for manganese and lead, all three methods were again successful in removing the interference.

CONCLUSIONS

A by no means exhaustive study of the interference of lithium on the determination of other elements has shown that significant interference occurs in many cases. If a fusion method such as the lithium fluoride–boric acid one is used for destruction of the solid prior to analysis of the sample with the atomic absorption method, then the possibility of lithium interference should be investigated. If present, it can be eliminated simply by the methods described above. The simplest approach, however, seems to be to add a large concentration of lithium to all test and standard solutions, as above about 1000 ppm, absorbance becomes independent of lithium concentration for all elements examined in this work.

The interference appears to be due to ionization of lithium and the mechanism is undoubtedly the same as that commonly observed with sodium and potassium.

Allan (*8*) has stated that ionization interference is minimized in cool flames, so the lack of interference reported for lithium on the absorbance of zinc (*6*) and lead (*7*) may be due to the use of cooler hydrogen–air and air–propane flames (See data in Table I).

RECEIVED for review August 18, 1970. Accepted September 25, 1970.

(7) R. M. Dagnall and T. S. West, *Talanta*, **11**, 1553 (1964).
(8) J. E. Allan, *Spectrochim. Acta*, **18**, 605 (1962).
(9) E. E. Angino and G. K. Billings, "Atomic Absorption Spectrometry in Geology," Elsevier, Amsterdam, 1967, p 37.

Spectrofluorimetric Determination of Traces of Fluoride Ion by Ternary Complex Formation with Zirconium and Calcein Blue

Tan Lay Har and T. S. West

Chemistry Department, Imperial College of Science and Technology, London, S.W.7., England

ALL SPECTROFLUORIMETRIC and, with two exceptions, all spectrophotometric procedures for the determination of fluoride ion are based on the ability of fluoride to abstract cations such as aluminium or zirconium from strongly absorbing or fluorescing complexes, thus liberating the free reagent. Such methods tend to be unselective. The two spectrophotometric methods which differ are kinetochromic spectrophotometry (*1*), which depends on the catalytic action of fluoride ion on the zirconium–xylenol orange reaction, and that based on the formation of a strongly absorbing 1:1:1 ternary complex with cerium(III) or lanthanum, alizarin complexan, and fluoride (*2*). The kinetochromic method allows fluoride to be determined down to 0.005 μg/ml with an "effective" molar absorptivity of 2×10^6 but must be operated under rigidly controlled conditions. The alizarin complexan ternary complex method is easy to apply, however, and in view of its high molar absorptivity, 3×10^4, its stability, and the fact that the reaction is not interfered with by other anions, it seemed logical to look for other ternary systems for the determination of fluoride. It was considered that the sensitivity could be improved even further by a fluorimetric method and this led us to an investigation of the effect of fluoride on the fluorescence intensity of the zirconium–Calcein Blue complex (*3*).

Since its almost simultaneous introduction by Eggers (*4*) and Wilkins (*5*), Calcein Blue has been used extensively as a metallofluorescent indicator for the complexometric titration of several metal ions with EDTA. Only recently (*3*) has it been used as a direct fluorimetric reagent for the determination of zirconium at pH 5.5. It was found that the addition of fluoride to the zirconium–Calcein Blue complex resulted in an enhancement of fluorescence intensity. In this paper we describe an investigation of this effect and the development of a method for the determination of fluoride based on this intensification of fluorescence

EXPERIMENTAL

Apparatus. Fluorescence measurements were made with a double monochromating spectrofluorimeter (Farrand Optical Co. No. 10244) fitted with a 150-W Xenon arc lamp (Hanovia Division No. 901 C-1) and RCA IP 28 photomultiplier and equipped with a Honeywell–Brown Recorder. Fused quartz cells (10 × 20 × 50 mm) were used throughout.

Reagents. SODIUM FLUORIDE SOLUTION $10^{-3}M$. Prepare a $10^{-3}M$ stock solution by dissolving 41.99 mg of analytical reagent grade sodium fluoride in a liter of distilled water. Ten milliliters of the stock solution were diluted to 1 liter to obtain a $10^{-4}M$ solution.

1 ml of $10^{-4}M$ $F^- \equiv 0.1899$ μg F

CALCEIN BLUE $10^{-4}M$. Prepare a $10^{-3}M$ solution by dissolving 160.2 mg of Calcein Blue (Hopkin and Williams) in a few drops of 0.1*M* potassium hydroxide and diluting to 500 ml with distilled water. Ten milliliters of this solution were diluted to 100 ml with distilled water to give a $10^{-4}M$ solution. After 2–3 days, all Calcein Blue solutions were discarded and fresh solutions were prepared.

ZIRCONYL CHLORIDE $10^{-4}M$. Prepare a $10^{-3}M$ solution by dissolving 32.2 mg of $ZrOCl_2$ in 100 ml of 3*M* HCl. It has been shown (*6*) that zirconium solutions 3*M* in HCl do not polymerize on standing. Solutions ($10^{-4}M$) were prepared by dilution with 3*M* HCl.

AMMONIA SOLUTION (APPROXIMATELY 1.5*M*). Eight milliliters of concentrated ammonia (18*M*) were diluted to 100 ml with distilled water.

Procedure. CALIBRATION CURVE. Transfer by pipet 5–30 ml (at suitable volume intervals) of $10^{-3}M$ sodium fluoride into 100-ml flasks. Add 2 ml of $10^{-4}M$ Calcein Blue and just sufficient NH_3 solution (*ca.* 3–4 ml of an approximately 1.5*M* NH_3 solution) to adjust the pH of the final solution to 2.5. Finally, add 2 ml of $10^{-4}M$ Zr in 3*M* HCl. Mix the contents of the flask and dilute to volume.

The fluorescence of the solutions was measured after 20–30 min at 410 nm with the excitation wavelength set at 350 nm.

Unknown solutions containing 0.9–6 μg F (or ≥0.01 ppm in concentration) were analyzed in a manner similar to that used to set up the calibration curves.

Because of day-to-day variation in lamp intensity, it is necessary to run two or three standards through with each batch of unknowns, as in all single beam fluorimetric procedures, to establish the position and slope of the calibration curve.

RESULTS AND DISCUSSION

Spectral Characteristics. Figure 1 shows the excitation and fluorescence emission spectra of a $2 \times 10^{-6}M$ solution of Calcein Blue at pH 2.5, (*a*) and (*b*), respectively, a 1:1 zirconium–Calcein Blue solution (*c*) and (*d*), respectively, and a 1:1:1 zirconium–Calcein Blue–fluoride solution (*e*) and (*f*), respectively, at the same concentration and pH, and obtained with identical instrumental settings of slit and gain, etc. These spectra are uncorrected for variations in the emission, characteristics of the 150-W Xenon arc lamp, the response characteristics of the IP 28 photomultiplier, and the diffraction gratings.

It will be seen that at pH 2.5 the addition of zirconium depresses the fluorescence originating from Calcein Blue at 450 nm and produces a new emission maximum of lower intensity at 410 nm. Similarly, the excitation maxima are changed from 325 nm for Calcein Blue to 350 nm for its zirconium complex. The addition of fluoride to the zirconium–Calcein Blue complex increases the fluorescence intensity, but the same maximum excitation and emission wavelengths are retained as for Zr:CB. This indicates that a ternary complex is formed and eliminates the possibility that

(1) M. L. Cabello-Tomas and T. S. West, *Talanta*, 16 781 (1969).
(2) M. A. Leonard and T. S. West, *J. Chem. Soc.*, 4477 (1960).
(3) R. V. Hems, G. F. Kirkbright, and T. S. West, ANAL. CHEM., 42, 784 (1970).
(4) J. H. Eggers, *Talanta*, 4 38 (1960).
(5) D. H. Wilkins, *ibid.*, p 182.
(6) B. C. Sinha and S. Das Gupta, *Analyst (London)*, 92, 558 (1967).

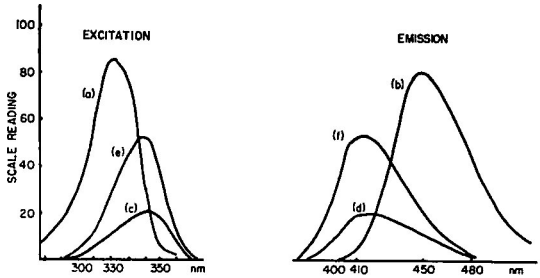


Figure 1. Fluorescence excitation and emission spectra for Calcein Blue, its 1:1 binary complex with Zr(IV) and its 1:1:1 ternary complex with fluoride and Zr(IV)

(a) CB excitation (fluorescence at 450 nm)
(b) CB fluorescence (excitation at 410 nm)
(c) CB–Zr excitation (fluorescence at 325 nm)
(d) CB–Zr fluorescence (excitation at 350 nm)
(e) CB–Zr–F excitation (fluorescence at 410 nm)
(f) CB–Zr–F fluorescence (excitation at 350 nm). Concentrations of CB/Zr/F at $2 \times 10^{-6}M$. pH 2.5

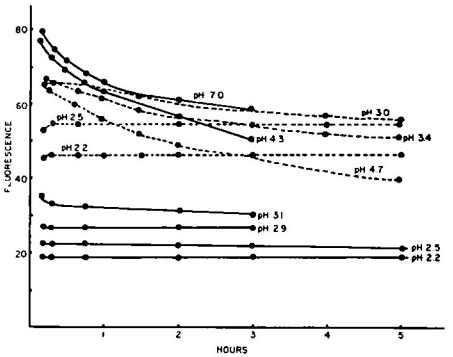


Figure 2. Fluorescence stability plots *vs.* time at specified pH values

Solid lines Zr:CB
Dotted lines Zr:CB:F
All other conditions as recommended in Procedure

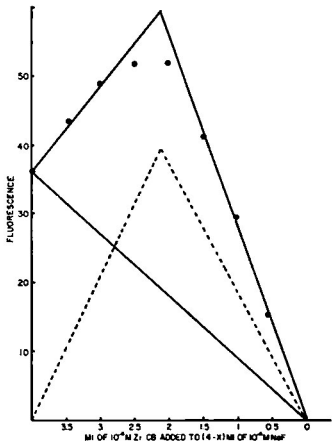


Figure 3. Continuous variations plot

F *vs.* Zr:CB
All other conditions as recommended in Procedure

the fluoride is simply abstracting zirconium from the 1:1 Zr:CB complex and releasing the more strongly fluorescent Calcein Blue. This was further confirmed by adding a 500-fold excess of fluoride to the Zr:CB complex which resulted in a decrease in fluorescence intensity at the excitation and emission maxima of the zirconium–Calcein Blue complex and an increase in fluorescence intensity at the emission and excitation maxima of the reagent itself.

Influence of pH on Stability of the Complex. Figure 2 shows the fluorescence intensity of a solution $2 \times 10^{-6}M$ with respect to both zirconium and Calcein Blue, at various pH values, plotted against time.

The dotted curves were obtained similarly, but with fluoride added in 1:1 proportion to the Zr:CB complex. The fluorescence of the solutions developed to a maximum value within 10 minutes. The Zr:CB binary complex shows maximum intensity at higher pH values than the ternary Zr:F:CB complex as shown previously (*3*). The drop in intensity with time at pH >3 is probably due to progressive hydrolysis of the zirconium complexes. At pH 2.5, all solutions showed no significant change in fluorescence intensities within 4 hours, and hence all experiments were carried out at this pH.

Nature of the Complex. Job's method of continuous variations was applied between the 1:1 zirconium–Calcein Blue complex and the fluoride ion (see Figure 3). This gave a binary complex to fluoride ratio of 1.2:1.

Mole ratio plots with varying concentrations of Calcein Blue against a fixed amount of a 1:1 zirconium fluoride solution and of zirconium solution showed that in excess Calcein Blue, the fluorescence due to the ternary complex is considerably diminished (see Figure 4). The decrease in the

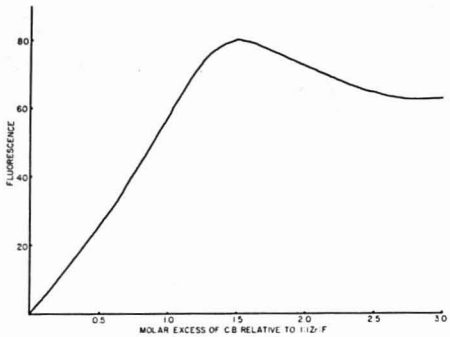


Figure 4. Effect of excess of Calcein Blue (relative to Zr) on the fluorescence of the ternary complex with fluoride

Table I. Study of Interferences

4μ of F by Recommended Procedure

Ion added, mole ratio Ion/F	Interference, %	Ion added mole ratio Ion/F	Interference, %
Cl^- (500)	0	Be^{2+} (50)	−33
NO_3^- (500)	0	Be^{2+} (5)	0
SO_4^{2-} (500)	+33	Ca^{2+} (500)	0
SO_4^{2-} (50)	+11	Mg^{2+} (50)	0
SO_4^{2-} (5)	0	Mn^{2+} (50)	Quenched (brown solution)
PO_4^{3-} (500)	Quenched	Mn^{2+} (5)	−13
PO_4^{3-} (50)	−67	Ag^+ (50)	White ppte
$B_4O_7^{2-}$ (500)	20	Ag^+ (5)	+10
$B_4O_7^{2-}$ (50)	0	Al^{3+} (50)	−39
MoO_4^{2-} (500)	−42	Al^{3+} (5)	−16
MoO_4^{2-} (50)	−9	Cd^{2+} (50)	0
MoO_4^{2-} (5)	0	Ni^{2+} (50)	0
WO_4^{2-} (500)	Quenched	Zn^{2+} (50)	0
WO_4^{2-} (50)	−87	Co(II) (50)	−22
WO_4^{2-} (5)	−21	Co(II) (5)	0
VO_3^- (500)	−75	Pb^{2+} (50)	0
VO_3^- (50)	0	Sb(III) (50)	−9
Oxalate (500)	−89	Sb(5)	0
Oxalate (50)	−80	AsV (50)	−16
Oxalate (5)	−55	AsV (5)	0
Tartrate (500)	−72		
Tartrate (50)	−66		
Tartrate (5)	−45		
Acetate	0		

presence of excess Calcein Blue (relative to Zr) may be explained by the breakdown of the ternary fluoride complex in favor of a polynuclear zirconium–Calcein Blue complex. Previous studies of the binary complex at pH 5.5 showed that excess CB had a depressant effect on the fluorescence also, although it was not so marked as for the ternary complex at pH 2.5. This depressing action of excess CB is safely accounted for, however, by formulating a 1:1 reaction with the fluoride ion.

From both the continuous variation and mole ratio plots, it was concluded that a 1:1:1 ternary complex was formed. The slightly high figure obtained for the Calcein Blue in the ratio was attributed to its partial decomposition when dissolved in alkali and its low assay because it is manufactured for use as a metallo-fluorescent indicator and could not be obtained 100% pure. Attempts at purification were not successful.

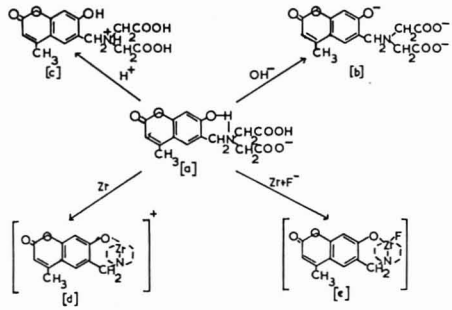


Figure 5. Structure of Calcein Blue at various pH values related to its fluorescence and suggested structure for the weekly fluorescent binary Zr:CB and moderately fluorescent Zr:CB:F ternary complexes

Order of Addition of Reagents. The effect of of the order of mixing of the solutions was investigated. It was found that the zirconium must be added after Calcein Blue; otherwise the fluoride produces no effect. The fluoride, however, could be added at any stage of the mixing.

Sensitivity of Method. The development of the method was carried out with test solutions $10^{-5}M$ in fluoride. However, the maximum instrumental sensitivity was not used and it was possible to determine down to $10^{-7}M$ concentrations in the final solution.

Interference Studies. The influence of up to 500-fold excess of a selection of 11 other anions likely to interfere by forming complexes or precipitates with zirconium was examined as were the effects of 13 cations likely to form preferential complexes with Calcein Blue or fluoride ion. The results of this study, which are summarized in Table I show that at a fivefold excess, tungstate, acetate, tartrate, and phosphate cause low results while, at 50-fold excess, molybdate also yields low recoveries and sulfate high recoveries. Among the cations, aluminum, manganese, and silver caused slight interference at fivefold excess, while at 50-fold excess, arsenic, antimony, beryllium, and cobalt caused low recoveries.

Nature of Complex Formation. The fluorescence of Calcein Blue at intermediate pH's has been attributed (*4*) to the formation of a hydrogen bridge between the phenolic oxygen and the nitrogen from the iminodiacetic acid group, Figure 5 (*a*), thus preventing torsion of the group about the C–CH_2 bond and minimizing nonradiative dissipation of energy. At high pH, deprotonation occurs, Figure 5 (*b*), and at low pH the *N* is protonated, Figure 5 (*c*), both resulting in breakage of the hydrogen bridge and freeing of the side chain, thus weakening the fluorescence yield by rotational dissipation of energy, etc.

Little is known about the chelate chemistry of zirconium, but it will be seen from the spectra presented in Figure 1 that at pH 2.5 the Zr:CB complex is less fluorescent than the reagent. This can be explained by the breakage of the H bridge on formation of a chelate complex with Zr, see Figure 5 (*d*). Thus, because of the largely ionic nature of the O–Zr bond the Zr:CB complex yields less fluorescence than the Calcein Blue alone at the same pH. The enhancement of fluorescence on addition of fluoride, Figure 5 (*e*), can be explained by the incorporation of fluoride ion in the coordination sphere of the zirconium, *i.e.*, replacement of coordinated H_2O molecules by the small fluoride ion, which has a

very high affinity for zirconium. The electrophilic effect of fluoride may cause withdrawal of electrons resulting in the formation of a more covalent O–Zr bond. This strengthening of the degree of covalency should favor stabilization of the excimer and, hence, increase the quantum efficiency of the fluorescence.

The above explanation is consistent with the observation that at higher pH's the binary Zr–Calcein Blue complex is more fluorescent than the reagent and addition of fluoride then has little or no effect.

CONCLUSIONS

The method suggested provides a positive fluorimetric method of very high sensitivity for the determination of trace amounts of fluoride in aqueous solution down to 0.01 ppm. Of the common anions, only phosphate interferes seriously at fivefold excesses. Very few cations interfere. A 1:1:1 ternary complex formation is responsible for fluorescence production. The increased fluorescence yield is attributed to conformational stabilization of the excimer of the fluorophore in the ternary complex. The method is rapid and the procedure is reproducible. Analyses show a precision of ±3% near the middle range of calibration curves.

RECEIVED for review May 12, 1970. Accepted September 22, 1970. We thank the Agricultural Research Council for a grant-in-aid of this work and the Science Research Council for a grant to purchase the spectrofluorimeter.

Fluorometric Methods for Determination of Europium and Terbium

Dora E. Williams and John C. Guyon
University of Missouri, Columbia, Mo. 65201

A VARIETY OF β-diketones have been used to form tetrakis chelates with europium and terbium for analytical purposes and as potential laser materials. Their utility as laser materials is limited by their high ultraviolet extinction coefficients, which would indicate good sensitivity in methods for the determination of europium and terbium. Since these chelates involve charge transfer from the chelating agent to the metal ion, the fluorescence wavelength is characteristic of the metal ion and provides a method for the determination of europium and terbium in the presence of other rare earth ions. Among those chelating agents previously tried are thenoyltrifluoroacetone (*1*) and trifluoroacetylacetone (*2*). Since trifluoro-β-diketones had been utilized, it was decided to try a hexafluoro-β-diketone, in the hope that more sensitive methods could be developed. This paper is a summary of the studies made upon the 1,1,1,5,5,5-hexafluoro-2,4-pentanedione chelates of europium and terbium.

EXPERIMENTAL

Apparatus. All fluorescence measurements were made on a Perkin-Elmer Fluorescence Spectrophotometer MPF-2A.

Reagents. The stock chelating agent solution was prepared by diluting 1 ml of Eastman 1,1,1,5,5,5-hexafluoro-2,4-pentanedione to 100 ml with 95% ethanol. A stock 100 ppm of europium solution was prepared by dissolving 11.6 mg of K & K europium oxide in 0.5 ml of 1.25*M* HCl, then diluting to 100 ml with 95% ethanol. A stock 100 ppm of terbium solution was prepared by dissolving 11.8 mg of K & K Tb_4O_7 in 5 ml of concd HCl and dilution to 100 ml with 95% ethanol. A 1-ppm solution of each lanthanide was prepared by dilution of 1 ml of each of the previous solutions to 100 ml with 95% ethanol, neutralizing the solution with alcoholic KOH prior to complete dilution. Finally, a 50-ppb working solution of each one was prepared by dilution of 25 ml of the 1-ppm solutions to 500 ml with 95% ethanol. Other rare earth solutions used in foreign ion study were rare earth chlorides supplied by K & K. The remainder of the foreign ion solutions reported were prepared from analytical reagent grade salts.

Table I. Effect of Rare Earth Ions

Rare earth	Added as	Tolerable level, ppm: Europium method	Tolerable level, ppm: Terbium method
Ce	$(NH_4)_2Ce(NO_3)_4$	1	1
Dy	$DyCl_3$	1	0.5
Er	$ErCl_3$	0.1	0.5
Eu	Eu_2O_3	...	1
Gd	$GdCl_3$	0.1	1
Ho	$HoCl_3$	0.1	1
La	$LaCl_3$	1	1
Nd	$NdCl_3$	1	1
Pr	$PrCl_3$	0.06	1
Sm	$SmCl_3$	0.06	1
Tb	$TbCl_3$	0.1	...
Tm	$TmCl_3$	1	1
Yb	$YbCl_3$	1	0.5

EUROPIUM METHOD

Procedure. Pipet an aliquot containing between 50 and 4000 ng of europium into a 50-ml volumetric flask. Neutralize the solution before the addition of chelating agent. If there is any deviation from neutrality at the time the chelating agent is added, the fluorescence intensity is reduced to that of the ethanol blank. Add 0.2 ml of the 1% chelating agent solution to the flask. This results in a final chelating agent concentration which gives the calibration curve the largest linear range.

Allow the solution to stand at room temperature for 10 minutes prior to dilution with 95% ethanol and 30 minutes after dilution to obtain maximum fluorescence intensity.

(1) E. C. Stanley, B. I. Kinneberger, and L. P. Varga, ANAL. CHEM., **38**, 1362 (1966).
(2) D. L. Ross and J. Blanc, *Advan. Chem. Ser.*, **71**, American Chemical Society, Washington, D. C., 1967, Chap. 12.

Table II. Effect of Foreign Ions

Ion	Added as	Tolerable level, ppm: Europium method	Tolerable level, ppm: Terbium method
NO_3^-	$NaNO_3$	1	1
NO_3^-	KNO_3	1	1
I^-	KI	1	1
Cr^{3+}	$Cr(NO_3)_3$	1	1
Al^{3+}	$AlCl_3$	1	1
Ba^{2+}	$Ba(Ac)_2$	1	...
Na^+	$NaNO_3$	1	...
K^+	KI	1	...
Pb^{2+}	$Pb(Ac)_2$	1	0.25
Hg^{2+}	$HgCl_2$	0.5	...
Fe^{3+}	$FeCl_3$	0.3	0.25
SiO_3^{2-}	Na_2SiO_3	0.3	...
CNS^-	KCNS	0.2	0.1
Mn^{2+}	$MnCl_2$	0.2	...
Br^-	KBr	0.1	0.5
Co^{2+}	$Co(NO_3)_2$	0.1	0.1
Cu^{2+}	$Cu(NO_3)_2$	0.1	1
Ni^{2+}	$Ni(NO_3)_2$	0.1	0.1
Y^{3+}	$Y(NO_3)_3$	0.1	...
SO_4^{2-}	Na_2SO_4	0.06	...
S^{2-}	Na_2S	0.06	...
F^-	NaF	0.00	...

Chelates prepared in 95% ethanol gave more intense fluorescence than those in methanol, acetone, water, and EtOH–H_2O mixtures less than 95% in ethanol. No significant increase in sensitivity resulted from using 100% ethanol. Measure the fluorescence intensity at 614 nm, with the excitation monochromator at 312 nm and a 430-nm cutoff filter in the emission path.

TERBIUM METHOD

Procedure. Similar variable studies were performed on the terbium chelate system as on the europium. The resulting procedure for Tb differs only slightly from that for Eu. The Tb chelate forms more readily and stabilizes more rapidly so the solution need stand only 5 minutes prior to dilution and may be read immediately thereafter. The Tb chelate solutions are read at emission wavelength of 544 nm and excitation wavelength of 312 nm.

DISCUSSION AND CONCLUSIONS

The 1,1,1,5,5,5-hexafluoro-2,4-pentanedione chelates of europium and terbium show intense fluorescence at wavelengths characteristic of the particular ion. This fluorescence, when used as the basis for the selective analysis of nanogram quantities of Eu and Tb, produces a more sensitive method than any previously reported for a trifluoro-β-diketone.

Calibration curves for both ions were prepared according to the methods outlined. Both methods have a sensitivity of 1 ppb. The europium calibration curve is linear between 1 and 50 ppb and is analytically useful to 80 ppb.

The foreign ions considered are listed in Tables I and II. The interferences of these ions were considered tolerable at the concentration level given if their presence altered the fluorescence intensity of a 4-ppb solution of Eu(Tb) by less than 6%. The data reported in Table I indicate that Eu and Tb can be selectively determined in the presence of large excesses (at least 15-fold) of other rare earth ions without separation procedure.

RECEIVED for review August 5, 1970. Accepted October 12, 1970.

Spectrophotometric Determination of Sulfide Ion with Organic Disulfides

Ray E. Humphrey, Willie Hinze, and William M. Jenkines III

Department of Chemistry, Sam Houston State University, Huntsville, Texas 77340

FEW SPECTROPHOTOMETRIC METHODS have been reported for the determination of hydrogen sulfide or sulfide ion. The procedure which appears to be the most widely used for this analysis involves the reaction of hydrogen sulfide with *p*-amino-*N*,*N*-dimethylaniline in the presence of ferric chloride to form methylene blue (*1*). This method is quite sensitive, the product having a molar absorptivity of about 35,000. In order to measure hydrogen sulfide in the parts per billion range, an indirect fluorescence method involving fluorescein mercuric acetate has been used (*2*).

The reaction of organic disulfides with sulfide ion was reported by Otto and Rössing (*3*). The following equation for this interaction was given:

$$RSSR + 2K_2S \rightarrow 2RSK + K_2S_2 \quad (1)$$

This reaction has apparently not been studied very extensively. We have found that a number of water-soluble organic disulfides, 2,2′-dithiodipyridine (2-PDS), 4,4′-dithiodipyridine (4-PDS), 2,2′-dithiodipyrimidine (2-PyDS), and 5,5′-dithiobis(2-nitrobenzoic acid) (DTNB), react with sulfide ion rapidly at room temperature to produce the thiol anion and elemental sulfur. This reaction is represented by the following equation:

$$RSSR + S^{-2} \rightarrow 2RS^- + S^0$$

This interaction has been found to be useful for the spectrophotometric determination of sulfide in the very low microgram per milliliter range. The disulfides DTNB, "Ellman's reagent," (*4*), 2-PDS and 4-PDS (*5*), and 2-PyDS (*6*) are used

(1) G. D. Patterson in "Colorimetric Determination of Non-Metals," D. F. Boltz, Ed., Interscience, New York, N. Y., 1958, pp 273–277.
(2) H. D. Axelrod, J. H. Cary, J. E. Bonelli, and J. P. Lodge, Jr., ANAL. CHEM., 41, 1856 (1969).
(3) R. Otto and A. Rössing, *Chem. Ber.*, 19, 3129 (1886).
(4) G. L. Ellman, *Arch. Biochem. Biophys.*, 82, 70 (1959).
(5) D. R. Grassetti and J. F. Murray, Jr., *Ibid.*, 119, 41 (1967).
(6) D. R. Grassetti and J. F. Murray, Jr., *Anal. Chim. Acta*, 46, 139 (1969).

Table I. Spectral Data for Thiol Anions

Disulfide	λ_{max} Thiol anion, nm[a]	Molar absorptivity[b]
2-PDS	340	7,000 (7060)
4-PDS	324	21,500 (19,800)
2-PyDS	275	16,000 (16,000)
DTNB	412	15,500 (13,600)

[a] The λ_{max} for the anion of 4-PDS shifts to 285 nm at pH 9 with a shoulder appearing at 324 nm. The λ_{max} for the 2-PyDS anion is at 268 nm at pH 9 and at 278 nm in distilled water.

[b] Literature values in parenthesis, reference (*5*) for 2-PDS, reference (*6*) for 2-PyDS, and reference (*8*) for DTNB.

for the spectrophotometric determination of sulfhydryl groups. Sulfite ion has also been determined with 4-PDS and DTNB (*7*).

EXPERIMENTAL

Apparatus. Absorption measurements were made with a Beckman DB-G spectrophotometer and spectra recorded using a Beckman DK-2A instrument. Polarograms were recorded with a Sargent Model XVI Polarograph.

Reagents. The disulfides 2-PDS, 4-PDS, and DTNB were obtained from Aldrich Chemical Co., Milwaukee, Wis., and were used without further purification. The disulfide 2-PyDS was obtained by iodine oxidation of 2-mercaptopyrimidine, also obtained from Aldrich. Stock solutions of the disulfides, approximately 0.001*M*, were generally made up in 95% ethanol. These solutions appeared to be quite stable. Stock solutions of sulfide ion, also about 0.001*M*, were prepared from $Na_2S \cdot 9H_2O$ by weighing crystals which had been washed with distilled water, dried, and dissolved in distilled water or a 0.001*M* solution of disodium ethylenediamine tetraacetate (EDTA) using a volumetric flask. The compound $Na_2S \cdot 9H_2O$ has been found to be a good working standard (*2*). We found that the concentrations as determined by an iodate–iodide procedure with a thiosulfate titration were essentially the same as those calculated from the weight and volume.

Buffer solutions were prepared from 0.025*M* Na_2HPO_4 and KH_2PO_4, pH 6.86, 0.01*M* $Na_2B_4O_7$, pH 9.18, and 0.05*M* $KHC_8H_4O_4$, pH 4.01. All other chemicals used were the best available reagent grade.

Procedure. Solutions were prepared by measuring the required volumes of the stock solutions of sulfide ion or disulfide by pipet and diluting to the final volume with a buffer solution or distilled water. For establishing or using a Beer's law plot, the disulfide was present in excess. All reactions were run at room temperature.

RESULTS AND DISCUSSION

Spectra. Spectral data for the disulfides and the corresponding thiol anions are presented in Table I. Spectra have been published for 2-PDS (*5*), 4-PDS (*5*, *7*), and DTNB (*7*, *8*). The oxidation product of sulfide ion, elemental sulfur, does not contribute to the absorption at the wavelength maximum for any of the thiol anions. The spectrum of every reaction solution using excess sulfide ion was essentially that of the respective thiol anion. The only disulfide which absorbs significantly at the wavelength maximum for the corresponding thiol anion at every pH used is 2-PyDS. It is desirable to make a correction for unreacted disulfide when using this compound. The wavelength maxima for all the thiol anions, except 4-thiopyridone, are not affected significantly by a change in pH. The compound 4-PDS is not as useful at pH 9, as the maximum for the thiol anion is shifted to shorter wavelengths and the interference of the disulfide is quite large. A shoulder at 324 nm can be used with a considerable decrease in sensitivity.

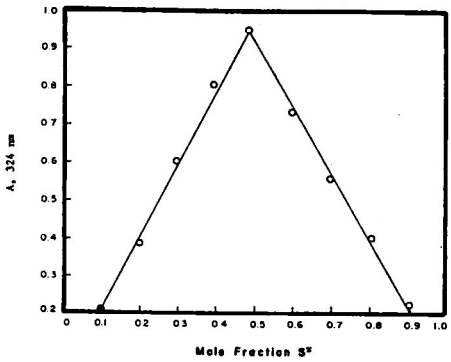


Figure 1. Continuous variations plot for the reaction of 4,4′-dithiodipyridine with sulfide ion

Stoichiometry. Mole ratio and continuous variations plots for the reaction of sulfide ion with these disulfides indicate that the stoichiometry in every case is 1:1 as shown in Equation 2. A continuous variations plot for the reaction of sulfide ion with 4-PDS is shown in Figure 1. There was little curvature in any of these plots indicating that the reactions were essentially complete when equimolar amounts of sulfide and disulfide were present. The reactions were quite fast and appeared to be practically complete within 5 minutes, and probably less, after adding the sulfide solution.

Polarography of Reaction Solutions. These disulfides all show a reduction wave at the dropping mercury electrode with a half-wave potential, $E_{1/2}$, in the region of −0.4 to −0.5 volts *vs.* the saturated calomel electrode (SCE). Sulfide ion shows an oxidation wave with $E_{1/2}$ of about −0.6 volt *vs.* SCE while elemental sulfur shows a reduction wave in the same region. These potential values are for solutions of pH 5 or slightly higher. Polarograms of reaction solutions with approximately equimolar reactants showed the loss or decrease of the reduction current for the disulfide group and the appearance of the reduction wave for elemental sulfur, characterized by a very steep slope. Oxidation current was also present at the less negative potentials due to any unreacted sulfide ion and the thiol anion produced by the reaction. Polarography confirmed that elemental sulfur is the oxidation product of sulfide ion and that the reaction is close to completion at 1:1 reactant ratios in many instances.

Effect of pH on the Reaction. Sulfide ion reacts readily with 2-PDS, 4-PDS, and 2-PyDS in distilled water and in buffers of pH 4, 7, and 9. The compound DTNB does not react in water or a pH 4 buffer but does react readily at pH 7 or 9. At pH values higher than 10, the disulfides are converted to the thiol anion, presumably by reaction with hydroxide ion (*9*).

(7) R. E. Humphrey, M. H. Ward, and W. Hinze, ANAL. CHEM., 42 698 (1970).

(8) G. L. Ellman, *Arch. Biochem. Biophys.*, 74, 443 (1958).

(9) A. J. Parker and N. Kharasch, *Chem. Rev.*, 59, 608 (1959).

Table II. Beer's Law Data for Sulfide Ion Determination

Sulfide, μg/ml	2-PDS		4-PDS		2-PyDS		DTNB	
	A 340 nm	ε[a]	A 324 nm	ε	A 275 nm	ε	A 412 nm	ε
0.23			0.29	39,000	0.20	26,000	0.19	25,500
0.46	0.17	11,500	0.56	38,000	0.38	25,500		
0.92	0.32	11,000	1.15	39,000	0.76	25,500	0.78	26,500
1.38	0.51	11,500			1.12	25,000	1.15	26,000
1.84	0.67	11,300					1.50	25,500

[a] These values are for a pH 7 buffer and are based on the molar concentration of sulfide ion.

Table III. Recovery of Sulfide from Synthetic Samples at pH 7

Sulfide present, μg/ml	Sulfide found, μg/ml	
	DTNB	4-PDS
0.32	0.35	0.31
0.44	0.44	0.43
0.57	0.55	0.56
0.70	0.72	0.68
0.83	0.84	0.82

Sensitivity. Molar absorptivity values for the determination of sulfide ion are listed in Table II. These values are based on the concentration of sulfide and confirm that two thiol anions are formed for every sulfide ion since the molar absorptivity values are quite close to twice that of the thiol anions. The molar absorptivity value using 4-PDS is somewhat higher than the methylene blue procedure while with the other disulfides the value is lower. Beer's law is followed in every case. The molar absorptivities do not vary appreciably at the different pH values. These compounds should be useful for the determination of sulfide ion over the range of approximately 0.05 to 2.0 μg/ml, the exact range depending on the disulfide used. Recovery of sulfide from synthetic samples is reasonably good, as shown in Table III.

Stability of Solutions. Disulfide solutions in 95% ethanol appear to be stable indefinitely. Solutions of DTNB are also quite stable in a pH 7 buffer. Solutions of sulfide ion in distilled water oxidize quite rapidly. A 0.001*M* solution of sulfide in distilled water was oxidized about 25% in 4 hours and 50% in 24 hours. Very dilute solutions, about 10^{-7} *M*, of Na_2S were reported to be oxidized to the extent of 3% in 6 hours when made up in 0.1*N* NaOH (*2*). We also found that sulfide solutions in 0.1*N* NaOH were reasonably stable, suffering less than 10% loss in 24 hours. However, sulfide solutions in NaOH were not used in most of this work to avoid adding hydroxide ion to the reaction solutions. In this work EDTA was found to stabilize the sulfide solutions considerably, the results being similar to those for sulfite solutions (*7*). Sulfide solutions which were 0.001*M* in EDTA were approximately 5% oxidized after 4 hours and slightly less than 15% after 24 hours. The extent of loss of sulfide had not increased appreciably from this after 10 days.

The thiol anions produced in the reaction are reasonably stable (*7*). There was little decrease in absorbance of these solutions on standing for 2–3 hours. Absorbance readings could probably be made anytime from 5 minutes to several hours after mixing the solutions and still give approximately the same result.

Interferences. These disulfides have been found to react with sulfite ion (*7*) and cyanide ion (*10*) and are useful for the determination of low concentrations of these substances. These ions could interfere in the analysis for sulfide ion. However, it seems likely that these interferences could possibly be avoided by choice of disulfide and pH to be used. Cyanide reacts very slowly at pH 8 or below unless present in much higher concentration than the disulfide. Sulfite will not react at pH 4 or below so that it might be possible to determine sulfide in the presence of sulfite using unbuffered solutions and either 2-PDS, 4-PDS, or 2-PyDS. These disulfides will also react with base at high pH values so that such solutions must be avoided.

Obviously any metal ion which will precipitate sulfide will be a serious interference. Determinations of sulfide at a level of 0.32 μg/ml were attempted using 4-PDS and having a metal ion, Cd(II), Cu(II), Fe(II), Hg(II), Ni(II), Pb(II), or Zn(II), present at 20 μg/ml. All of these ions interfered when no buffer was used for the reaction. Having EDTA present at 0.001*M* prevented the interference of Cd(II), Zn(II), Pb(II), and Ni(II) under these conditions. At pH 7, Cd(II), Cu(II), Hg(II), and Zn(II) interfered, while at pH 4, Fe(II), Hg(II), and Cu(II) showed interference. The presence of EDTA had no effect on the interferences in the buffer systems. In sulfide determinations using DTNB, all of the metal ions except Fe(II), Ni(II), and Pb(II) interfered. Results were the same at both pH 7 and 9 and with or without EDTA in the solution.

RECEIVED for review August 31, 1970. Accepted October 14, 1970. The authors express their appreciation to the Robert A. Welch Foundation of Houston, Texas for support of this research.

(10) R. E. Humphrey and W. Hinze, *Talanta*, in press.

Determination of Nitrite by Controlled-Potential Coulometry

J. E. Harrar

Chemistry Department, Lawrence Radiation Laboratory, University of California, Livermore, Calif. 94550

CLASSICAL TITRIMETRIC PROCEDURES for the determination of nitrite in acid solution are complicated by the instability and volatility of nitrous acid and its low rate of reaction with many titrants (*1*). For example, the recommended procedure for assaying reagent grade nitrite salts (*2*) is an indirect titration using both permanganate and ferrous ion standard solutions. Reported amperometric methods (*3*, *4*) are also subject to losses of nitrite in acid solution; however, they may be preferable for low concentrations. Constant-current coulometry eliminates the need for standard titrants, but two procedures that have been developed (*5*, *6*) require dual-intermediate back titrations and rather complex techniques.

This note describes a simple, accurate method in which nitrite is determined by coulometry at controlled potential. Nitrite is oxidized directly to nitrate at a platinum electrode in pH 4.7 acetate buffer solution. Possible loss of nitrous acid is not a factor in the analysis, and the reproducibility of the platinum electrode surface has a minor effect on the analytical results.

EXPERIMENTAL

Apparatus. The details of the construction and operation of the platinum-electrode electrolysis cell assembly are available elsewhere (*7*). The controlled-potential coulometer system (*8*) and the technique of predictive coulometry (*9*) have also been described. The predicted analytical results and the electrolytic rate constant data were both obtained by means of the analog predictor system.

Reagents. All chemicals were reagent grade or equivalent purity. Standard solutions of nitrite were prepared from a dried sample of J. T. Baker $NaNO_2$ sticks, which was assayed to American Chemical Society specifications (*2*). The $KMnO_4$ titrant was standardized against NBS $Na_2C_2O_4$. The $NaNO_2$ salt assayed 100.07%, with a combined estimate of 0.14% for the relative standard deviation [from the $KMnO_4$ solution standardization, the Fe(II) solution standardization, and the NO_2^- titration]. All volumetric glassware was calibrated or certified. Micropipets were used to take aliquots of the nitrite standard solutions for coulometric analysis.

Procedure. ELECTRODE PRETREATMENT. When the platinum working electrode is used for the first time, contamination is suspected, or the electrode has been anodized above +1.4 V *vs.* SCE, pretreat as follows. Immerse the electrode in boiling concentrated HCl; after 5 min, rinse with water, and place it in the coulometric cell assembly. Subsequent treatment with HCl is needed only when loss of electrolysis speed or high background currents appear.

With the 1*M* sodium acetate–1*M* acetic acid supporting electrolyte in the cell, polarize the working electrode at +1.10 V *vs.* SCE for 5 min. Replace the cell solution with a fresh portion of the supporting electrolyte and polarize the electrode at +0.95 V *vs.* SCE for 5 min. The background current should be less than 10 μA. If the electrode is not used for several hours, repeat the polarizations at +1.10 and +0.95 V before carrying out a determination.

COULOMETRIC ANALYSIS. Place sufficient 1*M* sodium acetate–1*M* acetic acid supporting electrolyte in the cell and in the two salt-bridge tubes. With stirring, pipet an aliquot of sample solution containing not more than 4 mg of nitrite into the cell. Electrolyze the solution at +0.95 *vs.* SCE and measure the integrator readout voltage when the current has decreased to 5–25 μA. The initial current should be 25–40 mA/mg NO_2^-.

Determine the background correction by electrolyzing the supporting electrolyte alone for the same length of time as required for the nitrite sample. This correction should not exceed the equivalent of 0.003 mg of nitrite for a 22-min electrolysis.

For a determination by predictive coulometry, first carry out a complete electrolysis to ascertain the time at which prediction accuracy is satisfactory. Correct the results for the background consisting of the accumulated charge at the time of prediction and the quantity $2i_b/k$ (*9*), where i_b is the constant background current and k is the electrolytic rate constant. The k value can be estimated with sufficient accuracy from the time of a complete electrolysis ($k = 6.9/t_{0.99\%}$), or it can be determined directly (*9*). The sum of the accumulated background charge ($i_b t$) and $2\,i_b/k$ should not exceed the equivalent of 0.003 mg of nitrite.

RESULTS AND DISCUSSION

Characteristics of Electrolysis of Nitrite. The results of recent voltammetric studies of the anodic oxidation of nitrite and nitrous acid in various media (*10*, *11*) have suggested that this reaction might form the basis of a controlled-potential coulometric method. Accordingly, the optimum conditions for the determination were sought, and the data shown in Figures 1 and 2 summarize these experiments.

At low pH, the error in the analysis (Figure 1) increases with the amount of time the nitrite solution is left in the cell before electrolysis is initiated. Thus, the negative bias is probably caused by the decomposition of nitrous acid. At the recommended pH of 4.7, no such loss could be detected for a period of 1 hour. Standard solutions of $NaNO_2$ in water, containing approximately 1 mg NO_2^-/ml, were also quite stable and remained within 0.1% titer for six weeks.

The maximum rate of electrolysis within each usable applied potential range decreased as the pH of the solution was raised. No electrolysis of nitrite was detected in 0.1*M* NaOH.

Confirming the reported voltammetric behavior (*10*, *11*), the oxidation of nitrite to nitrate was observed to be totally irreversible and the electrolysis rate to be strongly influenced by the extent of oxidation of the platinum electrode surface. As

(1) A. J. Clear and M. Roth, in "Treatise on Analytical Chemistry," Part II, Vol. 5, I. M. Kolthoff and P. J. Elving, Ed., Interscience, New York, N. Y., 1961, pp 276–278.
(2) "Reagent Chemicals," 4th ed., American Chemical Society Publications, Washington, D. C., 1968, pp 469, 548.
(3) J. T. Stock and R. G. Bjork, *Microchem. J.*, 6, 219 (1962).
(4) J. T. Stock and R. G. Bjork, *Talanta*, 11, 315 (1964).
(5) R. P. Buck and T. J. Crowe, ANAL. CHEM., 35, 697 (1963).
(6) R. Magno and M. Fiorani, *Ric. Sci.*, 38, 119 (1968).
(7) J. E. Harrar, *AEC Rep.*, *UCRL-50417*, Livermore, Calif., March 1968.
(8) J. E. Harrar and E. Behrin, ANAL. CHEM., 39, 1230 (1967).
(9) F. B. Stephens, F. Jakob, L. P. Rigdon, and J. E. Harrar, *ibid.*, 42, 764 (1970).
(10) E. Julien and M. Comtat, *Rev. Chim. Miner.*, 6, 885 (1969).
(11) G. Schmid and M. A. Lobeck, *Ber. Bunsenges. Phys. Chem.*, 73, 189 (1969).

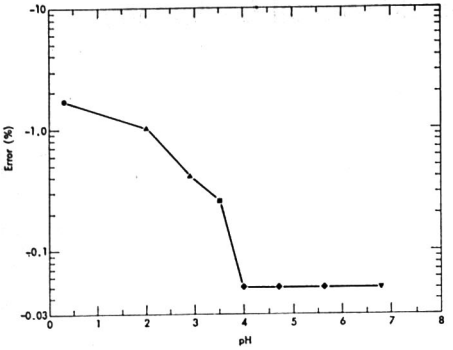


Figure 1. Error in controlled-potential coulometric determination of nitrite as a function of pH of supporting electrolyte. 1 mg of NO_2^- taken

- ● 0.5*M* H_2SO_4, E = +1.00 V *vs.* SCE
- ▲ 0.5*M* Na_2SO_4 + H_2SO_4, E = +0.95 V
- ■ 0.1*M* $KHC_8H_4O_4$ + H_2SO_4, E = +0.95 V
- ◆ 2*M* acetate buffer, E = +0.95 V
- ▼ 0.25*M* KH_2PO_4–0.25*M* Na_2HPO_4, E = +0.90 V

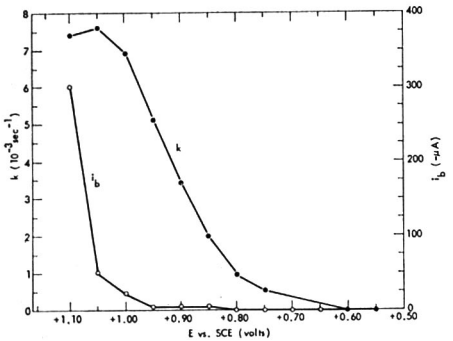


Figure 2. Electrolytic rate constant for oxidation of nitrite and background current in pH 4.7 acetate buffer supporting electrolyte

shown in Figure 2, this passivation phenomenon causes the electrolysis rate to reach a maximum and then decrease. This effect is even more pronounced in stirred solution voltammetry (*10*, *11*). The maximum rate of electrolysis is still slower, by at least a factor of three, than it would be if the process were controlled solely by mass transfer; thus, a complete electrolysis in the cell employed required 18–22 min at +0.95 V *vs.* SCE. The maximum rate of electrolysis is highest immediately after the pretreatment with boiling HCl; the electrode then ages in a few days to the condition represented in Figure 2.

The recommended pretreatment polarization of the electrode at +1.10 V *vs.* SCE rapidly stabilizes the background current at the analytical control potential of +0.95 V. However, if the electrode is polarized at still greater anodic potentials (*e.g.*, at +1.4 V), the electrode becomes even more passivated, and a complete electrolysis at +0.95 V requires 50–60 min. Measurements were also carried out with a pure gold working electrode, but no improvement in the rate of electrolysis was found. At corresponding applied potentials, the background current was lower with gold than with platinum, but the electrolysis rate peaked at the same value.

Table I. Analyses of Standard Solutions of Nitrite by Controlled-Potential Coulometry

1*M* HOAc–1*M* NaOAc supporting electrolyte, E = +0.95 V *vs.* SCE

Nitrite (mg)			Time of electrolysis min	Rel std dev %	Rel error %
Taken	Found	n			
4.017	4.016	8	23	0.03	−0.03
4.017	4.016[a]	5	11	0.05	−0.03
4.017	4.041[a]	5	8	0.14	+0.6
2.009	2.008	6	22	0.03	−0.05
2.009	2.009[a]	6	11	0.05	0.00
2.009	2.015[a]	6	8	0.07	+0.3
0.9474	0.9464	6	22	0.03	−0.11
0.4737	0.4729	6	22	0.03	−0.17
0.0882	0.0884	7	20	0.3	+0.2
0.0220	0.0219	5	17	0.8	−0.5
0.0220	0.0219[a]	5	4	0.7	−0.5

[a] Determination by predictive coulometry.

Because the oxidation of nitrite is totally irreversible, the background current at +0.95 V is low, and nitrite is stable in the recommended supporting electrolyte, the precision and accuracy of the analysis are not greatly dependent on the time of the electrolysis or the surface condition of the electrode. However, if desired, the time of electrolysis can be significantly shortened by predictive coulometry (*9*), since, for a given electrode condition and applied potential, the electrolytic rate parameter is relatively constant.

Analytical Accuracy and Precision. Table I illustrates the precision and accuracy obtained in analyzing standard nitrite solutions, by both conventional and predictive controlled-potential coulometry. The conditions of the determination and the low equivalent weight of NO_2^- allow extension of the procedure to fairly low levels with good results.

Interferences. Forty-five species were tested for their effect on the determination of nitrite, with the results summarized in Table II. Included are species commonly associated with nitrite, those reported to form complexes with nitrite (*12*), and those expected to be oxidized at +0.95 V *vs.* SCE. Among the untested substances which are known to be oxidized at this control potential are H_2O_2, Ir(III), Ru(III), Pu(III), and the lower oxidation states of osmium.

Most of the substances for which a level of interference was found were concomitantly oxidized with nitrite, and their contribution to the charge transferred was a simple additive function of the amount added. In addition, Mn(II), Sb(III), and SCN^- poisoned the working electrode—*i.e.*, not only was the rate of electrolysis of nitrite decreased considerably in the presence of these species, but subsequent electrolyses in their absence were also sluggish. The deposition of an insoluble material on the electrode is the probable cause of this behavior, since this is known to occur during the oxidation of Mn(II) (*13*) and Sb(III) (*14*). The recommended pretreatment with

(12) L. G. Sillen and A. E. Martell, "Stability Constants of Metal-Ion Complexes," 2nd ed., The Chemical Society, London, 1964, pp 164–166.
(13) C. O. Huber and L. Lemmert, ANAL. CHEM., **38**, 128 (1966).
(14) B. B. Baker and W. M. MacNevin, *J. Amer. Chem. Soc.*, **75**, 1473 (1953).

Table II. Tolerances of Diverse Substances in the Determination of Nitrite by Controlled-Potential Coulometry

1 mg NO_2^-, 1*M* HOAc–1*M* NaOAc supporting electrolyte, E = +0.95V *vs.* SCE

Substance	Added as	Amt to cause 0.3% rel error, mg	Substance	Added as	Amt to cause 0.3% rel error, mg
Cl^-	NaCl	>20	As(III)	$NaAsO_2$	0.005
Br^-	KBr	0.030	Au(III)	$HAuCl_4$	0.40
I^-	KI	0.002	Bi(III)	$Bi(NO_3)_3$	>1.0
NH_4^+	NH_4NO_3	>450	Cd(II)	$CdCl_2$	>1.5
N_2H_4	$N_2H_4 \cdot H_2SO_4$	0.010[a]	Ce(III)	$Ce(ClO_4)_3$	0.010
NH_2OH	$(NH_2OH)_2 \cdot H_2SO_4$	0.003[a]	Co(II)	$CoSO_4$	>1.0
N_3^-	NaN_3	0.004	Cr(III)	$Cr(ClO_4)_3$	0.002
NO_3^-	$NaNO_3$	>1500	Cu(II)	$CuSO_4$	>1.0
CN^-	NaCN	>0.5	Fe(II)	$Fe(NH_4)_2(SO_4)_2$	0.10[a]
SCN^-	NH_4SCN	0.001[b]	Fe(III)	$Fe(ClO_4)_3$	>10
OCN^-	KOCN	1.5	Hg(I)	$Hg_2(NO_3)_2$	0.025
Phthalate	$KHC_8H_4O_4$	>400	Hg(II)	$HgSO_4$	>1.5
$C_2O_4^{2-}$	$Na_2C_2O_4$	0.06	Mn(II)	$MnSO_4$	0.002[b]
CHO_2^-	$NaCHO_2$	0.75	Pb(II)	$Pb(OAc)_2$	>1.0[a]
ClO_4^-	$HClO_4$	>1200	Pd(II)	Na_2PdCl_4	0.007
PO_4^{3-}	Na_2HPO_4	>1000	Pt(II)	$PtCl_2$	0.020
PO_3^{3-}	Na_2HPO_3	>6	Pt(IV)	Na_2PtCl_6	>0.5
$H_2PO_2^-$	NaH_2PO_2	2.0	Rh(III)	$RhCl_3$	>0.5
SO_4^{2-}	Na_2SO_4	>1000	Sb(III)	$SbCl_3$	0.005[b]
SO_3^{2-}	Na_2SO_3	0.020[a]	Tl(I)	Tl_2SO_4	0.010
S^{2-}	$(NH_4)_2S$	0.010[a]	U(VI)	$UO_2(ClO_4)_2$	>5
SeO_3^{2-}	H_2SeO_3	>0.5	V(IV)	$VOSO_4$	0.005
Ag(I)	Ag_2SO_4	>10[c]			

[a] With preoxidation at +0.57V *vs.* SCE.
[b] Rate of electrolysis significantly decreased.
[c] Rate of electrolysis significantly increased.

hydrochloric acid was required to restore the working electrode to its normal condition.

With SO_3^{2-}, N_3^-, and Pt(II), which are oxidized at +0.95 V *vs.* SCE, and with $H_2PO_2^-$, Pd(II), and Au(III), which are not oxidized, a reaction with the nitrite was indicated by the appearance of a negative bias with increasing amounts of the interfering substance.

Several interferences were rapidly oxidized to a stable species at +0.57 V *vs.* SCE; thus, their tolerance levels may be raised by pre-electrolysis at this potential. However, most of these substances still cannot be tolerated at a very high level. Additional oxidation of the interference takes place at +0.95 V for hydroxylamine and sulfide, and there is evidence that both Fe(II) and hydrazine chemically reduce the platinum oxide film, increasing the background correction at +0.95 V. Iodide is quantitatively oxidized to I_2 at +0.57 V, but further to IO_3^- at +0.95 V; thus, little advantage is gained by preoxidation. Sulfite is oxidized to SO_4^{2-} at +0.57 V, but, because of its slow reaction with nitrite, moderate amounts still cause a significant bias.

A catalytic effect was observed when nitrite was oxidized in the presence of Pb(II) or Ag(I). No detectable oxidation of Pb(II) or Ag(I) occurred at +0.95 V *vs.* SCE, and no error was found in the determination at the interference levels indicated in Table II. However, the time for a complete electrolysis was reduced to 8 min, and, in the case of Pb(II), as with the poisoning effects noted above, the working electrode retained the catalytic activity. Thus, in certain circumstances it appears that it would even be desirable to include Pb(II) or Ag(I) in the supporting electrolyte for this determination.

Received for review September 14, 1970. Accepted October 29, 1970. Work performed under the auspices of the U. S. Atomic Energy Commission. Reference to a company or product name does not imply approval or recommendation of the product by the University of California or the U. S. Atomic Energy Commission to the exclusion of others that may be suitable.

Spectrophotometric Determination of Rhodium with Nitroso R.

Formula for the Rh(III)–Nitroso R Complex

Orville W. Rollins and Morris M. Oldham

Contribution from the Department of Chemistry, U. S. Naval Academy, Annapolis, Md. 21402

A CRITICAL EVALUATION of the known colorimetric methods for the determination of rhodium has been reported by Beamish (*1*). Subsequent to this review article, Nath and Agarwal (*2*) reported a spectrophotometric method for determination of this platinum metal employing nitroso R salt. We were unable to obtain satisfactory results in analyzing for rhodium by the aforementioned method. We have evaluated the method which was proposed by Nath and Agarwal and, after considerable modification of it, have developed a sensitive and useful colorimetric method for determination of rhodium using nitroso R salt.

EXPERIMENTAL

Apparatus. The absorption spectra shown in Figure 1 were obtained with a Carey Model 15 Spectrophotometer. All other absorbance measurements were made with a Beckman Model DU-2 Spectrophotometer.

A Sargent pH meter equipped with a combination electrode was used to measure pH.

Reagents. A standard rhodium(III) sulfate solution was obtained from Matthey Bishop, Inc., Malvern, Pa. It was prepared from sponge rhodium metal (99+% pure) and was certified to contain 69.04 ± 0.06 grams of the metal per liter of solution. The concentration of this solution was verified gravimetrically (to 2 ppt) by electrolytically depositing all of the Rh(III) from an aliquot onto a platinum gauze cathode. All solutions were prepared by appropriate dilutions of this standard rhodium sulfate solution.

The nitroso R salt which was used was obtained from K & K Laboratories, Inc. with a certified purity of 99% minimum. This was verified by potentiometric titration with standard NaOH solution. In a similar titration using a sample of Fisher Certified nitroso R salt, 80% of the calculated acidic hydrogen ions were titrated.

The following solutions were used to obtain the desired pH values: 33% sodium acetate, 6*M* acetic acid, 6*M* nitric acid, and dilute sodium hydroxide.

Deionized water was used throughout this study.

Absorbance Spectra. The absorbance spectra for solutions of the red Rh(III)–nitroso R complex and nitroso R itself are shown through a part of the visible region in Figure 1. The solution containing the complex was $6.039 \times 10^{-5} M$ with rhodium. Both solutions contained 5 ml of a nitroso R solution (0.500 g/100 ml), they were buffered at pH 5.5, then boiled for 70 minutes and cooled to room temperature before diluting to a final volume of 100 ml. The absorbance spectrum of the Rh(III)–nitroso R complex has not been reported heretofore.

Effect of pH. In order to determine the effect of pH on formation of the Rh(III)–nitroso R complex, solutions containing a fixed amount of Rh(III) and an excess of nitroso R were buffered at different pH values, boiled for 70 minutes, cooled, diluted to the same volume, and then their absorbance was measured. The results obtained at different wavelengths are shown in Figure 2.

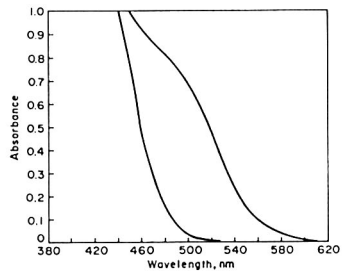


Figure 1. Absorption spectra of solutions at pH = 5.5

Upper curve. Rh(III)–nitroso R complex
Lower curve. Nitroso R blank

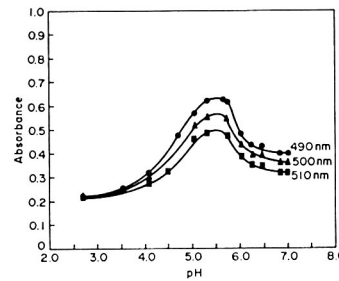


Figure 2. Effect of pH on formation of Rh(III)–nitroso R complex at wavelengths indicated

Effect of Heating. Solutions containing a fixed amount of Rh(III) and an excess of nitroso R were buffered at pH 5.5 and boiled for periods of 10, 30, 40, 50, 60, 70, and 80 minutes to determine the effect of heating on formation of the complex. Maximum absorbance was obtained (at 520 nm) after boiling for 60 minutes while approximately 75% of the color intensity was developed after boiling for 30 minutes. There was no appreciable formation of the colored complex at room temperature.

Determination of Formula for Rh(III)–Nitroso R Complex. The mole ratio method (*3*) was used to determine the formula for the Rh(III)–nitroso R complex. The final concentration of Rh(III) was $6.039 \times 10^{-5} M$ in each solution, they were buffered at pH 5.5, boiled for 70 minutes, cooled to room temperature, diluted to the same volume, and the absorbance was measured at 500 nm and 520 nm in 1-cm quartz cells with

(1) F. E. Beamish, *Talanta*, **12**, 789 (1965).
(2) S. Nath and R. P. Agarwal, *Chim. Anal. (Paris)*, **47** (5), 257 (1965).
(3) J. H. Yoe and A. L. Jones, IND. ENG. CHEM., ANAL. ED., **16**, 111 (1944).

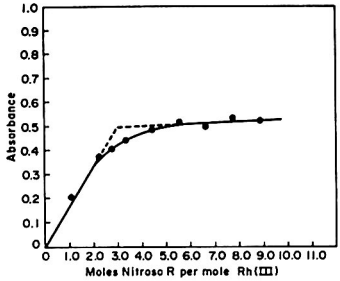


Figure 3. Determination of formula for the Rh(III)–nitroso R complex in solution at pH = 5.5

water as the reference. The results were the same at both wavelengths, and those obtained at 520 nm are displayed graphically as Figure 3, where it is clearly shown that the ratio of ligand to metal in this complex is 3 to 1.

Isolation of Sodium Salt of Rh(III)–Nitroso R Complex. Thirteen milliliters of a rhodium sulfate solution (0.389*M*, pH = 0.5) was pipetted into approximately 50 ml of a solution containing 7.34 grams of nitroso R (molar ratio of ligand to metal, 3.8 to 1.0), the pH was adjusted to 5.5 with sodium hydroxide and the resulting solution was boiled for 1 hour. This solution was then taken down to a volume of approximately 35 ml on a steam bath, and allowed to stand at room temperature whereupon red colored crystals of the product separated. These were recovered by suction filtration, washed with water followed by acetone, and air-dried. The product, $Na_6\{Rh[C_{10}H_4NO_2(SO_3)_2]_3\}\cdot Na_2SO_4\cdot 11.5\ H_2O$, weighed 3.3 grams.

Analysis of $Na_6\{Rh[C_{10}H_4NO_2(SO_3)_2]_3\}\cdot Na_2SO_4\cdot 11.5\ H_2O$. The sodium analysis was performed by flame photometry using a NIL Flame Photometer obtained from the National Instrument Laboratories, Inc. Rhodium was determined by the method being reported in this paper. Carbon, nitrogen, and sulfur were determined by Aldridge Associates & Co., Inc., Washington D. C. The dehydrations were carried out in an oven at 230 °C. *Anal.* Calcd. for $Na_6\{Rh[C_{10}H_4NO_2(SO_3)_2]_3\}\cdot Na_2SO_4\cdot 11.5\ H_2O$: Na, 11.64; Rh, 6.50; C, 22.8; N, 2.66; S, 14.2; H_2O, 13.1. Found: Na, 11.5$_4$, Rh, 6.4$_5$; C, 23.2; N, 3.12; S, 13.2; H_2O, 12.9.

Conformity to Beer's Law. Aliquots of exactly 2, 3, 4, 5, 6, and 7 ml were taken from a rhodium sulfate solution, $1.0064 \times 10^{-3}M$ with the metal, 5.0 ml of a nitroso R solution (0.500 gram per 100 ml) was added, and the solutions were buffered at pH 5.5 with NaAc and HAc. After boiling for 70 minutes, the solutions were cooled to room temperature, diluted to 100 ml, and their absorbance was measured against a blank of nitroso R which was prepared from 5 ml of that solution and which was treated in the same manner. Conformity to Beer's law is exhibited at wavelengths of 490 nm, 500 nm, and 520 nm through the concentration range $2.00 \times 10^{-5}M$ to $10.0 \times 10^{-5}M$—*i.e.*, 2.06 through 10.4 ppm of rhodium. The molar absorptivity for this complex at these wavelengths is 1.312×10^4, 1.175×10^4, and 8.350×10^3, respectively.

Effect of Foreign Ions. In order to determine the effect of various ions on this spectrophotometric method, solutions containing Rh(III) and the ion in question were treated exactly as described above. The final concentration of Rh(III) in all solutions was $4.026 \times 10^{-5}M$, the absorbance was measured at 520 nm against a nitroso R blank, also treated as described above. Boiling a solution of nitroso R at pH 5.5 for 70 minutes causes no change in its absorption spectrum in the region being studied (see Figure 1).

Table I. Effect of Foreign Ions

Foreign ion	Added as	Concentration, ppm
	No significant interference	
Ru(III)	$RuCl_3$	3.1
Os(VIII)	OsO_4	18.7
Pt(IV)	H_2PtCl_6	1.9
Ir(III)	$IrCl_3$	0.6
Y(III)	$Y(NO_3)_3$	16.5
Au(III)	$AuCl_3$	2.2
Ga(III)	$Ga(NO_3)_3$	6.0
Cd(II)	$CdSO_4$	14.0
Mn(II)	$MnCl_2$	6.5
Zn(II)	$Zn(NO_3)_2$	6.5
Mg(II)	$Mg(NO_3)_2$	4.9
In(III)	$In(NO_3)_3$	17.5
Zr(IV)	$Zr(SO_4)_2$	9.1
Cr(III)	$Cr(NO_3)_3$	6.0
MoO_4^{2-}	Na_2MoO_4	2.0
Al(III)	$Al(NO_3)_3$	27.0
Ce(IV)	$Ce(SO_4)_2$	5.8
Ce(III)	$Ce(NO_3)_3$	15.6
	Significant interference[a]	
Co(II)	$CoCl_2$	1.2
Cu(II)	$Cu(NO_3)_2$	1.2
Ce(IV)	$Ce(SO_4)_2$	11.5
Fe(III)	Fe(III) alum	1.0
WO_4^{2-}	Na_2WO_4	1.7
Ni(II)	$NiSO_4$	1.2
Au(III)	$AuCl_3$	11.0
Pd(II)	$Pd(NO_3)_2$	1.0
Ir(III)	$IrCl_3$	2.9

[a] The criterion for significant interference was an absorbance reading which varied more than 2.5% from the expected value.

Although the difference in absorbance between the Rh(III)–nitroso R complex and a blank is greater at 490 nm than it is at 520 nm, the absorbance readings were taken at 520 nm in order to take advantage of the very low absorbance of the blank (approximately 0.010 unit) as shown in Figure 1. The results of this study are summarized in Table I.

DISCUSSION

This spectrophotometric method for the determination of rhodium differs considerably from that proposed by Nath and Agarwal (*2*). First, we find that the Rh(III)–nitroso R complex is red and not blue as reported by those authors. Second, we find that the complex reaches its maximum absorbance in a narrow pH range (as shown in Figure 2) and is not stable and constant through the pH region 2.0 to 8.0 as reported. Third, we find that solutions containing rhodium(III) and nitroso R develop practically no color at room temperature and must be boiled for at least 1 hour to develop full color. Nath and Agarwal (*2*) have proposed that this platinum metal may be determined colorimetrically with nitroso R without heating the solutions, and they state that the color intensity of the complex is not modified from that developed at 25 °C by heating to 100 °C. This information was presented in table form where the colorimeter reading was shown to be the same for a solution heated to 25, 35, 40, 50, 60, 80, and 100 °C. Finally, those authors report that Beer's law is obeyed in the concentration interval of 1.03 to 41.2 ppm of rhodium, whereas we find that solutions of the complex show negative deviations from Beer's law above 10 ppm of rhodium.

The fact that solutions of Rh(III) containing nitroso R must be boiled for 1 hour in order for the reaction to go to

completion points to the extreme inertness of the hydrated Rh(III) ion. In fact, if these solutions were merely heated to 100 °C, and not boiled, there would be very little color development. This may be the reason for the fact that Nath and Agarwal did not observe the effect of continued boiling upon formation of the Rh(III)–nitroso R complex.

Nath and Agarwal used a Klett-Summerson colorimeter with filter number 54 (which transmits in the 520- to 580-nm region), so their study and ours were performed in essentially the same spectral region. Their source of rhodium(III) was its chloride (obtained from JM) which was assayed gravimetrically according to Scott (*4*).

Our solution studies show that the Rh(III)–nitroso R complex has a ligand to metal ratio of 3 to 1. This is depicted in Figure 3 where it is also evident that the complex dissociates appreciably at room temperature. The formula for the complex is also substantiated through the isolation and analysis of its sodium derivative. In a potentiometric titration of this derivative, we found no evidence for acidic hydrogen atoms which shows that the nitroso R is coordinating through the oxygen atoms of its naphthol group, a fact that is also supported by the sodium analysis. All of this evidence suggests that the nitroso R is functioning as a bidentate ligand in accord with the not unexpected coordination number of six for Rh(III). The amount of sodium sulfate which crystallized with the Rh(III) complex amounts to approximately a 10% "contamination" by weight in the final product.

The Rh(III)–nitroso R complex is so stable that solutions of it show no change in absorbance on standing for 24 hours.

(4) W. W. Scott, "Standard Methods of Chemical Analysis," D. Van Nostrand Co., New York, N. Y., 1964, Vol. I, p 746.

ACKNOWLEDGMENT

We thank Dr. Curtis D. Herron of Matthey Bishop, Inc. for the standard rhodium sulfate solution which was used in this research.

RECEIVED for review July 27, 1970. Accepted October 26, 1970. We are grateful to the United States Naval Academy Research Council for financial support for this work.

Determination of Polymeric Isocyanate in the Presence of Reactive Halides

Phillip M. Beazley

Marathon Oil Company, Denver Research Center, Littleton, Colo.

THE ISOCYANATE CONTENT of polymers derived from reactive halide intermediates (*1*) can not be determined by established amine titration procedures (*2–4*) because the residual halides react with the amines used. Kinetic studies showed that dicyclohexylamine reacts slowly with reactive halides and quickly with isocyanate. A titration technique using this amine was then developed.

Excess dicyclohexylamine is reacted with the isocyanate in dimethylformamide, DMF, for a prescribed time at room temperature. The excess amine is then titrated with HCl in isopropanol using bromcresol green indicator. Because the total amount of amine taken is known, the amine consumed by the sample is calculated by difference and is equivalent to the isocyanate content of the sample.

EXPERIMENTAL

Reagents. STANDARD 0.1*N* HCl. Dilute 9 ml of concentrated HCl to 1 liter with reagent grade isopropanol. Standardize this solution with tris-hydroxymethyl aminomethane using methyl red indicator.

DICYCLOHEXYLAMINE. Dilute 50 ml of dicyclohexylamine, Eastman White Label 4627, to 1 liter with dry DMF (*5*).

(1) P. A. Argabright, V. L. Sinkey, and B. L. Phillips, U. S. Patent 3,458,448 (1969).
(2) Sidney Siggia, "Quantitative Organic Analysis via Functional Groups," 3rd ed., John Wiley and Sons, New York, N. Y., 1963, p 558.
(3) R. Venkataraghavan and C. N. R. Rao, *Chemist–Analyst*, **51**, 49 (1962).
(4) Joe A. Vinson, ANAL. CHEM., **41**, 1661 (1969).
(5) E. Lieber, C. N. R. Rao, and T. S. Chao, *ibid.*, **29**, 932 (1957).

BROMCRESOL GREEN INDICATOR. Slurry 100 mg bromcresol green, Matheson, Coleman and Bell, Inc., with 1.5 ml of 1*N* NaOH and dilute to 100 ml with distilled water after all the indicator has dissolved in the hydroxide.

Procedure. Dissolve the sample containing about 1 mequiv of isocyanate in 5 ml of dry dimethylformamide. Pipet 10 ml of amine solution into the sample and after 2 minutes, add 40 ml of isopropanol and 8 drops of indicator. Titrate the unreacted amine with 0.1*N* HCl until the indicator remains yellow for at least 15 seconds. Run a blank to determine the total amount of amine taken and calculate the equivalent isocyanate content of the sample by subtracting the amount of unreacted amine from the total amount of amine taken.

RESULTS AND DISCUSSION

The reaction rates of benzyl bromide and *o*-tolylisocyanate with piperidine, dibutylamine, dicyclohexylamine, and diisopropylamine were compared. Equal portions of benzyl bromide in DMF were added to equal amounts of amine in DMF at room temperature. After 5 minutes, the reactions were quenched and the unreacted amines were titrated with HCl. The following results were obtained.

Amine	% Benzyl bromine reacted
Piperidine	96
Dibutylamine	84
Diisopropylamine	10
Dicyclohexylamine	6

In the same way, the reactions of *o*-tolylisocyanate with piperidine and dicyclohexylamine were compared.

Amine	% Isocyanate reacted
Piperidine	97.7
Dicyclohexylamine	97.0

A mixture of 61.9 mole % *o*-tolylisocyanate and 38.1 mole per cent benzyl bromide was next reacted with the same amines in the same way for various times. Both piperidine and dibutylamine reacted readily with the benzyl bromide but dicyclohexylamine reacted with very little of the bromide.

	Mole % mixture reacted		
Time, min	Piperidine	Dibutylamine	Dicyclohexyl-amine
1	94.4	68.7	60.6
2	95.4	71.3	61.4
4	98.1	79.1	62.2

A sample of polyisocyanate product (*I*) which contained 0.40% Cl and 0.47% Br (probably in the form of metal halides and benzylic halides) was reacted with dicyclohexylamine for various times.

Time, min	Mequiv/gram RNCO
1	5.88
2	6.05
4	6.04

From these data, it is evident that 2 minutes was sufficient time for dicyclohexylamine to react with all the isocyanate in the sample and yet not with a significant amount of benzylic halides.

To further test the applicability of dicyclohexylamine, the same product sample was spiked with 1.53 mequiv/gram of benzyl bromide, which represents the most reactive halide the product contains, and reacted with the amine for 2 minutes. The determined isocyanate content was 6.07 mequiv/gram. The error caused by this large amount of benzyl bromide was only 0.3%. Since the determined standard deviation of the method is 0.2%, the error caused by the bromide is nearly insignificant.

Two products containing different quantities of chlorine and bromine were analyzed using piperidine and dicyclohexylamine. Product A contained 0.33 mequiv/gram Br and no Cl. Product B contained 0.06 mequiv/gram Br and 0.11 mequiv/gram Cl based upon elemental analyses.

Amine	Mequiv/gram RNCO	
	A	B
Piperidine	6.20	5.66
Dicyclohexylamine	5.90	5.45

In each case, the result with piperidine was higher than the result with dicyclohexylamine by an amount nearly equal to the halide content of the products.

Product	Br + Cl, mequiv/gram	Piperidine–dicyclohexylamine, mequiv/gram
A	0.33	0.30
B	0.17	0.21

Finally, several isocyanates of diverse reactivity were assayed as received from Aldrich Chemical Co. using this procedure with piperidine and dicyclohexylamine.

	Isocyanate found, %	
Compound	Piperidine	Dicyclohexyl-amine
2,4-Toluene diisocyanate	99.7	99.4
Phenyl isocyanate	99.2	98.9
Allyl isocyanate	97.0	97.2
n-Butylisocyanate	98.2	87.4
Cyclohexyl isocyanate	96.3	91.2

It is evident that only cyclohexyl isocyanate and *n*-butylisocyanate did not react completely with dicyclohexylamine within the 2 minutes allowed. This method is, then, applicable to isocyanate–halide mixtures providing that the halides are no more reactive than benzyl bromide and the isocyanates are at least as reactive as allylisocyanate.

ACKNOWLEDGMENT

The author is grateful for the samples supplied by B. Phillips, and the helpful discussions with P. A. Argabright.

RECEIVED for review July 30, 1970. Accepted October 27, 1970.

Evaluation of Methods for Determination of Metallic Iron in Reduced Iron Ores

S. C. Blum and T. D. Searl

Esso Research and Engineering Company, Linden, N. J. 07036

IRON IS BEING PRODUCED in substantial quantities by the direct reduction of iron ores. The reduced ores contain gangue and iron oxides in addition to metallic iron. An accurate method for the determination of metallic iron in the reduced product is required for research and commercial purposes. Some procedures have been available in the past, and several have appeared recently. When these were used with reduced ores, conflicting results were obtained. Absence of a National Bureau of Standards' standard or similar standard of reduced iron ore necessitated the development of a technique for the evaluation of these methods. To do this, a series of iron ores in various stages of reduction were analyzed for all elements. In particular, the analysis for oxygen was considered to be essential. The availability of neutron activation equipment afforded the opportunity to measure oxygen. These analyses and the values for metallic iron and iron oxides obtained by the metallic iron method being evaluated were used to obtain a material and an oxygen balance.

Three basic analytical techniques for metallic iron with modifications of each were evaluated. The first (*1*) employed mercury(II) chloride. A variation of this is used as a standard by the Metal Powder Industry Federation (MPIF) (*2*). The second (*3*), which uses silver thiocyanate, has been employed by the Institute De Recherches De La Siderurgie (IRSID) in France. A modification (*4*) tested by the association of German Foundrymen (VDEh) was also studied. Finally, a bromine–methanol reagent with (*5*) and without (*6*) reflux was studied. The latter modification was rejected, as it was not applicable to reduced iron ores. A similar method (*7*) using a bromine–ethanol solution was not evaluated.

EXPERIMENTAL

Reference Samples. Large quantities of five reduced iron ores ranging from 90 to 30% in metallic iron content were ground to pass 100 mesh and were homogenized. Each sample had been reduced independently in a pilot plant; none were prepared by blending other samples. Complete chemical analyses were performed by four laboratories, in duplicate, for total iron, phosphorus, sulfur, carbon, and the gangue elements. Total oxygen content was determined by neutron activation at two laboratories and the average value was used.

Evaluation Technique. Reduced iron ores are composed of gangue, metallic iron, and iron(II, III) oxides. In evaluating a metallic iron procedure, material balances and oxygen balances are obtained on the series of reduced ores, by summing up the gangue values, calculated as the compounds, with the values obtained for metallic iron and the iron oxides by the procedure being studied. If a reagent did not dissolve all of the metallic iron, the remainder would be determined as iron oxides. The material balance in this case would total greater than 100%, and the oxygen calculated from the oxides would be greater than that determined by neutron activation. Conversely, if iron oxides were dissolved by a reagent and erroneously determined as metallic iron, the material balance would be less than 100%, and the calculated oxygen would be less than that determined by neutron activation.

Table I. Composition of Reduced Iron Ores

Sample	Total iron, %	Total gangue, %
2	93.7	5.4
4	91.6	4.7
5	87.5	7.4
6	88.6	4.6
7	78.7	5.1

Analytical Method. For the modified bromine–methanol procedure, 0.5 gram of the reduced ore was refluxed for 15 and 60 minutes with 100 ml of a solution of 5% bromine in methanol. The resultant iron bromide was separated from the insoluble iron oxides by filtration. The oxides were dissolved by refluxing with hydrochloric acid in a nitrogen atmosphere. Iron(II) was determined on one aliquot by direct titration with dichromate. Iron(II) and (III) was determined on a separate aliquot by reduction of Iron(III) with stannous chloride, followed by titration with dichromate. Bromine and methanol were removed by evaporating the filtrate to a low volume. Traces of organic matter were then destroyed by wet oxidation with nitric and sulfuric acid.

CAUTION: *Complete removal of alcohol and bromine are necessary before addition of nitric acid to avoid the possibility of a violent reaction.*

Metallic iron was determined on the filtrate by reduction with stannous chloride followed by dichromate titration.

RESULTS AND DISCUSSION

A summary of the elemental analysis of five reduced iron ores is presented in Tables I and II. Sample 5 contained 4.1% SiO_2 and 0.16 carbon, while Sample 2 contained 0.08% carbon. The gangue values for the other samples are close to the median.

A summary of the metallic iron results obtained by all the methods is presented in Table III. At low levels, the variation in metallic iron content is prohibitive. Although this variation diminishes with increasing metallic iron content, the range of values at the 90% level is still statistically significant.

The data obtained with the two silver thiocyanate procedures are given in Table IV. With the sample of highest metallization, the methods give comparable results although the value with the pH 4.5 reagent is a little higher. At the lower metallic iron level (higher iron oxide level) the results with the pH 4.5 reagent are over 2% higher. The material balance becomes poorer and the disparity between calculated

(1) E. Merck, *Z. Anal. Chem.*, **41**, 710 (1902).
(2) Metal Powder Industries Federation, New York, MPIF Standard 7-61.
(3) F. Marion and J. Aubrey, *Chem. Anal.*, **41**, #10 (1959).
(4) Dr. G. Kraft, Metallgesellschaft, Frankfurt (Main)/Postfach 2609, private communication, January 1965.
(5) G. Kraft and J. Fischer, *Z. Anal. Chem.*, **197**, 217 (1963).
(6) S. Wakamatzu, *Bunseki Kagaku*, **14**, 41 (1965).
(7) W. Classen, "Analysenverfahren für den Kraftswerksbetrieb," Vulkan-Verlag 5.625, Essen (1962).

Table II. Median Values of Gangue Components

Comp	SiO_2	Al_2O_3	TiO_2	CaO	MgO	MnO	P_2O_5	C	S
%	2.1	1.8	0.24	0.1	<0.05	<0.05	0.32	0.028	0.01

Table III. Comparison of Results Obtained by Metallic Iron Methods

Sample No.→	Metallic iron, %				
Method	2	4	5	6	7
$HgCl_2$, Wilner	89.5	78.7	71.2	64.7	26.1
$HgCl_2$, MPIF	...	76.9			
AgCNS, pH 5.1	91.1	82.1	77.4	72.8	40.0
AgCNS, pH 4.5	91.5	84.4			
Br-MeOH, 60 Min	91.3	80.6	74.5	69.6	29.9
Br-MeOH, 15 Min	91.3	80.7	74.3	69.8	28.9
Range	2.0	7.5	6.2	8.1	13.9

[a] Each value average of at least duplicate determinations.

Table IV. Evaluation of Silver Thiocyanate Method

pH of Solution →	Metallic iron, %		Calcd % oxygen			Material bal %	
	4.5	5.1	4.5	Measd[a]	5.1	4.5	5.1
Sample							
2	91.5	91.1	3.2	3.2	3.6	99.5	99.9
4	84.4	82.1	4.9	5.9	5.7	99.0	99.4
5		77.4		8.4	7.5		99.6
6		72.8		8.5	7.6		98.1
7		40.0		18.2	15.6		98.2

[a] By neutron activation.

Table V. Evaluation of Mercury(II) Chloride Method

Sample	Metallic iron, %	Wilner method: Oxygen, % Measured[a]	Wilner method: Oxygen, % Calcd	Material balance, %
2	89.5	3.2	4.1	100.6
4	78.7	5.9	6.7	100.6
5	71.2	8.4	9.0	100.2
6	64.7	8.5	10.1	100.9
7	26.1	18.2	19.7	100.9
		MPIF method		
4	76.9	5.9	7.2	100.8

[a] Neutron activation.

Table VI. Effect of Bromine–Methanol Reflux Time

Reflux, min	Metallic iron, %
2.5	22.7
5	27.1
15	28.9
30	29.3
60	29.4
240	33.0

and measured oxygen widens. This strongly suggests that the reagent attacks iron oxides and the effect is more pronounced at higher oxide levels and lower pH values.

The data obtained with the mercury(II) chloride method (*1*) are presented in Table V. In contrast to the silver thiocyanate method, the results do not appear to be influenced by the level of metallic iron present in the sample. Nevertheless, the fact that the material balances exceed 100%, combined with a consistently high calculated oxygen, suggests that the metallic iron values are erroneously low. This suggests the possibility that the mercury sludge occludes some metallic iron, rendering it unavailable to the reagent.

Bromine–Methanol Data. Data from a study made with Sample 7 on the effect of reflux time on metallic iron are presented in Table VI. As the data indicated that reaction times of 15 or 60 min gave small differences, both times were studied with the five samples (Table VII).

At high levels of metallic iron, both dissolution times gave equivalent results. Below 70%, some differences were observed. This was supported by increasing differences in the material balances. Since the material balance is poorer with decreasing metallic iron content when a 60-minute reflux time is used, it suggests that this reflux time may be too severe. However, no difference in oxygen balance was observed. In view of the relatively constant and nearly 100% material balance, it would appear that the 15-minute reflux time has some advantage over a wider range of metallic iron. It has a definite advantage in the shorter analytical time.

Iron carbide reacts like metallic iron in the bromine–methanol procedure, but its behavior with the other reagents is not known. However, the carbon content of the reduced ores, Table II, is low and would not affect the conclusions drawn from this study.

To obtain a measure of precision, the 15-minute methanol method was cooperatively tested by having four laboratories analyze the 5 samples in duplicate. The results presented in Table VIII show a standard deviation of 0.6.

Table VII. Evaluation of Bromine–Methanol Method

Reflux time, Min	Metallic iron 60	Metallic iron 15	Calcd % oxygen 60	Calcd % oxygen Measd[a]	Calcd % oxygen 15	Material balance, % 60	Material balance, % 15
Sample							
2	91.3	91.3	3.6	3.2	3.6	100.3	100.3
4	80.6	80.7	6.0	5.9	6.0	99.6	99.8
5	74.5	74.3	8.1	8.4	8.2	99.4	99.9
6	69.6	68.8	8.5	8.5	8.9	99.1	99.9
7	29.9	28.9	18.5	18.2	18.6	98.9	99.5
					Av	99.5	99.9

[a] Neutron activation.

Table VIII. Metallic Iron by Bromine Methanol Method-Variation Between Laboratories

Sample	Laboratory A	B	C	D	This work	$\bar{X}$	Std dev σ
2	XX	XX	90.7	91.2	91.3	91.1	0.3
3	88.7	89.1	89.3	88.8	89.0	89.0	0.2
5	73.3	74.1	74.0	74.4	74.3	74.0	0.4
6	70.9	70.1	69.4	69.5	68.8	69.7	0.8
7	28.8	30.2	29.7	30.7	28.9	29.6	0.8
						Av	0.6

In summary, the criteria used to establish the most accurate metallic iron values in reduced iron ore were material balances near 100% and calculated oxygen content which agreed with the direct determination. Based on this, it has been shown that the bromine–methanol procedure with 15-minute reflux time yields the most accurate results. The mercury(II) chloride procedure tends to be biased on the low side at all levels, while the silver thiocyanate method yields consistently high results, which worsen at lower metallic iron levels. The bromine methanol method has been in routine use in several laboratories for over three years. During that time many different types of ores in various degrees of reduction have been successfully analyzed.

RECEIVED for review August 6, 1970. Accepted October 22, 1970.

Amperometric Titration of Calcium and Magnesium Using the Lead Dioxide Electrode

C. O. Huber, K. Dahnke,[1] and F. Hinz[1]

Department of Chemistry and Laboratory for Surface Studies, University of Wisconsin—Milwaukee, Milwaukee, Wis. 53201

THE DETERMINATION of calcium and magnesium in the same solution is an important analytical chemistry problem because of the occurrence of both of these elements in drinking water, body fluids, etc. The concentrations encountered and the accuracy required are such that titration is often the most suitable method for analysis. Attempts have been made in the past to titrate the calcium specifically with EDTA (ethylenediaminetetraacetic acid) while preventing magnesium reaction by precipitating magnesium hydroxide at pH 12. Convenient and specific titration of calcium in the presence of magnesium has been demonstrated by Hildebrand, Schmid, and Reilley (*1*, *2*) using disodium EGTA (ethylene glycol bis-β-aminoethyl ether-*N*,*N*′-tetraacetic acid). When a suitable end point indicating system is available, the magnesium can subsequently be titrated using EDTA. Monnier and Roueche (*3*) performed such titrations amperometrically with a stationary mercury electrode at pH 10.5. Ordinary ammonia buffer systems are not permissible in their method because of mercury amino complex formations.

Here we report an amperometric titration method based on the anodic response of the lead dioxide electrode to EDTA and to EGTA. An ordinary ammonia–ammonium buffer system is used. The titration is rapid and convenient. Titrant concentration as low as millimolar can be used. Titration curve shapes are explained with reference to previously reported properties of the lead dioxide–solution interface.

EXPERIMENTAL

Apparatus. Except for the working electrode, conventional solid electrode amperometric apparatus was used. The cathode was a saturated calomel reference electrode connected by a salt bridge. The titration solutions were stirred with an electric motor driven magnetic stirrer.

The working electrode was PbO_2 plated onto approximately 12 × 1 mm platinum wire sealed in glass. The plating was done from 0.1*M* $Pb(NO_3)_2$ in 0.5*M* HNO_3. A suitable plate was obtained by plating at 6.0 mA for 30 minutes. The plating solution was stirred with a magnetic stirrer. Treatment of the platinum wire with concentrated HCl previous to plating the lead dioxide removed old PbO_2 and also improved the apparent quality of the PbO_2 plate. A stable and sensitive PbO_2 layer appeared almost black. Any exposed areas of platinum on the electrode resulted in spurious currents and could not be tolerated. Once prepared, the anode indicator electrode could be used for at least 20 titrations and often remained suitable for many more. When not in use, the electrode was stored in distilled water.

Reagents. Standard solutions of 0.01*M* EDTA and 0.01*M* Ca were prepared using reagent grade disodium EDTA salt and calcium carbonate. In order to remove any EDTA impurity in the reagent grade EGTA, it was recrystallized by acidifying an alkaline solution containing a small amount of magnesium. This was necessary because initial results showed persistently high results for calcium and low results for magnesium such as would be caused by EDTA as an impurity in the EGTA. Magnesium and EGTA solutions were standardized by titration with the standard EDTA and calcium solutions. The buffer solution was prepared to be one-tenth molar in both reagent grade ammonia and ammonium nitrate and then adjusted to pH 11 using sodium hydroxide. Standard serums were obtained commercially (Dade Reagents, Inc., Miami, Fla.) and used as purchased. Solutions were stored in polyethylene bottles.

Procedure. A 10.0-ml aliquot of the sample solution is added to 10 ml of 0.1*M* buffer solution in a 50-ml beaker which serves as the titration cell. After positioning the electrode and salt bridge, the applied voltage is adjusted to +1.2 volts *vs.* SCE. Titrant concentration is either 0.01*M* or 0.001*M* depending on sample concentration. Distinct changes in slope of the current *vs.* volume of titrant plots mark the equivalence points.

RESULTS AND DISCUSSION

Titration Curves. A typical titration curve for 0.001*M* titrant appears in Figure 1. The calcium end point is marked by the first stable drop in the anodic current. The titrant is then changed to EDTA, and the magnesium is titrated to the linearly extrapolated end point as shown.

Only a small excess of EGTA should be added after the first end point, less than 0.5 ml of 10^{-3}*M* EGTA if possible. Excess EGTA does not ruin the stoichiometry of the magnesium titration, but a larger excess tends to "round" the second titration equivalence point region because of conversion of MgEGTA to MgEDTA.

Titrations performed at various applied voltages between +0.8 and +1.4 volts *vs.* SCE give the same general shape of the titration curve shown in Figure 1. The choice of 1.2 volts

[1] Present address, Department of Chemistry, Purdue University, Lafayette, Ind. 47907

(1) G. P. Hildebrand and C. N. Reilley, ANAL. CHEM., 29, 258 (1957).
(2) R. W. Schmid and C. N. Reilley, *ibid.*, p 264.
(3) D. Monnier and A. Roueche, *Helv. Chim. Acta.*, 47, 103 (1964).

Table I. Titration Results

Sample	Present	Found	Est std dev	No. of titrations
$10^{-3}M$ Ca and Mg	408 ppm Ca	407 ppm Ca	1.7 ppm	5
	240 ppm Mg	239 ppm Mg	1.4	5
$10^{-3}M$ Ca and Mg	40.2 ppm Ca	40.0 ppm Ca	0.1	5
	24.0 ppm Mg	23.7 ppm Mg	0.3	5
Hard water	35.0 ppm Ca	34.2 ppm Ca	0.8	5
	11.2 ppm Mg	10.9 ppm Mg	0.3	5
Std serum	161 ppm Ca	159 ppm Ca	2.2	4
	50 ppm Mg	53 ppm Mg	2.0	4

is based on the observation that changes in current were slightly larger at this potential.

Titration Results. Results for titrations of various samples containing calcium and magnesium are shown in Table I. Hard water and blood serum can be titrated without previous separations. The accuracy and precision compare well with other methods at these concentration levels.

Relatively large amounts of phosphates and heavy metals would be expected to interfere. Results with the standard serums indicate, however, that for these samples, chloride, iron, and phosphate in concentrations at least equal to those for calcium and magnesium do not interfere.

Magnesium solutions titrated with EGTA behaved just as blank solutions. Also, calcium end points occur at the equivalence points even in the presence of magnesium at ten times the calcium concentration. These observations confirm that the calcium equivalence point indication is unaffected by the presence of magnesium in solution.

Electrode Response Mechanism. At the lead dioxide electrode EDTA and EGTA yield anodic currents at potentials more positive than about 0.8 V *vs.* SCE. The mechanism for this anodic current has been discussed previously (*4*). Part of that mechanism involves slow, but continuous reduction of the electrode material to the lead two state by the solvent system. Reoxidation of at least a portion of the divalent lead accounts for the relatively large anodic background current observed before the first equivalence point in Figure 1.

First End Point Signal. If titration is continued much beyond the first end point with EGTA, the initial drop in anodic current shown in Figure 1 reaches a minimum and then increasing anodic current is observed. Thus a limited amount of EGTA produces a descreasing current after which the increasing anodic current mechanism referred to earlier applies.

In fact, when $0.01M$ rather than $0.001M$ EGTA is used, this initial decrease just after the end point is not resolved and the anodic current begins to increase immediately giving the same general appearance for the first as for the second end point.

This limited decrease in anodic current at the first end point is attributed to chelation of divalent lead species in the reaction layer of the electrode by the excess chelating agent occurring after the equivalence point has been reached. This chelation prevents reoxidation of the divalent lead. The fact that this decrease is limited to a small amount of free EGTA indicates that only a restricted amount of divalent lead in the reaction layer is involved. The divalent lead would otherwise contribute to the background current as discussed above. One practical result of these observations is that the titrant concentration should be low enough so that the decrease in current is clearly observed or otherwise high enough so that the current clearly increases after the equivalence point. The effect itself should not be dependent on electrode area, therefore the choice of either $0.001M$ or $0.01M$ titrant used here can be recommended for other laboratories. Apparently at certain titrant concentrations between these values, a somewhat ambiguous first end point would be obtained.

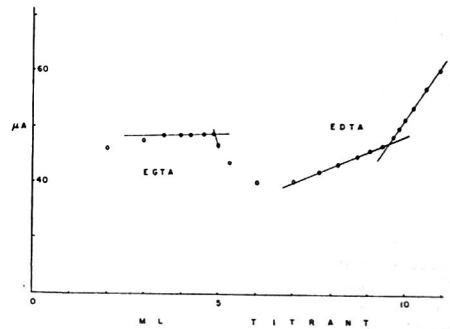


Figure 1. Titration curve

Electrode reactions in the vicinity of the end point were further studied using blank titrations. For both $0.001M$ EDTA and $0.001M$ EGTA, the sharp drop in current shown for the first equivalence point in Figure 1 is also observed upon the first additions of ligand to a blank solution. Thus, there is no measurable discrepancy between equivalence point and end point. This also shows that when used separately, an initial excess of either ligand first depletes lower oxidation state lead species in the reaction layer. In both cases after about 0.25 ml of $0.001M$ titrant had been added to the blank solution, the decreases in current were superseded by increases in current as described above.

Second End Point Signal. At the second equivalence point, the lower oxidation state lead species have already been depleted, so that only the increased anodic current can occur when the end point has been reached and excess EDTA is present.

Electrode Preparation and Storage. Variation of the current density when plating the lead dioxide electrode demonstrated that electrode sensitivity to free titrant increases with decreasing plating current density. Presumably lead dioxide layers deposited with lower current density contain more active sites in the lead dioxide lattice. The plating procedure adopted was based on obtaining adequate sensitivity without inconveniently long plating time.

Once prepared, storage of the electrode in distilled water

(4) D. R. Tallant and C. O. Huber, *J. Electroanal. Chem.*, **18**, 413 (1968).

results in a higher sensitivity than when stored in air. Such dependence on environment is not unexpected for an active electrode surface.

The results here suggest that the lead dioxide electrode is potentially applicable to the monitoring and investigation of a wide variety of titration reactions.

RECEIVED for review May 26, 1969. Accepted October 27, 1970. Presented at Division of Analytical Chemistry, 156th Meeting, ACS, Atlantic City, N. J., September 1968. Work supported in part by the National Science Foundation–Undergraduate Research Participation Program (GE-6510, GY-3044).

Determination of Nitrogen in Vanadium Nitrides and Uranium Nitride (UN)

Dean H. Bollman and D. M. Mortimore

Bureau of Mines, United States Department of the Interior, Box 70, Albany, Ore.

FOR THE KJELDAHL determination of nitrogen in refractory nitrides, one of the most exasperating problems is the inability in some cases to dissolve appropriate amounts of sample without loss of nitrogen.

Silve Kallmann *et al.* (*1*) have shown that a hydrofluoric acid–phosphoric acid–potassium dichromate combination will dissolve various refractory metals rather rapidly. The method is also applicable to most carbides and nitrides. However, no mention was made of vanadium nitride, which is particularly troublesome with regard to the problem mentioned above.

Other workers (*2*, *3*) have gone to modifications of the Dumas method for the determination of nitrogen in uranium nitride and vanadium nitride. Morgenthaler and Menichelli (*4*) used a gasometric determination requiring the use of chlorine.

E. T. Turkdogan and E. M. Fenn (*5*) used the Dumas method for determining the amount of nitrogen in vanadium nitrides when they were investigating the variation of composition with temperature of vanadium nitrides under one atmosphere of nitrogen. At 900 °C, a nitride contained 20.5% nitrogen, but at 1500 °C it had decreased to 17.1% nitrogen. They reported that the vanadium nitrides have distinct composition ranges, the beta ranging from $VN_{0.37}$ to $VN_{0.49}$, and the gamma from $VN_{0.71}$ to $VN_{1.00}$. The fact that the vanadium nitrides are not stoichiometric may be a factor in the nitrogen losses occurring during the regular Kjeldahl determination.

Meyer, Parry, and Davis (*6*) successfully used tube furnace ignition and gas chromatographic determination of the nitrogen for determining nitrogen in various refractory nitrides, including vanadium nitride.

For uranium, UO_2, and uranium nitrides, Joan Lathouse, F. E. Huber, Jr., and D. L. Chase (*7*) and others (*8*, *9*) have shown that loss of nitrogen can occur in the dissolution process for Kjeldahl determinations. Cupric selenate and hydrofluosilicic acid used in the dissolving process and De Varda's alloy used during distillation helped in some cases to prevent losses. However, Sinclair, Davies, and Melhuish (*10*) reported results which show that cupric selenate promotes loss of nitrogen when uranium–plutonium dioxides were dissolved in a mixture of phosphoric and sulfuric acids.

Turovtseva and Kunin (*11*) suggest that insoluble residues be fused with potassium sulfate crystals and a mixture of phosphoric and sulfuric acid. Our experience with bisulfate fusion of vanadium nitride has been that temperatures high enough to decompose the nitrides invariably led to nearly complete loss of nitrogen.

To obtain accurate and simplified methods for nitrogen in vanadium nitrides and UN, various procedures were attempted. Kjeldahl procedures for vanadium nitrides and uranium nitride are given below.

EXPERIMENTAL

Apparatus used were two semimicro Kjeldahl distillation flasks, 270-ml capacity; an Erlenmeyer flask, 4-liter, thick-walled, with Nichrome wire heating assembly mounted through a rubber stopper as a steam generator; an acid digestion bomb with Teflon (Du Pont) cup; and other conventional laboratory glassware and equipment.

Reagents were sodium hydroxide solution–40 % NaOH with H_2O, cool; sulfuric acid titrating solution–approximately 0.14*N*; boric acid solution, 1% with methyl red indicator. Combine 0.090 gram methyl red in 90 ml of ethyl alcohol, with 90 grams boric acid in 9 liters of H_2O. Make up and store in a $2\frac{1}{2}$ gallon solution bottle. The boric acid should be com-

(1) S. Kallmann, E. W. Hobart, H. K. Oberthin, and W. C. Brienza, Jr., ANAL. CHEM., **40**, 332–335 (1968).
(2) Research Group Rep. *AERE-R 4644;* Scientific Administration Office, Atomic Energy Research Establishment, Harwell, Didcot, Berkshire, England, August 1964.
(3) O. H. Kriege, *AEC Rep*, *LA-2306*, Los Alamos, N. M. Aug. 1959, p 38.
(4) L. P. Morgenthaler and R. P. Menichelli, ANAL. CHEM., **37**, 570–571 (1965).
(5) E. T. Turkdogan and E. M. Fenn, *J. Iron Steel Inst.*, **181**, 343–344 (1955).
(6) R. A. Meyer, E. P. Parry, and J. H. Davis, ANAL. CHEM., **39**, 1321–1323 (1967).
(7) Joan Lathouse, F. E. Huber Jr., and D. L. Chase, ANAL. CHEM., **31**, 1606–1607 (1959).
(8) Production Group Rep. *374(S)*, United Kingdom Atomic Energy Authority, Risley, Warrington, Lancashire, England, 1962.
(9) Harlan J. Anderson and James C. Langford, ANAL. CHEM., **35**, 1093–1094 (1963).
(10) V. M. Sinclair, W. Davies, and K. R. Melhuish, *Talanta*, **12**, 841–845 (1965).
(11) Z. M. Turovtseva and L. L. Kunin, "Analysis of Gases in Metals." Consultants Bureau, New York, 211–212 (1961).

Table I. Nitrogen in Vanadium Nitride, %

Sample	Nominal	Kjeldahl $HF-H_3PO_4-K_2Cr_2O_7$	Micro-combustion	Acid digestion bomb Kjeldahl 140 °C, HF
VN-10	8.84	6.6	9.6	8.26
powder	*a*	6.6	9.2	8.42
		6.8	9.7	8.16
			9.2	
VN-11	13.3	9.9	13.8	13.7
powder	*a*	10.2	14.0	13.8
		9.8	13.8	13.8
			13.7	
PC-285	21.2	10–17[c]	21.7	21.2
	b		21.2	21.4
			21.1	20.7
			21.4	

[a] Calculated from weight gain after exposure of high-purity vanadium to high-purity nitrogen at 1100–1200 °C.

[b] Reported value from laboratory supplying this material. Supplier also reported 78.6% V, 0.07% Fe, 0.07% O_2, and a few trace impurities; total = 99.94%.

[c] Kjeldahl, many runs made with various combinations of solvents (see discussion).

pletely dissolved and the solution made up to the full 9 liters before the indicator is poured in; otherwise a red precipitate will form.

Dissolution Procedures. VANADIUM NITRIDES. Weigh approximately 0.1-gram samples by difference into the Teflon cup of the acid digestion bomb. Add 10 ml of HF. Screw the cap of the bomb down tightly with the fingers and place the bomb in an oven maintained at 140–150 °C until the sample is dissolved. Up to four days has been required. The sample may be checked at any time by cooling the bomb to room temperature before opening and returning the bomb to the oven if the sample is not dissolved. When the sample has dissolved, transfer the solution quantitatively to the distillation apparatus.

URANIUM NITRIDE (UN). Weigh approximately 0.1-gram sample into a 50-ml beaker. Add 5 ml of phosphoric acid (H_3PO_4) and heat. After the H_2O has been driven off, heat covered until sample is in solution. Cool and dilute to 20 ml with H_2O. Stir carefully with a stirring rod to mix the water and acid. (The H_3PO_4 becomes thick and syrupy.) Transfer to the distillation apparatus when cool.

Description of Kjeldahl Distillation and Titration Method Used. Dissolved samples, made strongly alkaline with 40% NaOH solution were steam distilled in a semimicro Kjeldahl distillation apparatus. One hundred milliliters of distillate in each case were collected in a receiving beaker containing, originally, 10 ml of a 1% boric acid solution with methyl red indicator. Distillates were titrated with 0.14*N* sulfuric acid to the same end point (yellow to red). Deionized water was used to generate steam and used thoughout the determinations. The sulfuric acid was standardized with ammonium chloride carried through the distillation.

Blank Determinations. For high nitrogens (nitrides), blanks are not a significant factor (< 0.02% N with 0.1-gram sample). However, it is a good idea to carry a blank through the procedure to check for contamination.

Kjeldahl determinations should be made in an isolated area of the laboratory to prevent atmospheric contamination, and dissolved samples should not be allowed to stand around longer than necessary.

Safety Precautions. Care should be taken with the steam distillation apparatus to avoid any pressure buildups and exposure to hot steam.

RESULTS AND DISCUSSION

Table I gives the nitrogen content in vanadium nitride as determined by several methods. The Kjeldahl method, in any form other than with HF in the acid digestion bomb, failed with vanadium nitride. We suggest that molecular species (N_2) are formed in the dissolution process: samples were dissolved in airtight containers on a hot plate or in a water bath and cooled before opening, but results were still low. Also we tried many dissolution combinations involving HF, H_3PO_4, $HClO_4$, $K_2Cr_2O_7$, cupric selenate, and hydrofluosilicic acid. Either the sample would not dissolve or results were low and inconsistent.

When the ordinary Kjeldahl methods failed with vanadium nitrides, a simple microcombustion method was tried. Vanadium nitride samples were ignited in platinum boats in a microcombustion apparatus at 800 °C for 1 hour in flowing oxygen. Vanadium content was calculated from the weight of the V_2O_5 residues, and nitrogen obtained by difference. V_2O_5 residues were checked by the Kjeldahl procedure and were well under 100 ppm of nitrogen. It is recognized that the combustion technique may be valid only for rough approximations due to carbon, oxygen, or other impurities in the sample. For comparison purposes, the nitrogen values by this combustion method are shown in Table I, as are the nitrogen contents from the weight gain of high-purity vanadium as it was nitrided.

The Teflon-lined bomb values for the high-purity vanadium nitride (PC-285) indicate the Kjeldahl method is valid if vanadium nitride samples can be heated in a sealed container hot enough to dissolve with HF without an oxidizer.

Table II provides data of replicate runs of a uranium nitride sample over a period of 1 year. The Kjeldahl procedure was used after dissolving the sample in phosphoric acid only. The chromate method (5 ml H_3PO_4–15 ml HF–1 gram $K_2Cr_2O_7$ with about 0.1 gram of sample) is inadequate in this case. A loss of nitrogen results. We have found that H_3PO_4 alone is the most suitable solvent for uranium, UN, UC, and UN–UC–uranium oxide combinations.

Table II. Nitrogen in Uranium Nitride, UN Sample, %

Sample weight	Method	Number of determinations	Per cent, average	Per cent range	Stdard dev	Theoretical UN
0.1 g	Kjeldahl, H_3PO_4 solvent	28	5.78	5.71 to 5.84	0.035	5.56
0.1 g	Kjeldahl, Chromate method H_3PO_4-HF-$K_2Cr_2O_7$	8	3.48	3.28 to 3.74	0.164	5.56

RECEIVED for review April 1, 1970. Accepted October 27, 1970. Reference to specific brands is made to facilitate understanding and does not imply endorsement by the Bureau of Mines.

CORRESPONDENCE

Re: "Criteria for Judging Acceptability of Analytical Methods"

SIR: Earl F. McFarren, Raymond J. Lishka, and John H. Parker (*1*), the authors of this paper, propose a procedure for determining acceptability of an analytical method based on calculation of "total error." They then apply this proposed criteria to several analytical studies selected from the literature. One such study involved analysis of pesticide residues in water. The authors concluded in part: "... none of the pesticides studied could be determined satisfactorily by gas chromatography." They were, of course, referring only to the study results referenced in their paper but, by unfortunate inference, gave the impression that general pesticide residue GLC analysis was suspect. This is not true. There are, in fact, many published studies which have demonstrated the reliability of pesticide residue analysis and which produced acceptable results using the author's own criteria.

The "total error" has been calculated for a number of successful collaborative studies (*2–5*). These are summarized in Table I. As you will note, the results indicate that with few exceptions, pesticide residue GLC methodology is satisfactory, but could be improved.

Table I. Summary of AOAC Collaborative Study Data for Pesticides (*2–5*)

	No. of results	True, ppm	Mean, ppm	Mean error, ppm	Std dev, ppm	Total error, %
Butterfat (*2*)						
Heptachlor epoxide	20	0.261	0.293	+0.032	0.039	42.15
Dieldrin	20	0.266	0.255	−0.011	0.051	42.48
White potatoes (*3*)						
Aldrin	10	0.12	0.124	+0.004	0.013	25.00
DDE	10	4.90	4.95	+0.050	0.530	22.65
Methoxychlor	10	6.80	6.35	−0.450	0.750	28.68
Aldrin	10	0.04	0.0399	−0.0001	0.0039	19.75
DDE	10	0.70	0.704	+0.004	0.064	18.86
Methoxychlor	10	0.60	0.558	−0.042	0.050	23.67
Endive (*4*)						
Lindane	8	10.00	9.17	−0.830	0.780	23.90
Heptachlor	8	0.10	0.082	−0.018	0.015	48.00
DDD(TDE)	8	7.00	5.50	−1.500	1.030	50.86
Lindane	8	1.00	0.936	−0.064	0.105	27.40
Heptachlor	8	0.05	0.044	−0.006	0.006	36.00
DDD(TDE)	8	1.00	0.861	−0.139	0.120	37.90
Cauliflower (*4*)						
Lindane	8	10.00	9.57	−0.430	1.730	38.90
Heptachlor	7	0.10	0.094	−0.006	0.012	30.00
DDD(TDE)	6	7.00	5.98	−1.020	0.620	32.29
Lindane	7	1.00	0.883	−0.117	0.154	42.50
Heptachlor	7	0.05	0.041	−0.009	0.005	38.00
DDD(TDE)	5	1.00	0.864	−0.136	0.137	41.00
Apricots (*5*)						
BHC	12	4.04	4.18	+0.140	0.950	50.50
DDT	12	6.299	6.37	+0.071	0.580	19.54
Endrin	13	0.198	0.187	−0.011	0.023	28.79
BHC	12	0.879	0.93	+0.051	0.190	49.03
DDT	12	0.208	0.202	−0.006	0.020	22.12
Endrin	13	0.0496	0.049	−0.0006	0.006	25.40
Strawberries (*5*)						
BHC	12	4.219	4.31	+0.091	1.100	54.30
DDT	12	6.580	6.77	+0.190	0.680	23.56
Endrin	13	0.207	0.193	−0.014	0.022	28.02
BHC	12	0.918	0.96	+0.042	0.180	43.79
DDT	12	0.217	0.227	+0.010	0.023	25.81
Endrin	13	0.0518	0.052	+0.0002	0.010	38.99

TERRYL J. FARRELL

Department of Health, Education, and Welfare
Food and Drug Administration
1521 West Pico Boulevard
Los Angeles, Calif. 90015

RECEIVED for review June 12, 1970. Accepted August 31, 1970.

(1) E. F. McFarren, R. J. Lishka, and J. H. Parker, ANAL. CHEM., 42, 358 (1970).

(2) L. Y. Johnson, *J. Ass. Offic. Agr. Chem.*, 48, 668 (1965).
(3) R. T. Krause, *ibid.*, 49, 460 (1966).
(4) J. Gaul, *ibid.*, p 463.
(5) A. Davidson, *ibid.*, p 468.

Nonaqueous Electrochemical Cell Capable of Rigorous Exclusion of Water and Oxygen

Jerry L. Mills,[1] Roger Nelson,[2] Sheldon G. Shore, and Larry B. Anderson[3]

Department of Chemistry, The Ohio State University, Columbus, Ohio 43210

EVEN THOUGH AN EXTENSIVE amount of work has been done in aprotic and oxygen-free electrochemical systems, the most common methods of excluding the atmosphere have been to work in a self-contained glass system with continuous flushing by a predried inert gas, or to work in a dry-box (*1*, *2*). Neither of these techniques can compare with vacuum-line techniques in terms of their ability to exclude water or oxygen (*3*). Not only is total exclusion of H_2O and O_2 from a dry-box difficult to achieve, but there is often the greater problem of contamination by solvents and compounds used previously in the box. Cell designs for specific systems such as liquid ammonia or sulfur dioxide have been described (*4–6*), but one for a general cell for use where rigorous exclusion of H_2O and O_2 is necessary has not been previously published. The purpose of this paper is to describe an electrochemical cell which will minimize such contamination, and to describe methods for detecting and estimating water and oxygen contamination in electrochemical solvents at the $10^{-5}M$ level. The cell is moderately inexpensive to construct and simple to use when once assembled. Problems previously encountered using tetrahydrofuran as an aprotic electrochemical solvent (*7*) are easily rectified by use of the cell.

EXPERIMENTAL

Instrumental. Three-electrode polarograms were run on a commercially available instrument (Beckman Electroscan, Model "30"). Three-electrode cyclic voltammograms were taken with a Chemtrix type 300 Polarographic Unit and type 205 Time-Base Unit inserted in a Tektronix Model 564 oscilloscope.

Cell Description. The cell, shown in Figure 1, required the use of a standard high-vacuum line consisting of mechanical and mercury diffusion pumps with a pressure measuring device such as a McLeod gauge. The operating pressure of the vacuum line was 10^{-5} to 10^{-6} Torr. All vacuum line manipulations, *e.g.* vapor transfer of solvents, were standard (*3*).

The cell was vacuum tight. The platinum-glass seal in section *C* was coated on the exterior with Varian Associates high-vacuum epoxy, Torr Seal, to assure a vacuum seal and for mechanical strength. The stopcocks were Fischer and Porter high-vacuum Teflon stopcocks. All glass joints were standard. In solvents of high specific resistance (such as tetrahydrofuran), it is important to position the mercury drop as close as possible to the tip of the Luggin capillary. The DME capillary (6–12 second drop time) was constructed to meet that requirement. The seals connecting the DME capillary to the inner ⅌ 14/35 joint were made with Torr Seal (see Figure 1). To minimize free play between the DME and the inside of the joint prior to the epoxying process, Teflon (Du Pont) tape was wrapped around the capillary to form a snug fit at the top and bottom of the joint. The mercury reservoir was attached to the capillary by vacuum Tygon (No. R-3603). The silver reference electrode was made with a soft glass-platinum seal with silver wire attached to the platinum. The soft glass was attached to the joint with Torr Seal in the same manner as the DME described above.

Solvents. The grease-free storage vessel for solvents is shown in Figure 2. Tetrahydrofuran, THF (Baker, spectroscopic grade), was preliminarily dried over CaH_2. The vessel containing the THF was then attached to the vacuum line, the THF degassed and vapor transferred into a second solvent vessel which contained Na/K alloy (1 : 1 by weight). The Na/K alloy has several advantages for purification of THF for an electrochemical solvent: it removes both O_2 and H_2O, forming alkali-metal oxides or alkali-metal hydroxides plus hydrogen, respectively; it is easy to prepare and does not constitute the explosion hazard of drying with $LiAlH_4$; it has a self-cleaning surface that also serves as an indicator of absence of contamination by O_2 and H_2O. No evidence of significant reaction of the Na/K with the THF solvent was observed and such mixtures have been stored in borosilicate glass flasks for a month without detectable degradation in the electrochemical behavior of the vapor-transferred THF. The problems previously associated with the use of THF as an electrochemical solvent (*7*) are largely overcome by the procedures described herein.

Acetonitrile, AN (Matheson, Coleman and Bell, spectroscopic grade), was purified by the method of Osa and Kuwana (*1*). The solvent vessel containing the AN was attached to the vacuum line, and the AN degassed and vapor transferred to another vessel which contained crushed CaH_2.

Both of the solvent storage techniques (over Na/K for THF, and over CaH_2 for AN) utilize a highly reactive material which combines with the common solvent impurities as well as with the solvent to produce nonvolatile and/or nonelectroactive products. The very high electrochemical purities of both of the solvents studied in this work are probably due in large part to the final vapor transfer step.

Supporting Electrolyte. Tetrabutylammonium perchlorate, TBAP (Southwestern Analytical Inc., Austin, Texas, polarographic grade), was used as the supporting electrolyte in both solvents. (Tetrabutylammonium iodide is not sufficiently soluble in THF at 30 °C for most electrochemical uses as a background electrolyte.) It was dried *in vacuo* in small quantities (~10 g) at 90 °C, and once dried, was stored in the same vessel under vacuum. The supporting electrolyte solution was prepared by adding a known quantity of the dried TBAP (~2 g for 0.2 *M* background electrolyte in 30 ml of solvent) to a calibrated ampoule *B'* (see Figure 1). The ampoule was then attached to the vacuum line and held under ~10^5 Torr vacuum over-night. Gentle heating (heat gun or 90 °C oil bath) during this period will assure maximum H_2O removal, but is usually unnecessary if the perchlorate has been previously well dried and has undergone minimal exposure to the atmosphere during transfer. The solvent was then vapor transferred into the ampoule containing TBAP until the desired concentration was attained.

Reference Electrolyte Solution. The reference electrolyte

[1] University Postdoctoral Fellow, 1969–70.
[2] Graduate School Postdoctoral Fellow, 1968–69.
[3] Reprint requests should be directed to this author.

(1) T. Osa and T. Kuwana, *J. Electroanal. Chem.*, **22**, 389 (1969).
(2) K. S. V. Santhanam and A. J. Bard, *J. Amer. Chem. Soc.*, **88**, 2669 (1966).
(3) D. F. Shriver, "The Manipulation of Air-Sensitive Compounds," McGraw-Hill, New York, 1969.
(4) H. A. Laitinen and C. J. Nyman, *J. Amer. Chem. Soc.*, **70**, 2241 (1948).
(5) P. Arthur, D. S. Rulison, and K. D. Berlin, ANAL. CHEM., **40**, 1389 (1961).
(6) P. J. Elving, J. M. Markowitz, and I. Rosenthal, *J. Phys. Chem.*, **65**, 680 (1961).
(7) J. Badoz-Lambling and M. Sato, *Acta Chim. Hung.*, **32**, 191 (1962).

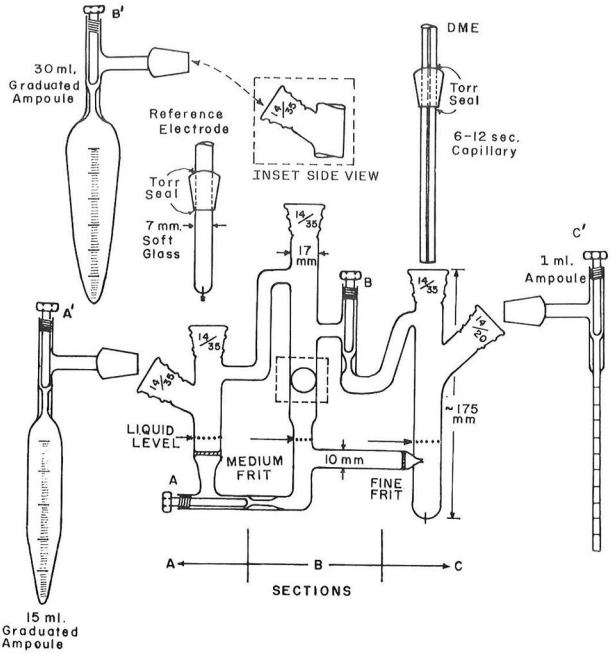


Figure 1. Vacuum-line electrochemical cell

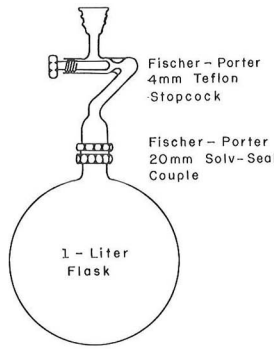


Figure 2. Grease-free solvent storage vessel

solution was prepared in an analogous manner to that of the supporting electrolyte solution. A known quantity of $AgClO_4$ (Alfa Inorganics, anhydrous) was added to ampoule *A'*. The ampoule was then attached to the vacuum line and continuously evacuated overnight. No heating of this material was attempted, because of the well known instability of heavy-metal perchlorates (*8*). An appropriate quantity of solvent was then vapor transferred into the vessel to achieve a 0.1*M* solution.

Sample Solutions. Known quantities of air-sensitive samples were introduced into ampoule *C'* (Figure 1) either by standard vacuum line techniques (*3*) (if the compound had sufficient volatility) or by syringe in a helium-atmosphere, Na/K dried dry-box (*3*). Solvent was then vapor transferred onto the sample until a convenient dilution was achieved.

Procedure of Cell Use. POLAROGRAPHY. Enough mercury is added to section *C* to cover the platinum wire and a small Teflon-clad stirring bar is floated on the mercury. With ampoules *A'*, *B'*, and *C'* in place and appropriately filled, the cell is attached to the vacuum line at the joint on the top of section *B*. The reference electrode is put into place and a plug is inserted where the DME would normally be placed. With the stopcocks on ampoules *A'*, *B'*, and *C'* closed and cell stopcocks *A* and *B* open, the cell is evacuated. The pressure is checked on the McLeod gauge, or leakage may be checked for simply by isolating the cell to a mercury manometer. After approximately 15 minutes when the pressure is sufficiently low and the adsorbed H_2O and O_2 has been pumped off, the plug is replaced by the DME and the cell is re-evacuated. During the evacuation, the mercury reservoir should be well below the capillary tip in order to prevent excessive pressure, and consequent streaming of mercury from the capillary tip. Stopcock *B* is closed and the cell is isolated from the vacuum line. Supporting electrolyte solution is added to the cell from ampoule *B'* (~15 *ml*, *vide infra*). Solution is allowed to flow through stopcock *A* until it touches the bottom of the frit in section *A*, and stopcock *A* is immediately closed. $AgClO_4$ solution is then added to section *A* from ampoule *A'* until the solution is at the level indicated by the dotted line in Figure 1. With the stopcocks on ampoules *A'* and *B'* closed, the cell is bled up through the vacuum line to atmospheric pressure with argon that has been purified by bubbling through Na/K alloy [alternately, research grade argon (99.999% pure) may be used directly]. The supporting electrolyte solution is thus forced through the frit and Luggin capillary into section *C* by the pressure differential. The mercury reservoir is quickly raised and, when the liquid levels in sections *B* and *C* are equal, stopcock *B* is opened. Ideally the liquid levels in sections *A*, *B*, and *C* should all be equal (as indicated by the dotted line in Figure 1), and this is achieved by initial addition of the proper amount of supporting electrolyte solution. When stopcock *A* is opened, the cell is ready for a background electrolyte scan. Compound is added from the calibrated ampoule *C'*. Alternately in place of ampoule *C'*, a vacuum-tight septum may be used for sample addition by syringe. The volume of solution in section *C* is measured when the cell is dismantled.

CYCLIC VOLTAMMETRY. Cyclic voltammograms may be taken with the cell by using the procedure described above and utilizing the dropping mercury electrode or a Pt-bead electrode. Results using the DMF at the higher scan rates (0.1 sec/volt) should be a fairly good approximation to behavior at a hanging mercury drop.

COULOMETRY. Coulometry may be carried out in the cell using basically the same method described above. The DMF is replaced by an auxiliary electrode and the mercury level in section *C* is raised until it almost touches the Luggin

(8) J. C. Schumacher, "Perchlorates, Their Properties, Manufacture, and Uses," Reinhold, New York, 1960.

capillary. By a slight modification of the cell, coulometry and polarography may be carried out simultaneously without changing the auxiliary and dropping mercury electrodes. An additional joint is placed on section *C* just opposite the Luggin capillary tip which will hold an auxiliary electrode similar to that described above. Then coulometry may be run on a sample, the electrode leads switched, and polarography or cyclic voltammetry run on the possible products.

SYSTEM EVALUATION

In order to evaluate the purification procedures and effectiveness of the cell in excluding atmospheric contamination, the following methods were utilized as checks. All potentials were measured against the Ag-wire/0.1*M* Ag^+ reference electrode in the appropriate solvent. However, in order to be as consistent as possible with the existing literature, all potentials are reported *vs.* the aqueous saturated calomel electrode, SCE. The Ag-wire/0.1*M* Ag^+ (THF) reference electrode was measured to be +0.49 V *vs.* SCE. The Ag-wire/0.1*M* Ag^+ (AN) reference electrode was measured to be +0.36 V *vs.* SCE.

Background Polarograms. In THF solution which was 0.2*M* in TBAP, the background polarogram indicated a small anodic wave at +0.14 V (presumably Cl^- ion) and a second unidentified impurity giving a small reversible cathodic wave at −1.2 V. The concentration of both of these impurities was estimated to be $\sim 1 \times 10^{-5} M$. The remaining background was a nearly linear rise of 0.07 μA/volt from 0.0 V to −3.1 V, presumably due to a charging phenomenon. A very sharp current rise appeared shortly after −3.1 V indicating discharge of solvent.

In AN solution which was 0.2*M* in TBAP, a scan of the background indicated a small impurity of approximately $1 \times 10^{-5} M$ at −0.6 V. The total, nearly linear, current rise from 0.0 V to −2.5 V was 0.2 μA, at which point the cathodic limit for the AN was reached, with a total current of 1.0 μA observed by −2.7 V.

Effect on Air-Sensitive Compounds. An evaluation of inherent H_2O and O_2 levels may be made by monitoring a polarographically reducible, H_2O–O_2 sensitive, compound at several concentrations. The zero-current intercept of a plot of i_d *vs.* concentration should indicate the order of magnitude of compound lost to reaction with H_2O or O_2. Such plots for hexaborane (10) and for several organoboranes (all of which are very O_2–H_2O sensitive), either had intercepts which could not be experimentally distinguished from zero or which indicated O_2–H_2O concentrations of $\sim 10^{-5} M$.

Effect of Addition of H_2O. Another method which may be used to check for the presence of H_2O is observation of the effect of H_2O addition on the background electrolyte scan mentioned above. In both THF and AN solvents, the addition of H_2O *did not* result in a specific reduction wave as reported previously (*1*), but had the effect of generally raising the level of the background current over the entire scanning region and also resulted in the current-rise being somewhat earlier and less precipitous. Addition of H_2O also caused a distinct increase in the charging current (*6*), as evidenced by the increased pen excursion observed during electrolysis on a single mercury drop. During the reduction scan of the pure background electrolyte solution (either THF or AN), the individual drops from the DME were not visible on the recorder until near the solvent cut-off (2.8 μA full-scale). However, the addition of $2 \times 10^{-5} M$ H_2O resulted in easily discernible drops. We tentatively attribute these charging effects to the orientation of the dipoles of H_2O molecules adsorbed on the mercury surface. The effects of H_2O addition mentioned above, *i.e.*, background current rise, solvent cut-off modification, and charging effects on the DME, were qualitatively proportional to H_2O concentration in the range 10^{-5} to $10^{-2} M$, and should provide useful diagnostics for the presence of H_2O in highly purified nonaqueous solvents systems.

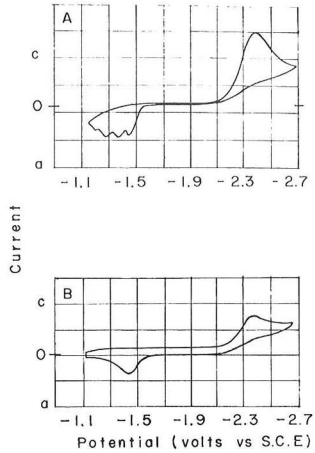


Figure 3. Cyclic voltammetry of 3,8-dimethyl-2-methoxyazocine, background electrolyte 0.2*M* TBAP

A. **$\sim 10^{-3} M$ azocine in DMF containing $\sim 10^{-2} M$ H_2O. Current sensitivity, 10 μA/div.** ***B.*** **$1.22 \times 10^{-4} M$ azocine in O_2–H_2O free THF. Current sensitivity, 2.0 μA/div.**

Azocine Systems. Azocines are known to reduce at the dropping mercury electrode, directly to the dianion (*9*). Such products of reduction of unsaturated organic compounds—anions and dianions—are often highly unstable to reactions with proton donors. Indeed, many of the presently available techniques for nonaqueous solvents were developed specifically for work in such organic systems. We have therefore used the highly unstable azocine dianion as a rigorous qualitative test of the low proton activity of the THF solvent and background electrolyte systems described here.

Figure 3 illustrates the effects of small amounts ($\sim 10^{-2} M$) of H_2O on the electrochemical behavior of 3,8-dimethyl-2-methoxyazocine in an incompletely dried DMF solvent system. The essentially ideal behavior of the parent–anion couple as obtained with the present nonaqueous cell system is also presented for comparison. No evidence is observed for multiple peaks on the anodic scan due to reoxidation of protonation products of the azocine dianion.

RECEIVED for review July 27, 1970. Accepted September 14, 1970. L.B.A. acknowledges the support of this work by the Petroleum Research Fund and by the Research Corporation. S.G.S. wishes to acknowledge, gratefully, the support of this work by the National Science Foundation.

(9) L. B. Anderson, J. F. Hansen, T. Kakihana, and L. A. Paquette, *J. Amer. Chem. Soc.*, in press.

Device to Overcome Spinning Difficulties with Nuclear Magnetic Resonance Sample Tubes at Variable Temperature

John Barzilay[1]

Unilever Research Laboratories, Vlaardingen/Duiven, The Netherlands

LIFTING OF THE SAMPLE tube during spinning is a common difficulty with the variable temperature probe in high resolution NMR spectrometers employing cylindrical turbine rotors. This is caused by the nitrogen flow that is used to control the temperature. Van Geet (*1*) has recently put forward a method of controlling this by using a cylindrical Teflon (Du Pont) weight sliding over the sample tube. However, for application to spectrometers with narrow pole gaps (*e.g.*, Varian HA-100), sufficient weight can be achieved only with an inordinately long and cumbersome cylinder.

We have overcome the problem by developing a small aluminum attachment (Dutch patent applied for.) (see Figure 1) which locks into the spinner housing of the Varian Probe V 4333 by means of a bayonet plug. From the four holes in the bottom of the attachment (see Figure 2), a gas stream gives a downward pressure on the top of the turbine rotor to overcome vertical movement of the sample tube. The air or nitrogen supply to this attachment is tapped by a T-piece junction from that used to control the spinning. No separate control of the gas supply to the attachment is necessary, since varying the gas pressure to alter the spinning speed of the sample tube apparently automatically compensates for the changing upward pressure.

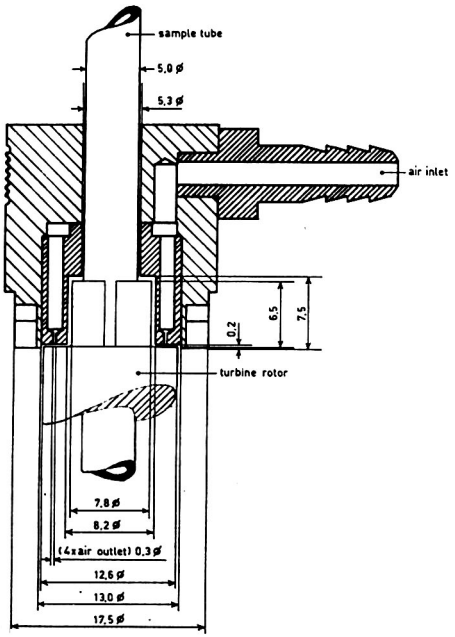


Figure 1. Aluminum attachment to spinner housing to prevent sample tube from lifting (sizes are in mm)

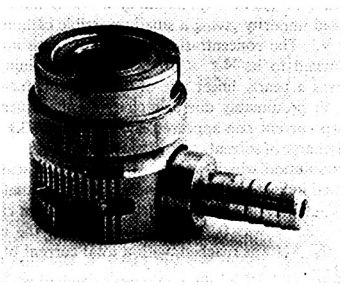


Figure 2. View of device showing the four air passages

With this system, we have found no difficulties in obtaining smooth and controllable spinning over the whole temperature range (−100 to +180 °C) and we now routinely operate the spectrometer at room temperature with the attachment in place. This has the further advantage that sample tubes are introduced into the probe without first attaching a turbine rotor, since this is already locked within the spinner housing.

ACKNOWLEDGMENT

Thanks are due to L. de Snayer and P. Oostveen for valuable discussions and technical assistance.

RECEIVED for review July 27, 1970. Accepted October 19, 1970.

[1] Author's address, Olivier van Noortlaan 120, Vlaardingen, The Netherlands.

(1) A. L. van Geet, ANAL. CHEM., 40, 1914 (1968).

Directory of Graduate Research 1969

Biennial publication of the ACS Committee on Professional Training

Covers the universities and colleges in the United States and Canada known to offer an organized curriculum leading to the doctoral degree in chemistry, biochemistry, chemical engineering, and pharmaceutical or medicinal chemistry.

The guide to graduate schools, research, and personnel in these areas.

201 Departments of Chemistry
165 Departments offering Biochemistry
106 Departments of Chemical Engineering
29 Departments of Pharmaceutical or Medicinal Chemistry

Lists 2807 full- and part-time staff members, each with outline of career, teaching and research specialties, and list of publications for the past two or five years.

Statistical data on departments include number of Ph.D. degrees conferred during the previous two years, number of staff members, and number of postdoctoral appointments.

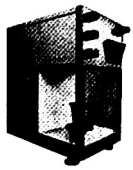
Other listings include interdisciplinary programs and doctoral theses accepted during previous two years.

1213 pp. with index of names paper bound (1970) $10.00 postpaid in U.S., plus 50 cents Canada and Pan America, plus 75 cents foreign.

Order from:
Special Issue Sales
American Chemical Society
1155 Sixteenth St., N.W.
Washington, D. C. 20036

Need a New Mettler Balance Catalog?





Easy-to-use analytical balances are covered in Mettler's newest catalog. There are 22 in all – from our $550 basic balance to our $2550 ultra-micro with ±0.1 microgram precision.

Sixteen digital readout, high speed top-loading balances are described in our 20-page catalog. All weigh unknowns, checkweigh, batch weigh, weigh-in and weigh below the balance.

For more information, circle number: Analytical Balances #1, Top-loading Balances #2, Demonstration #3.

Mettler Instrument Corporation
20 Nassau Street, Princeton, N.J. 08540

Mettler®

Circle No. 125 on Readers' Service Card

Analytical Chemistry

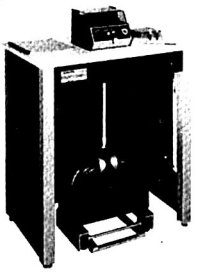
JANUARY 1971

Valid through MARCH 31, 1971

NEW PRODUCTS, NEW CHEMICALS, MFG. LITERATURE:

| | | |

New...Faraday Magnetic Susceptibility System for Under $3000.



Teaching... Quality Control... Basic and Applied Research ■ Detects Susceptibility to 0.5 x 10^{-6} cgs units

Applications include... ■ Teaching Fundamentals of Magnetochemistry; e.g., Comparing Properties of Dia-, Para-, Ferro- and Antiferromagnetic Materials. ■ Oxidation States of Transition Metals in Coordination Complexes. ■ Stereochemical Studies of Ionic and Covalent Structures. ■ Paramagnetic Susceptibility Changes with Temperature; Curie and Curie-Weiss Laws. Determination of Concentration in Solutions. ■ Thermomagnetic Studies of Oxidations and Reductions. ■ Solid State and Materials Research Studies. ■ Quality control—Determination of Ferromagnetic Impurities.

Milligram samples can be studied over a temperature range of 130°C below ambient to at least 300° above. The system's permanent magnet has a flux density of approximately 5700 gauss. ■ Standard readout is a visual digital display; recorder output is also provided. ■ Use the post card for more information.

Cahn Division/Ventron Instruments Corporation

7500 Jefferson St., Paramount, California 90723 • (213) 634-7840

Circle No. 33 on Readers' Service Card

here is the first complete, self-contained Mercury Analyzer System. Coleman Model MAS-50/$875.



It can be used in many scientific fields. Pollution: Air, water, food, soil, tissue. Clinical: Urine, blood, tissue. Industrial Control: Food, metal, soil, fertilizer.

- Sensitivity .01 μg of mercury, equal to or better than A.A.
- Direct reading in μg of mercury • Hatch and Ott procedure

This compact, self-contained, low-cost system makes determination of mercury in solids and solutions, organic or inorganic, or in air an inexpensive routine procedure. Coleman MAS-50 is so easy to operate, no special training is required. **Call or write today for free bulletin A-350.**

COLEMAN INSTRUMENTS
42 MADISON STREET
MAYWOOD, ILLINOIS 60153
(312 345-7500)

A DIVISION OF THE PERKIN-ELMER CORPORATION

COLEMAN

Circle No. 36 on Readers' Service Card

Name _____

Position _____

Company _____

Address _____

_____ Zip _____

☐ Industrial Firm ☐ Academic ☐ Government ☐ Other

FIRST CLASS
Permit No. 25682
Philadelphia, Pa.
19101

BUSINESS REPLY CARD
NO POSTAGE STAMP NECESSARY IF MAILED IN THE UNITED STATES

POSTAGE WILL BE PAID BY

ANALYTICAL CHEMISTRY

P. O. Box #8660

Philadelphia, Pennsylvania 19101

Analytical Chemistry **JANUARY 1971** Valid through MARCH 31, 1971

NEW PRODUCTS, NEW CHEMICALS, MFG. LITERATURE:

401 402 403 404 405 406 407 408 409 410 411 412 413 414 415
416 417 418 419 420 421 422 423 424 425 426 427 428 429 430
501 502 503 504 505 506 507 508 509 510 511 512 513 514 515
601 602 603 604 605 606 607 608 609 610 611 612 613 614 615
616 617 618 619 620 621 622 623 624 625 626 627 628 629 630
631 632 633 634 635 636 637 638 639 640 641 642 643 644 645

ADVERTISED PRODUCTS:

1	26	51	76	101	126	151	176	201	226	251	276	301
2	27	52	77	102	127	152	177	202	227	252	277	302
3	28	53	78	103	128	153	178	203	228	253	278	303
4	29	54	79	104	129	154	179	204	229	254	279	304
5	30	55	80	105	130	155	180	205	230	255	280	305
6	31	56	81	106	131	156	181	206	231	256	281	306
7	32	57	82	107	132	157	182	207	232	257	282	307
8	33	58	83	108	133	158	183	208	233	258	283	308
9	34	59	84	109	134	159	184	209	234	259	284	309
10	35	60	85	110	135	160	185	210	235	260	285	310
11	36	61	86	111	136	161	186	211	236	261	286	311
12	37	62	87	112	137	162	187	212	237	262	287	312
13	38	63	88	113	138	163	188	213	238	263	288	313
14	39	64	89	114	139	164	189	214	239	264	289	314
15	40	65	90	115	140	165	190	215	240	265	290	315
16	41	66	91	116	141	166	191	216	241	266	291	316
17	42	67	92	117	142	167	192	217	242	267	292	317
18	43	68	93	118	143	168	193	218	243	268	293	318
19	44	69	94	119	144	169	194	219	244	269	294	319
20	45	70	95	120	145	170	195	220	245	270	295	320
21	46	71	96	121	146	171	196	221	246	271	296	321
22	47	72	97	122	147	172	197	222	247	272	297	322
23	48	73	98	123	148	173	198	223	248	273	298	323
24	49	74	99	124	149	174	199	224	249	274	299	324
25	50	75	100	125	150	175	200	225	250	275	300	325

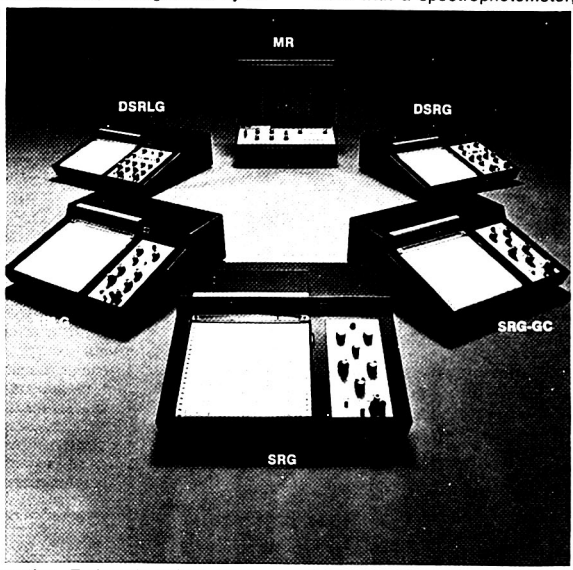
Potentiometric recorders: here's the picture.

Shown here, a portrait of all there is to know about potentiometric recorders. All from Sargent-Welch. And each deserves its own personality profile:

Model SRG: The basic recorder, distinguished by its advanced performance. Seven pre-calibrated spans. Three chart speeds. Guarded circuits and filtered inputs. Accuracy: ±0.25%. Reproducibility: ±0.1%. Full-scale pen response: Less than one second. Basic price: $975.

Model DSRG: The SRG times two. That is, a dual-pen recorder, with two linear channels, for recording two time-related variables, side by side or overlapping, on the same chart. Same matchless performance as the SRG, but only a few inches wider. Think of it as a space- and paper-saver. Basic price: $1675.

Model SRLG: The SRG taken one step further, with the addition of a logarithmic function. Eminently suited, therefore, for recording (say) the log of absorbance with a spectrophotometer. Precision, non-circular gears — which do the job much better than electrical approximations to the log function. Basic price: $1225.



Model DSRLG: Another logical move. Two SRLG's in one dual-pen recorder. Think of what that means if you work with a spectrophotometer, photometer, or densitometer — simultaneous recording of both transmittance *and* absorbance. Or linear/log recording of any two time-synchronized variables. Basic price: $2075.

Model SRG-GC: Something special, for use with a gas chromatograph. Fast response, high AC rejection, floating input, three chart speeds, and continuously variable wide-range spans. Optional integrator for precise measurement of areas under recorded curve. Basic price: $975 (with integrator, $1660).

Model MR: The ultimate recorder? Perhaps. Few can match it for precision, speed, sensitivity, and versatility. Measures and records (vs. time) any variable that can be translated into voltage or current, *or* that can be time-related by synchronous drive. Twelve ranges, twelve speeds. Basic price: $2650.

As we said, a complete picture of a complete line.

Now read the book.

0-214

Still, in all fairness, one picture and these few words don't do justice to our complete line of recorders. So we've prepared a fully illustrated, 30-page catalog. It's yours, without obligation, for returning the coupon. Do it now.

I'd like a copy of your recorder catalog. I'm especially interested in:

- ☐ Model SRG Recorder
- ☐ Model DSRG Dual-Pen Recorder
- ☐ Model SRLG Linear-Log Recorder
- ☐ Model DSRLG Dual-Pen Linear-Log Recorder
- ☐ Model SRG-GC Recorder for Gas Chromatographs
- ☐ Model MR Multi-Range Recorder

Name _____ Title _____

Organization _____

Address _____

City _____ State _____ Zip _____

Telephone _____ AC

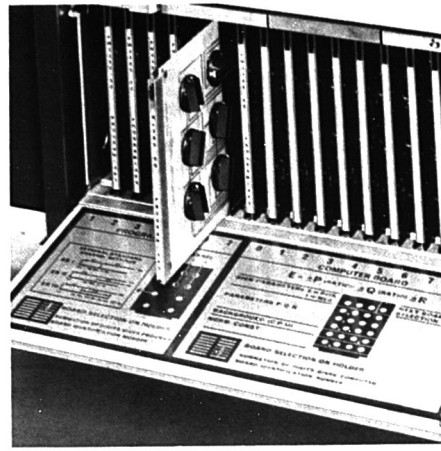
SARGENT-WELCH

Scientific instruments, apparatus, chemicals.
Sargent-Welch Scientific Company
7300 N. Linder Ave., Skokie, Illinois 60076

Chicago/Anaheim/Birmingham/Cincinnati
Cleveland/Dallas/Denver/Detroit
Springfield, N.J./Toronto/Montreal/Vancouver

Circle No. 167 on Readers' Service Card





There are 3 channel modules, 7 measurement programming boards, and 10 computing programming boards, in this improved Philips Automatic Liquid Scintillation Analyser

"... I'm sure all those modules and boards must save time and money, or you wouldn't have put them in. But what do they mean to a laboratory technician like me ... who must actually use the instrument?"
Fair question, young lady.
Yes, the new Philips Automatic, Multi-User Liquid Scintillation Analyser DOES save time and money for your laboratory. Its 21x20-sample capacity allows many more samples to be analysed in a workday. It optimises the use of the laboratory equipment budget ... and the precious time of the staff. But what's in this instrument for you?
Very simple. It does the routine work for YOU! Put in your samples ... turn it on ... read the results.
Don't worry about making mistakes ... THE INSTRUMENTS WON'T LET YOU! Once programmed, it will measure each sample tray with a different measuring and computing programme if you wish ... with no chance of error and no tiresome calculation. SIMPLIFIED OPERATION. FREEDOM FOR MORE PRODUCTIVE WORK. IMPROVED CHANCE FOR PROMOTION.

That's what's in it for you!
Why not ask your employer to send for our new brochure? Better still, order one for him. There's plenty in it for HIM too!

N.V. Philips' Gloeilampenfabrieken,
Analytical Equipment Department,
Eindhoven, the Netherlands.

PHILIPS ANALYTICAL EQUIPMENT



"That's really very nice... but what's in it for me?"

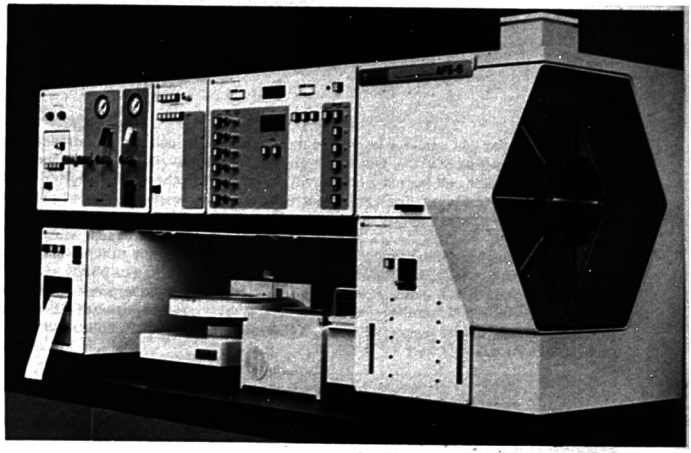
PHILIPS

Circle No. 159 on Readers' Service Card

NEW PRODUCTS

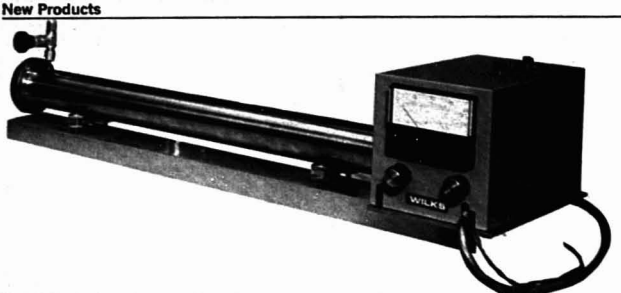
Equipment
Apparatus
Instruments

AFS-6 atomic fluorescence spectroscopy system offers six analytical channels; fluorescence and/or emission; automatic sample handling from preparation to digital printout; readout in direct concentration terms; and output rates as fast as 100 samples per hr. Standardization procedures are automatically performed by the system. The system uses hollow cathode lamps and electrodeless discharge tubes interchangeably; light sources are prealigned for snap-in/snap-out quick test changeover. There is great system flexibility and reliability. The instrument is scheduled for August delivery. The basic system costs $24,000. Technicon Instruments Corp., Tarrytown, N. Y. 10591. 914-631-8000 **401**





IBM System/7 is a low-cost, modular computer designed for taking readings from many measuring and testing devices and analyzing them almost instantaneously. Application notes describe its use in spectrometer operation, continuous process control, batch process control, instrument calibration, and process gas chromatograph operation. It can function as a self-contained system, or as part of a network in which it interacts with other IBM computers, such as the 1130, 1800, System/370, and most models of System/360. The system includes a processor module, input-output modules, and an operator station. Monthly rental is $352 for the smallest IBM System/7, including the processor, 2048 words of monolithic memory, and one input-output module. The purchase price is $16,060. Additional memory increments of 2048 words rent for $105, or can be bought for $3675. Initial customer shipments are scheduled for November 1971. International Business Machine Corp., 112 E. Post Rd., White Plains, N. Y. 10601. 914-696-1900 **402**



Model A-1 infrared gas analyzer has a one-meter pathlength cell and can detect and identify such gases as SO_2, CO, NO, and many hydrocarbons. Other models include one with a 10-meter cell having a sensitivity in ppm and others with shorter cells for higher concentrations. The instrument uses a circular variable filter to provide monochromatic radiation and a newly developed pyroelectric detector to measure its intensity. Up to 10× scale expansion is possible for increased sensitivity. Resolution is roughly equivalent to a rock salt prism and response time is less than one sec full scale. Scanning time is about 3 min for the complete spectral range (2–14.5 microns) or the instrument may be hand set to any absorption band and concentration vs. time recorded. Most versions of the gas analyzer are priced at less than $2000. Wilks Scientific Corp., 140 Water St., Box 441, South Norwalk, Conn. 06856. 203-838-4537 **403**

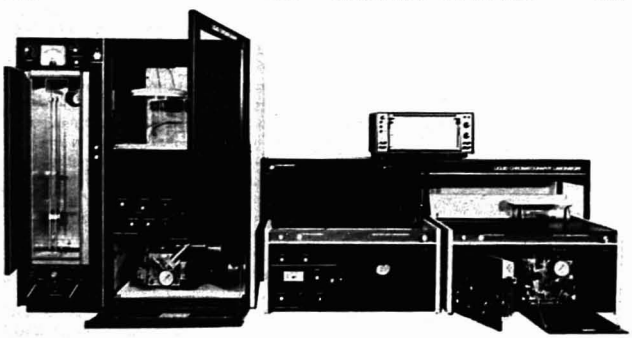
Viscometers

A new falling ball viscometer displays fall time on a five-digit Nixie register. Range of measurement is from 2 to 100,000 cs with a standard deviation of 0.1%. The instrument costs $7500.

A new laboratory viscometer measures viscosity of fluids in the control lab or in the plant for on-line samples. A sample is metered through a calibrated capillary at 56.6 cc/min in a constant temperature bath. Available in ranges from 0 to 2500 cP for ambient to 240°F bath temperatures, the unit costs $4000. Hallikainen, 750 National Ct., Richmond, Calif. 94804. 415-233-2010 **404**

Sodium Electrode

A new sodium electrode is said to respond faster to changes in sodium ion than any other commercially available electrode. A flat section of sodium-sensitive glass is set into a rugged epoxy body that protects the glass membrane from cracking, chipping, or shattering. The electrode is highly selective for sodium—said to be equal to or better than previous sodium electrodes. Two types are offered: Model 94-11, a dipping electrode ($150); and Model 96-11 ($195), a combination sodium and reference electrode. Orion Research Inc., 11 Blackstone St., Cambridge, Mass. 02139. 617-864-5400 **405**



Liquid chromatography laboratory provides three complete chromatographs to permit rapid, methodical analyses. System includes Model ALC/GPC-301 (left), ALC-202 with uv detector (center), and ALC-201, and two-pen chart recorder (top right). Price of the complete laboratory is under $20,000. Optional accessories include a digital curve translator for GPC data acquisition, recorders, an automatic fraction collector, a solvent programmer, and an additional detector. Waters Assoc., 61 Fountain St., Framingham, Mass. 01701. 617-879-2000 **406**

Electrophoresis Equipment

Laboratories using standard 8-sample electrophoresis systems can adapt their equipment so that they can apply all 8 samples simultaneously. The Sepratek conversion lid permits the use of the company's multiapplicator. The lid adapts the Beckman Microzone chamber to use the Sepratek multiapplicator. The latter ensures uniform sample application and maintains positive sample identification. The conversion lid costs $40; the multiapplicator, $115. Gelman Instrument Co., 600 S. Wagner Rd., Ann Arbor, Mich. 48106. 313-665-0651 **407**



Differential I light scattering photometer combines the latest advances in laser technology with solid-state electronics to automatically measure light scattered by microparticles as a function of the scattering angle. Light scattering characteristics are unique to certain classes of material and permit deduction of inherent structure features. The instrument also can be used for conventional turbidimetric and nephelometric measurements. The monochromatic, single-mode, highly collimated laser beam illuminates the liquid sample; a high quality photodetector automatically scans the scattered light over preselected ranges between 10 and 170 degrees. The recorded plot is of scattered light vs. angle. Special circuits and electronic design aid the processing of the data. The argon-ion laser, tunable to five wavelengths, is plane-polarized. Physical scientists use light scattering measurements for determining colloidal sizes, size distributions, and dielectric structure; also to determine molecular weights, refractive indices, etc. The instrument also has applications in microbiology and biochemistry. Price including laser and recorder is $9750. Science Spectrum, 1216 State St., P. O. Box 3003, Santa Barbara, Calif. 93105. 805-963-8605 **408**

Perkin-Elmer's new Atomax™ lamps fit any atomic absorption instrument you use.

Now, no matter what AA instrument you use, you no longer have to settle for second best in lamps.

Perkin-Elmer introduces Atomax hollow-cathode lamps, directly usable in all makes of atomic absorption equipment.

Perkin-Elmer has long led the field in atomic absorption; we ship more instruments worldwide than all eighteen other manufacturers put together. Much of this leadership is based on the quality of our Intensitron® hollow-cathode lamps. The Intensitrons, however, with a two-inch diameter, are hard to use in many AA's with restricted lamp space. Now, the new Atomax lamps give Intensitron performance in a smaller envelope with an octal socket. They fit directly into most atomic absorption spectrophotometers.

Advantages of Atomax lamps. Atomax lamps are available for every element that can be done by atomic absorption, and also in many multi-element combinations, including the famous seven-element lamp for Ca-Mg-Zn-Cu-Fe-Al-Si.

Rigid quality control assures that all lamps meet the same high standard for intensity, stability, and spectral purity. Shipment of lamps is fast, usually within eight working hours from receipt of order.

Lamp life. Atomax lamps contain more gas than the "necked-down" sources presently available so they offer longer performance. However, Perkin-Elmer's larger Intensitron lamps have endurance that smaller lamps cannot match, so users of Perkin-Elmer AA instruments should continue to employ Intensitrons.

Free gift offer. If you send for data now, you will receive a free Atomax Miniature Broadband Continuum source which radiates between 3800 and 8000 A. Hang it on your keychain. It also works as a flashlight.

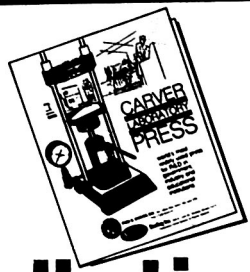
For data and free gift, write Instrument Division, Perkin-Elmer Corporation, 702 Main Avenue, Norwalk, Connecticut 06852.

PERKIN-ELMER



Circle No. 143 on Readers' Service Card

Get this new bulletin!

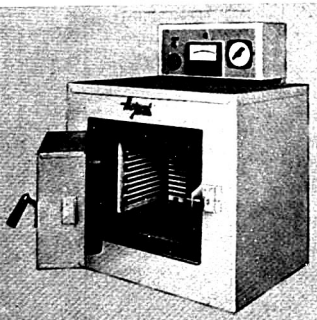


CARVER LABORATORY PRESSES

Complete description and prices of all models and accessories . . . including new air operated quick closer, constant pressure devices and complete motorization package. World's most widely used presses for R & D, testing, laminating, pelletizing, short run production. Capacities to 25 tons.

FRED S. CARVER, INC.
13 Chatham Road, Summit, New Jersey 07901
Sterlco a subsidiary of **Sterling, Inc.**
Milwaukee, Wisconsin

Circle No. 35 on Readers' Service Card

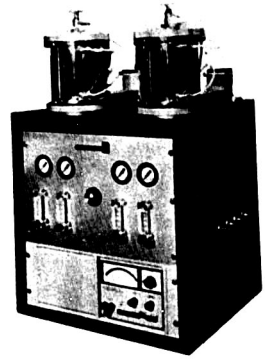


2350°F WORKHORSE

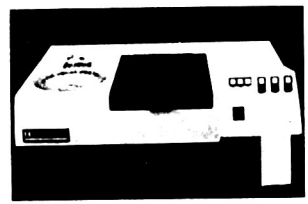
Model 7764 furnace gets the job done—any fusing, ashing, drying, enameling or heat treating job up to 2350° (1290°C)! An indicating-controlling instrument (for direct temperature setting) and a wattage selector put you in complete control at all temperatures. The fully insulated 3½ cu. ft. work chamber assures rapid heat-up and minimum heat loss. Sizes range from ½ to 8 cu. ft., write for complete literature today. Hotpack Corporation, 5004 Cottman Ave., Phila., Pa. 19135, (215) 333-1700. In Canada: Hotpack (Canada) Ltd., Waterloo, Ont.

Hotpack

Circle No. 87 on Readers' Service Card



Model DAT-T1 features a sample holder and temperature sensing circuit that has the sample and reference material thermocouples matched to within 3 μV. The instrument is able to resolve temperature differentials to 0.03°C/in. on the chart. The sample holder has capacities for micro- and macrosamples up to 1.25 cc. Provision for vacuum operation is included. Temperature range is from ambient to 1550°C. Harrop Laboratories, 3470 E. Fifth Ave., Columbus, Ohio 43219. 614-236-0291
409



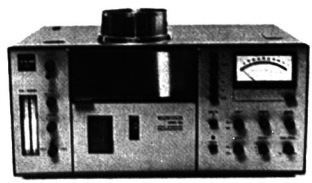
Coaglab system measures prothrombin time and partial thromoboplastin time simultaneously at a rate of 60 samples (120 determinations)/hr. Less than 0.2 ml of plasma is used; only 0.06 ml of reagent is required for each reaction. Following centrifugation of the blood in original collection tubes and insertion of the tubes into the sampler tray, no manual procedures are required to profile the samples. As each sample is aspirated into the system, it is deposited, with appropriate reagents, on a spot of magnetic iron oxide in which the reaction occurs. The opaque metallic particles in suspension act as a light barrier. Clot formation causes the iron particles to form a small lump, and the reaction is detected by means of light passage through the clarified liquid onto a photodetector cell. Cassettes of transparent tape provide a convenient, easily loaded medium for the iron oxide spots. Both test results are printed in digital

Very simply,
we'd like to say
that we are introducing
a new low cost
atomic absorption spectrophotometer
and that we'd like to emphasize
the combination of price,*
performance** and features.***
Thank you.

* Under $3,000.

** The new Varian Techtron Model 1000 is not only fully able to handle trace, major constituent and quantitative analyses for more than 66 elements, but is also an excellent teaching tool. With extreme sensitivity in just about any concentration units you need.

*** Built-in features include flame emission chopper, variable slits, four-lamp turret, tilt-out meter and automatic baseline correction.



The 1000.

For complete details, or a demonstration, write Varian Techtron, Walnut Creek, California 94598; NEVA Azabudai Bldg., Tokyo, Japan; Malton, Ontario, Canada; Crows Nest, N.S.W., Australia; or Zug, Switzerland.

varian techtron

Circle No. 191 on Readers' Service Card

FOR THINGS ULTRAVIOLET call on the specialist

NEW high intensity 280 nm lamp measures proteins. Miniature PENRAY® lamps calibrate photometers in space, sterilize devices in the laboratory. CHROMATO-VUE® darkrooms help diagnose afflicted children, analyze food impurities, help in the fight against cancer. BLAK-RAY® ultraviolet meters assure efficiency of germicidal lamps, measure UV dose in mutation studies, establish reproducibility of UV experiments in photochemistry and biological sciences.

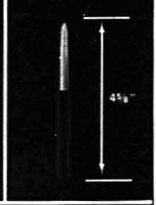
Every day our products solve similar problems. But then, other people's problems are "our thing." That's why we specialize in ultraviolet.

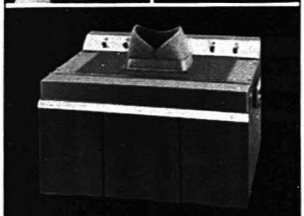
THE BROADEST ULTRAVIOLET LINE

HAND LAMPS
Many powerful MINERALIGHT® & BLAK-RAY® models.



PEN-RAY® LAMPS
Standard for wavelength calibration.



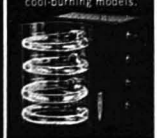


CHROMATO-VUE® & TRANSILLUMINATORS
Fluorescent darkrooms on a table top.

UV METERS—Positive check of germicidal lamp output.



P.C.Q.® LAMPS
Several intense, cool-burning models.



Write for new literature

ULTRA-VIOLET PRODUCTS, INC.

Specialist in specialty lamps since 1932

Suite 117 • 5114 Walnut Grove Avenue
San Gabriel, California 91778

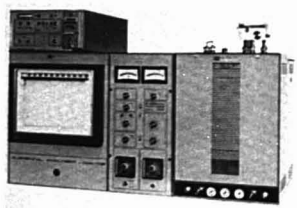
Circle No. 181 on Readers' Service Card

New Products

form to tenths of a second. The Coaglab system offers flexible modes of operation and can be used in conjunction with the company's AutoCounter (for platelet counting) or the new Hemolab system. The Coaglab without the platelet counting system costs $13,300; with platelet counting, $21,600. Technicon Instruments Corp., Tarrytown, N. Y. 10591. 914-631-8000 **410**



Chloride meter made by Evans Electroselenium, Ltd., of England (a new subsidiary of Corning Glass Works) provides readout accurate to ±1 meq/l. on a typical sample size of 0.2 ml. The instrument is designed for medical applications. Model 92 chloride meter costs $750. Corning Glass Works, Medfield, Mass. 02052. 607-962-4444 **411**

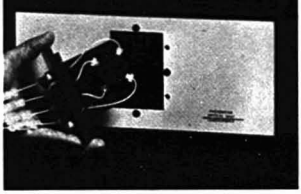


Automatic elemental analyzer for carbon, hydrogen, nitrogen, and oxygen, Carlo Erba Model 1102, features automatic sample injection for up to 23 samples. After loading the sample magazine, the analyses proceed automatically. The instrument uses automatic combustion through instantaneous flash pyrolysis and a unique oxygen injection technique. Two separate reactors, one for CHN and a second for O_2, as well as two chromatographic columns are used in the system. If used with the Model 1110 electronic integrator, peak integration is obtained simultaneously and automatically. The instrument will perform 23 complete analyses in 6 hr. Model 1102 costs $9800. Sanda, Inc., 130 Presidental Blvd., N., Bala Cynwyd, Pa. 19004. 215-839-0200 **412**

New UV Detector

- wide linear range
- high sensitivity
- O.D. and % T
- microflow cells





Chromatronix Model 200 UV Photometer combines a linear absorbance range up to 3.0 O.D. with very low noise and drift—less than .0004 O.D. Measurements can be made on any of ten absorbance ranges (from .01 O.D. full scale to 5.12 O.D. full scale) or on a single 0 to 100% transmittance scale. Recorder outputs of 1 mv and 10 mv are supplemented by a 0 to 1 ma output, which will drive low-cost galvanometric recorders. Two interchangeable plug-in flow cells are available: an 8-μl cell for micro-column analyses and a 32-μl cell for monitoring preparative separations, density-gradient centrifugation and electrophoresis.

Free new technical bulletin. A technical bulletin describing the use of ultrasensitive UV detectors in liquid chromatography is yours for the asking. Please address us at 2743 Ninth Street, Berkeley, California 94710. Phone (415) 841-7221.

CHROMATRONIX

Circle No. 32 on Readers' Service Card

FEBRUARY SESSIONS

The following ACS Short Courses are newly scheduled for February 1971. Two courses, including the premier session of "Interfacing the Minicomputer," are being offered in conjunction with the 22nd Pittsburgh Conference on Analytical Chemistry and Applied Spectroscopy.

To register or obtain complete information on the courses, convenient lodging, and student discounts, please write to Education Office, American Chemical Society, 1155—16th St., N.W., Washington, D.C. 20036. During the two-week period prior to a course, registration should be made by telephone: area code 202, 737-3337 ext. 258.

COLUMN SELECTION IN GAS CHROMATOGRAPHY

Feb. 6—Baltimore, Md. Dr. Harold M. McNair and Dr. Walter R. Supina; fee $60; in conjunction with ACS 6th Middle Atlantic Regional Meeting.

This course explores the critical step in gas chromatography, the selection of the proper column, from both the theoretical and practical point of view. Column material, length, diameter, solid support, and per cent liquid phase are discussed. The results obtained with different columns and different operating parameters are shown in chromatograms. Rules are developed to aid in choosing proper conditions. It is assumed that the registrant has been working with a gas chromatograph. No background in higher mathematics is required.

APPLIED POLYMER SCIENCE

Feb. 25–27—New York City area. Dr. Robert W. Lenz and Dr. Adi Eisenberg; fee $110 including lunches; required text, R. W. Lenz, "The Organic Chemistry of Synthetic High Polymers," John Wiley and Sons, Inc., 1967, $16.

This introductory course aims at providing a fundamental basis for a scientific approach to polymer preparations, properties, behavior, and applications. It surveys the important aspects of the synthesis of useful high molecular weight polymers, and the measurement and interpretation of the physical and mechanical properties most important for their utilization. Detailed consideration is given to the preparation and reactions of polymers, polymerization kinetics and mechanisms, rheology, and physical and mechanical properties. This is not a course in polymer engineering, which will be the subject of a future ACS Short Course.

AT PITTSBURGH ANALYTICAL CONFERENCE IN CLEVELAND, OHIO

GC/MS/COMPUTER TECHNIQUES

Feb. 27–28—Dr. Francis W. Karasek, Dr. William H. McFadden, and Walter E. Reynolds; fee $85; required text, L. S. Ettre and W. H. McFadden, eds., "Ancillary Techniques of Gas Chromatography," John Wiley and Sons, Inc., 1969, $17.50.

This course first reviews the fundamentals of gas chromatography and mass spectrometry, and then presents in more depth the principles important to the GC/MS combination instrumentation. Subject matter includes the characteristics of the different types of mass spectrometers, the GC/MS interfaces, discussion of instrumentation, the GC/MS combination, and computerization of the output. Although a B.S. in chemistry or related science is a desirable background, anyone with sufficient experience—or the assigned responsibility—to work with the instrumentation will benefit from the course.

INTERFACING THE MINICOMPUTER

Feb. 27–28—Dr. Raymond E. Dessy and David G. Larsen; fee $100; required text, H. Malmstadt and C. Enke, "Digital Electronics for Scientists," W. A. Benjamin, Inc., 1969, $9.50.

This new course demonstrates in detail how to interface analytical equipment and other instruments to a minicomputer. The goal is to enable the registrant to build his own multipurpose interface. The basic building blocks of an interface are displayed in actual operation. Then various interface packages are assembled, with closed circuit TV being used to allow viewing of all steps. Multiplexing, device-code addressing, computer timing cycles, and ADC/DAC elements are emphasized. Registrants should have some background in instrumentation.

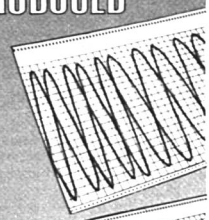
1200 SOLD IN 8 MONTHS

proves new Omnigraphic® recorder offers Versatility, Reliability and Price

and now... for added versatility



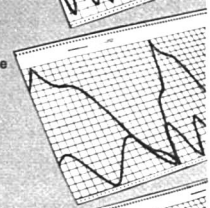
3 NEW FUNCTIONAL UNITS INTRODUCED



2 Pen Strip Chart

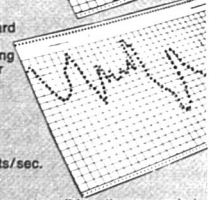
. . . for those applications requiring two simultaneous full scale recordings, the series 2-3300 is the ideal, economical recording tool.

Paper size:	10" (25cm) x 100'
9 pushbutton speeds:	.05 to 20 in/min.
Plug-in modules:	a dozen different signal conditioning modules are interchangeable between Y_1 and Y_2 axes.
Electric pen lift and event marker:	standard
Price:	Model 2-3300-52 $1205. plus selected Y axes modules.



Automatic Integration for GC

. . . is possible simply by plugging the new type 13 module into the Series 2-3300-52 recorder. The integral is recorded in the Y_2 channel, using the full 10" chart width for recording. The trace is "folded" at the bottom and top of the chart grid so that integration continues indefinitely, providing improved resolution. Type 13 Module costs $475. Write for brochure which fully describes the recorder, integration and peak area measurement.



Economical Point Plotter

. . . is achieved by plugging two modules into your standard model 3000 strip chart recorder. Modules 16 and 17 convert the strip chart to a true point plotter for handling data from Pulse Height Analyzer, Digital Oscilloscope or Averaging Computer. The cost is nominal, only $1695.

- 4 resolution selections: .025", .050", .075" and .100".
- Interchangeable Fibre Tip Colored Pen Points
- Maximum sensitivity setting 1 mv/in.
- At resolution setting of 40/in. plotting rate is 15 points/sec. (will plot 400 channels in approximately 27 sec.)

Write today for the newest Houston Instrument brochure describing the expanded variety of functions available to present users of the HI model 2000 X-Y and model 3000 strip chart recorders. Twelve plug-in modules available . . . and more in R&D.

®A registered trademark of Houston Instrument

houston instrument | DIVISION OF BAUSCH & LOMB

4950 TERMINAL AVENUE, BELLAIRE, TEXAS 77401
(713) 667-7403 CABLE HOINCO

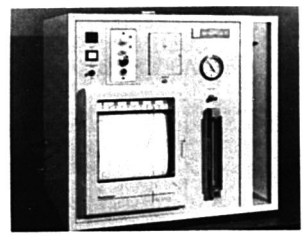
houston instrument | European Office | 8043 Unterfohring, München, Johanneskirchner Strasse 17, W. Germany (0811) 36-6300

Circle No. 86 on Readers' Service Card

New Products

Gc-Ir System

The Model 41B gc-ir analyzer is a fraction concentrator which momentarily traps a fraction and then injects it in concentrated form into the ir cell for analysis. With this system, any fraction having a total weight of between 10 and 50 μg and boiling below 250°C should produce a characteristic ir spectrum. The concentrator fits most infrared spectrophotometers and may be connected to output of any gas chromatograph. It is also available as an integrated system (Model 12-41B) including the gc-ir analyzer, a fast scan Model H-1200 Infragraph spectrophotometer, and related supplies. The Model 41B costs $2000. Wilks Scientific Corp., 140 Water St., Box 441, South Norwalk, Conn. 06856. 203-838 4537 **413**



Air monitor IV will detect and quantitate any one of six parameters: SO_2, total oxidants, NO_2, NO_x, H_2S, or fluoride. Analyses may be performed continuously, in ambient air, or in liquid-impinged samples introduced in the laboratory. Results can be presented in a digital printout, in direct concentration terms appropriate to the test. The system has integral data handling capability to permit transmission of results obtained in remote locations or direct input of results into a lab computer, and a two-speed pump, for either continuous remote sampling, or controlled laboratory analyses. The company has other air monitoring equipment including the Monitor IIA which completely automates wet chemical analyses. This instrument can be programmed by a change of manifold and colorimeter filters to perform SO_2 or NO_2. Built-in range expansion permits a selection of sensitivity ranges for SO_2 or NO_2 of 0–1 ppm, 0–0.5 ppm, and 0–0.2 ppm, and for H_2S of 0–170 ppb and 0–50 ppb. Price for the basic system of Monitor IIA is $4306. Monitor IV costs $5430 with the accessory for SO_2. Technicon Corp., Tarrytown, N. Y. 10591. 914-631-8000 **414**

Now! Turn your sulphuric acid ***instantly*** *into an efficient labware cleaner!*

CHROMERGE

mixes easily with sulphuric acid to clean safely, speedily.

Just pour one pre-measured bottle of Chromerge into a 9-lb. container of sulphuric acid, for a super-efficient chromic-sulphuric acid solution that removes stubborn deposits which resist other cleaners! Chemically and bacteriologically clean ...protects glass surfaces...gives a perfect miniscus for precise volumetric work!

19-089-01 — 6x25cc — $7.98
Case/4 per package — $28.80

NO HOOD. NO GLOVES. NO MIXING WITH WATER. NO BOILING!



Now Available in safe metal can, from your laboratory supply dealer.

MANOSTAT Division of Greiner Scientific Corp.
24 N. Moore Street, Dept. 521, New York, N.Y. 10013
Phone (212) 966-1190

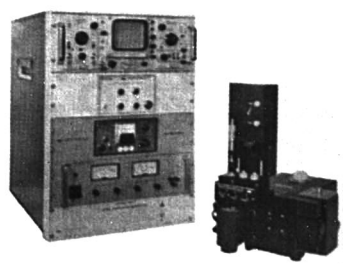
Circle No. 71 on Readers' Service Card

new stopped-flow spectrophotometric system

incorporating the Aminco-Morrow Stopped-Flow Apparatus and the New Aminco Grating Monochromator

- Permits reactions to be monitored after only 3 to 5 milliseconds' dead time
- Utilizes quantities as small as 100 μl from each of the two reservoirs
- Allows reactants in reservoirs to be changed quickly and easily without tools

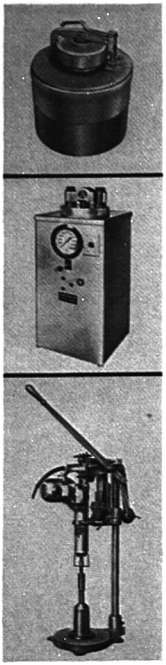
Other systems are available which incorporate the very versatile Aminco-Morrow Stopped Flow Apparatus and utilize instrumentation already in your laboratory. For further information about rapid-reactions instrumentation write to



AMINCO

AMERICAN INSTRUMENT COMPANY
A DIVISION OF TRAVENOL LABORATORIES, INC.
Silver Spring, Maryland 20910

Circle No. 9 on Readers' Service Card



Sample Preparation Equipment for Spectrochemical Analysis

Laboratory Disc Mills
for rapid, uniform sample grinding. These swing mills are ideal for specimen preparations. Three types: bench, enclosed and suspended production.

Hydraulic Briquetting Press
has automatic pressure regulator that assures uniform briquet densities. Uses molds to 1¾". A manual model also available.

Mortar and Pestle Assembly
is power driven for either electric or air hammer use. Gray iron, white iron or any brittle sample can be quickly crushed for analysis.

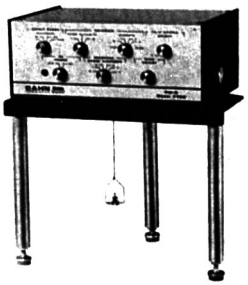
Ångstrom, Inc.
678 E. HURON RIVER DRIVE
P. O. BOX 256
BELLEVILLE, MICHIGAN 48111

Circle No. 1 on Readers' Service Card



Circle No. 105 on Readers' Service Card

New Products



RM-2 Recording Electrobalance measures weight changes as small as 5 μg. Major applications are thermogravimetry, static and dynamic surface tension, particle sedimentation, and magnetic susceptibility. The balance handles samples up to 10 g. Recorder outputs are 1, 7, and 10 mV to drive any standard strip chart of X-Y recorder and a 10-V/g output to operate a digital voltmeter or other digital recording devices. A wide range of accessory systems for specialized applications is available. $1350. Cahn Div./Ventron Corp., 7500 Jefferson St., Paramount, Calif. 90723. 213-634-7840 **415**

Programmable Desktop Calculators

Communication between desktop calculators and a wide variety of external devices is provided by a new plug-in interface for the HP Model 2570A coupler/controller. Instruments such as digital voltmeters, counters, and quartz thermometers can communicate with the calculator. The calculator can control instrument functions and produce formatted output with headings and labels on teleprinters. There is an extensive line of calculator peripherals which can be plugged in. The 2570A coupler/controller is $1625. Hewlett-Packard Co., 1601 California Ave., Palo Alto, Calif. 94304. 415-326-7000 **416**

X-Y Recorders

Plotamatic 805 and 815 are new 11- × 17-in. X-Y recorders for providing graphic output display in applications not requiring a time base. Primary users include chemical, analytical, and medical OEM producers, electronic laboratories, etc. These recorders are said to meet or exceed most current recorder specifications but are lower in price ($850 to $980). The recorders offer a zero adjustment of full scale plus 100% suppression and slewing speeds in excess of 20 in./sec. Bolt, Beranek and Newman, Inc., 1762 McGaw Ave., Santa Ana, Calif. 92705. 714-546-5300 **417**



THE SOPHIS-TICATES

Meet four of a myriad of research dewars custom-designed and carefully constructed* by Cryogenic Associates Inc. . . . research dewars most sought after by the chemist, the physicist, the biologist, the aerospace engineer . . . to mention a few.

These sophisticated non-nitrogen and nitrogen shielded helium research dewars are available as complete systems with Cryogenic Associates' *exclusive* custom flexible tube transfer lines, temperature and liquid level controllers, sensors and electronic power supplies.

Contact Cryogenic Associates . . . the team whose expertise has attracted the confidence of the most critical buyer.

*All products bear a *full guarantee* for one year on materials and workmanship.

CRYOGENIC ASSOCIATES INC.

". . . for the finest in Cryogenic Systems".

1718 North Luett Avenue
Indianapolis, Indiana 46222
Phone: (317) 632-2515

Catalog Available On Request

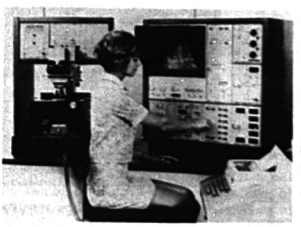
Circle No. 31 on Readers' Service Card

Floating Point Processor for PDP-12

A floating point processor for the PDP-12 laboratory computer does calculations as much as 39 times faster. The FPP-12 is designed for all types of floating point arithmetic. Typically, a three-word, 36-point floating point multiply took 1100 μsec when done by software, and 500 μsec when done by software and an Extended Arithmetic Element. An FPP-12-equipped PDP-12 can do the same calculation in 28 μsec. The price of the unit is $7500. The basic price of the PDP-12 which includes visual display, analog-to-digital converter, and two magnetic tape units, is $29,900. Digital Equipment Corp., Maynard, Mass. 01754. 617-897-5111 **418**

Low-Cost Digital Computer

The SPC-12 automation computer with 4K memory (expandable to 16K) is ideal for remote site, locally dedicated control applications. Priced at only $3600 the computer includes 4K words of 8-bit core memory, power supply, chassis, and front console. It also features four 12-bit hardware accumulators, three 12-bit hardware index registers, real-time clock, operations monitor alarm, a 12-bit parallel I/O channel, a serial I/O channel and teletypewriter interface, priority interrupt control with an interrupt line, DMA/DMT expansion capability, and a free comprehensive software support package. General Automation, Inc., 1055 S. East St., Anaheim, Calif. 92805. 714-778-4800 **419**



Quantimet 720 image analyzing computer performs pattern recognition tasks. Designed as a research instrument, the computer is of modular design and allows the easy addition of many extra modules to the basic system. The instrument will be shown at Nepcon '71 West at the Convention Center, Anaheim, Calif., Feb. 9 to 11. The instrument is made by Image Analysing Computers, Ltd., Melbourne, Royston, Hertfordshire. $35,000. The U.S. subsidiary is Imanco, 40 Robert Pitt Dr., Monsey, N. Y. 10952 420

this new booklet "figures" to help you



Send for FREE MC&B conversion booklet

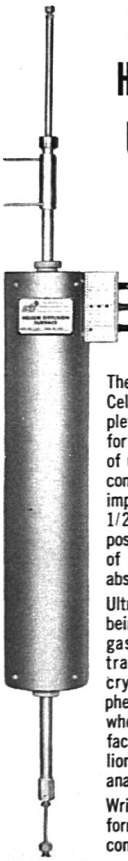
Order now and help will be on the way fast. Help in the form of hundreds of figuring formulae for quick and easy conversions. Included in our booklet is everything from Abcoulombs to Statcoulombs, yards to millimeters. Have we converted you? If so, fill out the handy coupon and mail.

MC/B MANUFACTURING CHEMISTS
Norwood, Ohio, Baton Rouge, La., East Rutherford, N.J., Los Angeles, Calif.

3-70 MCB
MC&B MANUFACTURING CHEMISTS
2909 Highland Avenue
Norwood, Ohio 45212
I'm converted! Send me your Conversion Booklet.
NAME_____
COMPANY_____
ADDRESS_____
CITY_____
STATE_____ ZIP_____

Circle No. 123 on Readers' Service Card

99.99995% PURE HELIUM



CONTINUOUS
HIGH OUTPUT
UNATTENDED
OPERATION
LOW COST
LONG LIFE

The ETI Helium Diffusion Cell Purifier is a complete equipment, ready for continuous production of ultra-pure helium from commercial grades. Total impurity levels as low as 1/2 part per million are possible without the use of liquid nitrogen-cooled absorbents.

Ultra pure helium is now being used extensively in gas chromatography, transistor processing, crystal growing atmospheres and other services where high purity helium facilitates parts per billion accuracy in critical analyses.

Write for additional information or engineering consultation.

Electron Technology, subsidiary of Esterline Corporation, 626 Schuyler Ave., Kearny, N.J. 07032 • (201) 998-8100

ELECTRON TECHNOLOGY

ESTERLINE

Circle No. 52 on Readers' Service Card

Here it is! The Perkin-Elmer Model 247

The moderate cost grating infrared spectrophotometer that gives you:

- 4,000^{cm-1} to 650^{cm-1} range
- 6 scan speeds
- 2^{cm-1} resolution at 1,000^{cm-1}
- built-in 4x abscissa expansion
- flatbed stripchart recorder
- continuous, unbroken recording
- automatic indexing
- time drive

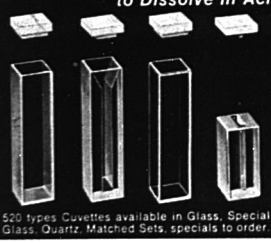
Write for full information on this modestly priced grating IR to: Instrument Division, Perkin-Elmer Corporation, 702 Main Avenue, Norwalk, Conn. 06852.

PERKIN-ELMER



Circle No. 145 on Readers' Service Card

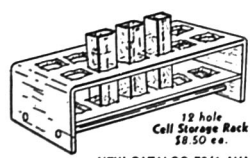
LOW PRICES ON QUALITY
ABSORPTION CELLS
Fully Fused—No Cemented Seams to Dissolve in Acid.



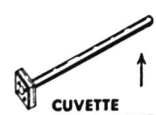
520 types Cuvettes available in Glass, Special Glass, Quartz. Matched Sets, specials to order.



CUVETTE WASHER-DRYER *The only fast way to wash and dry cuvettes without scratching or breaking. Completely assembled (without filtering flask) $16.00 ea.*



12 hole Cell Storage Rack $8.50 ea.



CUVETTE ADD-A-MIXER *used for adding small volumes of enzyme solution to reaction mixtures in spectrophotometer cuvettes $2.50 ea.*

NEW CATALOG 70/1 AVAILABLE

PRECISION CELLS, INC.
221 Park Ave. • Hicksville, N. Y. 11801
(516) 938-7772

Circle No. 133 on Readers' Service Card

NEW CHEMICALS

Tlc Reagent Proves Useful in Laser Technology

A dye, Rhodamine 6G, used routinely as a visualization reagent in tlc has now been reported to produce a continuous laser beam from a water solution of the dye excited by an argon ion laser. Rhodamine 6G has a molecular weight of 479.02 and is tunable from 570 to 625 microns. Eastman Kodak Co., Dept. 412L, Rochester, N. Y. 14650. 716-325-2000 **501**

Fluorocarbon 214

Fluorocarbon 214 (1,1,1,3-tetrachlorotetrafluoropropane) is a new commercial product said to be useful as a solvent in preparation of the stationary phase for reverse phase chromatography in the separation of tRNA's. Other suggested applications include its use as dielectric and heat transfer fluids. The chemical costs $11 for 25 g; $33, 100 g; $149, 500 g; and $264, 1 kg. PCR, Inc., P. O. Box 1466, Gainesville, Fla. 32601. 904-376-7522 **502**

Clinical Reagents

A new triglyceride set offers a reliable, fast, colorimetric method for the routine clinical lab determination of triglyceride. The reaction develops color that is stable for more than one hour. The extraction mixture is prepackaged in single use extraction tubes and the stable stock standard is supplied.

The T-4 tetraiodothyronine test as an indicator of thyroxine activity is often being used in place of PBI tests. A new T-4 set consists of disposable plastic columns filled and ready to use, a complete set of elution reagents, and color reagents for either manual or automated chemistry. A stable, primary T-4 standard is also supplied.

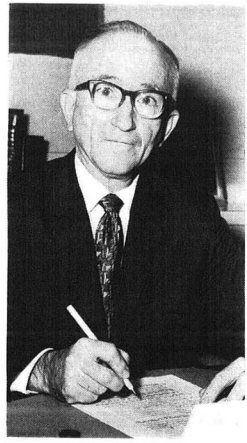
For more technical information on these sets and for data, write to Harleco, 60th & Woodland Ave., Philadelphia, Pa. 19143. 215-726-9600 **503**

Gc Support

A new ceramic support material for gas chromatography is designated Cera-Beads. Desirable properties include spherical shape, chemical inertness, thermal stability, uniform particle size, and low resistance to mass transfer. Analabs, Inc., 80 Republic Dr., North Haven, Conn. 06473. 203-288-3400 **504**

Samford University's, Dr. J. H. Langston:

"I evaluated analytical balances for a year... but it was a 15 minute TORBAL demonstration that sold me."



Dr. J. H. Langston, Chairman of the Chemistry Department at Samford University, needed some new analytical balances that could stand up under use by as many as twenty chemistry students per day. It took the Torsion representative just 15 minutes to point out that the no-knife-edge torsion design principle provides this kind of ruggedness—plus high accuracy and precision.

As a result of this demonstration, Samford University equipped their analytical lab with TORBAL EA-1 electronic analytical balances. The EA-1, with a capacity of 160 g and precision of 0.03 mg, features an electronic null indicator, which eliminates inaccuracies due to sensitivity variations, and complete digital readout to 0.1 mg for faster, easier reading.



We'd welcome the chance to demonstrate the EA-1 to you. Just call your nearest Torsion sales representative.

THE TORSION BALANCE CO. Dept. J. Main Office and Factory: Clifton, N.J.; Sales Offices: Chicago, Ill.; San Mateo, Cal.; Pittsburgh, Pa.; Plants and Offices in Montreal, Quebec; London, England and Waterford, Ireland

TORBAL

Circle No. 174 on Readers' Service Card



FASTEST GUN IN THE LAB!

Make an instant aerosol with any sprayable liquid! Apply reagents and indicators for thin layer and paper chromatography. Especially useful when reagents must be mixed for immediate or same-day use. Hundreds of everyday uses from sophisticated analyses to aerosol testing—and even touch-up painting.

Quixpray has *POWER!* It has all the power that's needed to produce a true aerosol mist from sprayable liquids. Other sprays, to hold down "flooding" with thin liquids, merely use a lot less pressure. We have a better approach. Each **Quixpray** head is equipped with a full bore dip tube for broad general use. As an accessory we offer a set of two flow regulating dip tubes—(1) Fine, for water-thin liquids and (2) Extra Fine for very thin liquids such as organic solvents. Now—whether you're spraying an alcoholic solution on a paper chromatogram or touch-up paint on a lab bench—you can be sure you're getting the complete dispersion produced by full power.

Quixpray Kit has one complete spray unit with 8 extra jars for storing stock liquids and 6 propellant refills. Also included are the two special flow regulating dip tubes mentioned above.

11160 **Quixpray Kit** $18/kit; 12 kits, $16/each

11175 **Quixpray**, Propellant refills, 15 oz Case of 12 $16.80/case

11170 **Quixpray**, Jars only, 4 oz Case of 12 $4/case

11165 **Quixpray**, Single spray unit (Head, propellant and jar with full bore dip tube) $3.25/unit

11180 **Quixpray**, Flow regulating dip tubes Set of 2 $3/set

PIERCE CHEMICAL COMPANY
P.O. Box 117 Rockford, Illinois 61105 U.S.A.
PHONE 815/968-0747 TWX 910-631-3419

Circle No. 134 on Readers' Service Card

CORCO

REAGENT CHEMICALS

ACIDS

Sulfuric
Nitric
Hydrochloric
Acetic
Perchloric
Phosphoric

BASES

Ammonium Hydroxide
Potassium Hydroxide
Sodium Hydroxide

SOLVENTS

Analytical
Electronic
Spectrophotometric

ELECTRONIC CHEMICALS

Dopants
Epitaxials
Acid Etches

STANDARD SOLUTIONS

Volumetric
Buffer
Percentage

SPECIALTY REAGENT CHEMICALS

Methoxides
Sodium Biphenyl
E.D.T.A.

CUSTOM CHEMICAL SYNTHESIS

CORCO
CHEMICAL CORPORATION
Manufacturers of
Reagent and Electronic Chemicals
Tyburn Road & Cedar Lane,
Fairless Hills, Pa. 19030
Phone: (215) 295-5006

Circle No. 37 on Readers' Service Card

New Chemicals

Chromatography Chemicals

For gas chromatography, new products available include a silylating reagent consisting of 3 parts by volume of trimethylsilylimidazole, 3 parts of bistrimethylsilylacetamide, and 2 parts of trimethylchlorosilane. It can make silyl ethers of sterically hindered OH groups on corticosteroids. New polyamide phases POLY-A103 and POLY-A101A are the first and only polyamides designed for gc. The phases have good thermal stability, low melting points, and high wetting characteristics. They are excellent for the separation of barbiturates, carbohydrates, and amino acids. Finally, a new packing, consisting of 10% EGSS-X on 100/120-mesh Gas Chrom Q is preconditioned and can be used immediately in the gc.

A new reagent for tlc detects monochain lipids. Used in conjunction with iodine the reagent will distinguish saturated lipids from the unsaturated.

New lipids available are the transisomers, brassidic acid and cholesteryl elaidate (both 99+% pure), and the glyceryl ethers, DL-2-hexadecyl and DL-2-octadecyl glyceryl ether. Applied Science Laboratories, Inc., P. O. Box 440, State College, Pa. 16801. 814-238-2406 **505**

Organic Reference Standards

Over 40 ultrapure organic solvents and solids with minimum assays of 99.9% absolute as established by both gc and a precise adiabatic calorimetric melting point technique are designated as Criterioquality standards. These high quality materials are applicable as organic reference standards in kinetic studies and other physical chemical investigations. Each liquid is accompanied by a chromatogram which states the actual purity, the amounts, and, when possible, the identity of the impurities. The calculated purity from the freezing point determination is also given. Solids have purity determined by mass spectrometry, ir, and melting point. MC&B, 2909 Highland Ave., Norwood, Cincinnati, Ohio 45212. 513-631-0445 **506**

New Organic Standard

Research quantities of 7-hydroxychlorpromazine are available. This compound is useful as a pharmaceutical intermediate and as an analytical standard in the metabolic study of the widely used tranquilizer, chlorpromazine. The company claims to be the sole worldwide source of this compound. Germantown Laboratories, Inc., 4150 Henry Ave., Philadelphia, Pa. 19144. 215-848-8600 **507**

The easiest syringes to read are now the easiest to find.

A few months ago, we introduced the patented Unimetrics Micro Syringe. Its totally unique, flat scale made it the easiest-to-read, most accurate GC syringe ever created.

Now we're improving it.

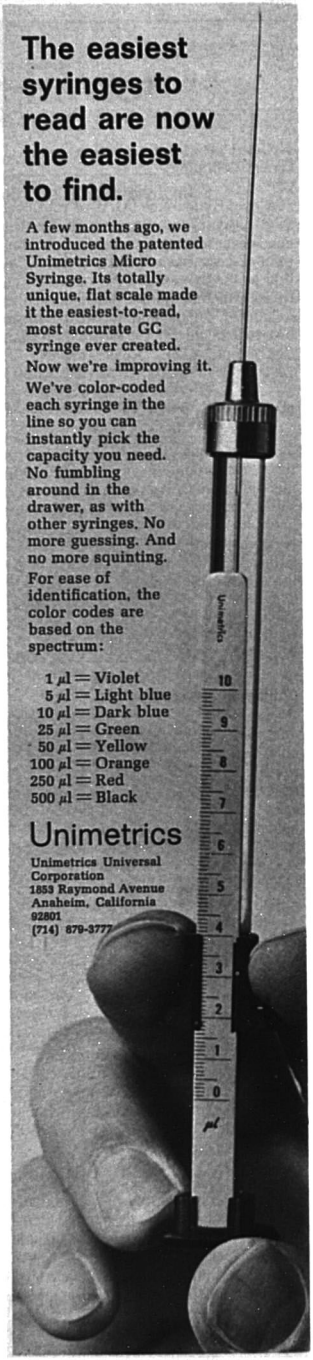
We've color-coded each syringe in the line so you can instantly pick the capacity you need. No fumbling around in the drawer, as with other syringes. No more guessing. And no more squinting.

For ease of identification, the color codes are based on the spectrum:

1 µl = Violet
5 µl = Light blue
10 µl = Dark blue
25 µl = Green
50 µl = Yellow
100 µl = Orange
250 µl = Red
500 µl = Black

Unimetrics

Unimetrics Universal Corporation
1853 Raymond Avenue
Anaheim, California
92801
(714) 879-3777



Circle No. 182 on Readers' Service Card

Bilirubin Reagents and Standard Set

A complete set of reagents and standard for the determination of both total and direct bilirubin levels in blood is available. A simple and rapid method developed by the company overcomes some of the usual obstacles in this type of testing. The set contains sufficient reagents for 120 direct and 120 total bilirubins using a macroprocedure; about twice as many assays may be done with a microprocedure. Harleco, 60th & Woodland Ave., Philadelphia, Pa. 19143. 215-726-9600 **508**

Clinical Reagents

Clinical reagents for blood chemistry packaged in a new Spoonpak unit containers are available. The disposable Spoonpak is designed for the accurate preparation of clinical chemistry solutions. Each unit contains an amount of reagent that is weighed to within 2% of the stated amount. The precisely measured quantity of reagent guarantees reproducibility in the formulation of solutions. Solutions are packed in lightproof containers with an inert layer of argon. Reagents now available are: bilirubin, phenyl phosphate, disodium salt, *p*-nitrophenyl phosphate, INT dye, fast red PDC salt, sodium nitrite, and 4-aminoantipyrine. J. T. Baker Chemical Co., Phillipsburg, N. J. 08865. 201-859-2151 **509**

Ultrahigh-Purity Metal Powders

A complete line of Marz- and VP-grade metal powders simplifies the preparation of high-purity alloys and compounds and has wide usage in powder metallurgy research, analytical chemistry, inorganic preparative chemistry, as well as pharmaceutical research. Starting metals are atomized to powder in an inert atmosphere yielding a uniform powder particle. Powders are available in mesh sizes to −325. Materials Research Corp., Route 303, Orangeburg, N. Y. 10962. 914-359-4200 **510**

New Reagent for Glucose and Uric Acid Determinations

A new reagent, SpecTru BCA, is useful for determinations of glucose and uric acid in automated systems. With the reagent, amine complexes of Cu(II) are readily reduced in dilute Na_2CO_3 solution to the deep lavender Cu(I) complex. In this reduction urate is effective at room temperature and glucose is effective with moderate heat. This reagent offers several advantages over the Cu-neocuproine method. Pierce Chemical Co., P. O. Box 117, Rockford, Ill. 61105. 815-968-0747 **511**

PRECISION SCIENTIFIC
SUBSIDIARY OF GCA CORPORATION

Auto-Aquatrator(TM)

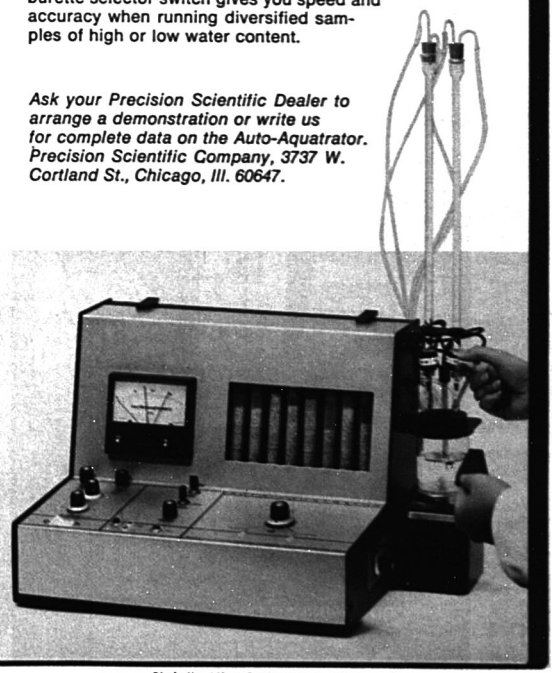
Accurate, automatic Karl Fischer titrations–unusually broad range of applications

With the Auto-Aquatrator, you get quick, accurate and consistent results—reproducible to 0.025 ml of titrant.

The ideal instrument to "automate" moisture determinations in a wide variety of applications: *blood, antibiotics, animal tissue, paper, foods, ethers, anti-freeze, nitroparaffines, hydrate formation in pipelines, phosphates, powders, pastes and liquids, light oils, lube oils, transformer oil, spent acid, alcohols, refrigerants, crystalline powder, propellants, procaine penicillin, crystalline penicillin, glycols, explosives, organic solvents, detergents, inorganic solids, lecithin, vegetable oils, corn syrup, cocoanut oil, benzene, toluene, styrene, nylon solutions, chlorinated solvents, turbine oils, protein, concentrated fruit juices, etc.*

The Auto-Aquatrator handles any organic or inorganic sample, utilizing standard Karl Fischer reagent, water-methanol solution or any suitable solvent, to establish water content by the conductometric method. Its unique burette selector switch gives you speed and accuracy when running diversified samples of high or low water content.

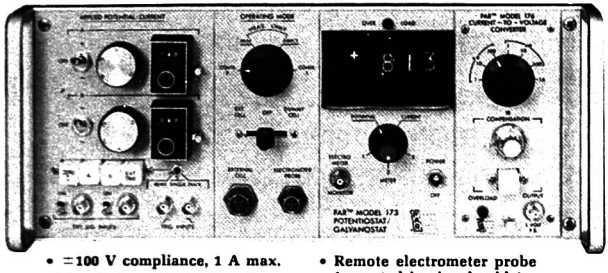
Ask your Precision Scientific Dealer to arrange a demonstration or write us for complete data on the Auto-Aquatrator. Precision Scientific Company, 3737 W. Cortland St., Chicago, Ill. 60647.



Circle No. 149 on Readers' Service Card

THE COMPLETE POTENTIOSTAT!

The new PAR™ Potentiostat/Galvanostat provides more features, modes of operation and flexibility than ever before available.



- **±100 V compliance, 1 A max.**
- **Two independent, internal potential sources**
- **High speed electronic potential switching**
- **Remote electrometer probe (mounted in signal cable)**
- **$10^{11}\Omega$ input impedance**
- **Slewing rate: 10V/μs**

Plug-in modules provide maximum flexibility in readout. Positive feedback IR compensation, high current measurement and galvanostatic capabilities up to 1 A are available. The Model 173 replaces a potentiostat, two voltage sources and a current-measuring device.

Price of the Model 173 is $2200 including probe. Digital version, $2560. Current readout module, $145. I-E converter, $550. 100 mA output version less than $2000. For more data, contact Princeton Applied Research Corp., Box 565, Princeton, N.J. 08540; telephone (609) 452-2111.

PAR PRINCETON APPLIED RESEARCH CORPORATION

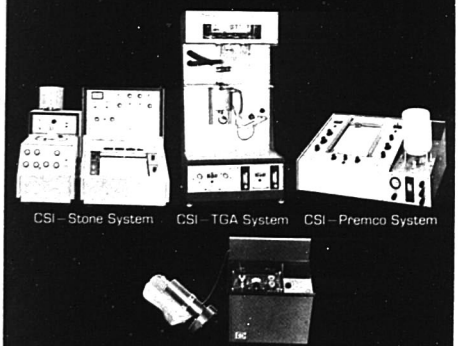
Circle No. 150 on Readers' Service Card

112

COLUMBIA SCIENTIFIC INDUSTRIES

STONE—PREMCO INSTRUMENTATION
TOTAL THERMAL ANALYSIS

DTA — EGA — TGA — DSC — Derivative DTA/TGA
26 Basic Models
Capabilities—160° C to 1600° C, 10⁻⁶ Torr, to 3000 P.S.I.



CSI—Stone System CSI—TGA System CSI—Premco System

Model 700 X-Ray Fluorescence Analyzer
Elemental Analysis—Calcium to Uranium
Detectable Limit Down to—0.01%-15 Second Test

FOR ADDITIONAL LITERATURE—WRITE OR TELEPHONE
COLUMBIA SCIENTIFIC INDUSTRIES
A & I Division, P. O. Box 6190, Austin, Texas 78702
512-926-1530

Circle No. 34 on Readers' Service Card

MANUFACTURERS' LITERATURE

Balances. A 32-page catalog carries descriptions and photographs of the company's full line of balances, weights, and accessories. New products included are the Dial-O-Gram Series 2000, magnetically damped, general purpose lab balances with dial-vernier readout to 0.1 μg, and the Model 6010PC, a moisture determination balance designed for pollution control. Ohaus Scale Corp., 29 Hanover Rd., Florham Park, N. J. 07932 **601**

Fluoride Ion Analyzer. Bulletin 4102, 8 pages, describes the principle of operation, electronic circuitry, and applications of the Model 900F fluoride ion analyzer. The instrument is designed for continuous measurement and control of fluorides in potable water and water pollution. Beckman Instruments, Inc., 2500 Harbor Blvd., Fullerton, Calif. 92634 **602**

Pressure Transducers. A guide for the use of pressure transducers, 32 pages, covers in detail how to establish pressure transducer specifications, testing pressure transducers, preferred circuits, practical considerations and precautions, and other information necessary for the successful use of these devices. Computer Instruments Corp., 92 Madison Ave., Hempstead, N. Y. 11550 **603**

Optical Components and Accessories. Catalog C-5, 36 pages, contains complete specification and price information on optical filters, custom filters, mirrors, and other electrooptical and optical products. Baird-Atomic, 125 Middlesex Turnpike, Bedford, Mass. 01730 **604**

Residual Gas Analyzers. An 8-page brochure describes two compact residual gas analyzers, the EAI QUAD 1100 and the new QUAD 1110 with built-in oscilloscope. Each system has a mass range from 1 to 300 atomic mass units. Varian, 611 Hansen Way, Palo Alto, Calif. 94303 **605**

Liquid Scintillation System. A 4-page bulletin, 7191, provides full specifications for the LS-230 liquid scintillation system, giving details of special features, such as the bidirectional sample changer, quench correction method, and readout options. Beckman Instruments, Inc., 2500 Harbor Blvd., Fullerton, Calif. 92634 **606**

Radiochemical Catalog. A 43-page catalog lists some of the labeled compounds available from the company. The catalog also describes the company's tritium-labeling service and its capability in the custom synthesis of labeled compounds. Biochemical and Nuclear Corp., P. O. Box 749, Burbank, Calif. 91503 **607**

Spectrophotometer. A 160-page brochure discusses the standard Model 14 which covers the uv-vis–near ir wavelength range, the 14UV (uv-vis range), and the company's spectroradiometer. Complete specifications and various accessories are included. Cary Instruments, 2724 S. Peck Rd., Monrovia, Calif. 91016 **608**

D/A and A/D Converters. An 8-page technical application note explains the principles of digital-to-analog converters based on the firm's new μDAC monolithic IC quad switch components, AD550, and thin film resistor packages, AD850. Analog Devices, Inc., 221 Fifth St., Cambridge, Mass. 02142 **609**

Data Acquisition and Computer Interface Products. An 8-page short-form catalog lists specifications and application summaries of converters, sample-hold modules, multiplexers, and other products for computer interfacing and data manipulation. Analog Devices, Inc., 221 Fifth St., Cambridge, Mass. 02142 **610**

Laser Systems Products. Publication JJ-2 describes the company's Q-switch solutions (reversibly bleachable dye solutions) for use with neodymium-doped lasers, and a solution for Q-spoiling ruby lasers. Other products for laser systems are included. Eastman Kodak Co., 343 State St., Rochester, N. Y. 14650 **611**

Tabletop Centrifuges. A 20-page catalog describes the company's line of eight tabletop centrifuges plus a broad selection of accessories. The units are the Clinette, Micro, Clinical, Chemical, MB. Micro-Capillary Tube Readers, HNS, and HT. International Equipment Co., 300 Second Ave., Needham Heights, Mass. 02194 **612**

Chromatography Catalog. A 108-page catalog gives detailed information on packings for gas, liquid, thin layer, and gel permeation chromatography; on components for the chromatography "do-it-yourselfer;" on a complete product line of instrumentation for liquid, gel permeation, and column chromatography; and on analytical and separation services and standards for identification, quality control, and production needs. Waters Assoc., Inc., 61 Fountain St., Framingham, Mass. 01701 **613**

Precision Balances. A 6-page brochure describes the Series HCE balances. The balances with capacities ranging from 1 kg to 50 kg have sensitivity ratios of 1 part in 10 million. Standard on all balances in this series is an electronic null indicator. Voland Corp., 27 Centre Ave., New Rochelle, N. Y. 10802 **614**

Tlc Supplies. A 60-page catalog lists hundreds of items for use in thin layer chromatography and thin layer and high voltage electrophoresis. Included are plates, adsorbents, developing tanks, drying equipment, sample streakers, uv lamps, etc. Camag, Inc., 2855 S. 163rd St., New Berlin, Wis. 53151 **615**

Lab-Crest/ANDREWS SCIENTIFIC DIVISION

MANUFACTURERS OF PRECISION INSTRUMENTS AND APPARATUS FOR THE ANALYTICAL CHEMIST

460 SERIES ROTAMETERS



These Flowmeters offer:

- Wide angle visibility
- High accuracy
- Tubes are easily removed by hand for cleaning or changing flow range.
- Available in stainless steel or aluminum, with or without the control valve.
- Clear plastic shield provided for tube protection and safety.

CHROMATOGRAPHY COLUMNS



- High Pressure columns manufactured of precision bore glass tubing and stainless steel fittings.
- Features: On-column sample injection. Contamination free construction.
- A complete line of low cost ascending or gravity feed columns with associated sample injection syringes.

GLASS & QUARTZ JOINTS

Offered in Three Styles

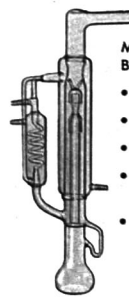


"SOLV-SEAL" JOINT

- ℨ Standard Taper, ℨ Ball & Socket and the patented "Solv-Seal"
- Easy disassembly
- Interchangeable parts
- Quartz or Borosilicate glass units in stock
- Low cost
- Immediate delivery

CUSTOM GLASS & QUARTZ

Fabrications to Meet all Analytical Requirements



Mastercraftsmen Glass-Blowers of:

- Condensers
- Distilling apparatus
- Extraction apparatus
- Custom applications & special requirements
- Guaranteed workmanship

Lab-Crest/ANDREWS SCIENTIFIC DIVISION

FISCHER & PORTER CO. 1511 COUNTY LINE RD., WARMINSTER, PA. 18974

Circle No. 63 on Readers' Service Card

Water Pollution. A 22-page catalog includes information on test kits for detergents, nitrogen, phosphate, and many other relevant ecology and pollution tests. Also illustrated is the company's direct reading engineer's laboratory for testing water in the field. Hach Chemical Co., Ames, Iowa 50010 **616**

Scientific Gases. A 26-page catalog includes prices, packaging, and purity specifications for chemical gases, rare gases, and other gases and gas mixtures. For a copy of the catalog, letterhead requests should be sent to MG Technical Products, Inc., 240 Madison Ave., New York, N. Y. 10016

Automatic XRF/NAA Analyzer. A 6-page folder introduces a new automatic X-ray fluorescence/neutron activation analysis system for both routine analysis and quick identification of unknowns. Atomic Energy of Canada, Ltd., Commercial Products, P. O. Box 93E, Ottawa, Canada **617**

Lab Furniture. A 12-page condensed catalog describes the Contempra laboratory furniture line. This colorful furniture includes base units, lab appliances, special-purpose base units, tables, under-counter cases, and fume hoods, stools, chairs, etc. Fisher Scientific Co., 312 Fisher Bldg., Pittsburgh, Pa. 15219 **618**

Analysis of Water, Wastes, and Process Liquids. Bulletin 7, 8 pages, lists a wide line of analyzers, monitors, and controllers for over 50 different water, processing, and pollution tests from acidity to zinc. Delta Scientific Corp., Lindenhurst, N. Y. 11757 **619**

Atomic Oxidizer. A 4-page technical brochure describes the PL-200 atomic oxidizer for rapid, low temperature dry ashing of samples for quality control analyses. Plasmatics, 2400 Wright Ave., Richmond, Calif. 94804 **620**

Liquid Chromatography Data Processing. A 4-page application note describes the use of a new computer interface system to linearize, integrate, and normalize data from liquid chromatographs. Princeton Applied Research Corp., P. O. Box 565, Princeton, N. J. 08540 **621**

Infrared Spectral Data Service. Publication JJ-165 includes detailed information and prices on the company's infrared data retrieval service. Eastman Kodak Co., 343 State St., Rochester, N. Y. 14650 **622**

Controlled Temperature Chambers. A 10-page catalog illustrates many models of custom-engineered equipment for all types of processing and testing. Temperatures, chamber sizes, and special features are given. Cincinnati Sub-Zero Products, Inc., 2612 Gilbert Ave., Cincinnati, Ohio 45206 **623**

Ultraviolet Products. Seven pages, "Things Ultraviolet," is a minicatalog identifying the wide range of ultraviolet spectral sources, hand lamps, intensity meters, spectral standards, and accessories available from the company. Ultra-Violet Products, Inc., 5114 Walnut Grove Ave., San Gabriel, Calif. 91778 **624**

Strip Chart Recorders. A 6-page brochure on 10 new recorders features the ultraspeed Mark II (1/6 sec full-scale); the Auto Attenuator (resets to the cor-

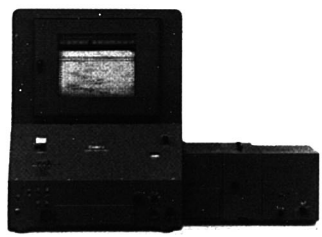
The Cary 14, 15, 16S and 17. Recording

In the whole world, there just isn't another group of comparable recording spectrophotometers.

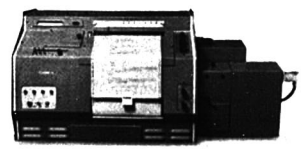
Each has been thoughtfully designed with a proven double monochromator and dual-beam photometric system. Each is precisely engineered throughout and meticulously tested. And each is the best recording spectrophotometer you can buy for the price.

First the venerable workhorse, the Cary 14. Using a prism-grating monochromator, the 14 rapidly and accurately records spectra in the ultraviolet, visible and near infrared from 186 to 2650 nm. Measures absorbance and transmittance directly. Adapts with accessories for reflectance, fluoresence, scattered transmission, and fixed-wavelength kinetics. Price: $19,600.*

Next, the Cary 15. Reliable, proven performer in such fields as the life sciences, pharmaceuticals and industrial research and quality control. Utilizes a double monochromator with two prisms to give exceptional UV penetration. Covers the UV-VIS range (185-800 nm). Features dual detectors to insure maximum photometric accuracy when measuring at high absorbances. Price: $12,950.*



CARY 14



CARY 15

rect input signal anywhere between 1 mV and 100 V); the Auto-Zero (selects automatically the optimum zero suppression voltage); and the linear/log recorder. Soltec Corp., 10747 Chandler Blvd., North Hollywood, Calif. 91601 **625**

Silane-Silicones. An 8-page catalog lists over 140 silanes and silicones having a variety of functional groups. These compounds have many uses including their use as reagents for gas chromatography and other analytical techniques. Marshallton Research Laboratories, Inc., Box 305, West Chester, Pa. 19380 **626**

Spectrograph. An 8-page bulletin covers the Jarrell-Ash 75-150, a versatile optical instrument that can be used as a spectrograph, a scanning spectrometer, or a direct-reading polychromator. Fisher Scientific Co., J308 Fisher Bldg., Pittsburgh, Pa. 15219 **627**

Electrophoresis. A 16-page booklet, "The New Look of Electrophoresis," Product Bulletin 300 B, describes the company's Separtek system for electrophoresis. Gelman Instrument Co., Ann Arbor, Mich. 48106 **628**

Company Periodicals

Requests for copies of the following publications should be sent directly to the address shown. Business or professional letterheads are requested.

Instrument News. Vol. 21, No. 1. This 16-page issue features an article on a novel application of frustrated multiple internal reflection (identification of stamp adhesives). Other articles deal with the feasibility of automating the white cell count differential counting procedure, double wavelength spectrophotometry, a new low-cost spectrophotometer, etc. Perkin-Elmer Corp., Main Ave., Norwalk, Conn. 06852

Labocopeia, No. 2, 8 pages, describes a variety of lab chemicals and other laboratory products of interest to many disciplines in analytical chemistry. Gallard-Schlesinger Chemical Mfg. Corp., 584 Mineola Ave., Carle Place, L. I., N. Y. 11514

Scientific Instrument News. Thermal Analysis Instrument Series. Vol. 2, No. 1. This issue carries two articles: "Low Temperature Micro-DTA Apparatus and Its Application" and "DT-GC Combination (Report 2), Analysis of Polystyrene." Shimadzu Seisakusho Ltd., 1, Nishinokyo Kuwabaracho, Nakagyo-ku, Kyoto, Japan

MPI Applications Notes. Vol. 5, No. 4, 4 pages, discusses the generation of analytical and nonanalytical functions. Three generation methods are explained: solution of differential equations, diode function generators, and curve followers. McKee-Pedersen Instruments, P. O. Box 322, Danville, Calif. 94526

Current Peaks. Vol. 2, No. 3, 4 pages, presents as its feature article "The Educational Gas Chromatograph: Essential Tool for Effective Teaching." Another article discusses the ACS pilot program called "ChemTec" whose members are developing a two-year curricula for students wishing to become chemical technicians. Dr. Robert Pecsok of UCLA directs the NSF-funded program. Carle Instruments, Inc., 1141 E. Ash Ave., Fullerton, Calif. 92631

pectrophotometry's awesome foursome.

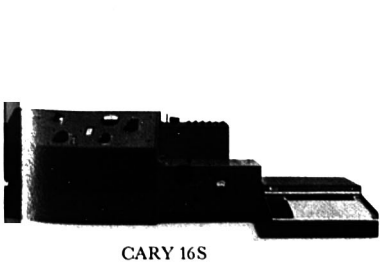
Then, the modular Cary 16S. A recording version of our renowned Cary 16 manual spectrophotometer. Designed for scanning and recording applications in the UV-VIS range where high stability and photometric accuracy are essential. To tailor a 16S system to specific requirements, pick and choose from a large group of modular accessories. Price of basic system: $10,970.*

Finally, the solid state Cary 17. It delivers all the performance of the Cary 14 plus such built-in extras as digitally coupled scan and chart drive, meters to indicate when operating conditions are optimum, and a multi-zero/multi-range slidewire. Does anything any spectrophotometer can. But better. Plus, it's completely computer-compatible for future closed loop operation. Range: 186-2650 nm. Price: $24,950.*

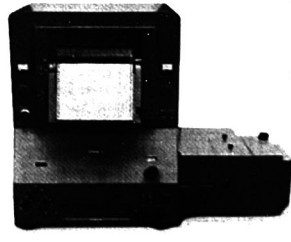
(We might also mention that for each of these instruments there's a SpectroSystem 100. A dedicated computer system for immediate processing of all spectral data.)

That's a brief look at Cary recording spectrophotometers. One just right for your work. And your budget. For complete specifications and prices, simply write Cary Instruments, a Varian subsidiary, 2724 South Peck Road, Monrovia, Calif. 91016. Ask for data file A101-11.

*All Prices F.O.B. Monrovia, California



CARY 16S



CARY 17

cary instruments

Circle No. 38 on Readers' Service Card

LABORATORY SUPPLY CENTER

BUYING A MASS SPECTROMETER ?
AND LOST IN A JUNGLE OF SPECIFICATIONS AND PRICES

AVOID COSTLY MISTAKES
by letting the experts help you select the optimum instrument to fit your needs and budget. Consultation with us will save you time, money and frustration.
WE ARE NOT AFFILIATED WITH ANY MANUFACTURER
For details, without obligation, write or phone:

MORGAN-SCHAFFER CORP.
5110 COURTRAI AVENUE, MONTREAL, QUE.
TEL. (514) 731 4652

LaMotte Chemical
Chestertown, Maryland 21620
Manufacturers of chemical testing equipment and accessories since 1919
Write Dept. AC for free catalog

ELECTRON MICROSCOPY ▲ MICROANALYSIS
SCANNING
TRANSMISSION
REPLICATION
ELECTRON MICROPROBE
X-RAY DIFFRACTION
ELECTRON DIFFRACTION
METALLOGRAPHY ▲ FRACTOGRAPHY ▲ FAILURE ANALYSIS
ERNEST F. FULLAM, INC. — *Scientific Consultants*
P.O. BOX 444 SCHENECTADY, N. Y. 12301 518-785-5533

FINALLY!!
A logical method for selecting columns for gas chromatography.
No more . . .
1. Lists of **polar** columns
2. Duplication of columns
3. Wasted time on obviously incorrect columns
4. Use of **obsolete** columns
But . . .
1. A list of numerically classified columns
2. A method for selecting columns based on structure of sample
3. **Examples** showing how system works
IT'S Free . . . and described in our 1971 catalog and in our column classification chart. Write for both. Self-addressed envelopes will speed up delivery.
SUPELCO, INC.
Supelco Park
Bellefonte, Pa. 16823
Phone (814) 359-2732

Acetonedicarboxylic Acid • Allyl Thiourea • ε-Aminocaproic Acid
Benzoic Anhydride • Chalcone • Chloroacetaldehyde • Cochineal
Desoxyribonucleic Acid • Diacetyl Monoxime • Dibenzyl Succinate
1,2-Diethoxyethane • Di-iso-propylxanthogen Disulfide • Dulcitol
Guanine • Hippuric Acid • α-Ketoglutaric Acid • Mandelic Acid
o-Phenanthroline • Phenylthiourea • Iso-Propenyl Acetate
Rhodanine • Salicin • Sodium Succinate • Succinimide • Taurine
Thymolphthalein • 2,2,2-Tribromoethanol • Urea Nitrate • Xylose
Write for list K-69 of other chemicals
Tel: 201 696-1700 TWX: 710 988-5831 Zip Code 07440
EASTERN CHEMICAL CORPORATION BOX K PEQUANNOCK, N. J.

Forty Six Distilled in Glass Solvents
BURDICK & JACKSON LABORATORIES, INC. 616 722 2310
MUSKEGON, MICHIGAN 49442

NMR SOLVENTS

Chloroform-d,	99.8% D	100g	$14.00
Acetone-d_6,	99.5% D	10g	$10.00
DMSO-d_6,	99.5% D	10g	$10.00

Request Catalog EJ-71
STOHLER
Stohler Isotope Chemicals
49 Jones Road
Waltham, Mass 02154
Tel: ICID 891-1827-8

ANALYTICAL SERVICES
MASS SPECTROMETRY
GAS CHROMATOGRAPHY—COMBINED GC-MS
INFRARED SPECTROPHOTOMETRY
THERMAL ANALYSIS—DTA-TGA-DSC
WEST COAST TECHNICAL SERVICE
1049 S. San Gabriel Blvd.
San Gabriel, California 91776
(213) 287-0926

GAS ANALYSES
Mass Spectrometry • Gas Chromatography
• Leak Detection
• Vacuum and Inert Gas Fusion
GOLLOB ANALYTICAL SERVICE INC.
47 Industrial Road, Berkeley Heights, N. J. 07922
201-464-3331

AMERICAN CHEMICAL SOCIETY

"Primary Publications on Microfilm"

Your Key to—

- Dramatic savings in archival space and dollars.
- Faster access to needed data.
- Unlimited distribution of copyrighted scientific data.

ACS publications in the program:

JOURNAL OF THE AMERICAN CHEMICAL SOCIETY (1879-1969)
INDUSTRIAL & ENGINEERING CHEMISTRY (1909-1969)
CHEMICAL & ENGINEERING NEWS (1923-1969)
ANALYTICAL CHEMISTRY (1929-1969)
JOURNAL OF PHYSICAL CHEMISTRY (1896-1969)
JOURNAL OF AGRICULTURAL & FOOD CHEMISTRY (1953-1969)
JOURNAL OF ORGANIC CHEMISTRY (1936-1969)
JOURNAL OF CHEMICAL AND ENGINEERING DATA (1956-1969)
CHEMICAL REVIEWS (1924-1969)
JOURNAL OF CHEMICAL DOCUMENTATION (1961-1969)
INDUSTRIAL & ENGINEERING CHEMISTRY—FUNDAMENTALS (1962-1969)
INDUSTRIAL & ENGINEERING CHEMISTRY—PROCESS DESIGN AND DEVELOPMENT (1962-1969)
INDUSTRIAL & ENGINEERING CHEMISTRY—PRODUCT R & D (1962-1969)
BIOCHEMISTRY (1962-1969)
INORGANIC CHEMISTRY (1962-1969)
JOURNAL OF MEDICINAL CHEMISTRY (1959-1969)
CHEMISTRY (1962-1969)
ENVIRONMENTAL SCIENCE & TECHNOLOGY (1967-1969)
ACCOUNTS OF CHEMICAL RESEARCH (1968-1969)
MACROMOLECULES (1968-1969)

For information on "ACS Primary Publications on Microfilm", write or call:

Mr. George Virvan
Special Issues Sales
American Chemical Society
1155 16th Street, N.W.
Washington, D.C. 20036
(202-737-3337)

INDEX TO ADVERTISERS IN THIS ISSUE

*Academic Press 51A
Flamm Advertising
A. E. L. Scientific Apparatus 18A
Streets Provinces
American Chemical Society 93A
*American Instrument 1A, 95A
Industrial Advertising Assoc.
*Analabs, Incorporated 60A
Deforte Art Associates, Inc.
*Angstrom, Incorporated 96A
Denham & Company, Inc.
*Applied Science Laboratories, Incorporated 108A
Media Services, Ltd.
Aztec Instruments 61A
A. B. W. Toft & Co.

*Bausch & Lomb—Analytical Systems Division 59A
Wolff Associates, Inc.
*Beckman Instruments, Incorporated. 37A
N. W. Ayer/Jorgensen/MacDonald, Inc.
*Bel Art Products 30A
Gallard Advertising Agency, Inc.
*James G. Biddle Company 4A
Shaifer, Scudder & Smith
Brinkmann Instruments, Incorporated OBC
The Shaller-Rubin Co., Inc.
Bruker Scientific, Incorporated 62A
Schwietzer Advertising
*Buchler Instruments Div., Sub. of G. D. Searle & Co. 78A
Selvin & Jaffe

*Cahn/Ventron Corporation 84A
Gordon Gelfond Associates, Inc.
*Carle Instruments, Incorporated 63A
Cochrane Chase & Company, Inc.
*Fred S. Carver, Inc., Sub. of Sterling, Inc. 90A
Scott, Inc. Advertising
*Chromatronix, Incorporated 92A
Bonfield Associates
*Coleman Instruments Corporation ... 84A
Mandabach & Simms, Inc.
Columbia Scientific Industries 102A
Corco Chemical Corporation 100A
Charles D. Karlsruher
Cryogenic Associates, Incorporated ... 97A
Bell-Catterlin & Hedgcock Advertising, Inc.

Digital Equipment Corporation 43A
Kalb & Schneider, Inc.

Eastman Kodak Company 19A
Rumrill-Hoyt, Inc.
Electron Technology 98A
Kniep Associates

Fabri-Tek Instruments, Incorporated .. 12A
Towell & Timmons, Inc.
*Fischer & Porter Company 103A
Furlong Promotions, Inc.
*Fiske Associates F1
** The Source

Greiner Scientific Corporation 95A
Fairfax, Inc.

*Hamamatsu TV Co., Ltd. 17A
Kairyusha Advertising Ltd.
*Hamilton Company 26A
Swain, Mealer & Emerson, Inc.
Heath Company 58A
Advance Advertising Service
*Hewlett-Packard 66A, 79A
Richardson, Thomas & Bushman, Inc.
Hewlett-Packard, San Diego Division 36A
Phillips Ramsey
*Hotpack Corporation 90A
Allyn H. Jackson
Houston Instrument 94A
Ray Cooley and Associates, Inc.

Illinois Water Treatment Company ... 50A
Cummings Brand McPherson Associates, Inc.
*Instrumentation Laboratory, Incorporated ..... IFC
Pazolt & Company Advertising
Instrumentation Specialties Company. 52A
Graham Printing & Advertising

Jeolco (U.S.A.) Incorporated 16A

*Kevex Corporation 54A
Bonfield Associates
*Kewaunee Scientific Equipment Corporation 96A
Phillips Associates
*Kontes Glass Company 46A
Aitkin-Kynett Co., Inc.

*Laboratory Data Control 57A
A. B. W. Toft & Co.
*Leeds & Northrup 25A
Gaynor & Ducas, Inc.

MC&B Mfg. Chemists 97A
Cooper, Strock, Scannell
*Mettler Instrument Corporation ... 10A, 83A
Harris D. McKinney, Inc.

*Nestler/Faust Mfg. Corp. 38A
deMartin-Marona & Associates
*Nuclear-Chicago, a subsidiary of G. D. Searle & Co. 53A
Sidney Clayton Associates, Inc.

*PCR, Incorporated 76A
Advertising Associates of Jacksonville, Inc.
*Perkin-Elmer 7A, 17A, 33A, 45A, 64A, 89A, 98A
Gaynor & Ducas, Inc.
*Pharmacia Fine Chemicals Div. 32A
Cummins, Macfail & Nutry, Inc.
*Philips Electronic Instruments 34A, 67A, 74A, 86A
** Marsteller, Inc.
*Photovolt Corporation 65A
Michel-Cather, Inc.
*Pierce Chemical Company 99A
Advertising Design
*Plenum Publishing 52A
Flamm Advertising
*Precision Cells, Incorporated 98A
Co-Ad Associates, Inc.
*Precision Scientific Company 101A
Tri-State Advertising Co., Inc.
*Princeton Applied Research Corporation 14A, 102A
Mort Barish Associates, Inc.

Raytheon Computer 5A
Durel Advertising

*Sargent-Welch Scientific Company. 35A, 85A
Sidney Clayton Associates, Inc.
*Schleicher & Schuell, Inc. 42A
Wildrick & Miller
*Scientific Glass Apparatus Co., Inc. . 77A
Sonic Engineering 55A
W. L. Towne

Technicon Corporation 56A
Mediad, Inc.
*Arthur Thomas Company 82A
*Torsion Balance 99A
Michel-Cather, Inc.

Ultra-Violet Products, Incorporated .. 92A
Philip J. Meany Company
*Unimetrics Universal Corporation ... 100A
Cochrane Chase & Co., Inc.

Van Waters & Rogers, Will Scientific 48A
Wolff Associates, Inc.
*Varian Aerograph 8A–9A
Chiat/Day, Inc.
*Varian Aid 47A
Chiat/Day, Inc.
*Varian Cary 104A–105A
Chiat/Day, Inc.
*Varian Techtron 91A
Chiat/Day, Inc.

Wang Laboratories, Incorporated 4A
Chirvag & Carns, Inc.
*Waters Associates ..... IBC
Thomas R. Sundheim Inc.
John Wiley & Sons 6A
Ed. McLean & Co., Inc.
Wilmad Glass Co., Incorporated 81A
Walsh Advertising Agency

▼ ▼ ▼

Laboratory Section 106A
Burdick and Jackson Laboratories, Inc.
Eastern Chemical Corporation
Ernest F. Fullam, Incorporated
Golbob Analytical Service
LaMotte Chemical Products Company
Morgan Schaffer Corporation
Stohler Isotope Company
Supelco, Incorporated
West Coast Technical Service, Incorporated

Advertising Management for the American Chemical Society Publications

CENTURY COMMUNICATIONS CORP.

Edward P. Blanchard, President, Thomas N. J. Koerwer, Executive Vice President. 142 East Avenue, Norwalk, Connecticut 06851 (Area Code 203) 853-4488

ADVERTISING SALES MANAGER
Thomas N. J. Koerwer

SALES REPRESENTATIVES

Chicago 60601 . . . Eugene Eldridge, Century Communications Corp., 307 North Michigan Avenue, 312-641-0890.

Cleveland 44113 . . . Michael Hayes, Century Communications Corp., 75 Public Square, 216-523-1930.

Dallas 75207 . . . Parker Harris, Roy McDonald Asso., 714 Stemmons Tower West, 214-637-2444.

Denver 80203 . . . Robert H. Heidersbach, Roy McDonald Asso., Inc., 846 Lincoln Street, 303-825-3325.

Houston 77006 . . . Frank N. Vickrey, Richard Clothier, Roy McDonald Asso., Inc., 3130 Southwest Freeway, 713-529-6711.

Los Angeles 90045 . . . Clay S. Holden, The Connecticut Century Communications Corp., Airport Arcade Bldg., 8820 S. Sepulveda Blvd., Suite 215, 213-776-0552

Norwalk 06851 . . . Don Davis, Richard Feary, Century Communications Corp., 142 East Avenue, 203-853-4488.

Philadelphia 19034 . . . James A. Byrne, Century Communications Corp., 535 Pennsylvania Avenue, Fort Washington, Pa., 215-643-2586.

Great Britain and Western Europe . . . Brayton Nichols, The American Magazine Group, 44 Conduit Street, London, W.1, England, Telephone Regent 4714.

Japan . . . Sumio Oka, International Media Representatives, Ltd., 1 Shiba-Kotohira-cho, Minatoku, Tokyo.

PRODUCTION DEPARTMENT
Production Director
Joseph P. Stenza
Advertising Production Manager
Penelope Mallach

*See ad in ACS Laboratory Guide

** *Companies so marked have advertisements in the foreign regional edition only*

FUTURE ARTICLES

Carbon Rod Atomizer in Atomic Absorption and Fluorescence Spectrometry
M. D. Amos, P. A. Bennett, K. G. Brodie, P. W. Y. Lung, and J. P. Matousek

High Sensitivity Internal Reflection Spectroelectrochemistry for Direct Monitoring of Diffusing Species Using Signal Averaging
N. Winograd and T. Kuwana

Use of a Modified Coulter Counter for Determining the Size Distribution of Macroinclusions Extracted from Plain Carbon Steels
D. A. Flinchbaugh

Expanded Capability of the Coulter Counter with a New Aperture Apparatus
D. A. Flinchbaugh

Use of Suspension Atomization in Atomic Absorption Spectrometry
W. W. Harrison and P. O. Juliano

Alternating Current Polarographic Method of Analysis in the Presence of Oxygen and Other Irreversibly Reduced Species
A. M. Bond and J. H. Canterford

Application of Photoelectron Spectrometry to Pesticide Analysis. II. The Photoelectron Spectro of Hydroxy-, and Halo-Alkanes and Halohydrins
A. D. Baker, D. Betteridge, N. R. Kemp, and R. E. Kirby

Some Analytical Characteristics of Organic Liquid Fuel Flame in Atomic Absorption Spectrometry
B. W. Bailey and J. M. Rankin

Automated Thermoanalytical Technique. An Automated Thermobalance
W. S. Bradley and W. W. Wendlandt

Improved Method for the Determination of Chlorinated Hydrocarbon Pesticide Residues in Whole Blood
S. J. Henderson, J. G. DeBoer, and H. M. Stahr

Known Addition Ion Selective Electrode Technique for Determining Simultaneously Fluoride and Chlorine in Calcium Halophosphate
L. G. Bruton

Separation of Perrhenate, Molybdate, and Selenite Ions on Silica Gel
A. M. Phipps

Spectrophotometric Determination of Cobalt with Benzil Mono-(2-Pyridyl) Hydrazone
R. T. Pflaum and E. Scott Tucker III

Simultaneous Coulometric Determination of Silver, Cadmium, and Indium in Ternary Alloys
A. Barello and G. R. Guidotti

Methyl-17 α-Acetoxy Progesterone Kinetic Study of the Beckmann Rearrangement of 6α-Methyl-17 α-Acetoxy Progesterone 3-Oxime by Cathode-Ray Polarography
A. P. Shroff and C. J. Shaw

Determination of Nitrogen and Hydrogen at Ppm Levels in Milligram Steel Samples
G. L. Hargrove, R. C. Shepherd, and H. Farrar IV

Fluorometric Determination of Submicrogram Quantities of Zirconium
T. D. Filer

Spectrofluorometric Determination of Europium, Samarium, and Terbium as Their Hexafluoroacetylacetone–Trioctylphosphine Oxide Complexes
R. P. Fisher and J. D. Winefordner

GAS-CHROM® Q

GAS-CHROM Q has been on the market for many years and is still the best support commercially available.

This high quality silane-treated support has broad applications as is shown in the literature. It is used extensively for analysis of pesticides, steroids, bile acids, alkaloids and fatty acid methyl esters. Use of GAS-CHROM Q minimizes peak tailing and catalytic decomposition of sensitive samples.

GAS-CHROM Q is made by treating GAS-CHROM P with dimethyldichlorosilane (DMCS) -- a process that is carefully controlled and tested. The finished support is evaluated both as a 10% DC 200 packing and as a 3% QF-1 packing.

Quality control is your assurance that GAS-CHROM Q will perform properly. Available in 3 mesh sizes: 60/80, 80/100, and 100/120.

THE FINEST SILANE-TREATED SUPPORT YOU CAN USE



Applied Science Laboratories Inc.

P.O. Box 440 / State College, Penna. 16801 / 814-238-2406

Circle No. 7 on Readers' Service Card

$20,000* buys you the most powerful liquid chromatography facility ever offered

Do prep work. Or high-speed, high-resolution chromatography. Or both.

Do size separations. Or affinity separations. Or partition, or ion exchange. Or any three.

Use UV or refractive index detection. Or both.

In short, take advantage of the analytical synergism provided by three liquid chromatographs working in close proximity to one another.

Use them simultaneously. Or sequentially. Or separately.

End backlogs. Speed research. Tackle real unknowns.

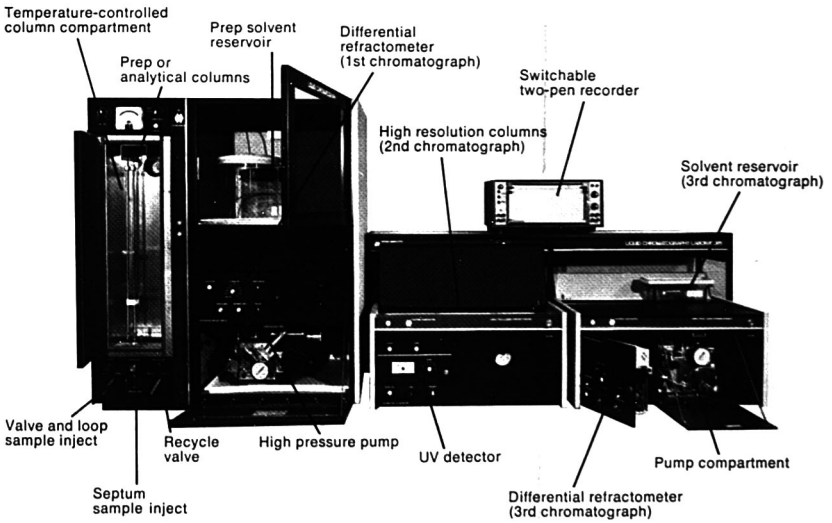
Telescope solvent programming by running three polarities simultaneously. Or recycle the sample for maximum resolution with minimum column length and operator manipulation. Use temperatures to 200°C, pressures to 3000 psig.

For sheer volume of work, or for variety of methods and parameters, the Liquid Chromatography Laboratory is *the* answer.

Write for complete specs and details to Waters Associates, Inc., 61 Fountain St., Framingham, Mass. 01701. Telephone (617) 879-2000. In Europe: Waters Associates, Ltd., Meadow Mills, Waters Street, Stockport, Cheshire, England; or Waters Messtechnik GmbH, 6 Frankfurt/Main, Savignystrasse 51, Germany.

*U.S. price, F.O.B. Framingham, $19,980

The Liquid Chromatography Laboratory, by Waters Associates.



WATERS ASSOCIATES

4954

Circle No. 199 on Readers' Service Card

This sleek, sophisticated new instrument is a phenomenal value. It's the Brinkmann/Metrohm pH-102...the first—and only—digital pH meter in its price range that offers 0.001 pH/0.1 mV sensitivity throughout the full span of 0 to 14 pH and −1.399 to + 1.399 mV.

The price is just $850, complete... and we mean complete—because the price includes shock-resistant combination electrode and stainless steel rod with mounting hardware, buffer solution and KCl.

At $650, model pH-101, delivers the same outstanding features with 0.01 pH and 1.0 mV sensitivity. The luxury look and luxury features are standard equipment in both models:

- Stable, all solid-state circuitry with built-in BCD and recorder output.
- Large, easy-to-use controls for temperature compensation, function, range and slope integration.
- All-digital readout.
- Automatic temperature control

For high precision pH metering, these features, and more, make the Brinkmann/Metrohm pH-101 and pH-102 unique in their field.

For all the facts, please write: Brinkmann Instruments, Cantiague Road, Westbury, N.Y. 11590.
In Canada: 50 Galaxy Boulevard, Rexdale (Toronto), Ontario.

BRINKMANN

Circle No. 20 on Readers' Service Card

pHantastic

